ALMA MATER STUDIORUM - UNIVERSITÀ DI BOLOGNA

SCUOLA DI INGEGNERIA E ARCHITETTURA

DIPARTIMENTO DI INGEGNERIA CIVILE, AMBIENTALE E DEI MATERIALI

CORSO DI LAUREA MAGISTRALE IN CIVIL ENGINEERING

TESI DI LAUREA

in
Advanced Design of Structures

SEMI-ENGINEERED EARTHQUAKE-RESISTANT STRUCTURES: ONE STORY BUILDINGS MADE WITH BHATAR CONSTRUCTION TECHNIQUE

CANDIDATO
Raffaele Carabbio

RELATORE:
Chiar.mo Prof. Ing. Stefano Silvestri

CORRELATORI
Dott. Ing. Luca Pieraccini

Anno Accademico 2015/2016

Sessione III

ACKNOWLEDGEMENTS

This thesis is focused on an engineering field; at the same time, it has been developed through multidisciplinary knowledge and eyes. The word Design involves all the fields I have ever appreciated. The word Design is the link-word, which connects all my academic path.

Ten years ago I started studying Industrial Design in Architecture atUniversità di Genova, then through the years I crossed civil and environmental studies, finishing focusing on Structural engineering curriculum in Bologna. Often the people thinks this is a strange path but I have never considered myself strictly pure. I have always considered varied and mix knowledge as a wealth.

I would like to thank my supervisor Prof. Ing. Stefano Silvestri, Arch. Martijn Schildkamp, Dot. Ing. Luca Pieraccini; I thank them for the support and time dedicated, for all of their guidance through this process; your discussion, ideas, and feedback have been absolutely invaluable.

I would like to thank Julio Alfredo Samayoa Avalos for his friendship and the time spent together studying and having fun and all my fellow students.

I would like to thank my family for the supports and the economic help for studying so long.

Thank you to my partner Antonio Coco, for all his love and support.

SOMMARIO

Questa tesi studia il comportamento statico e sismico di strutture semplici realizzate con un sistema costruttivo utilizzato da vari secoli , in zone piuttosto remote dei paesi che oggi vengono definiti come terzo mondo.A secondo delle zone il nome cambia.Per quanto riguarda le regioni Himalayane tra Nepal e Pakistán il nome comune è Bhatar. Questo sistema costruttivo vede come materiali utilizzati legno e pietra locali. Il Bhatar è costituito da pareti portanti composte da strati di pietra non perfettamente uniforme, i comuni muretti a secco, intervallati orizzontalmente da travi composte da elementi lignei i quali incastrati tra di loro risultano paragonabili a cordoli.Il sistema Bhatar è conosciuto come intrínsecamente antisísmico poichè esistono costruzioni di alcuni secoli che hanno resistito a fenomeni sismici importanti. Le analisi sono condotte con riferimento ad un edificio ad un piano, di dimensioni (pianta 3.60m x 3.6m) e con tetto in legno e terra. Questa tecnologia costruttiva, di carattere semi-ingegneristico, è già ampiamente utilizzata nelle regioni Himalayane, in Pakistan e India, ma è anche indirizzata alle popolazioni di nazioni in via di sviluppo poiché offre un vantaggio sia di tipo economico che di tipo tecnico rispetto ai materiali convenzionali (muratura in mattoni e cemento). Le informazioni ad oggi disponibili su questo genere di strutture sono molto limitate a causa della scarsa e poco approfondita ricerca eseguita sul tema.Di grande utilità è stato il materiale elaborato dall'architetto Tom Schacher technical advisor per la Swiss Agency for Development and Cooperation.Tom Schacher col suo lavoro ha stilato delle linee guida, tramite immagini per popolazioni semi-analfabete, che consigliano particolari dimensionamenti e rapporti tra dimensioni nella costruzione di sistemi a Bhatar.

L'obiettivo principale di questa ricerca è di definire gli aspetti principali del comportamento sismico di un edificio ad un piano composto secondo le linee guida dettate da Tom Schacher, con scopo di prevenire crolli causati da azioni sismiche e quindi ridurre il rischio sismico in quelle regioni del mondo dove questi disastri hanno intensità significative. Non esistono attualmente in letteratura ricerche specifiche su pareti costruite con il sistema Bhatar.

Per quanto riguarda le pareti , sono stati effettuati calcoli e analisi allo scopo di capire il comportamento statico e sismico. In analisi statica, è stata condotta una verifica a sforzo normale calcolando lo sforzo normale agente alla base del muro e la corrispondente capacità resistente.Per quanto riguarda l'analisi sismica del muro, si è studiato sia il comportamento nel piano sia quello fuori dal piano. Per l'analisi in piano ci si è concentrati sul materiale roccioso ed è stato utilizzato il modello di Barton che definisce la relazione non lineare che tra le tensioni normali e tangenziali nelle discontinuità degli ammassi rocciosi in presenza di pietre non uniformi.Per quanto riguarda l'analisi fuori dal piano l'attezione è stata rivolta alle connessioni degli elementi lignei che diventano fondamentali nelle reazioni a sollecitazioni di tipo orizzontale e prevengono ribaltamento e gli altri meccanismi di collasso, questo scopo le connessioni e le strutture in legno suggerite da Tom Schacher sono state esaminate alla luce delle norme tecniche Eurocodice 5 : Design of timber structures.

Grazie alle analisi effettuate è possibile avere una prima idea di quanto questo tipo di costruzioni siano effettivamente antisismiche. Importante è sottolineare che questa tesi è l'inizio di un lungo lavoro che per essere affrontato al meglio necessita di prove di laboratorio su materiali e prove di laboratorio su modelli in scala reale.

ABSTRACT

After the 2005 M7.6 Kashmir earthquake (Pakistan), field observations reported that several buildings manufactured with traditional techniques well resisted to this strong seismic event. Nonetheless, these techniques have never been deeply studied from a structural engineering point of view yet. The high number of people living in such structures highlights the importance of focusing on this subject.

This paper reports a full analytical study on the static and seismic behavior of simple one-storey buildings made with a typical construction technique commonly named as “Bhatar” system, used for several centuries and widely diffused in rather remote areas of the Himalayan regions like India, Nepal and Pakistan.

The Bhatar system consists of load-bearing walls made of common dry-stacked rubble stone masonry held together by horizontal wooden bands disposed at several levels (spaced at intervals of about 60 cm). It is widely adopted in developing countries due to its advantages from both economical and constructive point of view with respect to the conventional constructions techniques (i.e. brick masonry and concrete structures).

Despite its wide diffusion, the information currently available on the actual static and seismic behavior of such construction technique are very limited due to little attention paid on such topic.

In the present work, analytical analyses are conducted with reference to a one-storey building modulus characterized by a 3.6 m x 3.6 m square plan covered by an heavy wooden roof with 20 cm thick earth coverage, in order to investigate its response under both gravity and seismic inertial loadings. In detail, in-plane and out-of-plane response of a single wall under horizontal actions is discussed and particular attention is focused on the connections between the timber elements, which are fundamental for the transmission of the horizontal actions and for preventing overturning and other failure mechanisms.

The main aim is twofold: (i) to provide a first insight into the actual seismic response of such construction technique, as a basis for the specific design of ad-hoc laboratory tests on full-scale models, and (ii) to give some rules of thumb for a proper dimensioning and construction of this kind of structures.

INDEX

LIST OF FIGURES

Figure 12-1 Critical layers for the in-plane seismic analysis. Sliding...286

LIST OF TABLES

SIMBOLOGY

Symbols and abbreviations for Shorea Robusta EN388

$E_{0,mean}$ mean characteristic value of modulus of elasticity parallel to grain (in kN/mm2)

$E_{0,05}$ 5-percentile characteristic value of modulus of elasticity parallel to grain (in kN/mm2)

$E_{90,mean}$ mean characteristic value of modulus of elasticity perpendicular to grain (in kN/mm2)

$f_{c,0,k}$ characteristic value of compressive strength parallel to grain (in N/mm2)

$f_{c,90,k}$ characteristic value of compressive strength perpendicular to grain (in N/mm2)

$f_{m,k}$ characteristic value of bending strength (in N/mm2)

$f_{t,0,k}$ characteristic value of tensile strength parallel to grain (in N/mm2)

$f_{t,90,k}$ characteristic value of tensile strength perpendicular to grain (in N/mm2)

$f_{v,k}$ characteristic value of shear strength (in N/mm2)

G_{mean} mean characteristic value of shear modulus (in kN/mm2)

ρ_k characteristic value of density (in kg/m3)

ρ_{mean} mean value of density (in kg/m)

ANNEX A Determination of values

Tensile strength parallel to grain f_(t,0,k)=0,6*f_(m,k)

Compression strength parallel to grain fc,0,k = 5*(f m,k)^0,45

Shear strength

fv,k shall be taken from Table 1 Tensile strength perpendicular to grain

f_(t,90,k)=0,4 N/(mm^2) for softwoods

f_(t,90,k)=0,6 N/(mm^2) for hardwoods

Compressive strength perpendicular to grain

f_(c,90,k)=0,007 * ρ_k for softwoods

f_(c,90,k)=0,015 * ρ_k for hardwoods

Modulus of elasticity parallel to grain

E_0,05=0,67*E_(0,mean) for softwoods

E_0,05=0,84*E_(0,mean) for hardwoods

Mean modulus of elasticity perpendicular to grain

E_(90,mean)=E_(0,mean)/30 for softwoods

E_(90,mean)=E_(0,mean)/15 for hardwoods

Mean shear modulus G_mean=E_(0,mean)/16

Mean density ρ_(mean=1,2)*ρ_k

γ: Specific weight

λ: Slenderness

σ_N: Normal stress

τ= shear stress

μ= friction coefficient

As= Surface area

B= Base of the wall

c= cohesion

F_s= seismic force

H= Height of the wall

L= Length of the wall

M_{ext}: External moment

M_{sp}: moment due to the sprigs

t: Thickness

W_{roof}: Weight of the roof

W_t: Weight of the wall

M_{ytf} : Parasitic Bending moment along Y axis due to tension and flexion

M_{ycf} : Parasitic Bending moment along Y axis due to tension and flexion

M_{y1} Parasitic Bending moment along Y axis due to tension and flexion on external notch

M_{y2} Parasitic Bending moment along Y axis due to tension and flexion on internal notch

M_{z1} Parasitic Bending moment along Z axis due to compression and flexion

M_{z2} Parasitic Bending moment along Z axis due to compression and flexion

M_{x1} Parasitic Bending moment along X axis due to compression and flexion

M_{x2} Parasitic Bending moment along X axis due to compression and flexion

Wtb weight Timber Band

Wrs weight A - roof support

Wmb weight C - main block

Wof weight D - outer foundation

Ϭtb Stress under   Timber Band

Ϭrs Stress under A - roof support

Ϭmb Stress under C - main block

Ϭof Stress under C - main block

Wearth weight of Earth/clay

Wtwigs weight of Twigs

Wringstones weight of Ring of stones

Wplanks weight of Planks

Wrb weight of Roof beams

Wearth linear : linear load of Earth/clay

Wtwigs linear : linear load of Twigs

Wringstones linear : linear load of Ring of stones

Wplanks linear: linear load of Planks

Wrb linear: linear load of Roof beams

α is the load multiplier

$Wtot$ is the total weight of the box structure and of the roof

PGA is the peak ground acceleration

μi is the friction coefficient of the ith layer

Wi is the pertinent weight on the ith layer

β_j : is the distribution factor corresponding to the analyzed layer

W_j : is the weight corresponding to the analyzed layer

h_j : is the height corresponding to the analyzed layer

$\sum_{i=1}^{N} W_i * h_i + W_{roof} * H$: is the summation of all the of all the masses times the corresponding heights

μs_j is the friction coefficient obtained by the Barton models for rockfill corresponding to the analyzed layer

Nj is the pertinent normal force acting on the on the analyzed layer

Chapter 9

T_{min} is the minimum tension allowed for resisting to the seismic action

n is the total number of the rafters , for 3,6 m length wall = 12 (Each timber tie-beam is composed by 2 rafters)

M_{tot} is the total mass of the 3,6 m length wall

a_g is the seismic acceleration in g

g is the gravity acceleration constant = 9,81 m/s^2

Htchain is the height from the ground of the centroid of the roof rafter beam

H is the height of the centroid of the section of the wall

B is the horizontal component of the centroid of the section of the wall

E_{ext} is the external energy

E_{int} is the internal energy

β is the rotation angle for the overturning mechanism

$\delta 1$ is the displacement of the centroid

$\delta 2$ is the displacement of the application point of the considered seismic force (in same case just the roof force)

Δ is the proportional multiplier between 0 and 1

W_{roof} is the weight of the roof

W_{wall} is the weight of the wall

$\delta 3$ is the displacement of the application point of the considered seismic force of the wall

T_{min} is the minimum tension due to the seismic event on the roof tie timber beam

δt_{chain} is the displacement of the application point of the roof timber beams acting as a chain

Ht_{chain} is the height of the roof timber beams acting as a chain

Chapter 10

n : number of rigid joints n = 4

m : number members m = 4

r : support reactions r = 3

i : degree of indeterminacy i = ?

η_i : is the effective displacement in the effective structure

η_{i0} : is the displacement due to the primary system on the i released

X_i : is the unitary force in the position of the i released

η_{ik} : is the displacement of the point of application of the released X_i due to the redoundant $X_k = 1$

n : is the number of the released equal to the degree if indeterminacy i

$\eta_{ik} = \eta_{ki}$ due to Maxwell Theorem

$Mass_i$: is the mass involved for the specific tie-timber beam

g: is the gravity accelleration

α : is the seismic load multiplier

L : is the length of the wall

L : is the length of the wall equal to 3.6 m

l : is the length of the wall where the load is distributed, equal to 2.78 m

d : is the distances between all the timber elements, equal to 0.36 m

γ_b = 1.5 safety factor for the amplification of the seismic actions.

1 INTRODUCTION

1.1 Background

Bhatar system is a traditional method of construction which involves a vertical succession of dry stacked stones masonry and timber beam. Through the century and countries this kind of architecture has been used for many different purpose and different scale, temples for religions, forts for military camps and houses for civil use. Along the time some of these structures of the past are still standing after important earthquake, this suggest us that bhatar system has somehow a good seismic behavior. The different between the constructions that have survived and those who did not may be due to many factors. The knowledge of the know-how goes from an old generation to a new one, because of this there are many differences about materials, about the proper place where to build but most of all the differences about the techniques are the most important.

In the poor and lost areas where this kind of architecture is used is important to use local material and to avoid the use of material or component which need to be imported from somewhere else, this is not just because it is important to save money but most of all because there are no proper infrastructures and this means more obstacles and some time the impossibility to be done.

In order to give a reference point, international organizations such as ERRA , UN-HABITAT, SDC and FRC have published “Bhatar construction - An illustrated guide for craftsmen”.

Guidebook prepared by the Swiss Agency for Development and Cooperation SDC (Tom Schacher, technical advisor).In collaboration with: French Red Cross and Belgian Red Cross (technical research and development) UN Habitat, NSET and NESPAK (revisions) French Red Cross (Translation into Urdu) Mansehra, NWFP, April 2007

This guide shows how to built-up a bhatar house and the gross dimensions that must be satisfied.

Thus, this research was performed to ensure that this alternative building technique can be built in a seismic region knowing that it will be a safe structure and that can be used for a post-disaster reconstruction in developing countries.

1.2 Justification of the document and objectives

The use of bhatar system is a traditional technique in the construction field and it is widely used all over the Himalayan area due to some factors such as durability of the structure, low environmental impact, cost-effective ratio.

Considering the advantages that this system carries, it can be an alternative building technique and post-disaster reconstruction for houses in developing countries where it can be used for individual housing or for community facilities. Thereby, this technique can be built in remote areas, locations difficult to reach and poorly supplied areas with the advantage that gabion boxes are easily installed and that deployment can be performed without special equipment and there is no need of highly trained personnel.

On the other hand, from a seismic point of view, there will be "weight issues" because the bhatar are heavy due to the rocks (it's known that the seismic forces acting on the structure are proportional to the weight). Thus, the need of research has been identified in order to understand the static and seismic behavior of this kind of structures focusing on the limitations of the system and the structural safety under a certain seismic action.

1.2.1 General objectives

Based on the justification of this document, this dissertation aims at understand the behavior in-plane and out-of-plane under seismic actions of a modular box composed by walls built-up with bhatar method and to give practical suggestions and simple formulas for the dimensioning of the structure, satisfying structural safety conditions.

1.2.2 Specific objectives

- To comprehend the compression behavior and strength of a single Wall,composed by elementar modules under vertical loads.
- To verify the structural safety under seismic actions in-plane and out-of-plane of a wall build-up with bhatar system.
- Conduct analytical considerations to examine the effect of lateral forces on the behavior of a bhatar system.
- Propose constructions details and limitations to acquire an assure good seismic behavior of the structure
- To develop rules of thumb for a proper dimensioning and construction of this kind of structures in order to be a seismic resistant structure.

1.3 Organization of the thesis

The work has been organized starting from the elementary elements used in the Bhatar system thus starting from the geometry following the guide line of Architect Tom Schacher.

The following points shows the steps of the logic path followed in the work:

- Studies of Tom Sacher manual
- Definition of a single module

Definition of the wall

- Definition of one room module (box)
- Definition of material properties: Timber SHOREA ROBUSTA
- Definition of material properties: Stones LIMESTONE
- Studies on Rock discontinuities: Barton model –
- Connections - Eurocode 5 : EN 1995-1-1 :2004+A 1- DESIGN ULS
- Static Analysis
- Seismic analysis in plane – application of Barton model
- Seismic analysis out of plane – Overturning
- Seismic analysis out of plane – Bending
- Practical rules of thumb.

2 BHATAR

2.1 Traditional definition of Bhatar

Bhatar is a traditional construction system consisting of stone mortarless masonry walls reinforced with horizontal timber ladder-beams, which combine to resist and dissipate the energy and stresses induced during an earthquake.

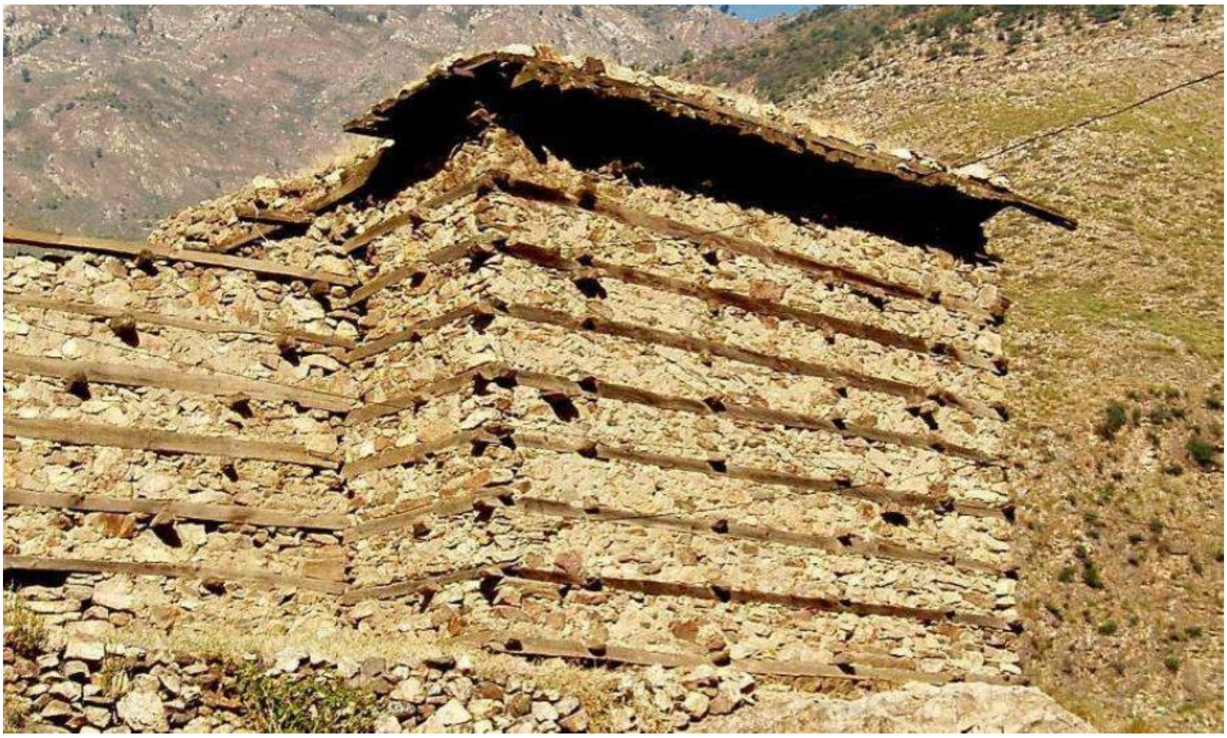

Figure 2-1 Project entry 2008 Asia Pacific - "Advocacy of traditional earthquake-resistant construction, North-West Frontier Province, Pakistan": "Bhatar" at Besham Fort.

Through the century and countries this kind of architecture has been used for many different purpose and different scale, temples for religions forts for military camp and houses for civil use.

Along the time some of these structures of the past are still standing after important earthquake, this suggest us that bhatar system has somehow a good seismic behavior. The different between the constructions that have survived and those who did not may be due to many factors. The knowledge of the know-how goes from an old generation to a new one, because of this there are many differences about materials, about the proper place where to build but most of all the differences about the techniques are the most important.

In the poor and lost areas where this kind of architecture is used is important to use local material and to avoid the use of material or component which need to be imported from somewhere else, this is not just because it is important to save money but most of all because there are no proper infrastructures and this means more obstacles and some time the impossibility to be done.

This type of construction has been extensively used in Turkey,Afghanistan, Pakistan, India and Nepal for many centuries, as shown in figure below.Nepal is the country taken as reference point for the local material.

Figure 2-2 Regions of the world where Bhatar is still used

Nepal is subjected to very strong earthquake because its characteristic positionas shown in the picture2-3.

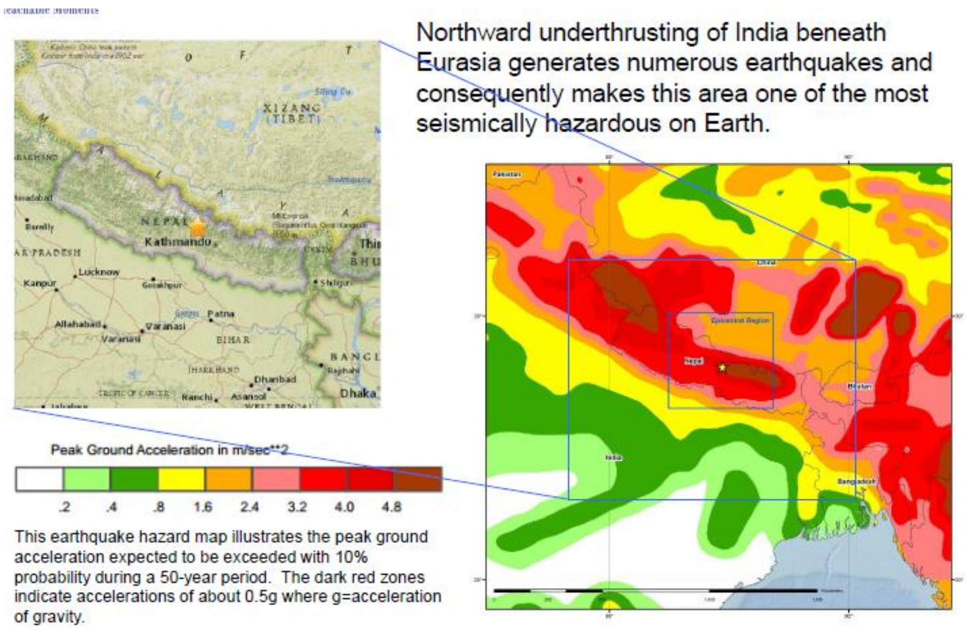

Figure 2-3 Nepal peak ground acceleration

2.2 Tom Schacher Manual : Bhatar construction - An illustrated guide for craftsmen

Arch Tom Schacher

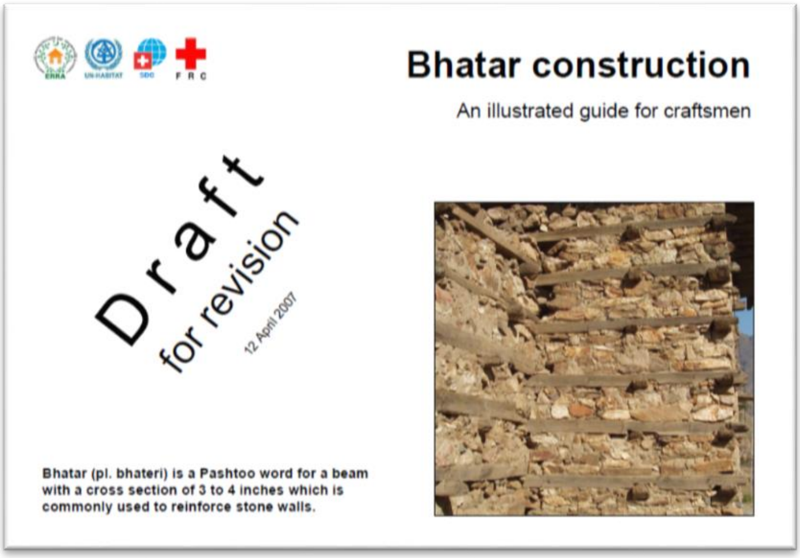

Figure 2-4 Bhatar construction-An illustrated guide for craftsmen

2.2.1 Gross shape and dimensions

The fisrt thing described is the position of the structure and the gross shape.As it is shown in the figure 2-5 it is always better to choose a simple and regular structure , if necessary it is better to subdivide it into rectangular parts.

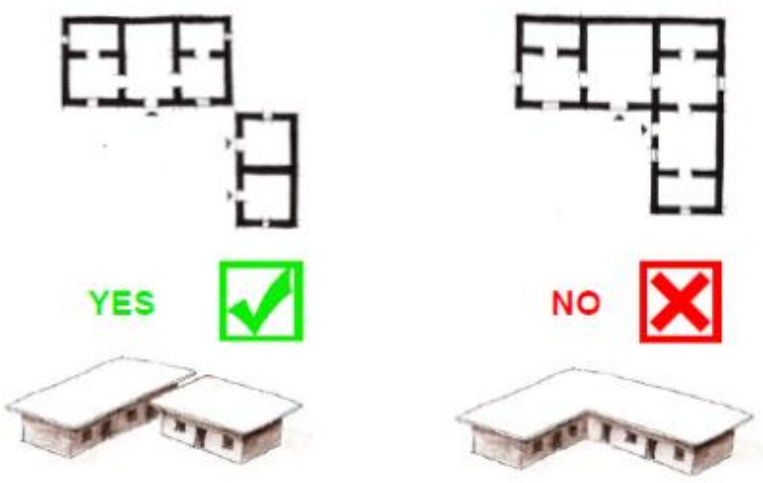

Figure 2-5 Divided rectangular structures

The first suggestion about the dimensions is the relation about the length and the width.The house must not be longer than three times the width , as it is shown in figure 2-6.

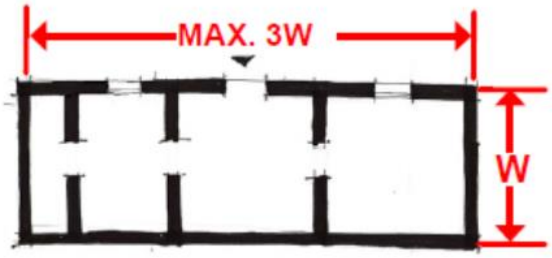

Figure 2-6 Gross dimension - ratio length/width

2.2.2 Foundation and plinth band

The foundation should be at least 2½ feet(0,762 m) wide and 3 feet (0,91 m) deep. The plinth band should be placed 1 foot (0,3 m) above the foundation (1 foot out of the ground) in order to avoid the contact with water, as it is shown in figure 2-7.

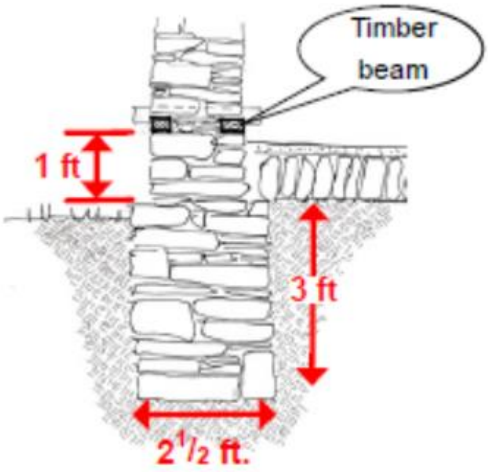

Figure 2-7 Foundations

The plinth band must pass under the door. It should be continous along all the perimeter (better if it is made in RC , it will not rot), , as it is shown in figure 2-8.

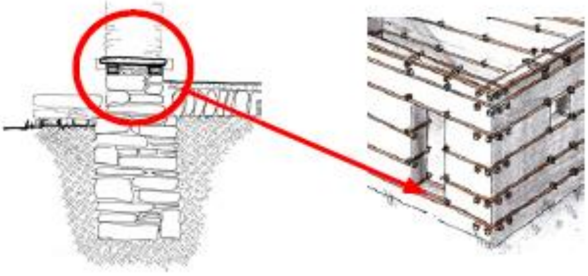

Figure 2-8 The plint

2.2.3 The Walls

The walls must be smaller than the values reported in the figure 2-9.

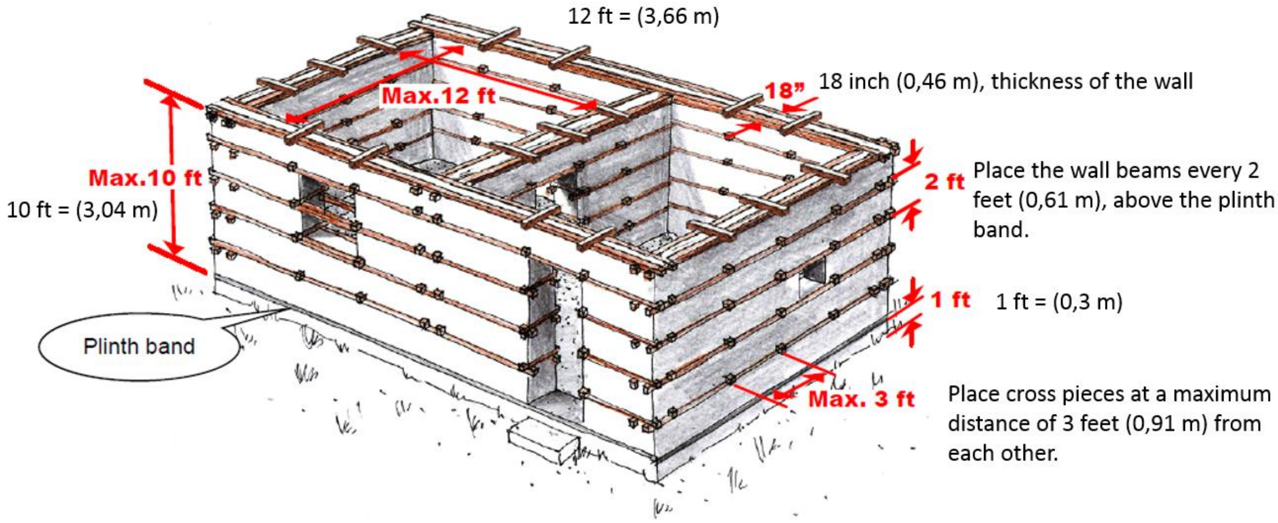

Figure 2-9 Wall dimensions

The drawing is not in scale, in a real scale it would be appreciated the fact that the spaces are quite small then the necessity to add the rooms.

2.2.4 Wall - joints

The timber elements may be not enough long to cover all the length of the wall so it is suggested to use scarf keyed joint along their length but taking into account that at each level they must be in different position and not along a vertical line as shown in figure 2-10., at the same time the position of the stones must be always laid down in order to have a dovetail as shown in figure 2-11

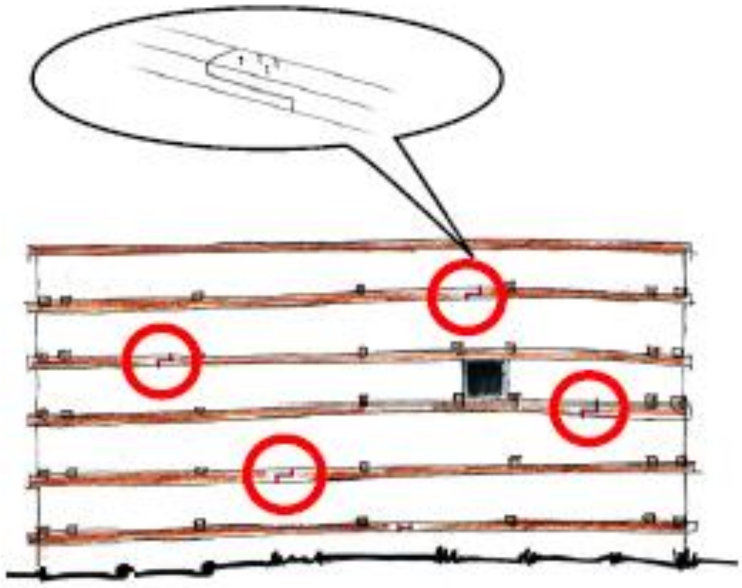

Figure 2-10 Spread the connection points.

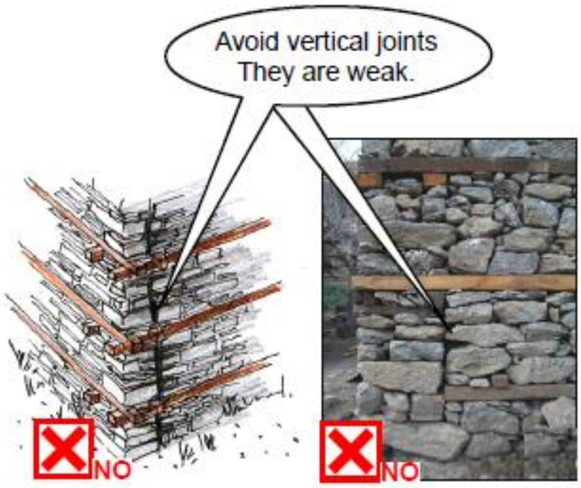

Figure 2-11 Raise all walls together to avoid vertical joints

2.2.5 Kashmiri joint or Keyed scarf joint

The joints in the timber element must be done with Kashmiri joint or normally known as keyed scarf joint as shown in figure2-12.

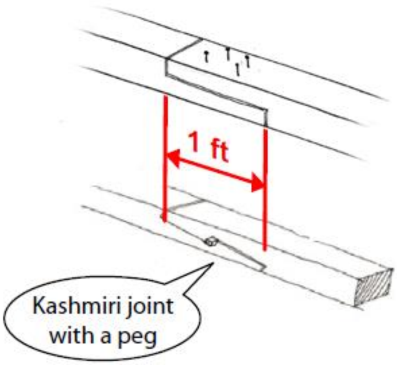

Figure 2-12 Kashmiri joint or Keyed Scarf Joint

2.2.6 Connections - Corners

The connections on the corners stand due to lap joints and Minimum size of beam is 3” (7,62 cm) high by 4” (10,16 cm)wide, as shown in figure 2-13.

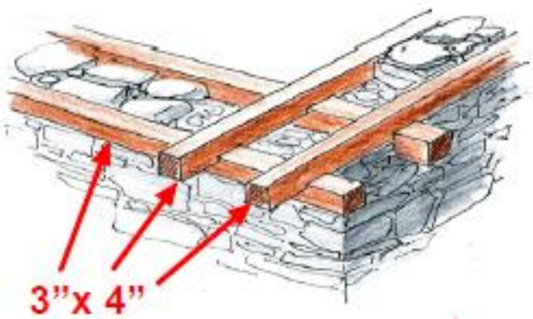

Figure 2-13 minimum size of the beams/rafters

Beams must be hooked together in the corners. Cut a notch of 1” (2,54 cm) into all four corner beams. Add 2 nails (3” =7,62 cm) for more security.Keep 4” (10,16 cm) of wood after all notches for strength.As shown in figure2-14.

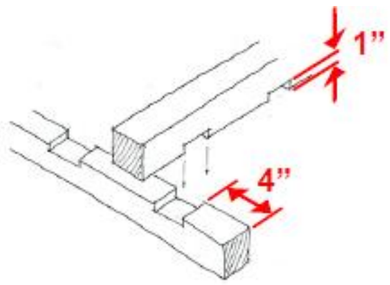

Figure 2-14 Lap joint – dimension

2.2.7 Connections – Cross Pieces

Along the wall cross pieces must be insert in order to assure stability. Cross pieces help to hold the beams and walls together.You need notches only on the cross pieces, but not on the main beams. As shown in figure2-15

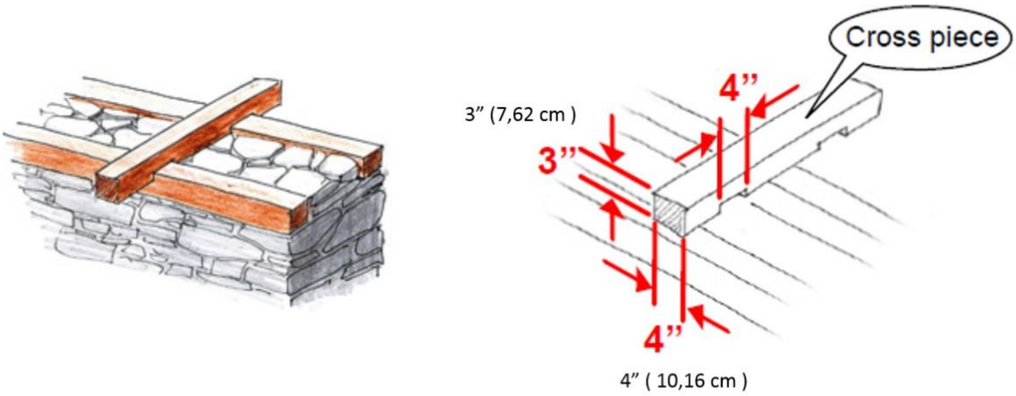

Figure 2-15 Cross Pieces

2.2.8 Connections – Internal wall

In case of double room they are specified how the connections between the walls must be done. Minimum size of beam is 3” (7,62 cm) high by 4” (10,16 cm)wide. Where internal walls connect, only notch the internal wall beams, not the main beams, as shown in figure2-16.

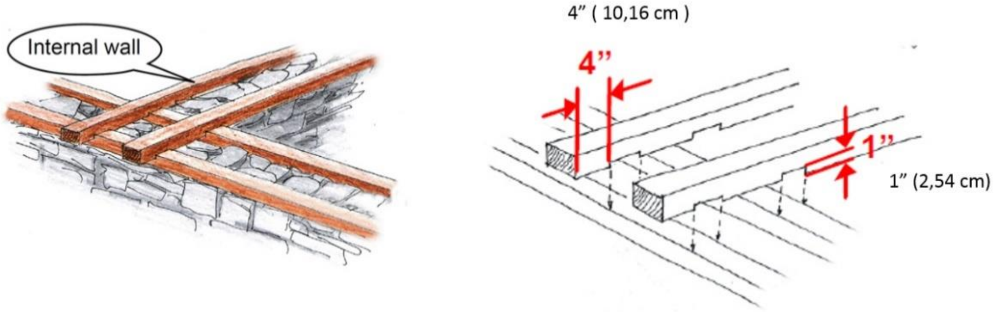

Figure 2-16 Internal wall joint

2.2.9 Openings

The distance between openings should be minimum 3 feet (0,91 m) ,windows and doors must not be wider than 3 feet (0,91 m) ,the windows must be between the beams. As shown in the figure2-17

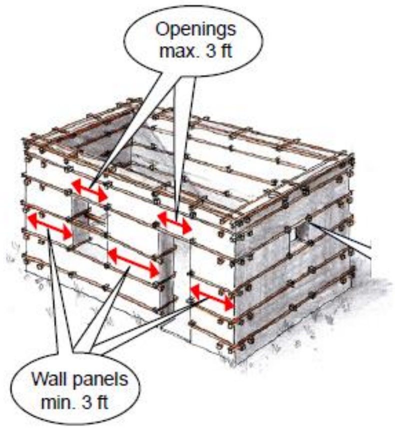

Figure 2-17 Openings

2.2.10 Doors

The integrity of the structure must be assured thus it must be avoided any modification and all the openings must be bounded with cross pieces as shown in figure 2-18

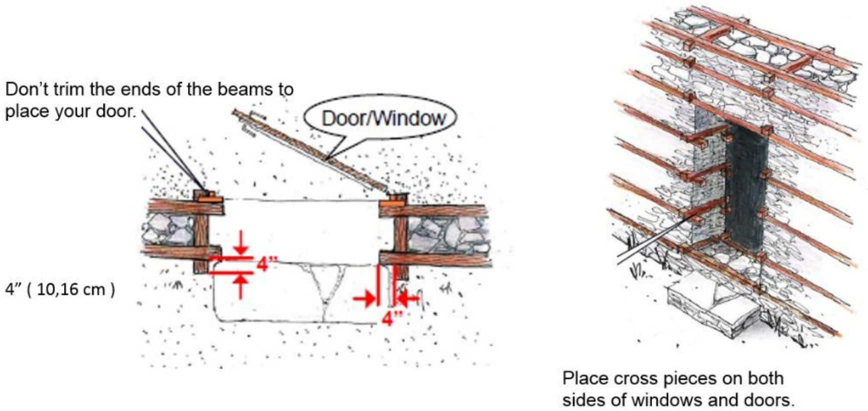

Figure 2-18 Openings 2

2.2.11 Windows

The windows must be reinforced with beams, for lintel must be added two pieces of wood in between the existing beams to support stones above. It must pass at least 1 foot(0,3 m) into masonry on each side of the opening, as shown in figure 2-19

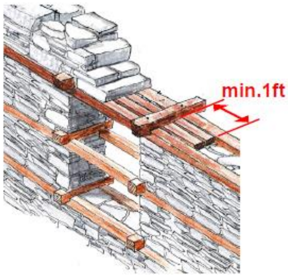

Figure 2-19 Lintel reinforcement

2.2.12 The Roof

The roof considered for this research is the flat heavy roof with earth cover which is the worst case but it does not need metal sheet to cover which are difficult te be found in far regions.

Some suggestions are given referring the figure below. 1-Let the top beams (bhateri) stick out of the wall 1 foot on each side. Connect them with nailed cross pieces. 2-Add the 4”x6”roof beams and let them too stick out 1 ft on each side (also over the retaining back-wall if there is) to protect the wall against rain. 3- Nail the planks on the roof beams leaving a half inch gap between each. 4-Place flat stones along the edge of the roof to contain the earth. 5- Add twigs and small branches in a layer 4 to 6 inch thick. 6 Cover with earth 4 to 6 inch thick. 7-Avoid to make the earth cover thicker over the years.

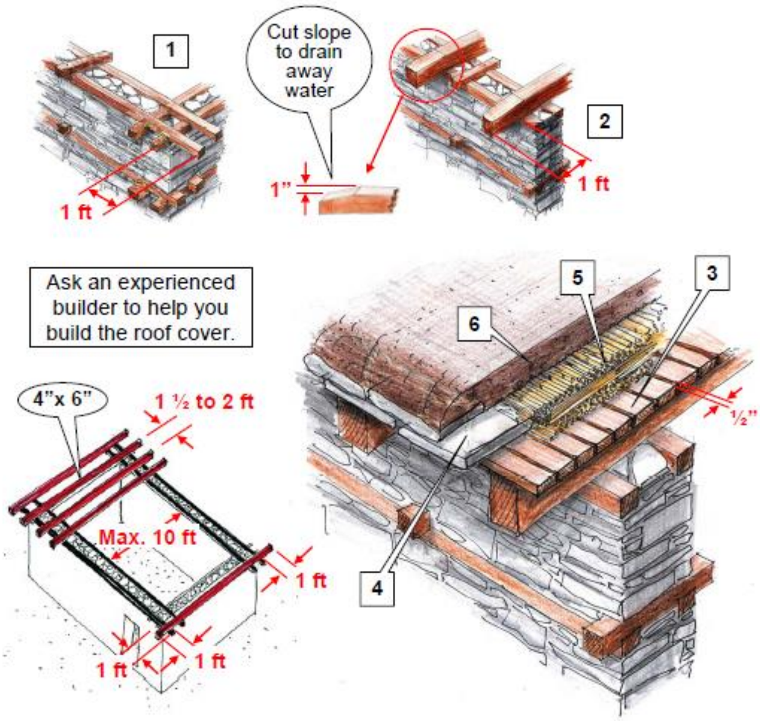

Figure 2-20 the flat heavy roof with earth cover

3 STUDY CASE

Following the Tom Schacher Manual

Following the guide lines given by Architect Tom Schacher it has been defined a basic module of the wall which can be used as modular unit in order to built square or rectangular housing unit.

3.1 Single modular unit

In accordance to the manual the single unit has been drawn starting from the ground layer until the roof support.The beams are placed every 60 cm exept the first beam from the bottom and the roof beam that are placed at 30 cm. The global measure are shown in the figure 3-1.

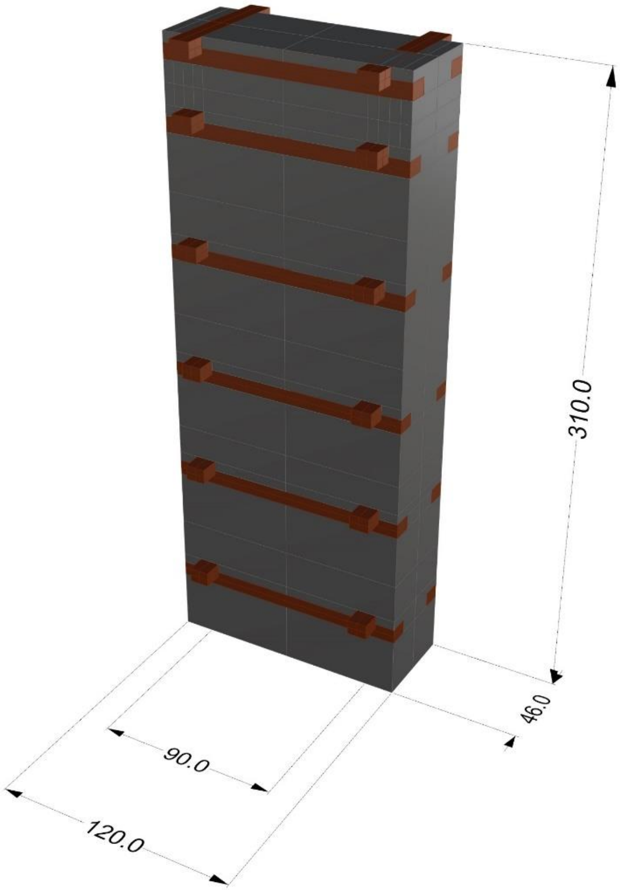

Figure 3-1 Modular unit-perspective

3.1.1 Orthogonal projection

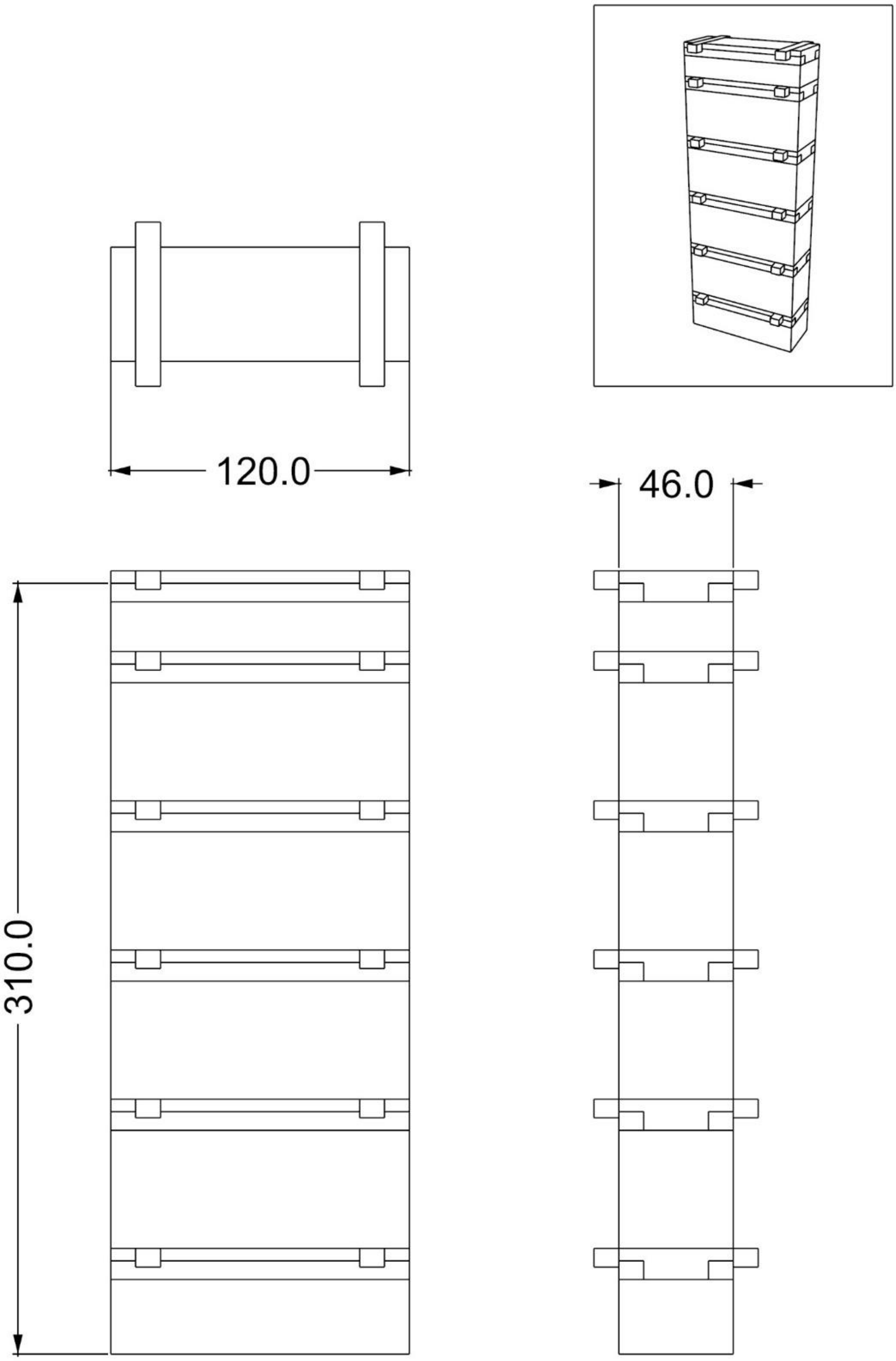

Figure 3-2 Modular unit - Orthogonal projection in cm

3.2 Single Wall

Using the modular unit it has been composed the largest wall suggested by the guide line. With a length of 12 feet it has been approximated to 3.6 m, width of 0,46 m and height of 3.1 m.

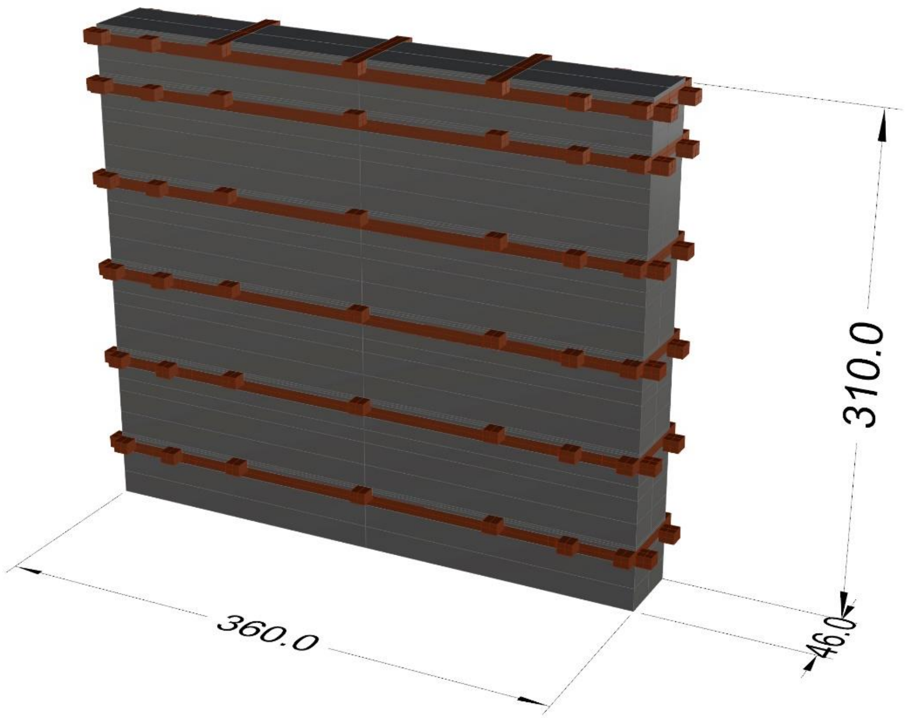

Figure 3-3Largest wall possible , length of 3.6m

3.2.1 Orthogonal projection

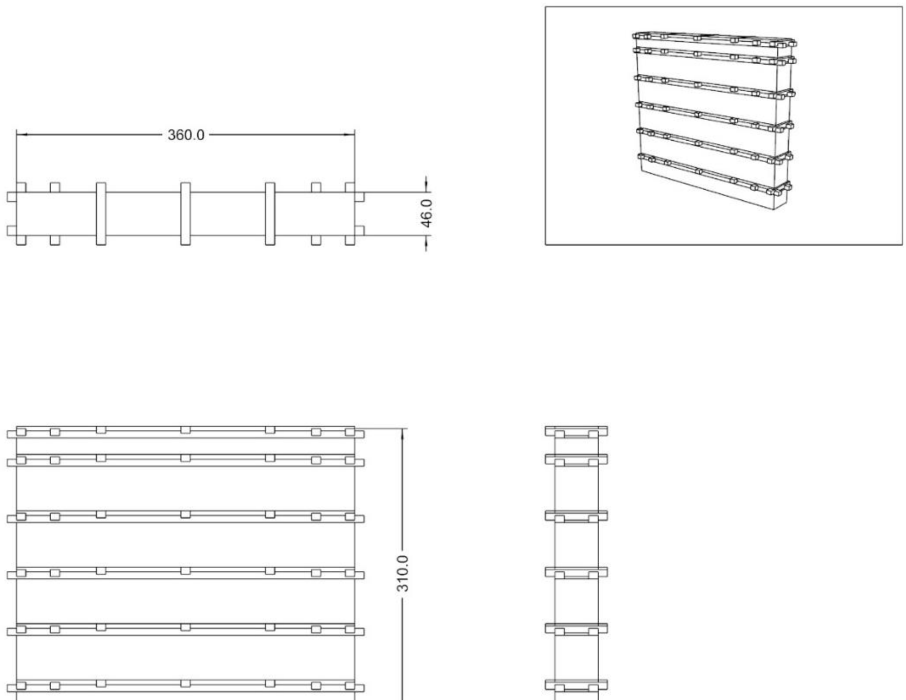

Figure 3-4 Wallt - Orthogonal projection in cm

3.3 One room box

Using four perimetric wall for a total around 12 modular units a room box have been defined. This room box is the largest single habitat unit which can be built with the use of the guide line.The one room box is composed by:

- Foundation and plinth band made of stones
- First seismic band made of wood
- Dimensions (length : 3,60 m ;Width : 3,60 m; Height 3,0 m)
- 1 door
- 2 window

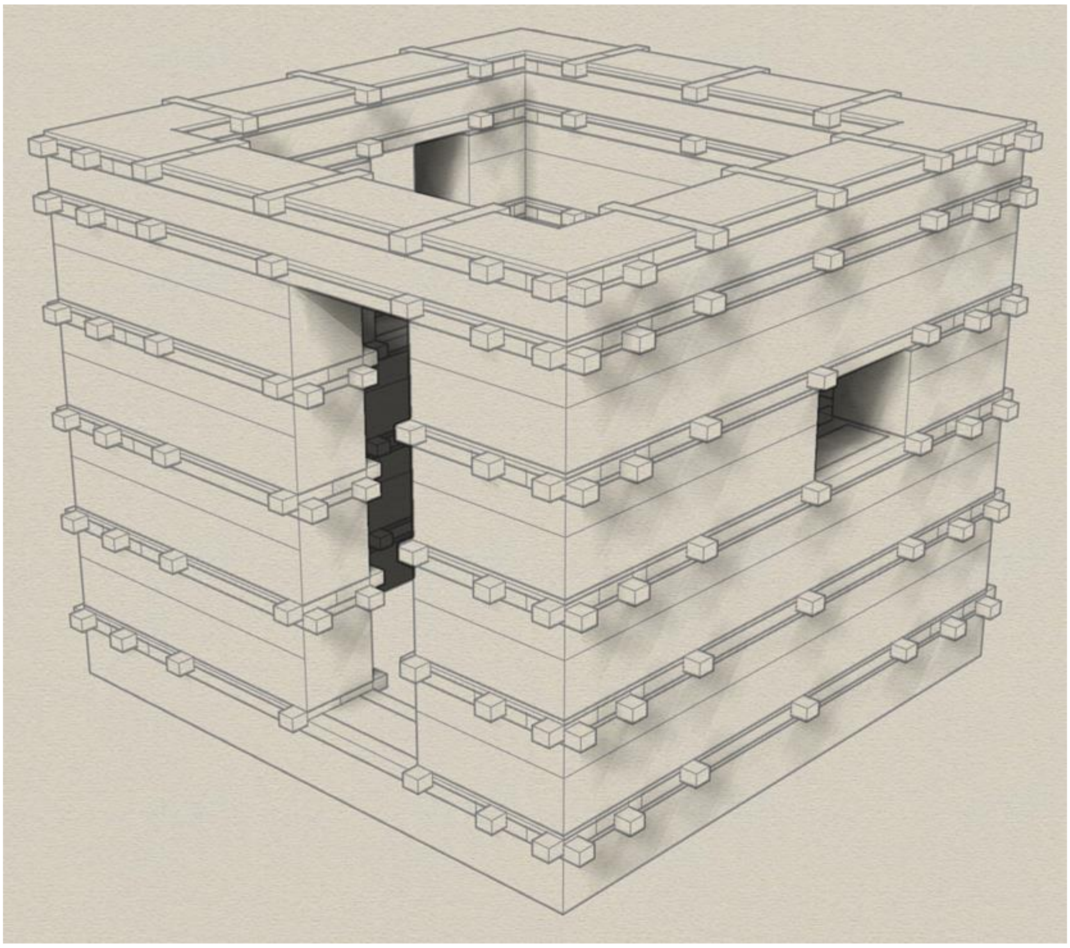

Figure 3-5 One room box

3.3.1 Orthogonal projection

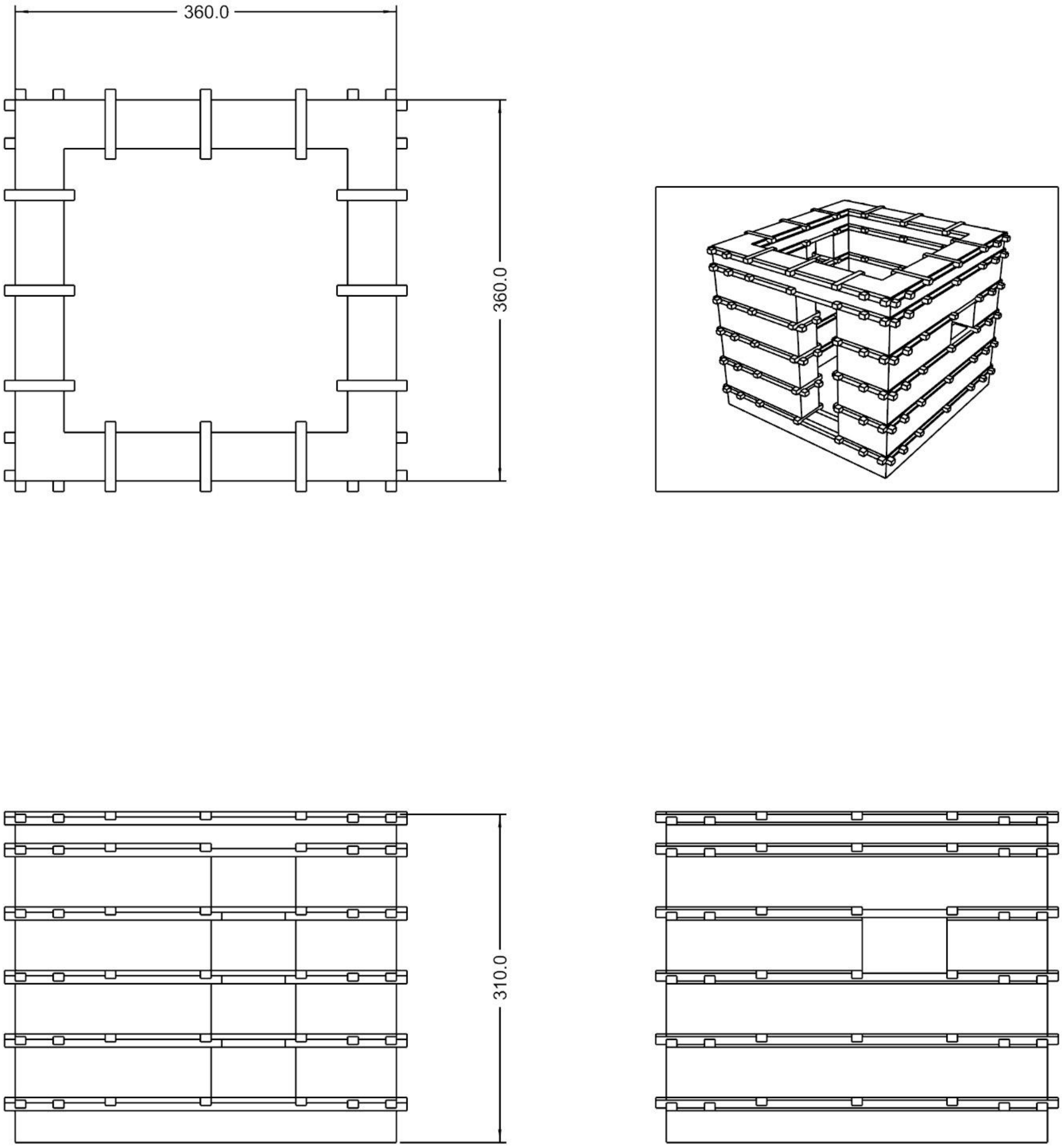

Figure 3-6 One room box orthogonal projections in cm

In the guide line is described the possibility of enlarging the structure adding walls in order to compose a second smaller habitat unit .The aim of the thesis is to understand the behavior of the basic structure thus all the studies regards the basic room box and in particular the behavior of the perimetric wall. As shown in the following figure the section AA represents the studied wall.

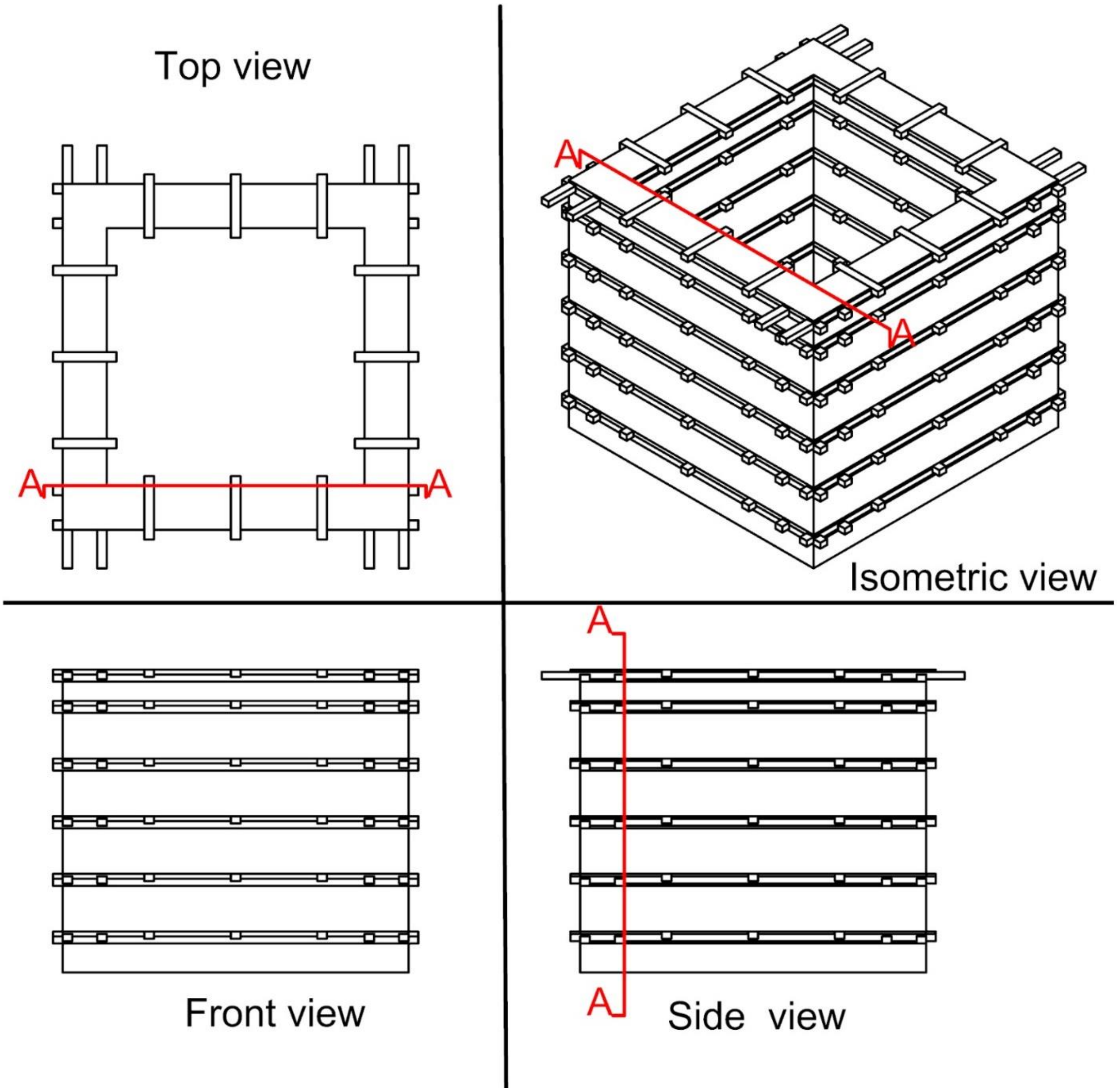

Figure 3-7 Section AA - studied wall

3.3.2 The Roof

The roof has been considered as flat heavy roof with earth cover which is composed , as show in the figure below, by (from the bottom):

- Last timber band
- Roof beams 10 cm height
- Planks 3 cm height
- Ring of flat stones 10 cm height
- Twigs 5 cm height
- Earth 20 cm height

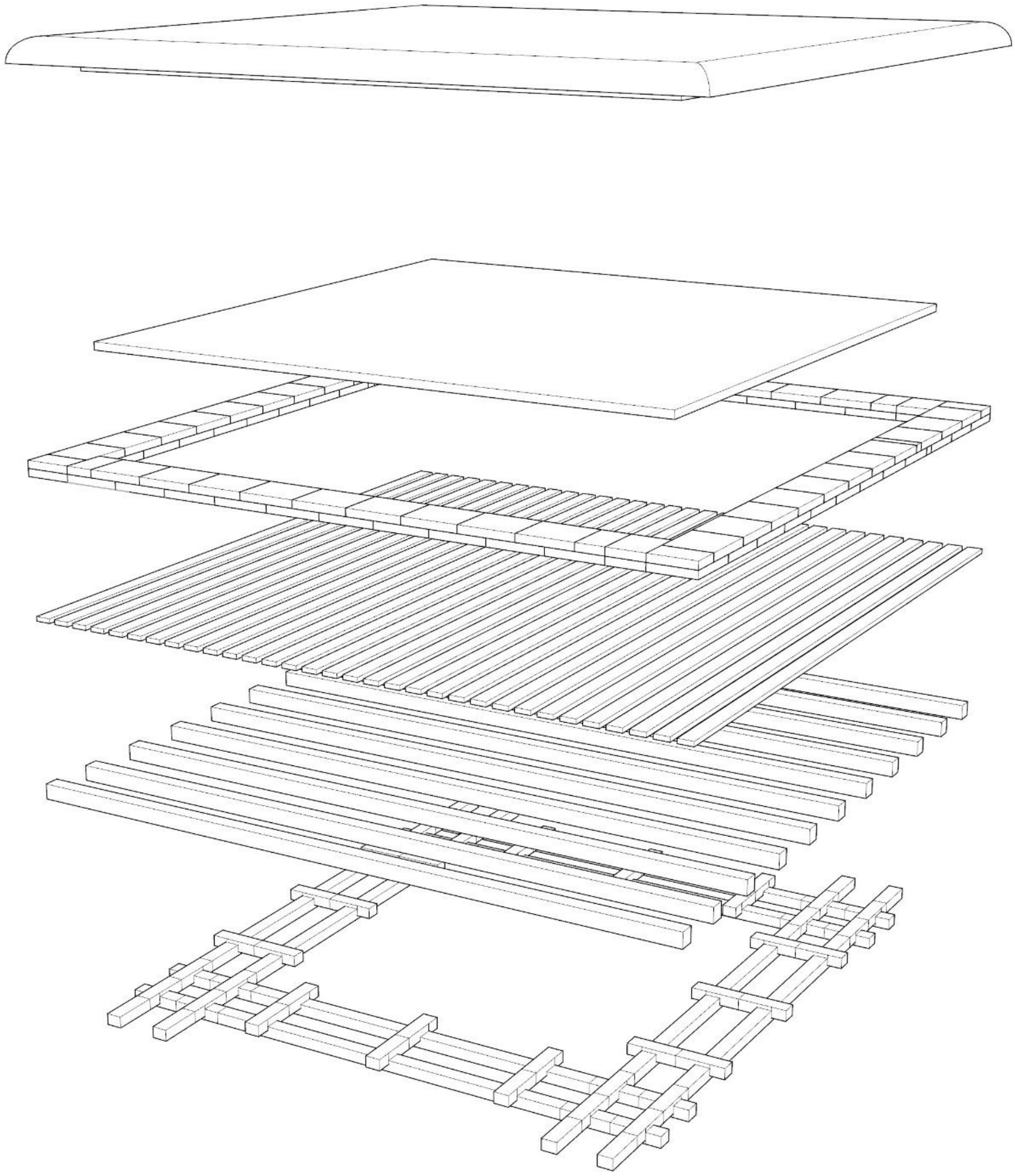

Figure 3-8 Flat earth heavy roof – exploded

4 MATERIALS

This chapter describe the two basic material, timber and stones used in the Nepal region.

4.1 Timber : Shorea Robusta

Thanks to the suggestions of Architect Martijn Schildkamp we know that exact timber traditionally used in Nepal to build Bhatar structures is the so called Shorea Robusta in Nepal language is called SAL.

4.1.1 Botanic Characteristics

Below in the figure are reported the botanic characteristics.

Kingdom :	Plantae
Division	Magnoliophyta
Class:	Magnoliopsida
Order :	Malvales
Family :	Dipterocarpaceae
Genus :	Shorea
Species :	S. robusta
Scientific Name :	Shorea robusta

Figure 4-1 Shorea Robusta – SAL

4.1.2 Mechanical properties of Shorea Robusta

In order to find the proper mechanical properties of Shorea Robusta it has been necessary a bibliographic research. This reaserch ended with 4 important sources which are listed below:

- Source 1 : MECHANICAL PROPERTIES AND DURABILITY OF SOME SELECTED TIMBER SPECIES (M. Bellal Hossain1 and A.S.M. Abdul Awal2*)
- Source 2 : STUDIES ON TENSILE STRENGTH PROPERTY OF COMMERCIAL TIMBER SPECIES OF SOLAN DISTRICT (Himachal Pradesh SEEMA BHATT, BUPENDER DUTT, RAJESH KUMAR MEENA and TASRUF AHMAD*)
- Source 3 : COMPARISON OF TEST RESULTS OF VARIOUS AVAILABLE NEPALESE TIMBERS FOR SMALL WIND TURBINE APPLICATIONS (R. Sharma1 1 1 , R. Sinha , P. Acharya , L. Mishnaevsky Jr. 2, P. Freere3)
- Source 4 : TECNOLOGIA DEL LEGNO (G. Giordano, UTET, Torino 1988.)

The different values found in the research have been averaged and they are reported in the following table.

Table 1 Shorea Robusta mechanical properties 1

Sal or Shorea robusta				
	Density ρ : (Kg/m3)	Specific gravity SG = ρsubstance / ρH2O	ultimate compressive strength σu (Mpa)	Tensile Ultimate stress longitudinal axis (MPa)
source 1	921	0,84	48	/
source 2	/	/	/	78,1
source 3	913 or 950	/	/	/
source 4	875	/	61	/
Average	914,75	0,84	54,5	78,1

Table 2 Shorea Robusta mechanical properties 2

Sal or Shorea robusta					
	Young's Modulus E : (Gpa)	Bending Strength (Mpa)	Minimum Static Bending Strength (Mpa)	Average Hardness (Mpa) Indentations : Incavatura	Minimum Hardness (Mpa)
source 1	/	/	/	/	/
source 2	/	/	/	/	/
source 3	12,55	83,85	61,7	87,5 (+o- 42,5)	45
source 4	15,6	121	/	medium/high	/
Average	14,075	102,425	61,7	87,5 (+o- 42,5)	45

4.1.3 Characteristic Values from EN 338

Comparison with Classification of timber in accordance with UNI EN 338 : 2009 Shorea Robusta is classified as D70 thus they have been used the following reference values.

Shorea Robusta		Hardwood species
		D70
Strength properties (in N/mm2)		
Bending	ƒm,k	70
Tension parallel	ƒt,0,k	42
Tension perpendicular	ƒt,90,k	0,6
Compression parallel	ƒc,0,k	34
Compression perpendicular	ƒc,90,k	13,5
Shear	ƒv,k	5,0
Stiffness properties (in kN/mm2)		
Mean modulus of elasticity parallel	E0,mean	20
5 % modulus of elasticity parallel	E0,05	16,8
Mean modulus of elasticity perpendicular	E90,mean	1,33
Mean shear modulus	Gmean	1,25
Density (in kg/m3)		
Density	ρk	900
Mean density	ρmean	1080

4.1.4 Design Values from EC 5 and en.1995.1.1.2004 and NICOLE – Istruzioni CNR_DT206_2007

Following the Eurocode 5 and the national codes for the design timber structure they have been selected and computed the following values.

Table 3 Design Value EC5-Nicole -1

DESIGN VALUE		
the partial factor for a material property	γm	1,5
Service class		2
modification factor taking into account the effect of the duration of load and moisture	Kmod permanent action	1,1
Depth factor	kh	From case

Table 4 Design Value EC5-Nicole -2

Strength properties (in N/mm2)		
Bending	ƒm,d	51,33
Tension parallel	ƒt,0,d	30,80
Tension perpendicular	ƒt,90,d	0,44
Compression parallel	ƒc,0,d	24,93
Compression perpendicular	ƒc,90,d	9,90
Shear	ƒv,d	3,67
Stiffness properties (in kN/mm2)		
Mean modulus of elasticity parallel	E0,d	13,33
5 % modulus of elasticity parallel	E0,05 d	11,20
Mean modulus of elasticity perpendicular	E90,d	0,89
Mean shear modulus	Gd	0,83
Density (in kg/m3)		
Density	ρk	900
Mean density	ρmean	1080

4.2 Stones : Main construction material since the Stone Age

In order to define the most probable stone largely used for the construction of bhatar the research has been started looking on which are the most common stones in the Nepal region taken as reference point. Thanks to Architect Martijn Schildkamp we know that people collect the stone from the ground and sometimes they take them directly to the quarries.

The most common rocks and their used in the Nepal region are listed below :

- marble, basalt, granite and red sandstones are cut into slabs and used in decoration;
- phyllite, slates, flaggy quartzite and schist are used for roofing;
- limestone, dolomite, quartzite, sandstone are used for aggregate in various construction works, road paving and flooring;

- vast quantities of river boulders, cobbles, pebbles and sands are mined as construction materials/ aggregates.

References :

DMG (Y.P. Sharma et al 1988) has evaluated such materials (boulders=347,006,000m3, cobbles=214,261,000m3 and pebbles=229,205,000m3) in the major rivers of Terai region.

MINERAL RESOURCES OF NEPAL AND THEIR PRESENT STATUS- Krishna P. Kaphle, Former Superintending Geologist, Department of Mines and Geology, Kathmandu, Nepal Former President, Nepal Geological Society

The world Housing Encyclopedia (WHE) specify that the rocks most used in wall and frame as rubble stones are Slates ,Limestone, Quartzite.

Architect Martijn Schildkamp collected pictures during the construction of a bhatar house. Comparing the pictures of the stones he sent and weaving togheter the possible material, it has been choosen the strongest one, limestone.

Figure 4-2 Architect Martijn Schildkamp - bhatar stones

Dolomite

Sandstone/Arenaria

Quartzite

Figure 4-3 Sedimentary rocks

The limestone/Calcarea has been choosen for the following steps of the thesis.

Limestone is good for building, and is generally the same either in masonry or building block. It is not a good fit for cobblestones because it is too soft.

Figure 4-4 Limestone/Calcarea

4.2.1 Limestone mechanical properties

In the context of this thesis the important parameters of the limestone are:

- Dry density
- Rebound Number with Schmidt hammer L-type (MATEST of Italy)
- Unconfined Compressive Strength (Miller's formula,1972)
- JCS, joint compressive strength (Miller's formula,1965)

The importance of these parameters will be explained in the Chapter 5 which will describe the surfaces behavior and the importance of the absence of the mortar.

In the table 5 are shown the results obtained by the research team of Dr. Ramli Nazir Faculty of Civil Engineering, Department of Geotechnics and Transportation, Universiti Teknologi Malaysia (Malaysia). The publication "Prediction of Unconfined Compressive Strength of Limestone Rock Samples Using L-Type Schmidt Hammer" has been really usefull in order to have preliminary laboratory data for the application of the Barton model which will be explained in the following Chapters.

Table 5 Rock characterization results

No.	Sample Type	Dry Density (kg/m3)	R : rebound number	**UCS: Miller`s correlation(MPa)**	**UCS:Obtained in Laboratory(MPa)**
1	Limestone	2817,0	36,0	72,0	72,9
2	Limestone	2748,0	35,9	76,0	72,9
3	Limestone	2646,0	31,5	55,0	58,5
4	Limestone	2777,0	31,5	60,0	60,6
5	Limestone	2671,0	28,9	49,0	52,2
6	Limestone	2773,0	30,4	56,0	56,4
7	Limestone	2676,0	37,7	79,0	76,7
8	Limestone	2683,0	36,8	76,0	75,7
9	Limestone	2748,0	34,8	71,0	72,5
10	Limestone	2707,0	35,6	72,0	69,6
11	Limestone	2759,0	36,6	79,0	78,1
12	Limestone	2704,0	33,9	66,0	63,5
13	Limestone	2726,0	35,1	71,0	75,7
14	Limestone	2796,0	37,9	88,0	83,3
15	Limestone	2822,0	36,4	82,0	85,6
16	Limestone	2730,0	36,0	74,0	76,2
17	Limestone	2720,0	36,0	71,0	74,8
18	Limestone	2887,0	35,0	72,0	70,5
19	Limestone	2699,0	39,0	81,0	83,6
20	Limestone	2679,0	37,0	76,0	73,4
Avarage		2738,4	35,1	71,3	71,6

Table 6 Miller's correlation 1972

Average data		
Miller`s correlation, 1972: $UCS = \sigma_c = 12{,}83 * e^{0{,}0487 * R_L}$		
Dry Density	2738,40	(kg/m3)
R : rebound number	35,10	/
UCS: Miller`s correlation	71,30	(MPa)
UCS:Obtained in Laboratory	71,64	(MPa)

Table 7Miller's correlation 1965

Miller`s correlation, 1965		
$Log10\, JCS = 0.00088 * (\gamma) * (R) + 1.01$ $JCS = 10^{0.00088 * (\gamma) * (R) + 1.01}$		
γ	26,85	kN/m^3
R	35,10	/
JCS	69,10	MPa

5 BARTON MODEL AND SHEAR STRENGTH OF ROCKFILL

One of the most peculiar aspect of the Bhatar system is the absence of mortar. This aspect is of great importance in the study of in plane behavior during an earthquake. The bhatar for its nature is already cracked. This means that micro displacements are possible.These micro movements must be considered as settlement. Micro slidings and displacements may be one of the reasons that allows the bhatar construction to dissipate energy.
From a safety engineering point of view in this thesis it has been studied the mechanism of resistance of the rock in the wall and the role of the absence of the mortar.This has meant to find a way to understand the behavior of rockfill. In order to do that the idea came reading the impressive work of BARTON, Nicholas R who studies the behavior of rock discontinuities in the field of Geotechnical engineering.

5.1 Interfaces between material : Timber-Stone and Stone-Stone

The behavior of the wall is strictly connected to the interfaces between the two main materials. The interaction stone-stone and timber-stone (see figure 5-1) is strongly related to the static frictional coefficients. The static frictional coefficient of the rocks is the most important for the aim of this work.

Figure 5-1 Stone layer (black box above) - Timber beam (black box below)

Due to the characteristics and dimensions of the rubble stones the behavior of the stone layers have been choosen as the peculiarity. The static frictional coefficient between the rocks is stongly higher than the static frictional coefficient between the stone and the timber. For this reason it has been made the hypothesis that the static frictional coefficient between the stone and the timber is negligible and the behavior of the wall in the layers where there are the timber bands has been studied using a reduction factor based on the areas of surfaces where the stones are in contact.

The reduction factor ξ has been computed as the ratio between the area of the section of the stones layer (Area) and the smaller area below the timber beam (Area*).

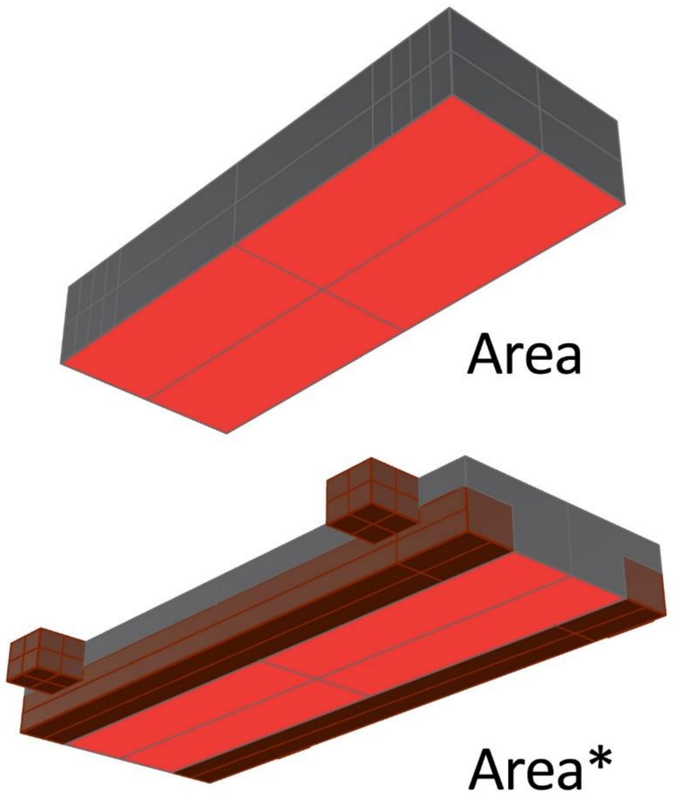

Figure 5-2 Contact surfaces

Table 8 Reduction factor due to the presence of the timber beam

Ratio between the areas

Contact Surface stones layer		
L module	1,2	m
Width	0,5	m
Area	0,6	m^2

Contact Surface below the timber beam		
L module	1,2	m
Width	0,3	m
Area*	0,3	m^2

Reduction factor ξ = Area/Area*	0,57

5.2 Shear strength of rock discontinuities

In the particular case of Bhatar it is necessary to evaluate the factors that control the shear strength of the discontinuities in a wall.

The following pages have the main intent to expose the principal theories and methods used in the analyses of stability for rock masses.

Starting from the Coulomb's law, it is shown how the behavior of a rock joint is described. Different authors defined their own methods to describe the rock joints behavior from more idealized scheme (linear) to more realistic scheme (non-linear).

The important aspect of the Barton's Method is the possibility to go from the rockjoint to the rock-fill joint.The idea is to use the same approach of the rock masses analysis, with rock-fill joint, in the strength analysis of the in plane behavior of the wall.

5.3 Plane smooth joint

The first basic case is the most idealized one.

Hypothesis : plane and smooth joint surface

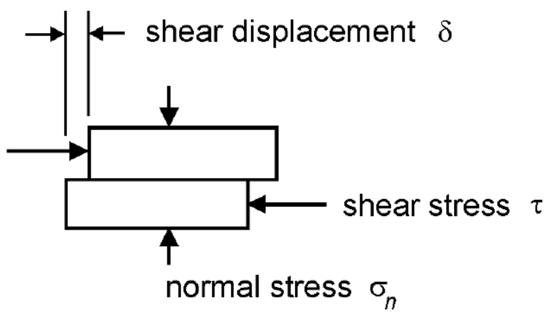

Figure 5-3 Plane and smooth joint surface

Observed mechanical behavior : shear stress quickly increases with deformation level, until a maximum value is reached; then, such value remains approximately constant.

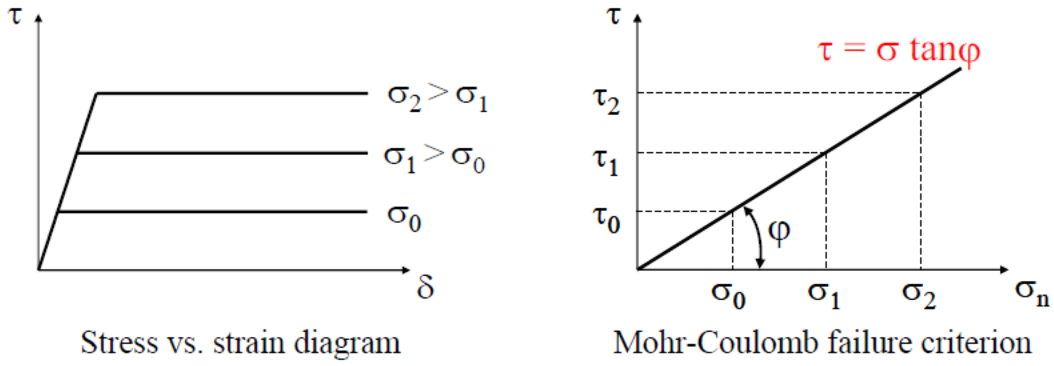

Figure 5-4 Stress vs Strain diagram and Mohr-Coulob failure criterion

- Linear friction model without cohesion: c* = 0
- Failure criterion (pure friction): $\tau = \sigma_n * tan\ (\phi)$

<u>Peak strength equal to residual strength</u>

<u>No dilatancy</u>

5.4 Idealised rough joint (Patton , 1966)

Hypothesis: regular " saw-tooth " roughness (asperities with inclination i).

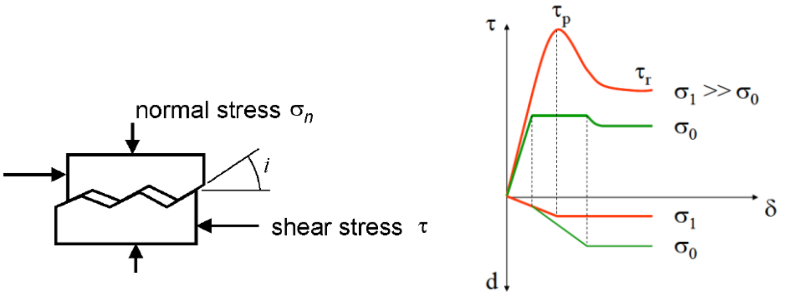

Figure 5-5 Rough joint surface

Observed mechanical behavior : shear stress quickly reaches a peak value. Then, increasing the deformation level, the shear stress stabilizes to a residual value.

<u>Dilatancy</u>

When a shear stress is applied on a rough surface joint, sliding occurs by climbing the asperities:

- to trigger a slide, it is at first required that the shear stress is capable to remove the embedding condition due to the asperities on the contact surface;
- the stress to apply is consequently higher than on a smooth surface.

<u>The shear strength of the joint will consequently increase;</u>

<u>The material (rock) will expand</u>

Sliding and dilatancy for low normal stresses

"Low" normal stresses:

- if the applied normal stress σn remains below a critical value $\sigma_{n,crit}$
- the upper rock block slides on the joint surface by climbing the asperity angle (in i direction)

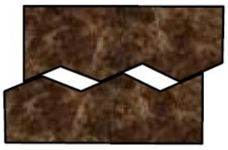

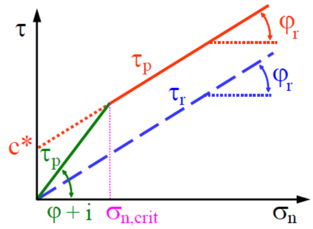

- the peak strength during sliding $\tau_p = \sigma_n * \tan(\phi + i)$
- the residual strength after sliding $\tau_r = \sigma_n * \tan \phi_r$

"High" normal stresses:

- if the applied normal stress σn is above the critical value σn,crit
- the asperities are sheared and the upper rock block moves almost horizontally (no dilatancy)

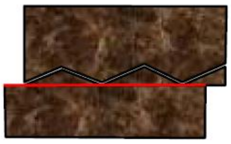

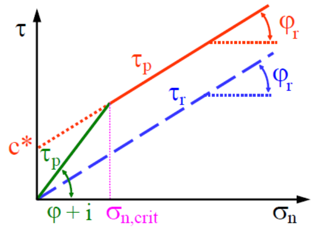

- the peak strength before shearing $\tau_p = \sigma_n * \tan(\phi_r) + c*$
- the residual strength after shearing $\tau_r = \sigma_n * \tan \phi_r$

« Low » normal stresses:

$$\sigma_n \leq \sigma_{n,criti}$$

$$\tau p = \sigma_n \tan(\phi + i)$$

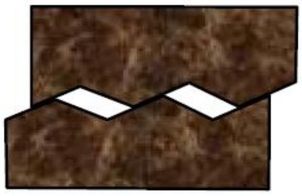

- Friction angle $(\phi + i)$
- Dilatancy d
- No cohesion

« High » normal stresses:

$$\sigma_n \geq \sigma_{n,criti}$$

$$\tau_p = \sigma_n * \tan(\phi_r) + c*$$

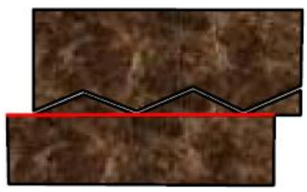

- Friction angle ϕ_r
- No dilatancy
- Cohesion $c*$

with $\sigma_{n,crit}$ the critical normal stress

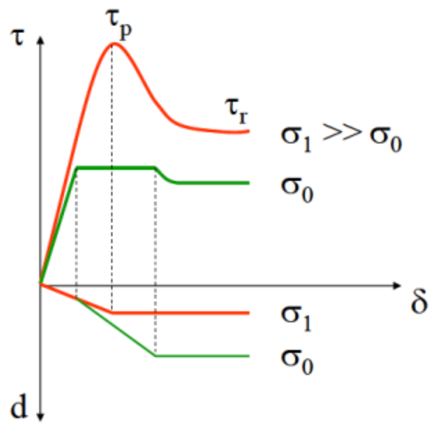

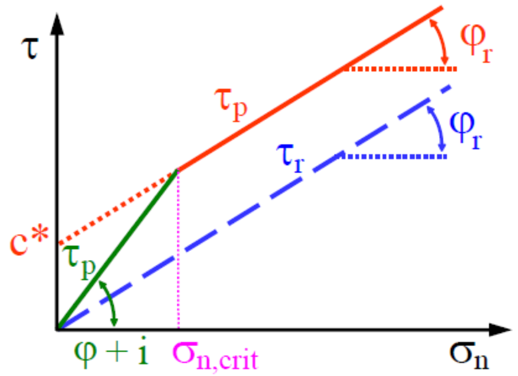

Given:

ϕ = friction angle on asperities surface

ϕ_r = friction angle on the joint surface

it can be assumed:

$$\phi = \phi r$$

The residual strength after the shearing of the asperities is:

$$\tau_p = \sigma_n * tan(\phi_r)$$

5.5 Real rough joint (Barton, 1973)

Hypothesis:

- the joint surface presents an irregular roughness (asperities with variable inclination i);

Observed mechanicalbehavior:

- progressive rupture of the asperities and some dilatancy
- The Mohr-Coulomb criterion is not fully applicable to describe the relation between shear strength and normal stress.

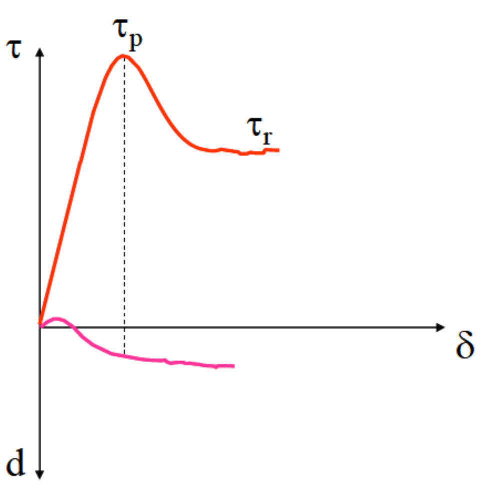

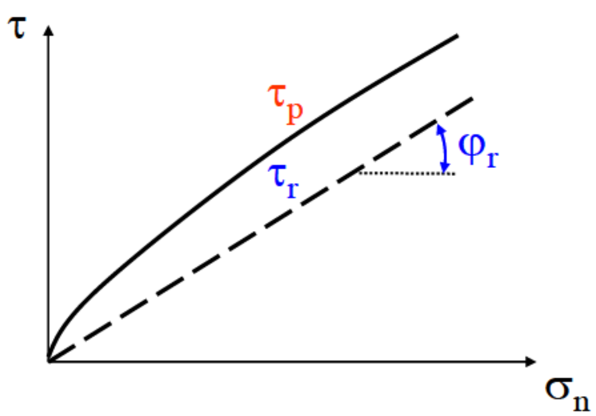

5.5.1 Barton's failure criterion

Laboratory results obtained by means of a shear testing machine. The test is performed keeping a constant applied normal stress. The circles represent the peak value of the shear strength, while the crosses describe the residual strength level.

5.5.2 Barton's empirical model:

$$\tau_p = \sigma_n * \tan\left(JRC * log_{10}\left(\frac{JCS}{\sigma_n}\right) + \phi_r\right)$$

τp = peak shear strength
σn = applied normal stress
JRC = Joint Roughness Coefficient
JCS = Joint wall Compressive Strength
ϕr = residual friction angle

5.5.2.1 Joint Roughness Coefficient (JRC)

JRC is a number varying in the interval 0 ÷ 20 and represents the relevance of roughness in defining rocks' shear strength (smooth surfaces: JRC = 0; very rough surfaces: JRC = 20).

JRC can be estimated by:

1. comparing the real profile of the asperities with standard profiles:
   - « Barton comb » is used on site to reproduce the real roughness profile;

Figure 5-6 45-D0566/A Profilometer (Barton comb), 150 mm length. ControlsGroup.

- the obtained profile is compared with the standard profiles;

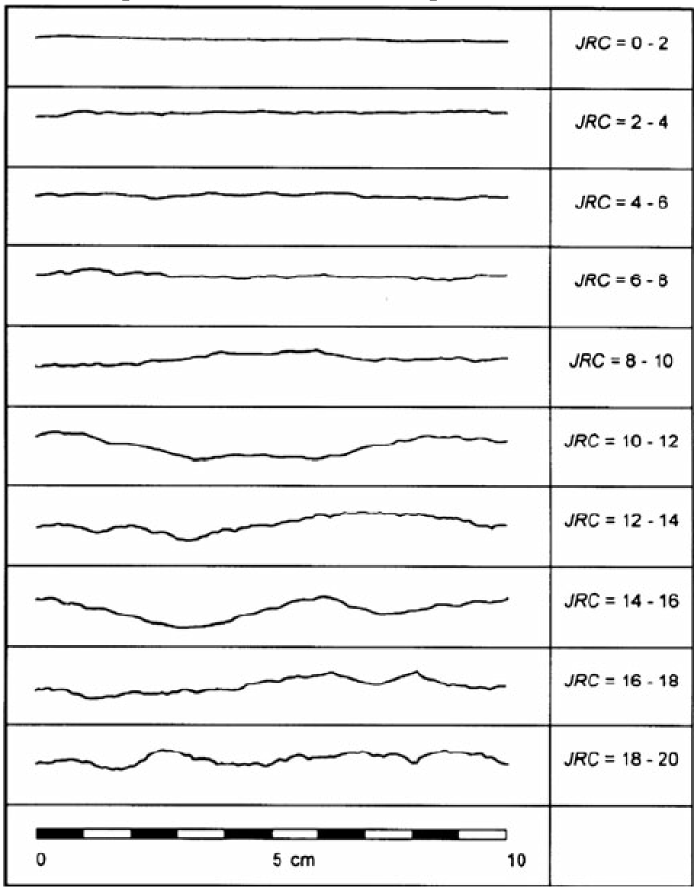

Figure 5-7 Roughness profiles and their corresponding JRC values (Barton and Choubey 1977)

- a value of JRC is assigned to evaluate the joint's roughness.

2. <u>performing a « tilt test »</u>
   - rock sample constituted by two parts separated by a joint;

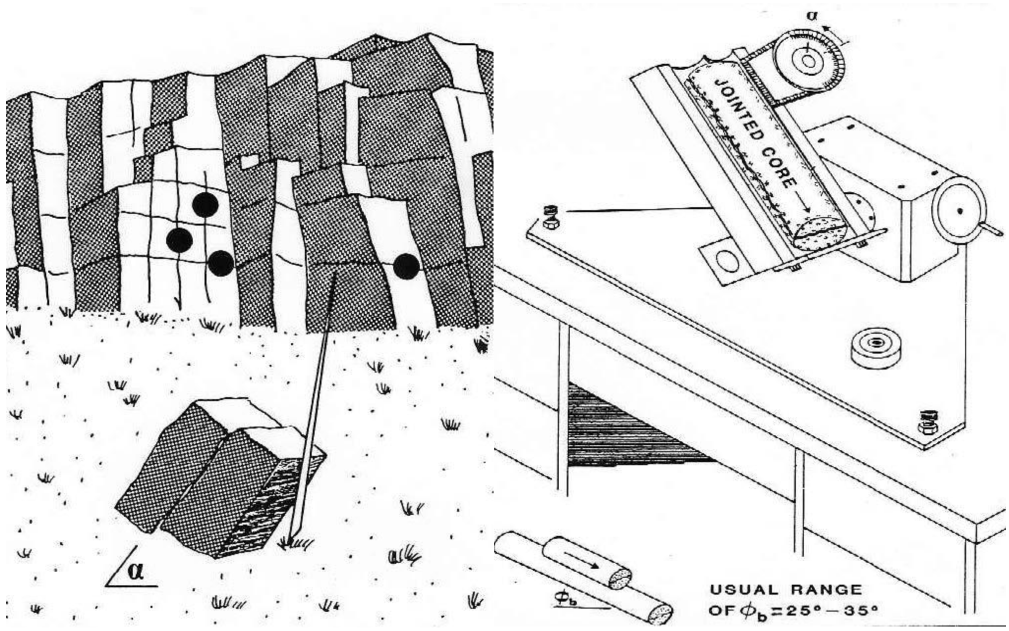

Figure 5-8 Tilt test (or self-weight gravity shear test) for characterizing rock joints. Note measurement

   - the sample is placed on a plane, slowly tilted until sliding between the parts occurs;

Figure 5-9 Tilt Test apparatus

- the angle of inclination α is measured;
- JRC is calculated by means of the equation:

$$JRC = (\alpha - \phi r) * \left(log_{10}\left(\frac{JCS}{\sigma_{n0}}\right)\right)^{-1}$$

where $\sigma_{n0} = \gamma * h * cos^2(\alpha)$ is the normal stress in situ on a surface inclined by α.

3. <u>measuring length and amplitude of the asperity profile and using a graphic correlation with JRC.</u>
    - the length of the asperity profile is measured;
    - the maximum amplitude of the asperity profile is measured;
    - a graphic correlation allows to determine the corresponding value of the Joint Roughness Coefficient (As shown below in figure 5-10).

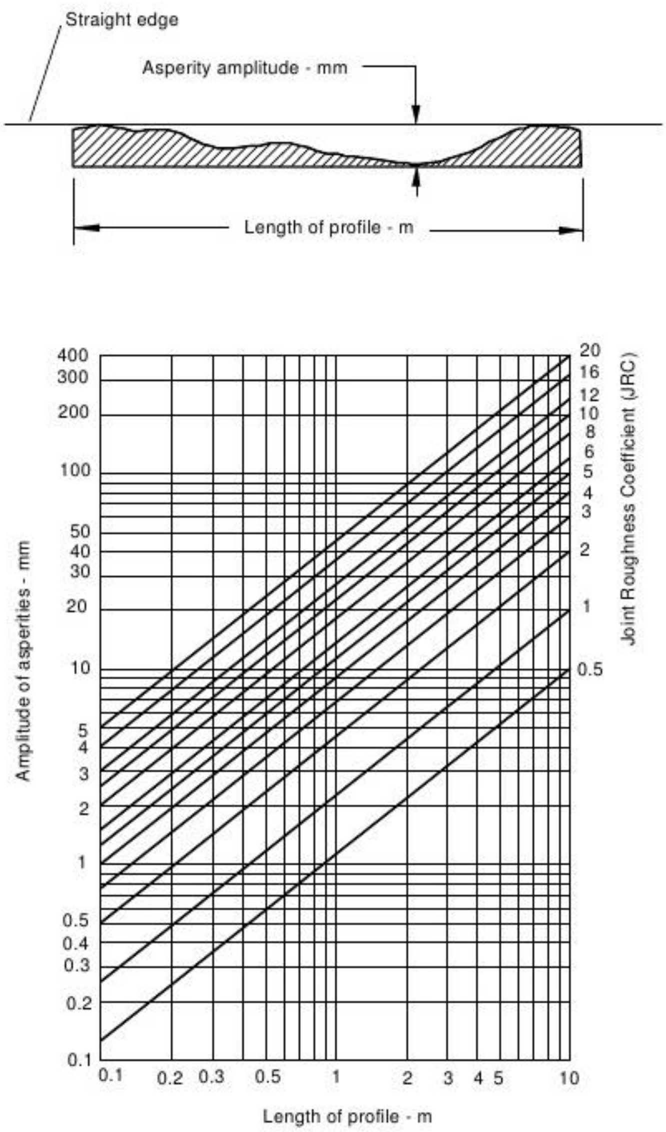

Figure 5-10 Alternative method for estimating JRC from Measuremens of surface roughness amplitude from a straight edge (Barton 1982).

5.5.2.2 Joint wall Compressive Strength (JCS)

JCS represents the compressive strength of the joint, measured on the wall of the joint itself.

JCS can be estimated by:

1. comparing the alteration degree of the joint with the degree of alteration of the rock;

   The degree of alteration of the joint is compared to the one of the rock. The value of JCS is then determined by means of a relation with the compressive strength of the intact rock.
   Degree of alteration of the joint surface:
   - - equal to rock: $JCS = \sigma c$ (rock)
   - - slighly higher than rock: $JCS = 0.5\ \sigma c$ (rock)
   - - much higher than rock: $JCS = 0.1\ \sigma c$ (rock)

2. performing on site measures with the Schmidt rebound hammer.

   The Schmidt rebound hammer is used in field observations to evaluate the Joint Compressive Strength. Depending on the inclination of the hammer, the measure allows to know the Schmidt hardness. This parameter is combined with the unit weight of the rock to obtain the value of JCS.

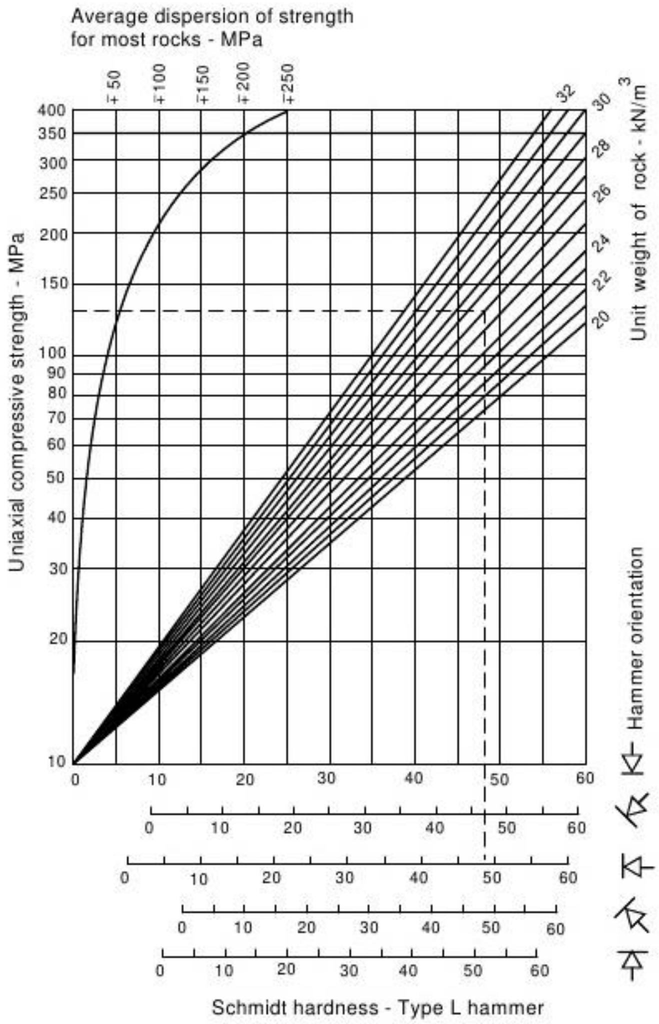

Figure 5-11 Estimate of joint wall compressive strength from Schmidt hardness

Barton's empirical model:

$$\tau_p = \sigma_n * \tan\left(\boxed{JRC * log_{10}\left(\frac{JCS}{\sigma_n}\right)} + \phi_r \right)$$

- the first term in parentheses represents the dilation angle δ (contribution of dilatancy to the shear strength)
- the more the joint surface is altered, the lower is the value of JRC and JCS and (as a consequence) of τ_p
- the less the joint's surfaces are embedded, the lower is the value of JRC (and τp)
- higher values of JRC give high dilation angles.

5.6 Shear Strength of Rockfill

The real contact stress levels are believed to be close to compressive failure where rock joint asperities and rockfill stones are in contact (e.g. Figure 5-12 for the case of rock joints). Therefore it is perhaps possible to use a common form of constitutive equation for extrapolating the strength measured at very low (index test) normal stress levels, to stress levels of engineering interest, as inside a large rockfill dam, inside a rock dump or under a rock slope formed of jointed rock.

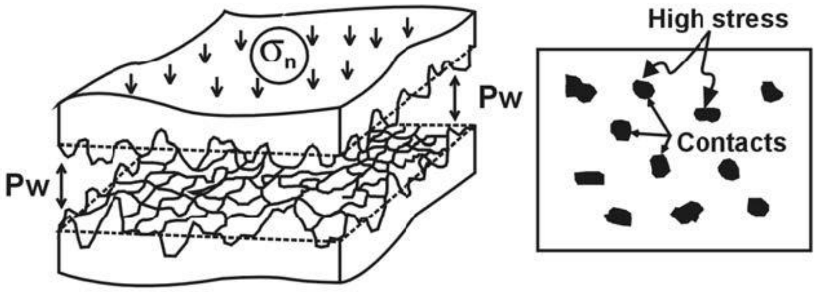

Figure 5-12 When peak shear strength is approached (joints and rockfill), the actual rock-to-rock contact stress levels are extremely high, due to small contact areas.

It is believed that the real ratios of $\sigma cn\ /JCS$ (contact normal stress/joint wall compressive strength, in the case of rock joints) and $\sigma cn\ /S$ (contact normal stress/particle strength,in the case of rockfill) are equal to the ratio A0 / A1 representing the ratio of true contact area/assumed contact area.

The terms JCS and S represent the joint compressive strength and the particle strength, respectively. In other words, contact area is a rock strength or particle strength regulated phenomenon at peak strength. Tilt tests are performed on a regular basis to characterise the roughness of rock joints.

The equation for back-calculating the effective roughness (R) of rockfill particles is shown in Figure 8 (diagram 5). Exactly the same format is used to back-calculate the joint roughness coefficient (JRC) for rock joints:

$$JRC\ =\frac{(\alpha_0-\ \varphi_r)}{log\left(\frac{JCS}{\sigma no}\right)} \qquad (1)$$

where σno represents the very low normal stress acting when sliding occurs between the two halves of a mating rock joint, at tilt angle αo. In the case of tilt tests on laboratory-scale joint samples, the normal stress is often as low as 0.001 MPa

A schematic example of tilt testing for rock joints has been explained before, while a suggested method for testing rockfill at full scale (without needing parallel grading curves) is shown in Figure 5-13, from Barton and Kjærnsli (1981).

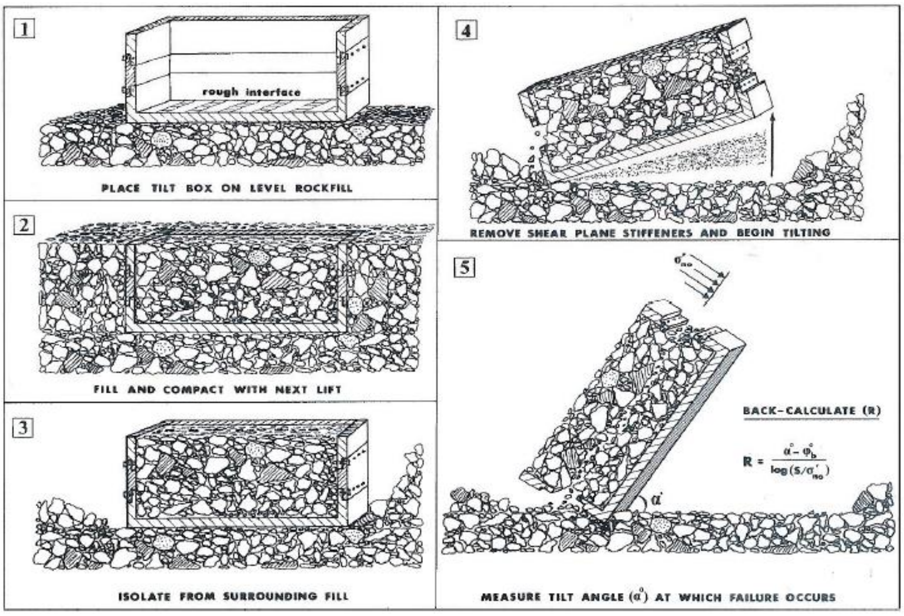

Figure 5-13 Illustration of the tilt test principle for rockfill (Barton and Kjærnsli, 1981)

5.6.1 The shear strength of rockfill as measured

Leps (1970) is responsible for assembling a significant number of large-scale triaxial shear test data for rockfills of various types.

The interpreted peak effective friction angles as a function of the estimated effective normal stress are shown in Figure 5-14 a.

We can 'fit' familiar values of JRC and JCS for rock joints (Figure 9b) that closely match the stress-dependent friction angles that (also) describe the shear strength of rockfills.

Mid-range JRC values (to correspond to an R-range of about 5 to 10, and low-to-high range JCS values (to correspond to an S-range of about 10 to 100 MPa) generated by medium weak to medium strong rock are seen to fit the test data.

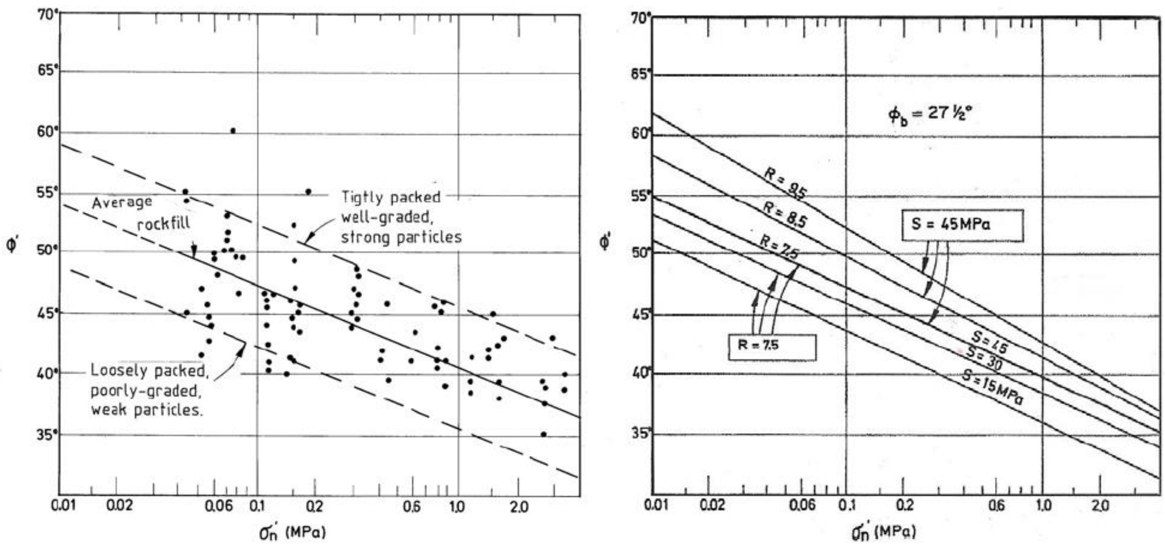

Figure 5-14 Leps (1970)

Left: Assembly of peak shear strength data for rockfills, from Leps (1970).

Right: Comparative JRC or R, and JCS or S values used to generate similar gradients to Leps 1970 data for rockfill.R = 5 to 10, and S = 10 to 100 MPa appear to cover the range of strengths assembled by Leps.

Less compacted rock dump materials will tend to have lower ‘R-values’ than the ‘tightly-packed’ particles, since there will generally be less interlocking.

The more conventionally plotted shear stress versus effective stress curves for rockfill, shown in Figure 5-15 from Marsal (1973), also confirm the similarities of the peak shear strength of rock joints and rockfill.

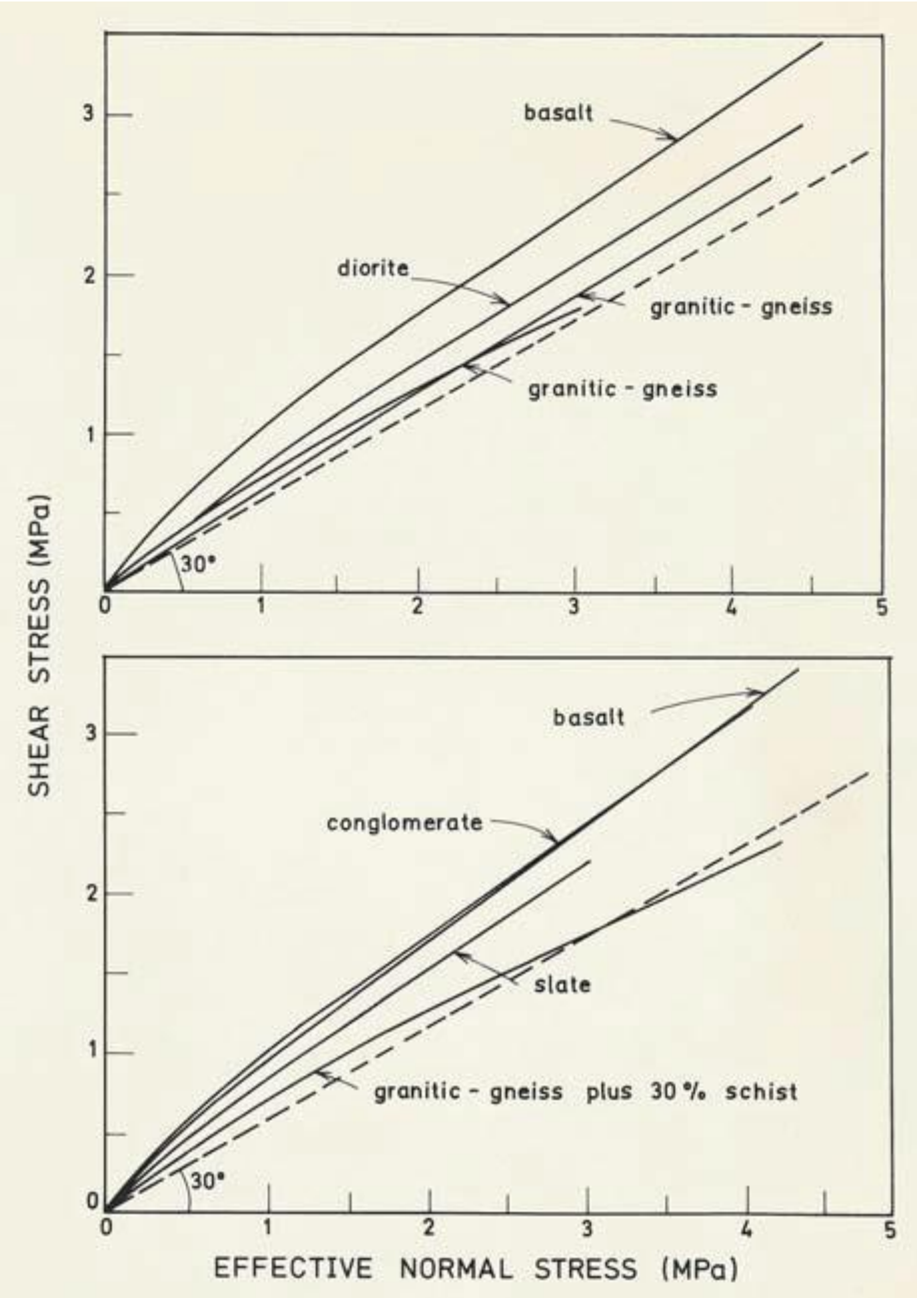

Figure 5-15 The peak shear strength envelopes for rockfill have remarkable similarity to those for medium rough, medium strength rock joints. Large-scale test data from Marsal (1973)

The large scale measurement of frictional strength of rock dump materials obtained from mines in the Chilean Andes shown in Figure 5-16 tend to further reinforce the idea of non-linear stress-dependent friction angles that are likely to apply to rock dumps in general (priv. comm., Sandra Linero, SRK).

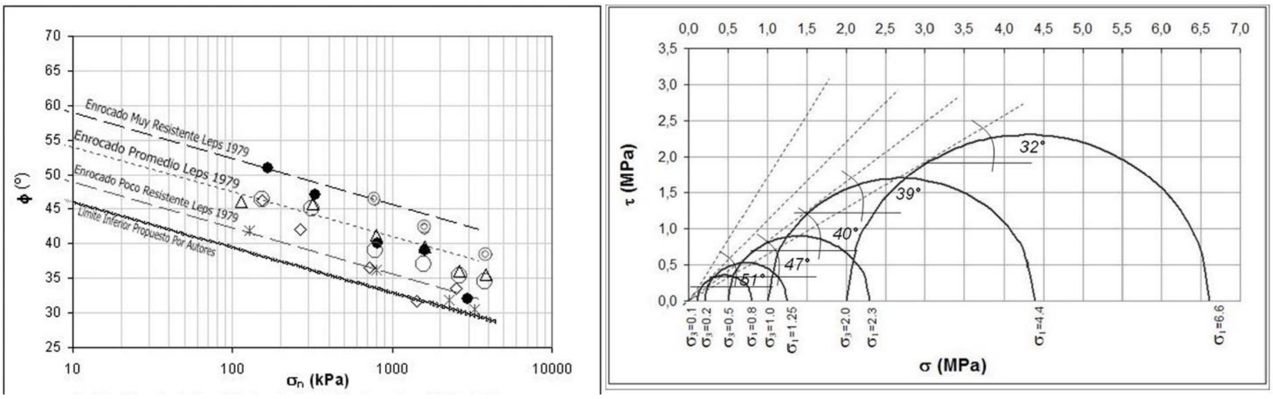

Figure 5-16 Large rock dumps are a familiar feature of mines in the Chilean Andes. Large-scale triaxial shear tests performed in Chile, with important results (black dots and Mohr circles) showing non-linear stress- ependent friction angles (Linero and Palma 2006)

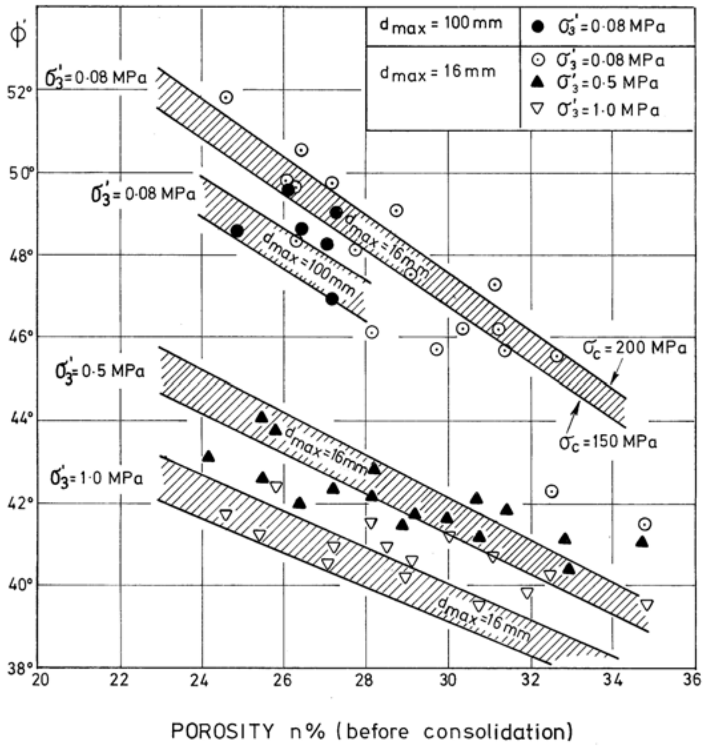

Figure 5-17 The same non-linearity with effective stress level is seen in large-scale triaxial tests performed at NGI (Strøm, 1974, 1975, 1978), with particle size-dependence, rock strength dependence, and porosity effects also indicated

For comparison, Figure 5-18 shows shear strength envelopes for rock joints that have been generated with the JRC-JCS model introduced in Figure 5-10. The strongly varying peak dilation angles, part of the reason for the non-linearity, are also shown on each envelope, except at lowest stress, where they may exceed 30°.

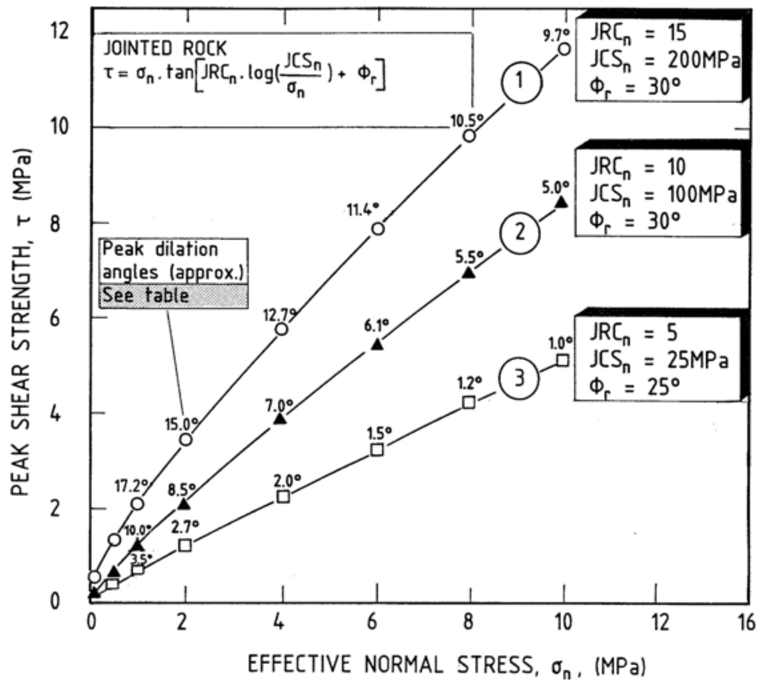

Figure 5-18 Shear strength envelopes (and peak dilation angles) predicted for rock joints, using the JRC-JCS non-linear model of Figure 5-10. Rockfill generally lies between curves #2 and #3

5.6.2 Estimating the shear strength of rockfill

As emphasised in all reports of rockfill shear strength, including Barton and Kjærnsli (1981), the degree of compaction and porosity achieved when building a dam or when preparing relevant laboratory samples is all important. The particle roughness and smoothness is also fundamental. Figure 5-19 illustrates an empirical scheme developed by the writer, for estimating the likely R-value for rockfills, whether for rounded gravels or for rough quarried rock. The high (relatively uncompacted) porosities in mining rock dumps clearly places such dumps in the middle-to right-hand areas of this diagram, and even sharp angular particles (relevant for waste rock, but perhaps not always for tailings) are unlikely to generate 'R-values' above 5 to 7, as also suggested in Figure 5-14.

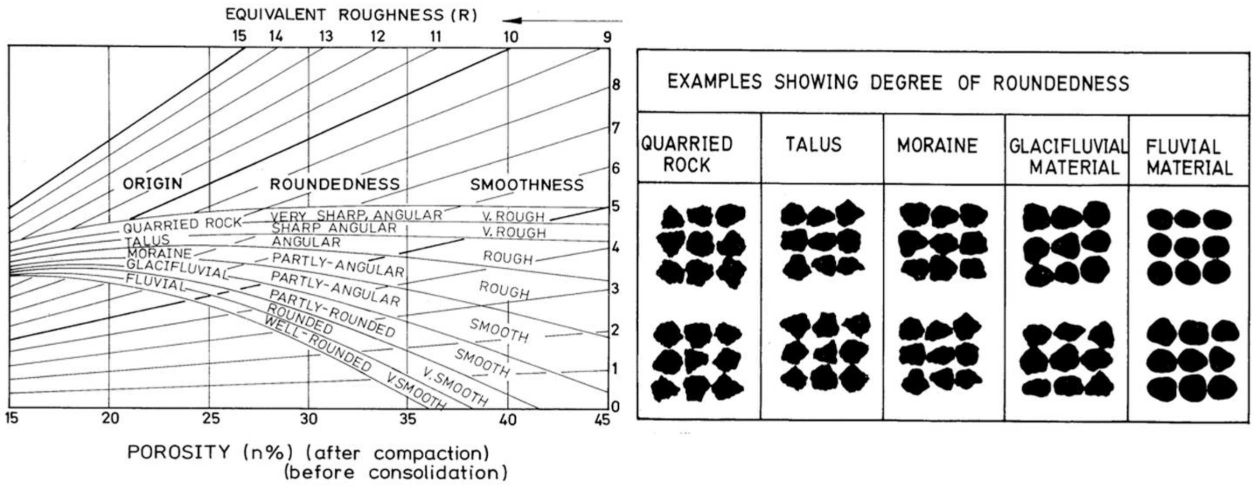

Figure 5-19 An empirical method for estimating the equivalent roughness R of rockfill as a function of porosity and particle origin, roundedness and smoothness. Barton and Kjærnsli (1981)

As a result of the literature survey of numerous rockfill test data, Barton, 1980 and Barton and Kjærnsli, 1981 developed a simple strength factoring scheme for estimating S as a function of UCS (or σc), when particle size (d50) varied over a wide range. The points A and B in Figure 15 were used to illustrate S-value estimation for a rock with UCS = 150 MPa, when d50 was 23 mm (S ≈ 0.3x150 = 50 MPa) and when d50 was 240 mm (S ≈ 0.2x150 = 30 MPa), in the case of interpreting triaxial strength data. Note the higher factors apparently needed when planar (and large-scale) shear is involved. Friction angles are typically several degrees higher (e.g. about 2° to 4°) when plane tests are compared with triaxial tests on the same material. There is noticeably less crushing of particles: hence the two empirical curves in Figure 5-20.

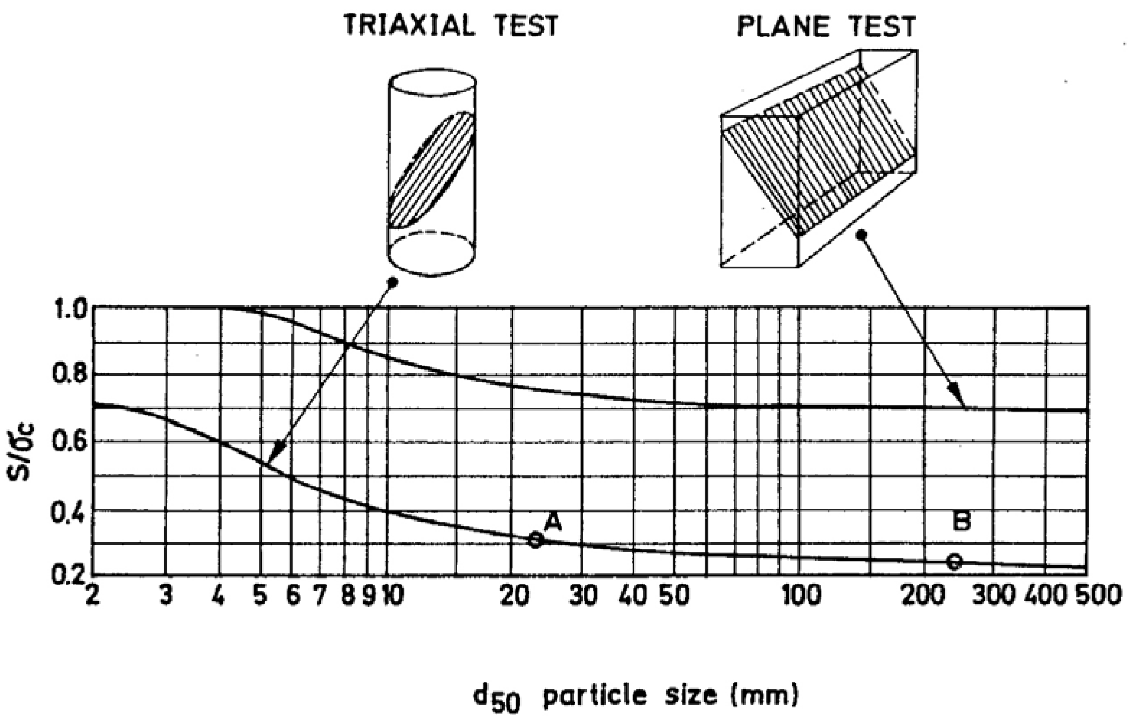

Figure 5-20 Particle size strongly effects the strength of contacts points in rockfill. Triaxial or plane shear also influencesbehavior. Empirical S/UCS reduction factors for estimating S when evaluating equation 3.

5.6.3 Interface shear strength

Interface shear strength, as between a (too smooth) rock foundation and a rockfill dam, seems to be governed by the 'weakest link' rule. If the roughness JRC of the interface, registered by amplitude/length profiling, is too low in relation to particle size (d50), the interface strength is controlled by JRC, and sliding occurs along the interface, as along the bottom face of a rock joint. If on the other hand, the interface roughness is sufficient to give good interlock to the rockfill particles, sliding will occur preferentially within the rockfill, in an 'R-controlled' particle smoothness or roughness dependent manner, with influence also of the porosity. A schematic illustration of the interface problem, and (probable) relevant controlling parameters is shown in Figure 5-21.

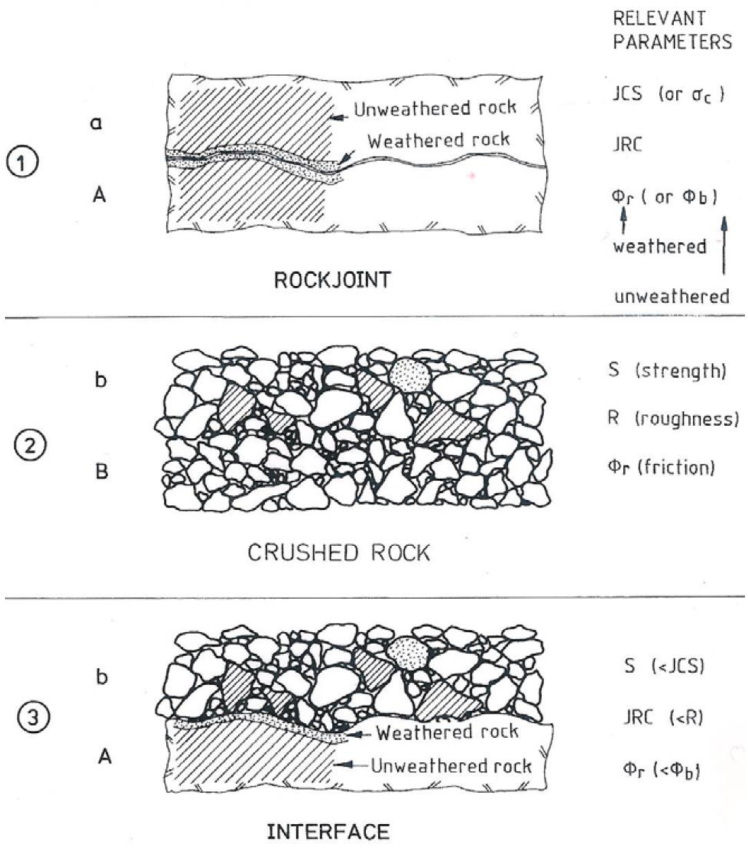

Figure 5-21 Asperity contact across stressed rock joints, and rockfill inter-particle contact, and rockfill lying on a rock foundation.

Asperity contact across stressed rock joints, and rockfill inter-particle contact, and rockfill lying on a rock foundation, are each examples of point-contact stress levels that are probably close to compressive failure, when peak shear strength is approached. For this reason the three cases have many points in common, including similar non-linear shear strength envelopes.

The peak shear strengths for rock joints, rockfill and interfaces are respectively:

Rock joints:

$$\tau_p = \sigma_n * \tan\left(JRC * log_{10}\left(\frac{JCS}{\sigma_n}\right) + \phi_r\right) \quad (2)$$

Rockfill:

$$\tau_p = \sigma_n * \tan\left(R * log_{10}\left(\frac{S}{\sigma_n}\right) + \phi_r\right) \quad (3)$$

Interface:

$$\tau_p = \sigma_n * \tan\left(JRC * log_{10}\left(\frac{S}{\sigma_n}\right) + \phi_r\right) \quad (4)$$

If the rockfill particles are not weaker than the rock foundation, as assumed in equation 4, then S > JCS, and the strength is determined by the weak foundation. In the case of rockfill or waste rock that is freshly blasted, the residual friction angle ϕ_r assumed, can (initially) be replaced by ϕ_b, which is usually a few degrees higher than the weathered value. Conservative, long-term design strength may nevertheless demand the use of ϕ_r for 'permanent' rock dumps and rockfill dams, as suggested in all three equations.

5.6.4 R-controlled or JRC-controlled behavior

As indicated above, the relative magnitudes of the interface parameters, and their possible contrast to the shear strength of the rockfill, will determine whether the interface (if very rough) causes 'R-controlled'behavior – meaning preferential failure through the rockfill, or 'JRC-controlled'behavior, meaning preferential shear along the interface. A review of interface tests, performed by Barton (1980) in response to doubts about the strength of a glacially-smoothed dam foundation in Norway, resulted in the separation of performance identified in Figure 5-22.

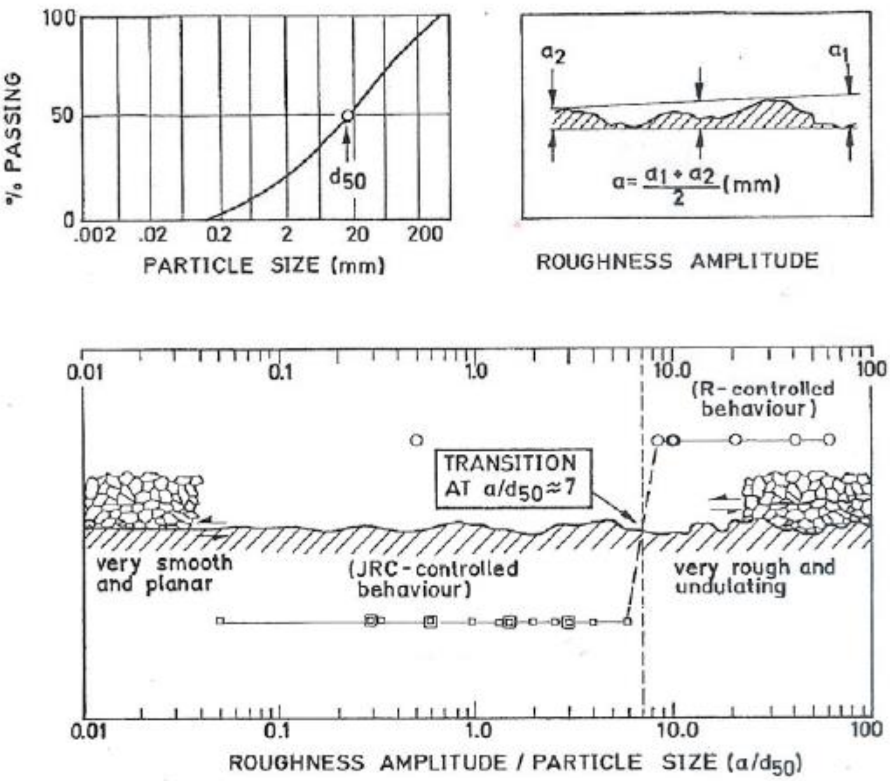

Figure 5-22 A review of interface shear tests was performed in response to concern over insufficient roughness for the rockfill dam foundation, in the glaciated mountain terrain in Norway.

5.7 Barton model applied on Bhatar system

The Barton model have been studied in two different configurations :

- Rockjoint
- Rockfill

In order to applied the Barton model and its equations they have been used the results about vertical normal stresses obtained in the static analysis which will be explained in the following chapters.

5.7.1 Rockjoint

In order to study the case of rockjoint interfaces of Bhatar construction we must refer to Case 1 of Figure 5-21 described by equation (2).

In this case we consider an ideal plane as a continuous joint. The whole interaction surface can be classified with the Barton parameters which are usually used to described a rock joint.

Different samples of stone may be tested and then It can be evaluated an average of the tanget: $tan\left(JRC * log_{10}\left(\frac{JCS}{\sigma_n}\right) + \phi_r\right)$ which, for the Bhatar thesis, is the coefficient of friction.

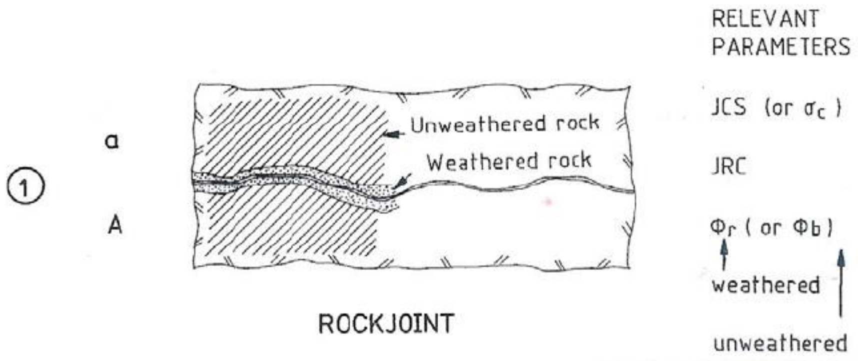

$$\tau_p = \sigma_n * \tan\left(JRC * log_{10}\left(\frac{JCS}{\sigma_n}\right) + \phi_r\right) \qquad (2)$$

where

τ_p = peak shear strength

σ_n = applied normal stress

JRC = Joint Roughness Coefficient

JCS = Joint wall Compressive Strength

ϕ_r = residual friction angle

5.7.2 Rockfill

Recalling what has been written until here, in order to study the case of rockfill interfaces of Bhatar construction we must refer to Case 2 of Figure 5-21 described by equation (3) :

$$\tau_p = \sigma_n * \tan\left(R * log_{10}\left(\frac{S}{\sigma_n}\right) + \phi_r\right) \qquad (3)$$

where

τp = peak shear strength
σn = applied normal stress
R = Roughness

S = Strength
ϕr = residual friction angle

In the case of rockfill or waste rock that is freshly blasted, the residual friction angle φr assumed, can (initially) be replaced by φb, which is usually a few degrees higher than the weathered value.

In order to estimate R :

$$R = \frac{\alpha^0 - \varphi_b}{log_{10}\left(\frac{S}{\sigma_n{}'}\right)}$$

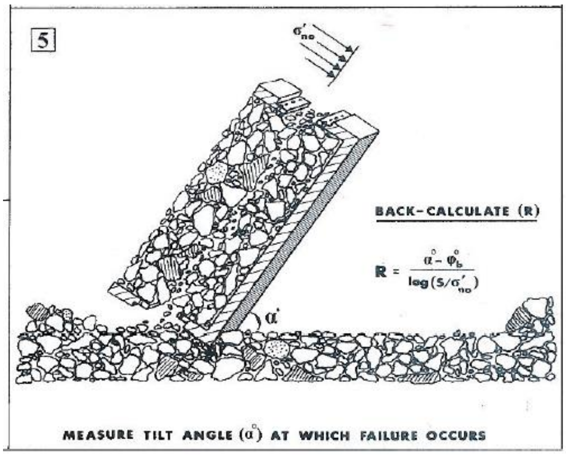

or

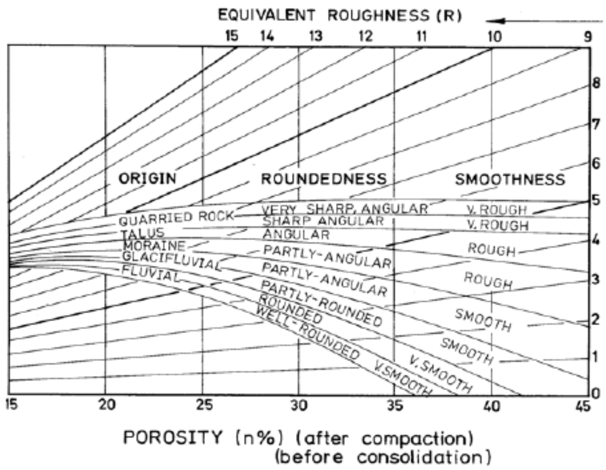

In order to estimate S :

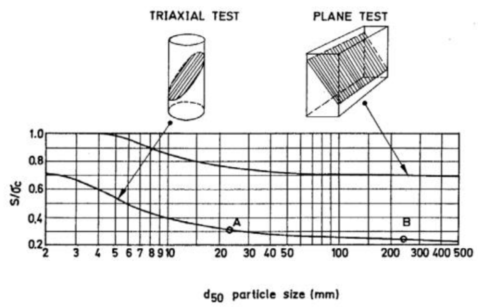

5.7.3 Voids ratio and Porosity

The *porosity* of the soil is the percent of void space.

$$n = 100 * \left(\frac{V_v}{V}\right)$$

Where

n is porosity (percentage)

V_v is volume of the void space (L^3 ; cm^3 ; m^3)

V is volume of the sample (L^3 ; cm^3 ; m^3)

The *void ratio* of the soil is the ratio of the volume of the voids to the volume of the solids.

$$e = \left(\frac{V_v}{V_s}\right)$$

Where

e is void ratio (percentage)

V_s is volume of the solids (L^3 ; cm^3 ; m^3)

The total volume is equal to the volume of the voids plus the volume of the solids.

$$V = V_v + V_s$$

The void ratio is closely related to the porosity if porosity is expressed as a ratio.

$n = \left(\frac{e}{1+e}\right)$ and $e = \left(\frac{n}{1-n}\right)$

5.7.4 Limestone Mechanical Properties for application of Barton model

In accordance to the previous chapter, they have been used the results of laboratory tests with the Schmidt hammer.

Table : Rock characterization results

No. (kg/m3) L	Sample Type	Dry Density (kg/m3)	R : rebound number	**UCS: Miller`s correlation(MPa)**	**UCS:Obtained in Laboratory(MPa)**
1	Limestone	2817,0	36,0	72,0	72,9
2	Limestone	2748,0	35,9	76,0	72,9
3	Limestone	2646,0	31,5	55,0	58,5
4	Limestone	2777,0	31,5	60,0	60,6
5	Limestone	2671,0	28,9	49,0	52,2
6	Limestone	2773,0	30,4	56,0	56,4
7	Limestone	2676,0	37,7	79,0	76,7
8	Limestone	2683,0	36,8	76,0	75,7
9	Limestone	2748,0	34,8	71,0	72,5
10	Limestone	2707,0	35,6	72,0	69,6
11	Limestone	2759,0	36,6	79,0	78,1
12	Limestone	2704,0	33,9	66,0	63,5
13	Limestone	2726,0	35,1	71,0	75,7
14	Limestone	2796,0	37,9	88,0	83,3
15	Limestone	2822,0	36,4	82,0	85,6
16	Limestone	2730,0	36,0	74,0	76,2
17	Limestone	2720,0	36,0	71,0	74,8
18	Limestone	2887,0	35,0	72,0	70,5
19	Limestone	2699,0	39,0	81,0	83,6
20	Limestone	2679,0	37,0	76,0	73,4
Avarage		2738,4	35,1	71,3	71,6

Average data		
Miller`s correlation, 1972: $$UCS = \sigma_c = 12{,}83 * e^{0{,}0487 * R_L}$$		
Dry Density	2738,40	(kg/m3)
R : rebound number	35,10	/
UCS: Miller`s correlation	71,30	(MPa)
UCS:Obtained in Laboratory	71,64	(MPa)

Miller`s correlation, 1965		
$Log10\,JCS = 0.00088 * (\gamma) * (R) + 1.01$ $JCS = 10^{\,0.00088*(\gamma)*(R)+1.01}$		
γ	26,85	kN/m^3
R	35,10	/
JCS	69,10	MPa

5.7.5 Rockjoint results

$$\tau_p = \sigma_n * \tan\left(JRC * log_{10}\left(\frac{JCS}{\sigma_n}\right) + \phi_r\right) \qquad (2)$$

where
τp = peak shear strength
σn = applied normal stress
JRC = Joint Roughness Coefficient
JCS = Joint wall Compressive Strength
ϕr = residual friction angle

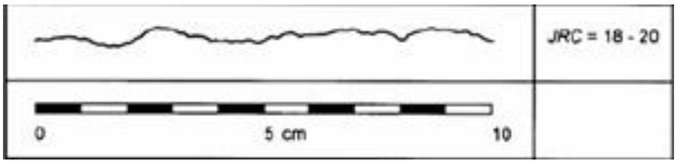

JCS

Comparing the alteration degree of the joint with the degree of alteration of the rock; The degree of alteration of the joint is compared to the one of the rock. The value of JCS is then determined by means of a relation with the compressive strength of the intact rock. Degree of alteration of the joint surface:

- equal to rock: $JCS = \sigma c$ (rock)

- slighly higher than rock: $JCS = 0.5\ \sigma c$ (rock)

- much higher than rock: $JCS = 0.1\ \sigma c$ (rock)

Table 9 Rockjoint data

Rockjoint		
Origin	Quarried rock	
Asperties	maximum	
JRC	20	
Ϭc (from lab tests)	71,6	MPa
JCS (Miller 1965)	69,1	MPa
JCS comparison	71,6	MPa
ϕr °	30	deg

$$\tau_p = \sigma_n \tan\left(20 \log\left(\frac{69.1}{\sigma_n}\right)\right)$$

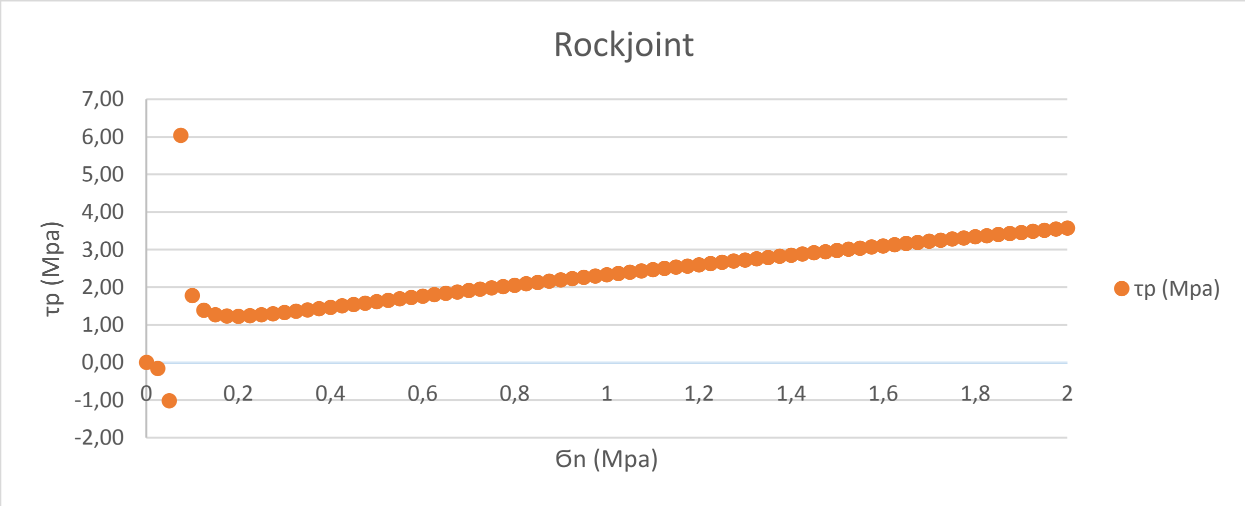

Figure 5-23 Rockjoint function for Bhatar

Table 10 Barton method for Rockjoint Bhatar results

Rockjoint				
Ϭn (Mpa)	τp (Mpa)	μ= τp/σn	rad	deg
0,036	-0,354468	-9,939	-1,47052	-84,255
0,045	-0,671098	-15,046	-1,50443	-86,198
0,056	-1,817527	-32,267	-1,53981	-88,225
0,068	-29,4048	-432,086	-1,56848	-89,867
0,080	3,661616	45,897	1,549012	88,752
0,090	2,264381	25,235	1,53119	87,731
0,093	2,076058	22,379	1,52614	87,441

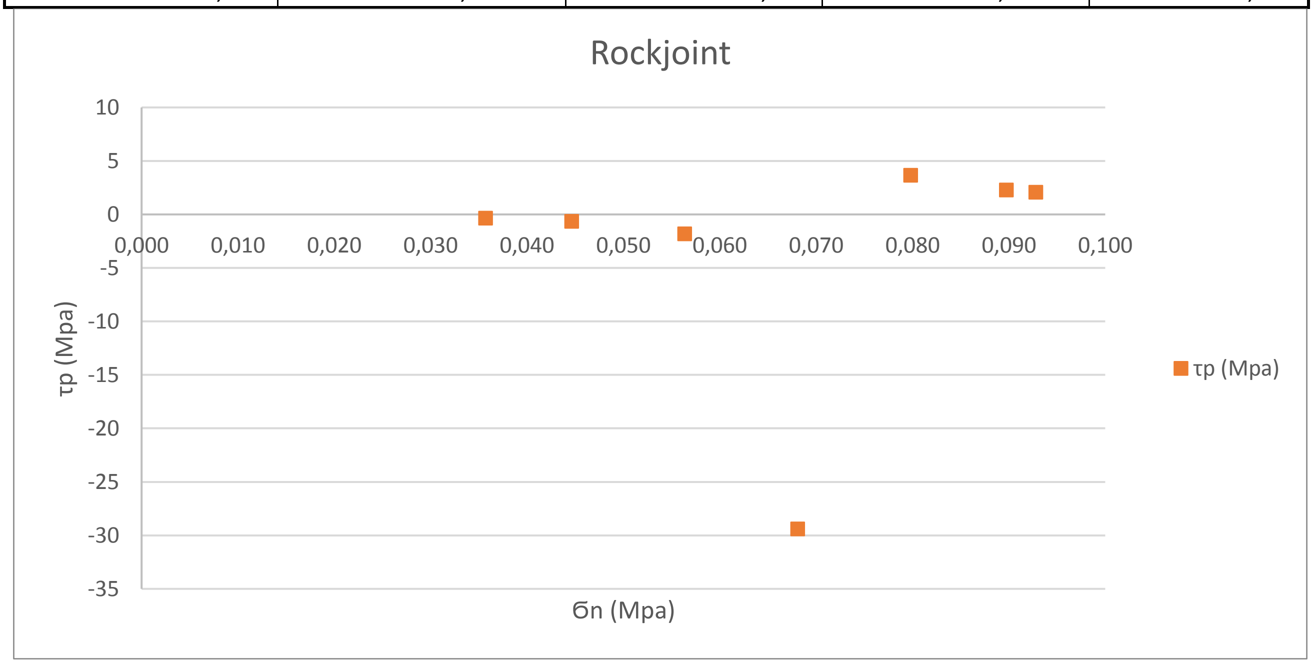

Figure 5-24 Rockjoint function for Bhatar range of interest

Asintoticbehavior, unreliable for our range of normal stress values.

5.7.6 Rockfill results

$$\tau_p = \sigma_n * \tan\left(R * log_{10}\left(\frac{S}{\sigma_n}\right) + \phi_r\right)$$

where

τp = peak shear strength
σn = applied normal stress
R = Roughness
S = Strength
ϕr = residual friction angle

In the case of rockfill or waste rock that is freshly blasted, the residual friction angle φr assumed, can (initially) be replaced by φb, which is usually a few degrees higher than the weathered value.

In order to estimate R :

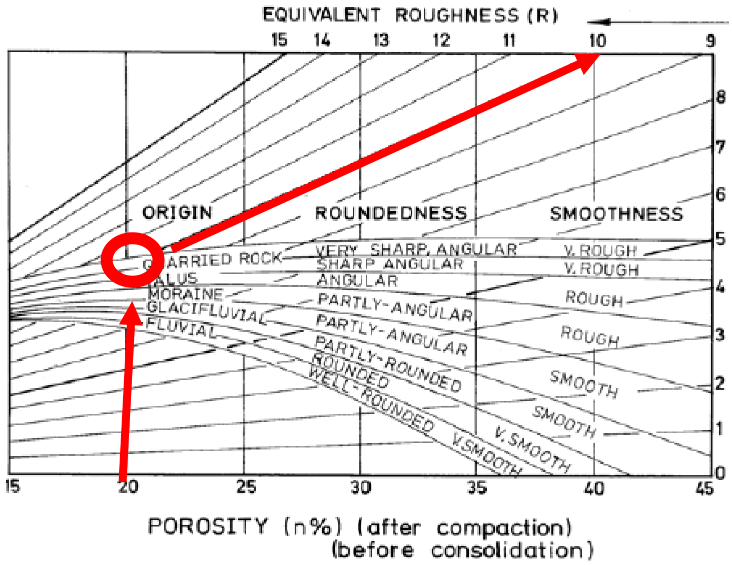

In order to estimate S :

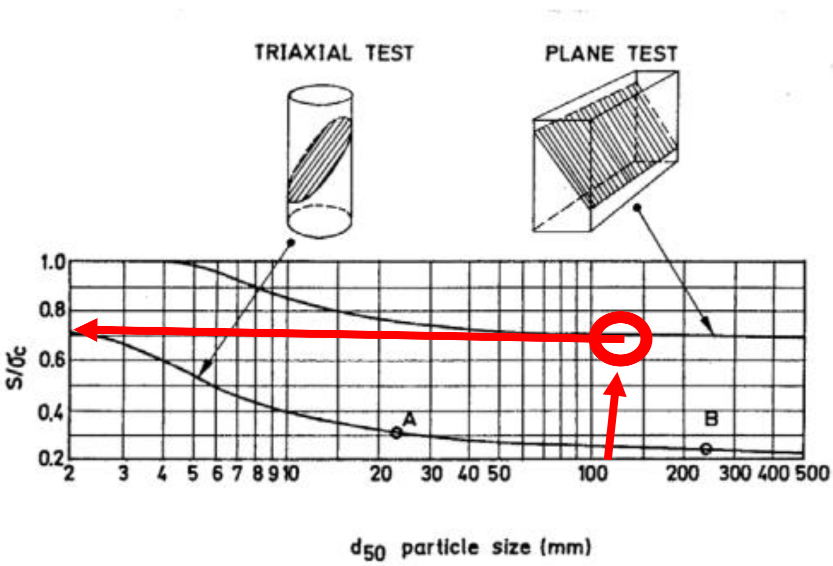

Table 11 Rockfill data

Rockfill		
n : porosity (%)	20	
Origin	Quarried rock	
R : Roughness =	10	
d50 Particle size	> 100 mm	
Ϭc (from lab tests)	71,6	MPa
S/Ϭc	0,7	
S : Strength =	50,12	MPa
φr °	30	deg

$$\tau_p = \sigma_n \tan\left(10 \log\left(\frac{50{,}12}{\sigma_n}\right)\right)$$

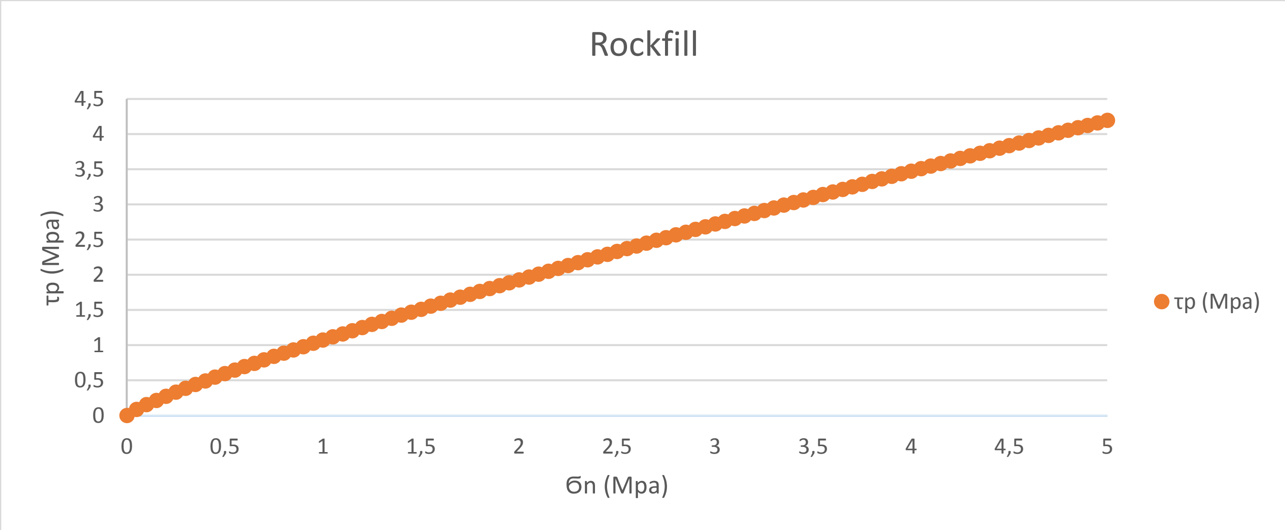

Figure 5-25 Rockfill function for Bhatar

Reliable for our range of normal stress values.

Table 12 Barton method for Rockfill Bhatar results

Normal Stress				Rockfill				
	KN/m^2	Kg/m^2	Kg/cm^2	Ϭn (Mpa)	τp (Mpa)	µ= τp/σn	rad	deg
σ1	34,99	3566,30	0,36	0,036	0,066	1,840	1,073	61,478
σ2	43,75	4460,24	0,45	0,045	0,079	1,768	1,056	60,507
σ3	55,26	5632,78	0,56	0,056	0,096	1,697	1,038	59,493
σ4	66,76	6805,31	0,68	0,068	0,112	1,643	1,024	58,672
σ5	78,26	7977,84	0,80	0,080	0,128	1,599	1,012	57,981
σ6	88,03	8973,09	0,90	0,090	0,141	1,568	1,003	57,471
σ ground	91,01	9277,01	0,93	0,093	0,145	1,559	1,001	57,326

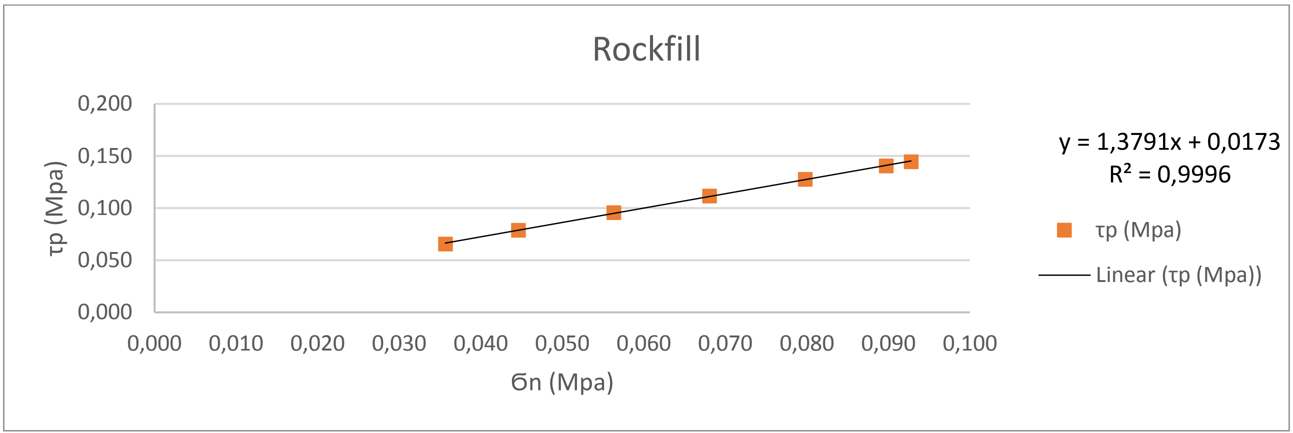

Figure 5-26 Rockfill function for Bhatar range of interest

Reliable for our range of normal stress values.

5.8 Conclusions

The behavior has been descripted by using two different version of Barton's method :

- Barton's method for Rock-joint
- Barton's method for Rock-fill

In the first case the resulting formula is not useful due to the fact that in the range of our interest the equation shows an asymptote which distorts the reliability of the results.

In the second case, with the evaluation of the rock-fill, the behavior of the joint is properly described in the range of our interest and it seems to be correct.

This approach must be verified by proper laboratory test on the different samples or if possible by the use of large scale module as shown in Barton's in situ tests.

Other kind of stones which are used in Nepal or different regions are :

- Dolomite
- Slates
- Sandstone
- Quartzite

The Barton's method for Rock-fill is one of the peculiar aspect of this thesis and it has been fundamental for the analysis of the in plane behavior of the Bhatar wall system.

6 TIMBER ELEMENTS AND CARPENTRY CONNECTIONS

6.1 Geometry of Timber elements

In accordance to the guidelines given in the Arch. Tom Schacher's manual they have been defined and studied all the timber elements Roof rafter beams, rafter beam and the cross piece. The modular unit is just an ideal module which allows us to study the static behavior. All the walls and the room box are built layer after layer with a vertical continuity from the plinth to the roof.

Figure 6-1 Continuous Bhatar wall

Figure 6-2 Carpentery connections

6.1.1 Rafter

The rafter is the most common timber element which compose the all structure and it is laid down on the stones layer parallel to the ground.

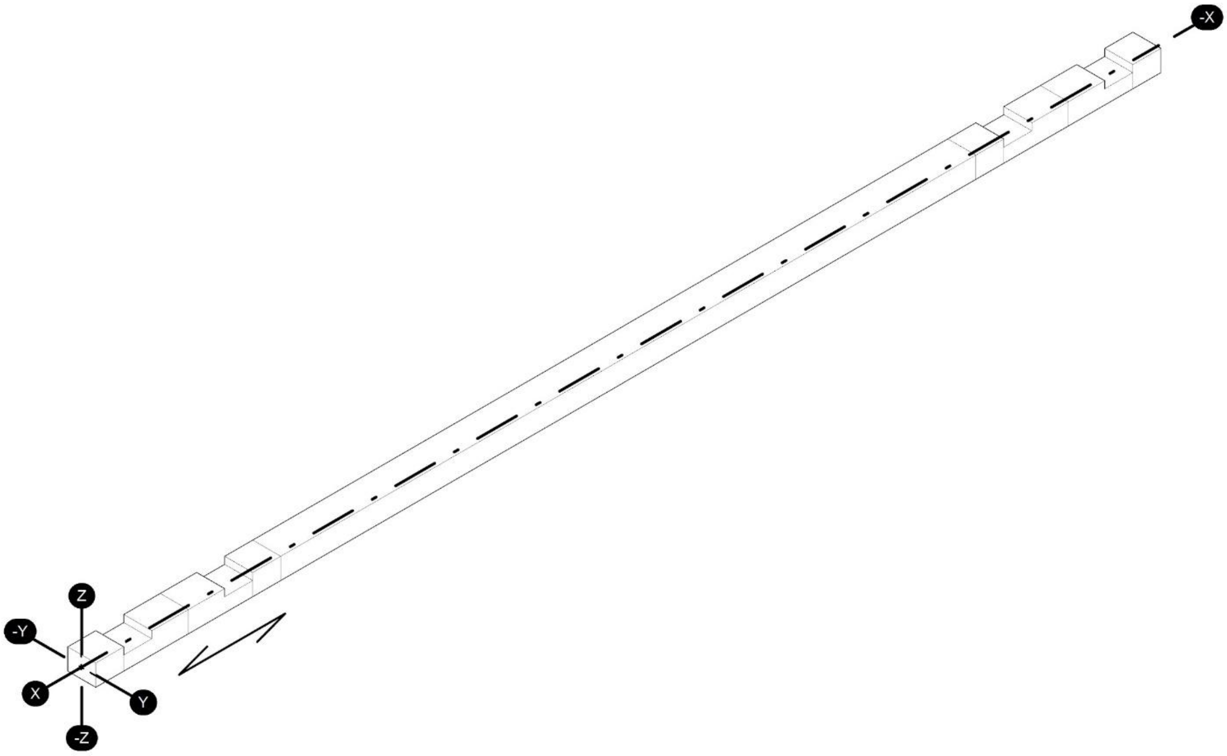

Figure 6-3 Rafter beam

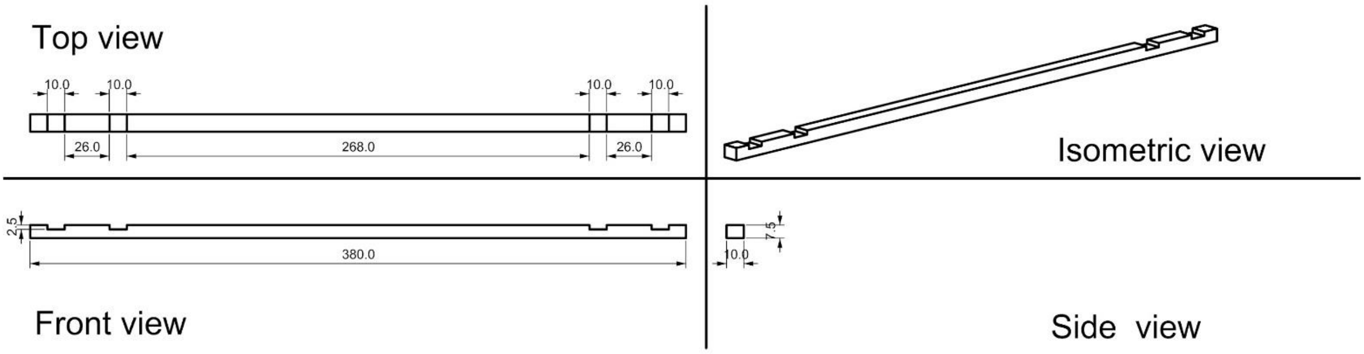

Figure 6-4 Rafter beam Orthogonal projections in cm

6.1.2 Roof rafter

The roof rafter beam is used just at the roof level and the difference with respect to the rafter beam is just the lengths of the two ends.The extremities are longer in order to support the heavy flat roof of earth.

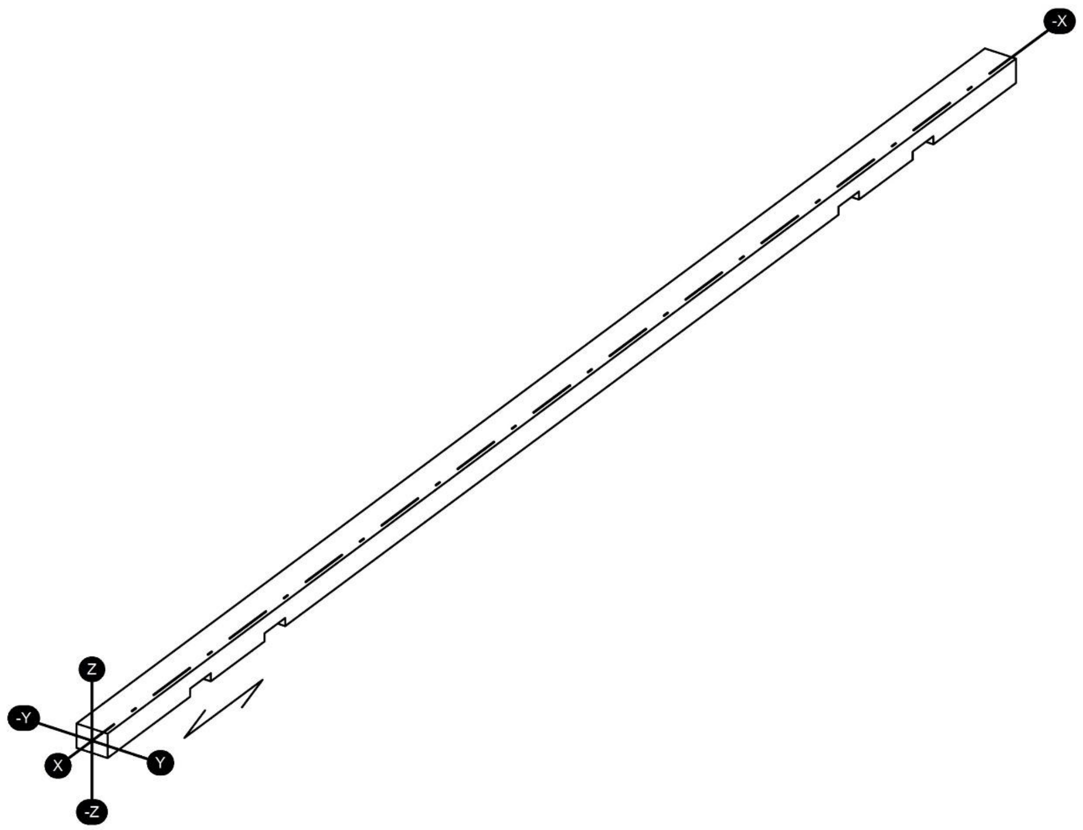

Figure 6-5 Roof rafter beam

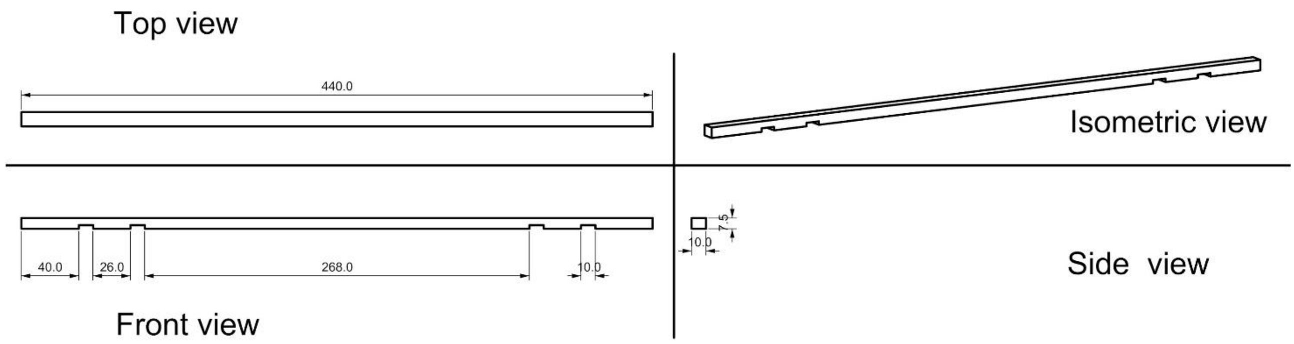

Figure 6-6 Roof rafter beam Orthogonal projections in cm

6.1.3 Cross piece

The cross pieces are the elements which assure stability. Cross pieces help to hold the beams and walls together. You need notches only on the cross pieces, but not on the main beams.

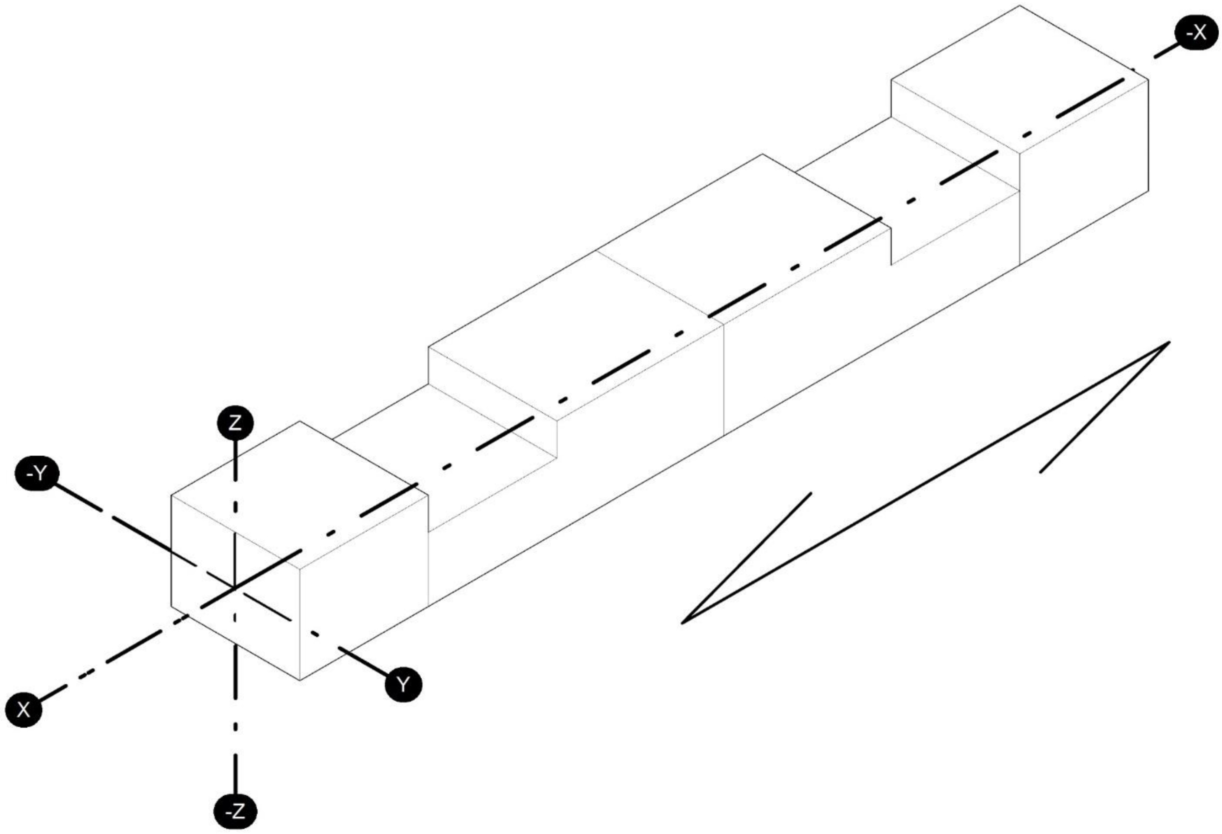

Figure 6-7Cross piece

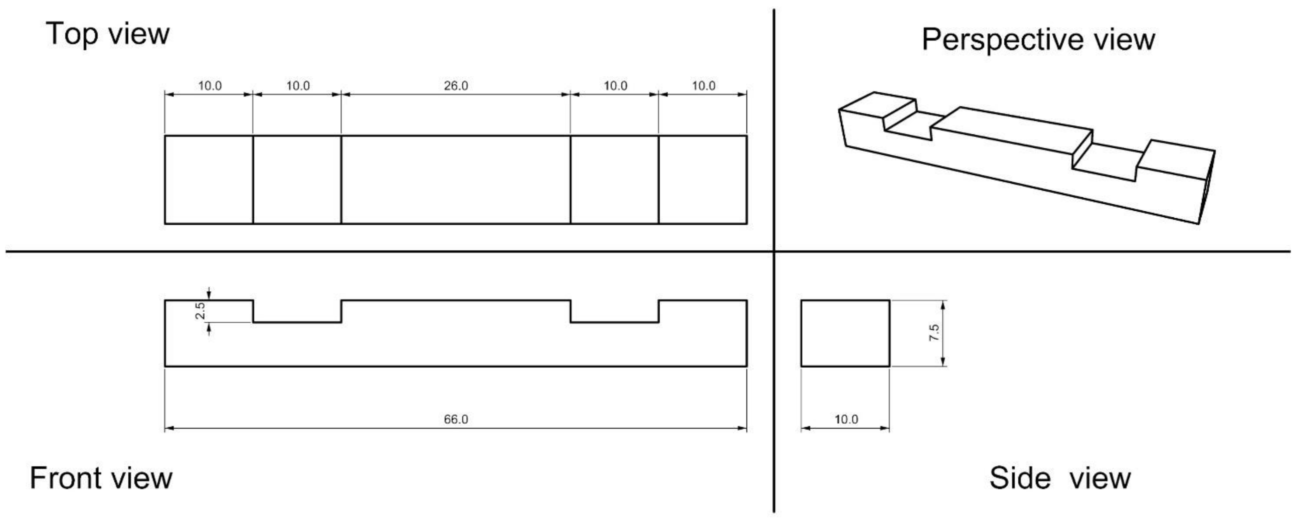

Figure 6-8 Cross Piece Orthogonal projections in cm

6.2 Assembling

Assembled timber band composed by Rafters and cross pieces

6.2.1 Timber Band

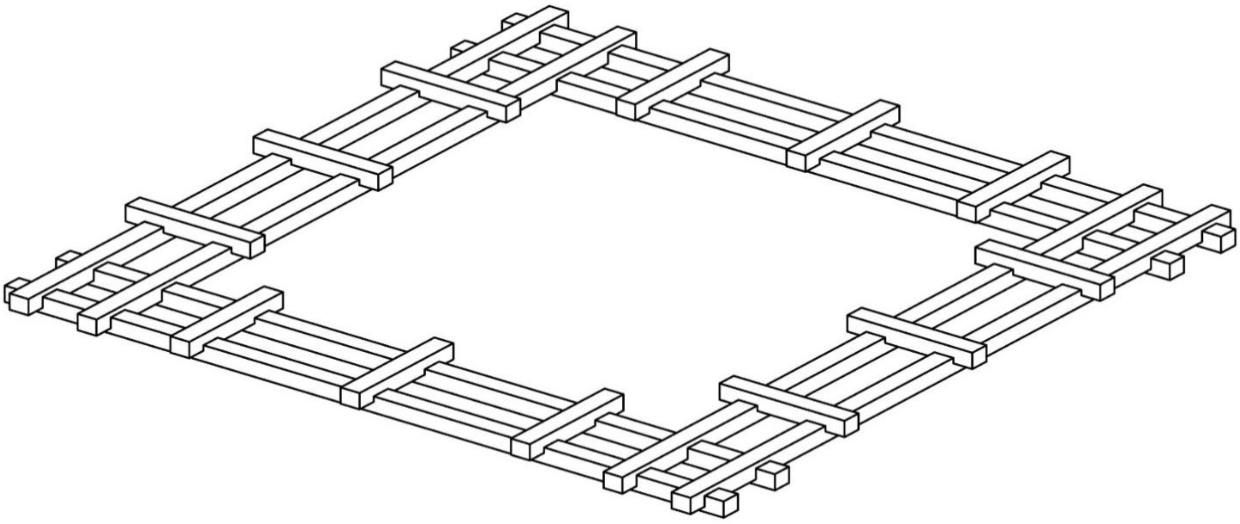

Figure 6-9 Timber Band

6.2.1.1 Rafter exploded

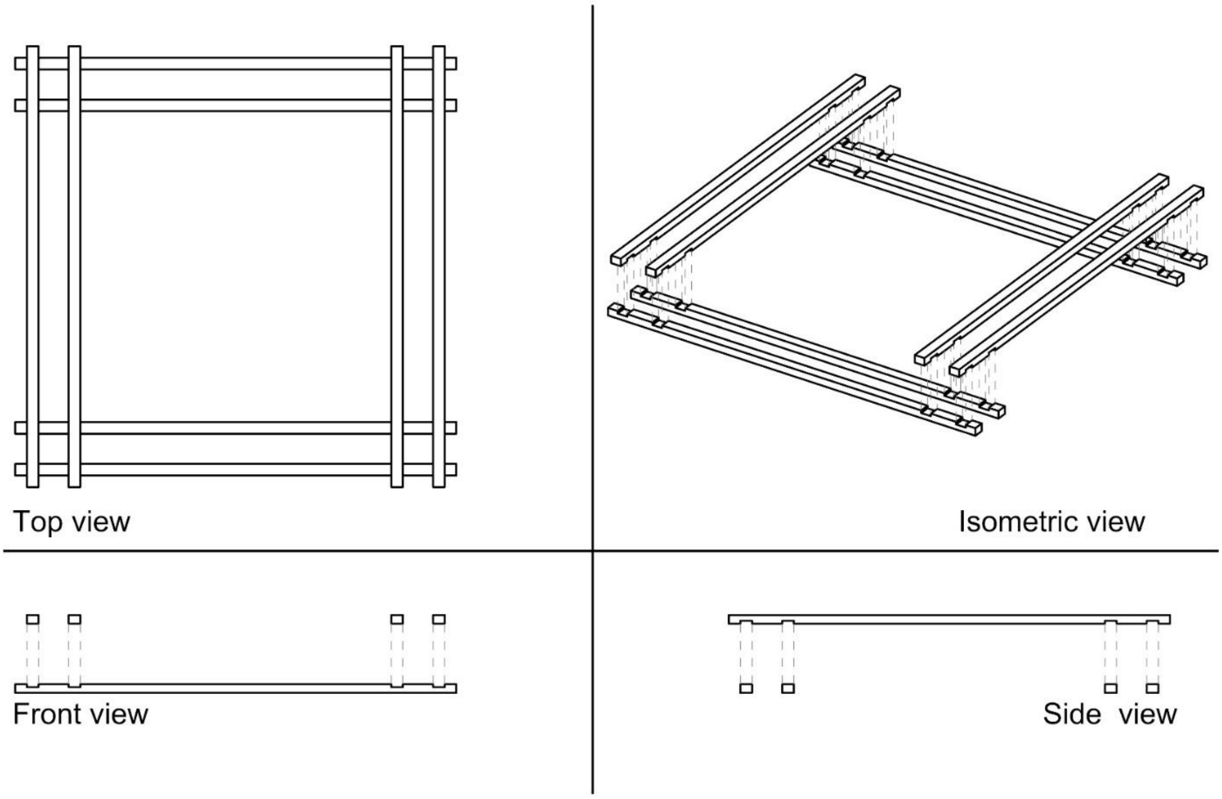

Figure 6-10 Timber band Rafter exploded

6.2.1.2 Cross pieces exploded

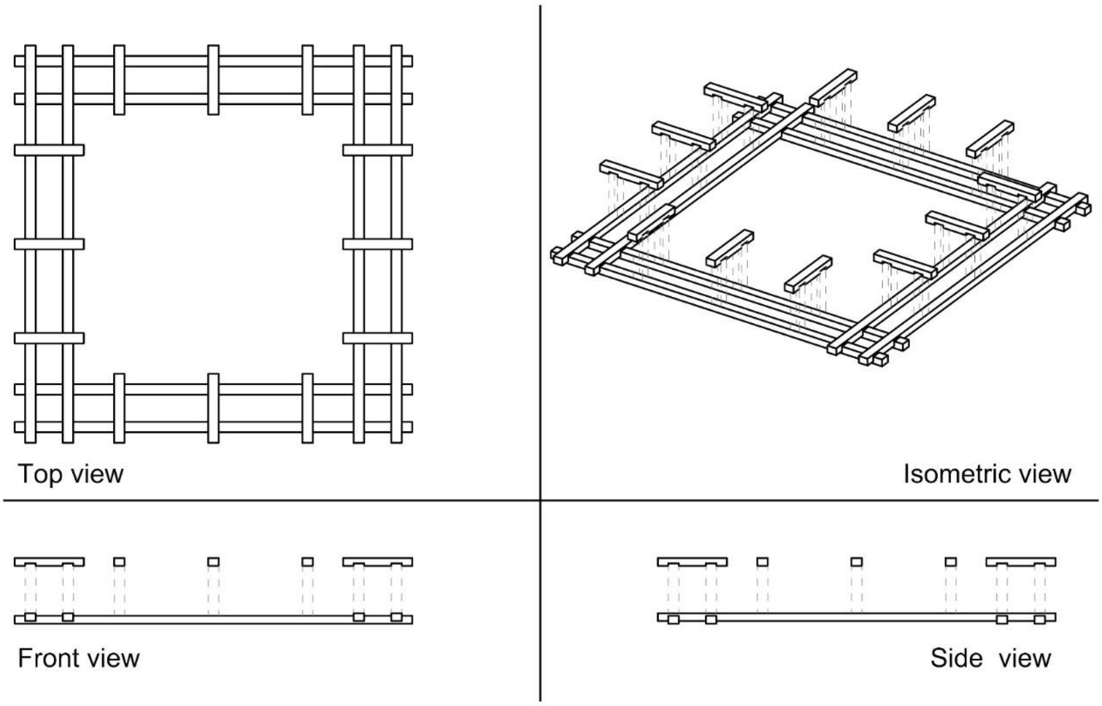

Figure 6-11 Timber band Cross pieces exploded

6.2.1.3 All exploded

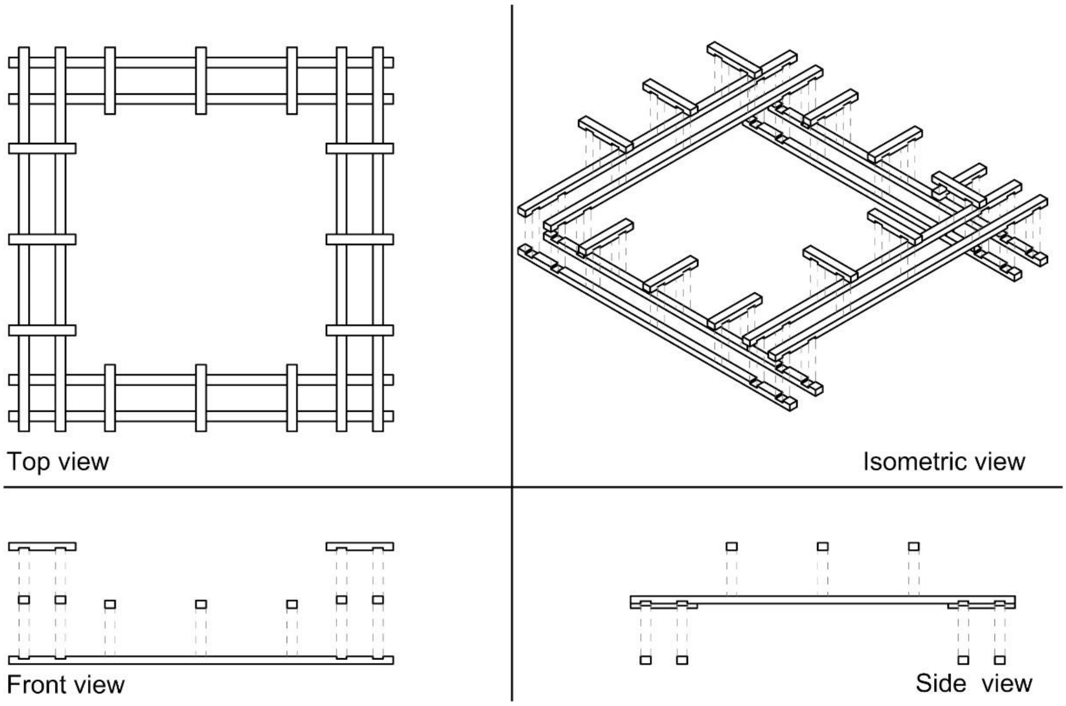

Figure 6-12 Timber band All exploded

6.2.2 Roof Timber Band

Assembled timber band composed by Roof rafters, Rafters and cross pieces.

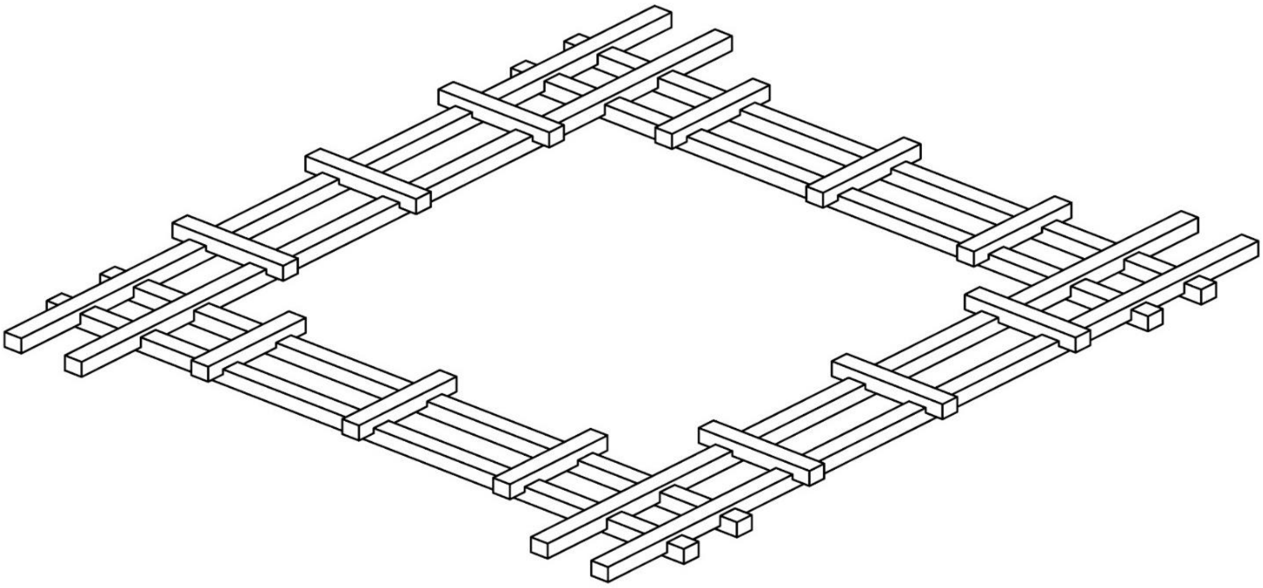

Figure 6-13 Roof Timber band

6.2.2.1 Roof Rafter explosed

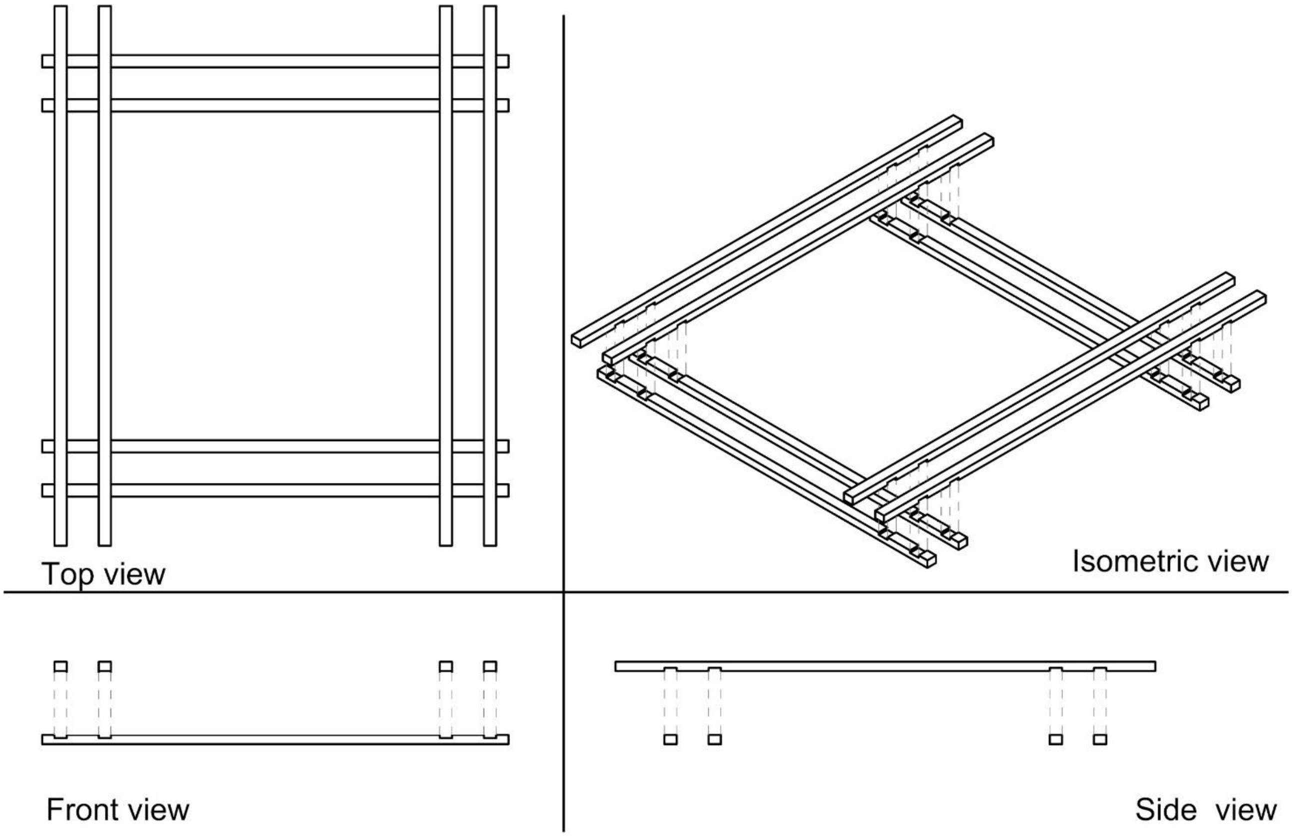

Figure 6-14Roof timber band Roof rafter exploded

6.2.2.2 Cross pieces explosed

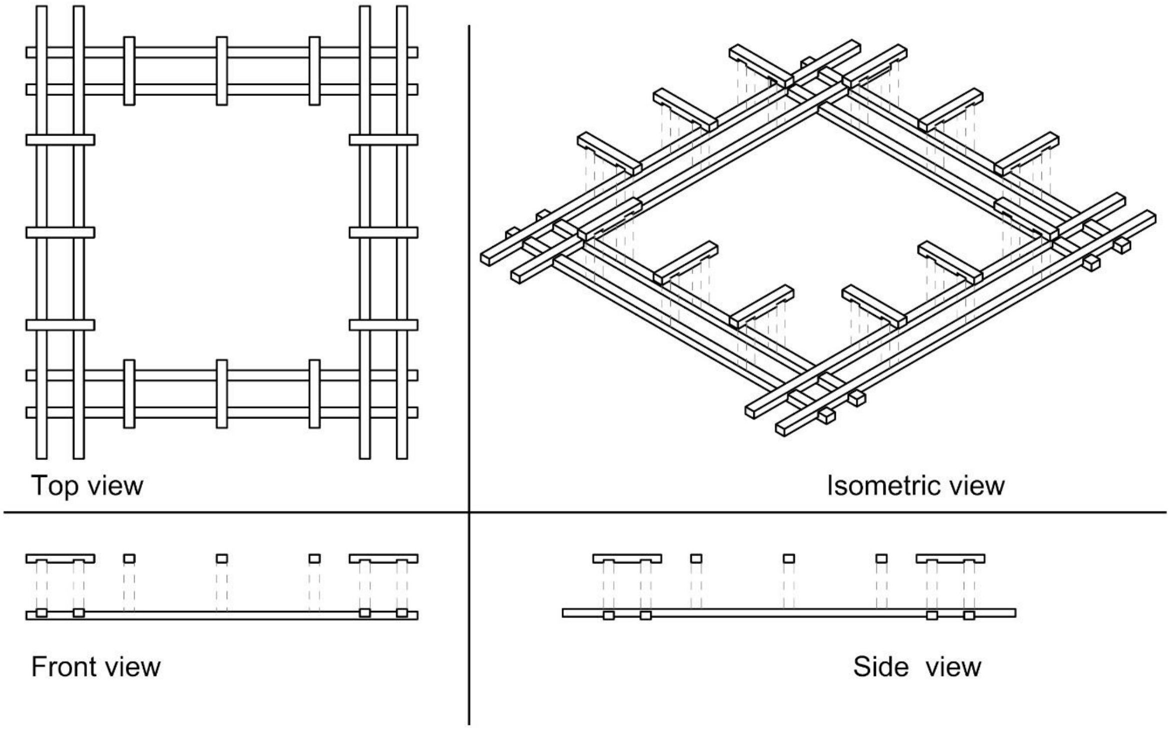

Figure 6-15 Roof timber band Cross pieces exploded

6.2.2.3 All explosed

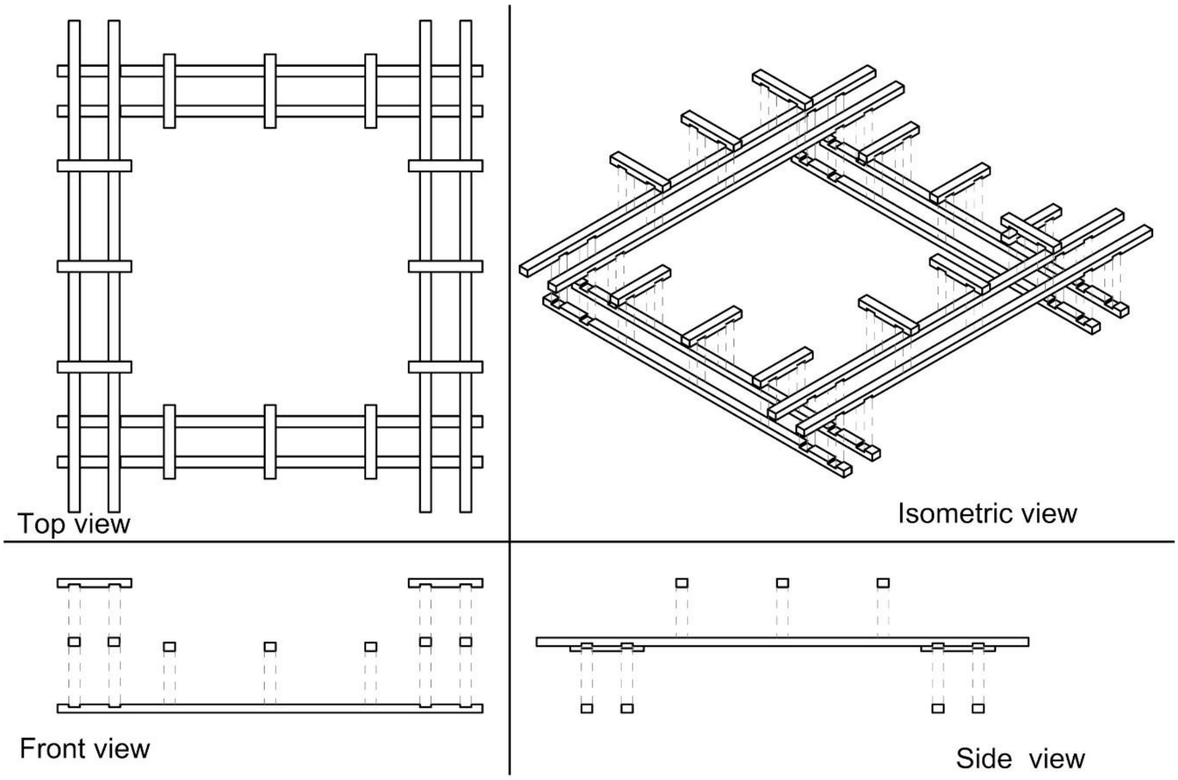

Figure 6-16 Roof Timber band All exploded

6.3 Portions of Rafter and Roof rafter

The rafters are composed by a central part which has been named rafter body and two ends which are exactly the same as the cross pieces. For the Roof rafter the heads are longer.

6.3.1 Rafter Head + Rafter Body + Rafter Head

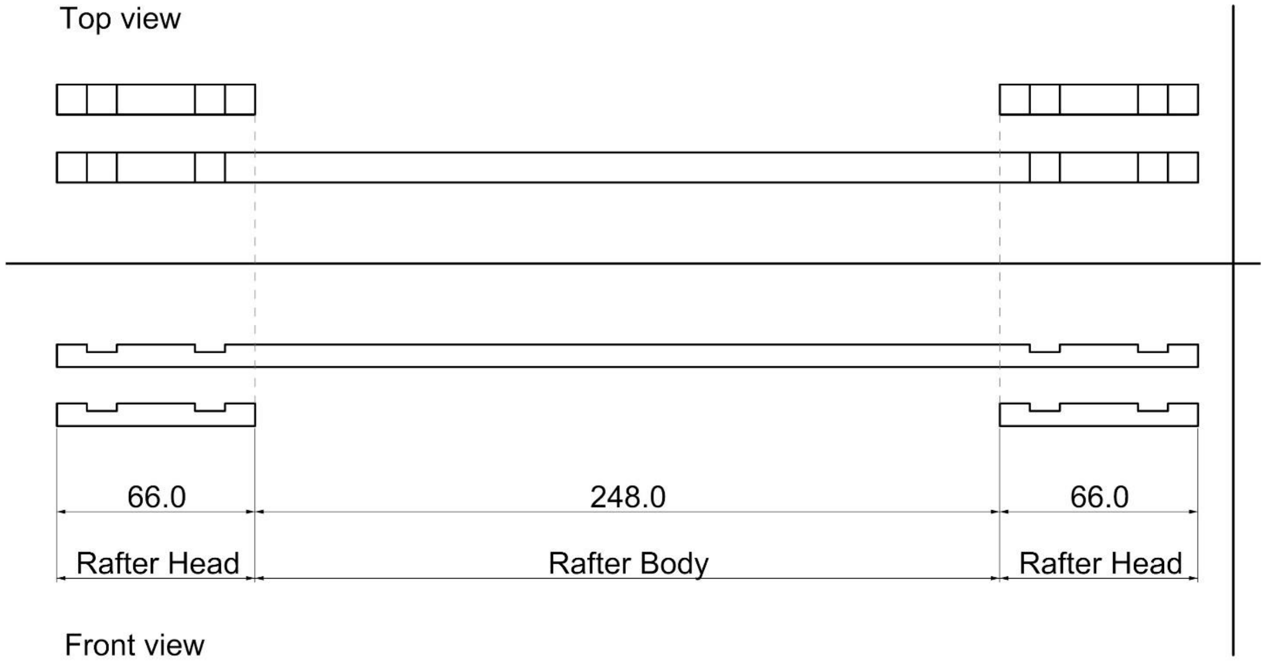

Figure 6-17 6.3.1 Rafter Head + Rafter Body + Rafter Head

6.3.2 Roof Rafter Head + Rafter Body + Roof Rafter Head

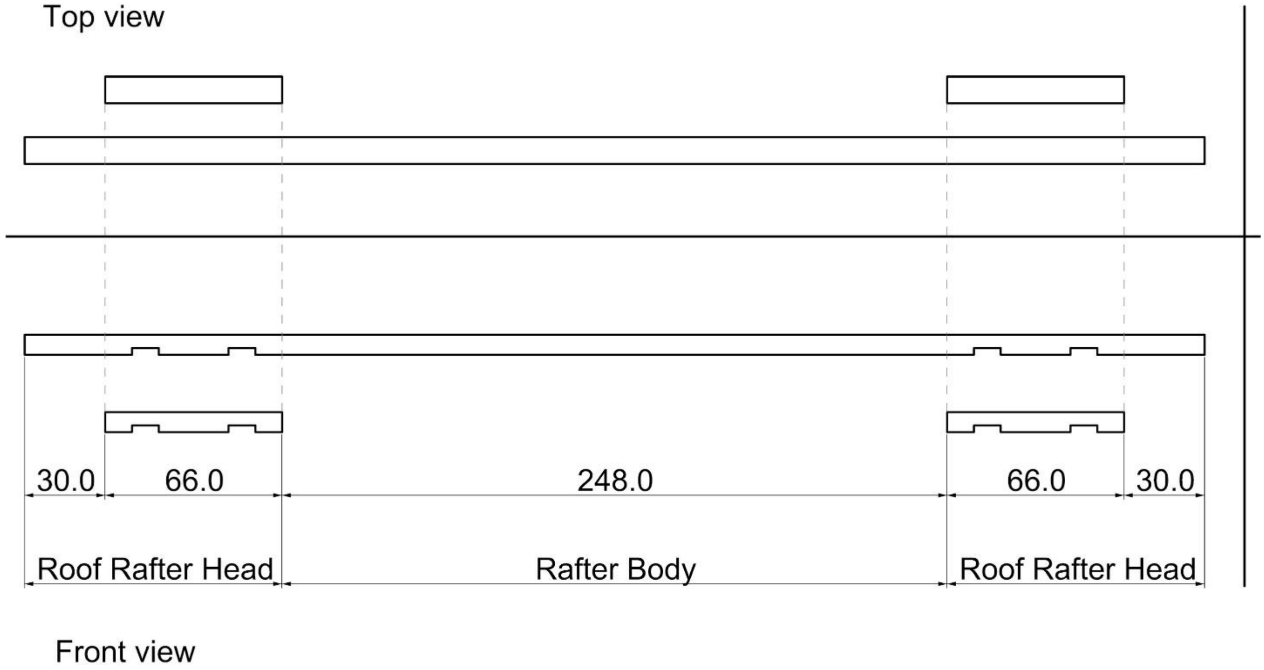

Figure 6-18 6.3.2 Roof Rafter Head + Rafter Body + Roof Rafter Head

6.3.3 Subdivisions of the timber elements

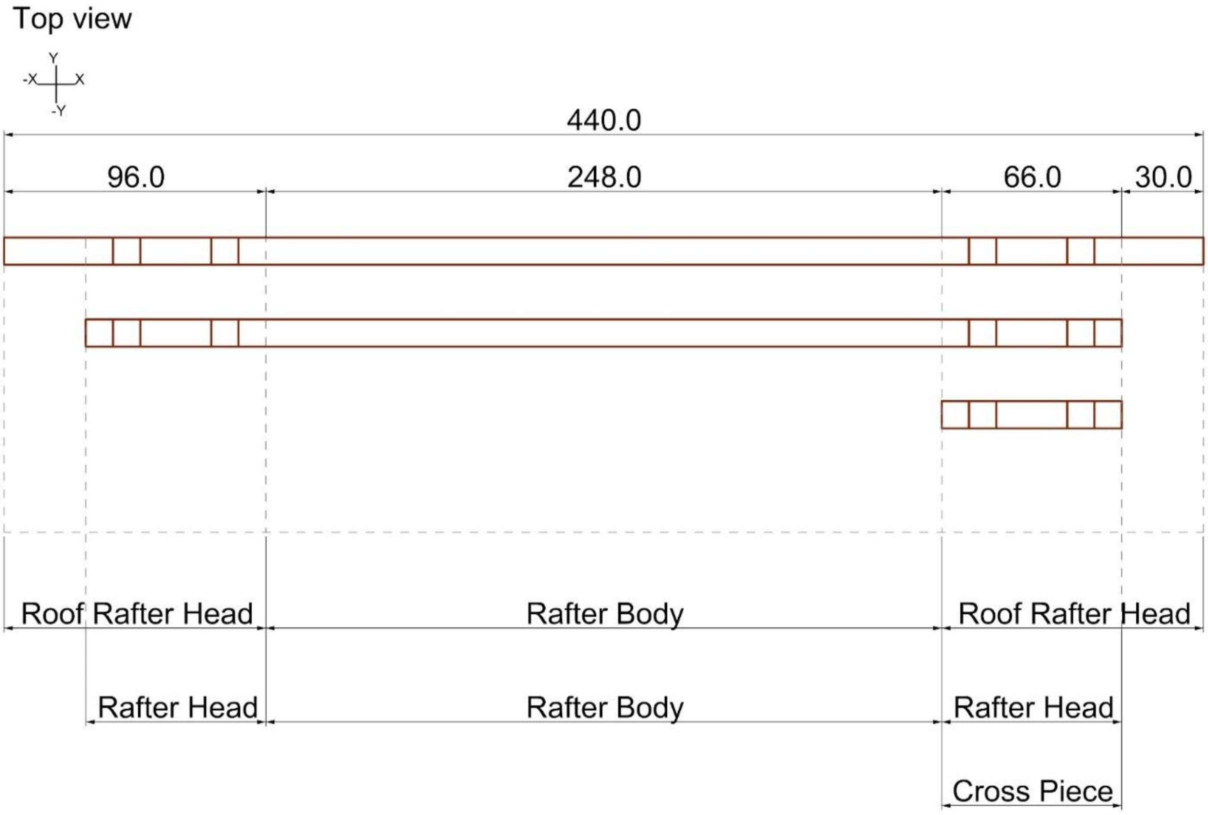

Figure 6-19 Subdivisions of the timber elements

6.4 Area under stresses

6.4.1 Cross Piece

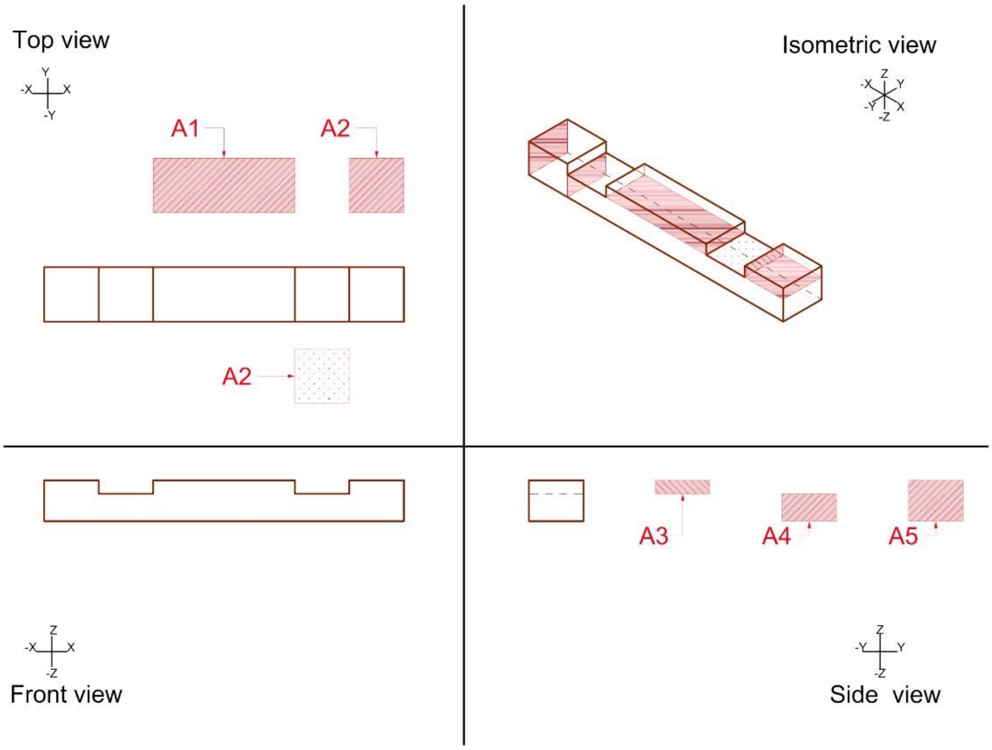

Figure 6-20 Area under stresses - Cross piece

6.4.1 Rafter

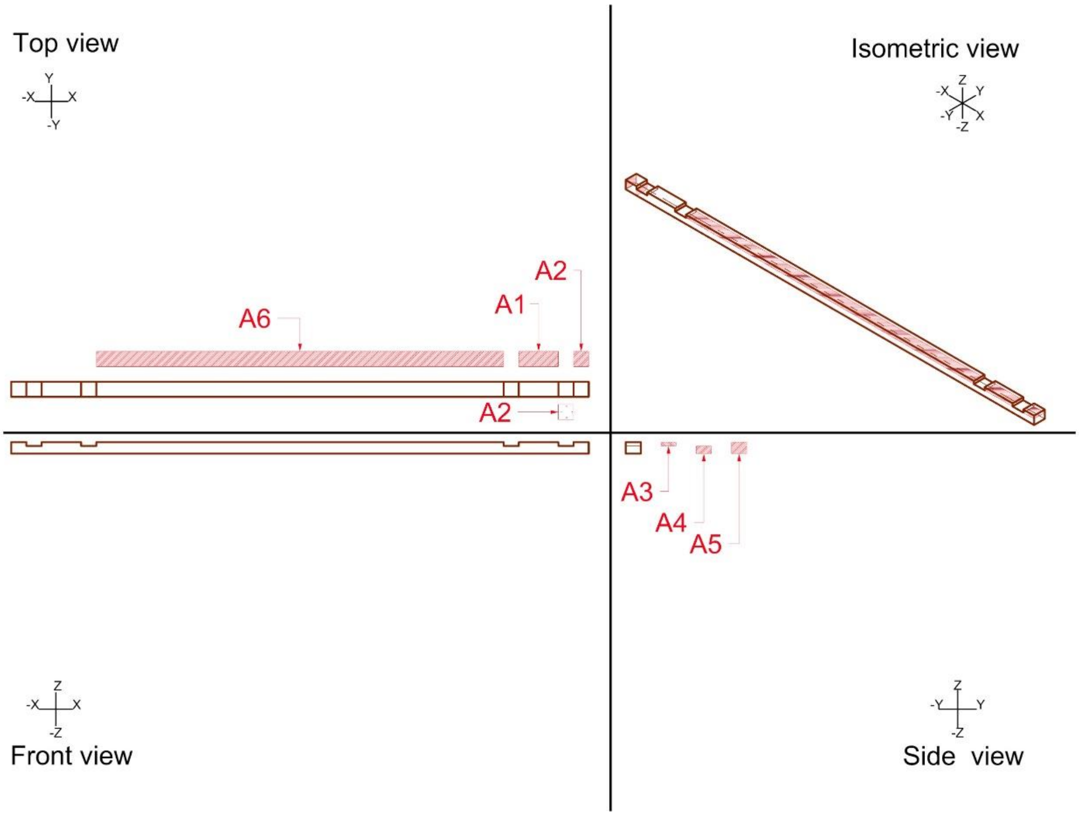

Figure 6-21 Area under stresses - Rafter

6.4.2 Roof Rafter

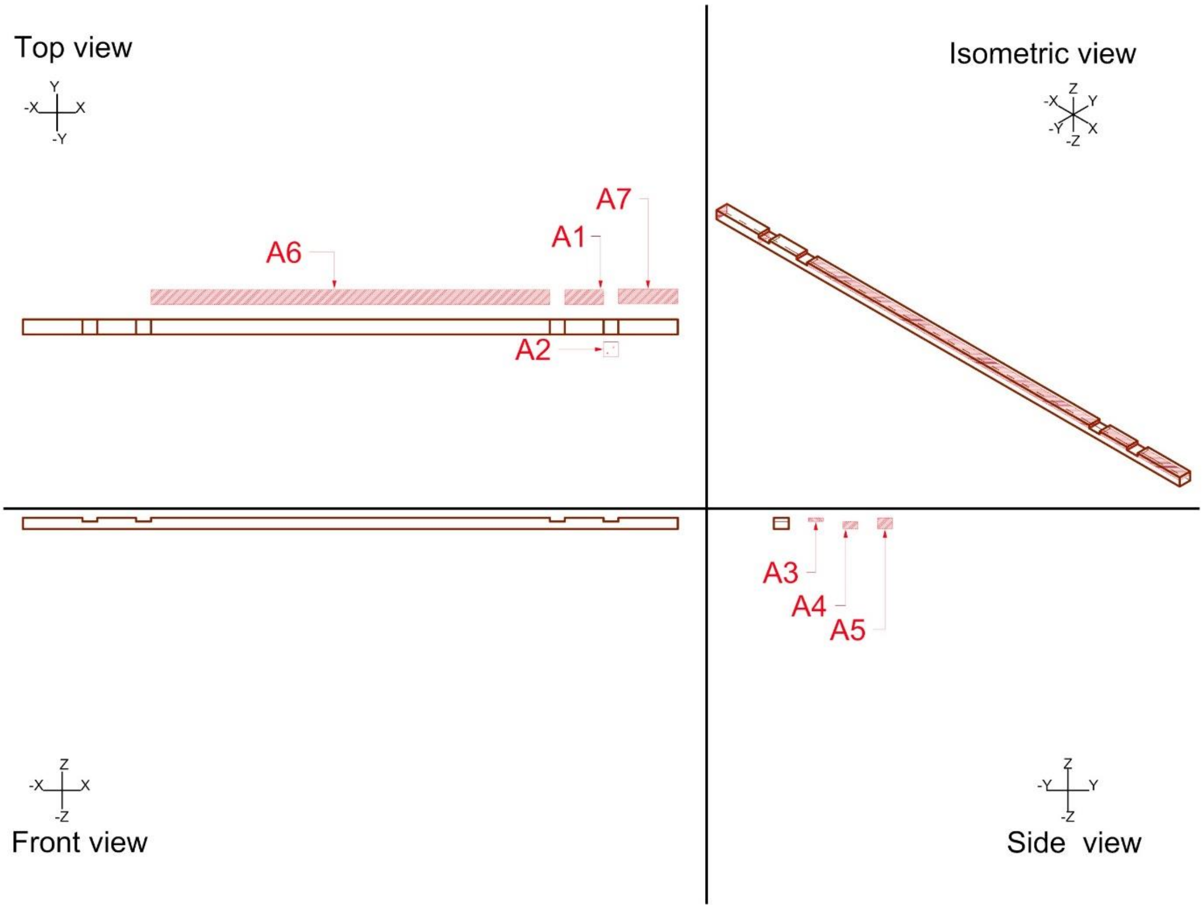

Figure 6-22 Area under stresses - Roof Rafter

6.4.3 Measures for area under stresses

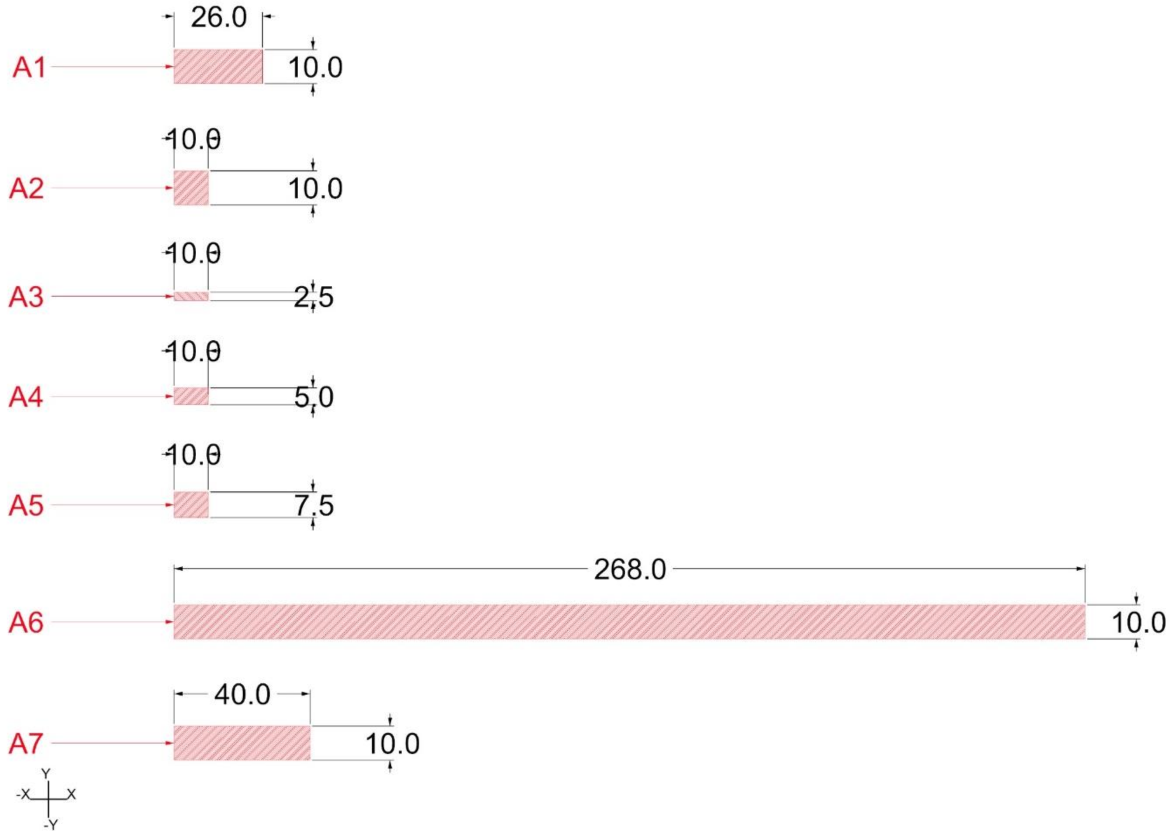

Figure 6-23 All areas under stresses

Table 13 Measures for all areas under stresses

	b	h	AREA		
	cm	cm	cm^2	m^2	mm^2
A1	26	10	260	0,026	26000
A2	10	10	100	0,01	10000
A3	10	2,5	25	0,0025	2500
A4	10	5	50	0,005	5000
A5	10	7,5	75	0,0075	7500
A6	268	10	2680	0,268	268000
A7	40	10	400	0,04	40000

6.5 Saint Venant for Timber elements

The distribution of the stresses in the section is mainly the same for the two roof rafter and for the normal rafter, the real different is in the notch of the cross piece as well in the rafter heads and in the roof rafter head.

6.5.1 Rafter

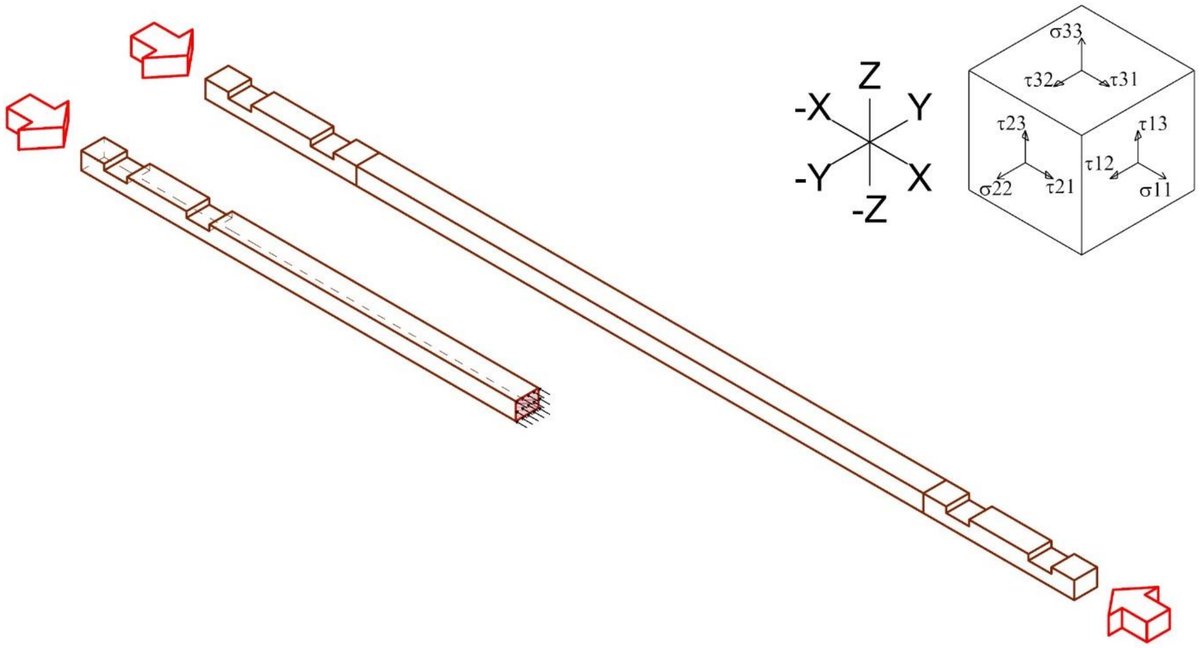

Figure 6-24 Rafter -Compression along X axis

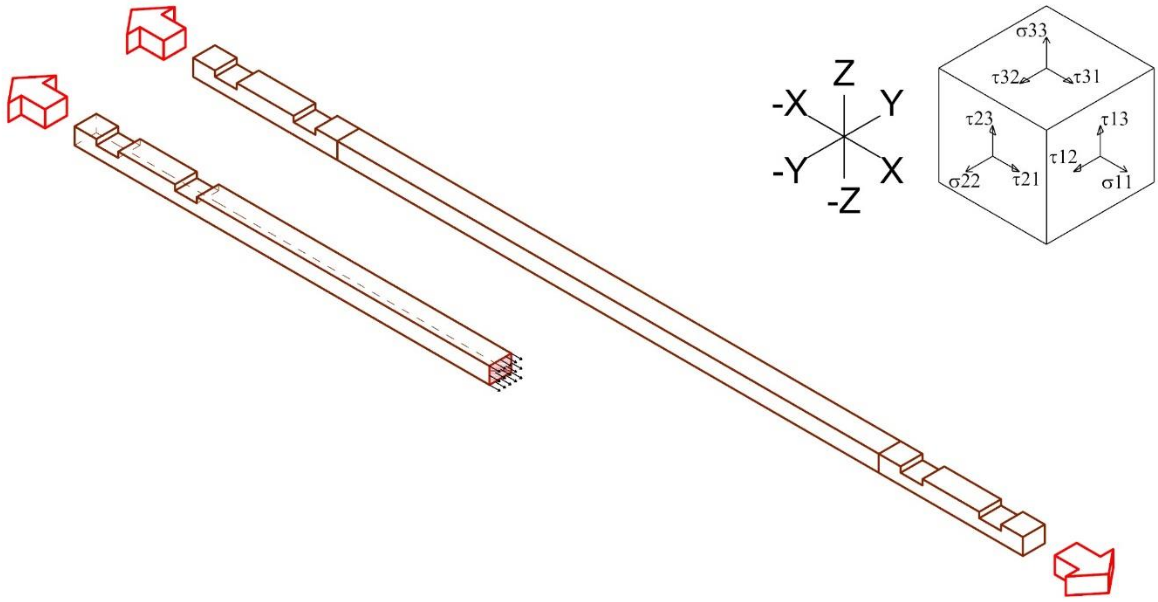

Figure 6-25 Rafter -Tension along X axis

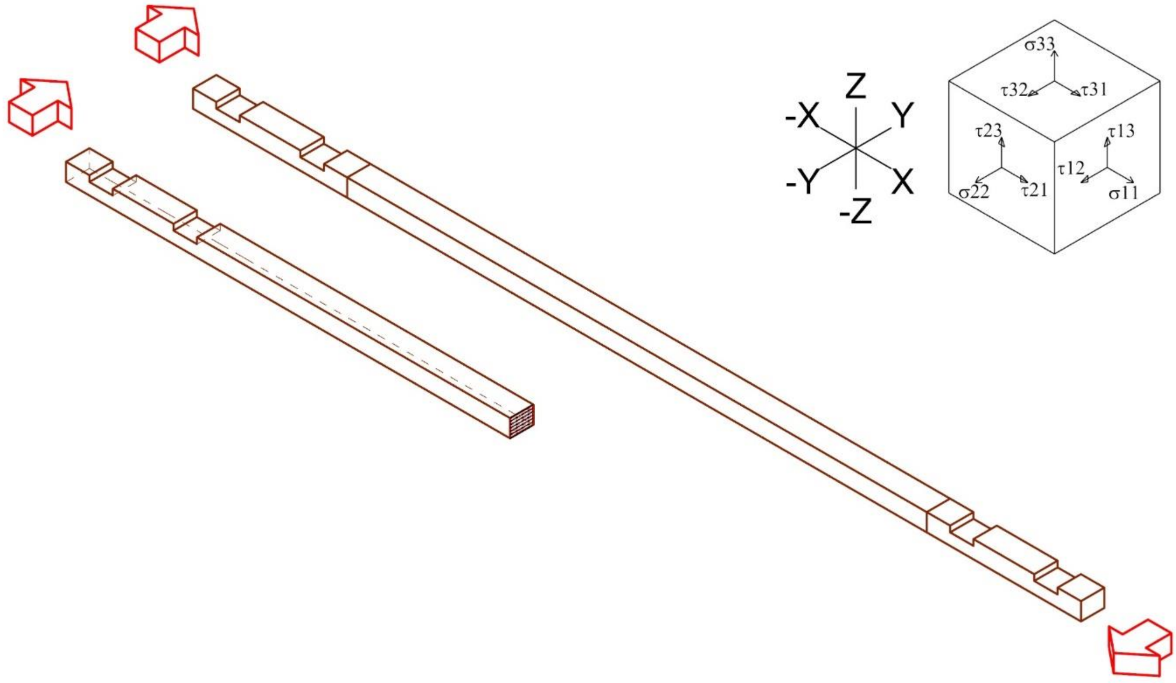

Figure 6-26 Rafter -Shear on Y axis

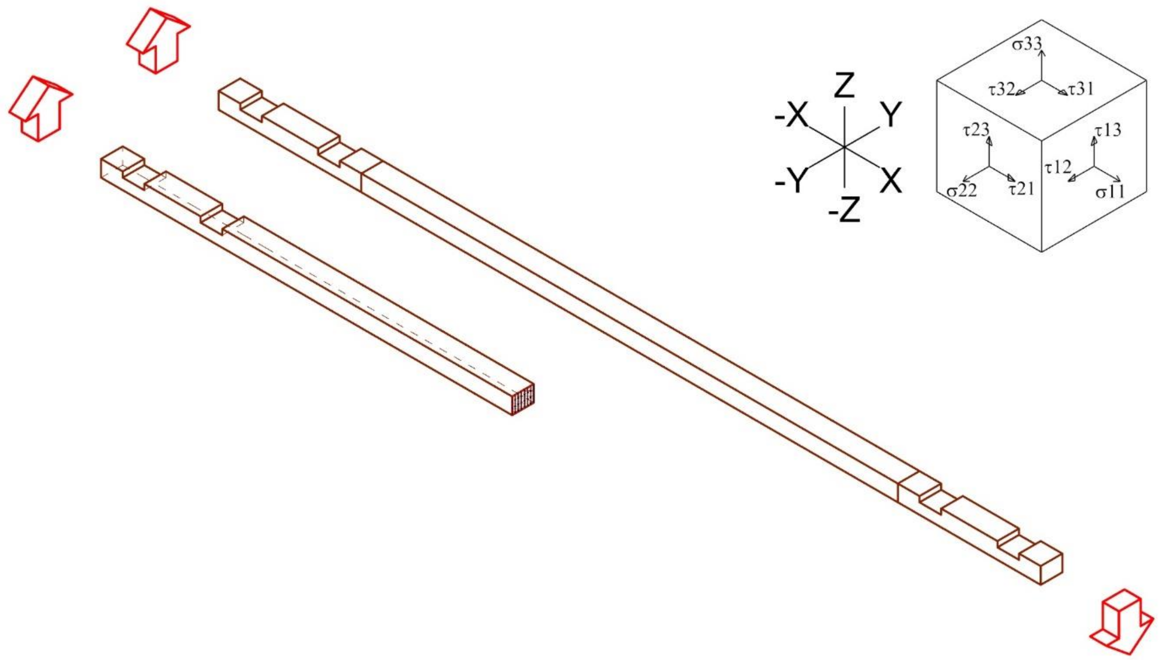

Figure 6-27 Rafter -Shear on Z axis

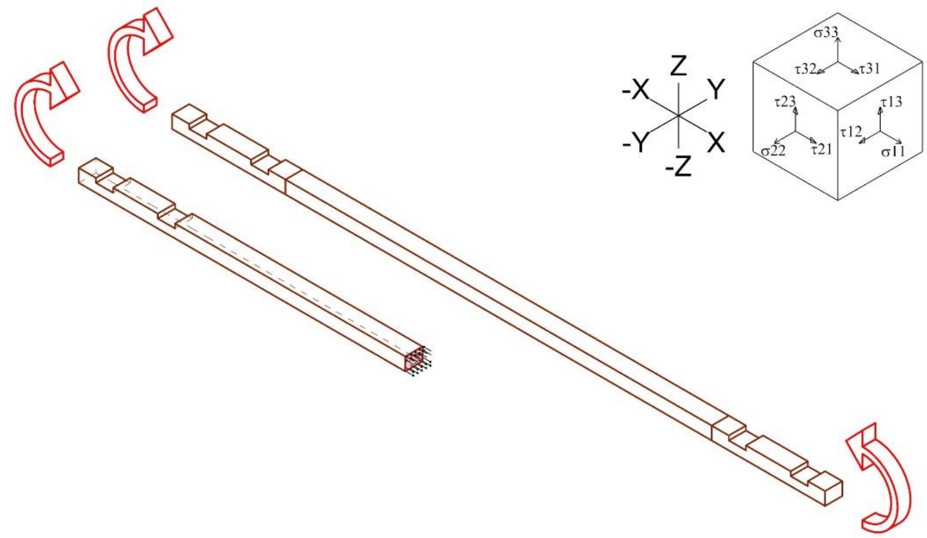

Figure 6-28 Rafter - Bending Moment My on Y axis

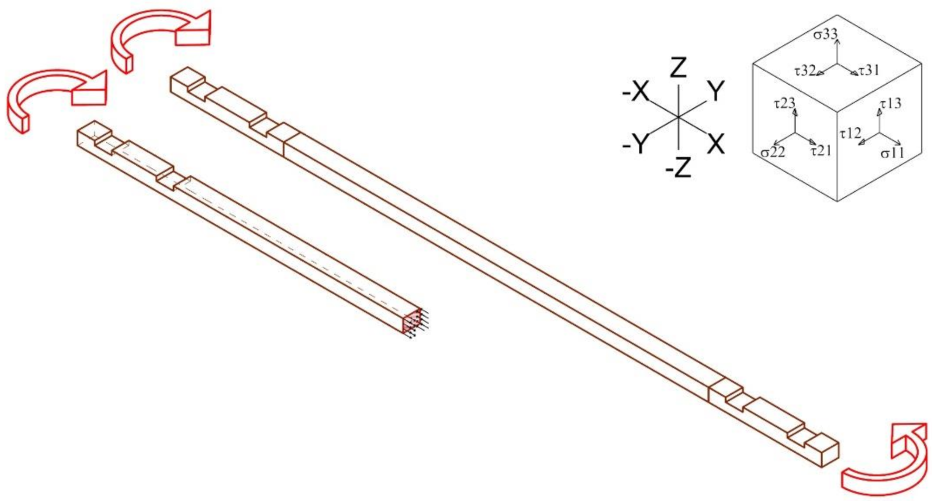

Figure 6-29 Rafter - Bending Moment Mz on Z axis

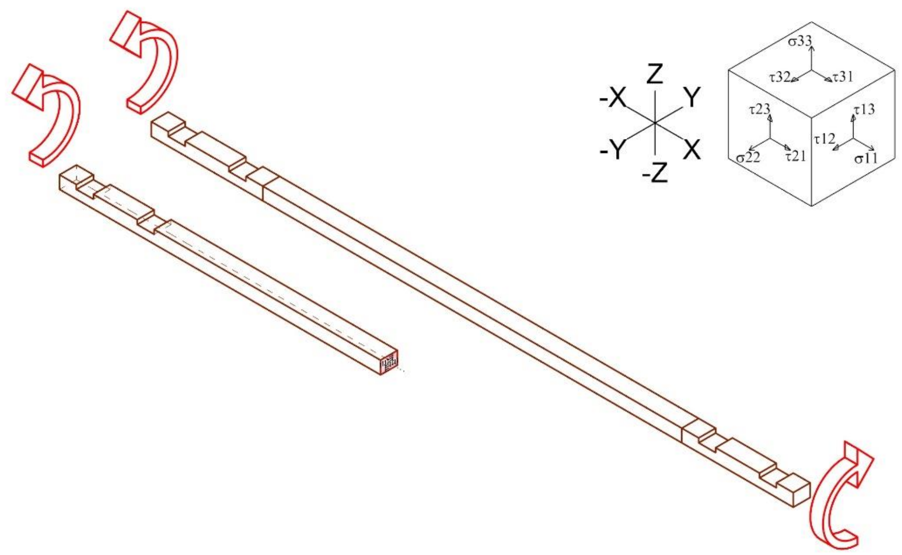

Figure 6-30 Rafter - Torsion: Mx on x axis

6.5.2 Roof rafter

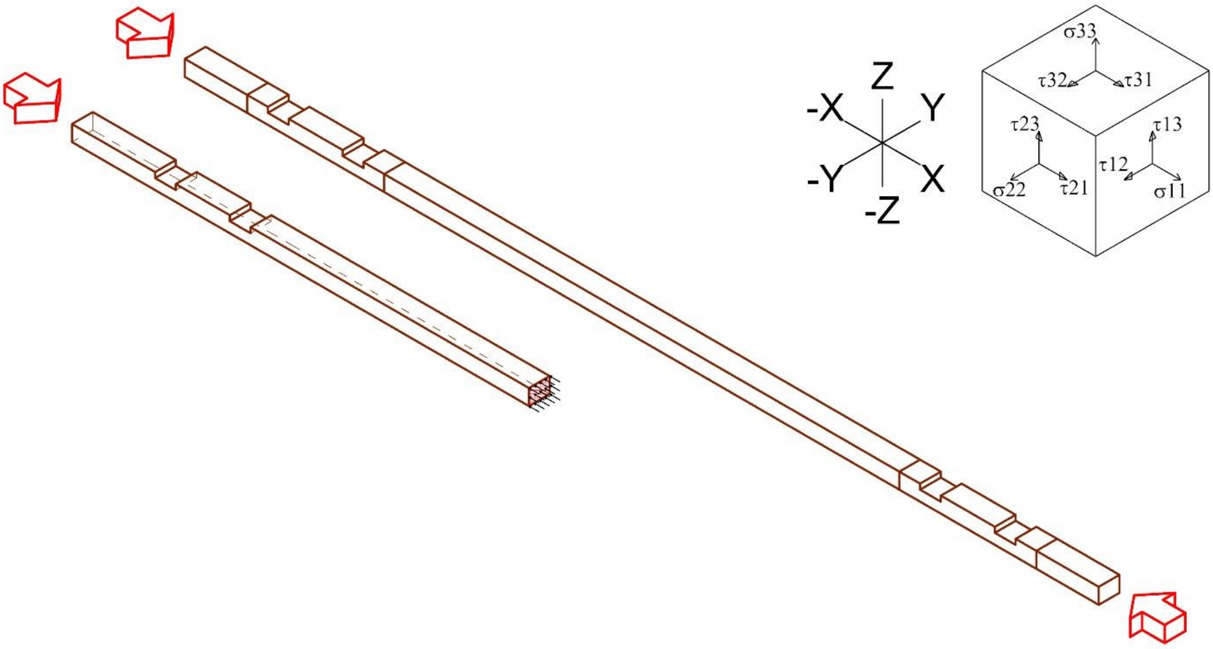

Figure 6-31 Roof Rafter -Compression along X axis

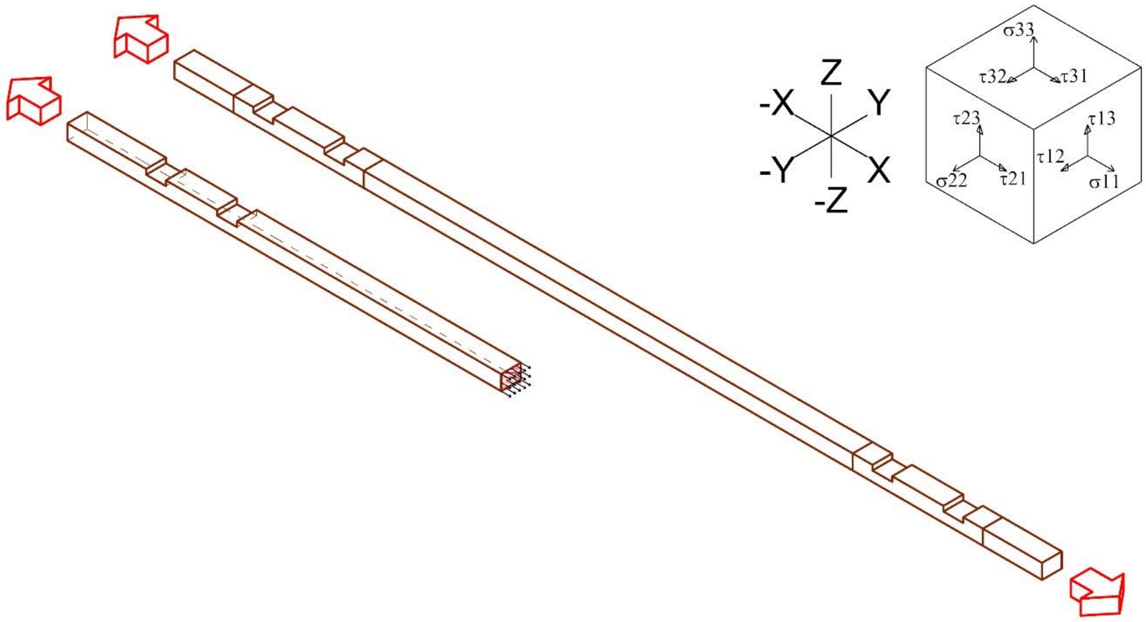

Figure 6-32 Roof Rafter -Tension along X axis

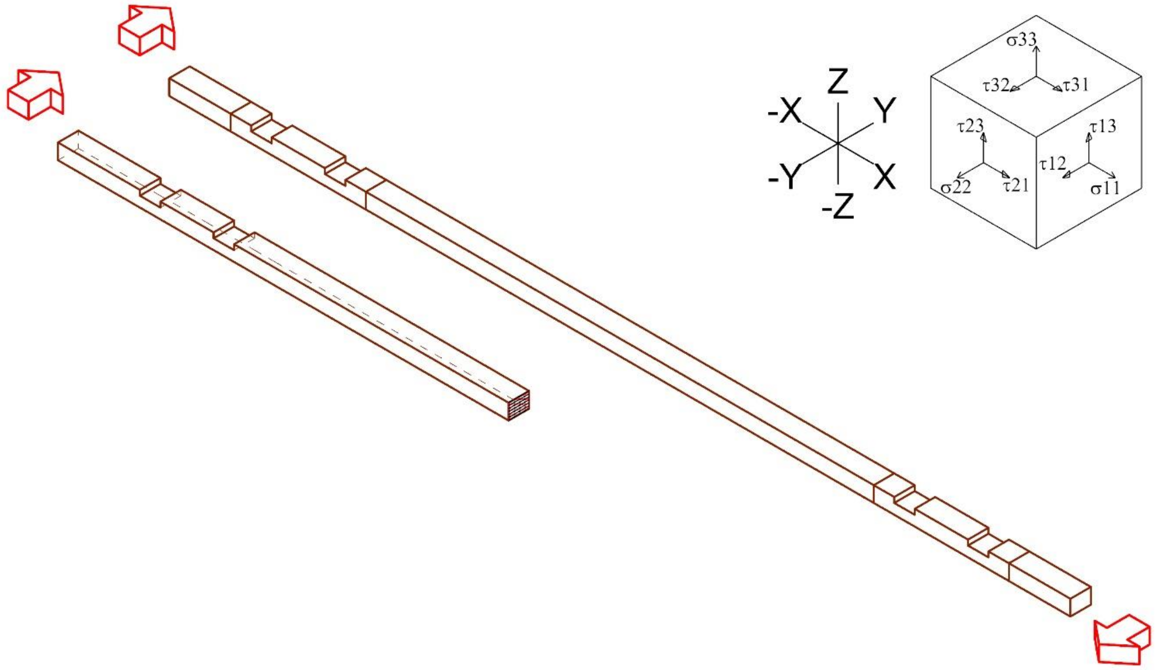

Figure 6-33 Roof Rafter -Shear on Y axis

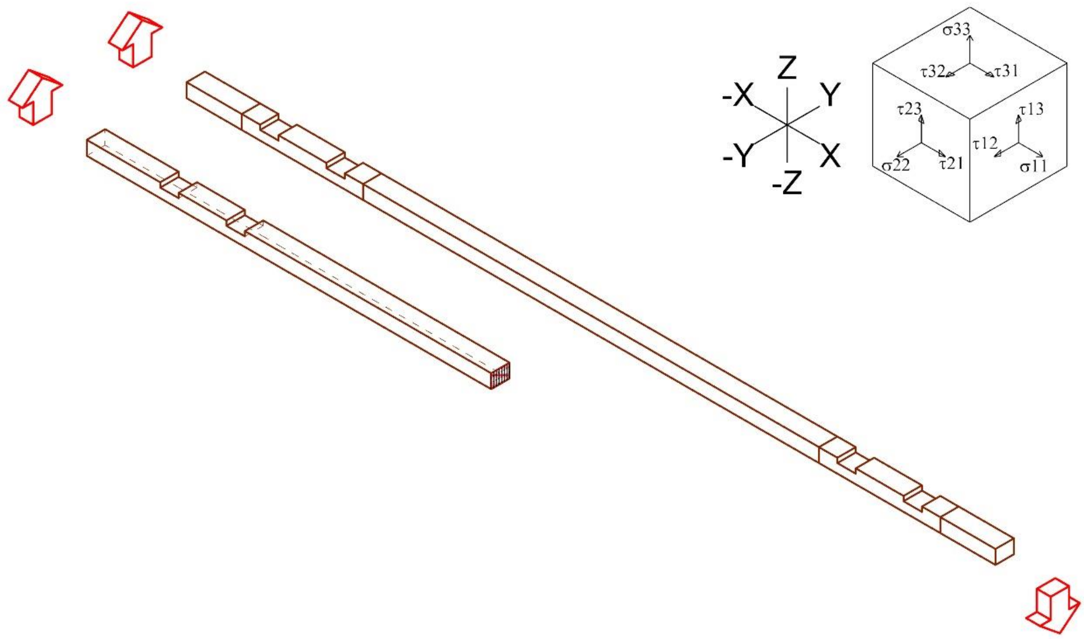

Figure 6-34 Roof Rafter -Shear on Z axis

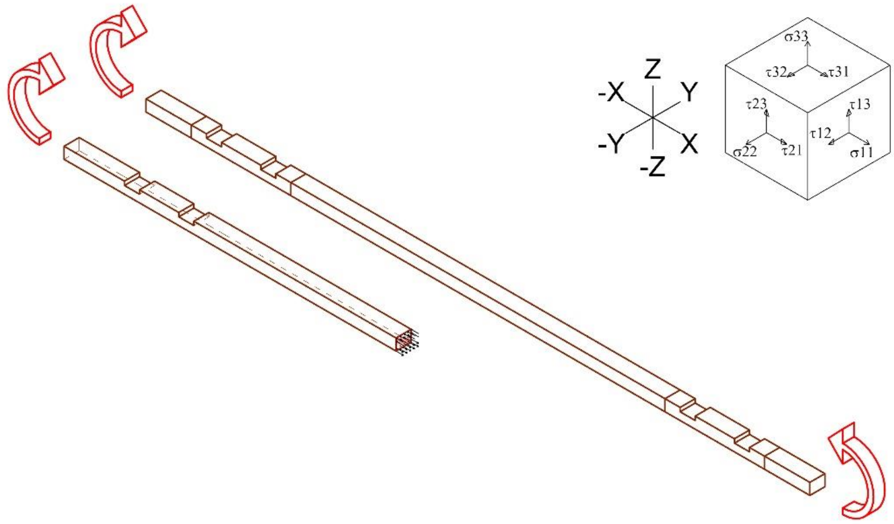

Figure 6-35 Roof Rafter - Bending Moment My on Y axis

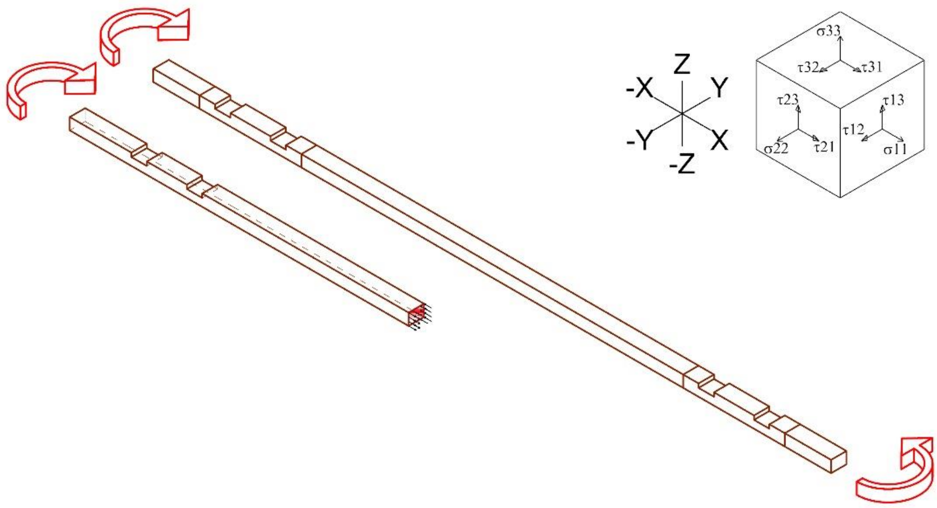

Figure 6-36 Roof Rafter - Bending Moment Mz on Z axis

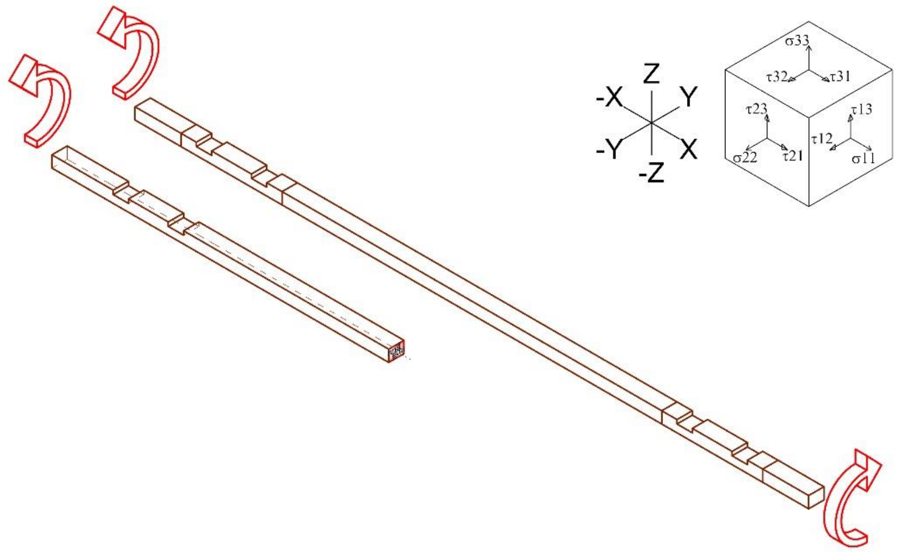

Figure 6-37 Roof Rafter - Torsion: Mx on x axis

6.5.3 Cross piece

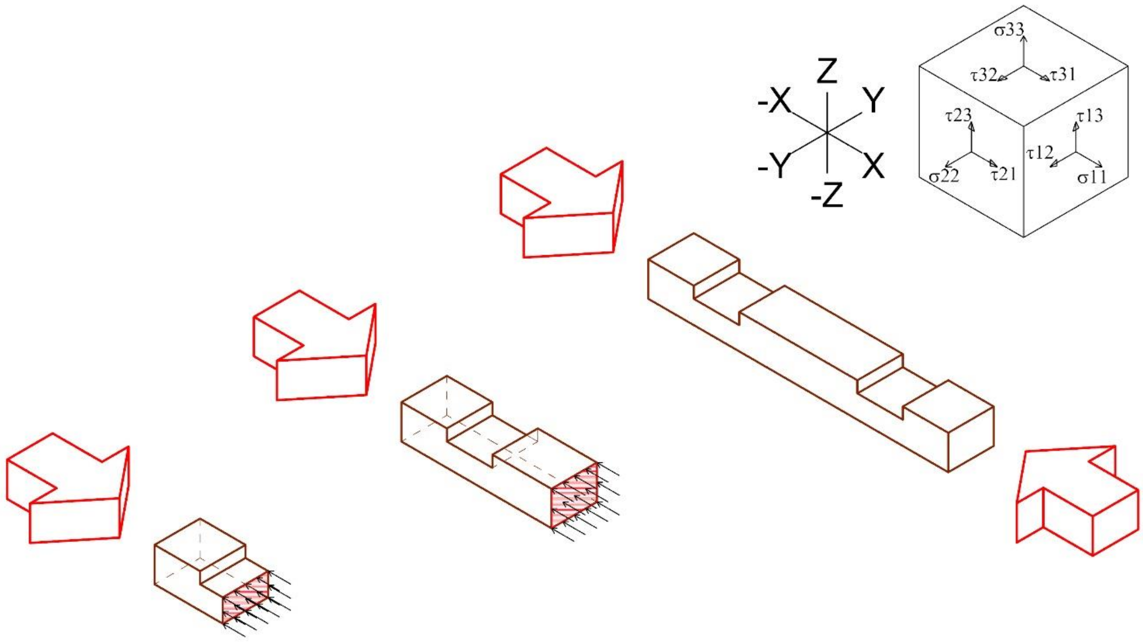

Figure 6-38 Cross Piece -Compression along X axis

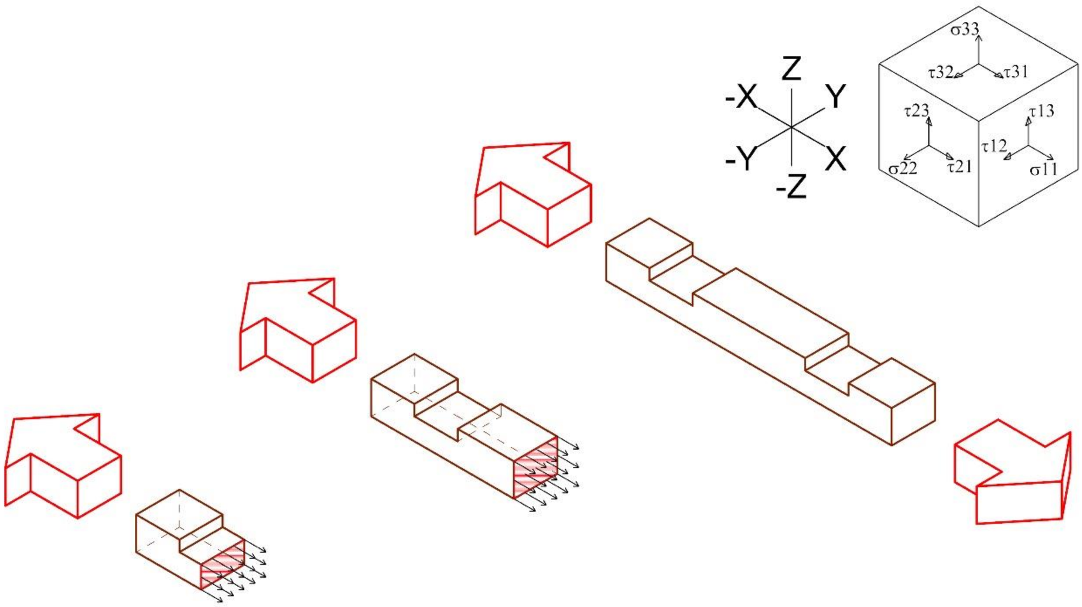

Figure 6-39 Cross Piece -Tension along X axis

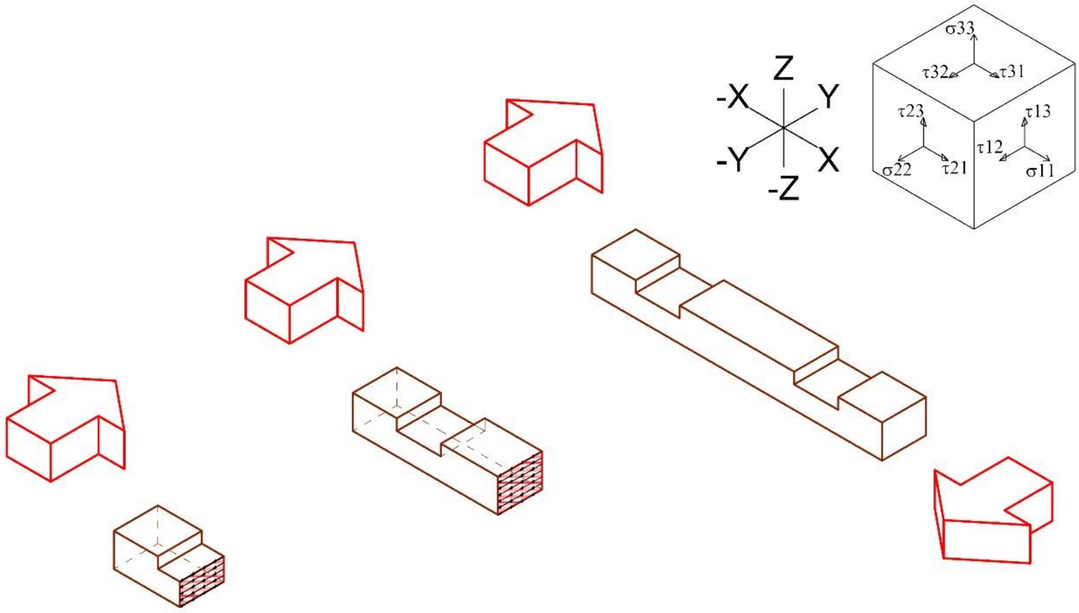

Figure 6-40 Cross Piece -Shear on Y axis

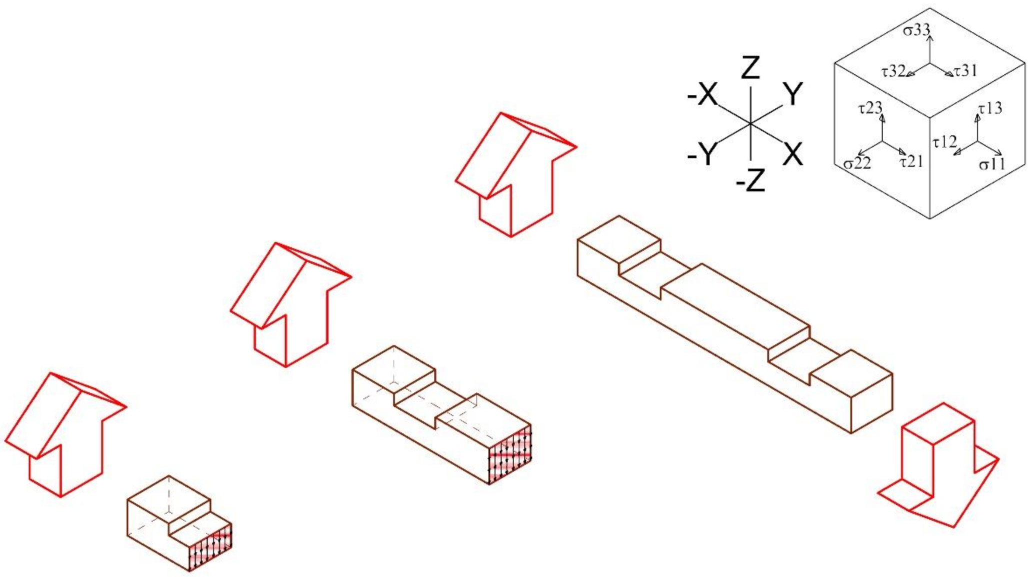

Figure 6-41 Cross Piece -Shear on Z axis

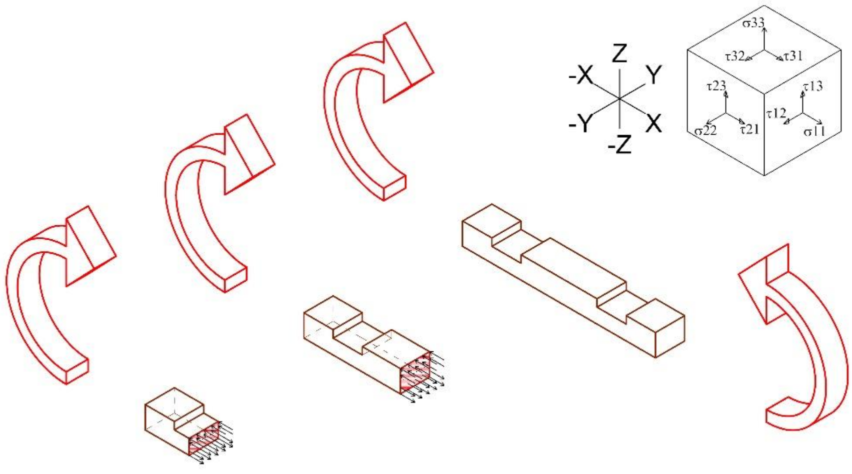

Figure 6-42 Cross Piece -Bending Moment My on Y axis

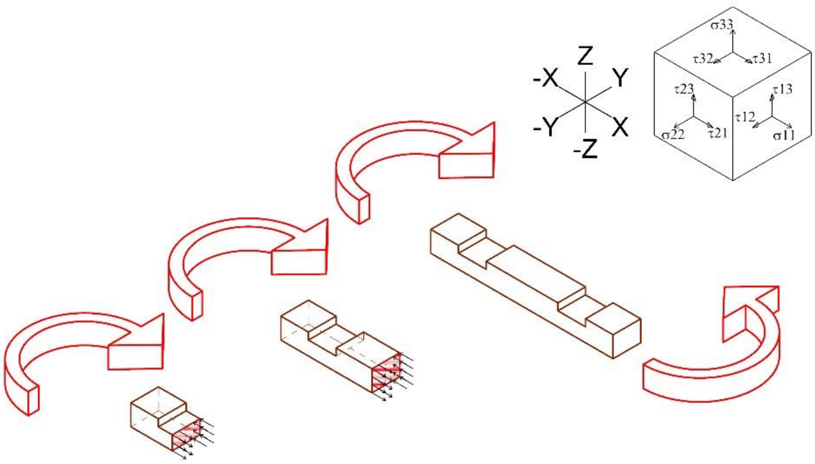

Figure 6-43 Cross Piece -Bending Moment Mz on Z axis

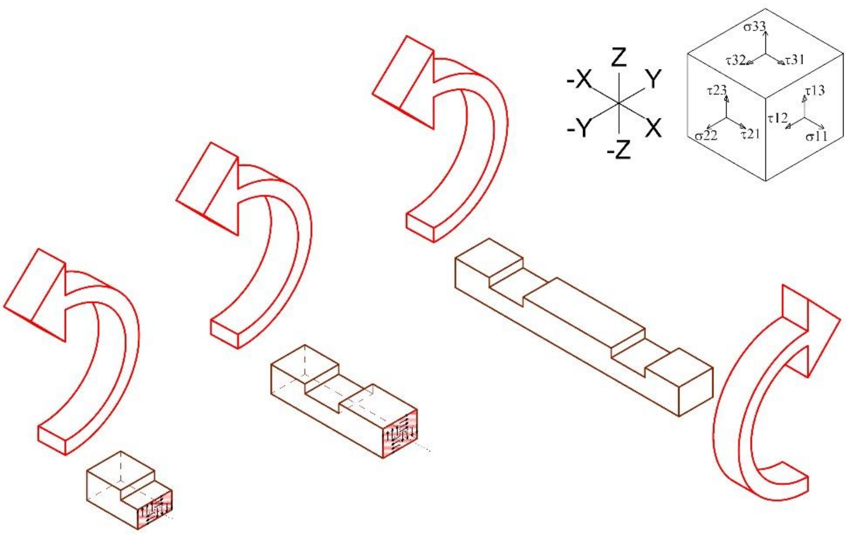

Figure 6-44 Cross Piece -Torsion: Mx on x axis

6.6 Eurocode 5 : EN 1995-1-1 :2004+A 1

In order to study the behavior of the timber elements connections the have been followed the verifications required in the Eurocode 5 and some additional verification required by the Italian code Nicole.

6.6.1 Tension parallel to the grain

$$\sigma_{t,0,d} \leq f_{t,0,d}$$

$\sigma_{t,0,d}$ is the design tensile stress along the grain

$f_{t,0,d}$ is the design tensile strength along the grain

$\sigma_{t0d} = \frac{N_{0d}}{A_{net,t}}$

N_{0d} is the design axial force parallel to the grain

$A_{net,t}$ is the net cross-sectional area perpendicular to the grain

$A_{net,v}$ is the net shear area in the parallel to grain direction

6.6.2 Tension parallel to the grain with keyed scarf joint

$$\sigma_{t,0,d} \leq f_{t,0,d} * R_{scarf}$$

$\sigma_{t,0,d}$ is the design tensile stress along the grain

$f_{t,0,d}$ is the design tensile strength along the grain

$\sigma_{t0d} = \frac{N_{0d}}{A_{net,t}}$

N_{0d} is the design axial force parallel to the grain

$A_{net,t}$ is the net cross-sectional area perpendicular to the grain

$A_{net,v}$ is the net shear area in the parallel to grain direction

$R_{scarf} = 0.11$ is the reduction factor for the presence of the keyed scarf joint.

6.6.3 Compression parallel to the grain

$$\sigma_{c,0,d} \leq f_{c,0,d}$$

$\sigma_{c,0,d}$ is the design tensile stress along the grain

$f_{c,0,d}$ is the design tensile strength along the grain

$\sigma_{c0d} = \frac{N_{0d}}{A_{net,t}}$

N_{0d} is the design axial force parallel to the grain

$A_{net,t}$ is the net cross-sectional area perpendicular to the grain

6.6.4 Compression perpendicular to the grain

$$\sigma_{c,90,d} \leq k_{c,90}\, f_{c,90,d}$$

$$\sigma_{c,90,d} \leq \frac{F_{c,90,d}}{A_{ef}}$$

$\sigma_{c,90,d}$ is the design compressive stress in the effective contact

$F_{c,90,d}$ is the design compressive load perpendicular to the grain

A_{ef} is the effective contact area in compression perpendicular

$f_{c,90,d}$ is the design compressive strength perpendicular to the grain

$k_{c,90} = 1{,}25\ or\ 1{,}5$ is a factor taking into account the load configuration, the possibility of splitting and the degree of compressive deformation

6.6.5 Tension perpendicular to the grain

This stress is not consistent for the bhatar constructions.

$$\sigma_{t90d} = \frac{N_{90d}}{A_{net,t}}$$

6.6.6 Bending

$$\frac{\sigma_{m,y,d}}{f_{m,y,d}} + k_m * \frac{\sigma_{m,z,d}}{f_{m,z,d}} \leq 1$$

$$k_m * \frac{\sigma_{m,y,d}}{f_{m,y,d}} + \frac{\sigma_{m,z,d}}{f_{m,z,d}} \leq 1$$

$\sigma_{m,y,d}\ and\ \sigma_{m,z,d}$ are the design bending stresses about the principal axes y and z.

$f_{m,y,d}\ and\ f_{m,z,d}$ are the corresponding design bending strengths.

$$\sigma_{m,y,d} = \frac{M_{y,d}}{W_y}$$

$M_{y,d}$ is the design bending moment on y axis

$W_y = \frac{b*h^2}{6}$ is the moment of resistance of the section around y axis

$$\sigma_{m,z,d} = \frac{M_{z,d}}{W_z}$$

$M_{z,d}$ is the design bending moment on z axis

$W_z = \frac{h*b^2}{6}$ is the moment of resistance of the section around z axis

NOTE: The factor km makes allowance for re-distribution of stresses and the effect of inhomogeneities of the material in a cross-section.

2) The value of the factor should be taken as follows:

- for rectangular sections: km = 0,7
- otherwise km = 1

6.6.7 Shear

For shear with a stress component parallel to the grain, see Figure 6.45(a), as well as for shear with both stress components perpendicular to the grain, see Figure 6.45(b), the following expression shall be satisfied:

$$\tau_d \leq f_{v,d}$$

τ_d is the design shear stress

$f_{v,d}$ is the design shear strength for the actual condition

$$\tau_d = \frac{3}{2} * \frac{V_{ad}}{b * h}$$

V_{ad} is the design shear force and "a" means the parallel axis

b is the width of the section

h is the height of the section

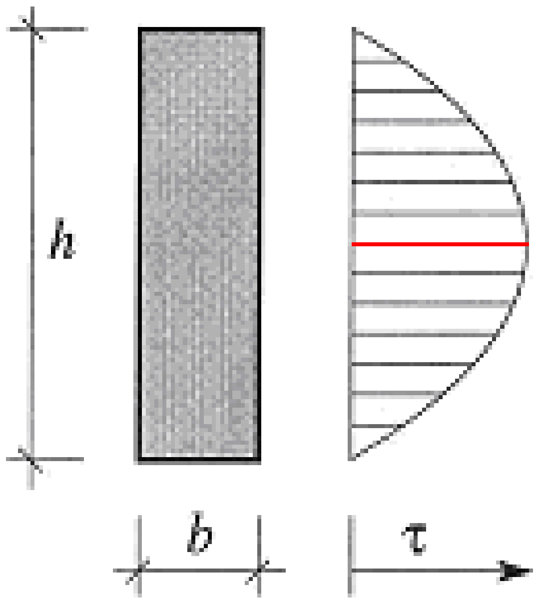

Figure 6-45 Jourawky stress distribution

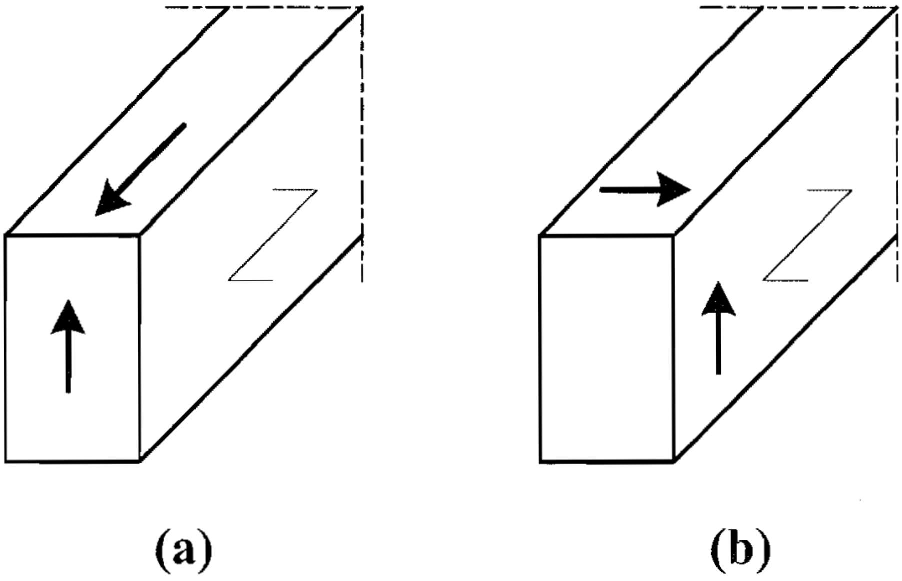

Figure 6-46 (a) Member with a shear stress component parallel to the grain (b) Member with both stress components perpendicular to the grain (rolling shear)

NOTE: The shear strength for rolling shear is approximately equal to twice the tensile strength perpendicular to grain. (2) For the verification of shear resistance of members in bending, the influence of cracks should be taken into account using an effective width of the member given as:

$$b_{ef} = k_{cr} * b$$

where b is the width of the relevant section of the member.$k_{cr} = 0{,}67$ for solid timber.

6.6.8 Torsion

The following expression shall be satisfied:

$$\tau_{tor,d} \leq k_{shape} * f_{v,d}$$

$$k_{shape} = \left\{ min \left\{ 1 + 0{,}15 * \frac{h}{b}; 2{,}0 \right\} \right\}$$

$\tau_{tor,d}$ is the design torsional stress
$f_{v,d}$ is the design shear strength
k_{shape} is a factor depending on the shape of the cross-section;
h is the larger cross-sectional dimension;
b is the smaller cross-sectional dimension.

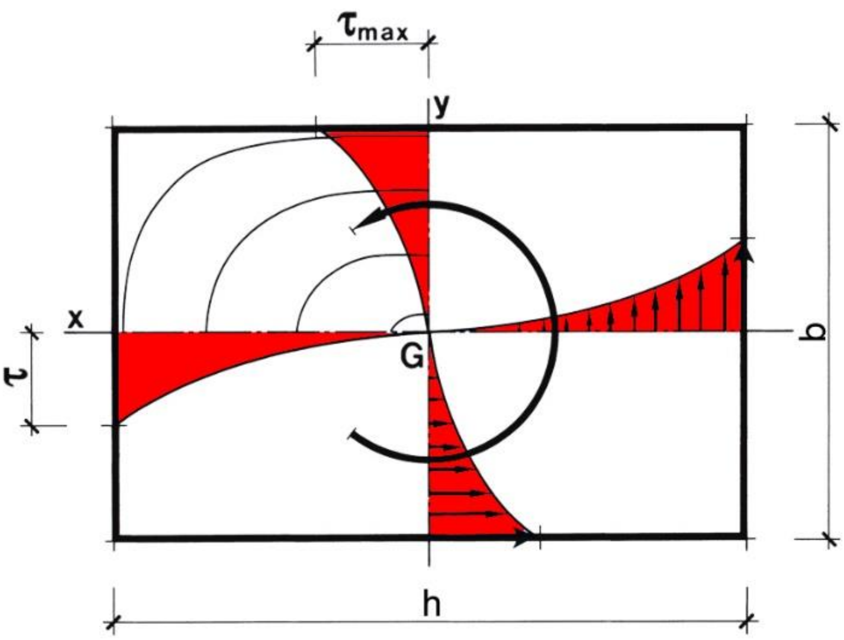

Figure 6-47 Torsional stress distribution

$$\tau_{tor,d} = \alpha * \frac{M_{x,d}}{h * b^2}$$

$M_{x,d}$ is the design torsional moment along x axis

α is a semi empirical coefficient which take into account the polar inertia of the section,the where h > b

$$\alpha = 3 + 1{,}8 * \frac{b}{h}$$

6.6.9 Combined bending and axial tension

$$\frac{\sigma_{t,0,d}}{f_{t,0,d}} + \frac{\sigma_{m,y,d}}{f_{m,y,d}} + k_m * \frac{\sigma_{m,z,d}}{f_{m,z,d}} \leq 1$$

$$\frac{\sigma_{t,0,d}}{f_{t,0,d}} + k_m * \frac{\sigma_{m,y,d}}{f_{m,y,d}} + \frac{\sigma_{m,z,d}}{f_{m,z,d}} \leq 1$$

For solid timber, glued laminated timber and LVL:

- for rectangular sections: km = 0,7
- otherwise km = 1

6.6.10 Combined bending and axial compression

$$\left(\frac{\sigma_{c,0,d}}{f_{c,0,d}}\right)^2 + \frac{\sigma_{m,y,d}}{f_{m,y,d}} + k_m * \frac{\sigma_{m,z,d}}{f_{m,z,d}} \leq 1$$

$$\left(\frac{\sigma_{c,0,d}}{f_{c,0,d}}\right)^2 + k_m * \frac{\sigma_{m,y,d}}{f_{m,y,d}} + \frac{\sigma_{m,z,d}}{f_{m,z,d}} \leq 1$$

For solid timber, glued laminated timber and LVL:

- for rectangular sections: km = 0,7
- otherwise km = 1

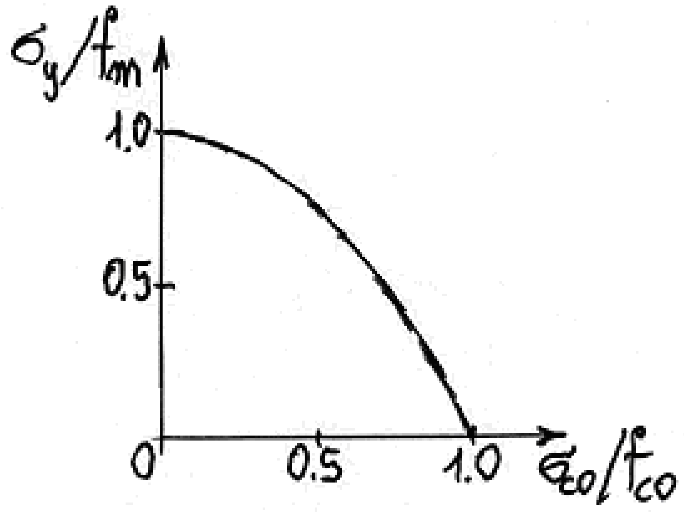

Figure 6-48 Combined bending with axial compression/tension

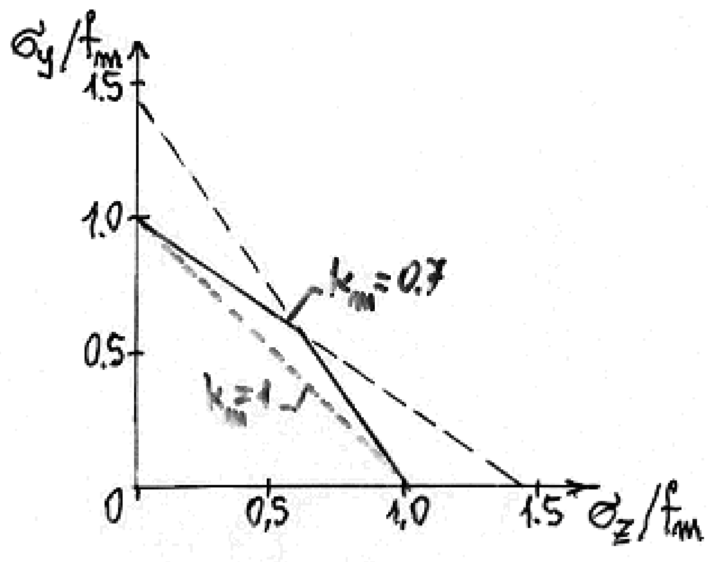

Figure 6-49 Combined biaxial bending with axial compression/tension :

6.6.11 Combined Torsion and Shear - CNR-DT 206/2007

$$\frac{\tau_{tor,d}}{k_{shape}*f_{v,d}} + \left(\frac{\tau_d}{f_{v,d}}\right)^2 \leq 1$$

τ_d is the design shear stress
$f_{v,d}$ is the design shear strength for the actual condition for a rectangular cross section :

$$k_{shape} = \left\{min\left\{1 + 0{,}15 * \frac{h}{b}; 2{,}0\right\}\right\}$$

$\tau_{tor,d}$ is the design torsional stress;
$f_{v,d}$ is the design shear strength;

k_{shape} is a factor depending on the shape of the cross-section;
h is the larger cross-sectional dimension;

b is the smaller cross-sectional dimension.

6.7 Resistances - Rafter Body

Appling the verification they have been computed the maximum resistance possible with the Arch.Tom Schacher's manual dimensioning.

6.7.1 Longitudinal to the grain

6.7.1.1 Rafter Body Compression: RB0comp and Rafter Body Tension: RB0tens

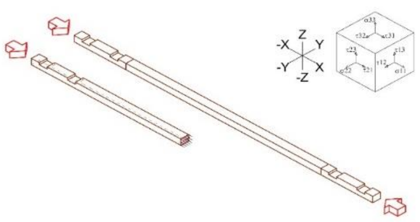

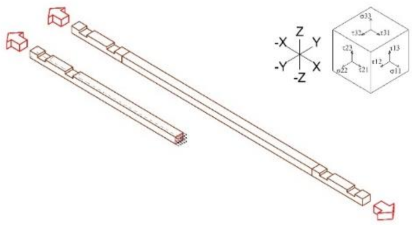

RB0comp		
N_0d	?	N
b	100,00	mm
h	75,00	mm
A_(net)	7500,00	mm
σ_(c,0,d)	#VALUE!	N/mm^2
f_(c,0,d)	24,93	N/mm^2
Verification	#VALUE!	
N_(0d)max	187,00	kN

RB0tens		
N_0d	?	N
b	100,00	mm
h	75,00	mm
A_(net)	7500,00	mm
σ_(t,0,d)	#VALUE!	N/mm^2
kh	1,08	
f_(t,0,d)	30,80	N/mm^2
Verification	#VALUE!	
N_(0d)max	231,00	kN

6.7.1.1 Rafter Body Shear in Z : RB0shearZ and Rafter Body Shear in Y: RB0shearY

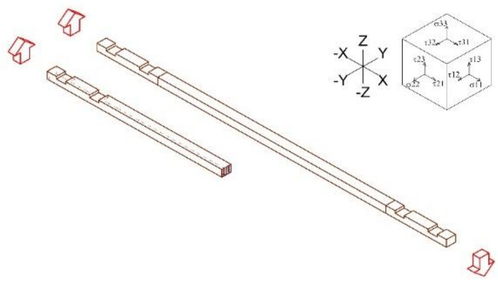

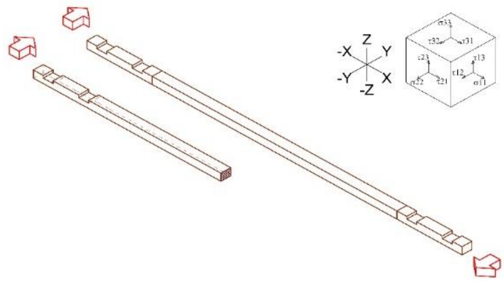

RB0shearZ with bending		
V_zd	?	N
K_cr	0,67	
A_(net)	5025,00	mm
τ_(d)	#VALUE!	N/mm^2
f_(v,d)	3,67	N/mm^2
Verification	#VALUE!	
V_zd max	12,28	kN

RB0shearY with bending		
V_yd	?	N
K_cr	0,67	
A_(net)	5025,00	mm
τ_(d)	#VALUE!	N/mm^2
f_(v,d)	3,67	N/mm^2
Verification	#VALUE!	
V_yd max	12,28	kN

RB0shearZ		
V_zd	?	N
A_(net)	7500,00	mm
τ_(d)	#VALUE!	N/mm^2
f_(v,d)	3,67	N/mm^2
Verification	#VALUE!	
V_zd max	18,33	kN

RB0shearY		
V_yd	?	N
A_(net)	7500,00	mm
τ_(d)	#VALUE!	N/mm^2
f_(v,d)	3,67	N/mm^2
Verification	#VALUE!	
V_yd max	18,33	kN

6.7.1.2 Rafter Body bending moment in Y: RB0mY and Rafter Body bending moment in Z: RB0mZ

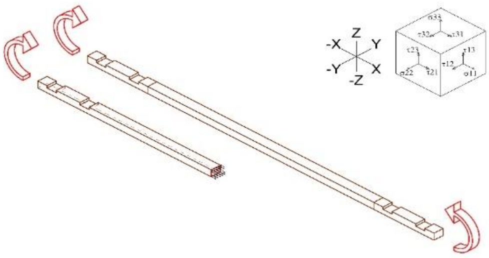

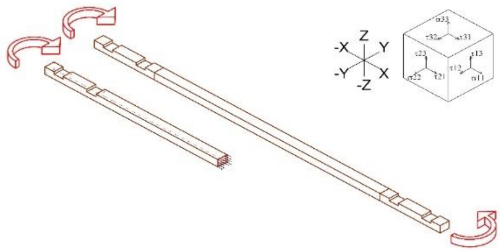

RB0mY		
M_(y,d)	?	Nmm
K_m	0,70	
b	100,00	mm
h	75,00	mm
W_(y,d)	93750,00	mm^3
σ_(m,y,d)	#VALUE!	N/mm^2
kh	1,15	
f_(m,d)	51,33	N/mm^2
f_(m,y,d)	58,97	N/mm^2
Verification	#VALUE!	
M_(y,d)max	5528110,83	Nmm
M_(y,d)max	5,53	kNm

RB0mZ		
M_(z,d)	?	Nmm
K_m	0,70	
b	100,00	mm
h	75,00	mm
W_(z,d)	125000,00	mm^3
σ_(m,z,d)	#VALUE!	N/mm^2
kh	1,08	
f_(m,d)	51,33	N/mm^2
f_(m,z,d)	55,67	N/mm^2
Verification	#VALUE!	
M_(z,d)max	6958693,87	Nmm
M_(z,d)max	6,96	kNm

6.7.1.3 Rafter Body torsional bending moment in X : RB0mX

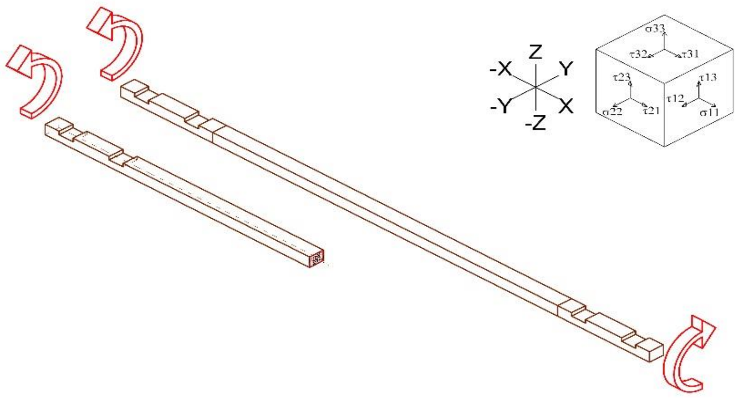

RB0mX		
M_(x,d)	?	Nmm
b	100,00	mm
h	75,00	mm
α	4,35	
τ_(tor,d)	#VALUE!	N/mm^2
K_shape	1,02	
f_(v,d)	3,67	N/mm^2
k_shape*f_(v,d)	3,74	N/mm^2
Verification	#VALUE!	
M_(x,d) max	483620,69	Nmm
M_(x,d) max	0,48	kNm

6.8 Resistances - Cross piece Notch

6.8.1 Longitudinal to the grain

6.8.1.1 Cross piece notch compression: CPNotch0comp and Cross piece notch tension: CPNotch0tens

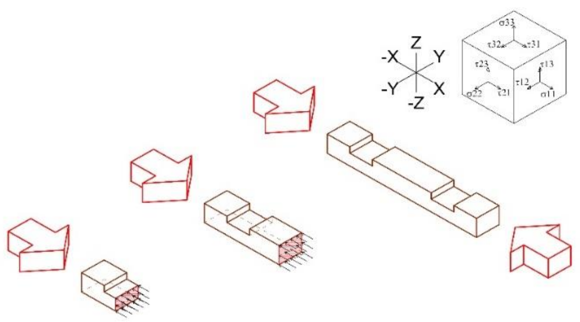

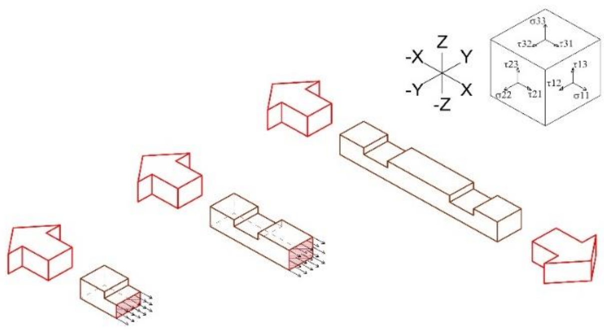

CPNotch0comp		
N_0d	?	N
b	100,00	mm
h	50,00	mm
A_(net)	5000,00	mm^2
σ_(c,0,d)	#VALUE!	N/mm^2
f_(c,0,d)	24,93	N/mm^2
Verification	#VALUE!	
N_(0d)max	124,67	kN

CPNotch0tens		
N_0d	?	N
b	100,00	mm
h	50,00	mm
A_(net)	5000,00	mm^2
σ_(t,0,d)	#VALUE!	N/mm^2
kh	1,08	
f_(t,0,d)	30,80	N/mm^2
Verification	#VALUE!	
N_(0d)max	154,00	kN

6.8.1.1 *Cross piece notch shear in Z: CPNotch0shearZ and Cross piece notch shear in Y: CPNotch0shearY*

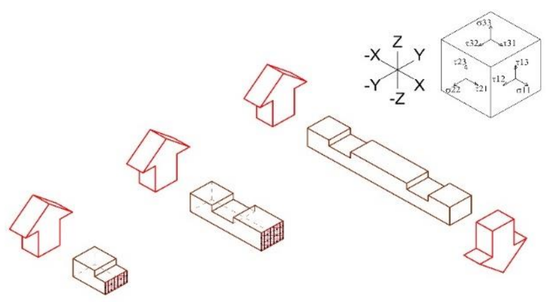

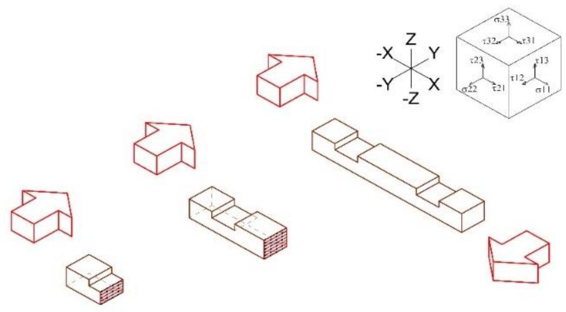

CPNotch0shearZ with bending		
V_zd	?	N
K_cr	0,67	
A_(net)	3350,00	mm^2
τ_(d)	#VALUE!	N/mm^2
f_(v,d)	3,67	N/mm^2
Verification	#VALUE!	
V_zd max	8,19	kN

CPNotch0shearY with bending		
V_yd	?	N
K_cr	0,67	
A_(net)	3350,00	mm^2
τ_(d)	#VALUE!	N/mm^2
f_(v,d)	3,67	N/mm^2
Verification	#VALUE!	
V_yd max	8,19	kN

CPNotch0shearZ		
V_zd	?	N
A_(net)	5000,00	mm
τ_(d)	#VALUE!	N/mm^2
f_(v,d)	3,67	N/mm^2
Verification	#VALUE!	
V_zd max	12,22	kN

CPNotch0shearY		
V_yd	?	N
A_(net)	5000,00	mm
τ_(d)	#VALUE!	N/mm^2
f_(v,d)	3,67	N/mm^2
Verification	#VALUE!	
V_yd max	12,22	kN

6.8.1.2 *Cross piece notch bending moment in Y: CPNotch0mY and Cross piece notch bending moment in Z: CPNotch0mZ*

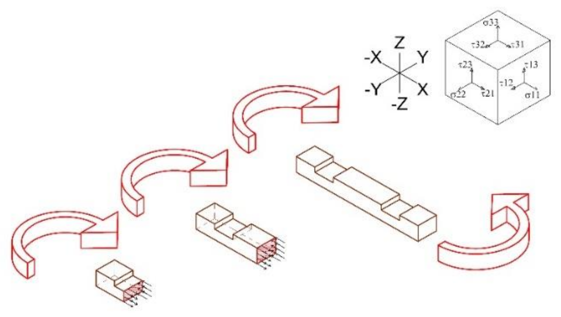

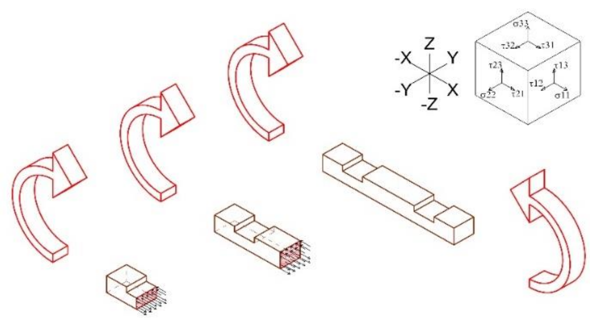

CPNotch0mY		
M_(y,d)	?	Nmm
K_m	0,70	
b	100,00	mm
h	50,00	mm
W_(y,d)	41666,67	mm^3

CPNotch0mZ		
M_(z,d)	?	Nmm
K_m	0,70	
b	100,00	mm
h	50,00	mm
W_(z,d)	83333,33	mm^3

σ_(m,y,d)	#VALUE!	N/mm^2
kh	1,25	
f_(m,d)	51,33	N/mm^2
f_(m,y,d)	63,95	N/mm^2
Verification	#VALUE!	
M_(y,d)max	2664480,07	Nmm
M_(y,d)max	2,66	kNm

σ_(m,z,d)	#VALUE!	N/mm^2
kh	1,08	
f_(m,d)	51,33	N/mm^2
f_(m,z,d)	55,67	N/mm^2
Verification	#VALUE!	
M_(z,d)max	4639129,24	Nmm
M_(z,d)max	4,64	kNm

6.8.1.3 Cross piece notch torsional bending moment in X: CPNotch0mX

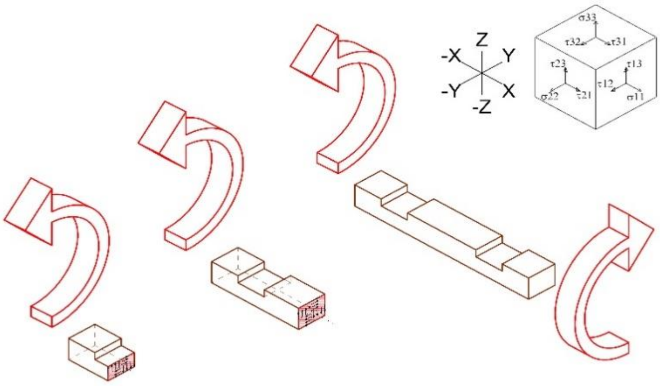

CPNotch0mX		
M_(x,d)	?	Nmm
b	100,00	mm
h	50,00	mm
α	3,90	
τ_(tor,d)	#VALUE!	N/mm^2
K_shape	1,03	
f_(v,d)	3,67	N/mm^2
k_shape*f_(v,d)	3,78	N/mm^2
Verification	#VALUE!	
M_(x,d) max	242094,02	Nmm
M_(x,d) max	0,24	kNm

6.9 Activation of the chains

The possible failure mechanisms, which will be described in the following chapters, have shown the necessity of defining and naming the reaction in the corner joints at the roof level. In this chapter it is shown the overturning mechanism in order to make the reader understand the specific elemnts involved in the description.

6.9.1 Overturning Mechanism

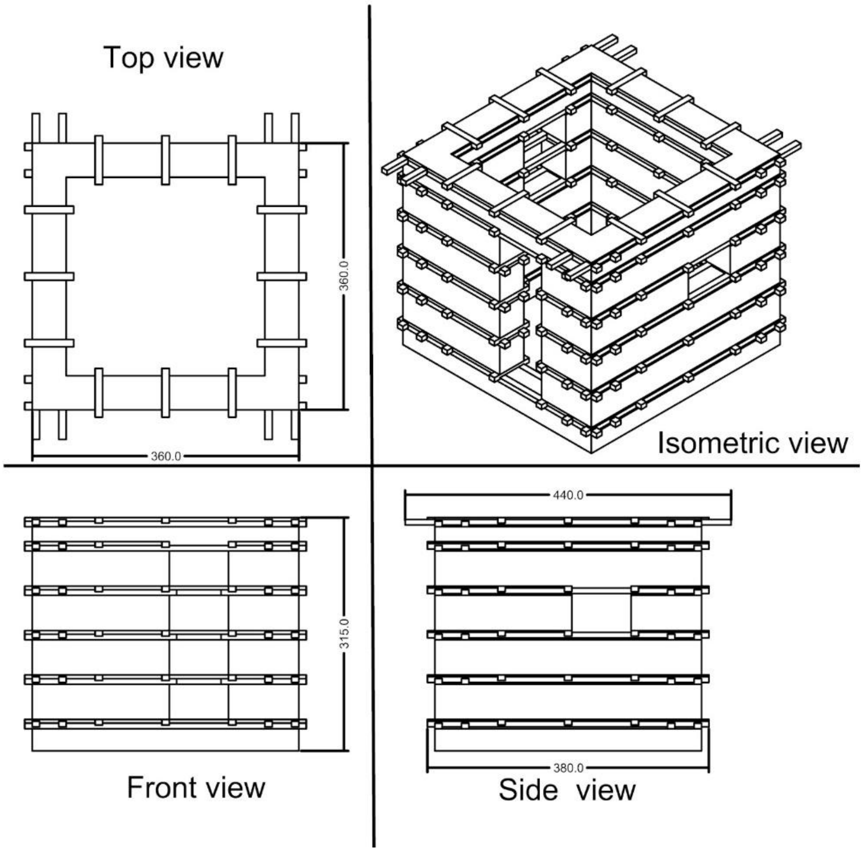

Figure 6-50 Overview of the room box

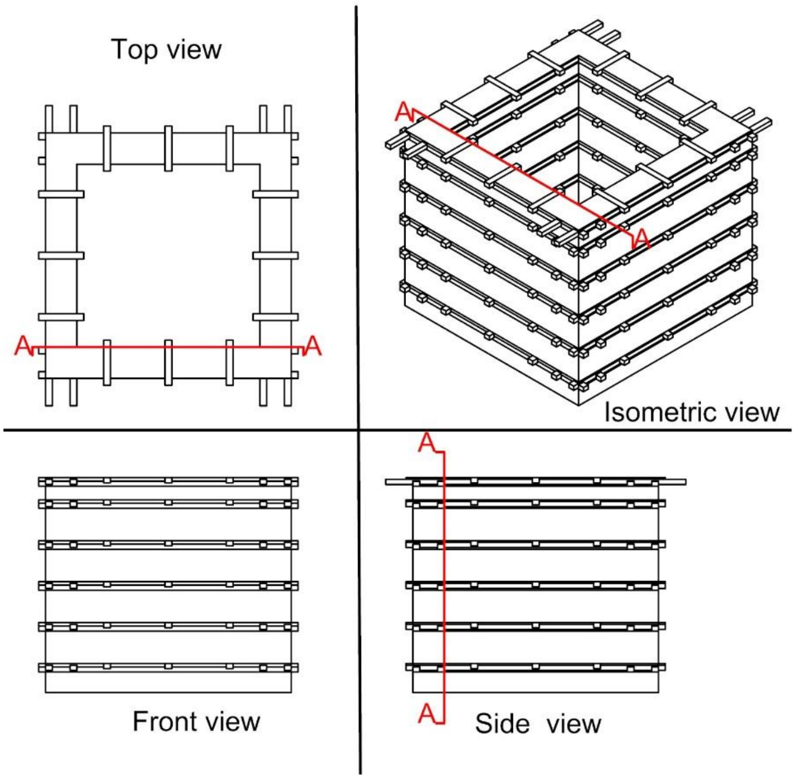

Figure 6-51Section of the studied wall

During the seismic event it may happen the overturning mechanism due to the inertia of the wall, because the mass is subjected to the movement of the ground defined as the peak ground acceleration. This phenomenon is shown in the following figures.

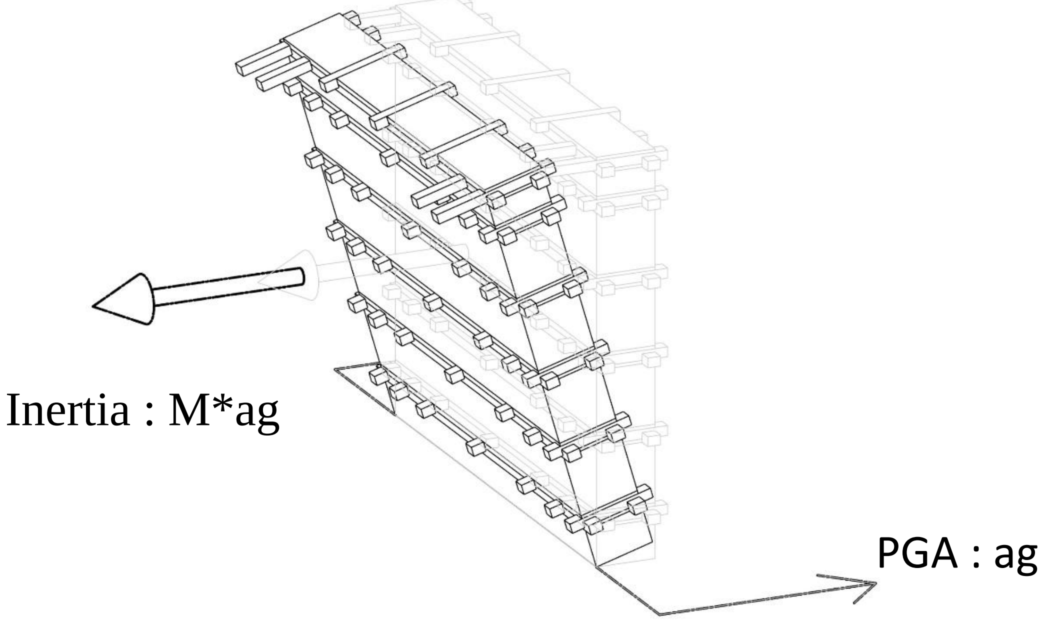

Figure 6-52 Overturning mechanism

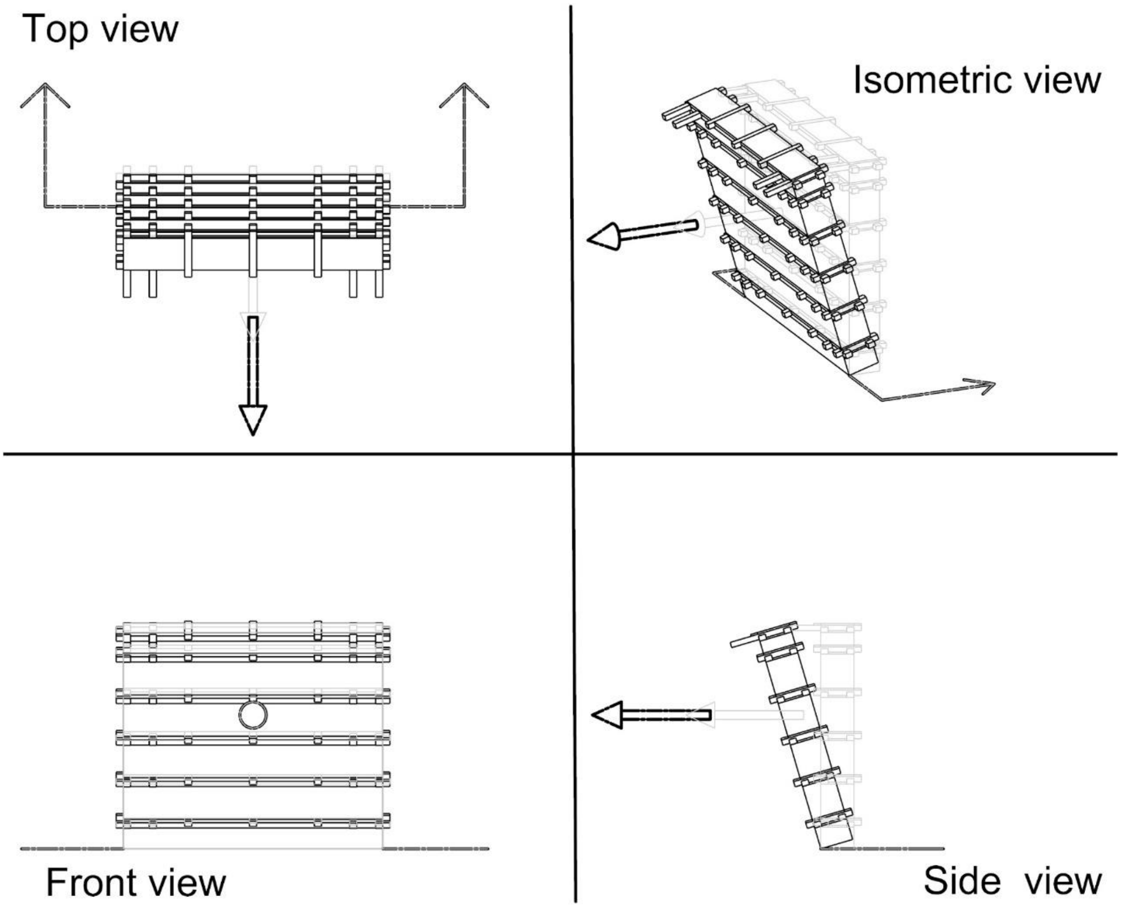

Figure 6-53Overturning mechanism - Orthogonal projections

6.9.2 Activation of the chain along Roof Rafter Head

The failure mechanism activate the timber elements at the roof level. The Roof rafters start to work as chain. In the following pictures the two red arrow show the forces developed by the chains.

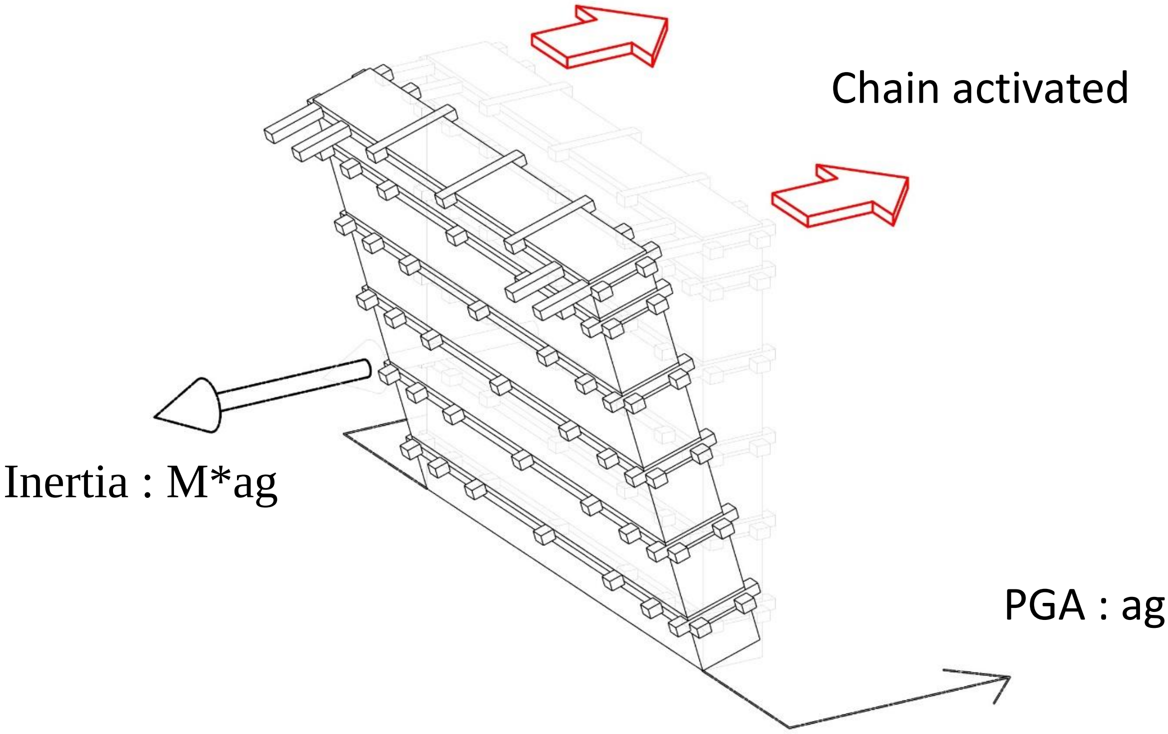

Figure 6-54 - activation of the chains Overturning mechanism

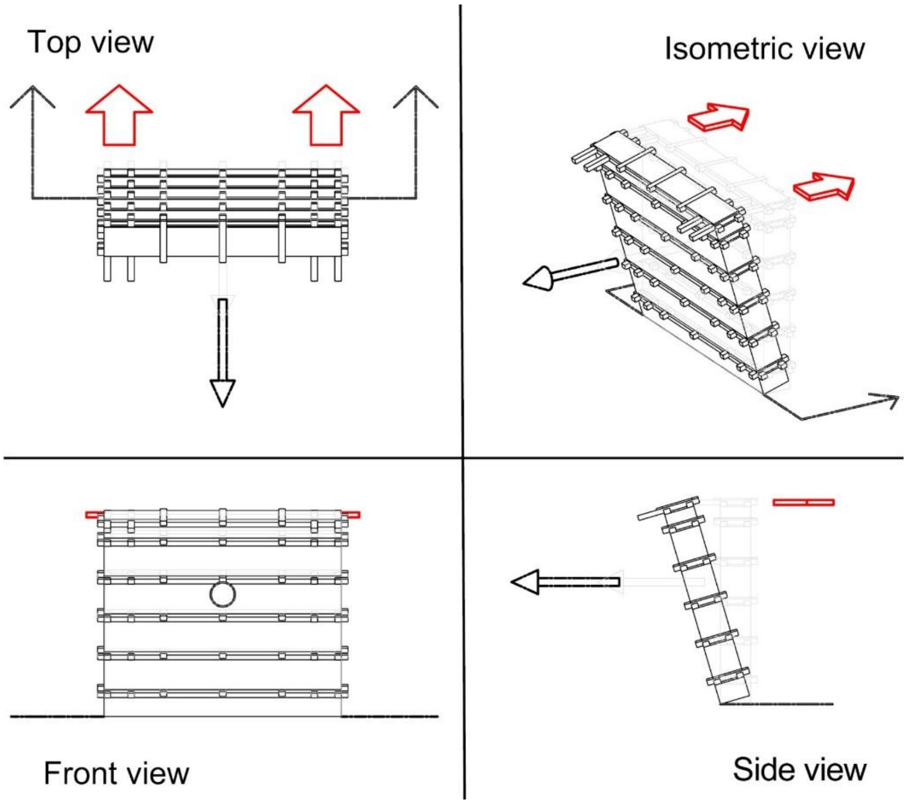

Figure 6-55 Figure 6 53Overturning mechanism - Orthogonal projections activation of the chains

The forces developed in the chains are sheared in the rafters, this repartitions will be described in the following chapters because it is different for the different failure mechanisms.

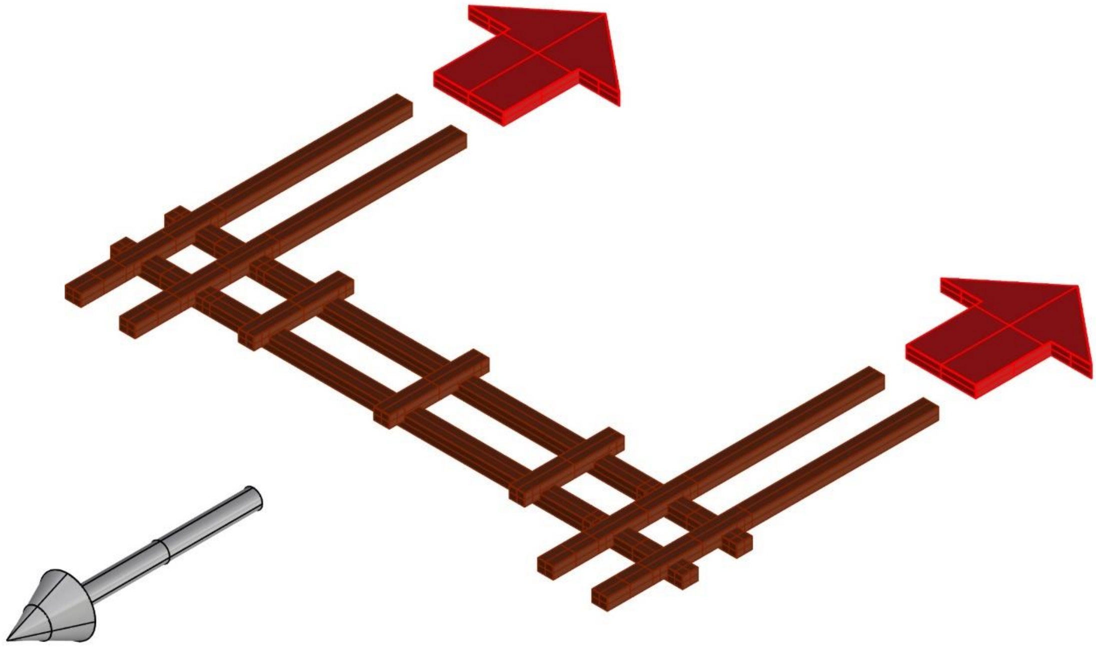

Figure 6-56 Roof timber beam subjected to seismic actions

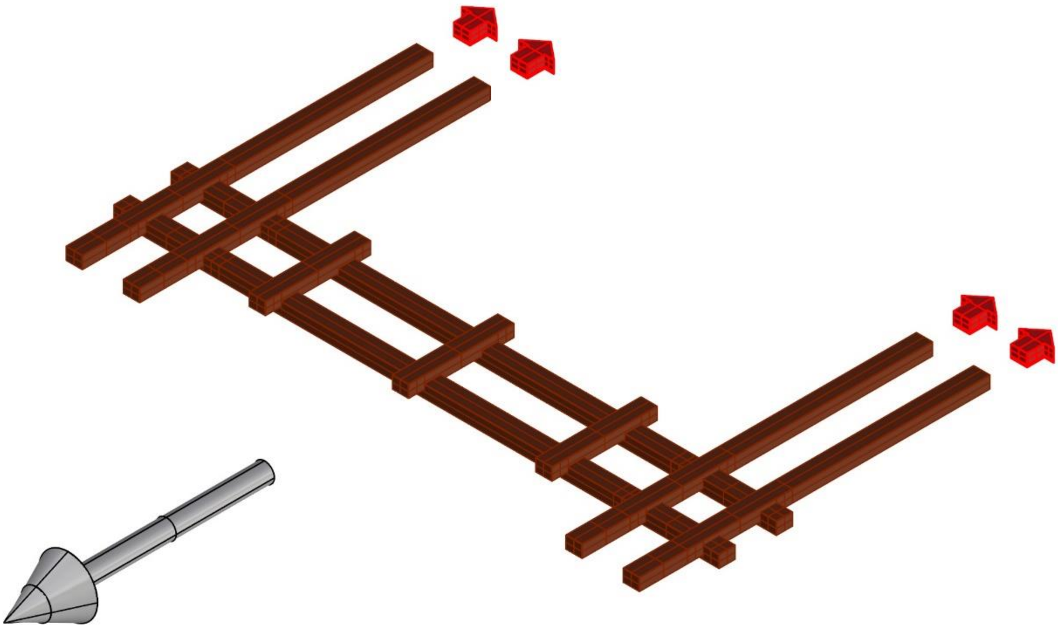

Figure 6-57 Repartitions of forces - Roof timber beam subjected to seismic actions

In order to describe the behavior of the corner joint at the roof level they have been named the four rafters crossed in the corner joint, considering that the behavior of the structure in symmetric.The numbering always start from the external element to the internal.

The elements belonging to the failing wall have been named R# due to the fact that they are passive resisting elements. The rafter belonging to the timber beam working as a chain have been named T# due to the fact that they are subjected mainly to tension.

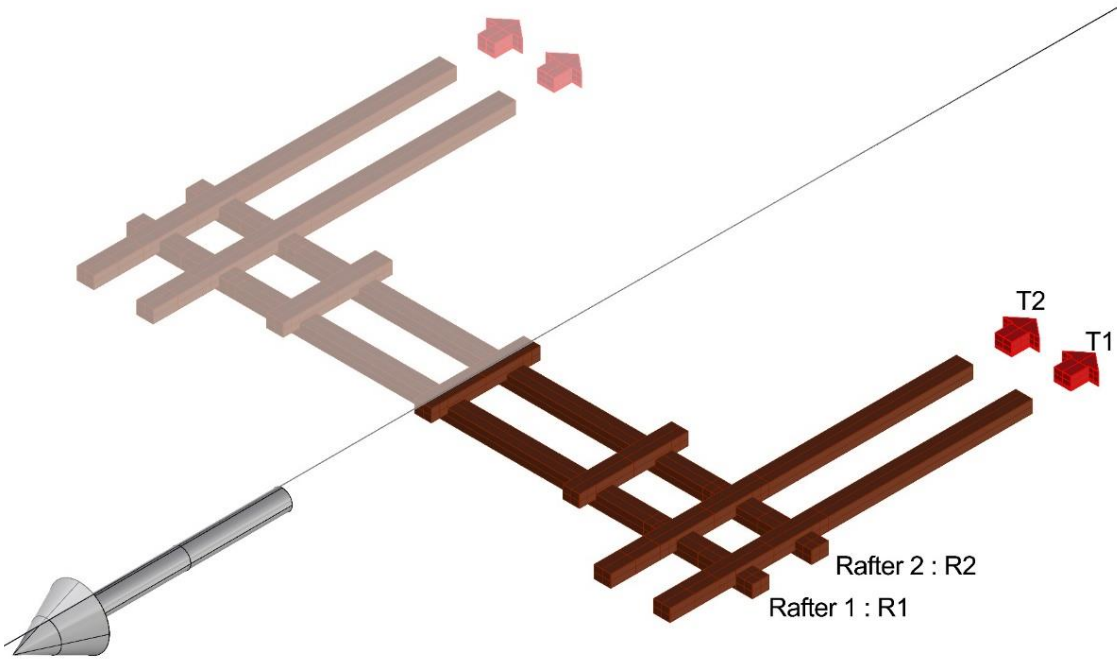

Figure 6-58 Descriptions of the rafters crossed at the roof timber beam

Each intersection have been recolled as the summations of the names of the crossing rafters, as shown in the picture below.

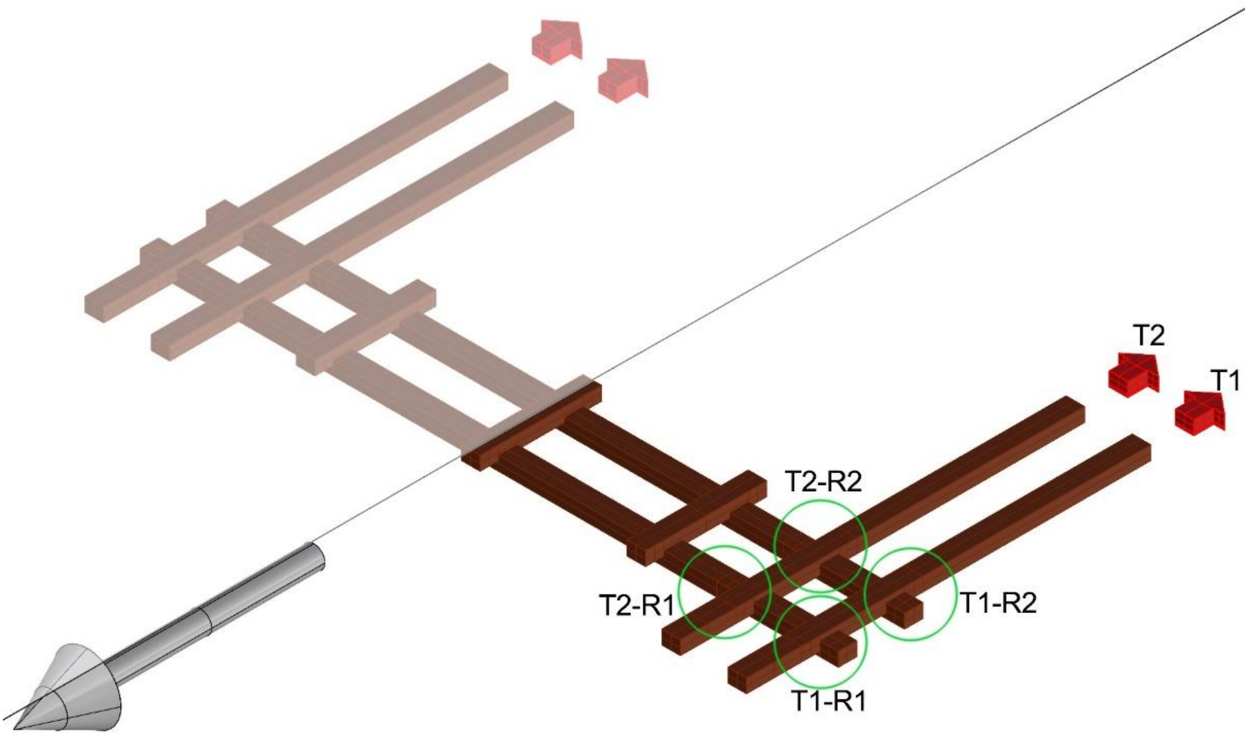

Figure 6-59 Description of the crossing rafters at roof level

6.9.2.1 Axial forces

In the following pages they are described the stressed part of the timber elements and the hierarchy of the forces due to the activation of the chains .

6.9.2.1.1 Axial stresses

The following tables reports the values of the maximum allowed stresses and their position are shown in the following figures.

To be clear names must be read like these examples :

- RRH0tension : Roof Rafter Head - 0 = along the fibers – tens : in tension - A# stressed area
- RRH0compression : Roof Rafter Head - 0 = along the fibers – compression : in compression - A# stressed area
- RRH90compression : Roof Rafter Head - 90 = perpendicular to the fibers – compression : in compression - A# stressed area

Table 14 Roof rafter Head and Rafter head

RRH0tension	A4	
N_0d	?	N
b	100,00	mm
h	50,00	mm
A_(net)	5000,00	mm^2
σ_(t,0,d)	#VALUE!	N/mm^2
kh	1,08	
f_(t,0,d)	30,80	N/mm^2
Verification	#VALUE!	
N_(od)max	154,00	kN

RRH0compression	A3	
N_0d	?	N
b	100,00	mm
h	25,00	mm
A_(net)	2500,00	mm^2
σ_(c,0,d)	#VALUE!	N/mm^2
f_(c,0,d)	24,93	N/mm^2
Verification	#VALUE!	
N_(od)max	62,33	kN

RH90compression	A3	
N_90d	?	N
b	100,00	mm
h	25,00	mm
A_(net)	2500,00	mm^2
σ_(c,90,d)	#VALUE!	N/mm^2
k_(c,90)	1,50	
f_(c,90,d)	9,90	N/mm^2
Verification	#VALUE!	
N_(90d)max	16,50	kN

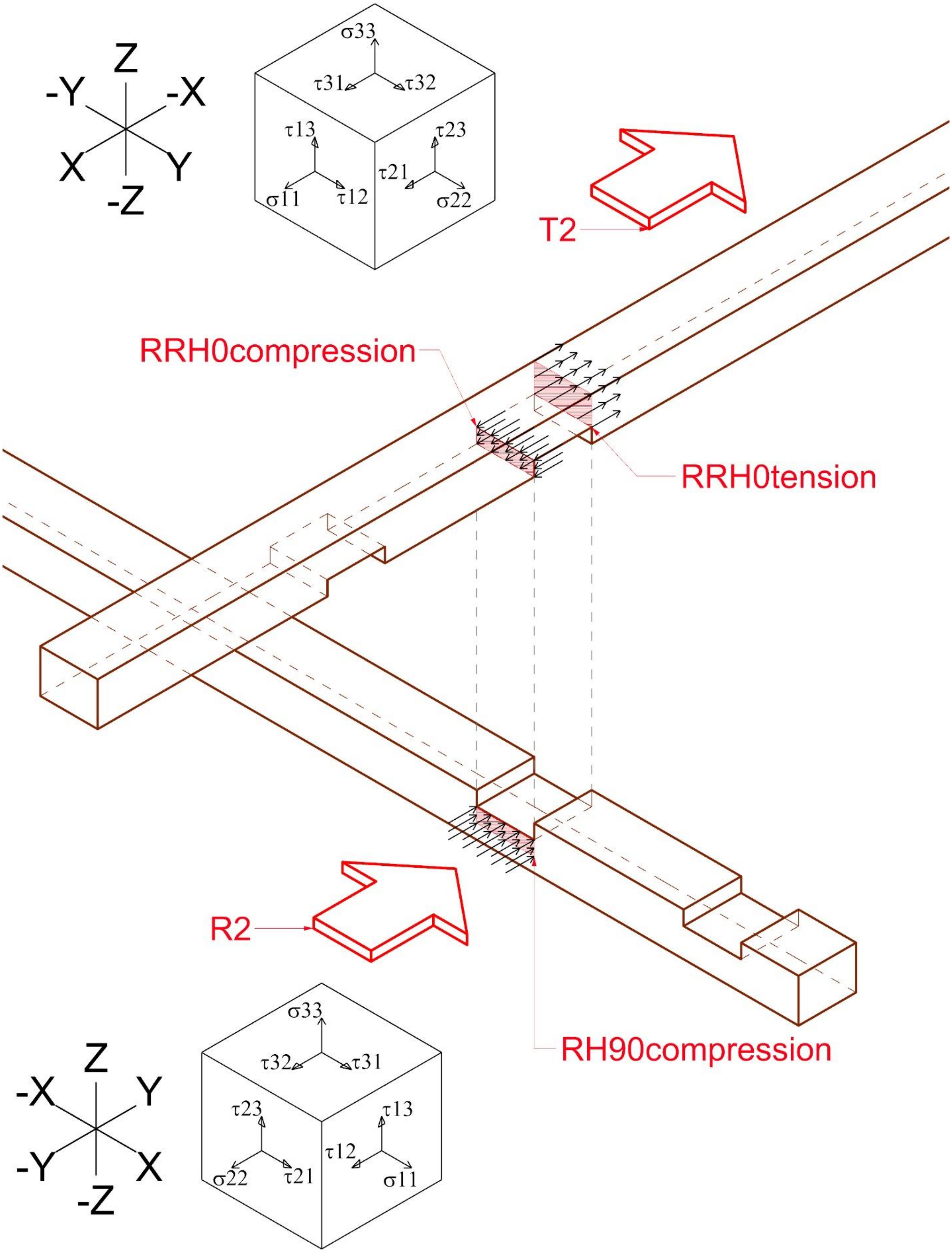

Figure 6-60 Roof Rafter Head Axial stresses : Crossing rafters T2-R2

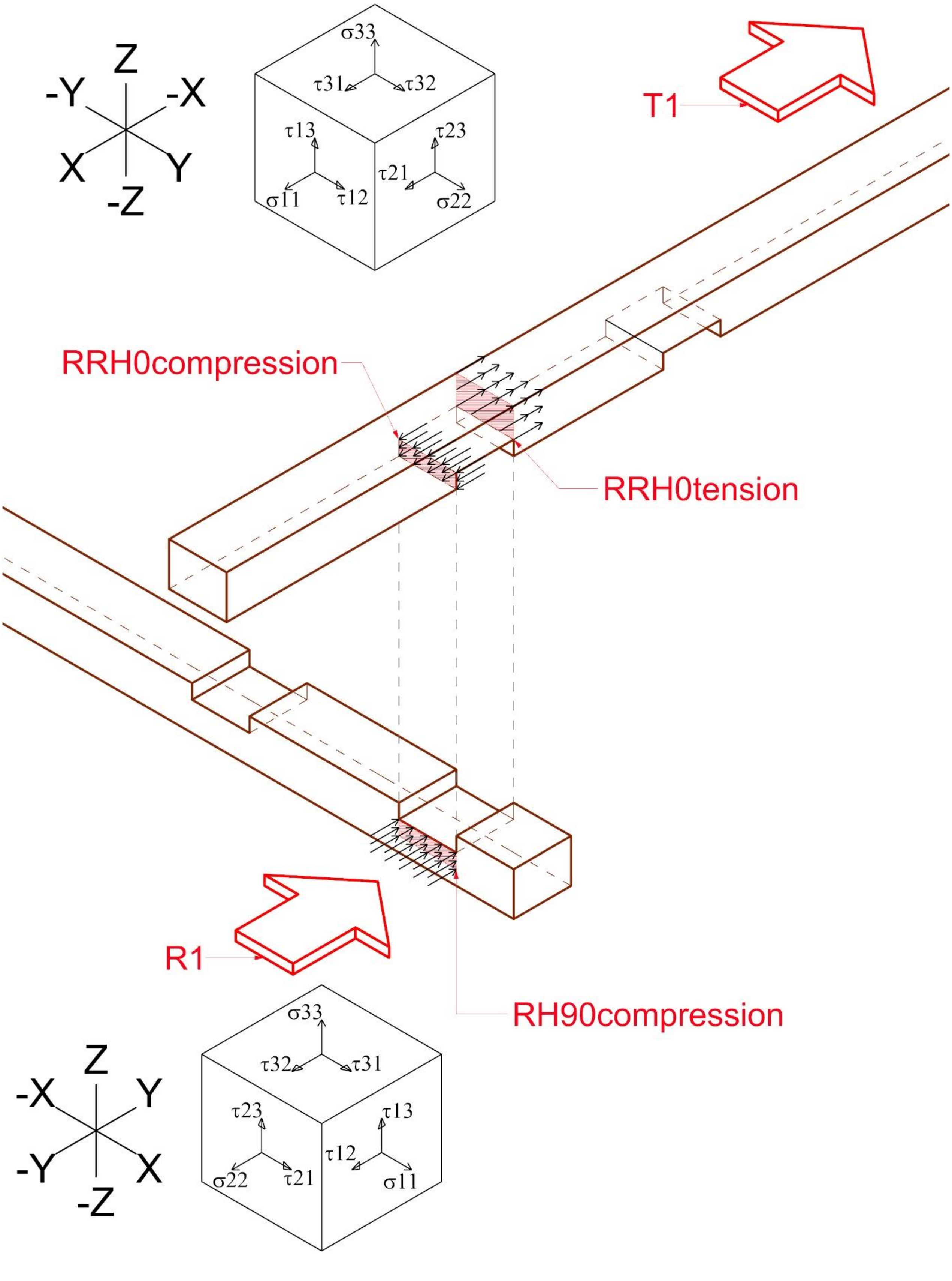

Figure 6-61 Roof Rafter Head Axial stresses : Crossing rafters T1-R1

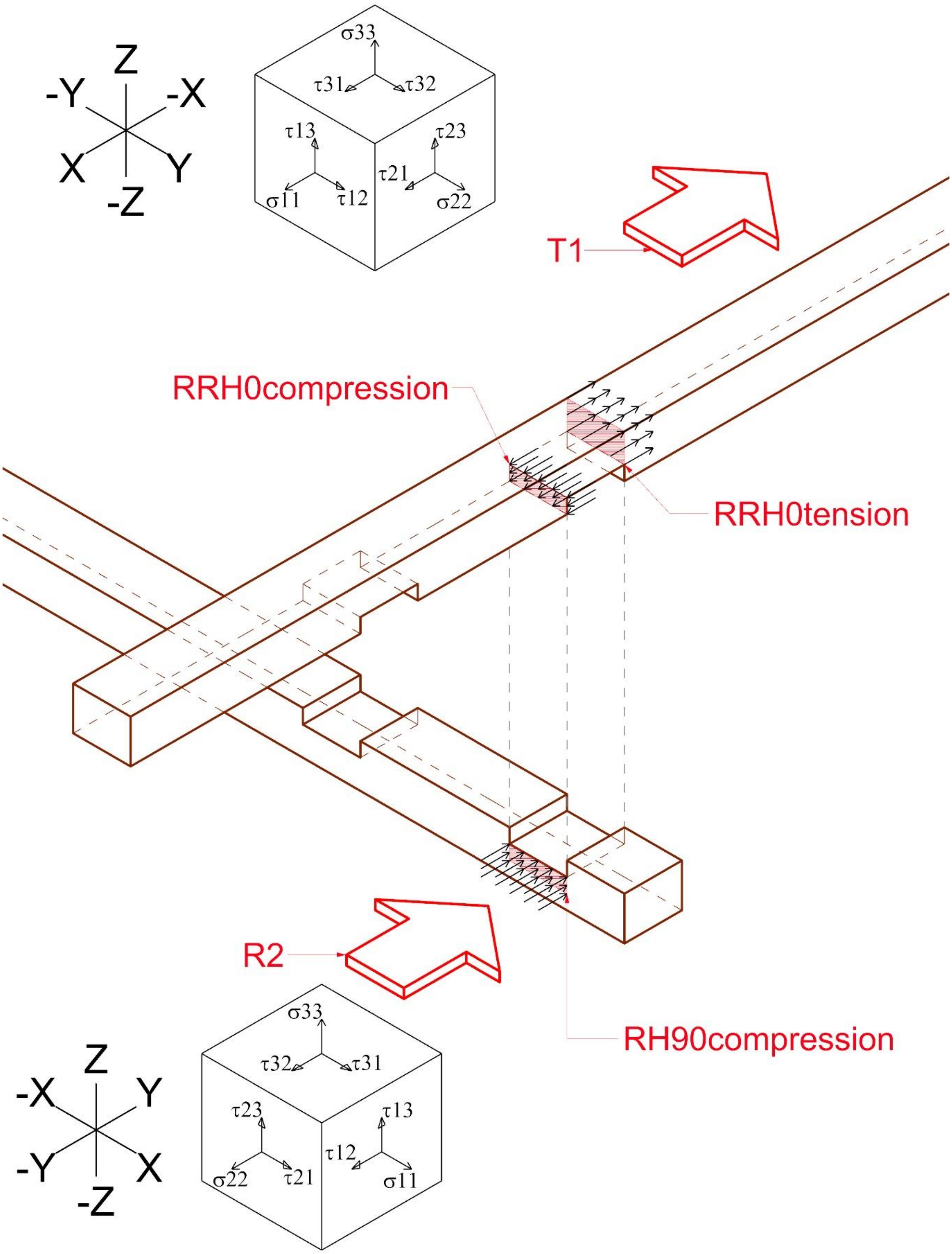

Figure 6-62 Roof Rafter Head Axial stresses : Crossing rafters T1-R2

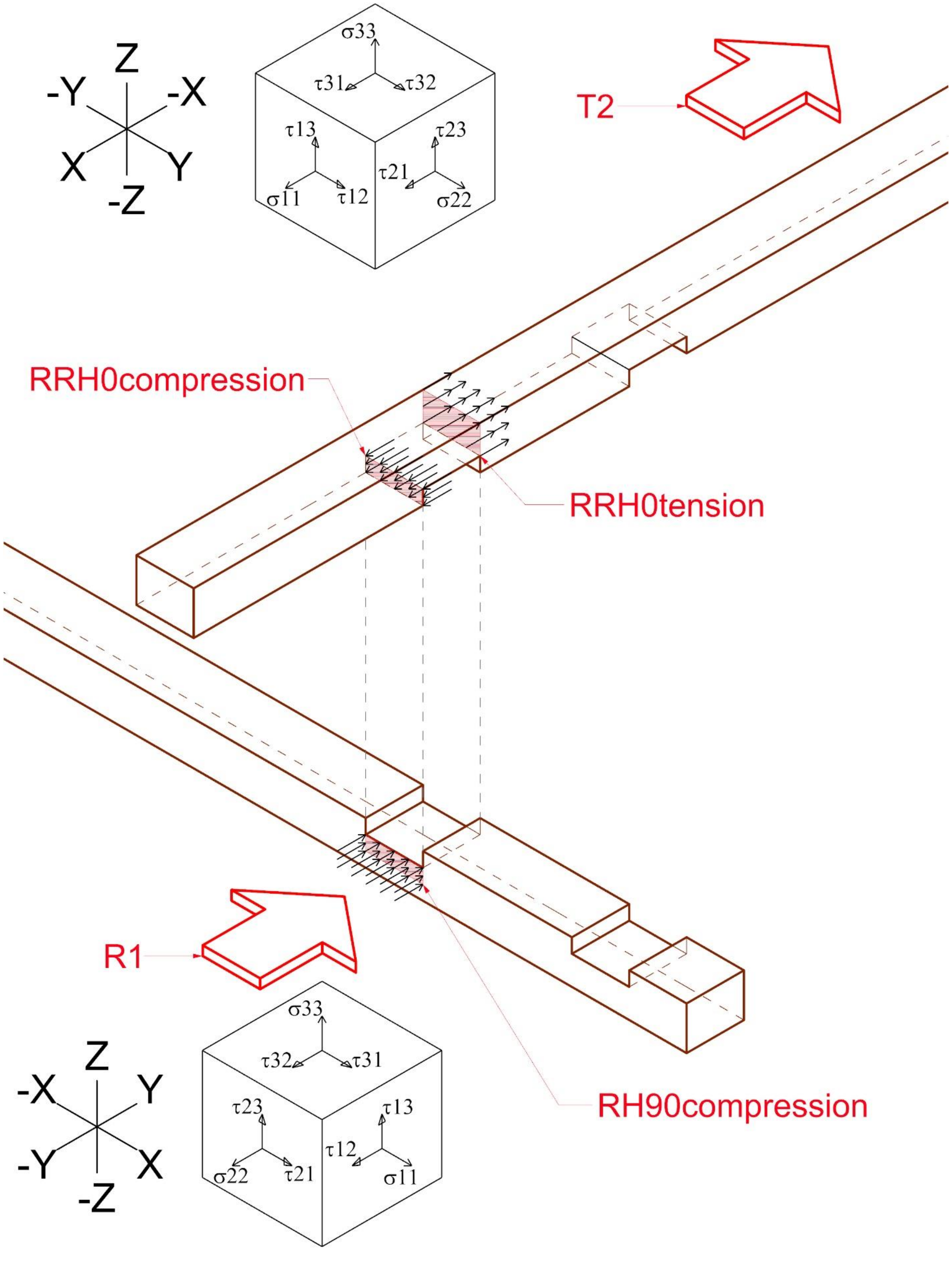

Figure 6-63 Roof Rafter Head Axial stresses : Crossing rafters T2-R1

6.9.2.1.2 Tangential stresses

As before the names are related to the timber elements and to the subjected stresses.

- RRH0shearEXT : Roof Rafter Head - 0 = along the fibers – shear : under shear force – EXT : external surface - A# stressed area
- RRH0shearINT : Roof Rafter Head - 0 = along the fibers – shear : under shear force – INT : internal surface - A# stressed area
- RH90shear : Rafter Head - 90 = perpendicular to the fibers – shear : under shear force - A# stressed area
- RRH0shearEXT, RRH0shearINT, and RH90shear: are computed in case of just pure shear force or shear force and bending moment acting at the same time.

RRH0shearEXT	A7	
with bending		
V_0d	?	N
K_cr	0,67	
A_(net)	26800,00	mm^2
τ_(d)	#VALUE!	N/mm^2
f_(v,d)	3,67	N/mm^2
Verification	#VALUE!	
V_0d max	65,51	kN

RRH0shearINT	A1	
with bending		
V_0d	?	N
K_cr	0,67	
A_(net)	17420,00	mm^2
τ_(d)	#VALUE!	N/mm^2
f_(v,d)	3,67	N/mm^2
Verification	#VALUE!	
V_0d max	42,58	kN

RRH0shearEXT	A7	
V_0d	?	N
A_(net)	40000,00	mm^2
τ_(d)	#VALUE!	N/mm^2
f_(v,d)	3,67	N/mm^2
Verification	#VALUE!	
V_0d max	97,78	kN

RRH0shearINT	A1	
V_0d	?	N
A_(net)	26000,00	mm^2
τ_(d)	#VALUE!	N/mm^2
f_(v,d)	3,67	N/mm^2
Verification	#VALUE!	
V_0d max	63,56	kN

RH90shear	A5	
with bending		
V_90d	?	N
K_cr	0,67	
A_(net)	5025,00	mm^2
τ_(d)	#VALUE!	N/mm^2
ft,90,d	0,44	N/mm^2
f_(v,d)	0,88	N/mm^2
Verification	#VALUE!	
V_90d max	2,95	kN

RH90shear	A5	
V_90d	?	N
A_(net)	7500,00	mm^2
τ_(d)	#VALUE!	N/mm^2
ft,90,d	0,44	N/mm^2
f_(v,d)	0,88	N/mm^2
Verification	#VALUE!	
V_90d max	4,40	kN

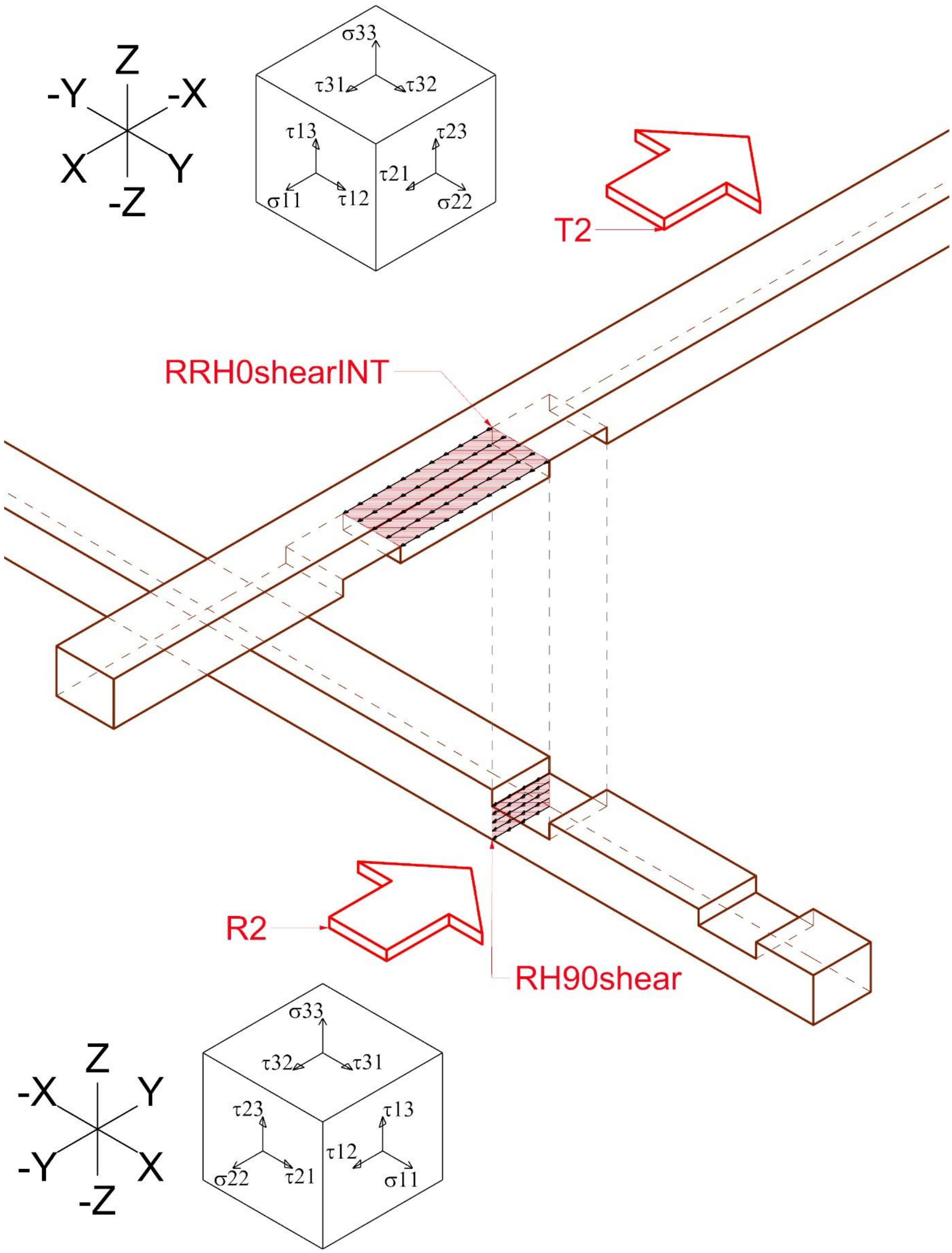

Figure 6-64 Roof Rafter Head Tangential stresses: Crossing rafters T2-R2

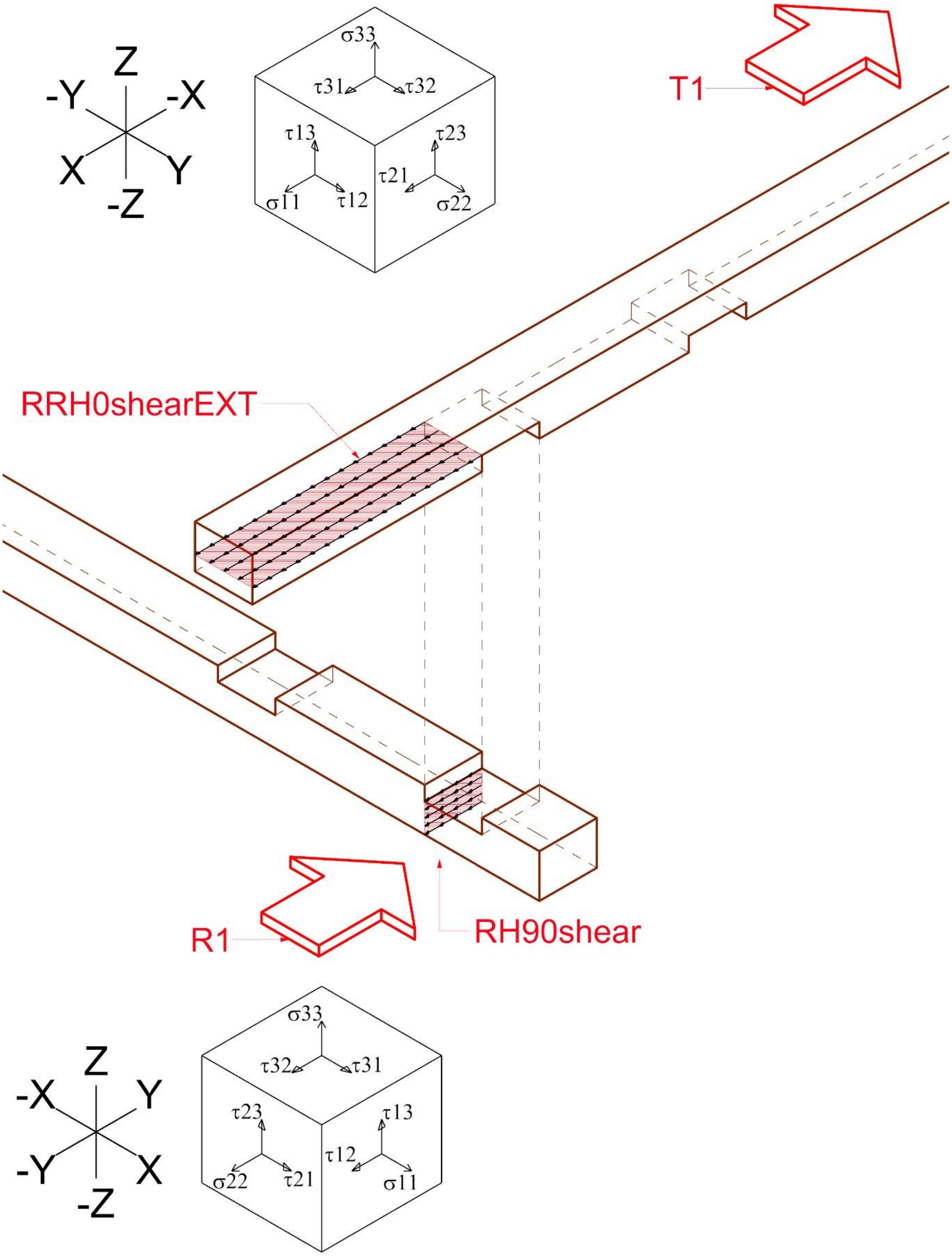

Figure 6-65 Roof Rafter Head Tangential stresses: Crossing rafters T1-R1

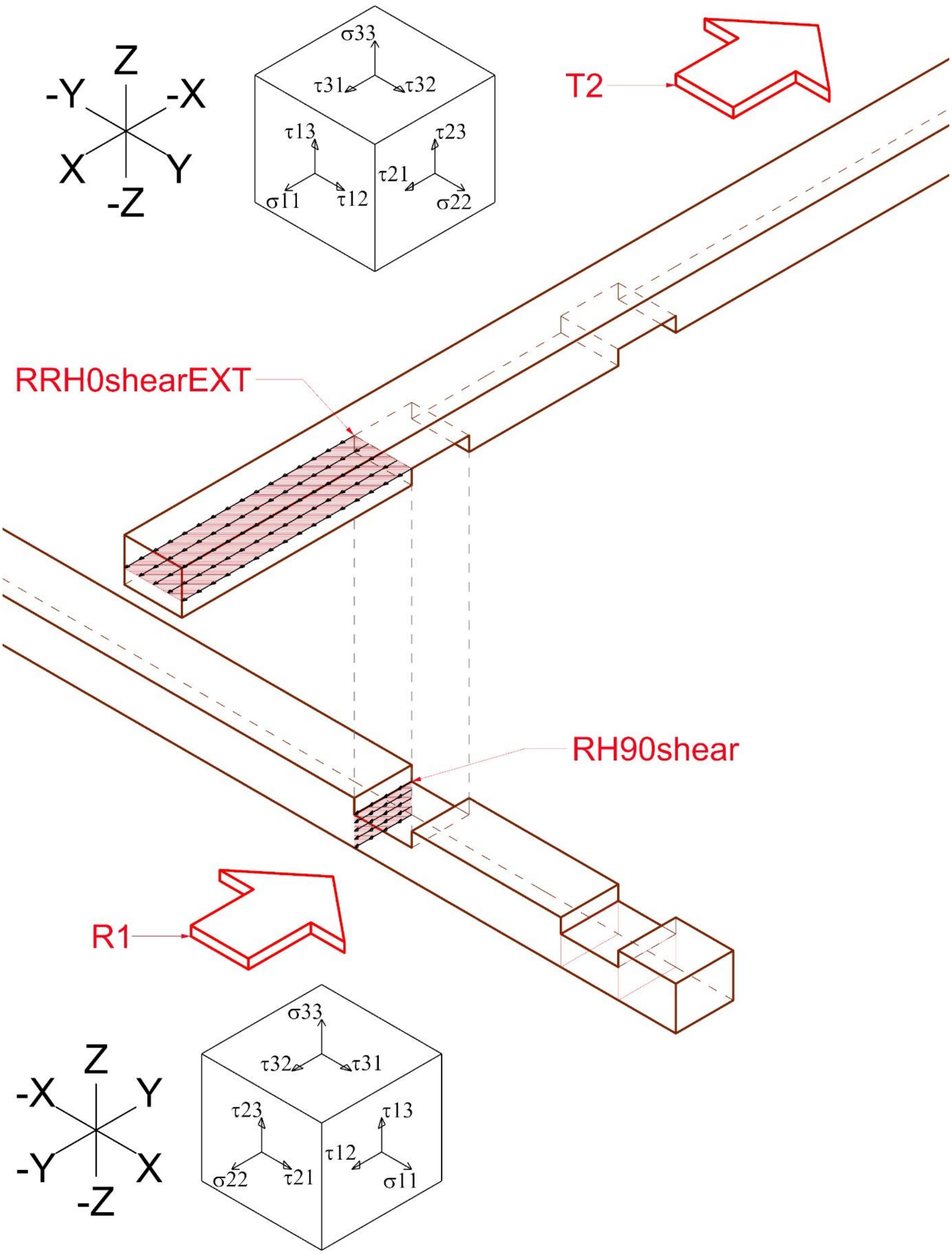

Figure 6-66 Roof Rafter Head Tangential stresses: Crossing rafters T1-R2

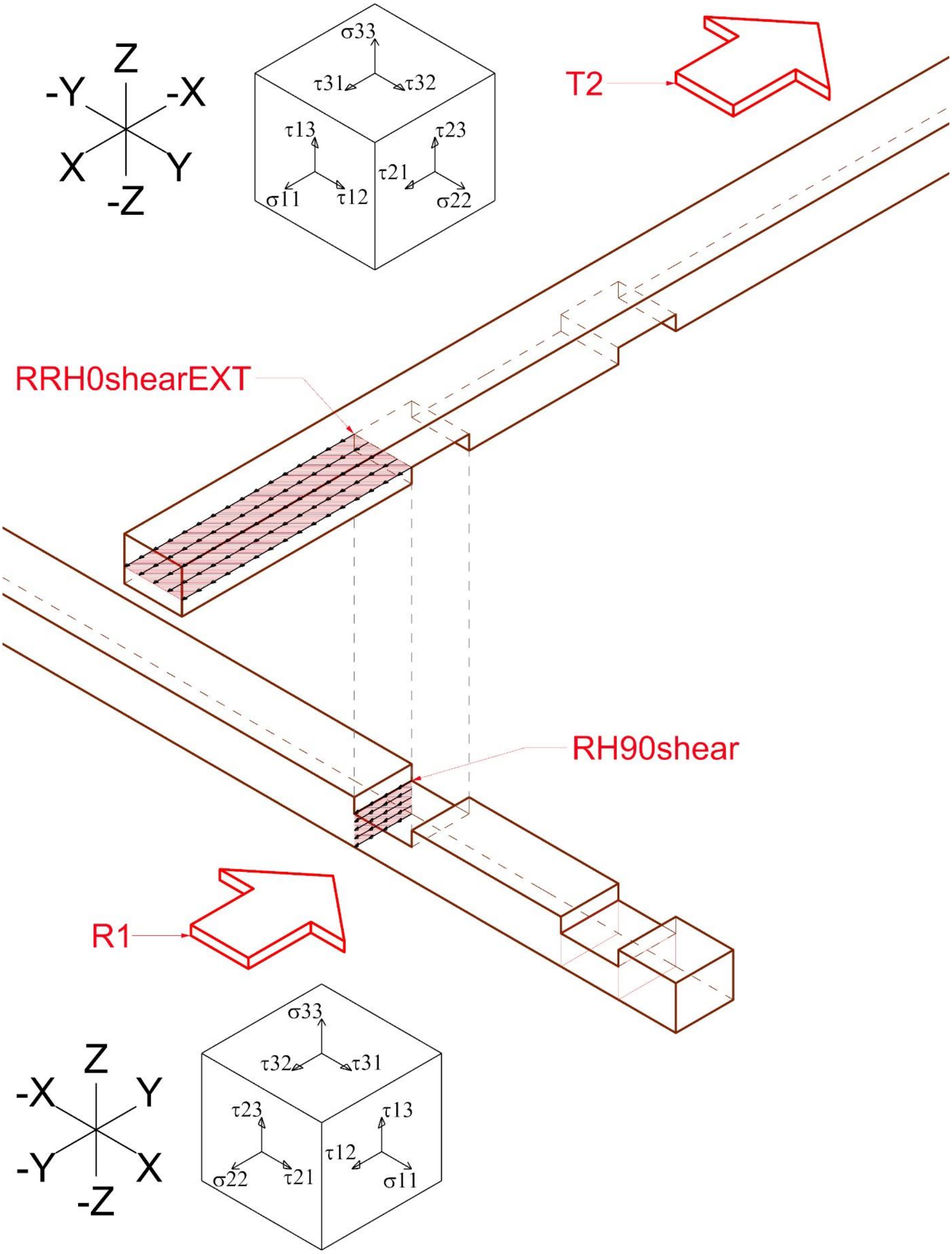

Figure 6-67 Roof Rafter Head Tangential stresses: Crossing rafters T2-R1

6.9.2.2 Bending Moments

In the following figures are shown the "parasitic" bending moments developed congruently with the geometry of the timber elements and the applied actions. In the following paragraph it will be shown how the values of each bending moment has been computed.

6.9.2.2.1 Bending Moments : Axial stresses

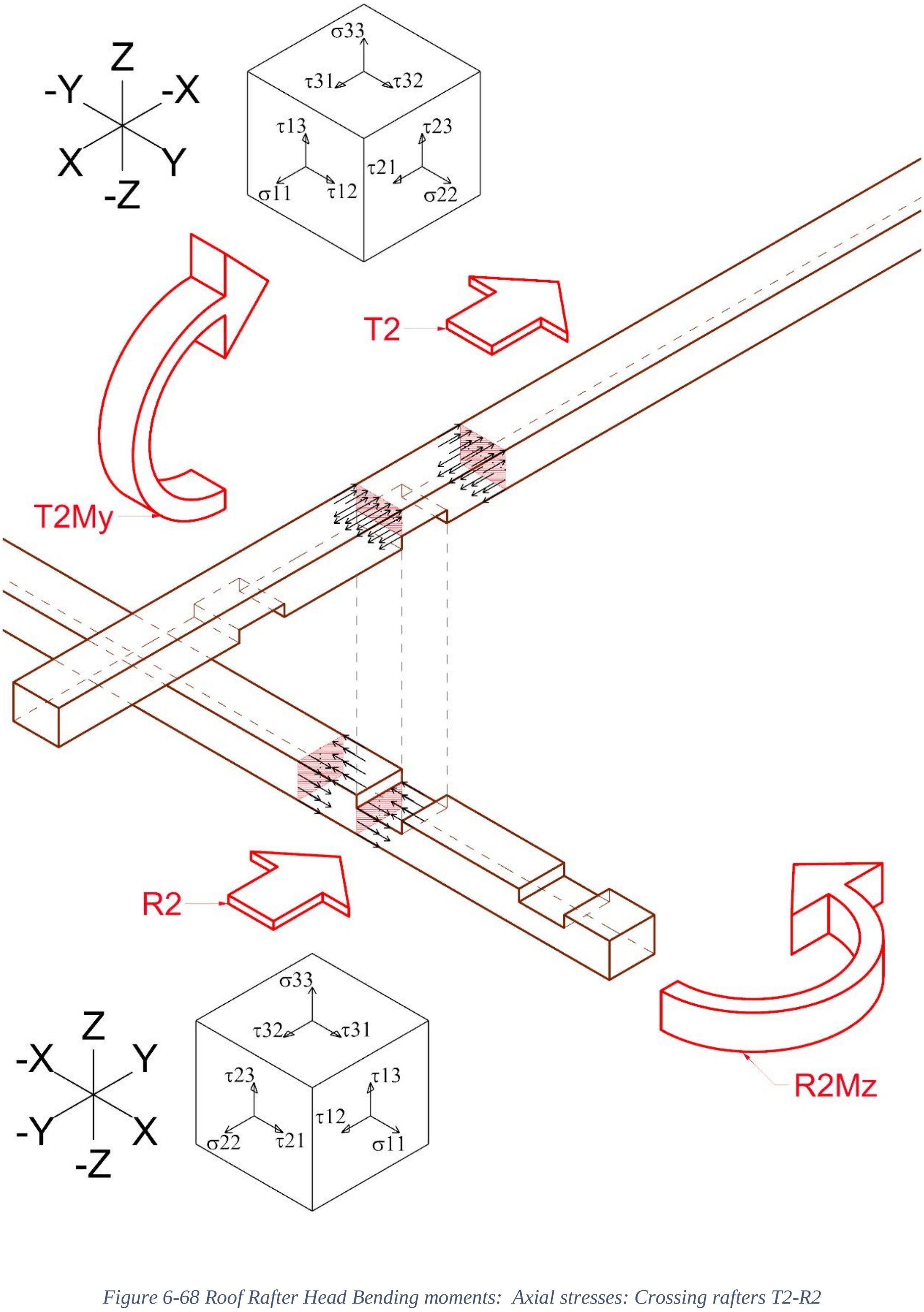

Figure 6-68 Roof Rafter Head Bending moments: Axial stresses: Crossing rafters T2-R2

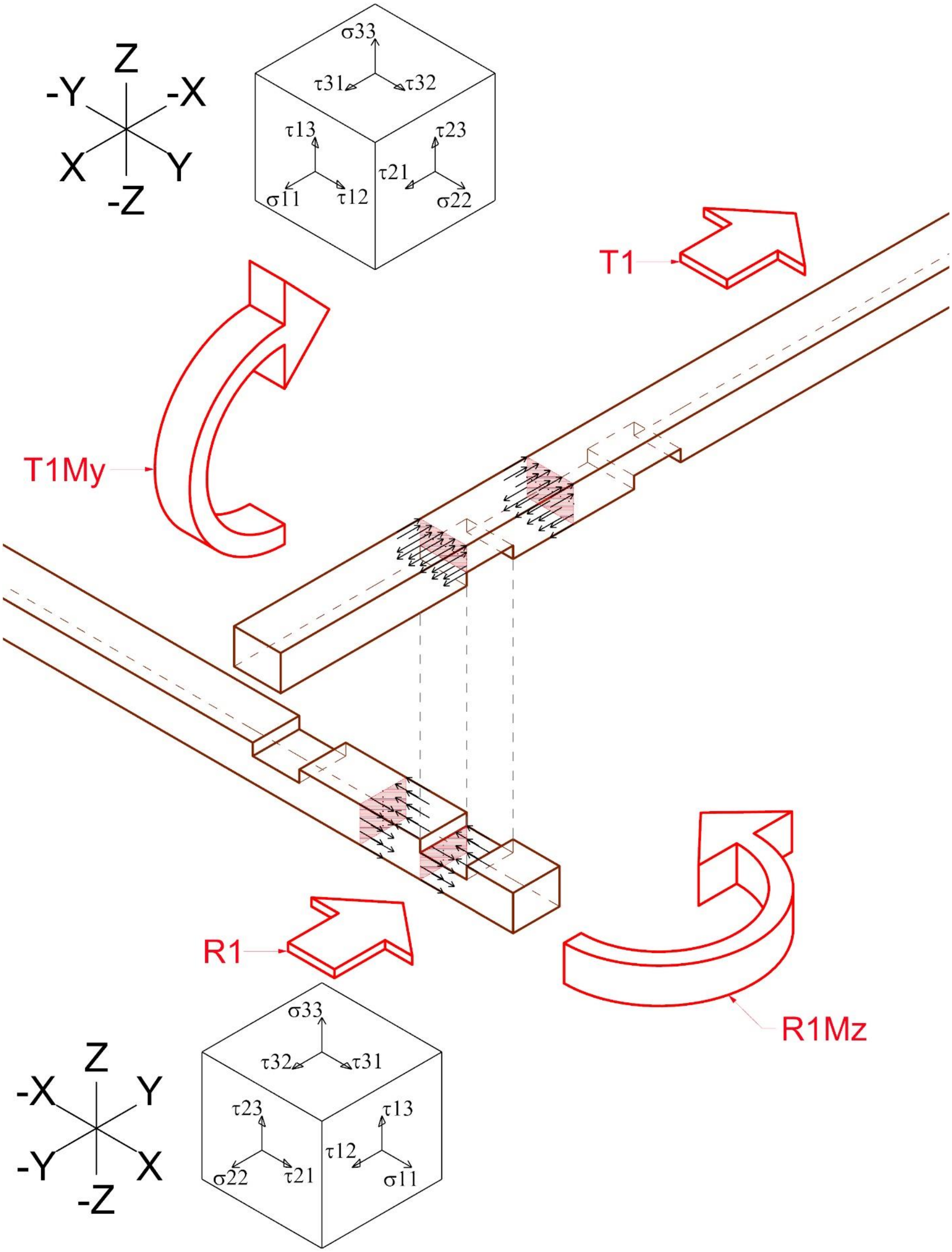

Figure 6-69 Roof Rafter Head Bending moments: Axial stresses: Crossing rafters T1-R1

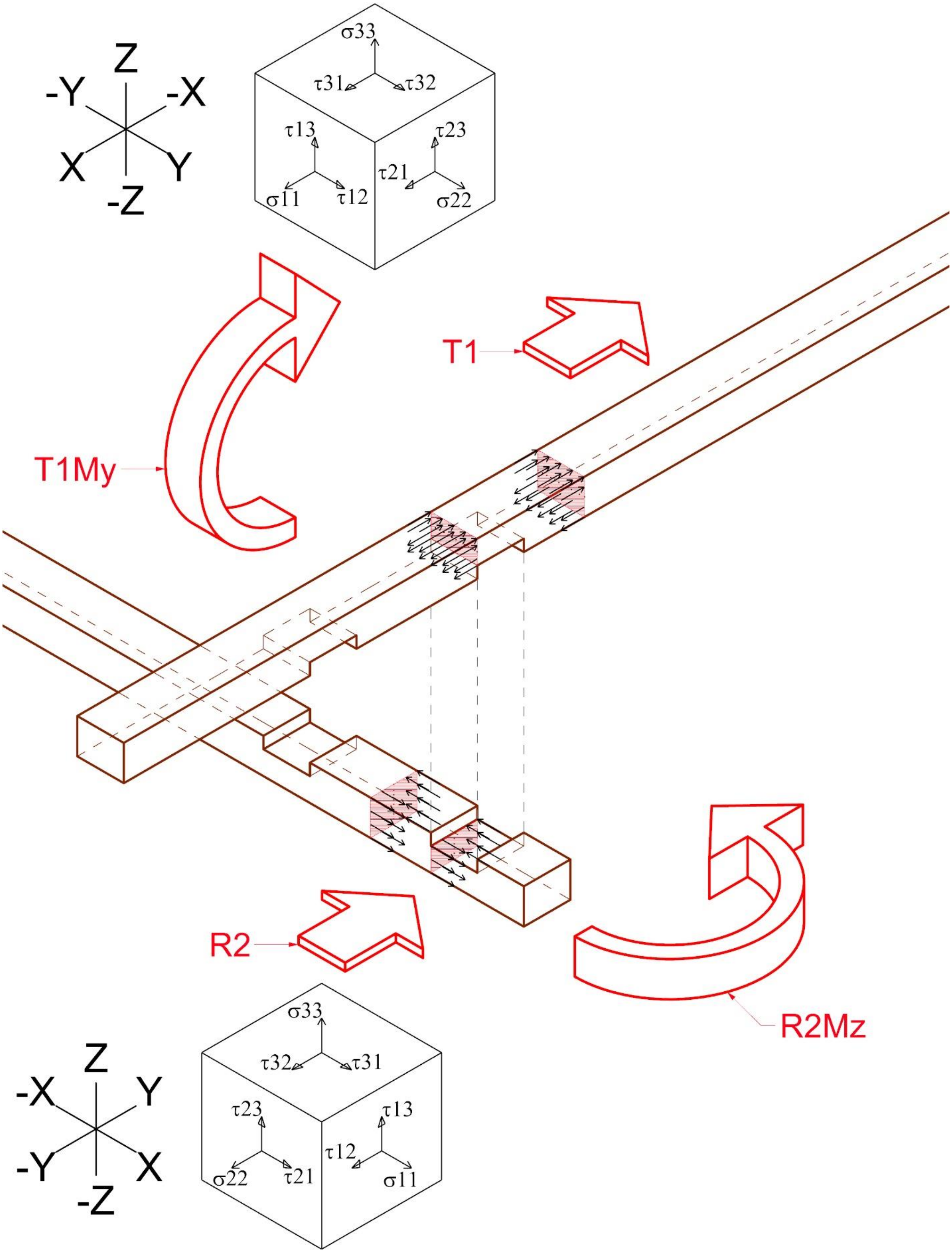

Figure 6-70 Roof Rafter Head Bending moments: Axial stresses: Crossing rafters T1-R2

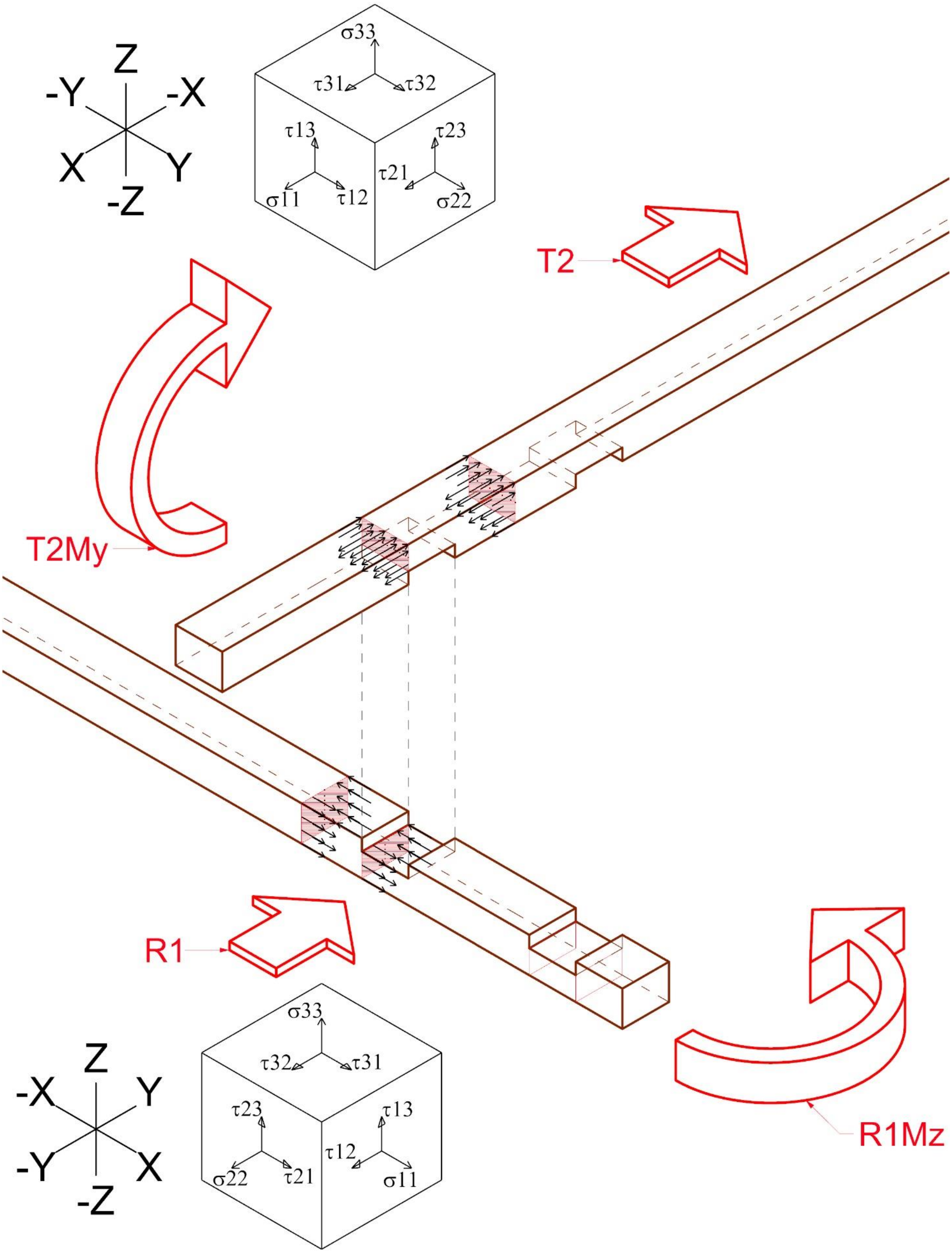

Figure 6-71 Roof Rafter Head Bending moments: Axial stresses: Crossing rafters T2-R1

6.9.2.2.2 Torsnion : Tangential stresses

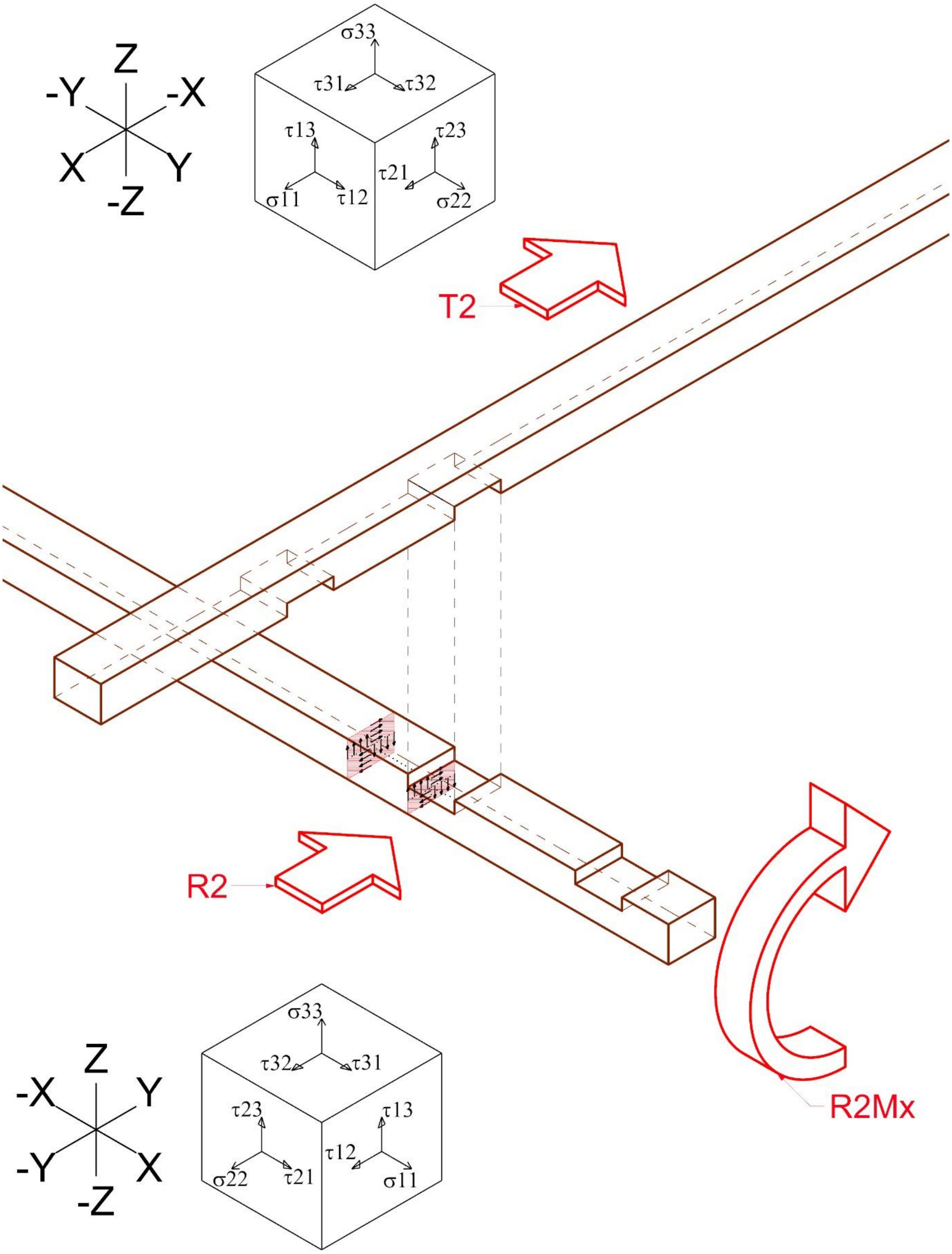

Figure 6-72 Roof Rafter Head Bending moments: Torsnion : Tangential stresses : Crossing rafters T2-R2

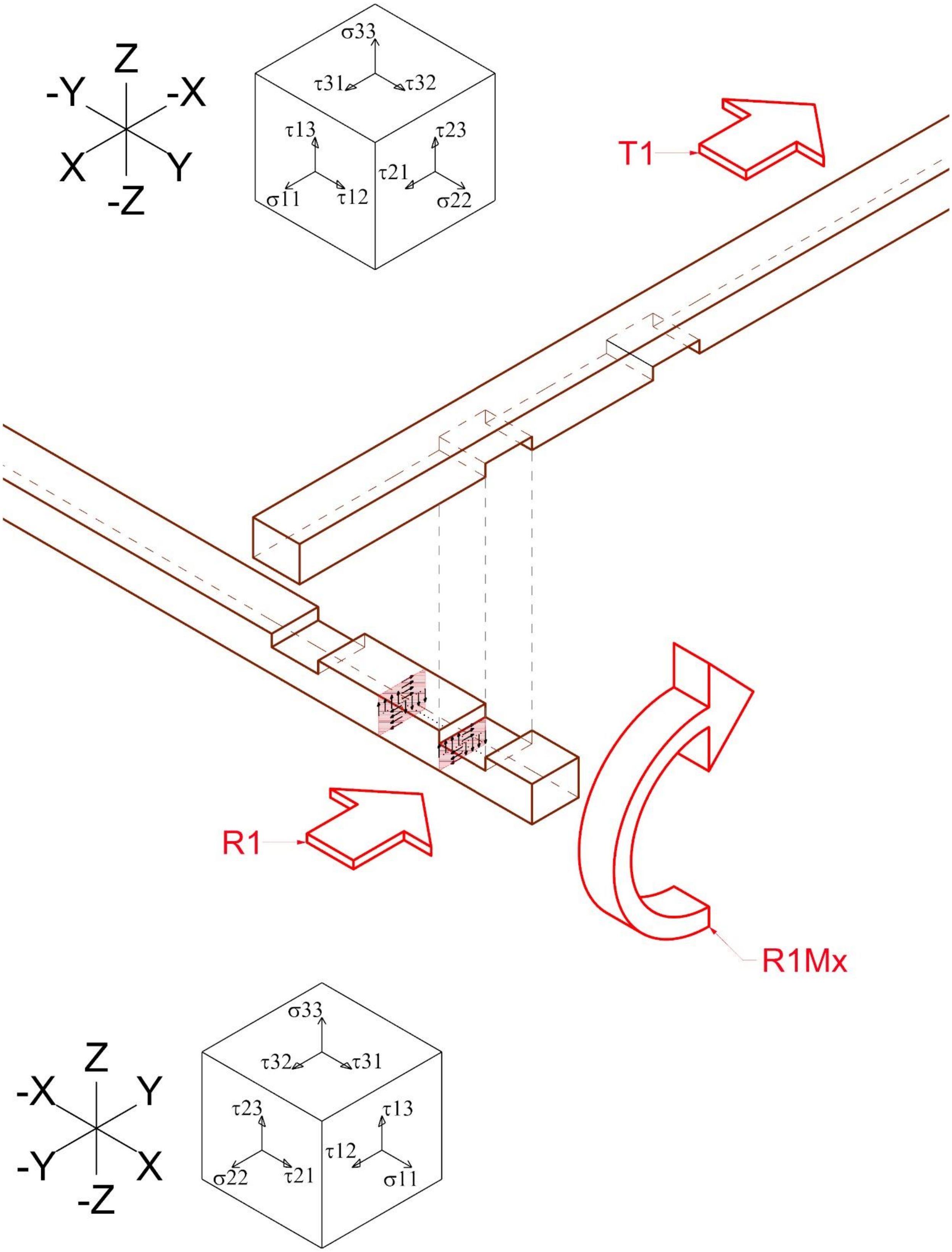

Figure 6-73 Roof Rafter Head Bending moments: Torsion: Tangential stresses: Crossing rafters T1-R1

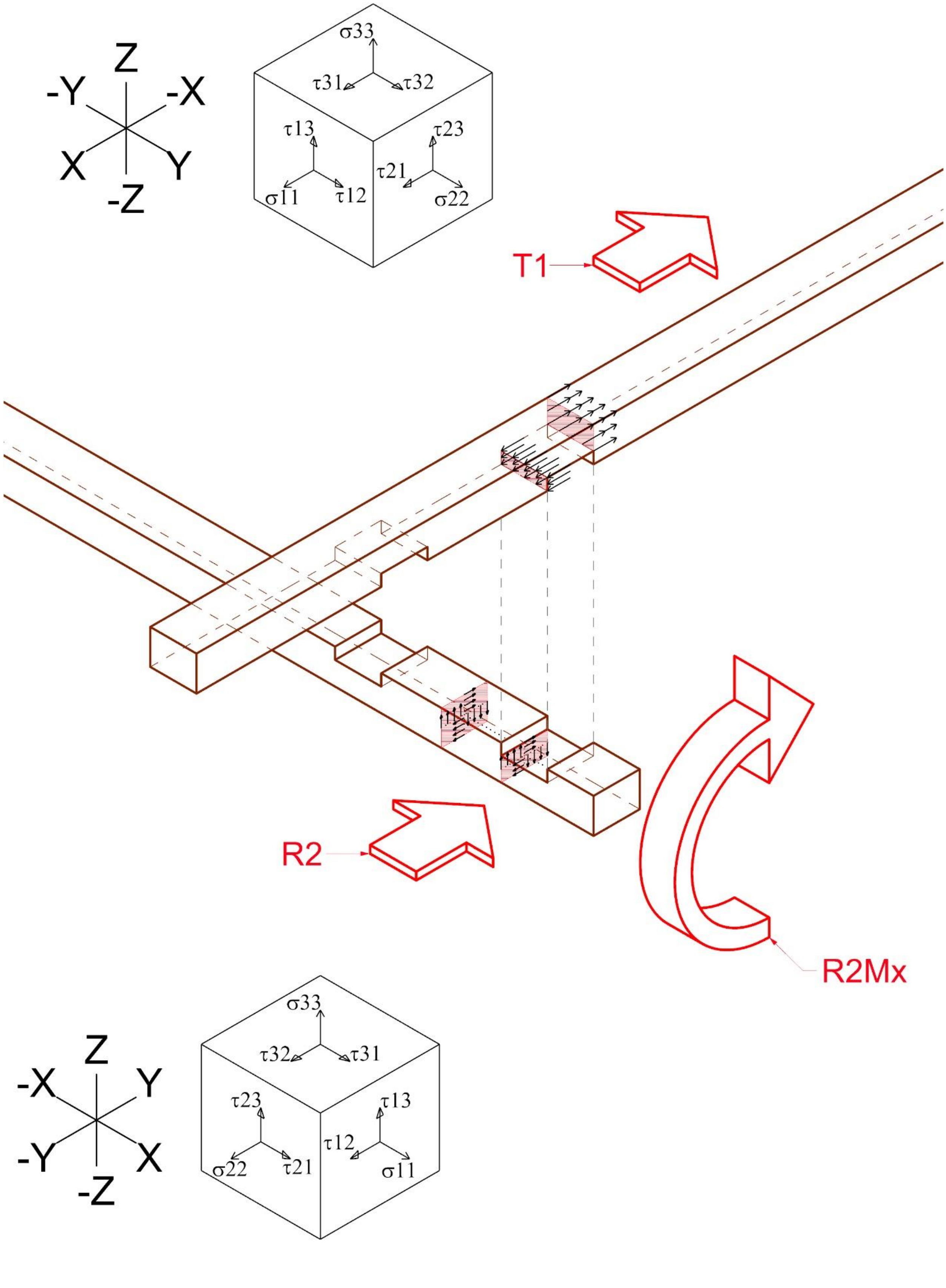

Figure 6-74 Roof Rafter Head Bending moments: Torsion: Tangential stresses: Crossing rafters T1-R2

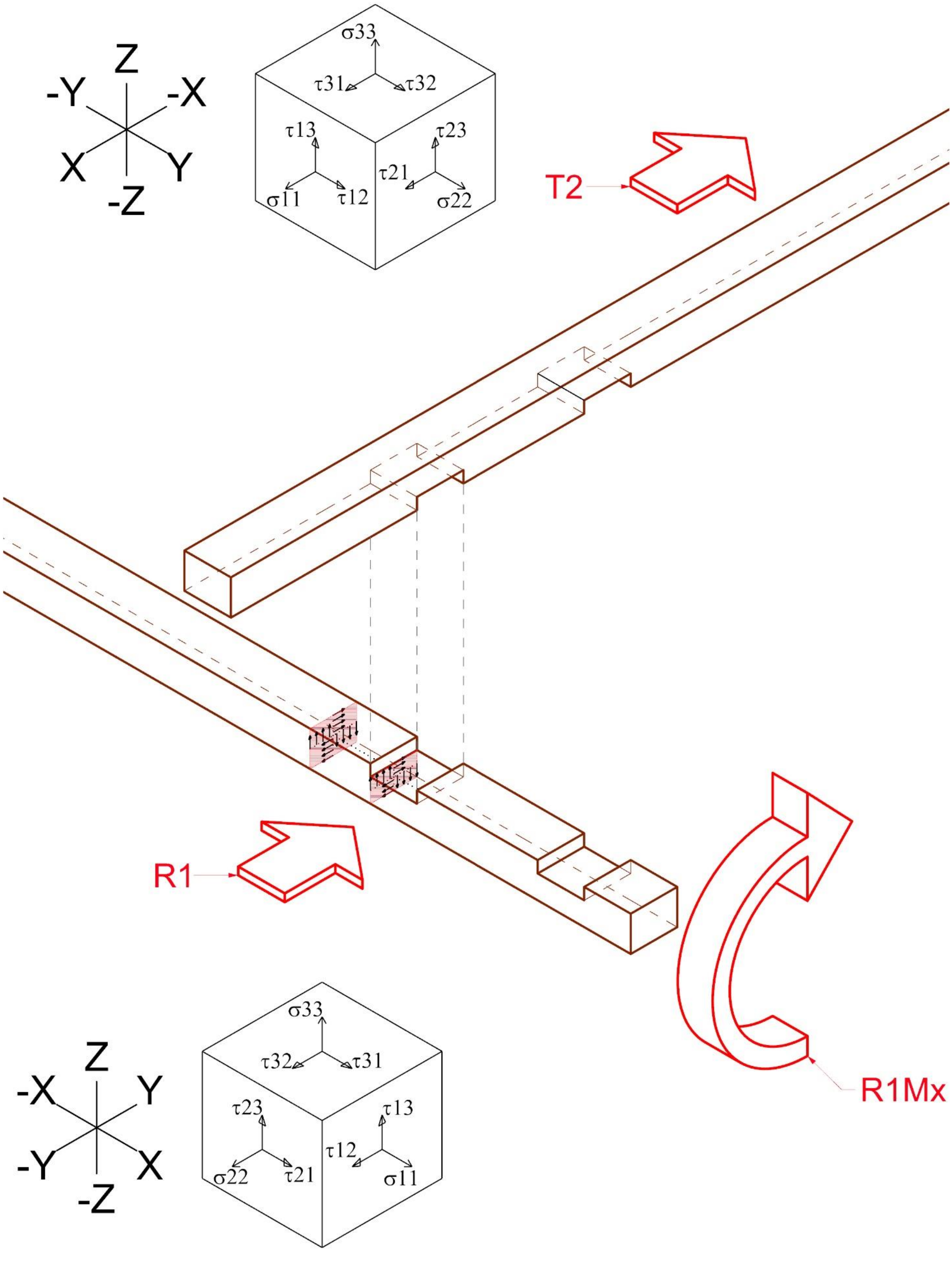

Figure 6-75 Roof Rafter Head Bending moments: Torsion: Tangential stresses: Crossing rafters T2-R1

6.9.3 Activation of the chain along Rafter Head

In accordance to what has been written for the roof rafter head it has been studied in the same way the behavior of the rafter head because the failure mechanism may be activated in the perpendicular direction studied for the roof rafter head.

The forces developed in the chains are sheared in the rafters, this repartitions will be described in the following chapters because it is different for the different failure mechanisms.

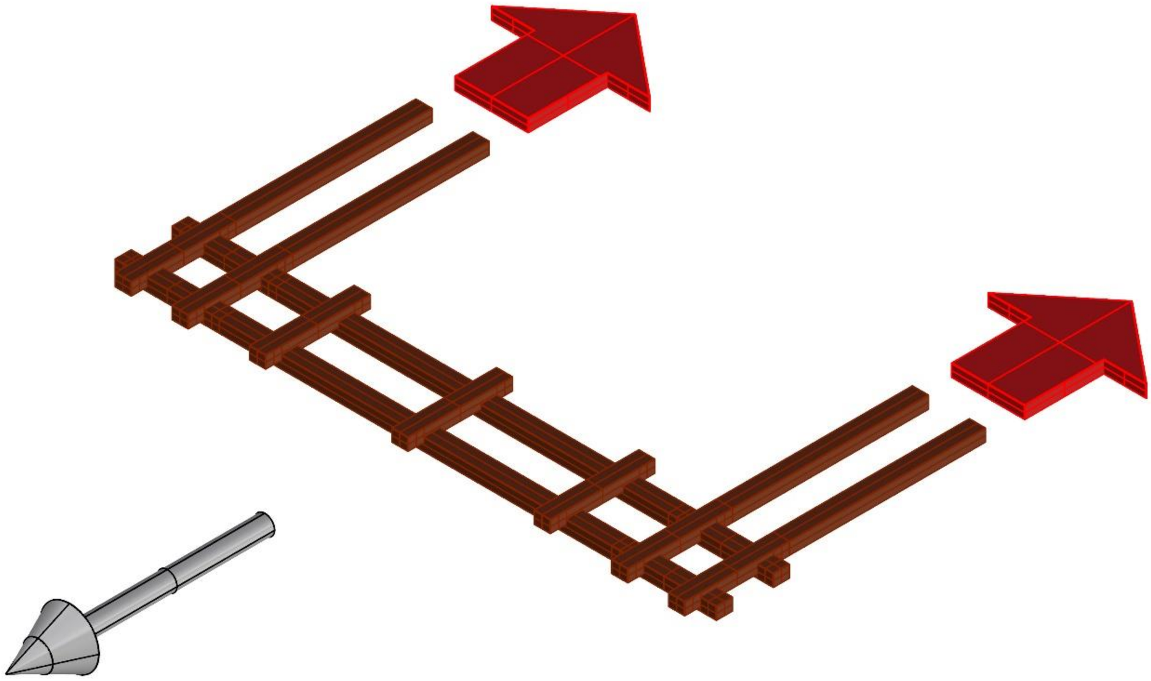

Figure 6-76 Roof timber beam subjected to seismic actions (normal rafter)

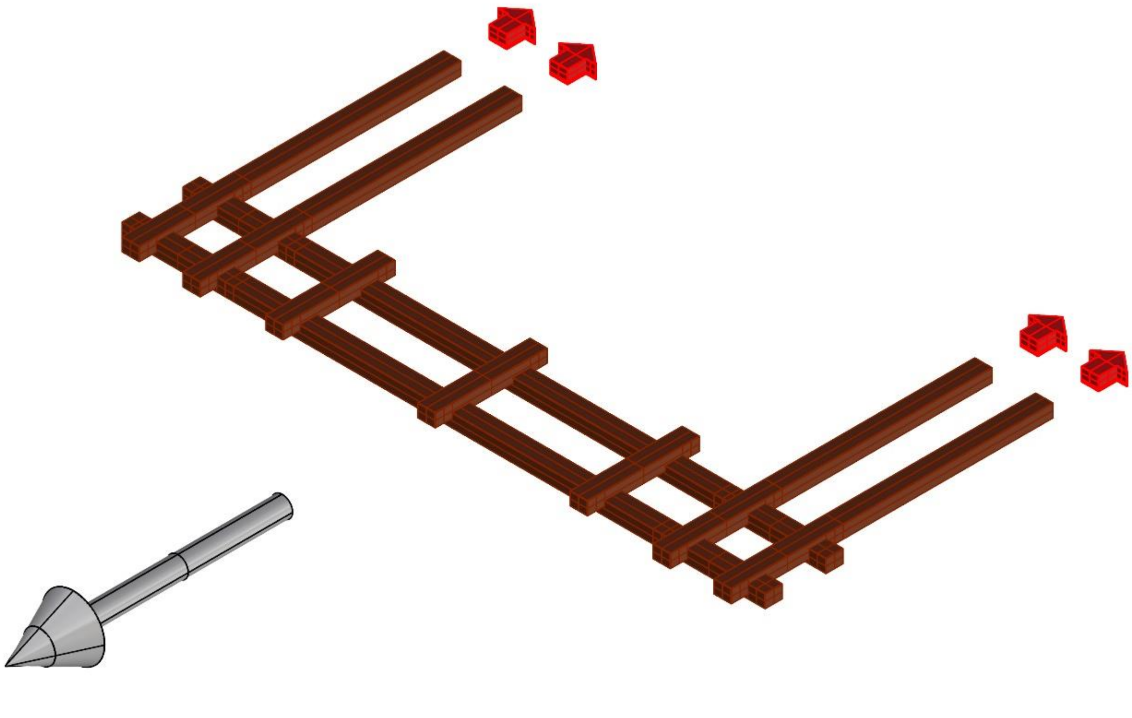

Figure 6-77 Repartitions of forces - Roof timber beam subjected to seismic actions (normal rafter)

In order to describe the behavior of the corner joint at the roof level they have been named the four rafters crossed in the corner joint, considering that the behavior of the structure in symmetric.The numbering always start from the external element to the internal.

The elements belonging to the failing wall have been named R# due to the fact that they are passive resisting elements. The rafter belonging to the timber beam working as a chain have been named T# due to the fact that they are subjected mainly to tension.

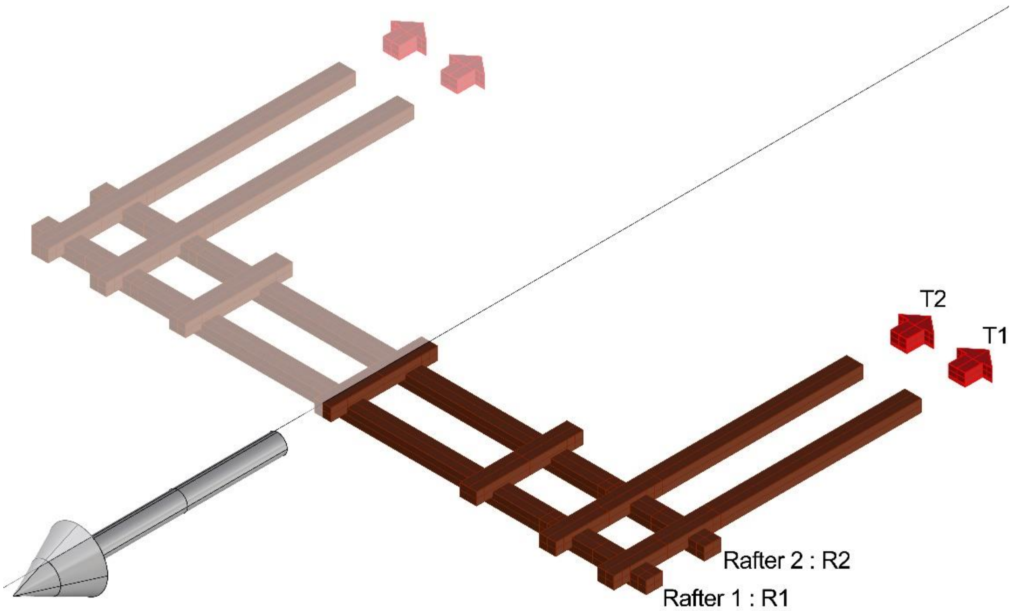

Figure 6-78 Descriptions of the rafters crossed at the roof timber beam actions (normal rafter)

Each intersection have been recolled as the summations of the names of the crossing rafters, as shown in the picture below.

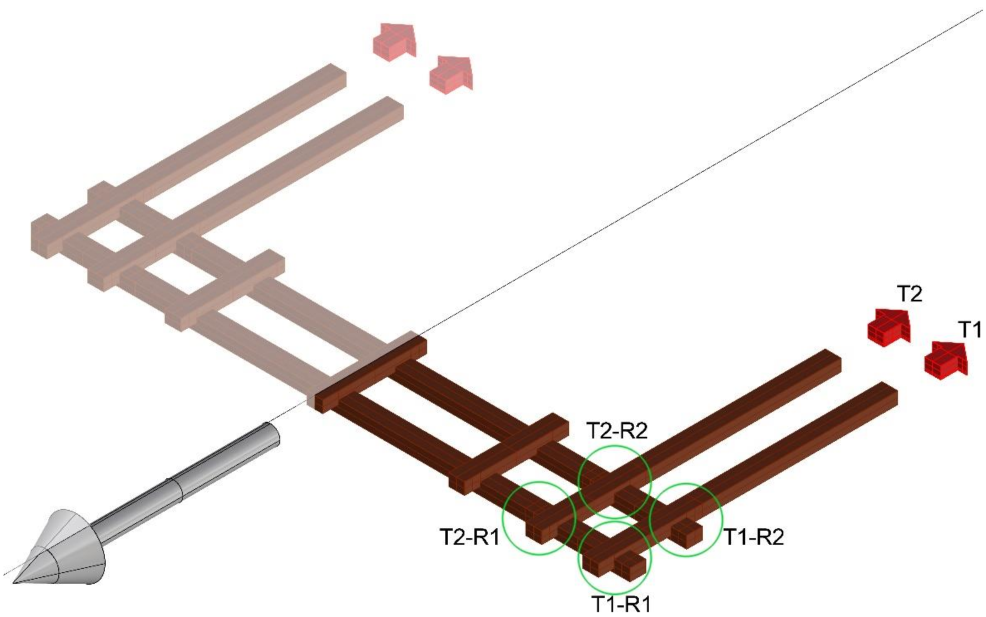

Figure 6-79 Description of the crossing rafters at roof level actions (normal rafter)

6.9.3.1 Axial forces

In the following pages they are described the stressed part of the timber elements and the hierarchy of the forces due to the activation of the chains .

6.9.3.1.1 Axial stresses

The following tables reports the values of the maximum allowed stresses and their position are shown in the following figures.

To be clear names must be read like these examples :

- RRH0tension : Roof Rafter Head - 0 = along the fibers – tens : in tension - A# stressed area
- RRH0compression : Roof Rafter Head - 0 = along the fibers – compression : in compression - A# stressed area
- RRH90compression : Roof Rafter Head - 90 = perpendicular to the fibers – compression : in compression - A# stressed area

Table 15 Roof rafter Head and Rafter head

RH0tension	A4	
N_0d	?	N
b	100,00	mm
h	50,00	mm
A_(net)	5000,00	mm^2
σ_(t,0,d)	#VALUE!	N/mm^2
kh	1,08	
f_(t,0,d)	30,80	N/mm^2
Verification	#VALUE!	
N_(od)max	154,00	kN

RH0compression	A3	
N_0d	?	N
b	100,00	mm
h	25,00	mm
A_(net)	2500,00	mm^2
σ_(c,0,d)	#VALUE!	N/mm^2
f_(c,0,d)	24,93	N/mm^2
Verification	#VALUE!	
N_(od)max	62,33	kN

RH90compression	A3	
N_90d	?	N
b	100,00	mm
h	25,00	mm
A_(net)	2500,00	mm^2
σ_(c,90,d)	#VALUE!	N/mm^2
k_(c,90)	1,50	
f_(c,90,d)	9,90	N/mm^2
Verification	#VALUE!	
N_(90d)max	16,50	kN

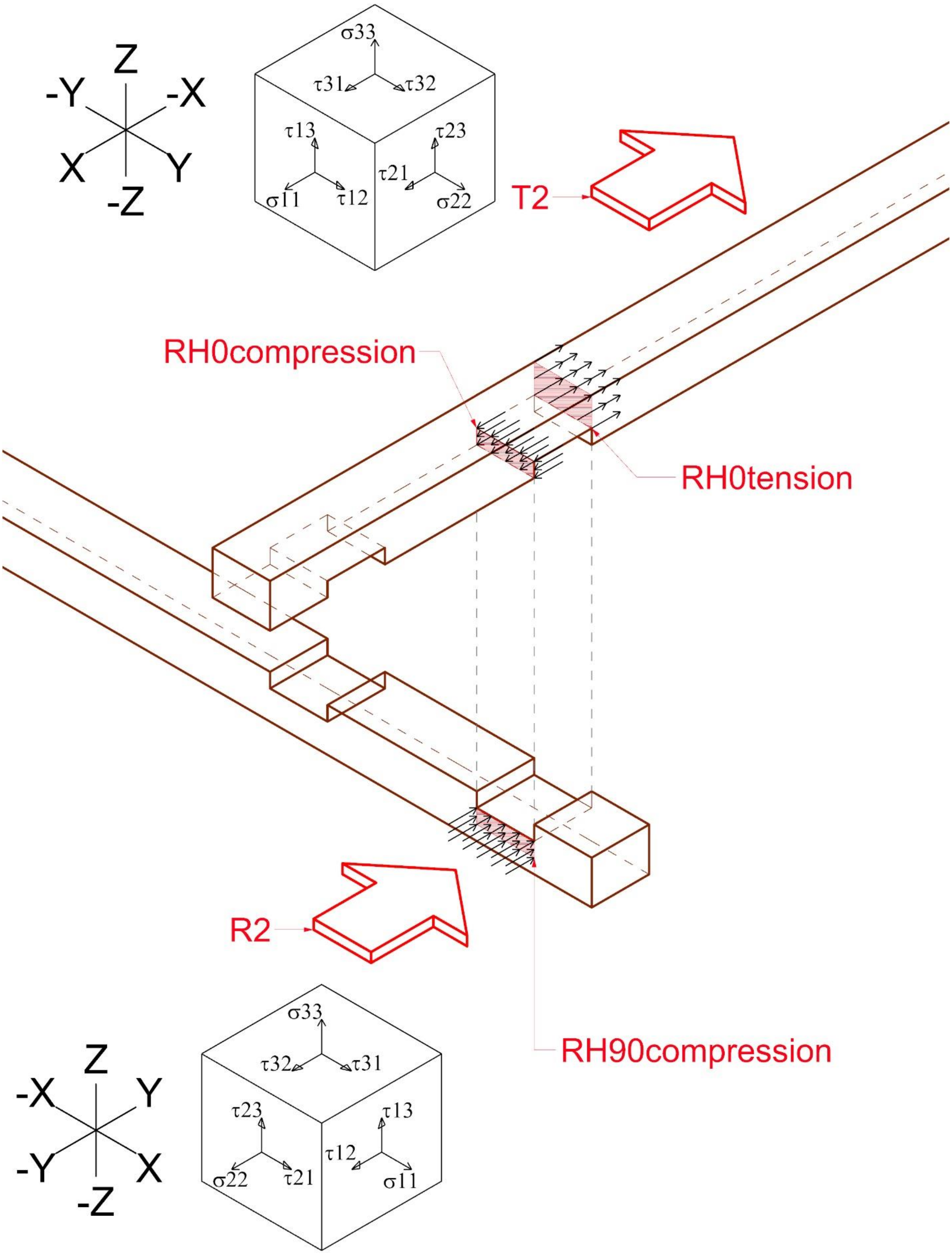

Figure 6-80 Rafter Head Axial stresses: Crossing rafters T2-R2

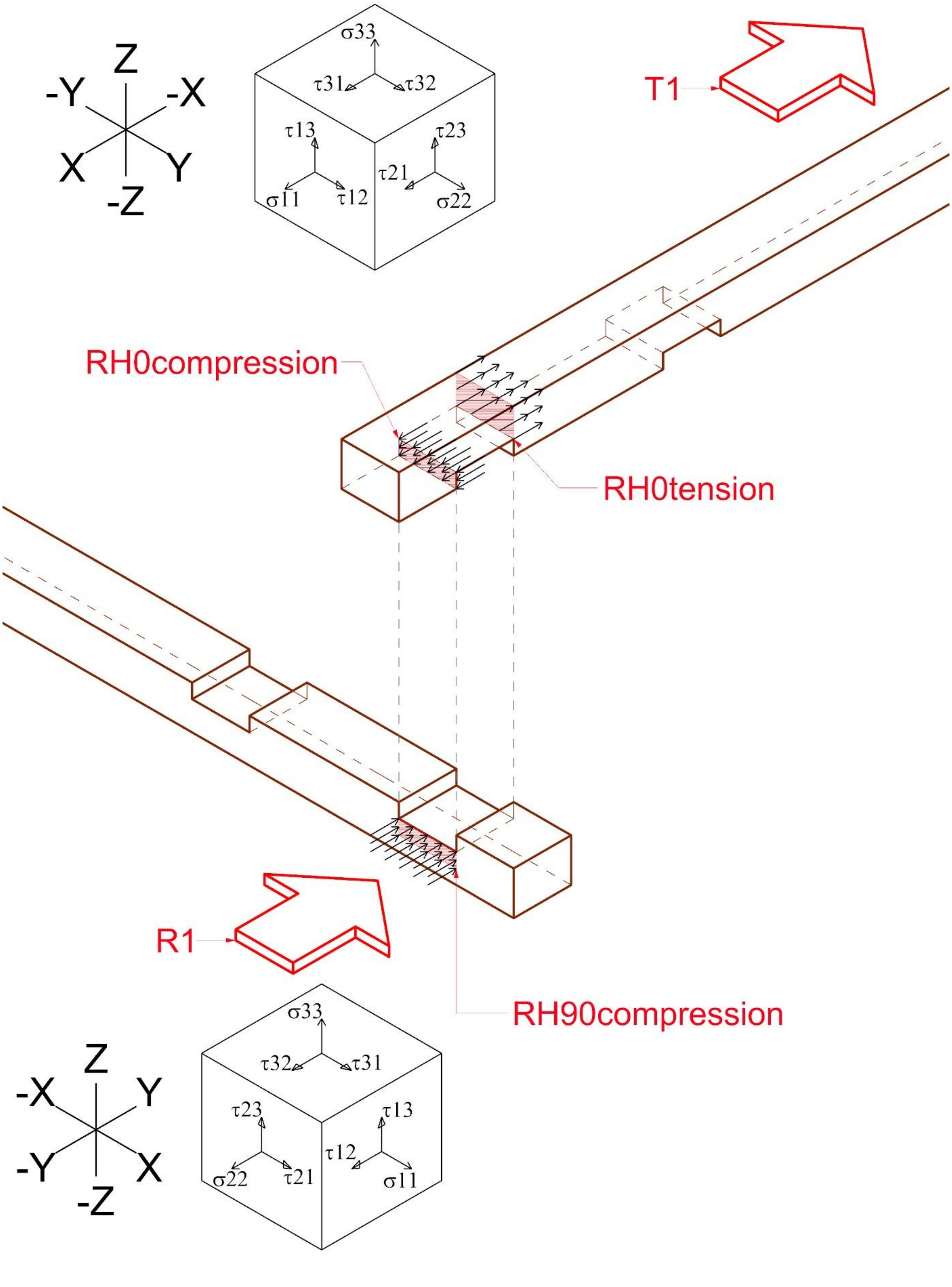

Figure 6-81 Rafter Head Axial stresses: Crossing rafters T1-R1

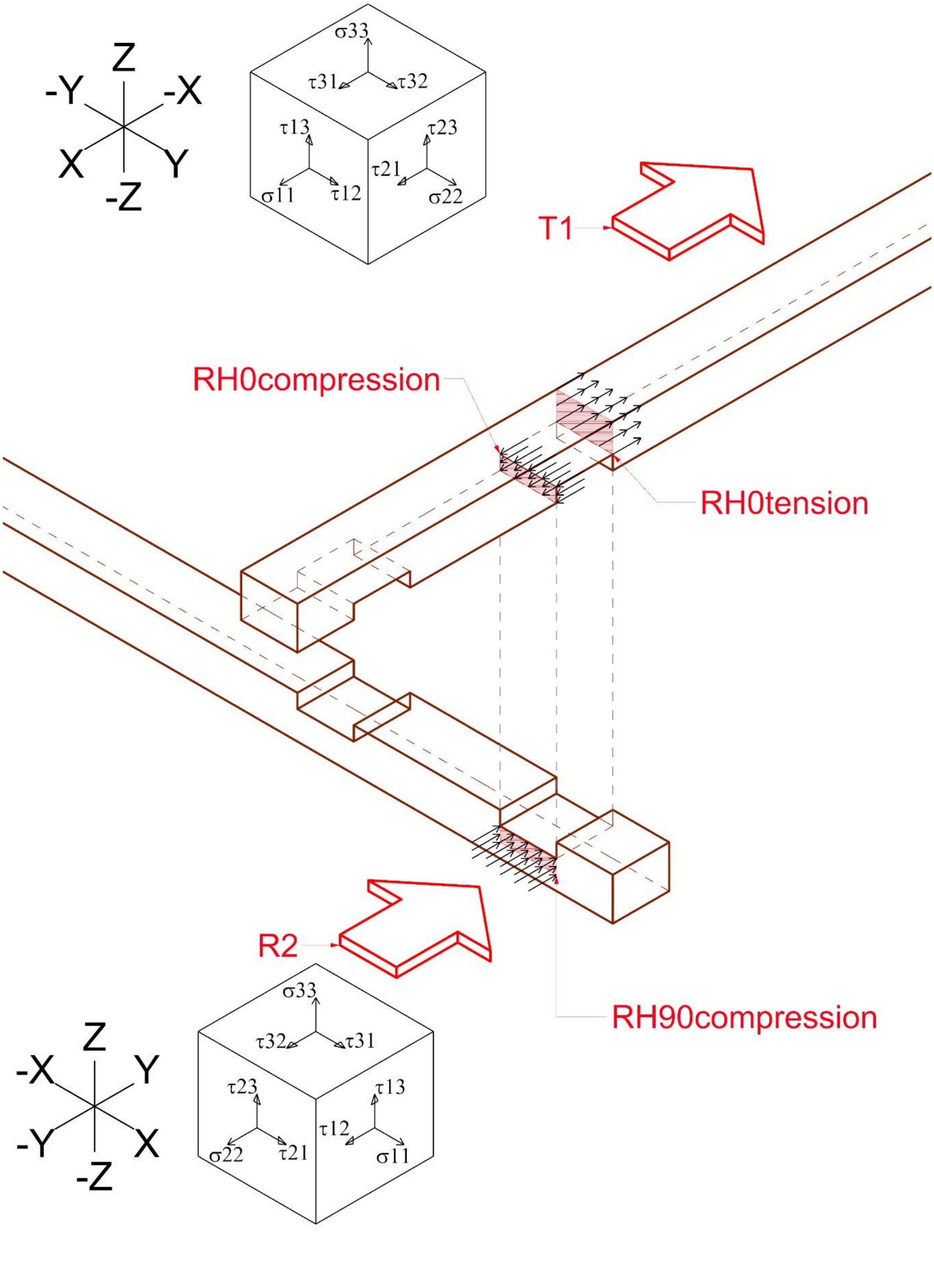

Figure 6-82 Rafter Head Axial stresses: Crossing rafters T1-R2

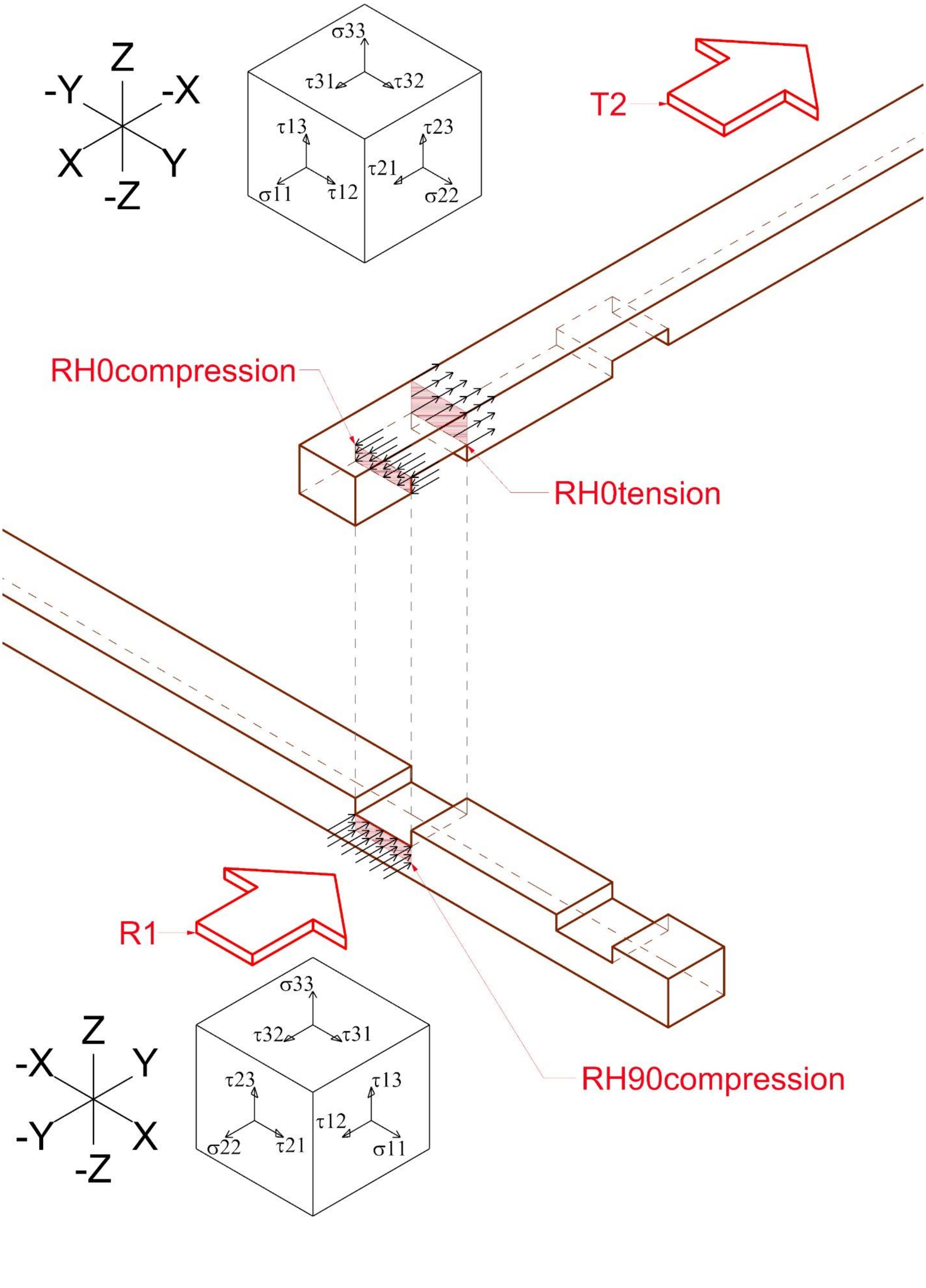

Figure 6-83 Rafter Head Axial stresses: Crossing rafters T2-R1

6.9.3.1.2 Tangential stresses

As before, the names are related to the timber elements and to the subjected stresses.

- RH0shearEXT : Rafter Head - 0 = along the fibers – shear : under shear force – EXT : external surface - - A# stressed area
- RH0shearINT : Rafter Head - 0 = along the fibers – shear : under shear force – INT : internal surface - - A# stressed area
- RH90shear : Head - 90 = perpendicular to the fibers – shear : under shear force - A# stressed area
- RH0shearEXT, RH0shearINT, and RH90shear: are computed in case of just pure shear force or shear force and bending moment acting at the same time.

RH0shearEXT	A2	
with bending		
V_0d	?	N
K_cr	0,67	
A_(net)	6700,00	mm^2
τ_(d)	#VALUE!	N/mm^2
f_(v,d)	3,67	N/mm^2
Verification	#VALUE!	
V_0d max	16,38	kN

RH0shearINT	A1	
with bending , " = RRH0shearINT "		
V_0d	?	N
K_cr	0,67	
A_(net)	17420,00	mm^2
τ_(d)	#VALUE!	N/mm^2
f_(v,d)	3,67	N/mm^2
Verification	#VALUE!	
V_0d max	42,58	kN

RH0shearEXT	A2	
V_0d	?	N
A_(net)	10000,00	mm^2
τ_(d)	#VALUE!	N/mm^2
f_(v,d)	3,67	N/mm^2
Verification	#VALUE!	
V_0d max	24,44	kN

RH0shearINT	A1	
V_0d	?	N
A_(net)	26000,00	mm^2
τ_(d)	#VALUE!	N/mm^2
f_(v,d)	3,67	N/mm^2
Verification	#VALUE!	
V_0d max	63,56	kN

RH90shear	A5	
with bending		
V_90d	?	N
K_cr	0,67	
A_(net)	5025,00	mm^2
τ_(d)	#VALUE!	N/mm^2
ft,90,d	0,44	N/mm^2
f_(v,d)	0,88	N/mm^2
Verification	#VALUE!	
V_90d max	2,95	kN

RH90shear	A5	
V_90d	?	N
A_(net)	7500,00	mm^2
τ_(d)	#VALUE!	N/mm^2
ft,90,d	0,44	N/mm^2
f_(v,d)	0,88	N/mm^2
Verification	#VALUE!	
V_90d max	4,40	kN

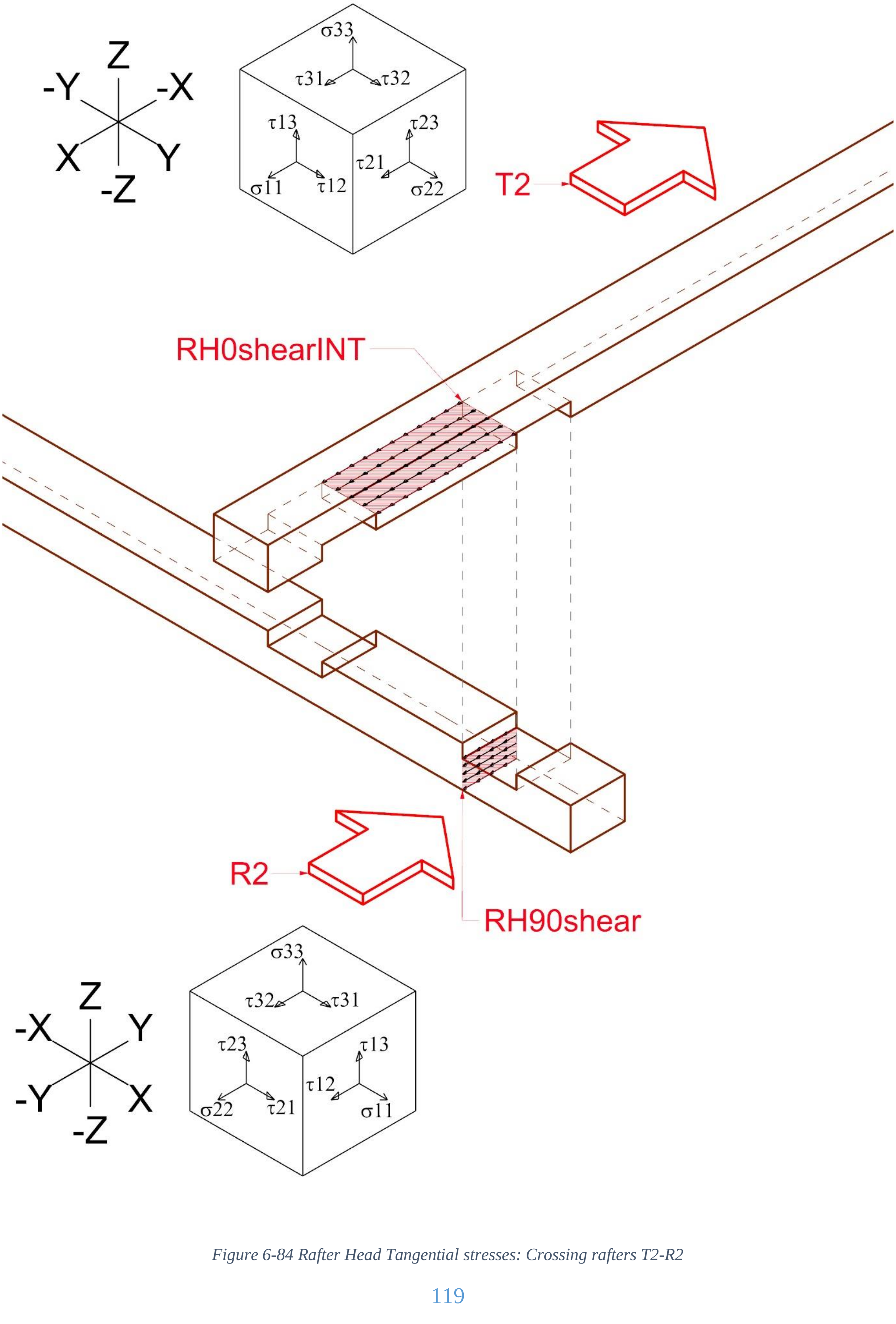

Figure 6-84 Rafter Head Tangential stresses: Crossing rafters T2-R2

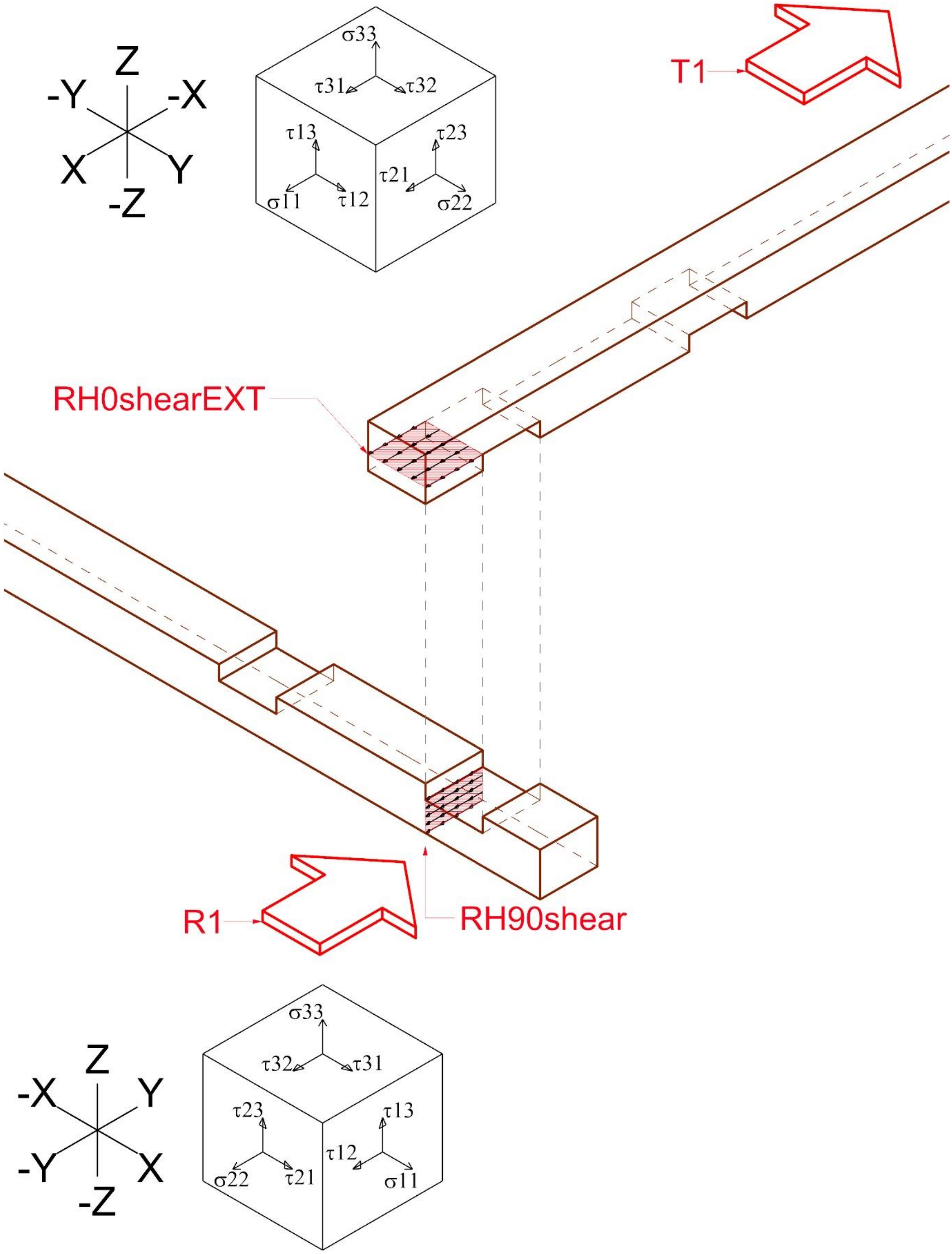

Figure 6-85 Rafter Head Tangential stresses: Crossing rafters T1-R1

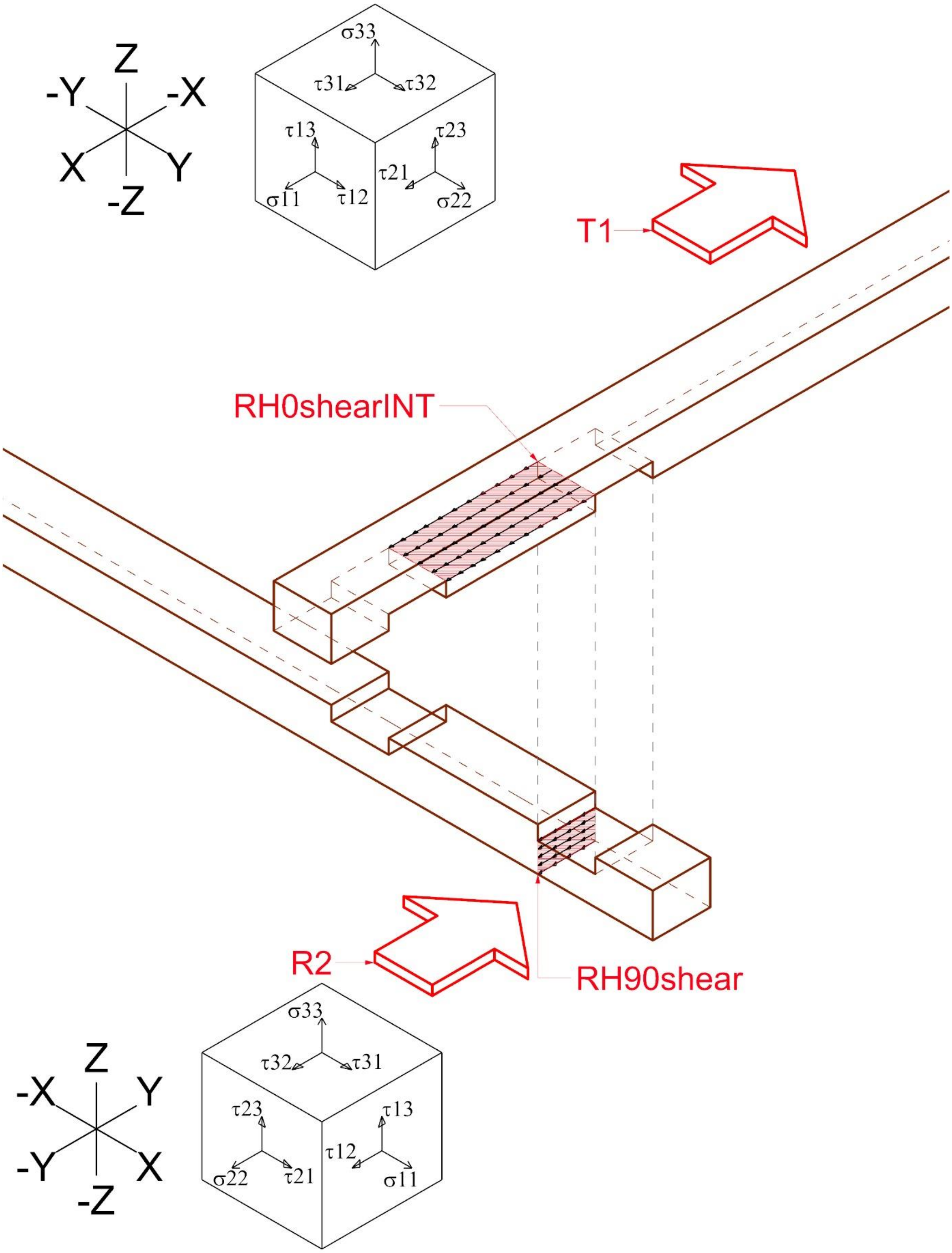

Figure 6-86 Rafter Head Tangential stresses: Crossing rafters T1-R2

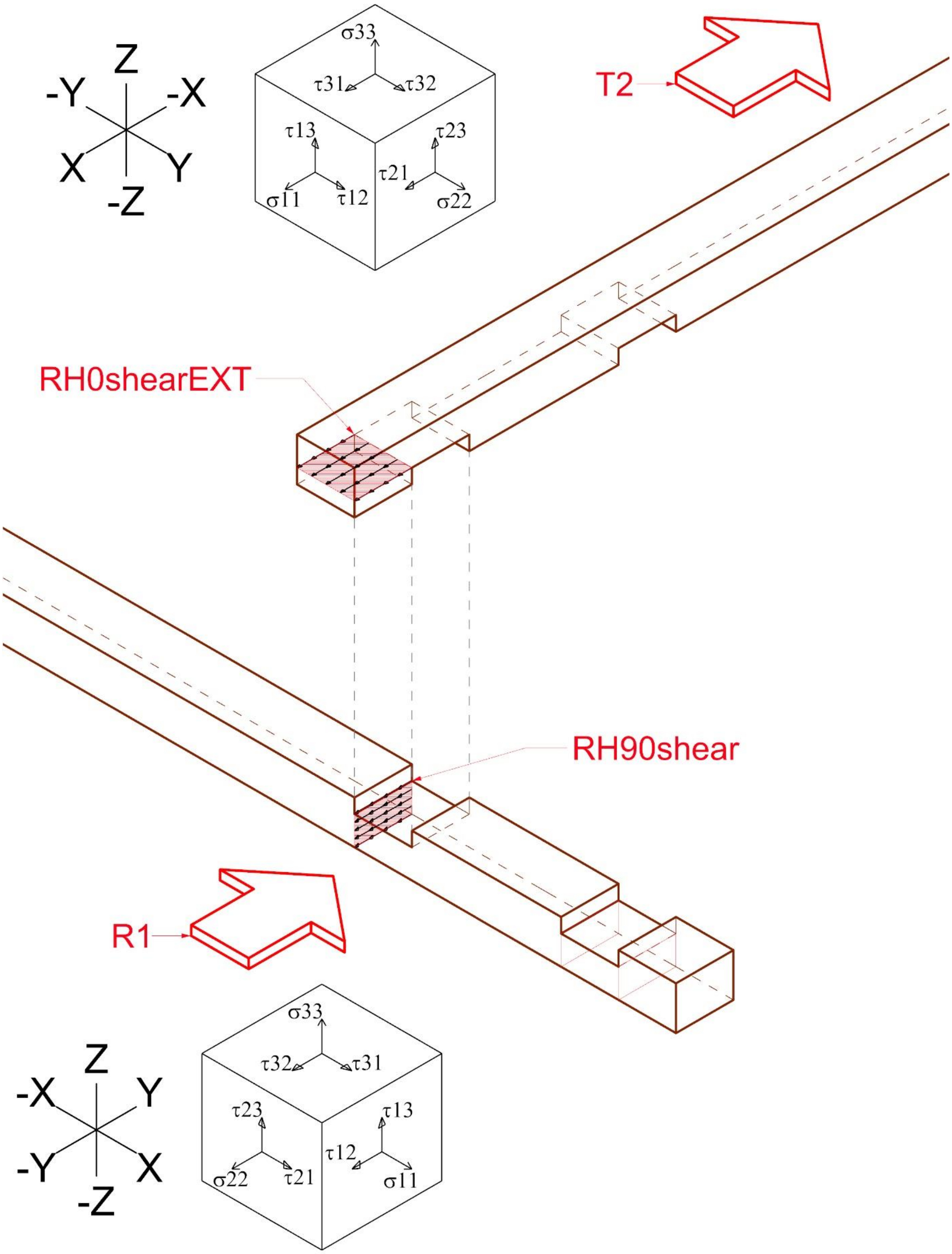

Figure 6-87 Rafter Head Tangential stresses: Crossing rafters T2-R1

6.9.3.2 Bending Moments

In the following figures are shown the “parasitic” bending moments developed congruently with the geometry of the timber elements and the applied actions. In the following paragraph it will be shown how the values of each bending moment has been computed.

6.9.3.2.1 Bending Moments : Axial stresses

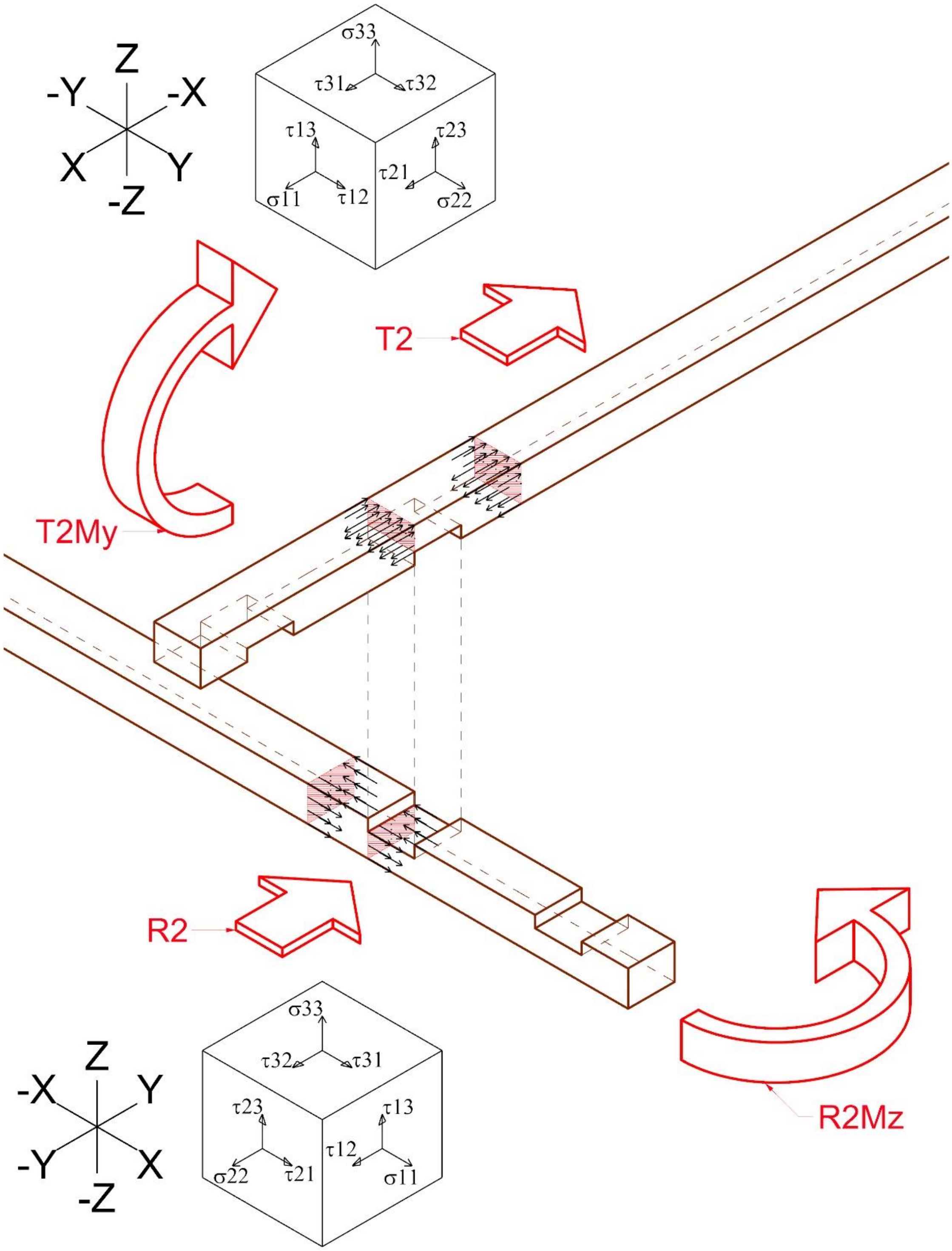

Figure 6-88 Rafter Head Bending moments: Axial stresses: Crossing rafters T2-R2

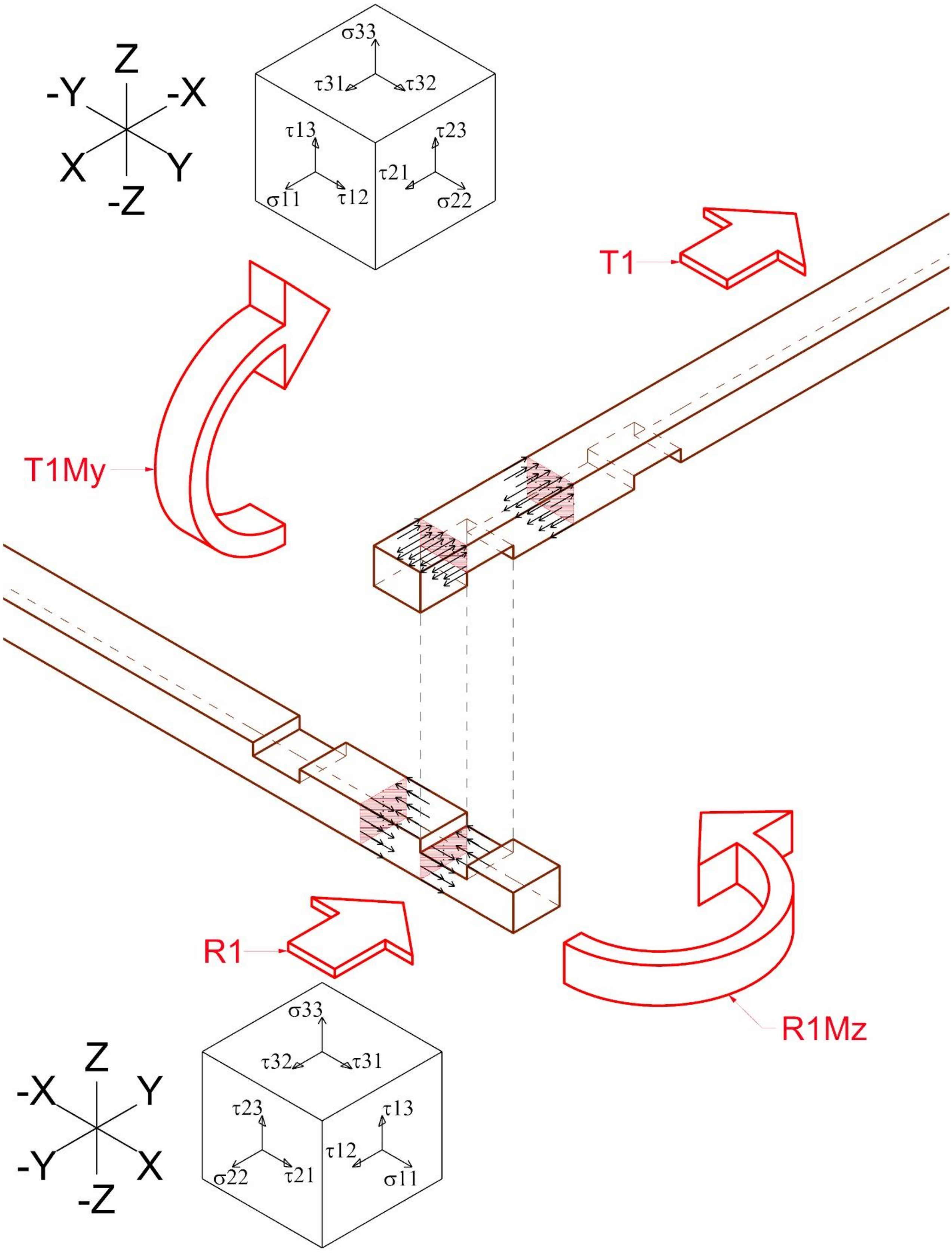

Figure 6-89 Rafter Head Bending moments: Axial stresses: Crossing rafters T1-R1

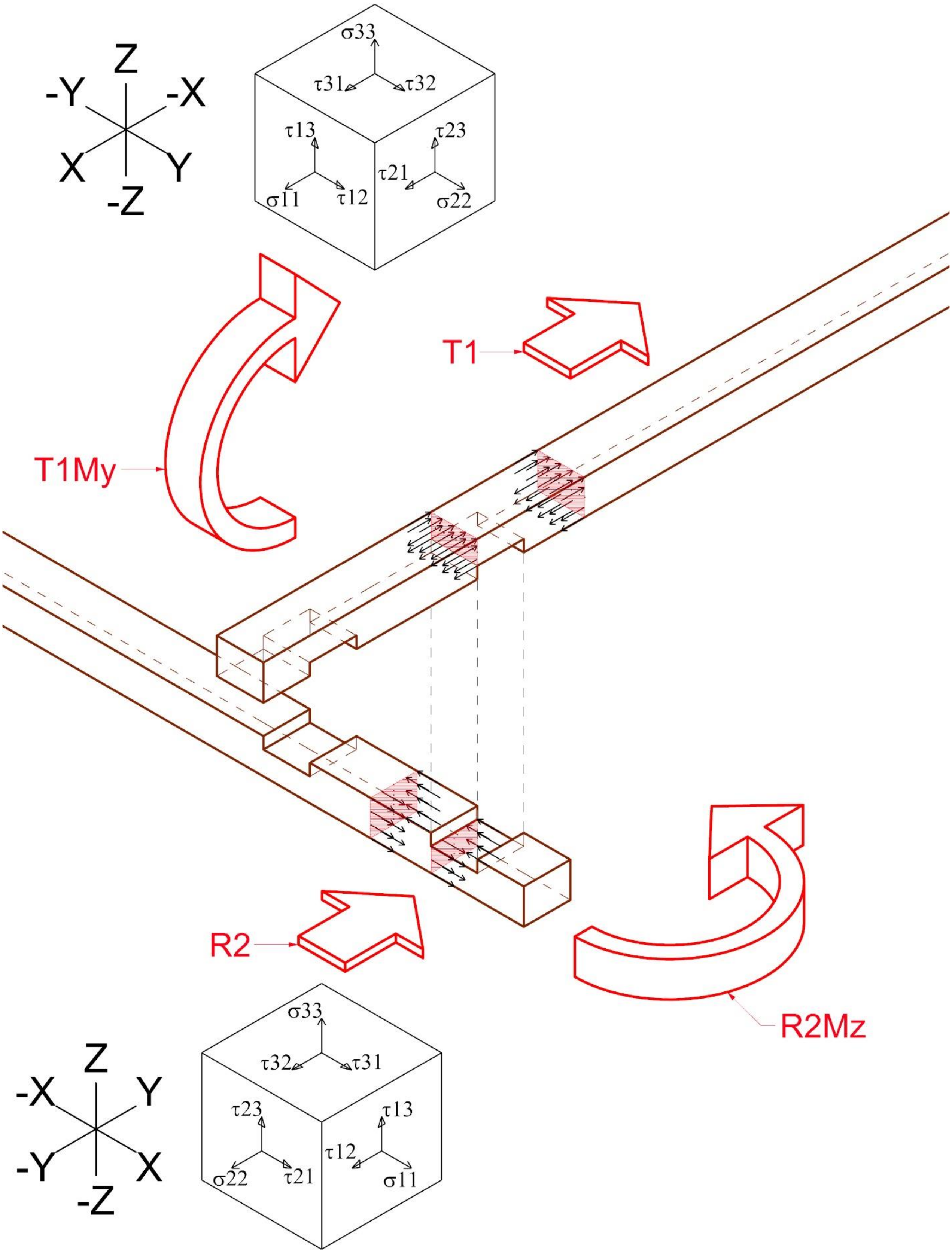

Figure 6-90 Rafter Head Bending moments: Axial stresses: Crossing rafters T1-R2

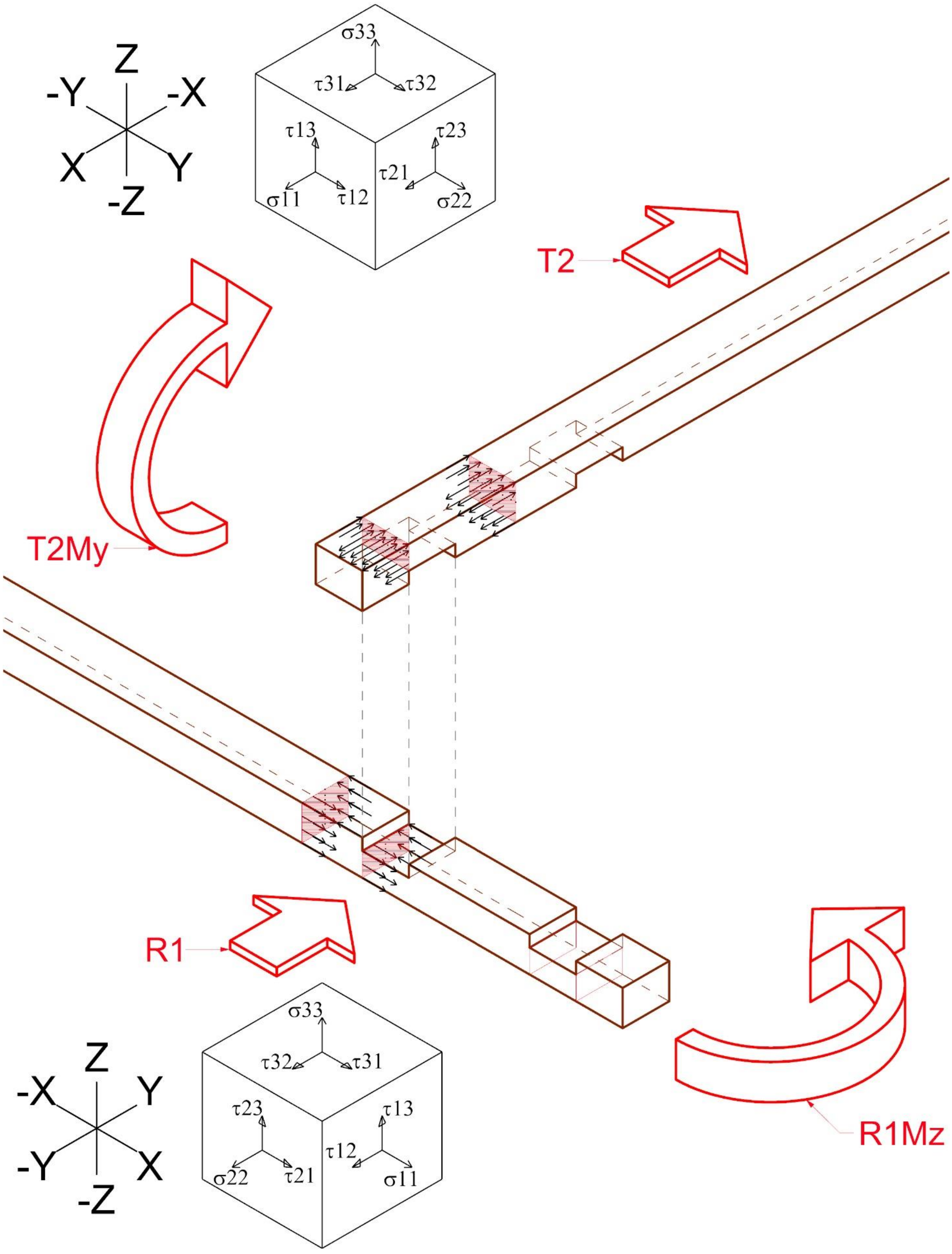

Figure 6-91 Rafter Head Bending moments: Axial stresses: Crossing rafters T2-R1

6.9.3.2.2 Torsnion : Tangential stresses

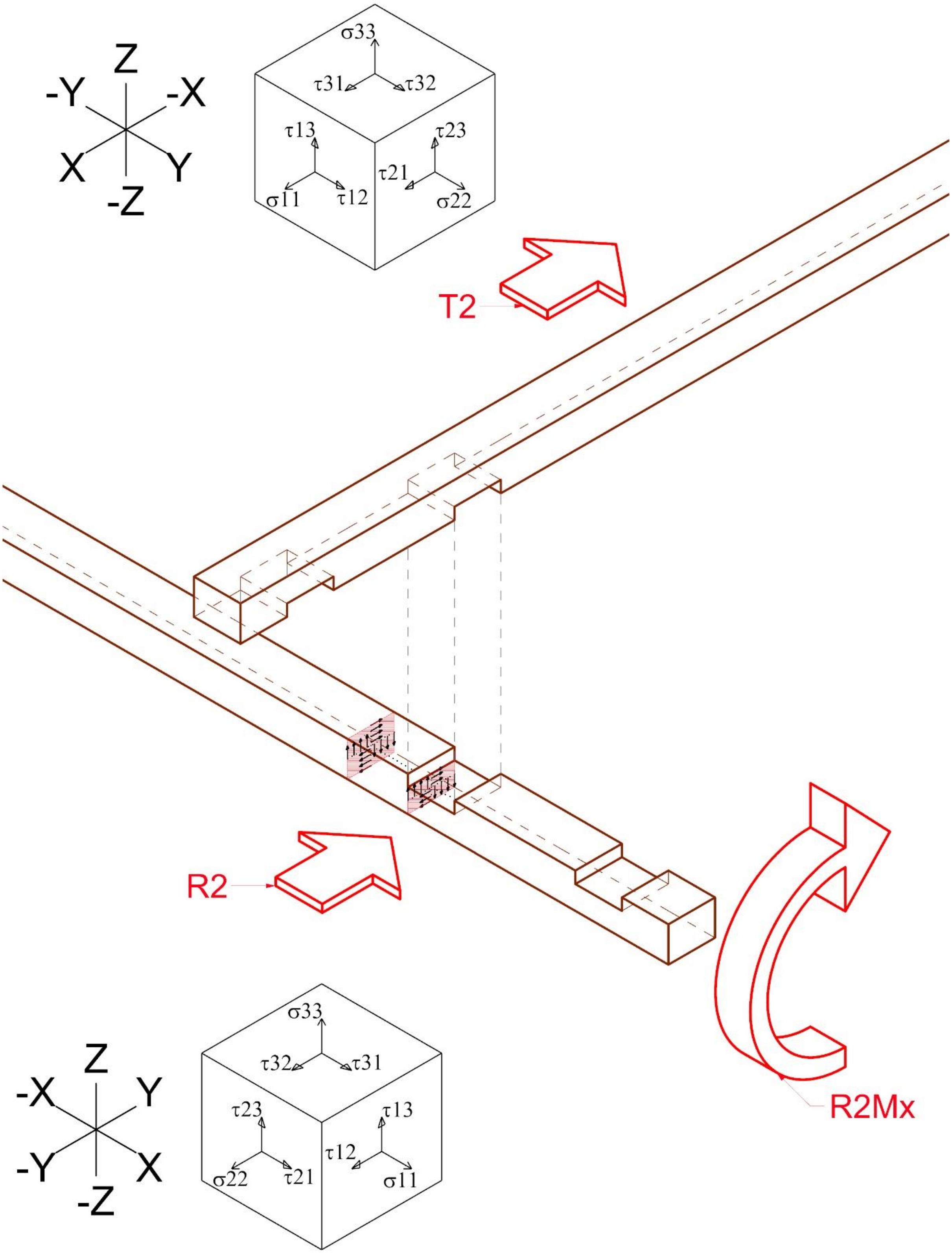

Figure 6-92 Rafter Head Bending moments: Torsnion : Tangential stresses : Crossing rafters T2-R2

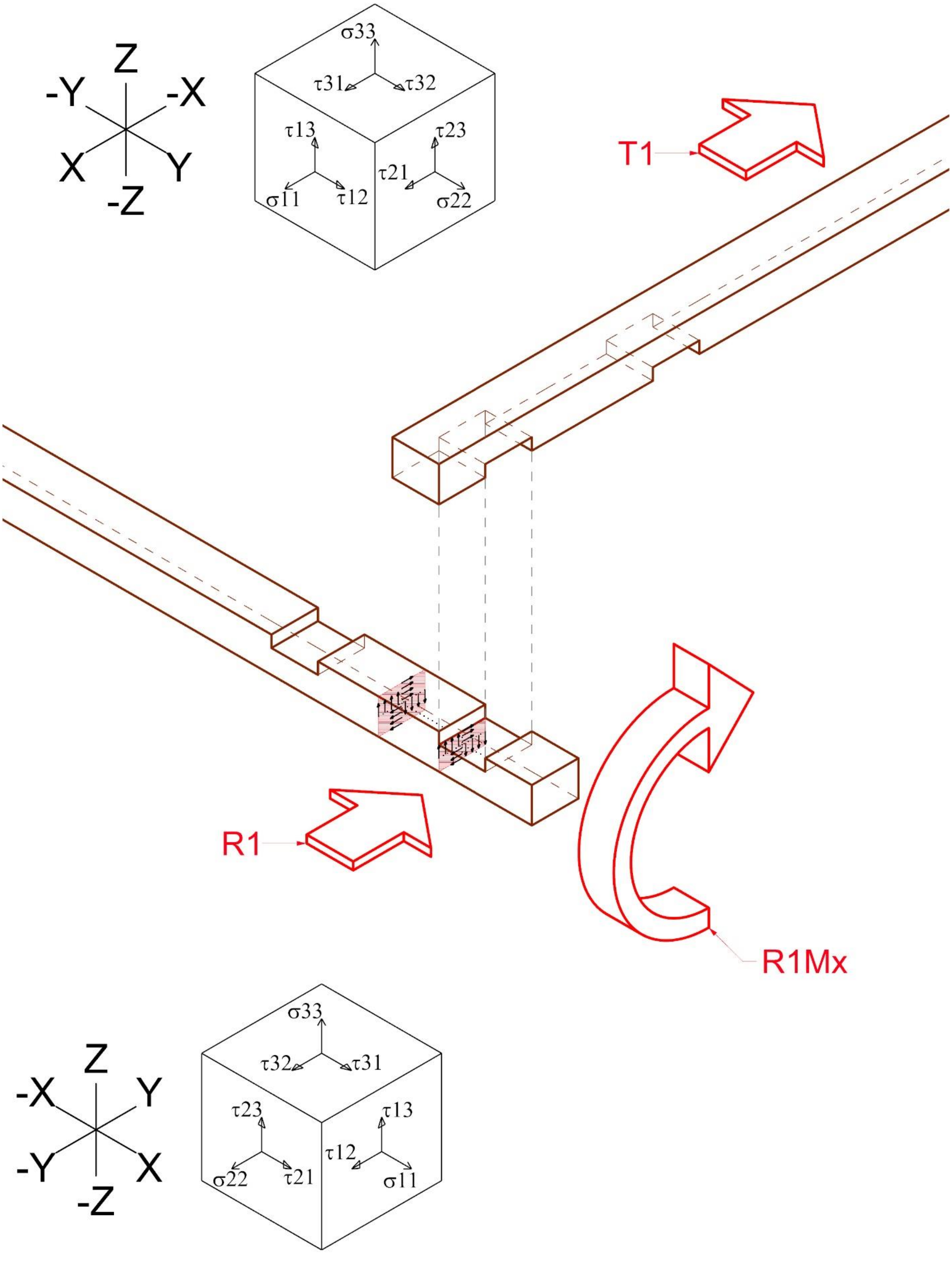

Figure 6-93 Rafter Head Bending moments: Torsion: Tangential stresses: Crossing rafters T1-R1

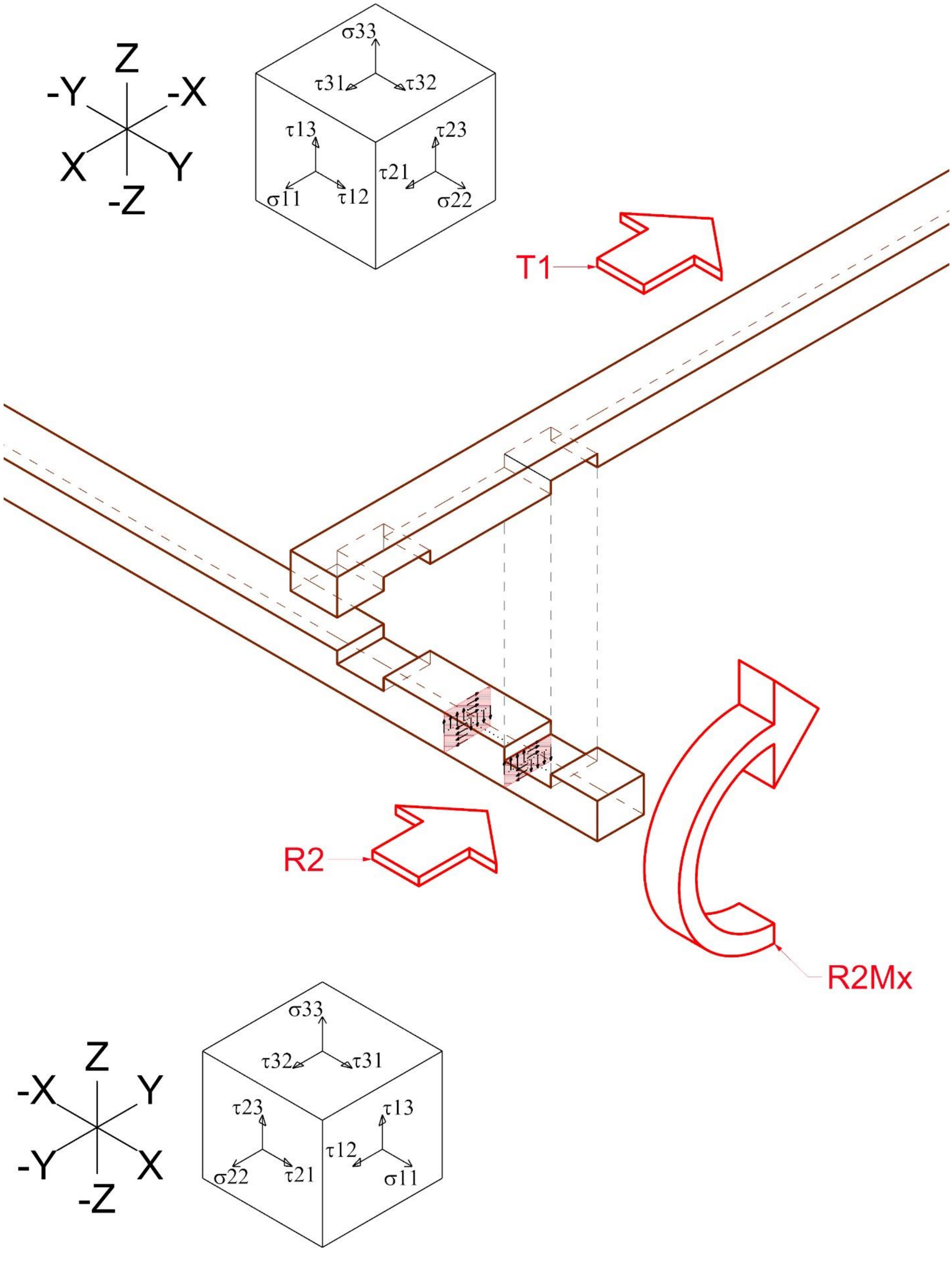

Figure 6-94 Rafter Head Bending moments: Torsion: Tangential stresses: Crossing rafters T1-R2

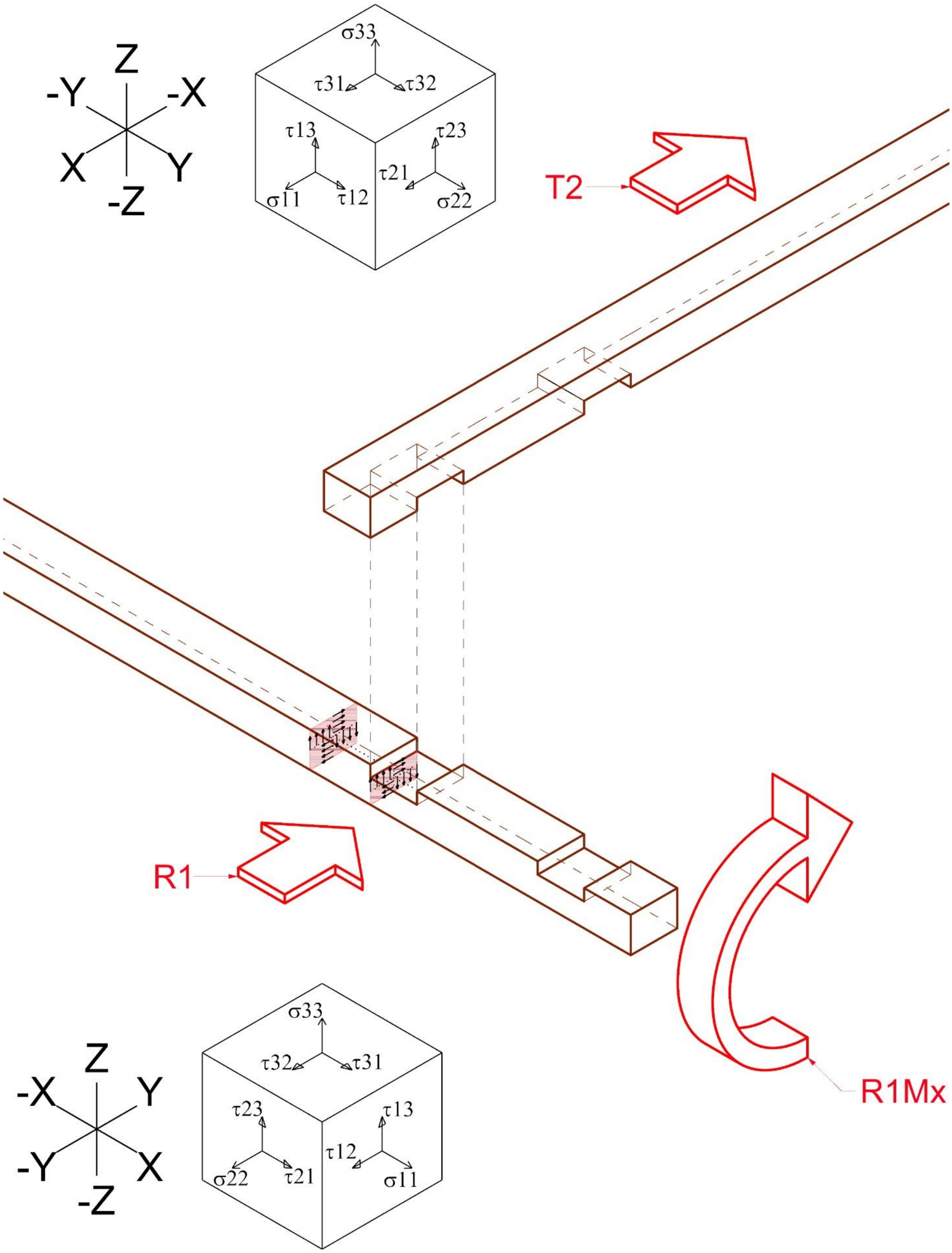

Figure 6-95 Rafter Head Bending moments: Torsion: Tangential stresses: Crossing rafters T2-R1

6.9.1 Possible actions along cross pieces

For further information they have been studied three possible actions along the cross pieces. The cross pieces may be subjected to compression, to tension or to a third case which has named “friction/inertia” and which subject the cross piece to a shear stress due to contrast of the timber beam and the inertia of the stones layer.

6.9.1.1 Compression

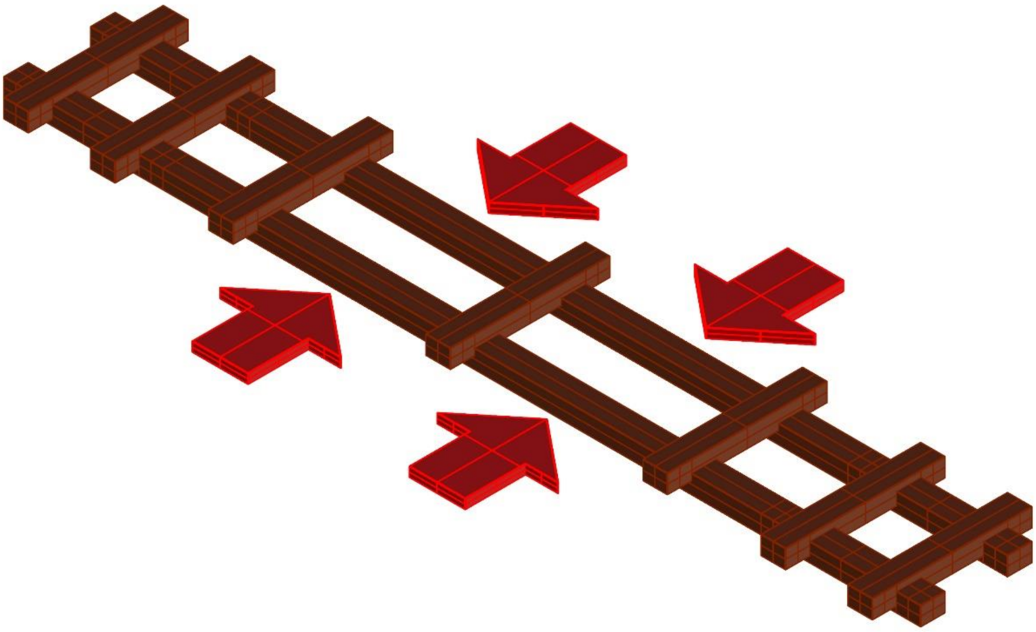

Figure 6-96 Cross Piece – Compression

As before the names are related to the timber elements and to the subjected stresses.

- CP0compression : Cross piece - 0 = along the fibers – compression : under compression - A# stressed area
- RB90compression : Rafter Body - 90 = perpendicular to the fibers – compression : under compression - A# stressed area
- RB90shear : Rafter Body - 90 = perpendicular to the fibers – shear : under shear force - A# stressed area
- RB90shear : is computed in case of just pure shear force or shear force and bending moment acting at the same time.

CP0compression	A3	
N_0d	?	N
b	100,00	mm
h	25,00	mm
A_(net)	2500,00	mm^2
σ_(c,0,d)	#VALUE!	N/mm^2
f_(c,0,d)	24,93	N/mm^2
Verification	#VALUE!	
N_(0d)max	62,33	kN

RB90compression	A3	
N_90d	?	N
b	100,00	mm
h	25,00	mm
A_(net)	2500,00	mm^2
σ_(c,90,d)	#VALUE!	N/mm^2
k_(c,90)	1,50	
f_(c,90,d)	9,90	N/mm^2
Verification	#VALUE!	
N_(90d)max	16,50	kN

RB90shear	A5	
with bending		
V_90d	?	N
K_cr	0,67	
A_(net)	5025,00	mm^2
τ_(d)	#VALUE!	N/mm^2
ft,90,d	0,44	N/mm^2
f_(v,d)	0,88	N/mm^2
Verification	#VALUE!	
V_90d max	2,95	kN

RB90shear	A5	
V_90d	#VALUE!	N
A_(net)	7500,00	mm^2
τ_(d)	#VALUE!	N/mm^2
ft,90,d	0,44	N/mm^2
f_(v,d)	0,88	N/mm^2
Verification	#VALUE!	
V_90d max	4,40	kN

6.9.1.1.1 Axial stresses

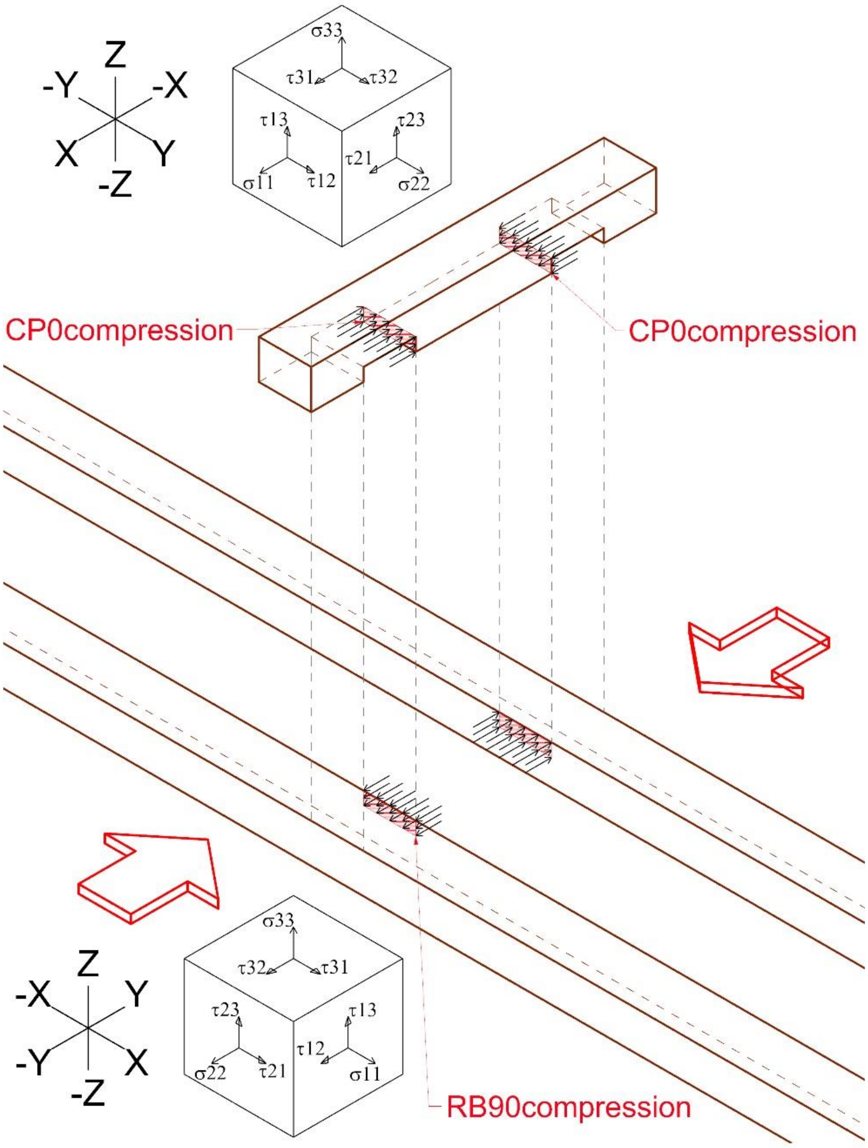

Figure 6-97 Cross Piece - Compression - Axial stresses

6.9.1.1.2 Tangential stresses

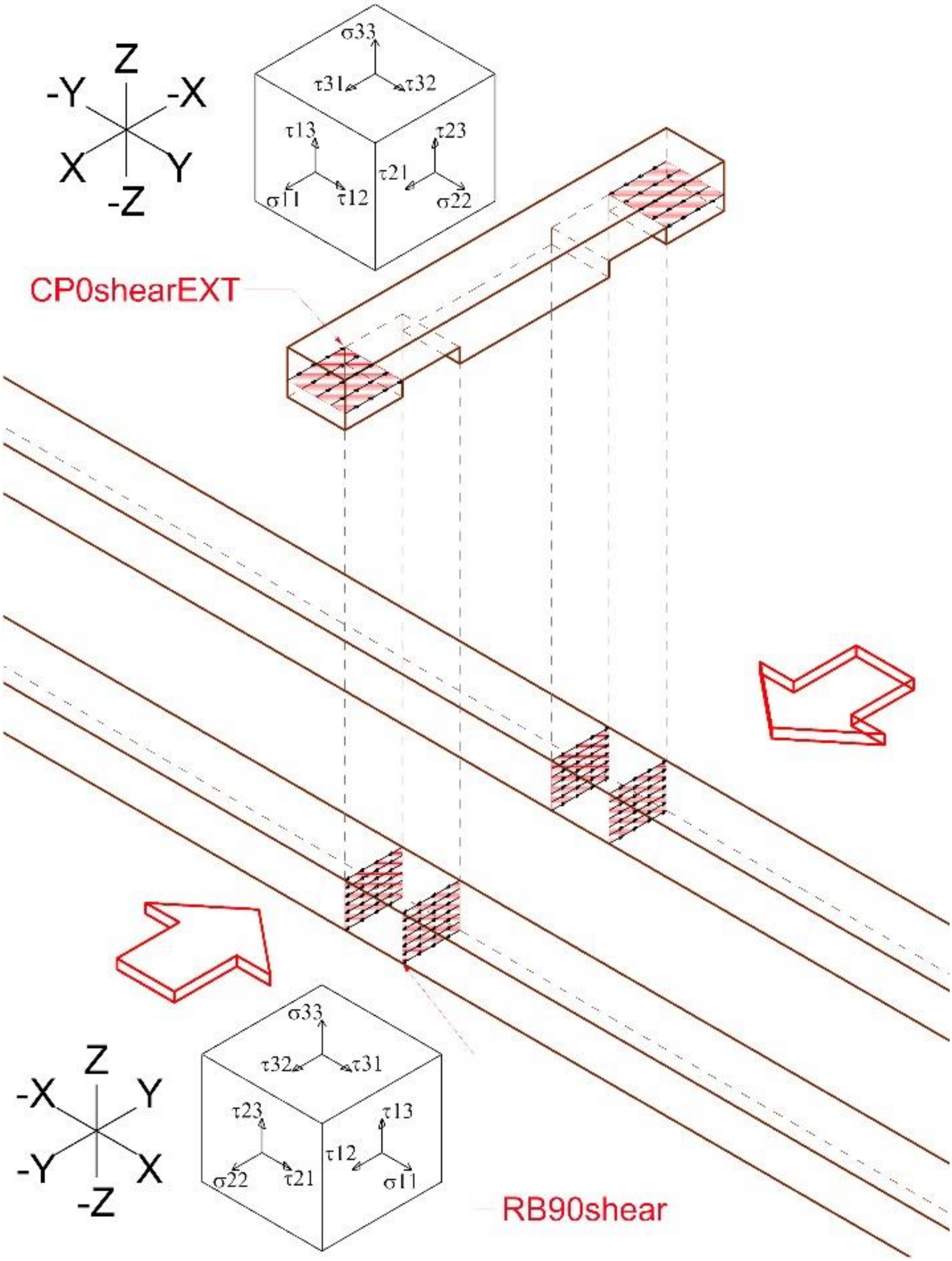

Figure 6-98 Cross Piece - Compression - Tangential stresses

6.9.1.2 Tension

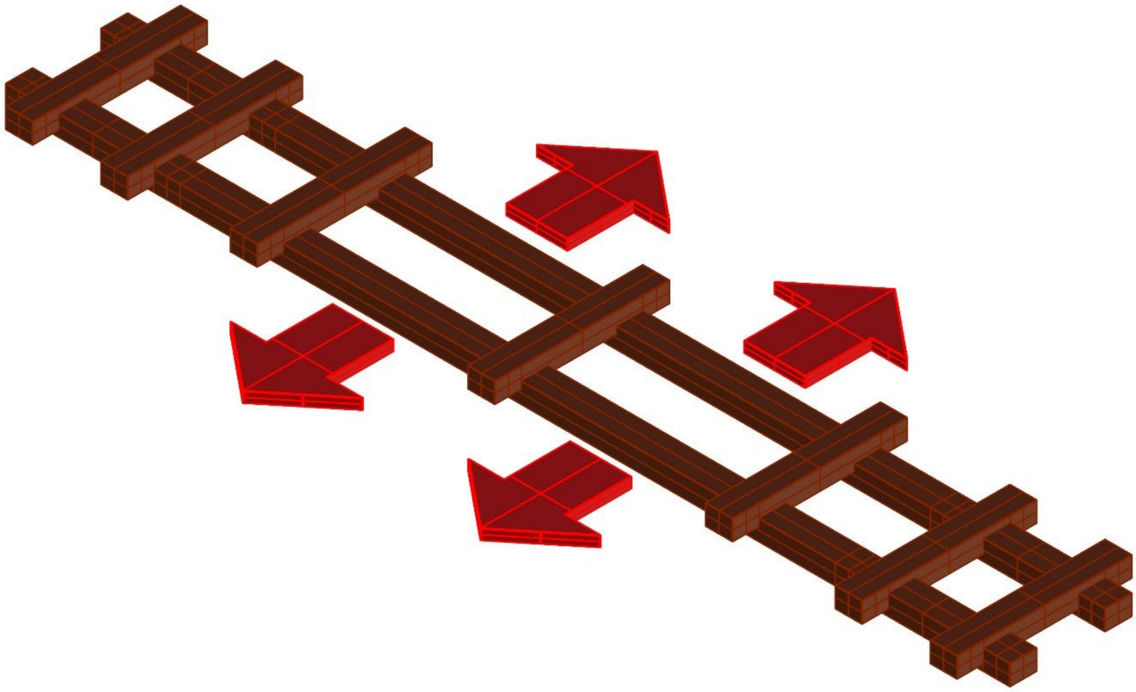

Figure 6-99 Cross Piece – Tension

- CP0tension : Cross piece - 0 = along the fibers – tension : under tension - A# stressed area
- CP0compression : Cross piece - 0 = along the fibers – compression : under compression - A# stressed area
- RB90compression : Rafter Body - 90 = perpendicular to the fibers – compression : under compression - A# stressed area
- CP0shearEXT:Cross piece - 0=along the fibers – shear : under shear force – EXT : external surface - A# stressed area
- RB90shear : Rafter Body - 90 = perpendicular to the fibers – shear : under shear force - A# stressed area
- CP0shearEXT and RB90shear : are computed in case of just pure shear force or shear force and bending moment acting at the same time.

CP0tension	A4	
N_0d	?	N
b	100,00	mm
h	50,00	mm
A_(net)	5000,00	mm^2
σ_(t,0,d)	#VALUE!	N/mm^2
kh	1,08	
f_(t,0,d)	30,80	N/mm^2
Verification	#VALUE!	
N_(0d)max	154,00	kN

CP0compression	A3	
N_0d	?	N
b	100,00	mm
h	25,00	mm
A_(net)	2500,00	mm^2
σ_(c,0,d)	#VALUE!	N/mm^2
f_(c,0,d)	24,93	N/mm^2
Verification	#VALUE!	
N_(0d)max	62,33	kN

RB90compression	A3	
N_90d	?	N
b	100,00	mm
h	25,00	mm
A_(net)	2500,00	mm^2
σ_(c,90,d)	#VALUE!	N/mm^2
k_(c,90)	1,50	
f_(c,90,d)	9,90	N/mm^2
Verification	#VALUE!	
N_(90d)max	16,50	kN

CP0shearEXT	A2	
with bending		
V_0d	?	N
K_cr	0,67	
A_(net)	6700,00	mm^2
τ_(d)	#VALUE!	N/mm^2
f_(v,d)	3,67	N/mm^2
Verification	#VALUE!	
V_0d max	16,38	kN

RB90shear	A5	
with bending		
V_90d	?	N
K_cr	0,67	
A_(net)	5025,00	mm^2
τ_(d)	#VALUE!	N/mm^2
ft,90,d	0,44	N/mm^2
f_(v,d)	0,88	N/mm^2
Verification	#VALUE!	
V_90d max	2,95	kN

CP0shearEXT	A2	
V_0d	#VALUE!	N
A_(net)	10000,00	mm^2
τ_(d)	#VALUE!	N/mm^2
f_(v,d)	3,67	N/mm^2
Verification	#VALUE!	
V_0d max	24,44	kN

RB90shear	A5	
V_90d	#VALUE!	N
A_(net)	7500,00	mm^2
τ_(d)	#VALUE!	N/mm^2
ft,90,d	0,44	N/mm^2
f_(v,d)	0,88	N/mm^2
Verification	#VALUE!	
V_90d max	4,40	kN

6.9.1.2.1 Axial stresses

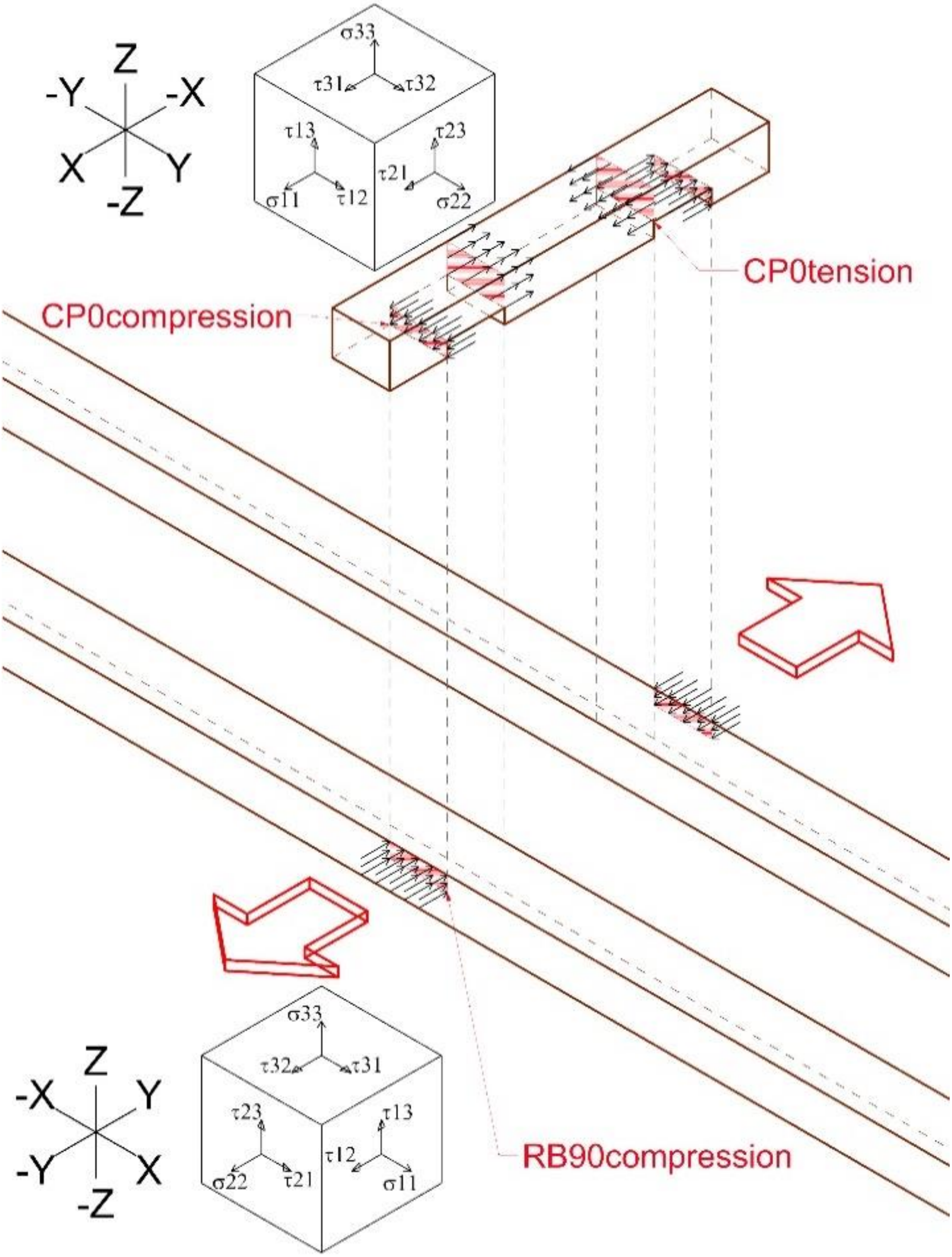

Figure 6-100 Cross Piece - Tension - Axial stresses

6.9.1.2.2 Tangential stresses

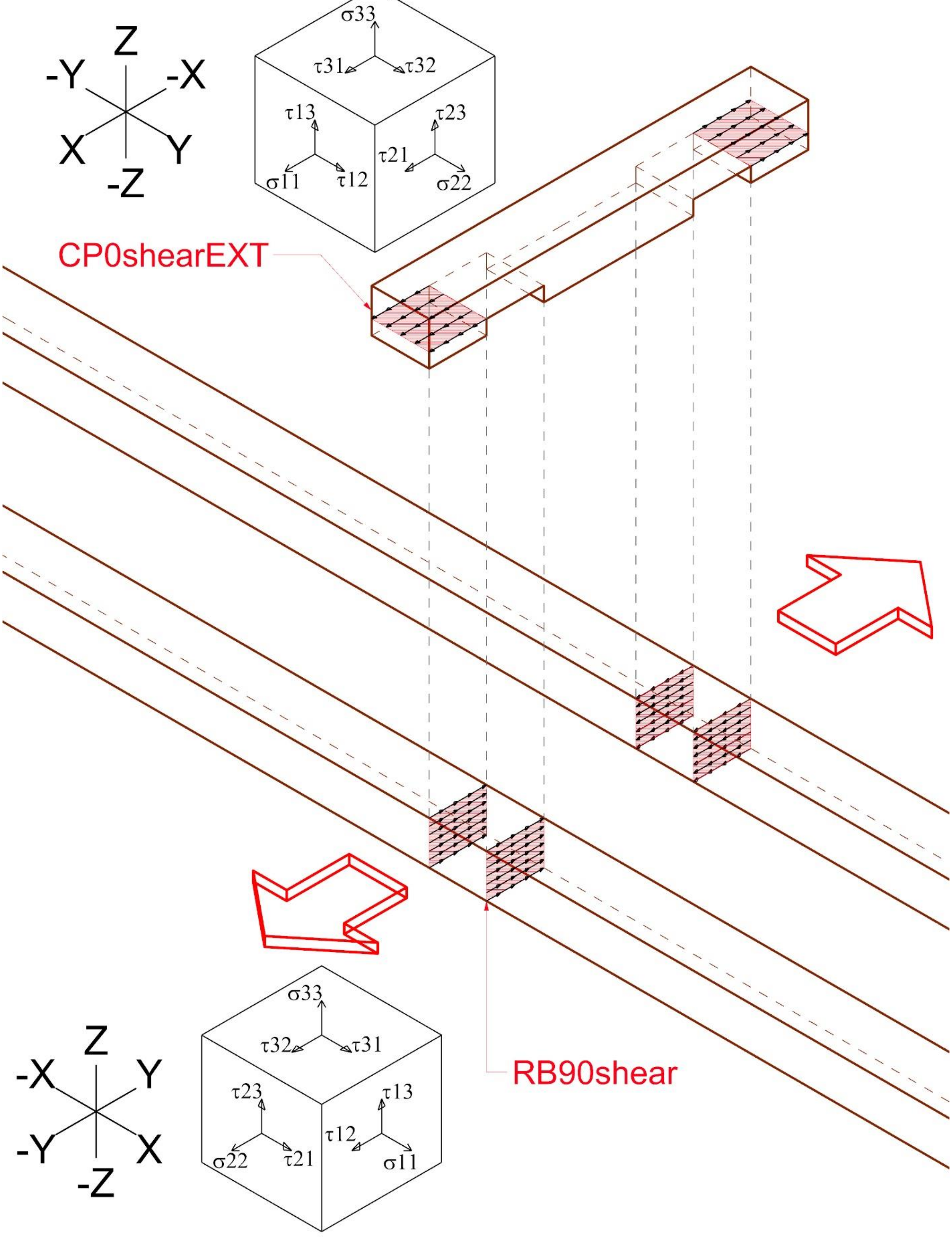

Figure 6-101 Cross Piece - Tension - Tangential stresses

6.9.1.3 Friction/Inertia

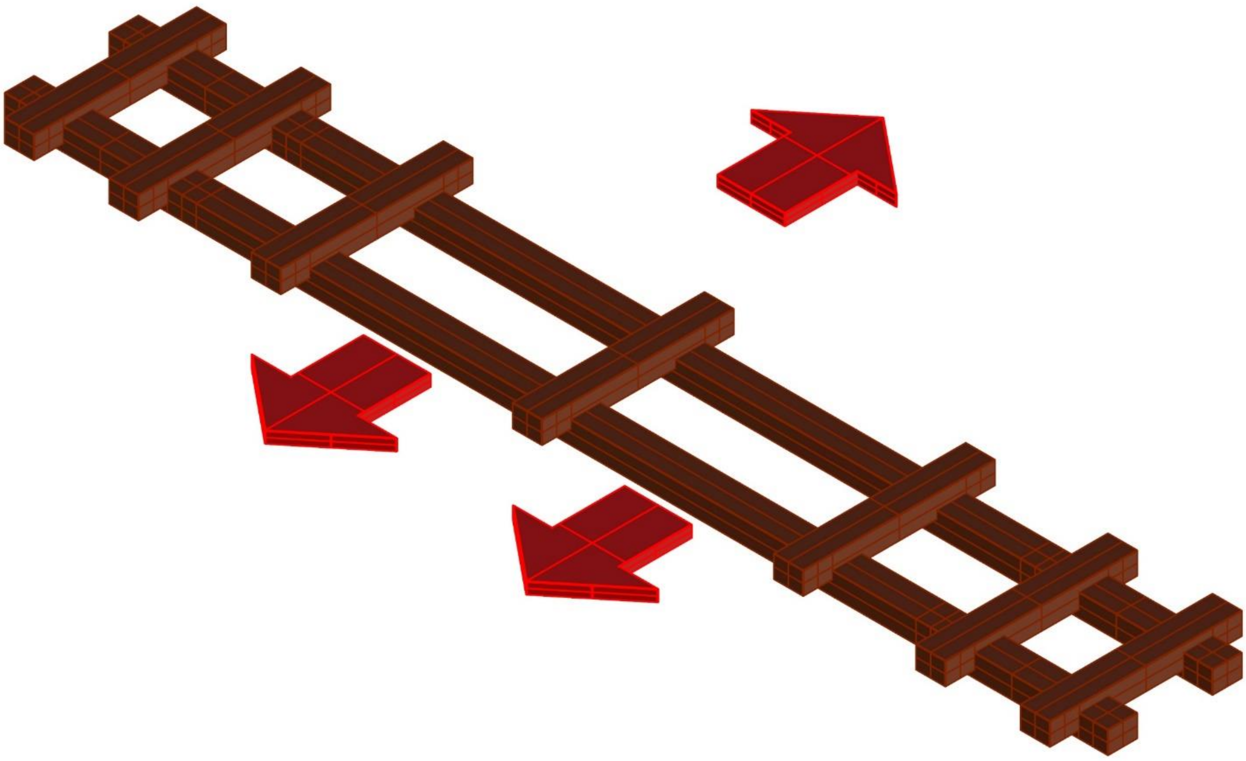

Figure 6-102 Cross Piece – Friction/Inertia

The names are reported in the previous paragraphs except for :

- CP0shearINT:Cross piece - 0=along the fibers – shear : under shear force – INT : internal surface - A# stressed area
- CP0shearINT, CP0shearEXT and RB90shear : are computed in case of just pure shear force or shear force and bending moment acting at the same time.

CP0shearINT	A1	
with bending		
V_0d	?	N
K_cr	0,67	
A_(net)	17420,00	mm^2
τ_(d)	#VALUE!	N/mm^2
f_(v,d)	3,67	N/mm^2
Verification	#VALUE!	
V_0d max	42,58	kN

CP0shearINT	A1	
V_0d	#VALUE!	N
A_(net)	26000,00	mm^2
τ_(d)	#VALUE!	N/mm^2
f_(v,d)	3,67	N/mm^2
Verification	#VALUE!	
V_0d max	63,56	kN

6.9.1.3.1 Axial stresses

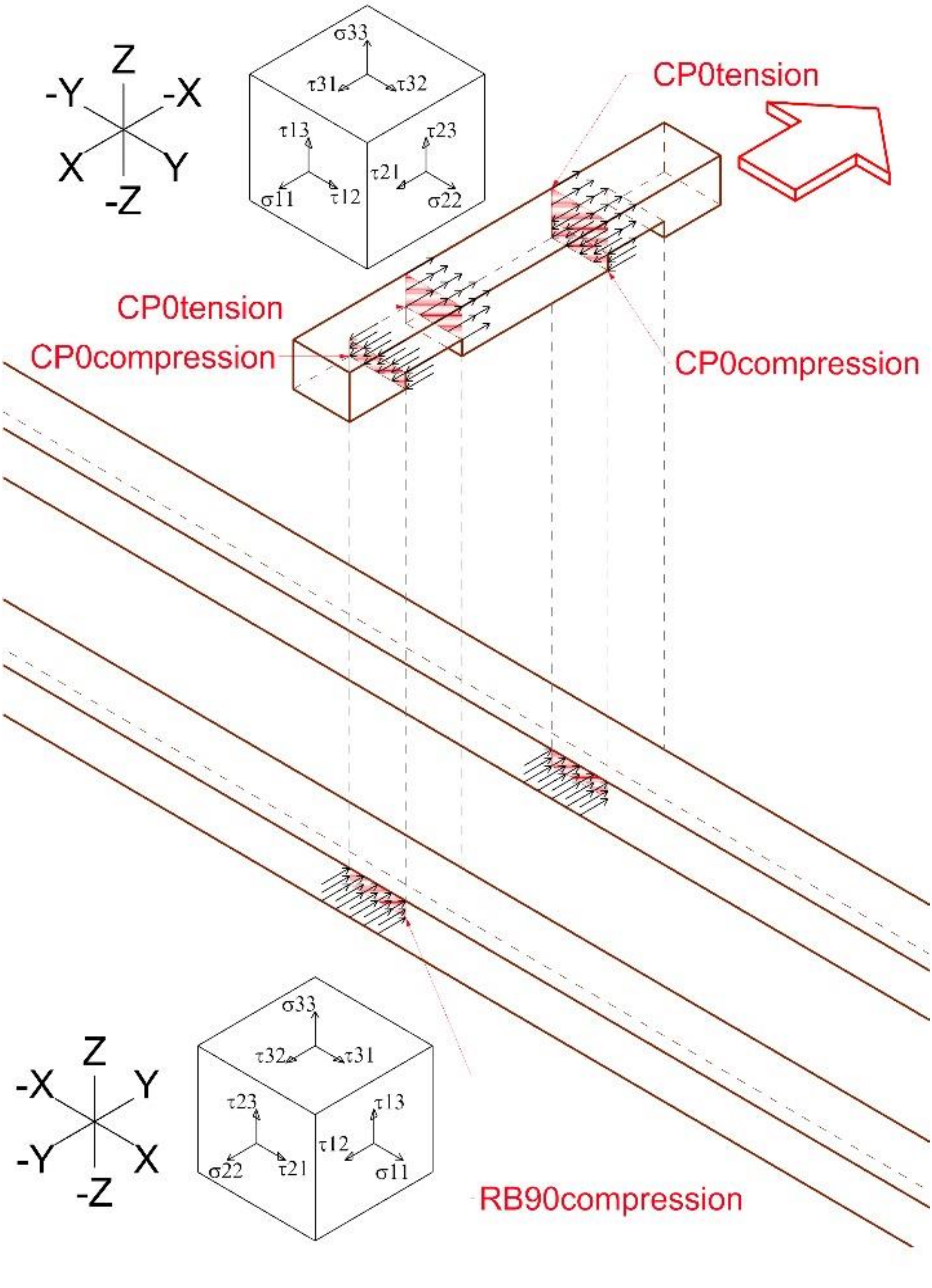

Figure 6-103 Cross Piece - Friction/Inertia - Axial stresses

6.9.1.3.2 Tangential stresses

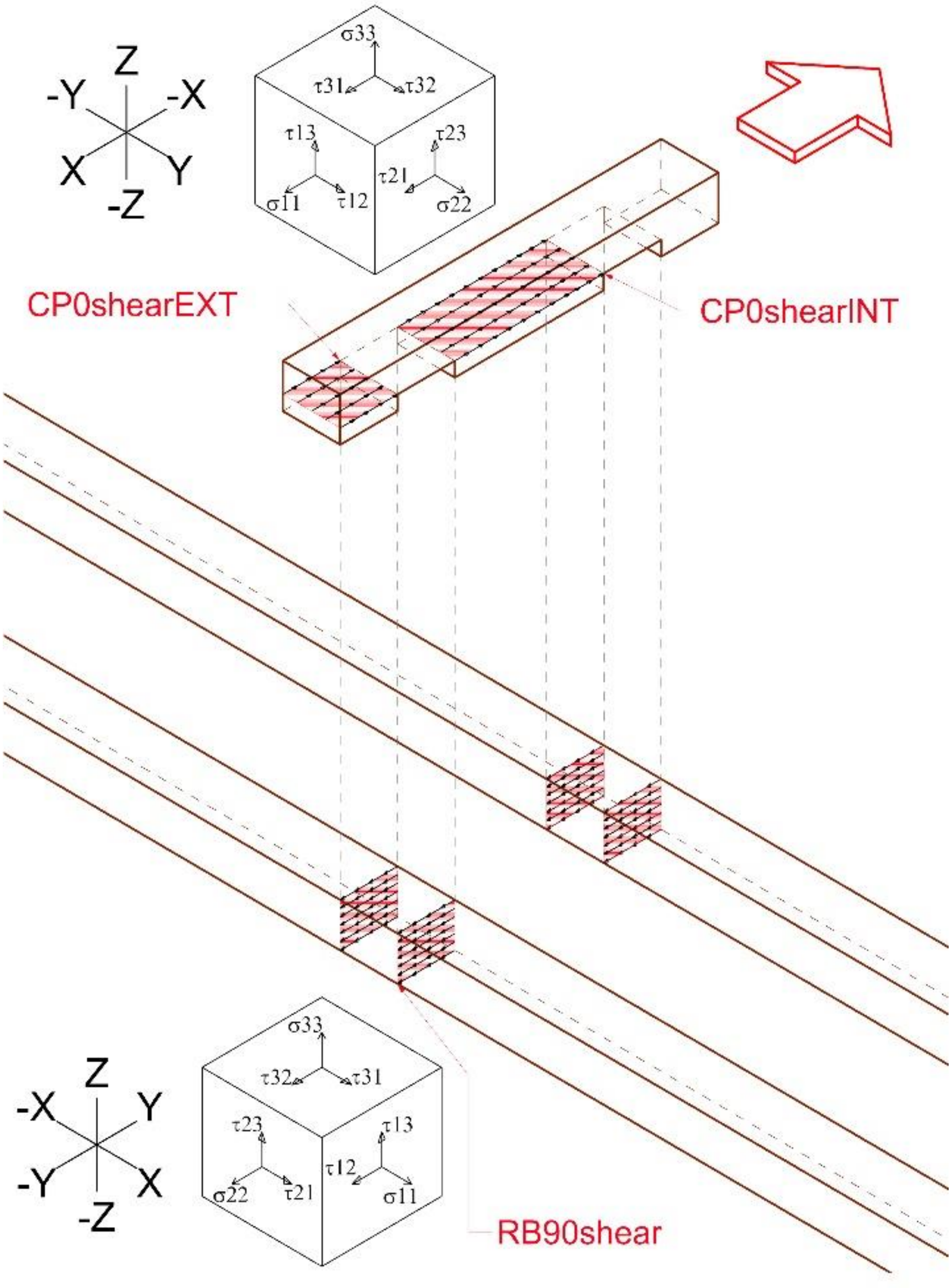

Figure 6-104 Cross Piece - Friction/Inertia - Tangential stresses

6.10 Internal developed bending moments

In the following paragraphs are reported the considerations about the "parasitic" bending moments developed internally to the timber elements. The parasitic bending moments are computed in correspondence of the notch and they come from equilibrium considerations. The positions of the parasitic bending moments have been reported before, look at the figure 6-88 to figure 6-95.

In the excel computations it has been used the following nomenclature :

- Body0mY : Body : section of the body – 0 =along the fibers – mY : bending moment around Y axis
- Body0mZ : Body : section of the body – 0 =along the fibers – mZ : bending moment around Z axis
- Body0mX : Body : section of the body – 0 =along the fibers – mX : bending moment around X axis
- Notch0mY : Notch = section of the notch – 0 =along the fibers – mY : bending moment around Z axis
- Notch0mZ : Notch = section of the notch – 0 =along the fibers – mZ : bending moment around Y axis
- Notch0mX : Notch = section of the notch – 0 =along the fibers – mX : bending moment around X axis

6.10.1 Mytf bending moment due to tension

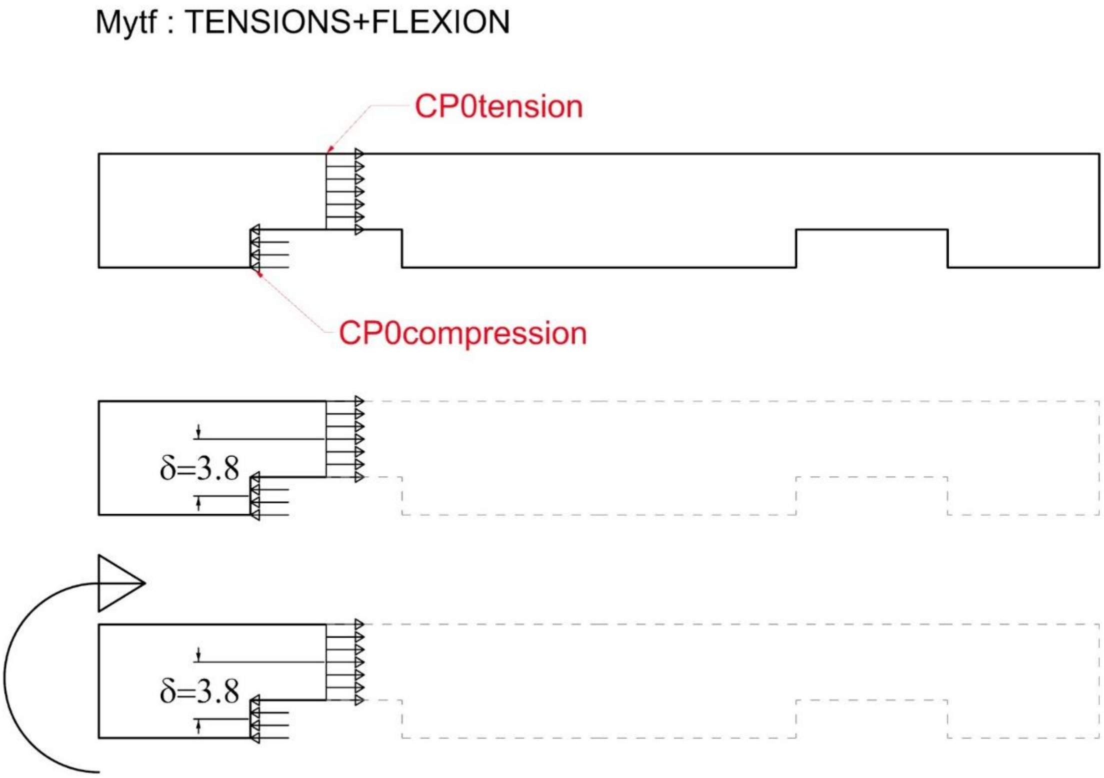

Figure 6-105 Parasitic Bending moment along Y axis due to tension and flexion

Depenings on the position and on the tension force applied the calculations have been based on the following formulas where δ is the lever arm, or the distance between the two geometric centroids of the areas where the stresses are applied:

- M_{y1} Parasitic Bending moment along Y axis due to tension and flexion on external notch

$$M_{y1} = T_1 * \delta = T_1 * 0{,}038m$$

- M_{y2} Parasitic Bending moment along Y axis due to tension and flexion on internal notc

$$M_{y2} = T_2 * \delta = T_2 * 0{,}038m$$

In the figure 6-105 CP0tension and CP0compression are the stresses which develop T1 force.

6.10.2 Mycf bending moment due to compression

The same considerations have been adopted to the compression case.

M_{ycf}: Parasitic Bending moment along Y axis due to tension and flexion

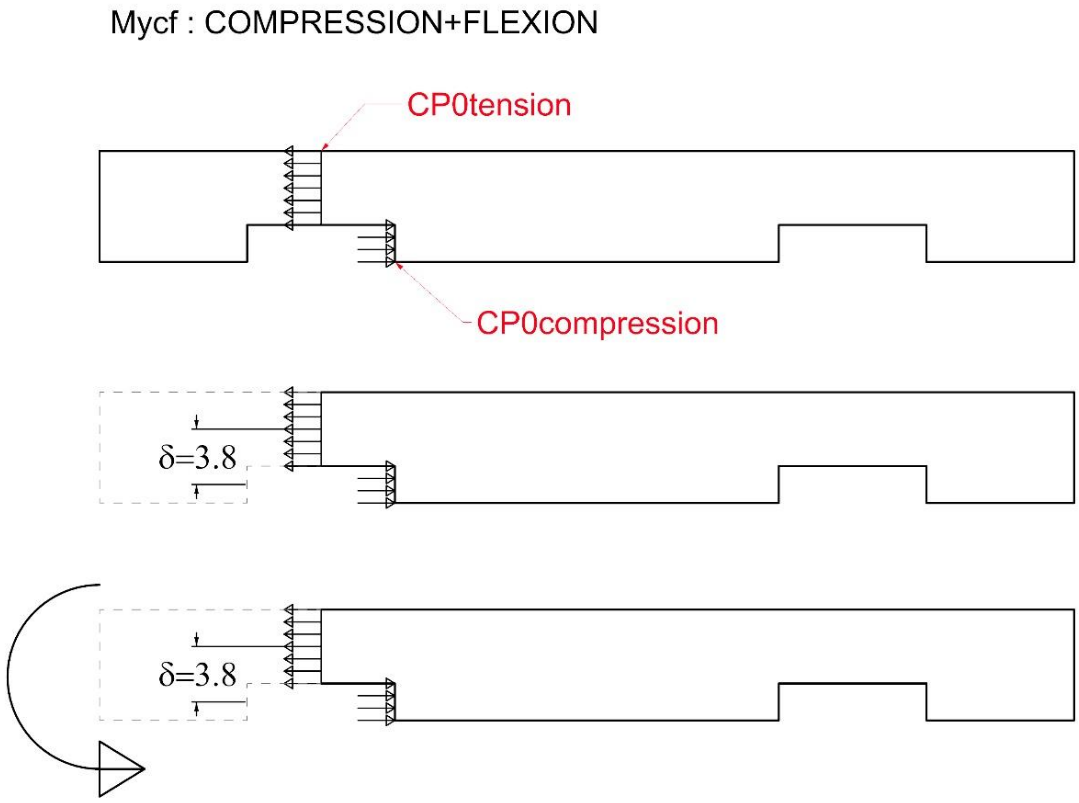

Figure 6-106 Parasitic Bending moment along Y axis due to compression and flexion

The same consideration of CP0tension and CP0compression are the same explained before.

6.10.3Mz bending moment

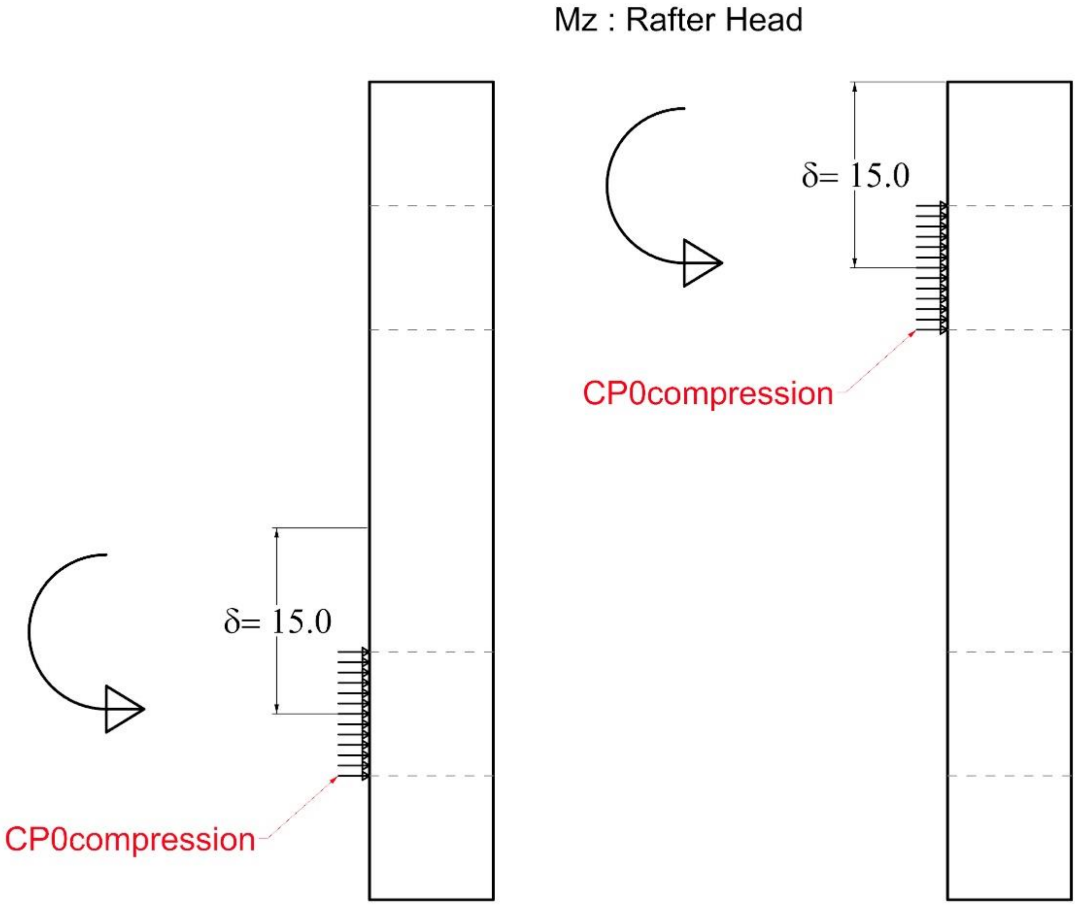

Figure 6-107 Parasitic Bending moment along Z axis due to compression and flexion

Depenings on the position and on the tension force applied the calculations have been based on the following formulas where δ is the lever arm, or the distance between the two geometric centroids of the areas where the stresses are applied:

- M_{z1} Parasitic Bending moment along Y axis due to tension and flexion

$$M_{Z1} = T_1 * \delta = T_1 * 0{,}015m$$

- M_{z2} Parasitic Bending moment along Y axis due to tension and flexion (considering the addition of M_{z1})

$$M_{Z2} = M_{Z1} + T_2 * \delta = M_{Z1} + T_2 * 0{,}015m$$

In the figure 6-107 CP0compression is the stress which develop T1 and T2 forces.

6.10.4 Torsional Mx

The torsional moments have been studied as the effect of compression of the rafter T, acting as a chain, on the R rafter. The instantaneous torsional moment develops on the notch. In the larger section of the rafter head the torsional moment will be verified as consequence of the moment on the notch. The lever arm δ_{tor} is the distance between the centroid of the notch section and the point where the force is applied. This distance is 12mm.

6.10.4.1 Mx Notch

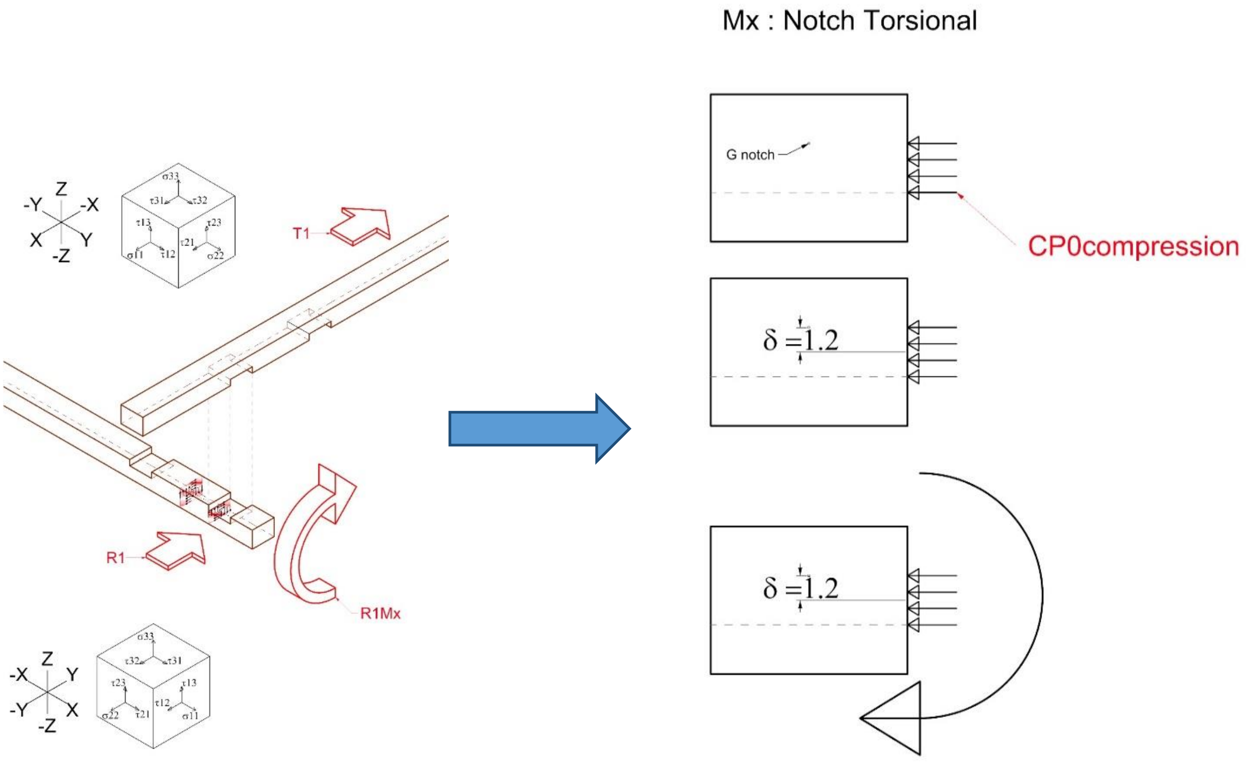

Figure 6-108 Parasitic Torsional Bending moment along X axis due to compression on the notch

- M_{x1} Parasitic Bending moment along X axis due to compression and flexion

$$M_{x1} = R_1 * \delta_{tor} = R_1 * 0{,}012m$$

- M_{x2} Parasitic Bending moment along X axis due to compression and flexion

$$M_{x2} = R_2 * \delta_{tor} = R_2 * 0{,}012m$$

6.10.4.2 Mx Rafter Head

In the case of of the body section the lever arm δ_{tor} ,the distance between the centroid of the notch section and the point where the force is applied, is null then the verification will be done just on the notch section which is the weaker.

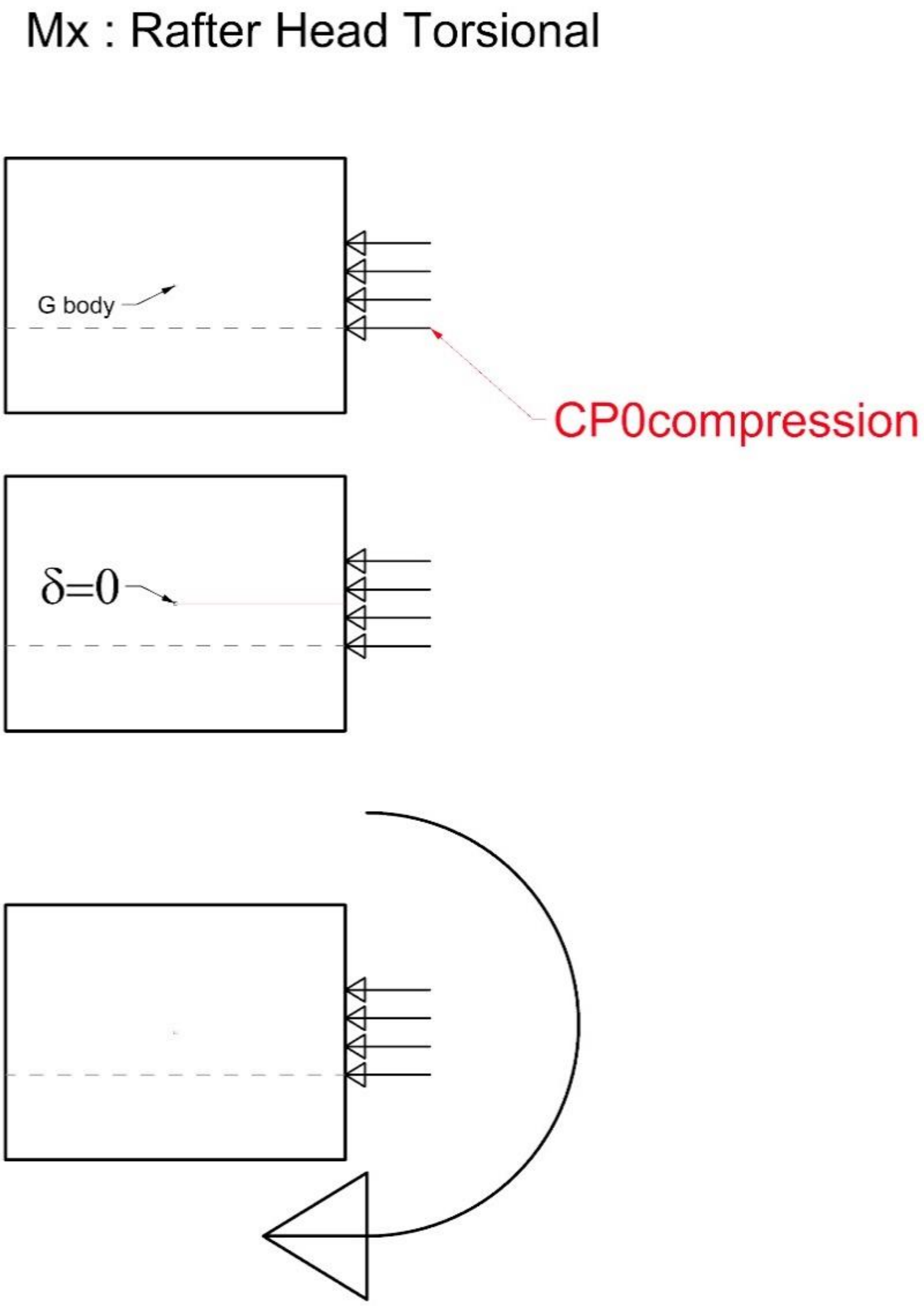

Figure 6-109 Parasitic Torsional Bending moment along X axis due to compression on the body section

6.10.4.3 Mx Rafter Body

For further information it has been studied the parasitic torsional bending moment due to the friction inertia case,and the proper lever arm which is $\delta_{tor} = 0.025$mm.

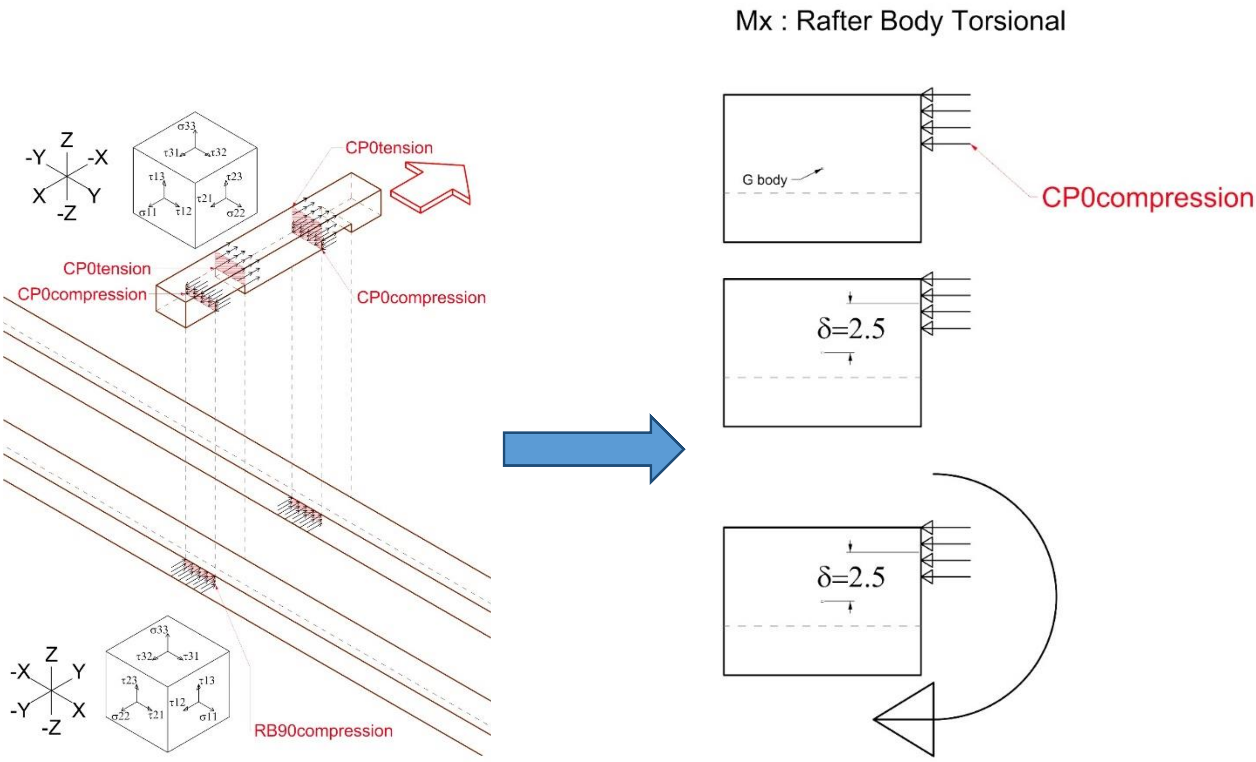

Figure 6-110 Figure 6 109 Parasitic Torsional Bending moment along X axis due to Friction/Inertia case on the body section

6.11 Keyed scarf joint

6.11.1 Geometry and resistance

The presence of a keyed scarf joint on a timber element under tension affects the resistance of the element, from laboratory tests it has been defined the reduction factor Rscarf., references from Strutture in legno .Piazza M., Tomasi R, Modena R.

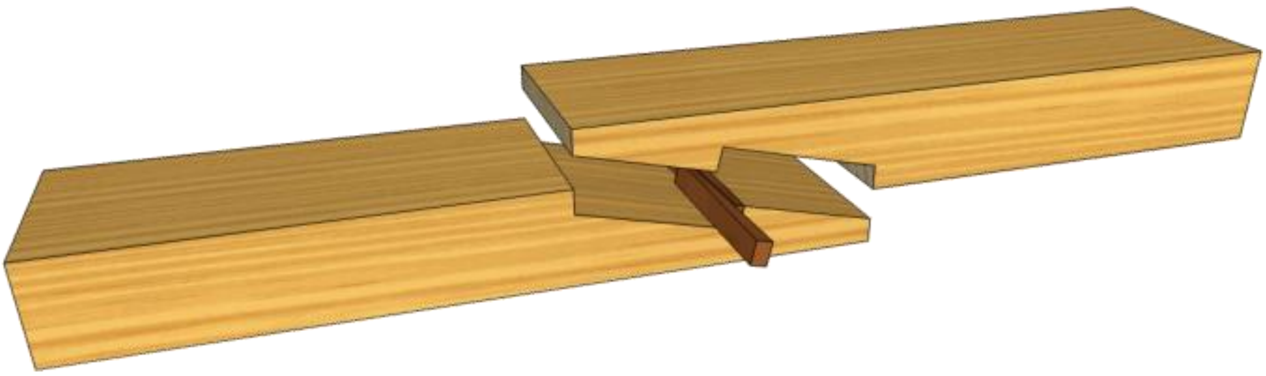

Figure 6-111 Kashmir Joint or Keyed Scarf Joint

From Laboratory test Rscarf has been defined as :

$$R_{scarf} = \frac{Stength\ of\ the\ element\ with\ joint}{Stength\ of\ the\ element} = 0{,}11$$

6.11.2 Influence of keyed scarf joint on element subjected to tension

Recalling the Eurocode paragraph it has been reported the maximum tension force allowed on the timber rafter without and with a keyed scarf joint.

$$\sigma_{t,0,d} \leq f_{t,0,d} * R_{scarf}$$

$\sigma_{t,0,d}$ is the design tensile stress along the grain

$f_{t,0,d}$ is the design tensile strength along the grain

$\sigma_{t0d} = \frac{N_{0d}}{A_{net,t}}$

N_{0d} is the design axial force parallel to the grain

$A_{net,t}$ is the net cross-sectional area perpendicular to the grain

$A_{net,v}$ is the net shear area in the parallel to grain direction

$R_{scarf} = 0.11$ is the reduction factor for the presence of the keyed scarf joint.

RB0tens		
N_0d	?	N
b	100,00	mm
h	75,00	mm
A_(net)	7500,00	mm
σ_(t,0,d)	0,00	N/mm^2
kh	1,08	
f_(t,0,d)	30,80	N/mm^2
Verification	Not defined	
N_(0d)max	231,00	kN

Influence of keyed scarf joint		
Verification	Not defined	
N_(0d)max	25,41	kN

7 STATIC ANALYSIS

7.1 Aim of static analysis

The aim of the static analysis is to understand thebehavior of the structure subjected to the vertical loads due to the roof and the self-weight.

In order to be consistent with the preliminary considerations shown in the previous chapter The analysis has been conducted in two peculiar positions:

- the criticalbehavior in the middle of the stones layers;
- the critical behavior immediately below the timber band .

The wall has been decomposed in modular unit with dimensions 1,20m x 0,46m x 3,0 m as shown in Study Case chapter.

Each module has been decomposed in subparts.

7.2 Single modular unit

In order to study the single modular unit in the static analysis they have been defined the volumes of each element which composes each layer, they have been used the material properties described in the chapter 4 thus they have been obtained the weights of the elements.

7.2.1 Material properties

Table 16 Material Properties for single modular unit

SPECIFIC WEIGHT - DENSITY		
	KN/m^3	Kg/m^3
Ystone	26,86	2738,02
Y rubble stone	19,88	2026,14
Ytimber	8,97	914,75

e: void ratio	0,26
n : porosity (%)	0,20

Contact Surface		
L module	1,20	m
Width	0,46	m
Area	0,55	m^2

7.2.2 Volumes

The model have been drawn with the Rhinoceros 3D computer graphics and computer-aided design (CAD) application software. This software allowed to have information about the geometrical properties of the designed 3d models.

The single modular unit has been decomposed in its elementary parts as shown in the figure below.

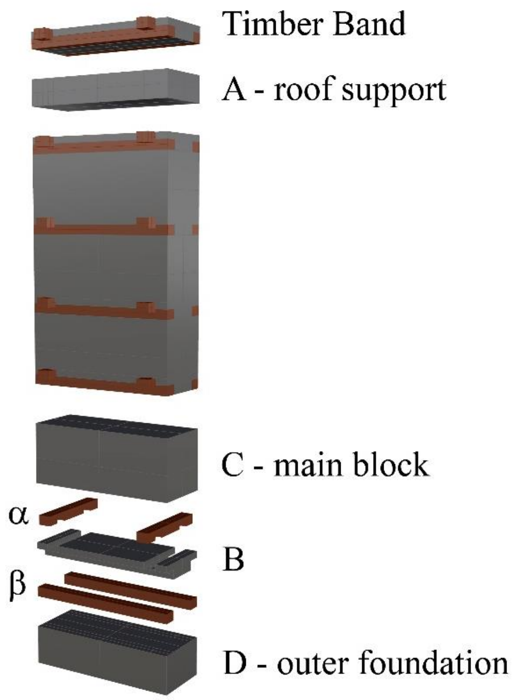

Figure 7-1 Single modular unit – Decomposed

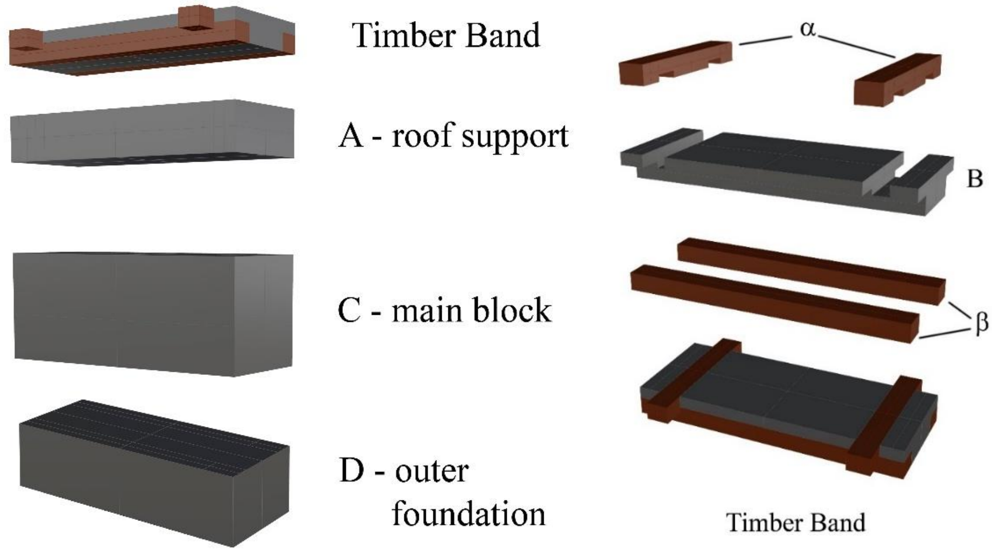

Figure 7-2 Single modular unit – Large -Decomposed

Table 17 Elementary parts of single modular unit - Volumes

VOLUMES	
	m^3
A - roof support	0,11040
B - rubble stone band	0,04510
C - main block	0,26220
D - outer foundation	0,16560
α - cross pieces	0,00900
β- timber rafter	0,00445

Timber Band	
volume percentage	%
timber	37,36
rubble stones	62,64

7.2.3 Weights and stresses

They have been computed the weights of the elementary parts multiplying each volume for the proper specific weight, then the stresses immediately below each layers have been obtained dividing the mass over the contact surface.

Table 18 Elementary parts of single modular unit - Weights and stresses

WEIGHTS Timber Band		
	KN	Kg
Wtb	1,14	115,99

WEIGHTS A - roof support		
	KN	Kg
Wrs	2,19	223,69

WEIGHTS C - main block		
	KN	Kg
Wmb	5,21	531,25

WEIGHTS D - outer foundation		
	KN	Kg
Wof	3,29	335,53

Stress under Timber Band		
	KN/m^2	Kg/m^2
σtb	2,06	210,12

Stress under A - roof support		
	KN/m^2	Kg/m^2
σrs	3,98	405,23

Stress under C - main block		
	KN/m^2	Kg/m^2
σmb	9,44	962,41

Stress under C - main block		
	KN/m^2	Kg/m^2
σof	5,96	607,84

7.1 Roof

The same approach used for the single modular unit has been adopted for the roof.In order to study the roof in the static analysis they have been defined the volumes of each element which composes each layer, they have been used the material properties described in the chapter 4 thus they have been obtained the weights of the elements.

7.1.1 Material properties

In the following table are reported some new properties of materials which have not been described before like the earth/clay and the twigs. For these two material the properties have been choosen roughly in respect to the others because the uncertainties of which are the exact material used in the chosen Nepal regions by the way still suggested by Arch Tom Schacher's guide.

Table 19 Material Properties for roof

SPECIFIC WEIGHT - DENSITY		
	KN/m^3	Kg/m^3
ϒstone	26,86	2738,02
ϒtimber	8,97	914,75
ϒearth/clay	22,56	2300,00
ϒtwigs	0,50	50,97

e : void ratio	0,00
n : porosity (%)	0,00

Contact Surface roof plane		
L roof	3,90	m
Width	3,90	m
Area	15,21	m^2

Contact Surface roof module		
L roof	1,20	m
Width	0,46	m
Area	0,55	m^2

7.1.2 Volumes

As for the single modular unit Rhinoceros 3D has been used to have information about the geometrical properties of the designed 3d models.

The heavy flat roof has been decomposed in its elementary parts as shown in the figure below.

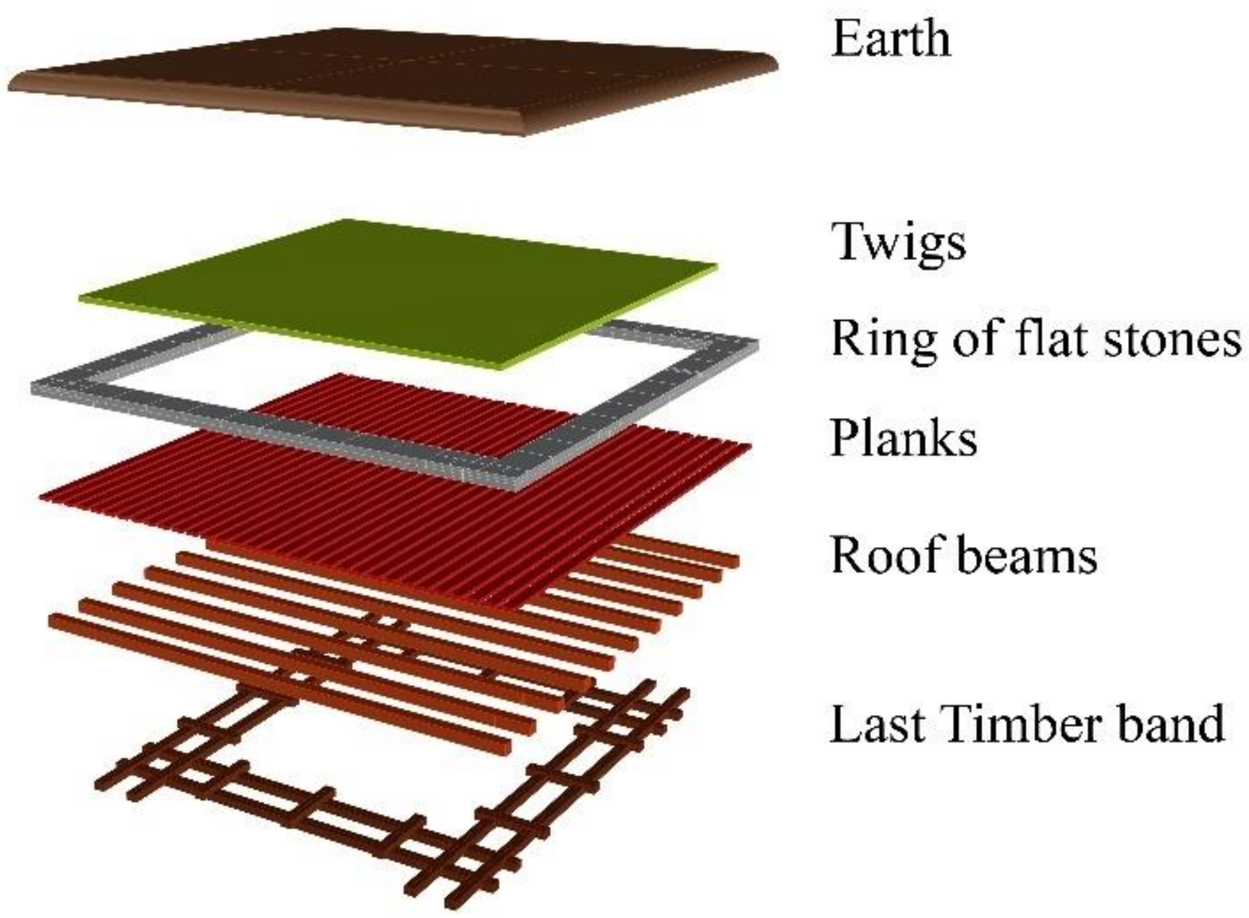

Figure 7-3 Roof – Decomposed

Table 20 Elementary parts of Roof - Volumes

VOLUMES	
	m^3
Earth/clay	3,58
Twigs	0,73
Ring of stones	0,49
Planks	0,42
Roof beams	0,48

7.1.3 Weights and linear load

They have been computed the weights of the elementary parts multiplying each volume for the proper specific weight, then the linear load immediately below each layers have been obtained dividing the mass over the roof area .

Table 21 Elementary parts of Roof - Weights and linear load

WEIGHTS Earth/clay		
	KN	Kg
Wearth	80,68	8224,63

WEIGHTS Twigs		
	KN	Kg
Wtwigs	0,36	37,19

WEIGHTS Ring of stones		
	KN	Kg
Wringstones	13,28	1353,68

Load Earth/clay		
	KN/m	Kg/m
Wearth linear	5,30	540,74

Load Twigs		
	KN/m	Kg/m
Wtwigs linear	0,02	2,44

Load Ring of stones		
	KN/m	Kg/m
Wringstones linear	0,87	89,00

WEIGHTS Planks		
	KN	Kg
Wplanks	3,79	386,39

WEIGHTS Roof beams		
	KN	Kg
Wrb	4,34	442,74

Load Planks		
	KN/m	Kg/m
Wplanks linear	0,25	25,40

Load Roof beams		
	KN/m	Kg/m
Wrb linear	0,29	29,11

Looking at the Arch. Tom Schacher's manual, the roof is sustained by the roof beams, which are supported by two walls. The total weight of the roof have been studied applied to the two wall perpendicular to the roof beams. Successively the roof weight has been counted to a single modular unit.

Table 22 Total weight of roof on wall and on module

Roof total weight

WEIGHT ROOF		
	KN	Kg
Wroof	102,46	10444,63

WEIGHT ON 1 WALL (3,6m)		
	KN	Kg
Wroof wall	51,23	5222,31

WEIGHT ON 1 MODULE (1,2m)		
	KN	Kg
Wroof module	17,08	1740,77

7.2 Normal Stresses

The normal stresses due to the vertical load have been studied in two peculiar position. The first case is the surfaces in the middle of each the stones layers, this because the rubble stones are not confined and thus it is a weaker position. The second case is the surfaces immediately below the timber beam, this because the contact surfaces between the stones is smaller due to the reduction factor obtained by the ratio between the areas described in the chapter 5 paragraph 1.

7.2.1 Normal Stress inside stones layer

Considering the hypothesis made about interfaces between stones, they have been computed the stresses on each layer as shown in the figure.

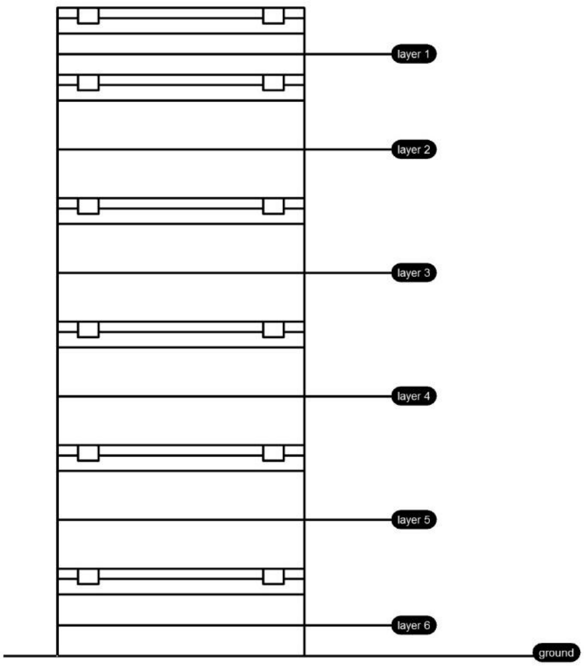

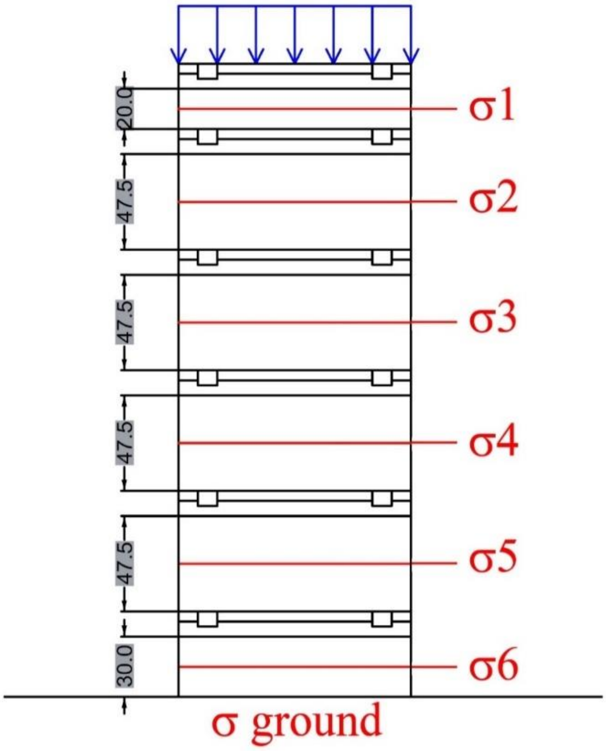

Figure 7-4 Normal stresses - Inside stones layers - Studied surfaces *Figure 7-5 Normal stresses - Inside stones layers - Sigma Stresses*

Table 23 Normal stresses - Inside stones layers - Sigma Stresses

Normal Stress				
	KN/m^2	Kg/m^2	Kg/cm^2	MPa
σ1	34,99	3566,30	0,36	0,036
σ2	43,75	4460,24	0,45	0,045
σ3	55,26	5632,78	0,56	0,056
σ4	66,76	6805,31	0,68	0,068
σ5	78,26	7977,84	0,80	0,080
σ6	88,03	8973,09	0,90	0,090
σ ground	91,01	9277,01	0,93	0,093

7.2.2 Normal Stress below timber beam

They have been computed the stresses on each layer below the timber beam as shown in the picture.

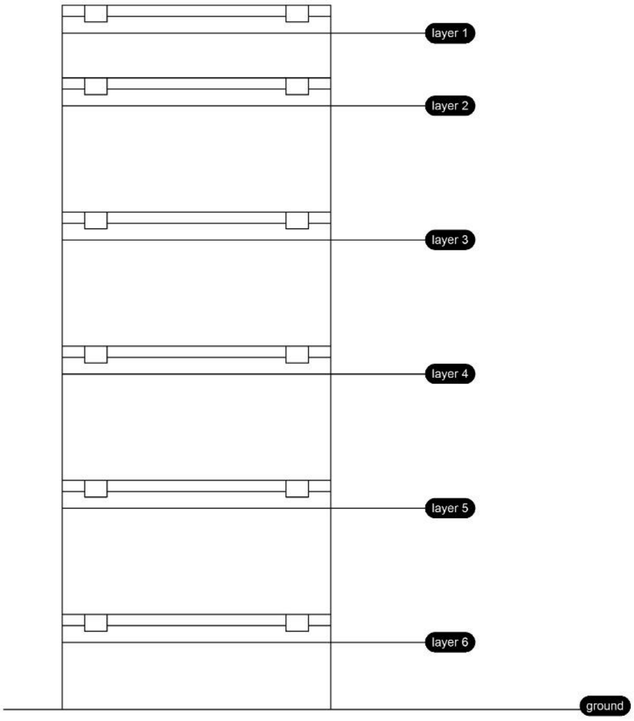

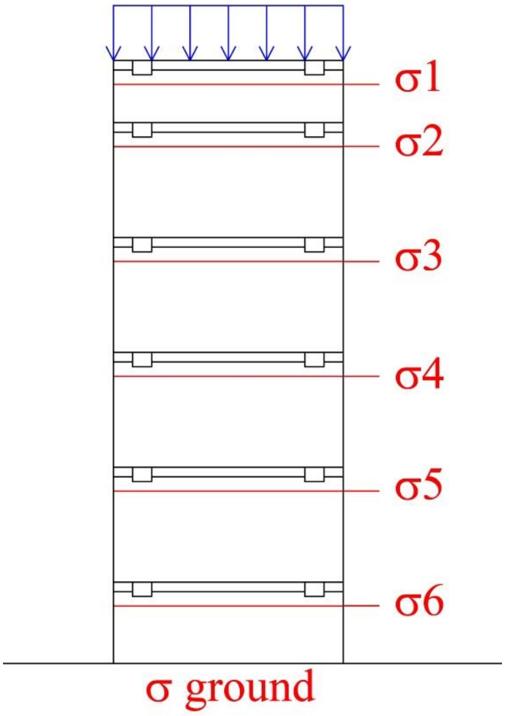

Figure 7-6 Normal stresses - Below timber beam - Sigma Stresses Figure 7-7 Normal stresses - Below timber beam - Studied surfaces

Table 24 Normal stresses - Below timber beam - Sigma Stresses

Normal Stress				
	KN/m^2	Kg/m^2	Kg/cm^2	MPa
σ1	33,00	3363,69	0,34	0,034
σ2	39,03	3979,04	0,40	0,040
σ3	50,54	5151,57	0,52	0,052
σ4	62,04	6324,10	0,63	0,063
σ5	73,54	7496,64	0,75	0,075
σ6	85,04	8669,17	0,87	0,087
σ ground	91,01	9277,01	0,93	0,093

8 SEISMIC ANALYSIS IN PLANE

The effect of an earthquake on a structure is schematize as an horizontal action.The seismic actions are proportional to the mass of the structure and to the peak ground acceleration at the base of the structure. There are different schematization for representing the distribution of these forces on the building. In this thesis they have been selected the three case possible by hand calculation:

- Force applied at the top of the wall ;
- Triangular lateral distribution over the height of the wall ;
- Uniform lateral distribution over the weight of the wall.

As it has been explained in the initial chapters the bhatar system is composed by rubble stones masonry , this means that the structure is already cracked.The seismic analysis in plane is based on the application of the Barton's empirical model for the rock fill presented in the chapter 5. This non-linear model permits to have values of the friction coefficient μ, which develops at each studied layer due to the vertical load and the self-weight. These friction coefficients have been used to described the resisting behavior of each layers subjected to the horizontal forces due to the seismic event.

8.1 Shear strength for rockfill with Barton empirical model

The Barton model is described by a function which described the shear stress in function of the normal stresses and others parameters described in the chapter 5.The peculiar thing is that the non-linearity of the function strictly depends on the normal stresses. For each studied surface the normal stresses have been taken from the static analysis described in the chapter 7. Thus they have been obtained values of friction coefficient μ for each critical surface. They have been reported the corresponding friction angles.

8.1.1 Normal Stress and Coefficients of friction inside stones layer

Table 25 Normal Stress and Coefficients of friction inside stones layer

Normal Stress					Barton empirical model for rockfill - Friction coefficient μ				
	KN/m^2	Kg/m^2	Kg/cm^2	MPa	Ϭn (Mpa)	τp (Mpa)	μ= τp/σn	rad	deg
σ1	34,99	3566,30	0,36	0,036	0,04	0,07	1,84	1,07	61,52
σ2	43,75	4460,24	0,45	0,045	0,04	0,08	1,77	1,06	60,58
σ3	55,26	5632,78	0,56	0,056	0,06	0,09	1,70	1,04	59,59
σ4	66,76	6805,31	0,68	0,068	0,07	0,11	1,65	1,03	58,78
σ5	78,26	7977,84	0,80	0,080	0,08	0,12	1,61	1,01	58,11
σ6	88,03	8973,09	0,90	0,090	0,09	0,14	1,58	1,01	57,60
σ ground	91,01	9277,01	0,93	0,093	0,09	0,14	1,57	1,00	57,46

8.1.2 Normal Stress and Coefficients of friction below timber beam

Table 26 Normal Stress and Coefficients of friction below timber beam

Normal Stress					Barton empirical model for rockfill - Friction coefficient μ				
	KN/m^2	Kg/m^2	Kg/cm^2	MPa	Ϭn (Mpa)	τp (Mpa)	μ= τp/σn	rad	deg
σ1	33,00	3363,69	0,34	0,034	0,034	0,06	1,86	1,08	61,73
σ2	39,03	3979,04	0,40	0,040	0,040	0,07	1,81	1,07	61,06
σ3	50,54	5151,57	0,52	0,052	0,052	0,09	1,73	1,05	59,97
σ4	62,04	6324,10	0,63	0,063	0,063	0,11	1,67	1,03	59,10
σ5	73,54	7496,64	0,75	0,075	0,075	0,12	1,62	1,02	58,37
σ6	85,04	8669,17	0,87	0,087	0,087	0,14	1,58	1,01	57,75
σ ground	91,01	9277,01	0,93	0,093	0,093	0,14	1,57	1,00	57,46

8.2 Seismic load multiplier

The aim of this analysis is to understand the point at which the structure shows a critical behavior, which may cause a failure. The failure happens when the the seismic force is larger than the resisting shear force of the wall. The seismic force has been defined with the term Fs and the resisting shear force with the term Rs. In order to study the problem it has been introduced the seismic load multiplier α applied to the seismic force Fs. The subscript term i is to specify the considered layer.

8.2.1 Critical multiplier for inside stones layer

The analyzed layers are shown in the following figure.

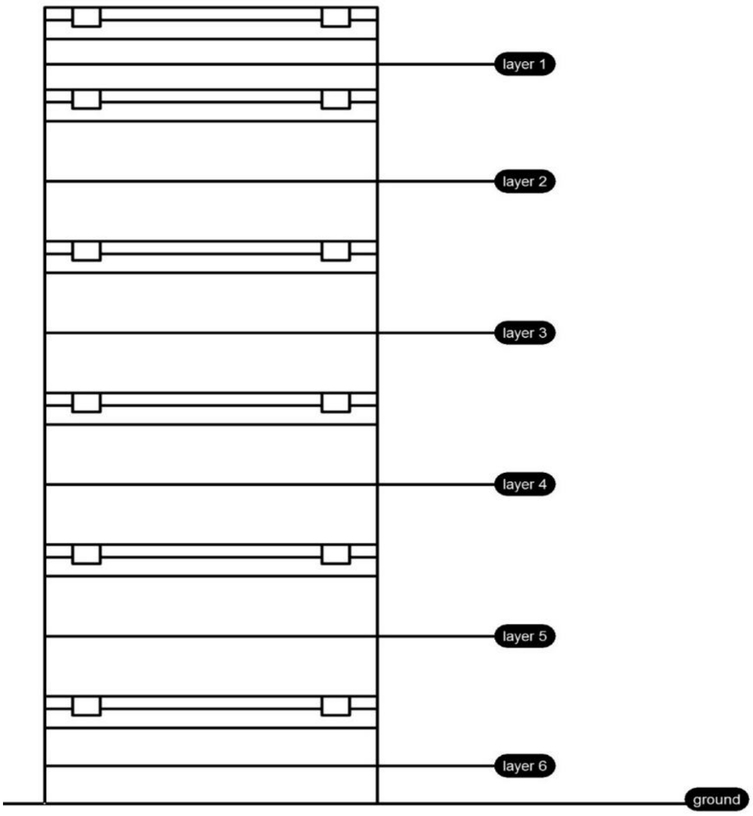

Figure 8-1 Analyzed layers for inside stones layer case

8.2.1.1 Force applied at the top of the wall

Figure 8-2 Force applied at the top of the wall

The system has a safe behavior if

$$Fs < Rs$$

Where the forces can be written as:

$$\alpha * \frac{Wtot}{2} * PGA < \mu i * Wi$$

α is the load multiplier

$Wtot$ is the total weight of the box structure and of the roof

PGA is the peak ground acceleration

μi is the friction coefficient of the i^{th} layer

Wi is the pertinent weight on the i^{th} layer

The critical load multiplier for each surfaces can be written as :

$$\alpha \leq \frac{(\mu i * Wi)}{(Wtot/2 * PGA)}$$

Table 27 Force applied at the top of the wall - Data

Total Weight of the box+roof		
	KN	Kg
Wbox	313,91	31999,28
Wroof	102,46	10444,63
Wtot	416,37	42443,90
Peak Ground Accelleration		
PGA	1	g

Fs=	Wtot/2*PGA=	208,19	kN

In the following table are reported values of the limit values of load multiplier for a safe behavior,

$$\alpha \text{ such that } \quad \frac{Fs}{Rs} < 1$$

The resisting shear forces Rsi have been obtained multiplying the normal force acting on the layer time the pertinent friction coefficient.

Table 28 Safe limit multipliers - Force applied at the top of the wall -inside stones layer case

	Wi = Ni	Rsi = τi = Ni*μi	α <
	kN	kN	
layer1	57,94	106,81	0,51
layer2	72,46	128,49	0,62
layer3	91,51	155,91	0,75
layer4	110,55	182,43	0,88
layer5	129,60	208,26	1,00
layer6	145,77	229,71	1,10
ground	150,71	236,19	1,13

8.2.1.2 Triangular lateral distribution over the height of the wall

In the case of a triangular lateral distribution they have been defined the distributions factors depending on the mass and the height of the analyzed layer.

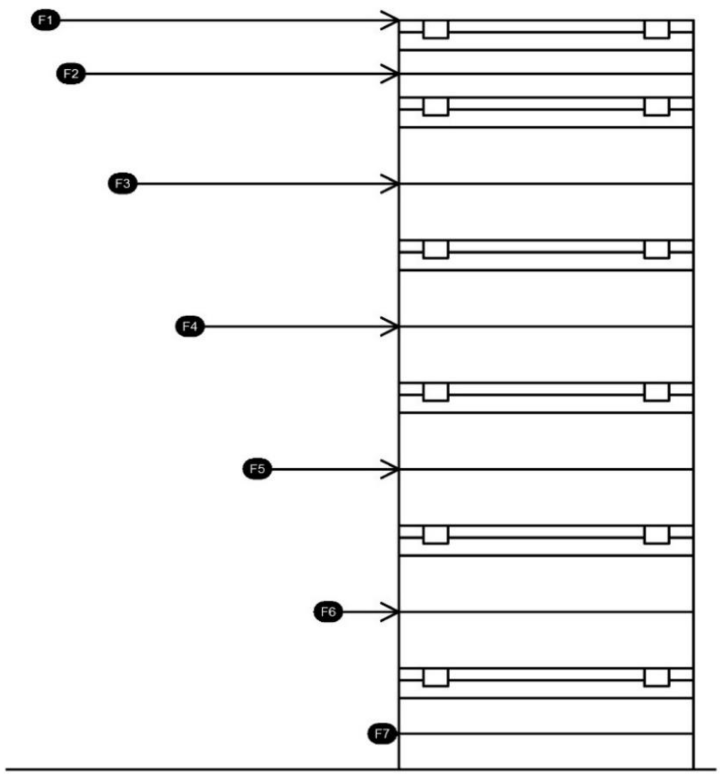

Figure 8-3 Triangular lateral distribution over the height of the wall for inside stones layer

The seismic force Fs has been computed as in the first case, thus it has been distributed multiplying by the distribution factor β. The distribution factors have been obtained using the following formula:

$$\beta_j = \frac{W_j * h_j}{\sum_{i=1}^{N} W_i * h_i + W_{roof} * H}$$

Where

β_j : is the distribution factor corresponding to the analyzed layer

W_j : is the weight corresponding to the analyzed layer

h_j : is the height corresponding to the analyzed layer

$\sum_{i=1}^{N} W_i * h_i + W_{roof} * H$: is the summation of all the masses times the corresponding heights

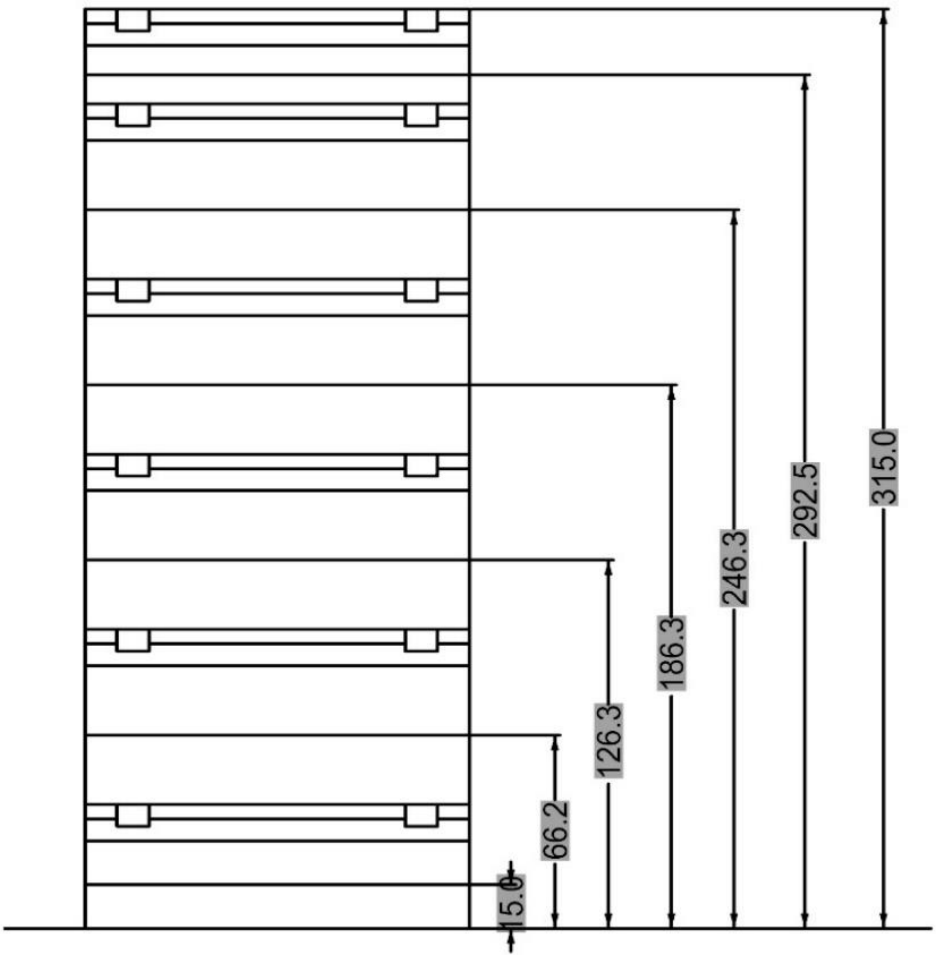

Figure 8-4 Triangular lateral distribution over the height of the wall for inside stones layer- Heights (cm)

The force Fj applied to each layer has been obtained using the following formula:

$$F_j = F_s * \beta_j = F_s * \frac{W_j * h_j}{\sum_{i=1}^{N} W_i * h_i + W_{roof} * H}$$

Seismic Force		
Fs= Wtot/2*PGA	201,24	kN

Table 29 Triangular distribution of the forces - inside stones layer case

Distribution of the forces			
	W	Height of Force : hi	Wi * hi
Wi	kN	m	kN*m
Wroof	17,08	3,15	53,79
W1	2,23	3,15	7,04
W2	4,84	2,93	14,16
W3	6,35	2,46	15,64
W4	6,35	1,86	11,83
W5	6,35	1,26	8,02
W6	5,39	0,66	3,57
W7	1,65	0,15	0,25

Distribution factors and Forces		
Fj	βj	Fj=Fs*βj
	/	kN
F1	0,53	110,81
F2	0,12	25,79
F3	0,14	28,49
F4	0,10	21,55
F5	0,07	14,61
F6	0,03	6,50
F7	0,002	0,45

The system has a safe behavior if

$$Fs < Rs$$

Where the forces can be written as:

$$\alpha * PGA * \frac{1}{2} * \left(W_T + W_{roof}\right) * \sum_{i=i}^{j} \frac{W_j * h_j}{\sum_{i=1}^{N} W_i * h_i + W_{roof} * H} \leq \mu s_j * Nj$$

α is the load multiplier

$Wtot$ is the total weight of the box structure and of the roof

PGA is the peak ground acceleration

μi is the friction coefficient of the i^{th} layer

Wi is the pertinent weight on the i^{th} layer

μs_j is the friction coefficient obtained by the Barton models for rockfill corresponding to the analyzed layer

Nj is the pertinent normal force acting on the on the analyzed layer

The critical load multiplier for each surfaces can be written as :

$$\alpha \leq \frac{\mu s_j * Nj}{PGA * \frac{1}{2} * (W_T + W_{roof}) * \sum_{i=i}^{j} \frac{W_j * h_j}{\sum_{i=1}^{N} W_i * h_i + W_{roof} * H}}$$

In the following table are reported values of the limit values of load multiplier for a safe behavior,

$$\alpha \; such \; that \quad \frac{Fs}{Rs} < 1$$

Table 30 Safe limit multipliers- Triangular lateral distribution-inside stones layer case

Computing α such that Fs< Rshear			
Layer	Nj	Rshear = N*μs	α <
	kN	kN	
Layer1	57,94	106,81	0,96
Layer2	72,46	128,49	0,94
Layer3	91,51	155,91	0,94
Layer4	110,55	182,43	0,98
Layer5	129,60	208,26	1,03
Layer6	145,77	229,71	1,11
Layer_ground	150,71	236,19	1,13

8.2.1.1 Uniform lateral distribution over the height of the wall

In the case of a triangular lateral distribution they have been defined the distributions factors depending on the mass and the height of the analyzed layer.

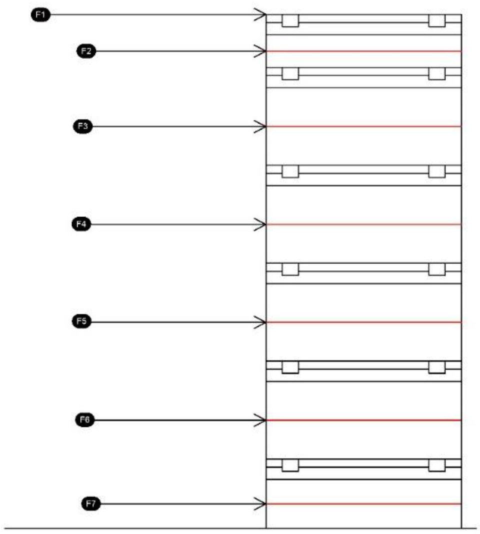

Figure 8-5 Uniform lateral distribution over the height of the wall for inside stones layer

The seismic force Fs has been computed as in the first case, thus it has been distributed multiplying by the distribution factor β. The distribution factors have been obtained using the following formula:

$$\beta_j = \frac{W_j}{\sum_{i=1}^{N} W_i + W_{roof}}$$

Where

β_j : is the distribution factor corresponding to the analyzed layer

W_j : is the weight corresponding to the analyzed layer

$\sum_{i=1}^{N} W_i + W_{roof}$: is the summation of all the masses

The force Fj applied to each layer has been obtained using the following formula:

$$F_j = F_s * \beta_j = F_s * \frac{W_j}{\sum_{i=1}^{N} W_i + W_{roof}}$$

Seismic Force		
Fs= Wtot/2*PGA	201,24	kN

Table 31 Uniform Distribution of the forces - inside stones layer case

Distribution of the forces	
	W
Wi	kN
Wroof	17,08
W1	2,23
W2	4,84
W3	6,35
W4	6,35
W5	6,35
W6	5,39
W7	1,65
Sum	50,24

Distribution factors and Forces		
Fj	βj	Fj=Fs*βj (kN)
	/	
F1	0,38	80,03
F2	0,10	20,06
F3	0,13	26,31
F4	0,13	26,31
F5	0,13	26,31
F6	0,11	22,33
F7	0,03	6,82

The system has a safe behavior if

$$Fs < Rs$$

Where the forces can be written as:

$$\alpha * PGA * \frac{1}{2} * \left(W_T + W_{roof}\right) * \sum_{i=i}^{j} \frac{W_j}{\sum_{i=1}^{N} W_i + W_{roof}} \leq \mu s_j * Nj$$

α is the load multiplier

$Wtot$ is the total weight of the box structure and of the roof

PGA is the peak ground acceleration

μi is the friction coefficient of the i^{th} layer

Wi is the pertinent weight on the i^{th} layer

μs_j is the friction coefficient obtained by the Barton models for rockfill corresponding to the analyzed layer

Nj is the pertinent normal force acting on the on the analyzed layer

The critical load multiplier for each surfaces can be written as :

$$\alpha \leq \frac{\mu s_j * Nj}{PGA * \frac{1}{2} * \left(W_T + W_{roof}\right) * \sum_{i=i}^{j} \frac{W_j}{\sum_{i=1}^{N} W_i + W_{roof}}}$$

In the following table are reported values of the limit values of load multiplier for a safe behavior,

$$\alpha \text{ such that } \quad \frac{Fs}{Rs} < 1$$

Table 32 Safe limit multipliers- Triangular lateral distribution-inside stones layer case

Computing α such that Fs< Rshear			
Layer	Nj	Rshear = N*µs	α <
	kN	kN	
Layer1	57,94	106,81	1,33
Layer2	72,46	128,49	1,28
Layer3	91,51	155,91	1,23
Layer4	110,55	182,43	1,19
Layer5	129,60	208,26	1,16
Layer6	145,77	229,71	1,14
Layer_ground	150,71	236,19	1,13

8.2.2 Critical Multiplier below the timber band

Following the same procedure described in the previous paragraph, they have been analyzed the surfaces on the layers immediately below the timber bands. The positions of the new layers are shown in the figure below.

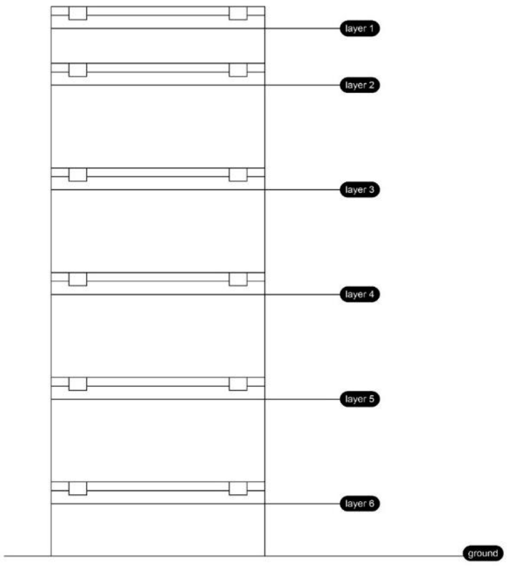

Figure 8-6 Analyzed layers for the below timber bands case

8.2.2.1 Force applied at the top of the wall

The resisting shear forces Rsi have been obtained multiplying the normal force acting on the layer by the pertinent friction coefficient and by the reduction factor ξ.

In the following table are reported values of the limit values of load multiplier for a safe behavior,

$$\alpha \text{ such that } \quad \frac{Fs}{Rs} < 1$$

Table 33 Safe limit multipliers - Force applied at the top of the wall –below timber band case

	Wi = Ni	Rsi = τi = N*μi *ξ	α <
	kN	kN	
layer1	54,64	57,44	0,28
layer2	64,64	66,08	0,32
layer3	83,69	81,83	0,39
layer4	102,74	97,01	0,47
layer5	121,79	111,76	0,54
layer6	140,83	126,16	0,61
ground	150,71	133,50	0,64

8.2.2.2 Triangular lateral distribution over the height of the wall

Following the same procedure described in the previous paragraph.

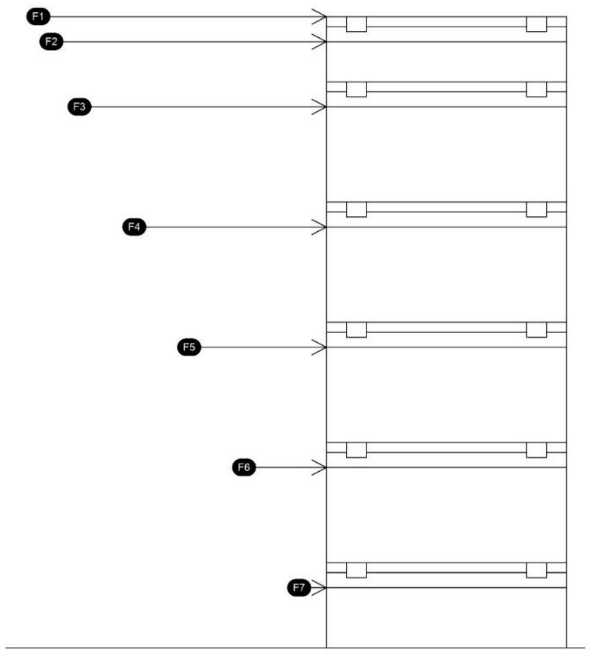

Figure 8-7 Triangular lateral distribution over the height of the wall for below timber bands

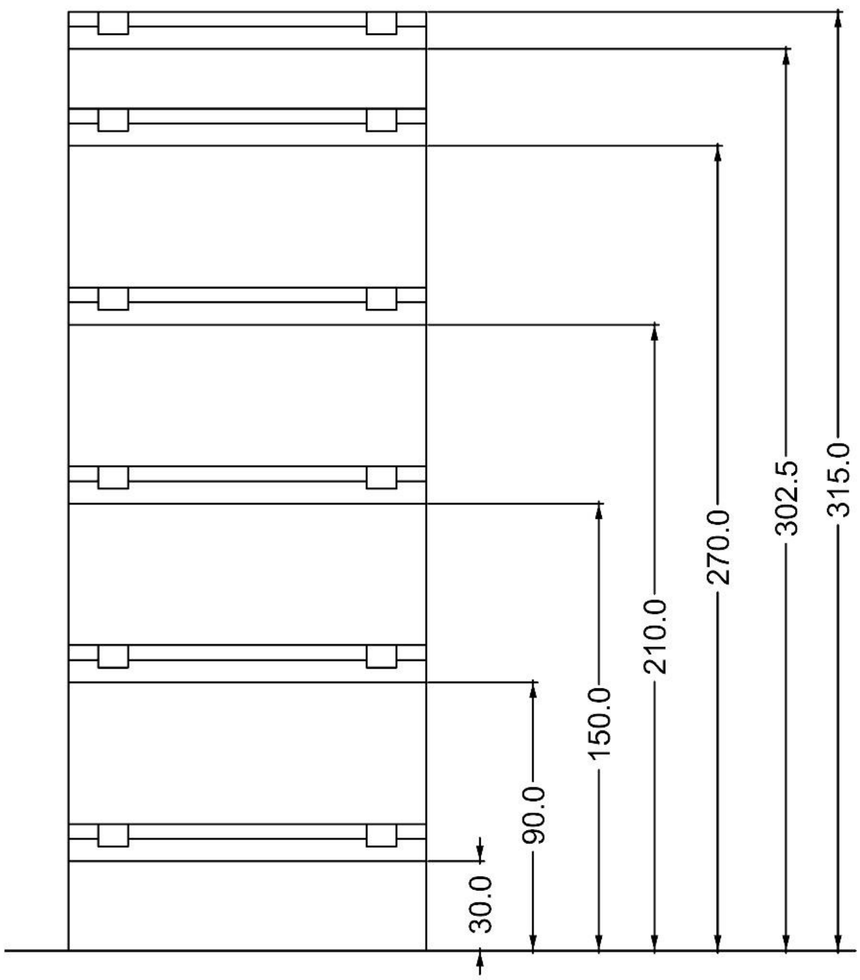

Figure 8-8 Triangular lateral distribution over the height of the wall for below timber bands - Heights

Seismic Force		
Fs= Wtot/2*PGA	201,24	kN

Table 34 Triangular distribution of the forces – below the timber bands case

Distribution of the forces			
	Weight	Heigth of Force : hi	Wi * hi
Wi	kN	m	kN*m
Wroof	17,08	3,150	53,79
W1	1,14	3,150	3,58
W2	3,33	3,025	10,08
W3	6,35	2,700	17,14
W4	6,35	2,100	13,33
W5	6,35	1,500	9,52
W6	6,35	0,900	5,71
W7	3,29	0,300	0,99

Distribution factors and Forces		
Fj	βj	Fj=Fs*βj
	/	
F1	0,50	104,63
F2	0,09	18,38
F3	0,15	31,26
F4	0,12	24,32
F5	0,08	17,37
F6	0,05	10,42
F7	0,01	1,80

In the following table are reported values of the limit values of load multiplier for a safe behavior,

$$\alpha \text{ such that } \quad \frac{Fs}{Rs} < 1$$

Table 35 Safe limit multipliers- Triangular lateral distribution- below timber bands case

Computing α such that Fs< Rshear			
Layer	Nj	Rshear = N*μs*ξ	α <
	kN	kN	
Layer1	54,64	57,44	0,55
Layer2	64,64	66,08	0,54
Layer3	83,69	81,83	0,53
Layer4	102,74	97,01	0,54
Layer5	121,79	111,76	0,57
Layer6	140,83	126,16	0,61
Layer_ground	150,71	133,50	0,64

8.2.2.1 *Uniform lateral distribution over the height of the wall*

Following the same procedure described in the previous paragraph.

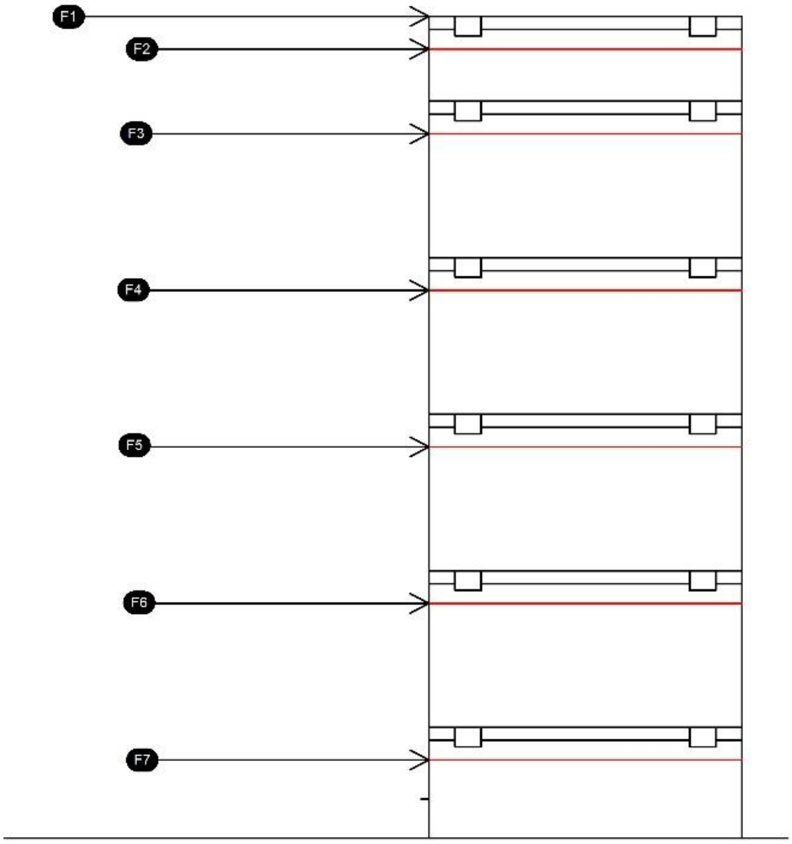

Figure 8-9 Triangular lateral distribution over the height of the wall for below timber bands

Seismic Force		
Fs= Wtot/2*PGA	201,24	kN

Table 36 Uniform distribution of the forces – below the thimber bands case

Distribution of the forces	
	Weight
Wi	kN
Wroof	17,08
W1	1,14
W2	3,33
W3	6,35
W4	6,35
W5	6,35
W6	6,35
W7	3,29
Sum	50,24

Distribution factors and Forces		
Fj	βj	Fj=Fs*βj
	/	kN
F1	0,36	75,49
F2	0,07	13,81
F3	0,13	26,31
F4	0,13	26,31
F5	0,13	26,31
F6	0,13	26,31
F7	0,07	13,64

In the following table are reported values of the limit values of load multiplier for a safe behavior,

$$\alpha \; such \; that \qquad \frac{Fs}{Rs} < 1$$

Table 37 Safe limit multipliers- Triangular lateral distribution- below timber bands case

Computing α such that Fs< Rshear			
Layer	Nj	Rshear = N*μs*ξ	α <
	kN	kN	
Layer1	54,64	57,44	0,55
Layer2	64,64	66,08	0,54
Layer3	83,69	81,83	0,53
Layer4	102,74	97,01	0,54
Layer5	121,79	111,76	0,57
Layer6	140,83	126,16	0,61
Layer_ground	150,71	133,50	0,64

8.2.1 Conclusions on seismic analysis in-plane

Recalling the results, they have been identified the critical layers for the in plane seismic analysis. The color red identified the critical load multiplier smaller than the Nepal peak ground acceleration, which is 0,5 g.

Table 38 Summary of results for the in-plane seismic analysis

	Critical Multiplier for inside stones layer case		Critical Multiplier below the timber band case	
Force applied at the top of the wall	**Layer**	**α <**	**Layer**	**α <**
	layer1	0,51	layer1	0,28
	layer2	0,62	layer2	0,32
	layer3	0,75	layer3	0,39
	layer4	0,88	layer4	0,47
	layer5	1,00	layer5	0,54
	layer6	1,10	layer6	0,61
	Layer_ground/Foundation	1,13	Layer_ground/Foundation	0,64
Triangular lateral distribution over the height of the wall	**Layer**	**α <**	**Layer**	**α <**
	Layer1	0,96	Layer1	0,55
	Layer2	0,94	Layer2	0,54
	Layer3	0,94	Layer3	0,53
	Layer4	0,98	Layer4	0,54
	Layer5	1,03	Layer5	0,57
	Layer6	1,11	Layer6	0,61
	Layer_ground/Foundation	1,13	Layer_ground/Foundation	0,64
Uniform lateral distribution over the height of the wall	**Layer**	**α <**	**Layer**	**α <**
	Layer1	1,33	Layer1	0,76
	Layer2	1,28	Layer2	0,74
	Layer3	1,23	Layer3	0,71
	Layer4	1,19	Layer4	0,68
	Layer5	1,16	Layer5	0,66
	Layer6	1,14	Layer6	0,65
	Layer_ground/Foundation	1,13	Layer_ground/Foundation	0,64

8.2.1.1 Critical Multiplier for inside stones layer case

Considering the Nepal peak ground acceleration given PGA = 0,5 g the seismic force results smaller than resisting shear force in both the sliding configurations.

The most critical one is the first configuration of «Force applied at the top of the wall» at the roof level but still on the safe side with a critical multiplier α =0,51 thus resisting to Nepal PGA.

8.2.1.2 Critical Multiplier below the timber band case

Considering the Nepal peak ground acceleration given PGA = 0,5 g the behavior shown is different in the sliding configurations examined .

The most critical one is the first configuration of «Force applied at the top of the wall”, which shows problems at the following layers:

- Layer 1
- Layer 2
- Layer 3
- Layer 4

As shown in the picture below

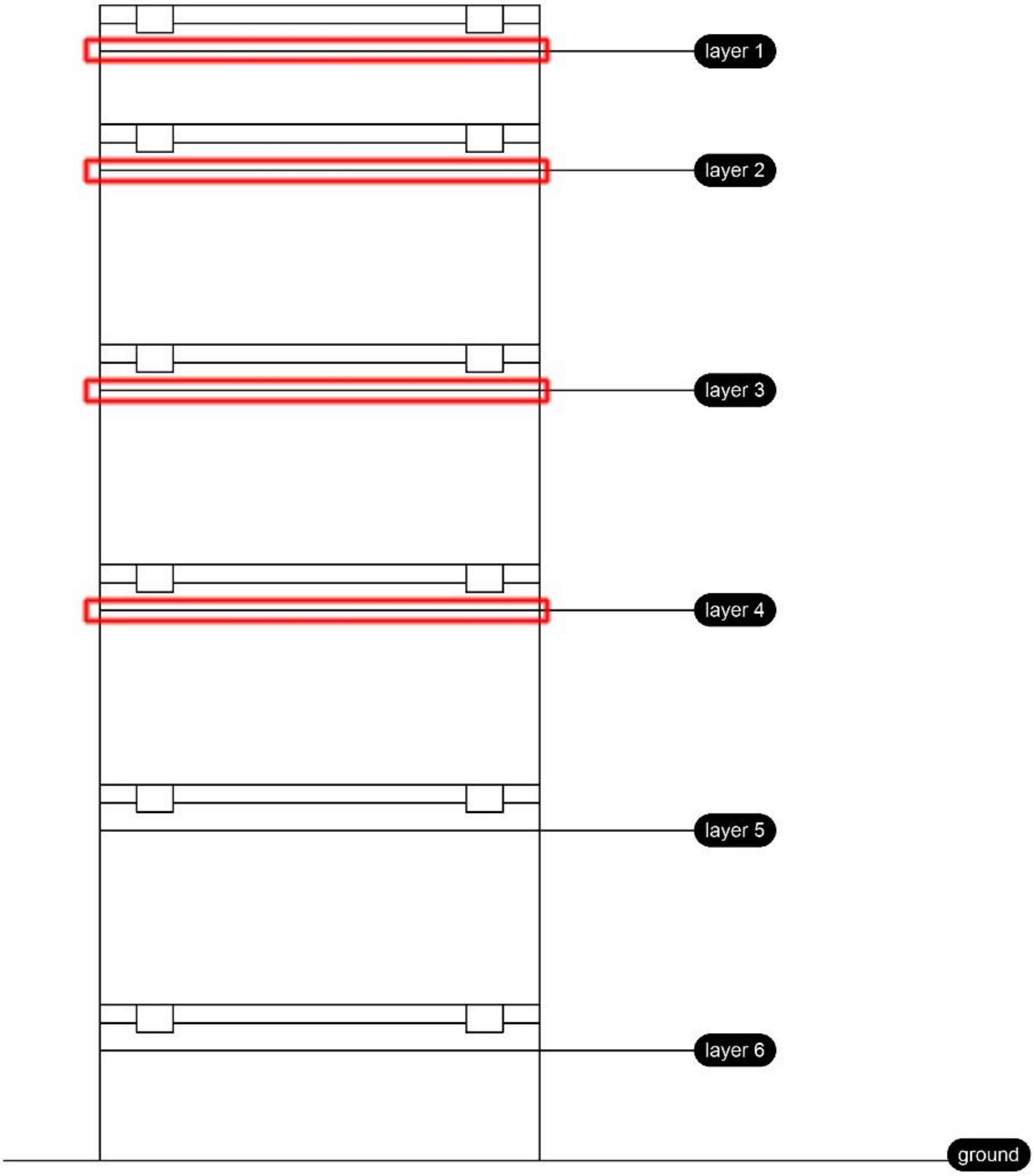

Figure 8-10 Critical layers for the in-plane seismic analysis

8.2.1.3 Safety Factor

In-plane analysis have been conducted without the use of any safty factors. The designer can only analyze for what he knows to be true. Philosophically and practically speaking it is impossible to know everything. Using a safety factor is an admission to this ignorance. Thus it has been applied to the results a safety factor γ_b = 1.5 in order to amplify the seismic actions.

Table 39 Summary of results for the in-plane seismic analysisReduced by Safety factor γ_b = 1.5

	Critical Multiplier for inside stones layer case		Critical Multiplier below the timber band case	
Force applied at the top of the wall	**Layer**	**α <**	**Layer**	**α <**
	layer1	0,34	layer1	0,18
	layer2	0,41	layer2	0,21
	layer3	0,50	layer3	0,26
	layer4	0,58	layer4	0,31
	layer5	0,67	layer5	0,36
	layer6	0,74	layer6	0,40
	Layer_ground/Foundation	0,76	Layer_ground/Foundation	0.76
Triangular lateral distribution over the height of the wall	**Layer**	**α <**	**Layer**	**α <**
	Layer1	0,64	Layer1	0,37
	Layer2	0,63	Layer2	0,36
	Layer3	0,63	Layer3	0,35
	Layer4	0,65	Layer4	0,36
	Layer5	0,69	Layer5	0,38
	Layer6	0,74	Layer6	0,41
	Layer_ground/Foundation	0,76	Layer_ground/Foundation	0.76
Uniform lateral distribution over the height of the wall	**Layer**	**α <**	**Layer**	**α <**
	Layer1	0,89	Layer1	0,51
	Layer2	0,86	Layer2	0,49
	Layer3	0,82	Layer3	0,47
	Layer4	0,80	Layer4	0,46
	Layer5	0,78	Layer5	0,44
	Layer6	0,76	Layer6	0,43
	Layer_ground/Foundation	0,76	Layer_ground/Foundation	0,43

9 SEISMIC ANALYSIS OUT OF PLANE – OVERTURNING RIGID BEHAVIOR

The failure mechanisms due to the seismic action may happen in the perpendicular direction in respect to the length of the wall. In this chapter will be explained what is defined as the overturning mechanism of the wall.

9.1 Hypothesis of rigid body behavior

The wall has been considered as it was composed by rigid blocks, which may overturn around ideal hinges set in different positions over the height of the wall. The figure below is recalled from the chapter 6 where they were explained the timber tie-beam chain activation.

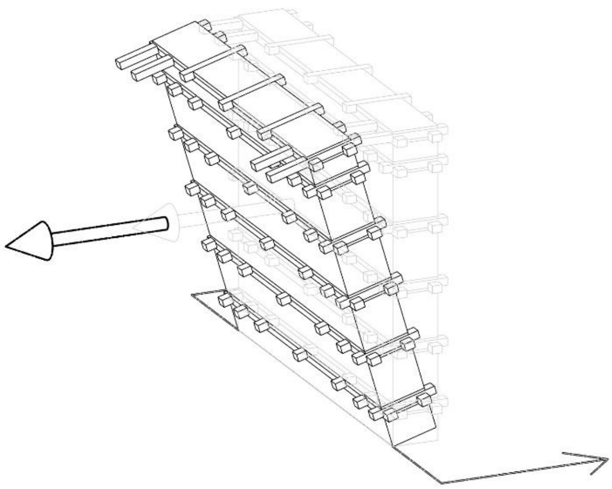

Figure 9-1 Overturning mechanism – example scheme

The stabilizing traction is equally divided between the to parallel tie-timber beam chains which are composed by 2 roof rafters or 2 rafters.

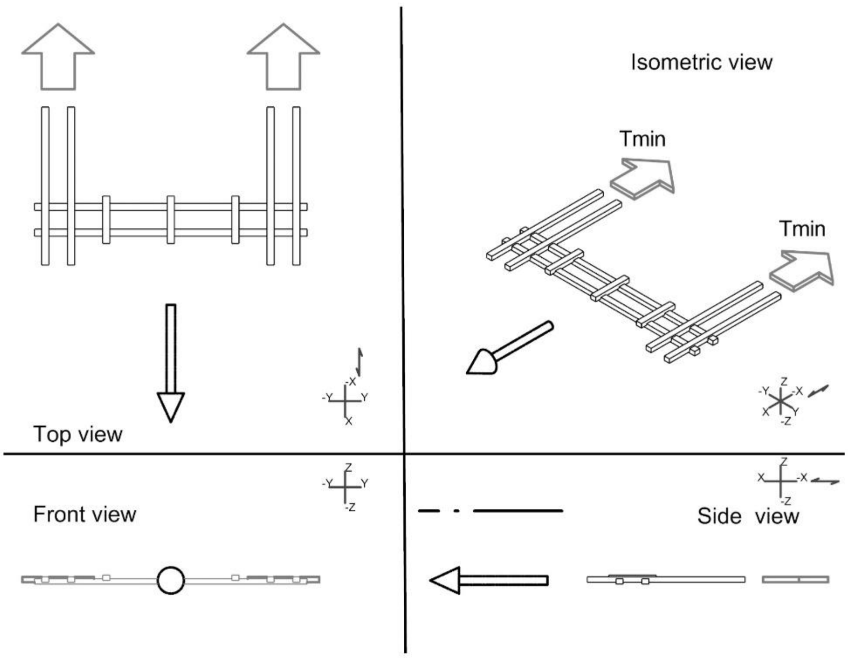

Figure 9-2 Overturning mechanism - tie-timber beam chains activation

9.2 Rigid body over rigid soil by Equilibrium – Tmin as function of α load multiplier - Hand calculation

Using the equilibrium method, they have been analyzed the horizontal and rotational equilibrium. They have been obtained equations in function of the load multiplier in order to get the values of the applied to the rafters. These tensions are the limit values needed to avoid the failures.

The main data used for this aim are reported below.

Table 40 Masses of each analyzed layer

Mass for each Force 3 module		
	KN	Kg
Wroof module	51,23	5222,31
W1	6,70	683,48
W2	14,52	1480,36
W3	19,05	1941,72
W4	19,05	1941,72
W5	19,05	1941,72
W6	16,17	1648,13
W7	4,94	503,29

Table 41 Total weight and mass of the wall composed by 3 single modular unit

Total Weight 1 wall (3 module)		
	KN	Kg
Wtot	150,71	15362,73

Table 42 Heights of the considered rafters

Height of Force : hi	
Hi	m
Hroof	3,10
H1	3,10
H2	2,78
H3	2,18
H4	1,58
H5	0,98
H6	0,38
Htchain	3,0875

Where Htchain is the height from the ground of the centroid of the roof rafter beam.

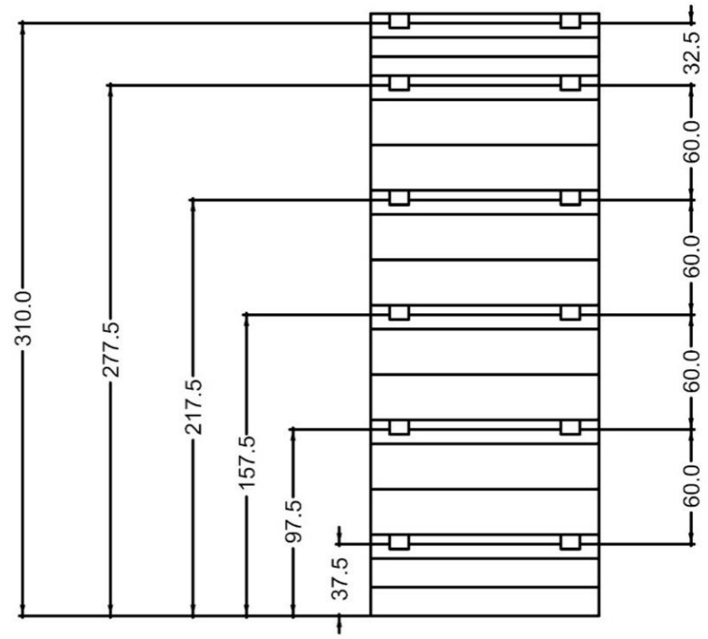

Figure 9-3 Heights of the rafters and distances between the timber beams bands

9.2.1 Horizontal equilibrium

The horizontal equilibrium has been computed for completeness and it is unlikely. It is the only one case where all the rafters have been considered as working at the same time. For the analysis the tensions defined in the drawing as T1 until T6 has the identic values then it will be named with just a single name like Tmin.

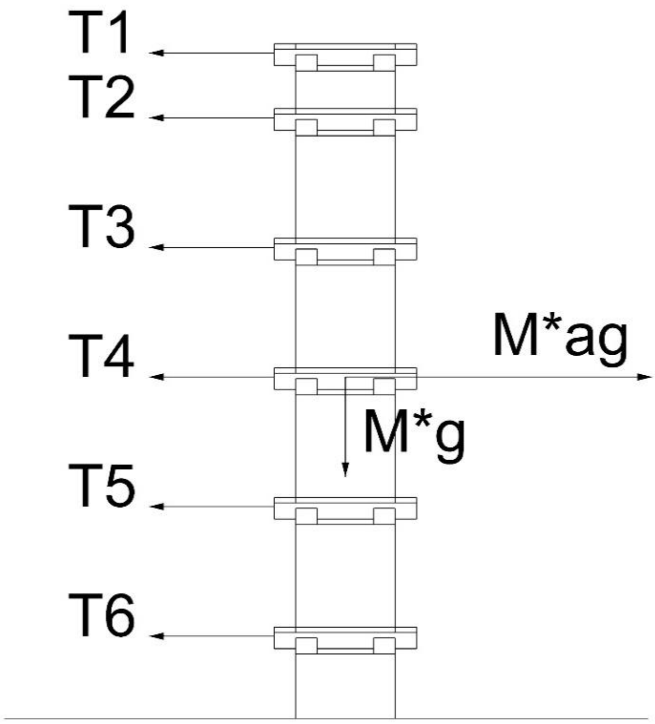

Figure 9-4 Horizontal equilibrium – equilibrium method

9.2.1.1 Minimum Traction dependent on α

Equations for computing the Minimum tensions as function of α load multiplier are shown below:

$$T_{min} * n = M_{tot} * a_g * \alpha$$

$$a_g = g \ then$$

$$T_{min} = \frac{M_{tot} * a_g}{n} * \alpha = \frac{W_{tot}}{n} * \alpha$$

Where

T_{min} is the minimum tension allowed for resisting to the seismic action

n is the total number of tie timber beams, for 3,6 m length wall = 12 (Each timber tie-beam is composed by 2 rafters)

M_{tot} is the total mass of the 3,6 m length wall

a_g is the seismic acceleration in g

g is the gravity acceleration constant = 9,81 m/s^2

Results are reported in the following table.

Table 43 Horizontal equilibrium - minimum tensions

Minimum Tension dependent on α	
α	Tmin (kN)
0	0,00
0,1	1,26
0,2	2,51
0,3	3,77
0,4	5,02
0,5	6,28
0,6	7,54
0,7	8,79
0,8	10,05
0,9	11,30
1	12,56

9.2.2 Rotational equilibrium

The rotational equilibrium has been computed by the equilibrium method, in this case they have been considered just the two tie timber beam at the roof level, as shown in the figure below.

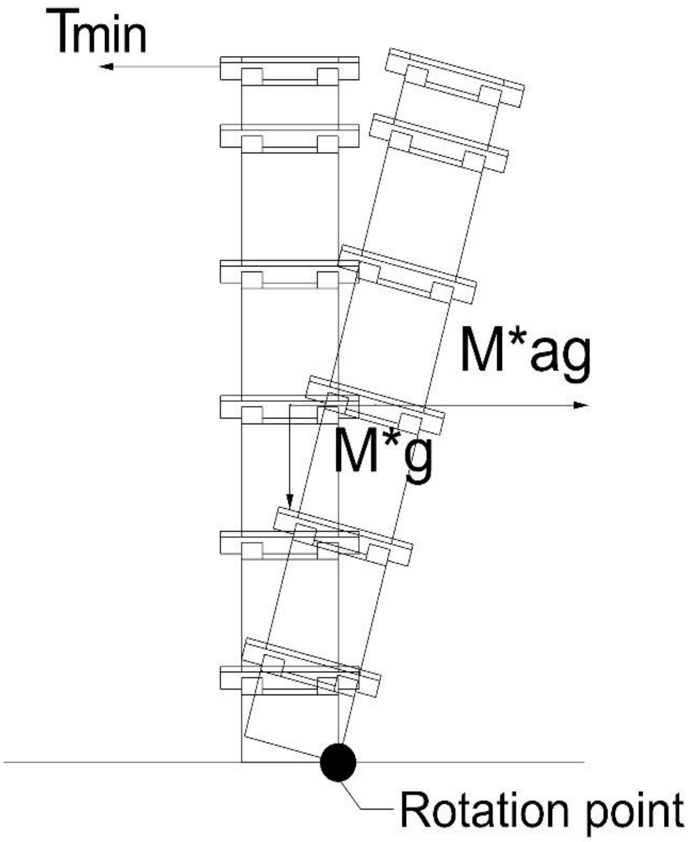

Figure 9-5 Rotational equilibrium – equilibrium method

9.2.2.1 Minimum Traction dependent on α

Equations for computing the minimum tensions as function of α load multiplier are shown below:

$$2 * T_{min} * Ht_{chain} = M_{tot} * a_g * \frac{H}{2} * \alpha - M_{tot} * g * \frac{B}{2}$$

$$a_g = g$$

$$T_{min} = \frac{M_{tot} * a_g * \frac{H}{2} * \alpha - M_{tot} * g * \frac{B}{2}}{2 * Ht_{chain}}$$

Where the new parameters in respect to the horizontal equilibrium are :

H is the height of the centroid of the section of the wall

B is the horizontal component of the centroid of the section of the wall

Table 44 Centroid of the section of the wall - data

H centroid	1,583	m
B centroid	0,23	m

Table 45 Rotational equilibrium - minimum tensions

Minimum Tension dependent on α	
α	Tmin (kN)
0	~~-5,61~~
0,1	~~-1,75~~
0,2	2,11
0,3	5,98
0,4	9,84
0,5	13,70
0,6	17,57
0,7	21,43
0,8	25,29
0,9	29,16
1	33,02

9.3 Rigid body over rigid soil by PVW - α load multiplier - Hand calculation

The overturning mechanism has been studied with the principle of virtual work method, which consider the relations about the energies involved in the mechanism. In order to ensure the equilibrium the external energies must be equal to the internal energies developed by the mechanism. The principle of virtual work method has been used for different configurations of the forces as well for different configurations of the position of the hinges (or rotation points).

In the following paragraphs are reported two configuration of forces:

- Unique seismic force on the top ;
- Roof force + Wall force, this means that the force developed from the inertia of the roof mass has been considered distinguished and applied at the roof level while the wall mass has been set applied at the centroid of the section of the wall.

The two force configurations have been studied for different cases:

- α critical – for this case the activation of the tie-timber beam chains has been neglected with the aim of understanding the behavior of the free wall;
- Tmin – for this case they have been applied all the value of the seismic load multiplier from 0,0 to 1,0 with steps of 0,1 in order to know the values of the tension applied to the rafters by the seismic event.

The analysis has been conducted considering a rigid block behavior, for accuracy, it is important to underline that in the following pages, the behavior of the whole wall is the last case of the blocks analysis but it has been described apart.

9.3.1 Unique seismic force on the top

The main data used for this aim are reported below.

Table 46 Weights and masses pertinent to studied blocks

Weights in 3 modulus		
	KN	Kg
Wroof on timber 1	57,94	5905,80
W2 on timber 2	72,46	7386,16
W3 on timber 3	91,51	9327,88
W4 on timber 4	110,55	11269,59
W5 on timber 5	129,60	13211,31
W6 on timber 6	145,77	14859,44
W7 on ground	150,71	15362,73

Table 47 Heights and ratios for Δ proportional multiplier between 0 and 1

Heights and ratios for Δ proportional multiplier between 0 and 1				
Hinge	H	Δhi	Δ	H*(1-ΔH)
2	3,15	0,325	0,103175	2,825
3	3,15	0,925	0,293651	2,225
4	3,15	1,525	0,484127	1,625
5	3,15	2,125	0,674603	1,025
6	3,15	2,725	0,865079	0,425

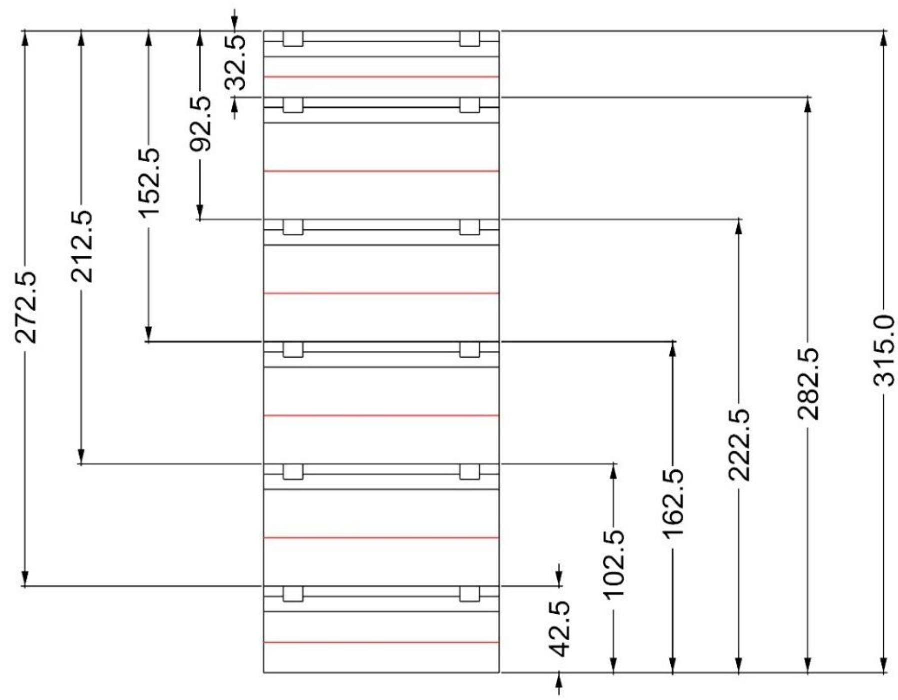

Figure 9-6 Hinges posotions

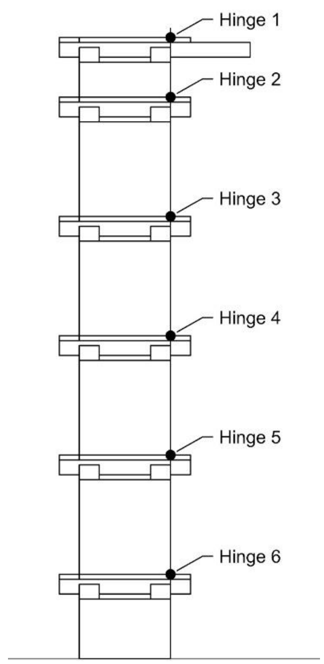

Figure 9-7 Hinges heights and Blocks Heights

9.3.1.1 Overturning Wall - α critical

Equations for computing the critical α load multiplier are shown below:

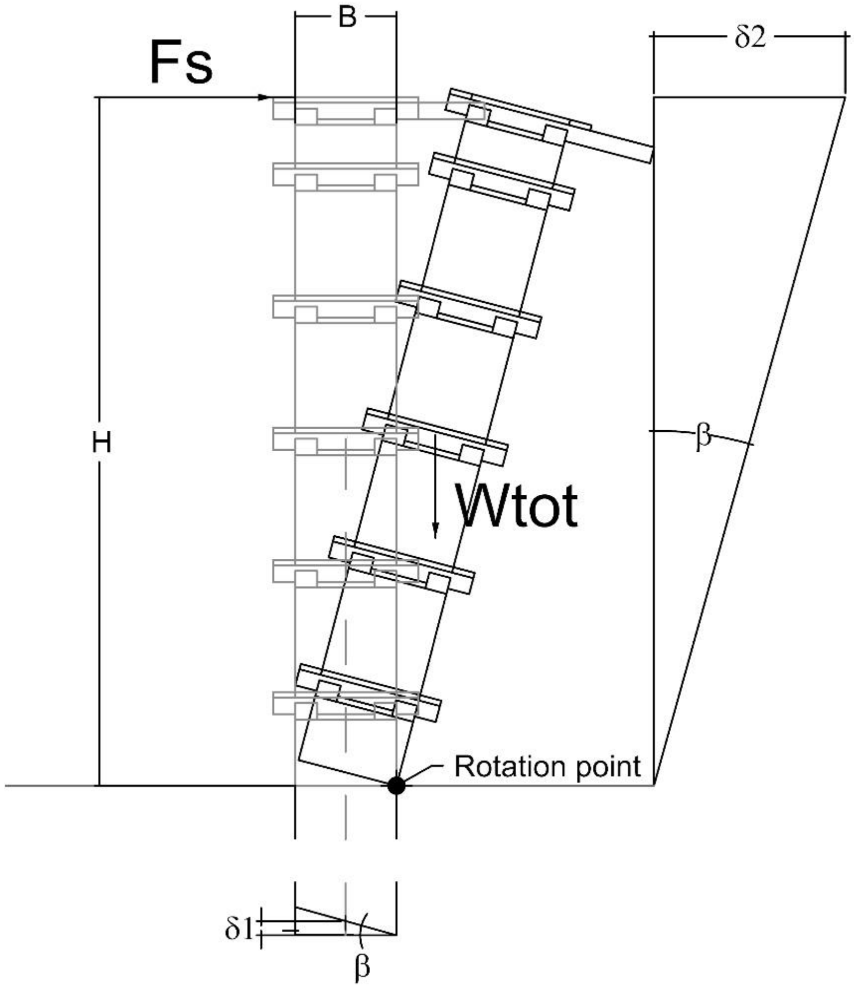

Figure 9-8 Unique seismic force on the top - Overturning Wall - α critical

$$E_{ext} - E_{int} = 0$$

$$F_s * \delta 2 - W_{tot} * \delta 1 = 0$$

$$\alpha * (W_{tot}) * H * \beta - W_{tot} * \frac{B}{2} * \beta = 0$$

$$\alpha = \frac{W_{tot} * B}{W_{tot} * 2 * H}$$

$$\alpha = \frac{B}{2 * H}$$

$$\alpha = \frac{0.46}{2 * 3{,}15} = 0.073$$

Where

E_{ext} is the external energy

E_{int} is the internal energy

β is the rotation angle for the overturning mechanism

$\delta 1$ is the displacement of the centroid

$\delta 2$ is the displacement of the application point of the considered seismic force

9.3.1.2 Overturning Blocks - α critical

The critical load multiplier for the configuration of the unique seismic force applied on the top of the wall for the analysis of the blocks is the same of the entire wall case. This is due to the fact that the computation end up with a ratio of the same geometrical component.

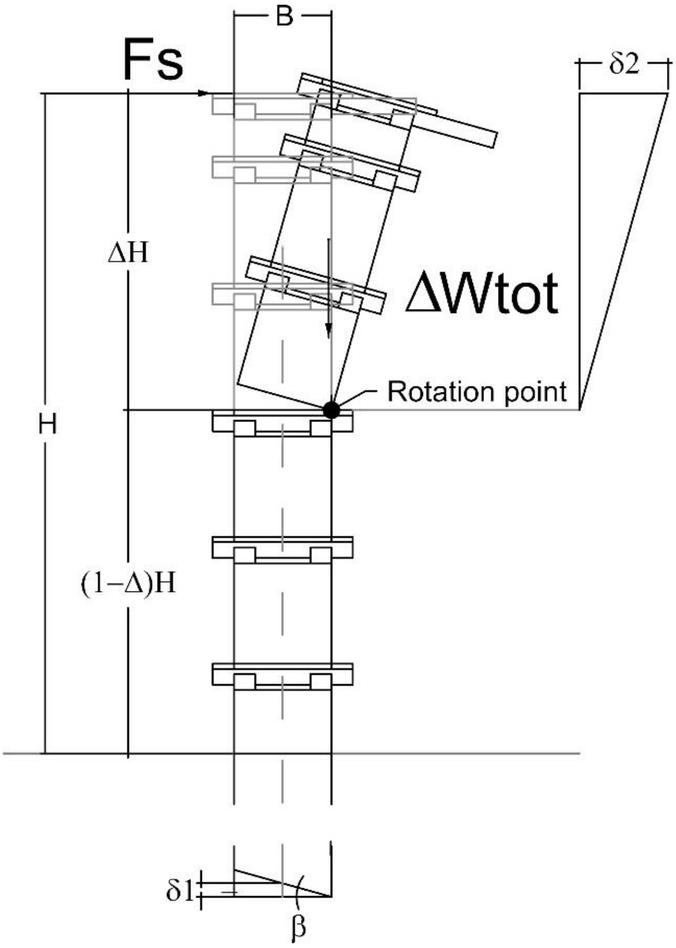

Figure 9-9 Unique seismic force on the top - Overturning Blocks - α critical

$$F_s * \delta 2 - \Delta W_{tot} * \delta 1 = 0$$

$$\alpha * (W_{tot}) * \Delta * H * \beta - \Delta * W_{tot} * \frac{B}{2} * \beta = 0$$

$$\alpha = \frac{\Delta * W_{tot} * B}{\Delta * W_{tot} * 2 * H}$$

$$\alpha = \frac{B}{2 * H}$$

$$\alpha = \frac{0.46}{2 * 3{,}15} = 0.073$$

where

Δ= proportional multiplier between 0 and 1 based on the position of the hinges and the heights of the blocks.

9.3.2 Roof force + Wall force

9.3.2.1 Overturning Wall - α critical

Equations for computing the critical α load multiplier are shown below:

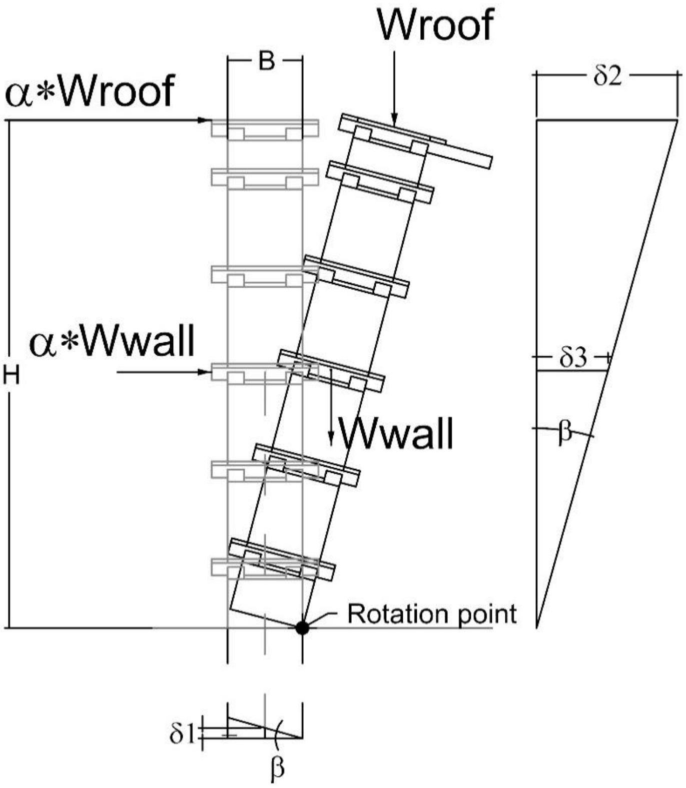

Figure 9-10 Roof force + Wall force - Overturning Wall - α critical

$$\alpha * W_{roof} * \delta 2 + \alpha * W_{wall} * \delta 3 - \left(W_{roof} + W_{wall}\right) * \delta 1 = 0$$

$$\alpha * W_{roof} * H * \beta + \alpha * W_{wall} * \frac{H}{2} * \beta - \left(W_{roof} + W_{wall}\right) * \frac{B}{2} * \beta = 0$$

$$\alpha * H * \left(W_{roof} + \frac{W_{wall}}{2}\right) = \frac{\left(W_{roof} + W_{wall}\right) * B}{2}$$

$$\alpha = \frac{B}{2 * H} * \frac{\left(W_{roof} + W_{wall}\right)}{\left(W_{roof} + \frac{W_{wall}}{2}\right)}$$

$$\alpha = 0{,}1055$$

W_{roof} is the weight of the roof

W_{wall} is the weight of the wall

$\delta 1$ is the displacement of the centroid

$\delta 2$ is the displacement of the application point of the considered seismic force of the roof

$\delta 3$ is the displacement of the application point of the considered seismic force of the wall

9.3.2.2 Overturning Blocks - α critical

Equations for computing the critical α load multiplier are shown below:

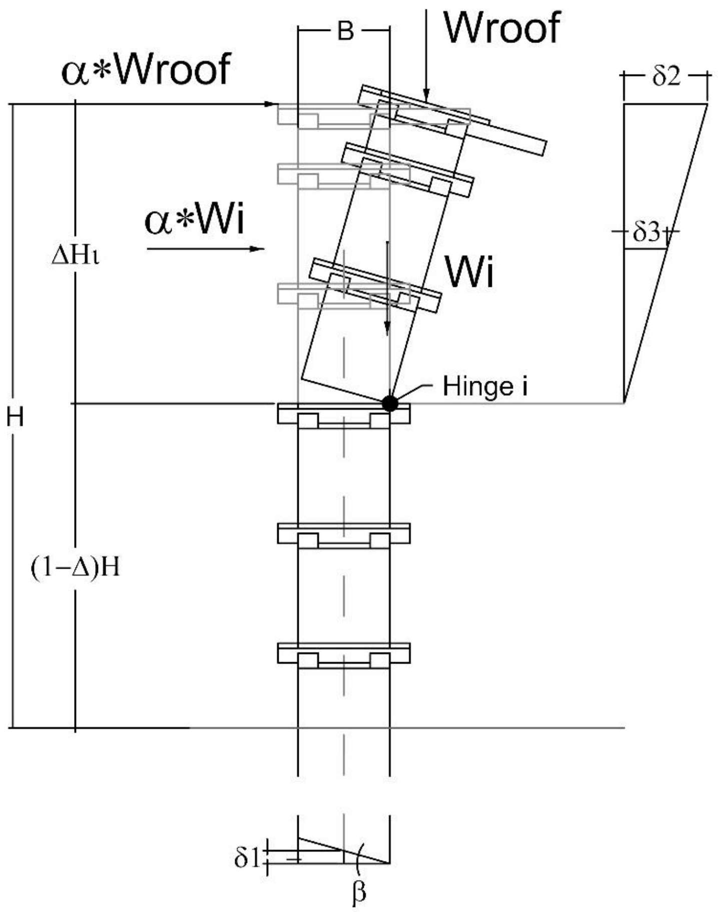

Figure 9-11 Roof force + Wall force - Overturning Blocks - α critical

$$\alpha * W_{roof} * \delta 2 + \alpha * W_i * \delta 3 - \left(W_{roof} + W_i\right) * \delta 1 = 0$$

$$\alpha * W_{roof} * \Delta H_i * \beta + \alpha * W_i * \frac{\Delta H_i}{2} * \beta - \left(W_{roof} + W_i\right) * \frac{B}{2} * \beta = 0$$

$$\alpha = \frac{B}{2 * \Delta H_i} * \frac{\left(W_{roof} + W_i\right)}{\left(W_{roof} + \frac{W_i}{2}\right)}$$

Where

W_i is the weights of the pertinent block.

Table 48 Roof force + Wall force - Overturning Blocks - α critical multipliers

	Weights in 3 modulus							
hinge i	Wi	KN	Kg	H	Δhi	Δ	H*(1-ΔH)	α
hinge 1	Wroof on timber 1	57,94	5905,80	/	/	/	/	/
hinge 2	W2 on timber 2	72,46	7386,16	3,15	0,325	0,103	2,825	0,79
hinge 3	W3 on timber 3	91,51	9327,88	3,15	0,925	0,294	2,225	0,30
hinge 4	W4 on timber 4	110,55	11269,59	3,15	1,525	0,484	1,625	0,20
hinge 5	W5 on timber 5	129,60	13211,31	3,15	2,125	0,675	1,025	0,15
hinge 6	W6 on timber 6	145,77	14859,44	3,15	2,725	0,865	0,425	0,12

The α critical load multipliers reported must be read as maximum limit value beyond which the failure mechanism happens.

9.3.3 Unique seismic force on the top with timber tie-beams - Minimum Tension dependent on α

In the following pages, it is reported the calculus procedure used to obtain the minimum tension acting on the tie-timber beam chains due to different α load multipliers.

The main data used for this aim are reported below.

Table 49 Weights and masses pertinent to studied blocks - Tmin

Weights in 3 modulus		
	KN	Kg
Wroof on timber 1	57,94	5905,80
W2 on timber 2	72,46	7386,16
W3 on timber 3	91,51	9327,88
W4 on timber 4	110,55	11269,59
W5 on timber 5	129,60	13211,31
W6 on timber 6	145,77	14859,44
W7 on ground	150,71	15362,73

Table 50 Heights and ratios for Δ proportional multiplier between 0 and 1 - Tmin

Heights of the mass and forces						
Heights of the mass				Height of Force : Ht		
Block	Δhi	Δ	H of hinge : H*(1-Δ)	Hti	m	Δhti (m)
roof	0	0	3,15	Htroof	3,100	/
Timber1	0	0	3,15	Ht1	3,100	/
Timber2	0,325	0,103174603	2,825	Ht2	2,775	0,2625
Timber3	0,925	0,293650794	2,225	Ht3	2,175	0,8625
Timber4	1,525	0,484126984	1,625	Ht4	1,575	1,4625
Timber5	2,125	0,674603175	1,025	Ht5	0,975	2,0625
Timber6	2,725	0,865079365	0,425	Ht6	0,375	2,6625
Wall	3,15	1	0	Htchain	0,000	3,0875
				Sum	10,975	3,0875

9.3.3.1 Overturning Wall – Tmin

Equations for computing the minimum tensions as function of α load multiplier are shown below:

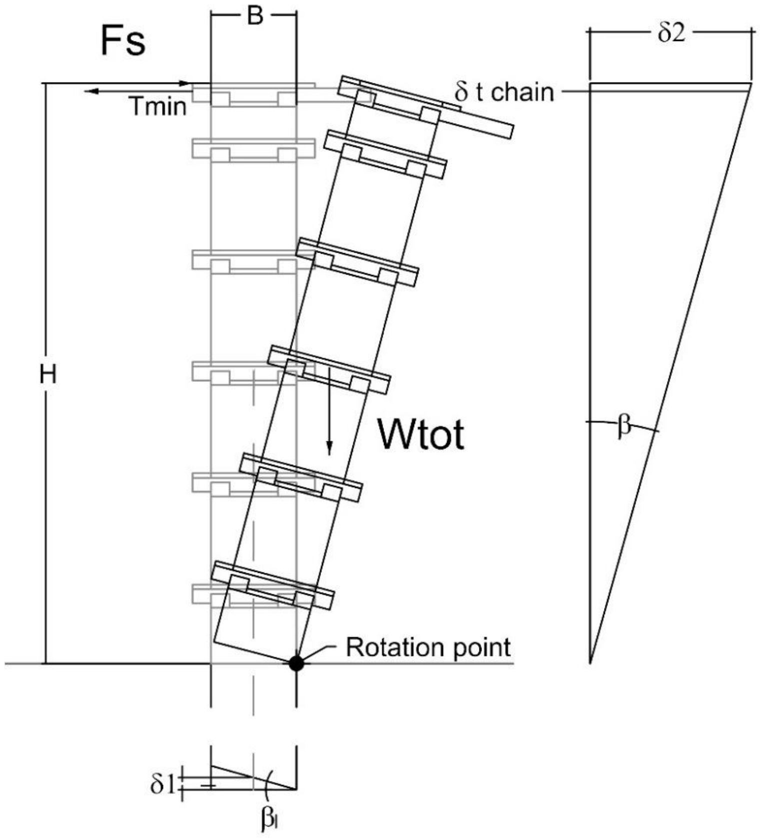

Figure 9-12 Unique seismic force on the top - Overturning Wall - Tmin

$$F_s * \delta 2 - W_{tot} * \delta 1 - 2 * T_{min} * \delta t_{chain} = 0$$

$$\alpha * (W_{tot}) * H * \beta - W_{tot} * \frac{B}{2} * \beta - 2 * T_{min} * Ht_{chain} * \beta = 0$$

$$T_{min} = \frac{W_{tot} * H * \alpha \ - \ W_{tot} * \frac{B}{2}}{2 * Ht_{chain}}$$

Where

T_{min} is the minimum tension due to the seismic event on the roof tie timber beam

δt_{chain} is the displacement of the application point of the roof timber beams acting as a chain

Ht_{chain} is the height of the roof timber beams acting as a chain

Table 51 Unique seismic force on the top - Overturning Wall - Tmin

Minimum Tension dependent on α	
α	Tmin (kN)
0	-5,61
0,1	1,95
0,2	9,52
0,3	17,08
0,4	24,65
0,5	32,22
0,6	39,78
0,7	47,35
0,8	54,91
0,9	62,48
1	70,05

9.3.3.2 Overturning Blocks – Tmin

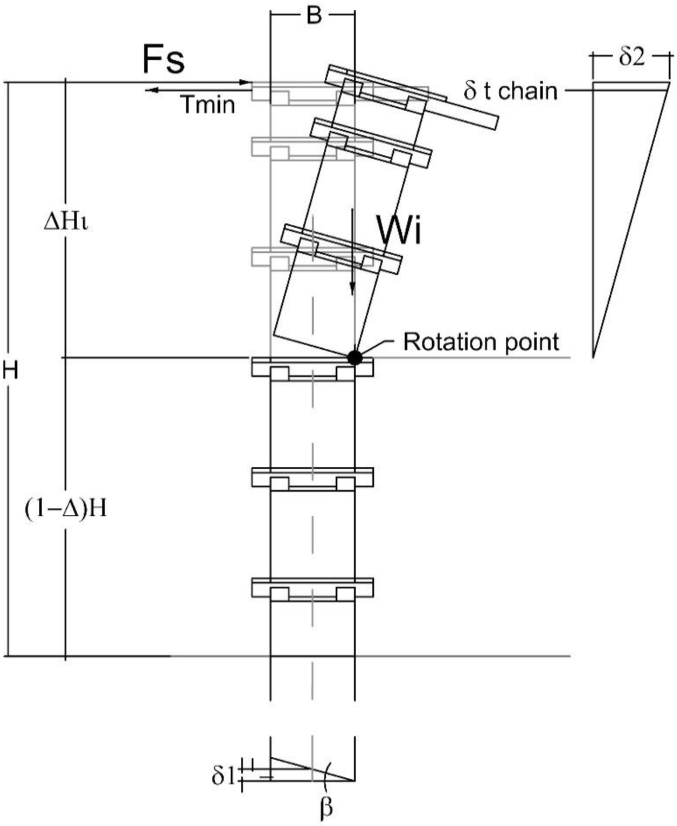

Figure 9-13 Unique seismic force on the top - Overturning Blocks - Tmin

$$F_s * \delta 2 - W_{on\ timber} * \delta 1 - 2 * T_{min} * \delta t_{chain} = 0$$

$$\alpha_i * (W_i) * \Delta H_i * \beta - W_i * \frac{B}{2} * \beta - 2 * T_{min} * Ht_{chain} * \beta = 0$$

$$T_{min} *= \frac{\alpha_i * W_i * \Delta H_i - W_i * \frac{B}{2}}{2 * Ht_{i-chain}}$$

Table 52 Unique seismic force on the top - Overturning Blocks - Tmin -data and results

Tmin for Unique seismic force on top														
hinge i	Wi		Δhi	Δhti-chain	α=									
		kN	(m)	(m)	0,1	0,2	0,3	0,4	0,5	0,6	0,7	0,8	0,9	1
hinge 1	Wroof on timber 1	57,94	/	/	/	/	/	/	/	/	/	/	/	/
hinge 2	W2 on timber 2	72,46	0,325	0,26	-27,26	-22,77	-18,29	-13,80	-9,32	-4,83	-0,35	4,14	8,63	13,11
hinge 3	W3 on timber 3	91,51	0,925	0,86	-7,29	-2,39	2,52	7,43	12,33	17,24	22,15	27,05	31,96	36,87
hinge 4	W4 on timber 4	110,55	1,525	1,46	-2,93	2,83	8,60	14,36	20,13	25,89	31,65	37,42	43,18	48,95
hinge 5	W5 on timber 5	129,60	2,125	2,06	-0,55	6,13	12,80	19,48	26,16	32,83	39,51	46,19	52,86	59,54
hinge 6	W6 on timber 6	145,77	2,725	2,66	1,16	8,62	16,08	23,54	31,00	38,46	45,92	53,38	60,84	68,30

Table 53 Unique seismic force on the top - Overturning Blocks - Tmin

Tmin=f(α) [kN]	α=									
	0,1	0,2	0,3	0,4	0,5	0,6	0,7	0,8	0,9	1
hinge 1	/	/	/	/	/	/	/	/	/	/
hinge 2	-27,26	-22,77	-18,29	-13,80	-9,32	-4,83	-0,35	4,14	8,63	13,11
hinge 3	-7,29	-2,39	2,52	7,43	12,33	17,24	22,15	27,05	31,96	36,87
hinge 4	-2,93	2,83	8,60	14,36	20,13	25,89	31,65	37,42	43,18	48,95
hinge 5	-0,55	6,13	12,80	19,48	26,16	32,83	39,51	46,19	52,86	59,54
hinge 6	1,16	8,62	16,08	23,54	31,00	38,46	45,92	53,38	60,84	68,30

The negative values must be considered with no physical meanings.

9.3.4 Roof force + Wall force with timber tie-beams - Minimum Traction dependent on α

9.3.4.1 Overturning Wall – Tmin

Equations for computing the minimum tensions as function of α load multiplier are shown below:

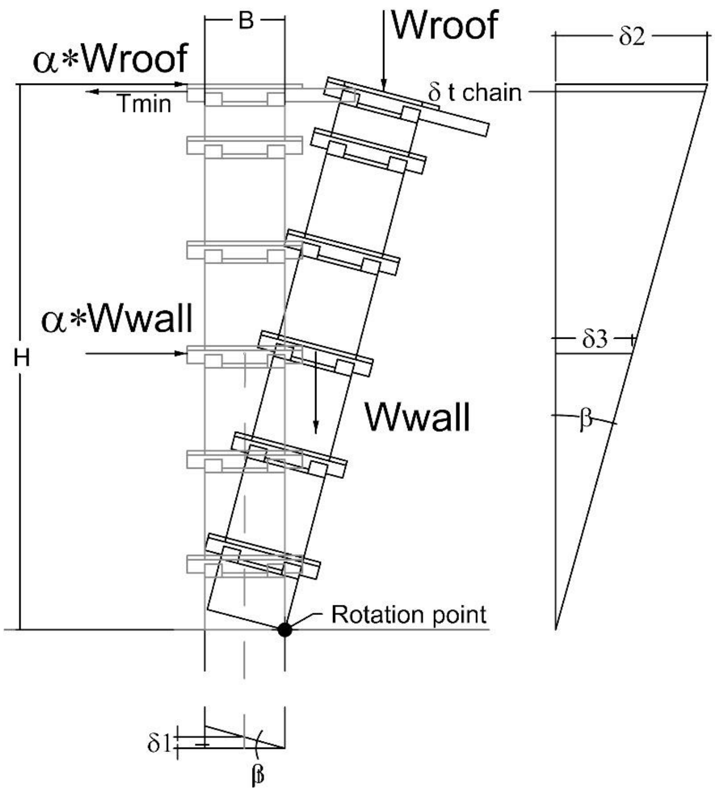

Figure 9-14 Roof force + Wall force - Overturning Wall - Tmin

$$\alpha * W_{roof} * \delta 2 + \alpha * W_{wall} * \delta 3 - \left(W_{roof} + W_{wall}\right) * \delta 1 - 2 * T_{min} * \delta t_{chain} = 0$$

$$\alpha * W_{roof} * H * \beta + \alpha * W_{wall} * \frac{H}{2} * \beta - \left(W_{roof} + W_{wall}\right) * \frac{B}{2} * \beta - 2 * T_{min} * Ht_{chain} * \beta = 0$$

$$\alpha * H * \left(W_{roof} + \frac{W_{wall}}{2}\right) = \frac{(W_{roof}+W_{wall})*B}{2} + 2 * T_{min} * Ht_{chain}$$

$$T_{min} = \frac{\alpha * H * \left(W_{roof} + \frac{W_{wall}}{2}\right) - \left(W_{roof} + W_{wall}\right) * \frac{B}{2}}{2 * Ht_{chain}}$$

Table 54 Roof force + Wall force - Overturning Wall - Tmin

Minimum Tension dependent on α	
α	Tmin (kN)
0	-7,77
0,1	-1,08
0,2	5,61
0,3	12,30
0,4	18,99
0,5	25,69
0,6	32,38
0,7	39,07
0,8	45,76
0,9	52,45
1	59,14

9.3.4.2 Overturning Blocks – Tmin

Equations for computing the minimum tensions as function of α load multiplier are shown below:

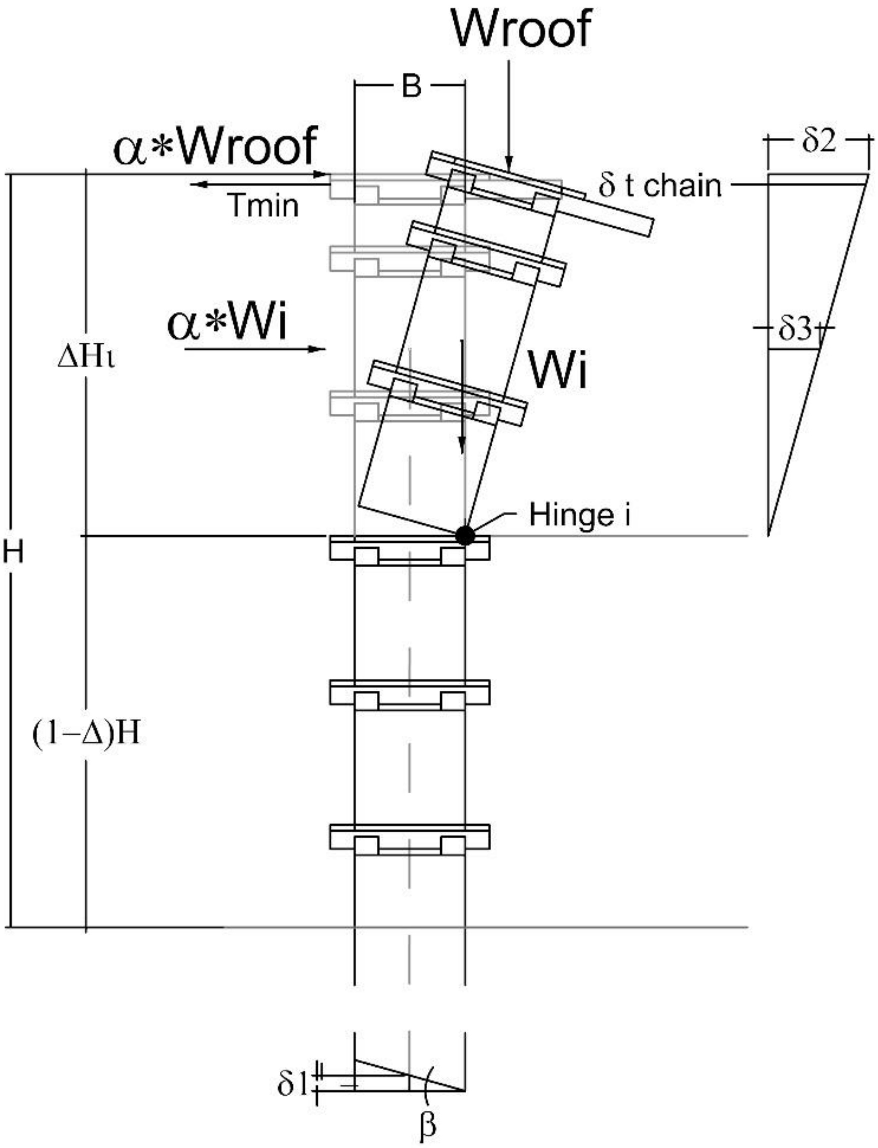

Figure 9-15 Roof force + Wall force - Overturning Blocks – Tmin

$$\alpha_i * W_{roof} * \delta 2 + \alpha_i * W_i * \delta 3 - \left(W_{roof} + W_i\right) * \delta 1 \; - 2 * T_{min} * \delta t_{i-chain} = 0$$

$$\alpha_i * W_{roof} * \Delta H_i * \beta + \alpha_i * W_i * \frac{\Delta H_i}{2} * \beta - \left(W_{roof} + W_i\right) * \frac{B}{2} * \beta \; - 2 * T_{min} * Ht_{i-chain} * \beta = 0$$

$$T_{min} = \frac{\alpha_i * \Delta H_i * \left(W_{roof} + \frac{W_i}{2}\right) - \left(W_{roof} + W_i\right) * \frac{B}{2}}{2 * Ht_{i-chain}}$$

Table 55 Roof force + Wall force - Overturning Blocks - Tmin -data and results

Tmin for Seismic force due to wall(in the centroide) and roof (on top)														
hinge i	Wi		Δhi	Δhti-chain	α=									
		KN	(m)	(m)	0,1	0,2	0,3	0,4	0,5	0,6	0,7	0,8	0,9	1
hinge 1	Wroof timber 1	57,94	/	/	/	/	/	/	/	/	/	/	/	/
hinge 2	W2 on timber 2	72,46	0,325	0,26	-27,71	-23,67	-19,64	-15,60	-11,56	-7,53	-3,49	0,54	4,58	8,62
hinge 3	W3 on timber 3	91,51	0,925	0,86	-8,19	-4,19	-0,18	3,83	7,83	11,84	15,85	19,85	23,86	27,87
hinge 4	W4 on timber 4	110,55	1,525	1,46	-4,30	0,09	4,48	8,88	13,27	17,66	22,05	26,45	30,84	35,23
hinge 5	W5 on timber 5	129,60	2,125	2,06	-2,40	2,43	7,27	12,10	16,93	21,76	26,59	31,42	36,25	41,08
hinge 6	W6 on timber 6	145,77	2,725	2,66	-1,08	4,13	9,34	14,55	19,76	24,98	30,19	35,40	40,61	45,83

Table 56 Roof force + Wall force - Overturning Blocks – Tmin

Tmin=f(α) [kN]	α=									
	0,1	0,2	0,3	0,4	0,5	0,6	0,7	0,8	0,9	1
hinge 1	/	/	/	/	/	/	/	/	/	/
hinge 2	-27,71	-23,67	-19,64	-15,60	-11,56	-7,53	-3,49	0,54	4,58	8,62
hinge 3	-8,19	-4,19	-0,18	3,83	7,83	11,84	15,85	19,85	23,86	27,87
hinge 4	-4,30	0,09	4,48	8,88	13,27	17,66	22,05	26,45	30,84	35,23
hinge 5	-2,40	2,43	7,27	12,10	16,93	21,76	26,59	31,42	36,25	41,08
hinge 6	-1,08	4,13	9,34	14,55	19,76	24,98	30,19	35,40	40,61	45,83

9.4 Conclusions about the highest required tension strength Tmin

9.4.1 Horizontal equilibrium and Rotational equilibrium – Tmin

The values reported on the Rotational equilibrium ,focused on Minimum Traction dependent on α, show how much the chain at the roof level needs to bear.

In order to resist a PGA of 0,5 g the chain must bear at least 13,70 kN.

Minimum Tension dependent on α	
α	Tmin (kN)
0	~~-5,61~~
0,1	~~-1,75~~
0,2	2,11
0,3	5,98
0,4	9,84
0,5	13,70
0,6	17,57
0,7	21,43
0,8	25,29
0,9	29,16
1	33,02

9.4.2 Unique seismic force on the top - α critical

In the kinetic approach both the studied cases, entire wall mechanism and block by block mechanism, show the same critical seismic multiplier. This multilpier is quite low but it seems to be correct due to the fact of the absence of the mortar and neither any other stabilizing devices.

$$\alpha = 0.073$$

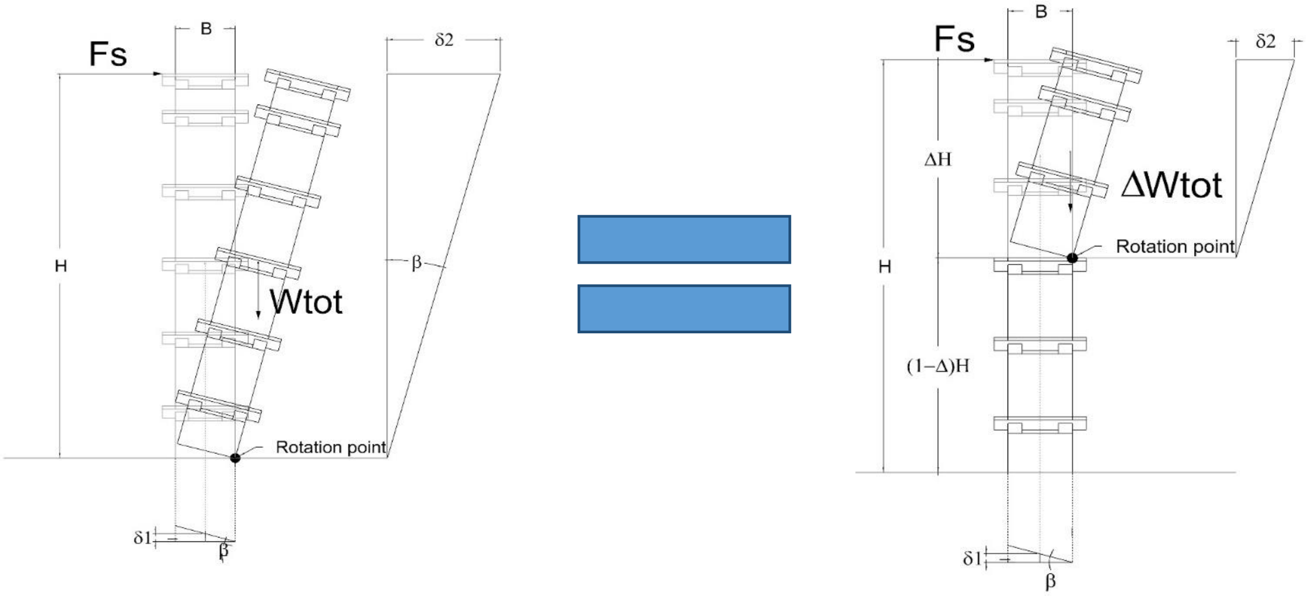

9.4.3 Roof force + Wall force - α critical

In the kinetic approach both the studied cases, entire wall mechanism and block by block mechanism, show the different critical seismic multipliers. In the case of block by block mechanism:

	Weights in 3 modulus							
hinge i	Wi	KN	Kg	H	Δhi	Δ	H*(1-ΔH)	α
hinge 1	Wroof on timber 1	57,94	5905,80	/	/	/	/	/
hinge 2	W2 on timber 2	72,46	7386,16	3,15	0,325	0,103	2,825	0,79
hinge 3	W3 on timber 3	91,51	9327,88	3,15	0,925	0,294	2,225	0,30
hinge 4	W4 on timber 4	110,55	11269,59	3,15	1,525	0,484	1,625	0,20
hinge 5	W5 on timber 5	129,60	13211,31	3,15	2,125	0,675	1,025	0,15
hinge 6	W6 on timber 6	145,77	14859,44	3,15	2,725	0,865	0,425	0,12

The most critical case is the one of the entire wall mechanism :

$$\alpha = 0.1055$$

9.4.4 Unique seismic force on the top with timber tie-beams - Tmin

In the kinetic approach the entire wall mechanism with the unique seismic force at the top of the wall is the most critical. This is due to the facts that the whole mass of the wall takes part to the mechanism and the lever arm is the maximum possible. Minimum Tension dependent on α considering the chain only at the roof level.

In order to resist a PGA of 0,5 g the chain must bear at least 32,22 kN.

Minimum Tension dependent on α	
α	Tmin (kN)
0	-5,61
0,1	1,95
0,2	9,52
0,3	17,08
0,4	24,65
0,5	32,22
0,6	39,78
0,7	47,35
0,8	54,91
0,9	62,48
1	70,05

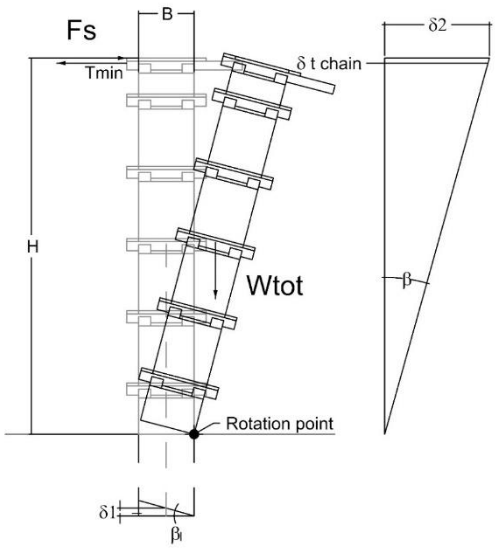

9.4.5 Roof force + Wall force with timber tie-beams - Tmin

Wall mechanism and block by block mechanism have been studied by the kinetic approach. The most critical case is the entire wall mechanism where the minimum traction of the chain in function of α isreported in the recall table

In order to resist a PGA of 0,5 g the chain must bear at least 25,69 kN .

Minimum Tension dependent on α	
α	Tmin (kN)
0	-7,77
0,1	-1,08
0,2	5,61
0,3	12,30
0,4	18,99
0,5	25,69
0,6	32,38
0,7	39,07
0,8	45,76
0,9	52,45
1	59,14

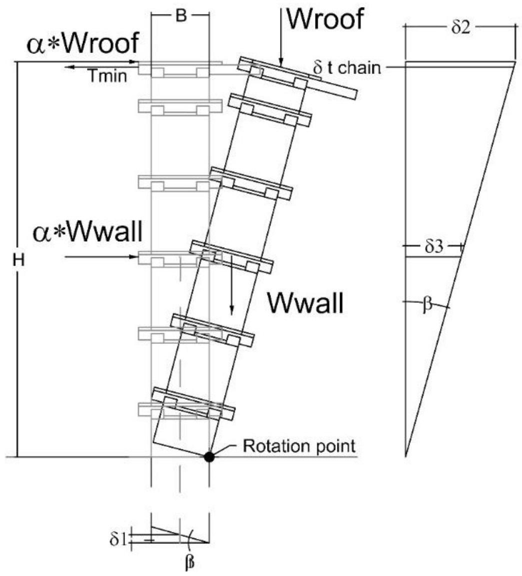

9.5 Verifications for Overturning Rigidbehavior

The verifications have been performed considering the worst case with load seismic multiplier α = 1 thus Tmin= 70,05 kN and considering that the reactions in the joint are equally distributed between the Tie-timber chain and the tie-timber beam of the failing wall.

9.5.1 Analyzing the worst case : Unique seismic force on the top with timber tie-beams - Tmin

Minimum Tension dependent on α	
α	Tmin (kN)
0	-5,61
0,1	1,95
0,2	9,52
0,3	17,08
0,4	24,65
0,5	32,22
0,6	39,78
0,7	47,35
0,8	54,91
0,9	62,48
1	70,05

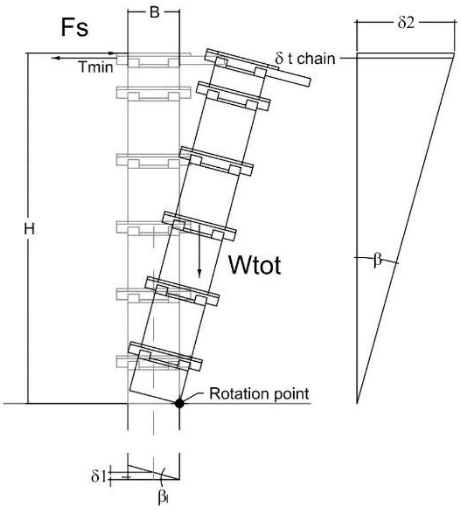

9.5.2 Equal distribution of the reactions T1=T2 and R1=R2

In order to be clear they are recalled the hypothesis asserted in the chapter 6 , and the equal distribution of the reactions on corner joint.

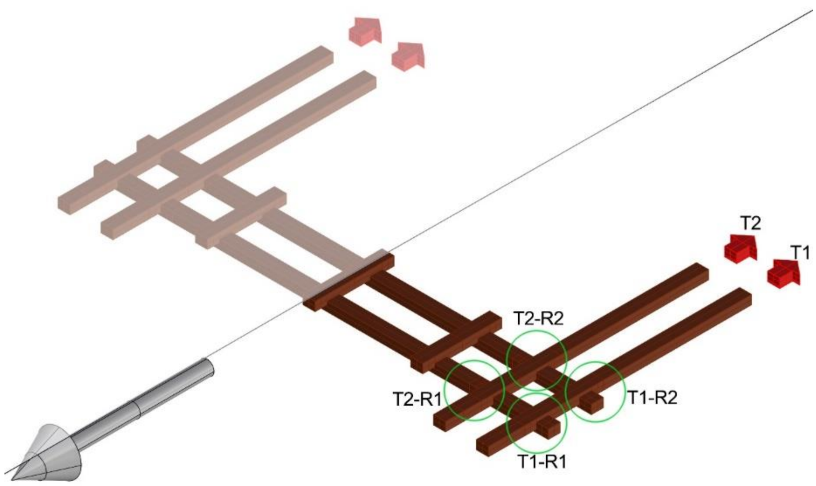

$$T_1 = T_2 = \frac{T_{min}}{2}$$

$$(T_1R_1) = (T_1R_2) = (T_2R_1) = (T_2R_2) = \frac{T_{min}}{4}$$

Thebehavior of the rafters chain 1 and 2 is the same thus the verifications on T1 is equal to T2.

Thebehavior of rafters belonging to the overturning wall is the same thus the verifications on R1 is equal to R2.

The verifications have been performed on the biggest section of the rafters, the body, which refers to a section of area equal to A5. The same verifications have been performed considering the smallest section, the notch, of area equal to A4.

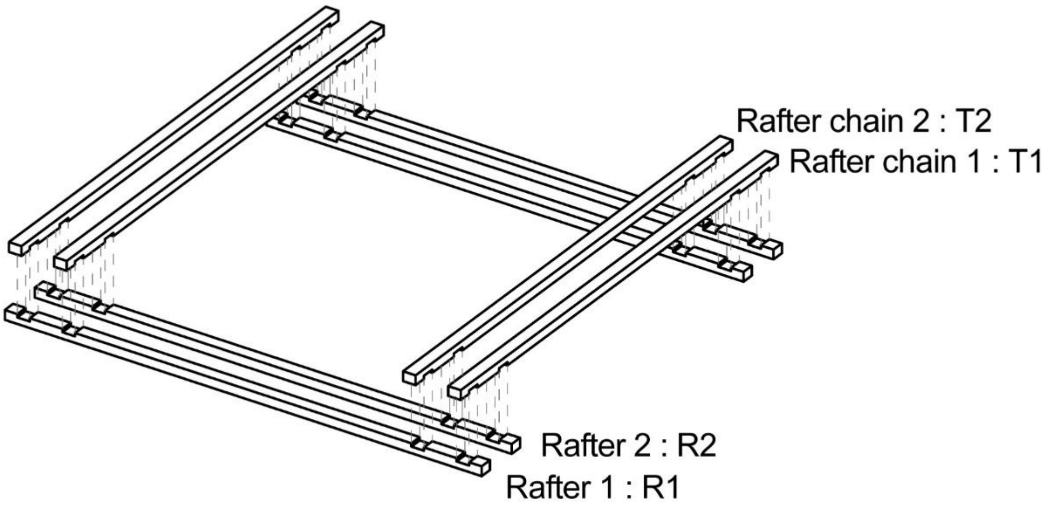

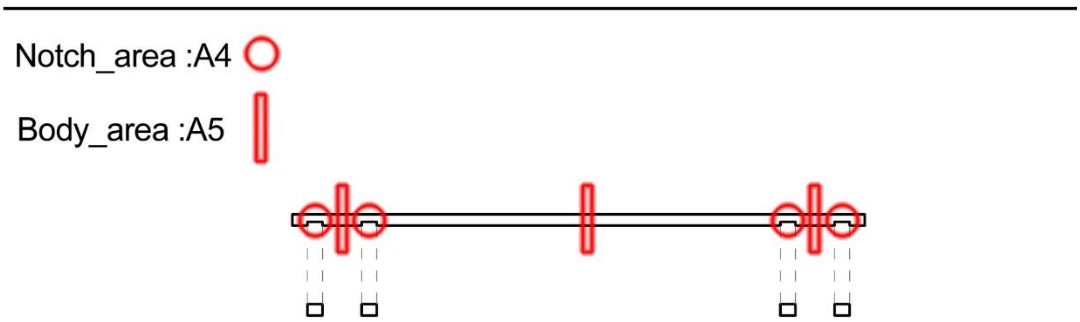

Table 57 Geometric dimensions for Notch and Body Areas

	b	h	AREA net		
	mm	mm	mm^2	cm^2	m^2
A4	100	50	5000	50	0,005

	b	h	AREA net		
	mm	mm	mm^2	cm^2	m^2
A5	100	75	7500	75	0,0075

All the verifications have been done considering the highest load multiplier, thus α=1 .In the cases where the verification is not satisfied the load multiplier has been reduced until the verification was verified.

9.5.3 Verifications T1=T2

All the verifications have been

9.5.3.1 Body

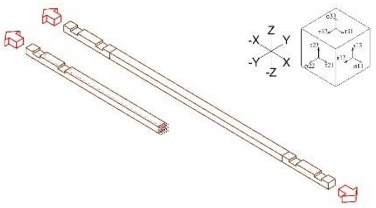

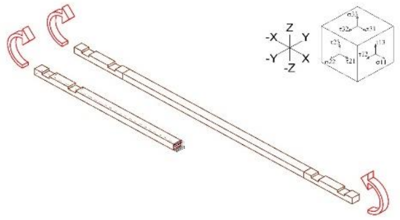

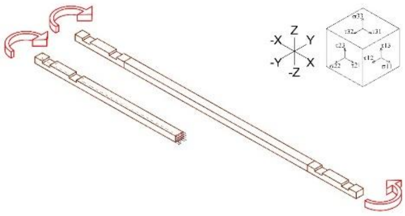

RB0tens		
N_0d	35022,92	N
b	100,00	mm
h	75,00	mm
A_(net)	7500,00	mm
σ_(t,0,d)	4,67	N/mm^2
kh	1,08	
f_(t,0,d)	30,80	N/mm^2
Verification	VERIFIED	
N_(0d)max	231,00	kN

Influence of keyed scarf joint		
Verification	NOT VERIFIED	
N_(0d)max	25,41	kN

RB0mY		
M_(y,d)	1330870,94	Nmm
K_m	0,70	
b	100,00	mm
h	75,00	mm
W_(y,d)	93750,00	mm^3
σ_(m,y,d)	14,20	N/mm^2
kh	1,15	
f_(m,d)	51,33	N/mm^2
f_(m,y,d)	58,97	N/mm^2
Verification	VERIFIED	
M_(y,d)max	5528110,83	Nmm
M_(y,d)max	5,53	kNm

RB0mZ		
M_(z,d)	0,00	Nmm
K_m	0,70	
b	100,00	mm
h	75,00	mm
W_(z,d)	125000,00	mm^3
σ_(m,z,d)	0,00	N/mm^2
kh	1,08	
f_(m,d)	51,33	N/mm^2
f_(m,z,d)	55,67	N/mm^2
Verification	VERIFIED	
M_(z,d)max	6958693,87	Nmm
M_(z,d)max	6,96	kNm

RB0tens is satisfied for a load seismic multiplier α = 0.7

9.5.3.2 Body Combinations

Combined bending and axial tension

$$\frac{\sigma_{t,0,d}}{f_{t,0,d}} + \frac{\sigma_{m,y,d}}{f_{m,y,d}} + k_m * \frac{\sigma_{m,z,d}}{f_{m,z,d}} \leq 1$$

$$\frac{\sigma_{t,0,d}}{f_{t,0,d}} + k_m * \frac{\sigma_{m,y,d}}{f_{m,y,d}} + \frac{\sigma_{m,z,d}}{f_{m,z,d}} \leq 1$$

For solid timber, glued laminated timber and LVL:

- for rectangular sections: km = 0,7
- otherwise km = 1

Combination of RB0tens and RB0mY are satisfied for a load multiplier α = 1

Combination of RB0tens and RB0mZ are satisfied for a load multiplier α = 1

9.5.3.3 Notch

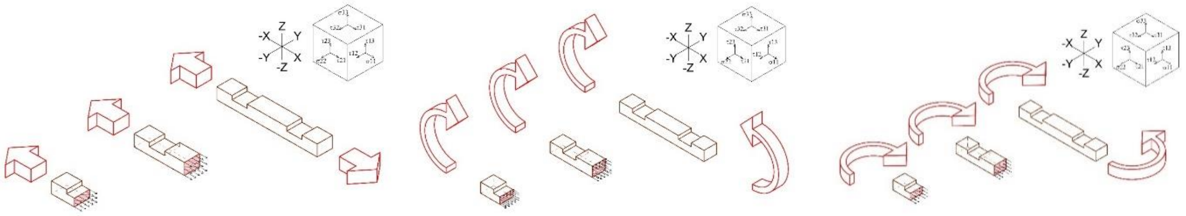

CPNotch0tens		
N_0d	35022,92	N
b	100,00	mm
h	50,00	mm
A_(net)	5000,00	mm^2
σ_(t,0,d)	7,00	N/mm^2
kh	1,08	
f_(t,0,d)	30,80	N/mm^2
Verification	VERIFIED	
N_(0d)max	154,00	kN

CPNotch0mY		
M_(y,d)	1330870,94	Nmm
K_m	0,70	
b	100,00	mm
h	50,00	mm
W_(y,d)	41666,67	mm^3
σ_(m,y,d)	31,94	N/mm^2
kh	1,25	
f_(m,d)	51,33	N/mm^2
f_(m,y,d)	63,95	N/mm^2
Verification	VERIFIED	
M_(y,d)max	2664480,07	Nmm
M_(y,d)max	2,66	kNm

CPNotch0mZ		
M_(z,d)	0,00	Nmm
K_m	0,70	
b	100,00	mm
h	50,00	mm
W_(z,d)	83333,33	mm^3
σ_(m,z,d)	0,00	N/mm^2
kh	1,08	
f_(m,d)	51,33	N/mm^2
f_(m,z,d)	55,67	N/mm^2
Verification	VERIFIED	
M_(z,d)max	4639129,24	Nmm
M_(z,d)max	4,64	kNm

It is important to underline that in the notch section, the keyed scarf joint has not been considered.

9.5.3.1 Notch Combinations

Combined bending and axial tension

$$\frac{\sigma_{t,0,d}}{f_{t,0,d}} + \frac{\sigma_{m,y,d}}{f_{m,y,d}} + k_m * \frac{\sigma_{m,z,d}}{f_{m,z,d}} \leq 1$$

$$\frac{\sigma_{t,0,d}}{f_{t,0,d}} + k_m * \frac{\sigma_{m,y,d}}{f_{m,y,d}} + \frac{\sigma_{m,z,d}}{f_{m,z,d}} \leq 1$$

For solid timber, glued laminated timber and LVL:

- for rectangular sections: km = 0,7
- otherwise km = 1

Combination of CPNotch0tens and CPNotch0mY are satisfied for a load multiplier α = 1

Combination of CPNotch0tens and CPNotch0mZ are satisfied for a load multiplier α = 1

9.5.4 Verifications R1=R2

9.5.4.1 Body

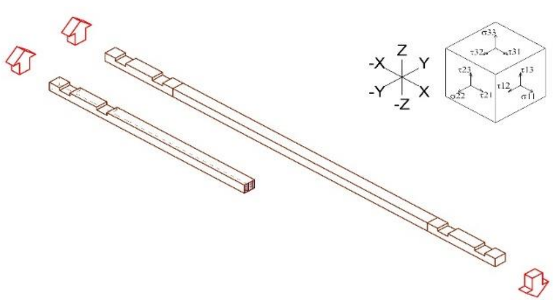

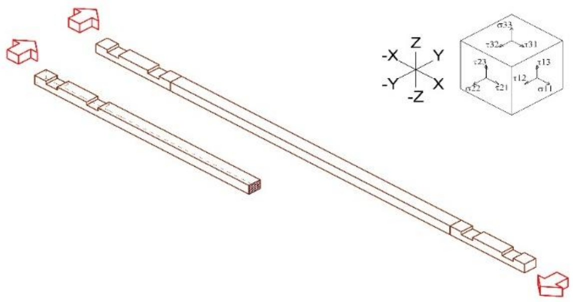

RB0shearZ with bending		
V_zd	0,00	N
K_cr	0,67	
A_(net)	5025,00	mm
τ_(d)	0,00	N/mm^2
f_(v,d)	3,67	N/mm^2
Verification	VERIFIED	
V_zd max	12,28	kN
RB0shearZ		
V_zd	0,00	N
A_(net)	7500,00	mm
τ_(d)	0,00	N/mm^2
f_(v,d)	3,67	N/mm^2
Verification	VERIFIED	
V_zd max	18,33	kN

RB0shearY with bending		
V_yd	35022,92	N
K_cr	0,67	
A_(net)	5025,00	mm
τ_(d)	10,45	N/mm^2
f_(v,d)	3,67	N/mm^2
Verification	NOT VERIFIED	
V_yd max	12,28	kN
RB0shearY		
V_yd	35022,92	N
A_(net)	7500,00	mm
τ_(d)	7,00	N/mm^2
f_(v,d)	3,67	N/mm^2
Verification	NOT VERIFIED	
V_yd max	18,33	kN

RB0shearY with bending and RB0shearY are satisfied for a load seismic multiplier $\alpha = 0.35$

9.5.4.2 Notch

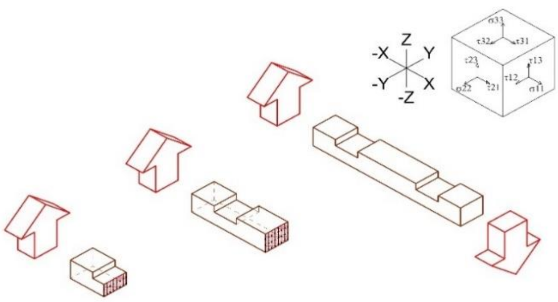

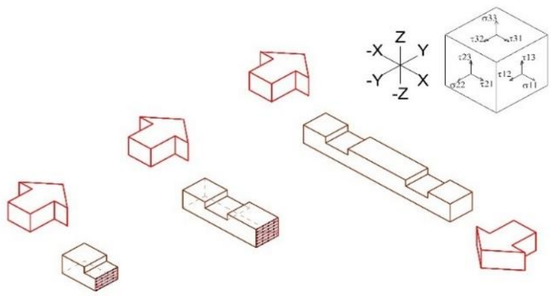

CPNotch0shearZ with bending		
V_zd	0,00	N
K_cr	0,67	
A_(net)	3350,00	mm^2
τ_(d)	0,00	N/mm^2
f_(v,d)	3,67	N/mm^2
Verification	VERIFIED	
V_zd max	8,19	kN

CPNotch0shearY with bending		
V_yd	35022,92	N
K_cr	0,67	
A_(net)	3350,00	mm^2
τ_(d)	15,68	N/mm^2
f_(v,d)	3,67	N/mm^2
Verification	NOT VERIFIED	
V_yd max	8,19	kN

CPNotch0shearZ		
V_zd	0,00	N
A_(net)	5000,00	mm
τ_(d)	0,00	N/mm^2
f_(v,d)	3,67	N/mm^2
Verification	VERIFIED	
V_zd max	12,22	kN

CPNotch0shearY		
V_yd	35022,92	N
A_(net)	5000,00	mm
τ_(d)	10,51	N/mm^2
f_(v,d)	3,67	N/mm^2
Verification	NOT VERIFIED	
V_yd max	12,22	kN

CPNotch0shearY with bending and CPNotch0shearY are satisfied for a load seismic multiplier α = 0.2

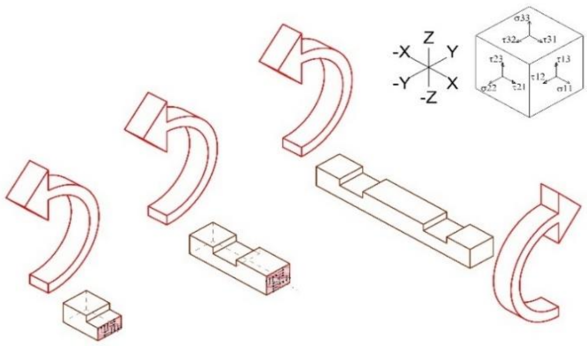

CPNotch0mX		
M_(x,d)	420275,03	Nmm
b	100,00	mm
h	50,00	mm
α	3,90	
τ_(tor,d)	6,56	N/mm^2
K_shape	1,03	
f_(v,d)	3,67	N/mm^2
k_shape*f_(v,d)	3,78	N/mm^2
Verification	NOT VERIFIED	
M_(x,d) max	242094,02	Nmm
M_(x,d) max	0,24	kNm

CPNotch0mX is satisfied for a load seismic multiplier α = 0.5

9.5.4.3 Notch Combinations

Combined Torsion and Shear - CNR-DT 206/2007

$$\frac{\tau_{tor,d}}{k_{shape} * f_{v,d}} + \left(\frac{\tau_d}{f_{v,d}}\right)^2 \leq 1$$

Combination of CPNotch0mX and CPNotch0shearZ are satisfied for a load multiplier α = 0.5

Combination of CPNotch0mX and CPNotch0shearY are satisfied for a load multiplier α = 0.2

9.5.5 Verifications on corner joint, seismic event parallel to Roof Rafter

In order to report the verification on the corner joint at the roof level they have been recalled the hypothesis done in the chapter 6.

9.5.5.1 Scheme

As well they have been reported all the data collected in the previous chapter to verify all the sections.

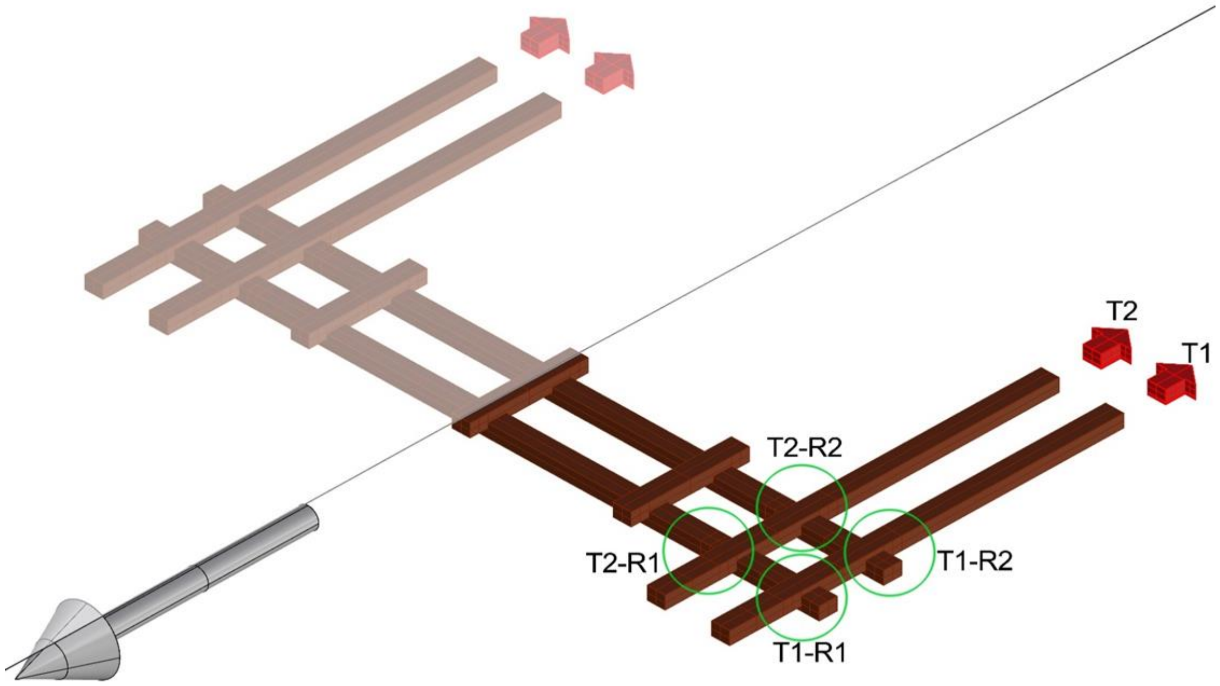

Tmin	70045,84	N	70,05	kN
α	1,00			
T1R1=T1R2=T2R1=T2R2=Tmin/4=	17511,46	N	17,51	kN

	Design Actions				
Compression	N_0d	17511,46	N	17,51	kN
Tension	N_0d	17511,46	N	17,51	kN
Shear Z	V_zd	17511,46	N	17,51	kN
Shear Y	V_yd	17511,46	N	17,51	kN
Bend.MY	M_(y,d)	665435,47	Nmm	0,67	kNm
Bend.MZ	M_(z,d)	5253437,94	Nmm	5,25	kNm
Torsion.MX	M_(x,d)	210137,52	Nmm	0,21	kNm

lever arm	δ for My	38,00	mm
lever arm	δ1 for Mz1	150,00	mm
lever arm	δ2 for Mz2	150,00	mm
lever arm	δnotch for Mxnotch	12,00	mm
lever arm	δbody for Mxbody	25,00	mm

9.5.5.2 Axial stresses: Compression and Tension

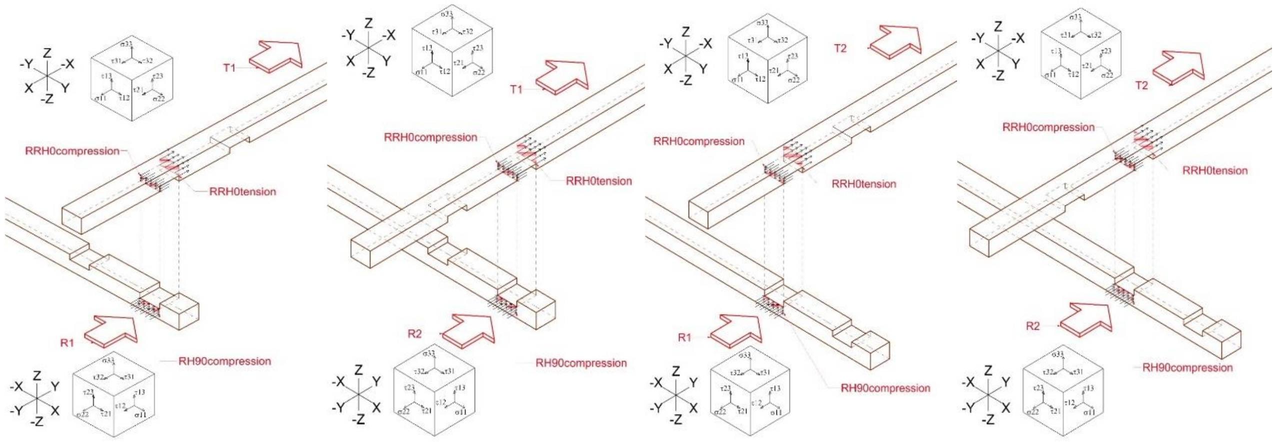

RRH0tension	A4	
N_0d	17511,46	N
b	100,00	mm
h	50,00	mm
A_(net)	5000,00	mm^2
σ_(t,0,d)	3,50	N/mm^2
kh	1,08	
f_(t,0,d)	30,80	N/mm^2
Verification	VERIFIED	
N_(od)max	154,00	kN

RRH0compression	A3	
N_0d	17511,46	N
b	100,00	mm
h	25,00	mm
A_(net)	2500,00	mm^2
σ_(c,0,d)	7,00	N/mm^2
f_(c,0,d)	24,93	N/mm^2
Verification	VERIFIED	
N_(od)max	62,33	kN

RH90compression	A3	
N_90d	17511,46	N
b	100,00	mm
h	25,00	mm
A_(net)	2500,00	mm^2
σ_(c,90,d)	7,00	N/mm^2
k_(c,90)	1,50	
f_(c,90,d)	9,90	N/mm^2
Verification	VERIFIED	
N_(90d)max	16,50	kN

9.5.5.3 Tangential stresses: Shear

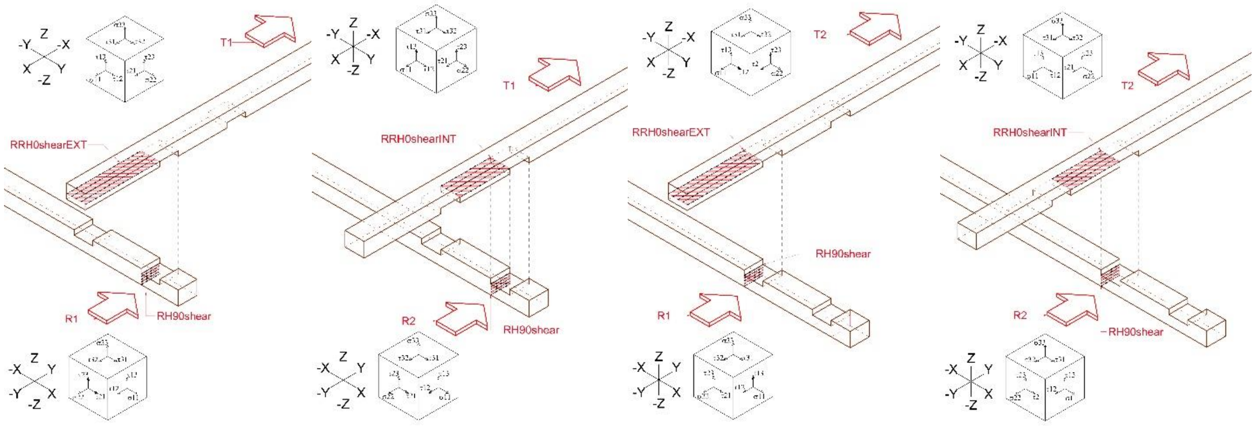

RRH0shearEXT	A7	
with bending		
V_0d	17511,46	N
K_cr	0,67	
A_(net)	26800,00	mm^2
τ_(d)	0,98	N/mm^2
f_(v,d)	3,67	N/mm^2
Verification	VERIFIED	
V_0d max	65,51	kN

RRH0shearINT	A1	
with bending		
V_0d	17511,46	N
K_cr	0,67	
A_(net)	17420,00	mm^2
τ_(d)	1,51	N/mm^2
f_(v,d)	3,67	N/mm^2
Verification	VERIFIED	
V_0d max	42,58	kN

RH90shear	A5	
with bending		
V_90d	17511,46	N
K_cr	0,67	
A_(net)	5025,00	mm^2
τ_(d)	5,23	N/mm^2
ƒt,90,d	0,44	N/mm^2
f_(v,d)	0,88	N/mm^2
Verification	NOT VERIFIED	
V_90d max	2,95	kN

RRH0shearEXT	A7	
V_0d	17511,46	N
A_(net)	40000,00	mm^2
τ_(d)	0,66	N/mm^2
f_(v,d)	3,67	N/mm^2
Verification	VERIFIED	
V_0d max	97,78	kN

RRH0shearINT	A1	
V_0d	17511,46	N
A_(net)	26000,00	mm^2
τ_(d)	1,01	N/mm^2
f_(v,d)	3,67	N/mm^2
Verification	VERIFIED	
V_0d max	63,56	kN

RH90shear	A5	
V_90d	17511,46	N
A_(net)	7500,00	mm^2
τ_(d)	3,50	N/mm^2
*f*t,90,d	0,44	N/mm^2
f_(v,d)	0,88	N/mm^2
Verification	NOT VERIFIED	
V_90d max	4,40	kN

RH90shear with bending is satisfied for a load multiplier α = 0.15

RH90shear is satisfied for a load multiplier α = 0.2

9.5.5.4 Bending moments My and Mz

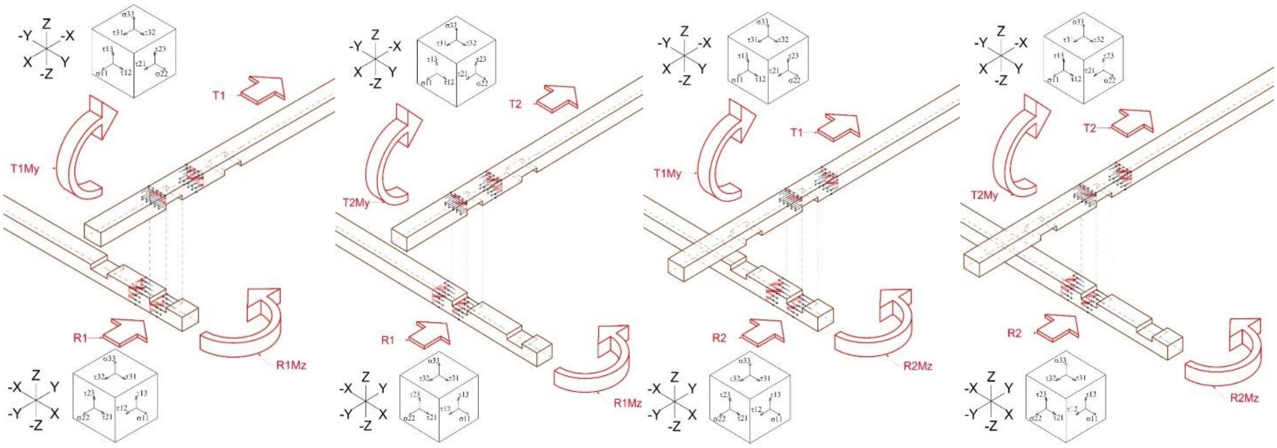

Notch0mY		
N_0d	17511,46	N
δ for My	38,00	mm
M_(y,d)	665435,47	Nmm
K_m	0,70	
b	100,00	mm
h	50,00	mm
W_(y,d)	41666,67	mm^3
σ_(m,y,d)	15,97	N/mm^2
kh	1,25	
f_(m,d)	51,33	N/mm^2
f_(m,y,d)	63,95	N/mm^2
Verification	VERIFIED	
M_(y,d)max	2664480,07	Nmm
M_(y,d)max	2,66	kNm

Notch0mZ1		
V_90d	17511,46	N
δ1 for Mz1	150,00	mm
M_(z,d)	2626718,97	Nmm
K_m	0,70	
b	100,00	mm
h	50,00	mm
W_(z,d)	83333,33	mm^3
σ_(m,z,d)	31,52	N/mm^2
kh	1,08	
f_(m,d)	51,33	N/mm^2
f_(m,z,d)	55,67	N/mm^2
Verification	VERIFIED	
M_(z,d)max	4639129,24	Nmm
M_(z,d)max	4,64	kNm

Notch0mZ2		
V_90d	35022,92	N
δ2 for Mz2	150,00	mm
M_(z,d)	5253437,94	Nmm
K_m	0,70	
b	100,00	mm
h	50,00	mm
W_(z,d)	83333,33	mm^3
σ_(m,z,d)	63,04	N/mm^2
kh	1,08	
f_(m,d)	51,33	N/mm^2
f_(m,z,d)	55,67	N/mm^2
Verification	NOT VERIFIED	
M_(z,d)max	4639129,24	Nmm
M_(z,d)max	4,64	kNm

Body0mY		
N_0d	17511,46	N
δ for My	38,00	mm
M_(y,d)	665435,47	Nmm
K_m	0,70	
b	100,00	mm
h	75,00	mm
W_(y,d)	93750,00	mm^3
σ_(m,y,d)	7,10	N/mm^2
kh	1,15	
f_(m,d)	51,33	N/mm^2
f_(m,y,d)	58,97	N/mm^2
Verification	VERIFIED	
M_(y,d)max	5528110,83	Nmm
M_(y,d)max	5,53	kNm

Body0mZ1		
V_90d	150,00	N
δ1 for Mz1	510,00	mm
M_(z,d)	76500,00	Nmm
K_m	0,70	
b	100,00	mm
h	75,00	mm
W_(z,d)	125000,00	mm^3
σ_(m,z,d)	0,61	N/mm^2
kh	1,08	
f_(m,d)	51,33	N/mm^2
f_(m,z,d)	55,67	N/mm^2
Verification	VERIFIED	
M_(z,d)max	6958693,87	Nmm
M_(z,d)max	6,96	kNm

Body0mZ2		
V_90d	35022,92	N
δ2 for Mz2	150,00	mm
M_(z,d)	5253437,94	Nmm
K_m	0,70	
b	100,00	mm
h	75,00	mm
W_(z,d)	125000,00	mm^3
σ_(m,z,d)	42,03	N/mm^2
kh	1,08	
f_(m,d)	51,33	N/mm^2
f_(m,z,d)	55,67	N/mm^2
Verification	VERIFIED	
M_(z,d)max	6958693,87	Nmm
M_(z,d)max	6,96	kNm

Notch0mZ2 is satisfied for a load multiplier α = 0.8

9.5.5.5 Torsion

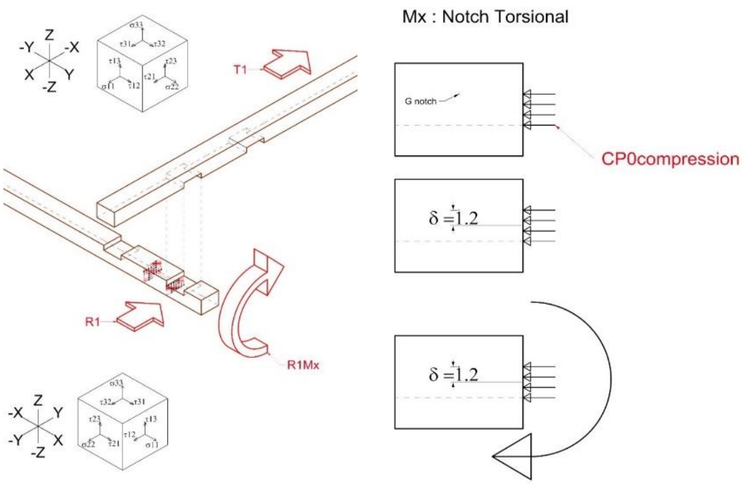

Notch0mX		
V_90d	1,75E+04	N
δnotch for Mxnotch	12,00	mm
M_(x,d)	210137,52	Nmm
b	100,00	mm
h	50,00	mm
α	3,90	
τ_(tor,d)	3,28	N/mm^2
K_shape	1,03	
f_(v,d)	3,67	N/mm^2
k_shape*f_(v,d)	3,78	N/mm^2
Verification	VERIFIED	
M_(x,d) max	242094,02	Nmm
M_(x,d) max	0,24	kNm

Body0mX		
V_90d	1,75E+04	N
δnotch for Mxnotch	12,00	mm
M_(x,d)	210137,52	Nmm
b	100,00	mm
h	75,00	mm
α	4,35	
τ_(tor,d)	1,63	N/mm^2
K_shape	1,02	
f_(v,d)	3,67	N/mm^2
k_shape*f_(v,d)	3,74	N/mm^2
Verification	VERIFIED	
M_(x,d) max	483620,69	Nmm
M_(x,d) max	0,48	kNm

9.5.5.6 *Combinations*

Combined bending and axial tension

$$\frac{\sigma_{t,0,d}}{f_{t,0,d}} + \frac{\sigma_{m,y,d}}{f_{m,y,d}} + k_m * \frac{\sigma_{m,z,d}}{f_{m,z,d}} \leq 1$$

$$\frac{\sigma_{t,0,d}}{f_{t,0,d}} + k_m * \frac{\sigma_{m,y,d}}{f_{m,y,d}} + \frac{\sigma_{m,z,d}}{f_{m,z,d}} \leq 1$$

For solid timber, glued laminated timber and LVL:

- for rectangular sections: km = 0,7
- otherwise km = 1

Combination of Notch0tens and Notch0mY are satisfied for a load multiplier α = 1

Combination of Notch0tens and Notch0mZ2 are satisfied for a load multiplier α = 1

Combination of Body0tens and Body0mY are satisfied for a load multiplier α = 1

Combination of Body0tens and Body0mZ2 are satisfied for a load multiplier α = 1

Combined bending and axial compression

$$\left(\frac{\sigma_{c,0,d}}{f_{c,0,d}}\right)^2 + \frac{\sigma_{m,y,d}}{f_{m,y,d}} + k_m * \frac{\sigma_{m,z,d}}{f_{m,z,d}} \leq 1$$

$$\left(\frac{\sigma_{c,0,d}}{f_{c,0,d}}\right)^2 + k_m * \frac{\sigma_{m,y,d}}{f_{m,y,d}} + \frac{\sigma_{m,z,d}}{f_{m,z,d}} \leq 1$$

For solid timber, glued laminated timber and LVL:

- for rectangular sections: km = 0,7
- otherwise km = 1

Combination of Notch0comp and Notch0mY are satisfied for a load multiplier α = 1

Combination of Notch0comp and Notch0mZ2 are satisfied for a load multiplier α = 1

Combination of Body0comp and Body0mY are satisfied for a load multiplier α = 1

Combination of Body0comp and Body0mZ2 are satisfied for a load multiplier α = 1

Combined Torsion and Shear - CNR-DT 206/2007

$$\frac{\tau_{tor,d}}{k_{shape} * f_{v,d}} + \left(\frac{\tau_d}{f_{v,d}}\right)^2 \leq 1$$

Combination of Notch0mX and Notch90shearY are satisfied for a load multiplier α = 0.8

Combination of Body0mX and Body90shearY are satisfied for a load multiplier α = 1

9.5.6 Verifications on corner joint, seismic event parallel to Rafter

9.5.6.1 Scheme

The difference between the roof rafter and the rafter is the length of the head.

The length of the normal rafter is shorter and the difference affects the longitudinal shear resistance of the element.

For all the other verifications nothing changes, that is why in the following, they are reported only the verifications about the shear resistance.

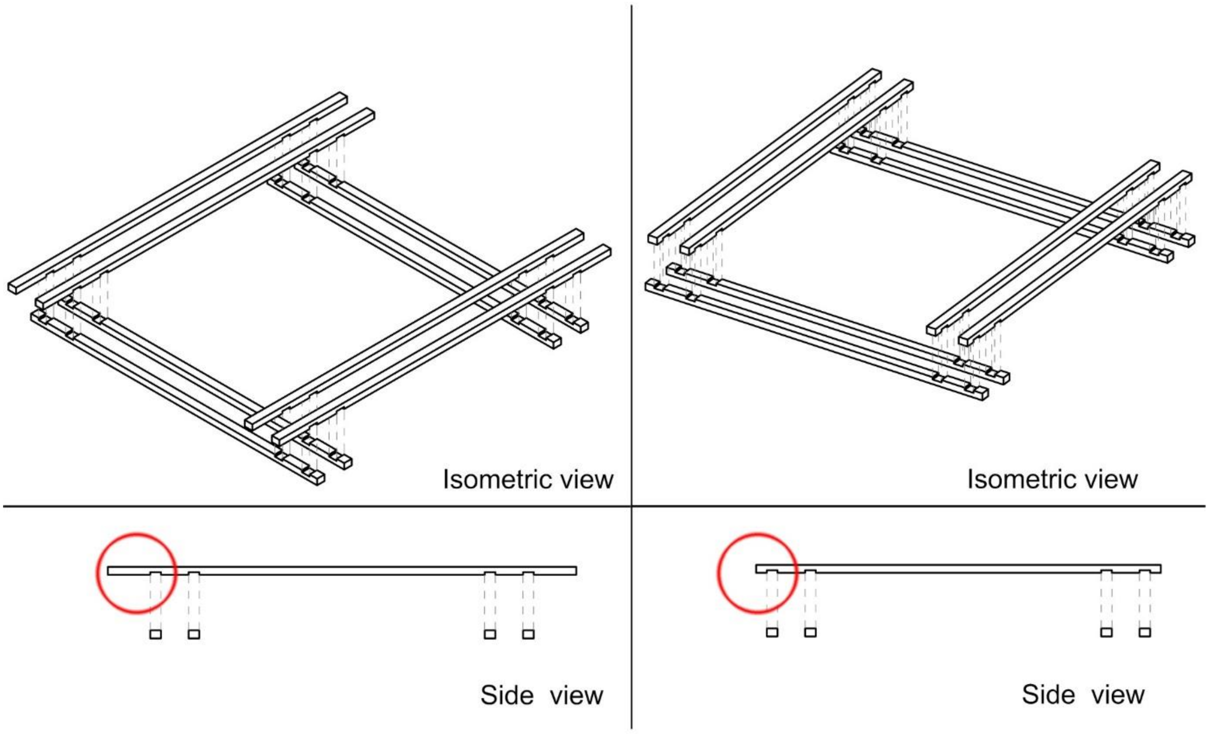

9.5.6.2 Tangential stresses: Shear

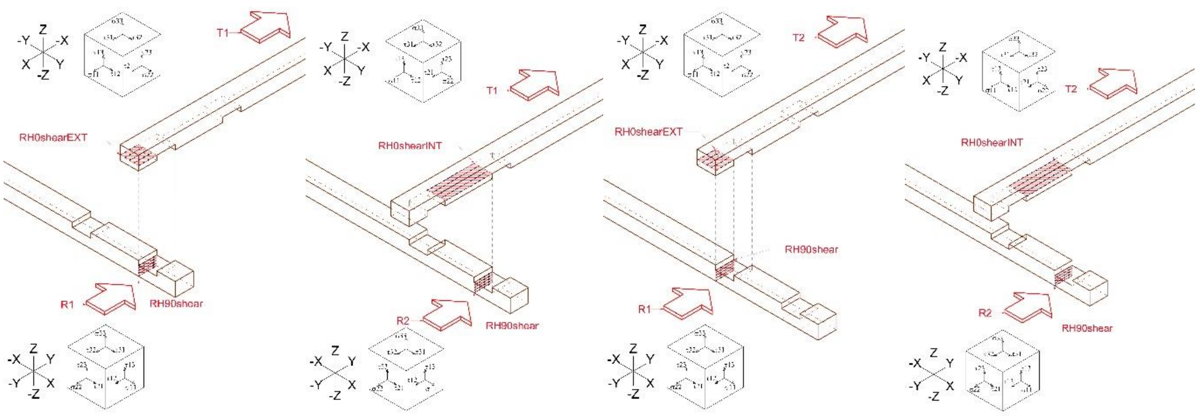

RH0shearEXT	A2	
with bending		
V_0d	17511,46	N
K_cr	0,67	
A_(net)	6700,00	mm^2
τ_(d)	3,92	N/mm^2
f_(v,d)	3,67	N/mm^2
Verification	NOT VERIFIED	
V_0d max	16,38	kN

RH0shearINT	A1	
with bending , " = RRH0shearINT "		
V_0d	17511,46	N
K_cr	0,67	
A_(net)	17420,00	mm^2
τ_(d)	1,51	N/mm^2
f_(v,d)	3,67	N/mm^2
Verification	VERIFIED	
V_0d max	42,58	kN

RH90shear	A5	
with bending		
V_90d	17511,46	N
K_cr	0,67	
A_(net)	5025,00	mm^2
τ_(d)	5,23	N/mm^2
ft,90,d	0,44	N/mm^2
f_(v,d)	0,88	N/mm^2
Verification	NOT VERIFIED	
V_90d max	2,95	kN

RH0shearEXT	A2	
V_0d	17511,46	N
A_(net)	10000,00	mm^2
τ_(d)	2,63	N/mm^2
f_(v,d)	3,67	N/mm^2
Verification	VERIFIED	
V_0d max	24,44	kN

RH0shearINT	A1	
" = RRH0shearINT "		
V_0d	17511,46	N
A_(net)	26000,00	mm^2
τ_(d)	1,01	N/mm^2
f_(v,d)	3,67	N/mm^2
Verification	VERIFIED	
V_0d max	63,56	kN

RH90shear	A5	
V_90d	17511,46	N
A_(net)	7500,00	mm^2
τ_(d)	3,50	N/mm^2
ft,90,d	0,44	N/mm^2
f_(v,d)	0,88	N/mm^2
Verification	NOT VERIFIED	
V_90d max	4,40	kN

RH0shearEXT with bending is satisfied for a load multiplier $\alpha = 0.9$

RH90shear with bending is satisfied for a load multiplier $\alpha = 0.15$

RH90shear is satisfied for a load multiplier $\alpha = 0.25$

9.6 Conclusions on seismic analysis out of plane – Overturning

9.6.1 Safetybehavior under seismic multiplier α=0,15

All the verifications have been computed in function of the seismic load multiplier α.

Summing up the results it can be noticed that the timber elements with the function of chain is not particularly affected by the keyed scarf joint and it has an high strengthbehavior, this is due to the shorea robust properties.

The most critical section is in the rafters of the timber beam belonging to overturning wall.

This section has been named RH90shear and it is shown in the figure below.

The verification of this section is satisfied for a seismic load multiplier α = 0,15

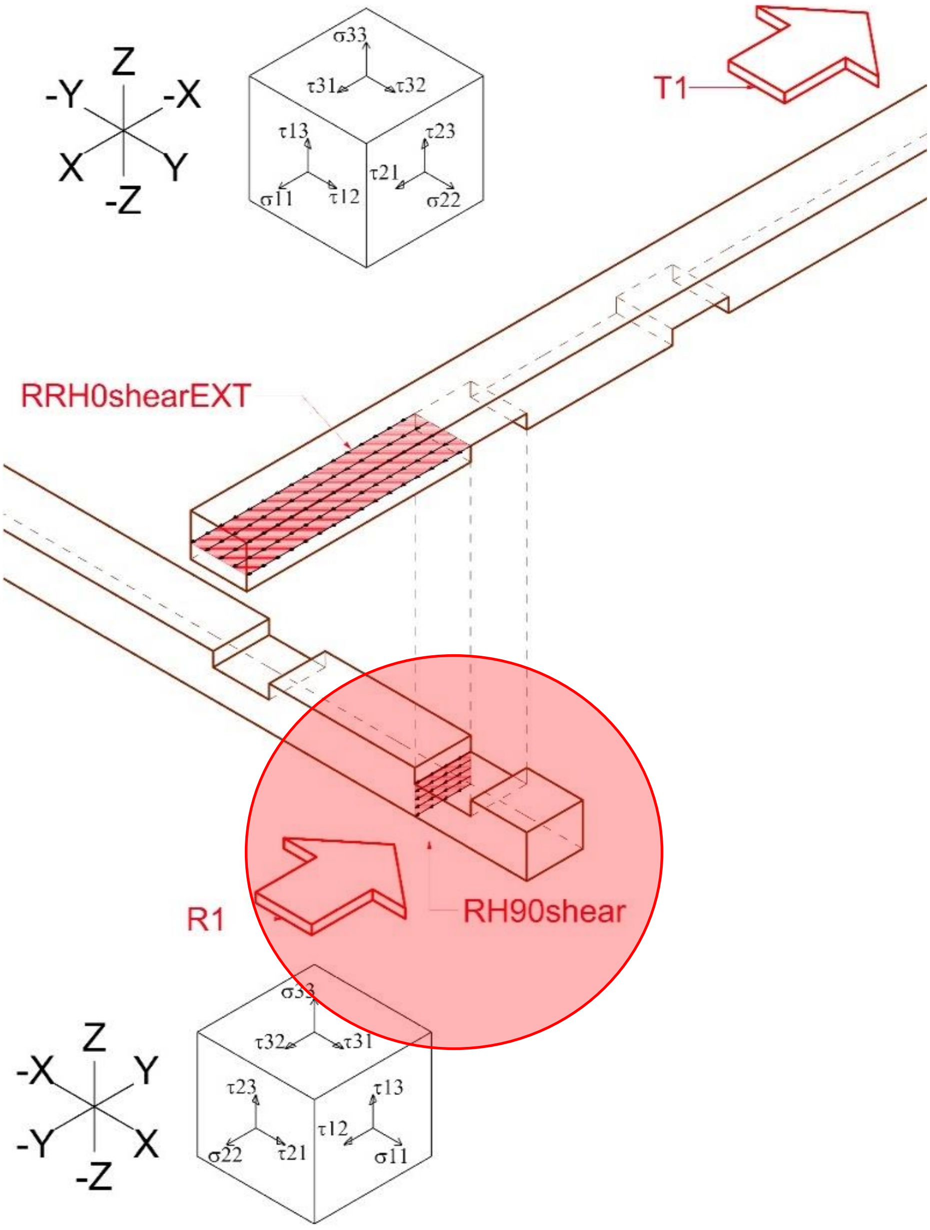

Figure 9-16 Overturning - RH90Shear most critical section

10 SEISMIC ANALYSIS OUT OF PLANE - FLEXIBLE RESPONSE BENDING BEHAVIOR

10.1 Hypothesis of Flexible response – Bending behavior

The wall has been considered as it was composed by flexible layers, which may bend in the plane parallel to the ground. The figure below shows the analyzed failure mechanism in the flexible configuration .

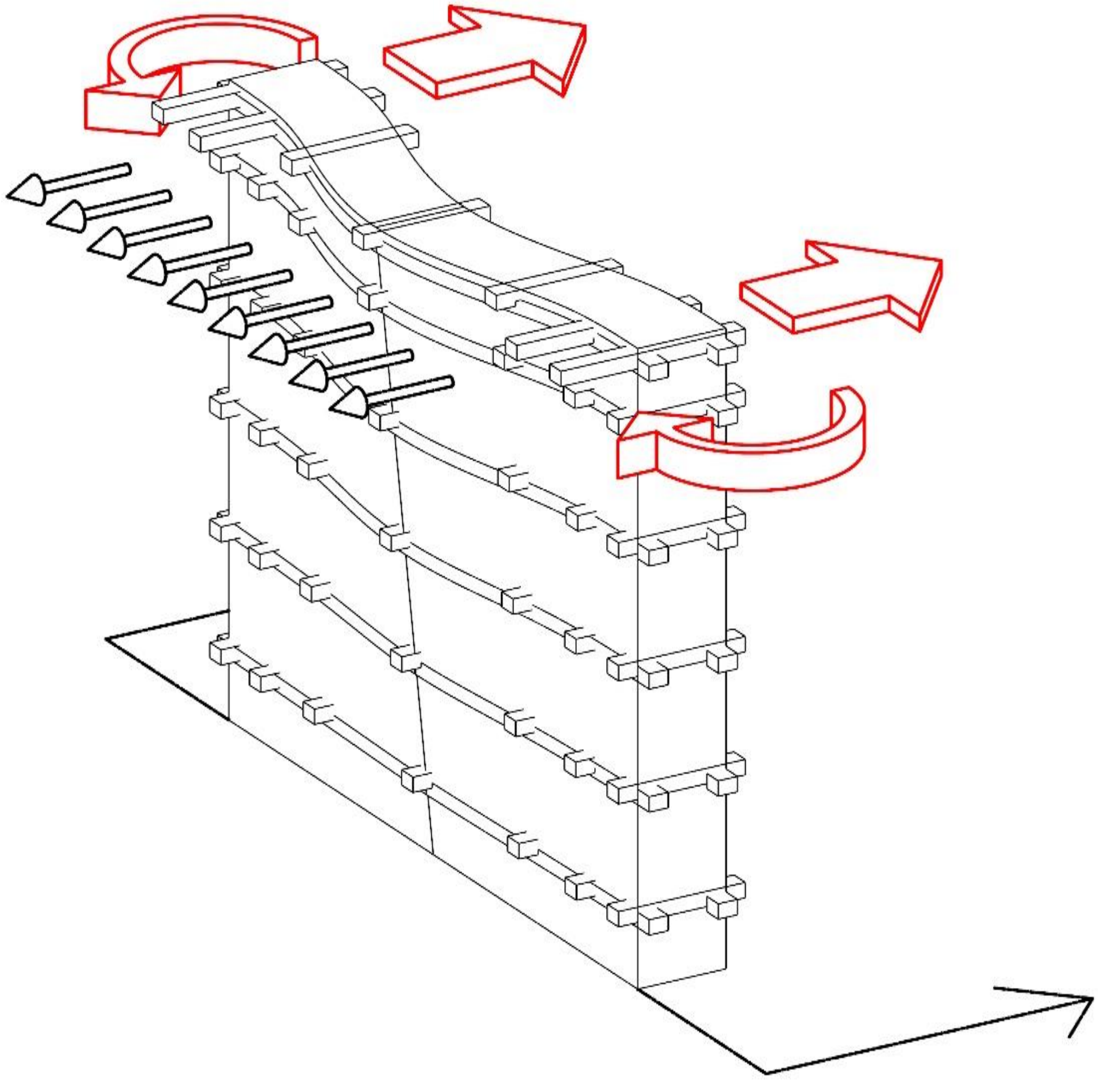

Figure 10-1 Flexible mechanism – example scheme

In this configuration, the activation of the tie-timber beam chain has been analyzed in a different way respect to the overturning configuration.

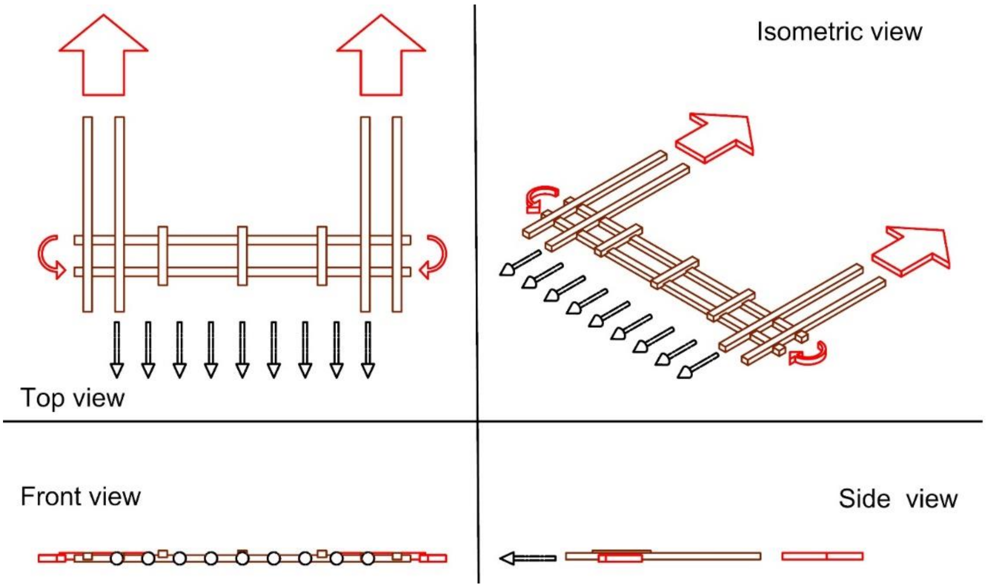

Figure 10-2 Flexible mechanism - tie-timber beam chains activation

10.1.1 Hypothesis of Flexible behavior

The load is distributed along the tie-timber beam and it is due to a portion of the total mass around each tie-timber beam.

In order to know the reactions of each timber beam it is necessary to study the end connections composed by 2 rafters perpendicular to others 2 roof rafter or 2 rafters.

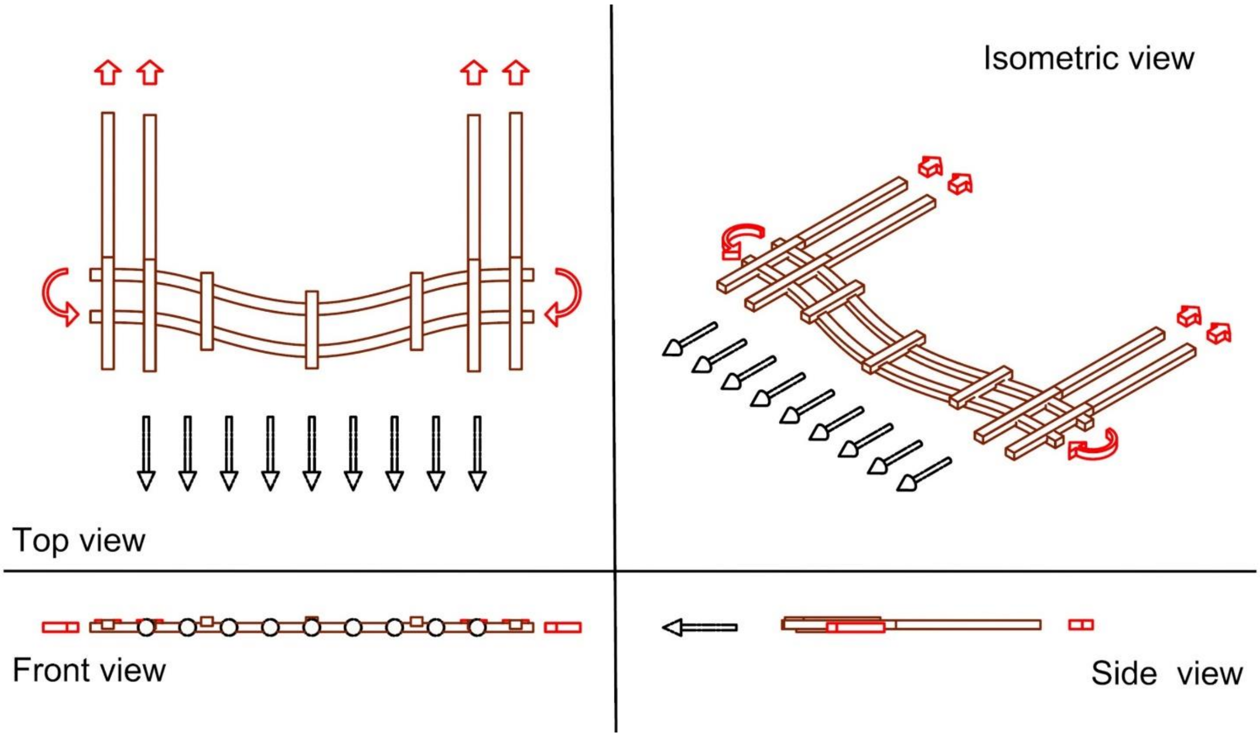

Figure 10-3 Flexible mechanism - deformed tie-timber beam chains and activation

10.1.2 Static scheme of the timber tie- beam

For each timber band in the wall, it has been defined an equivalent static scheme (clamped-clamped) and they have been defined the masses involved for each mechanism.

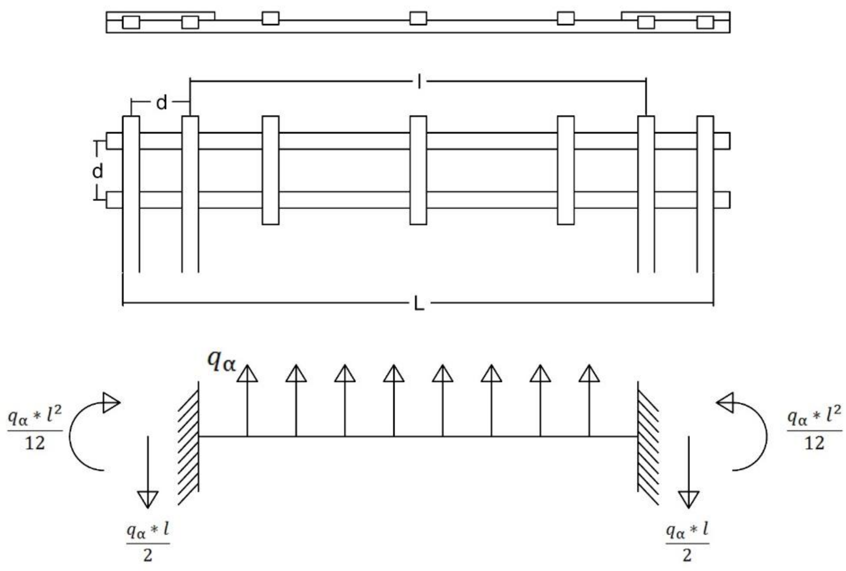

Figure 10-4 Static scheme of the timber tie-beam (clamped ends)

Reactions used in the scheme :

- Seismic load :

$$q_\alpha = \frac{Mass_i * \alpha * g}{L}$$

- T chain, shear force :

$$T_{chain} = \frac{q_\alpha * l}{2}$$

- M chain , bending moment :

$$M_{chain} = \frac{q_\alpha * l^2}{12}$$

All the this terms will be explained in the following sub-chapters.

10.1.3 Hyperstatic scheme of the corner joint and actions from static scheme of the timber tie- beam

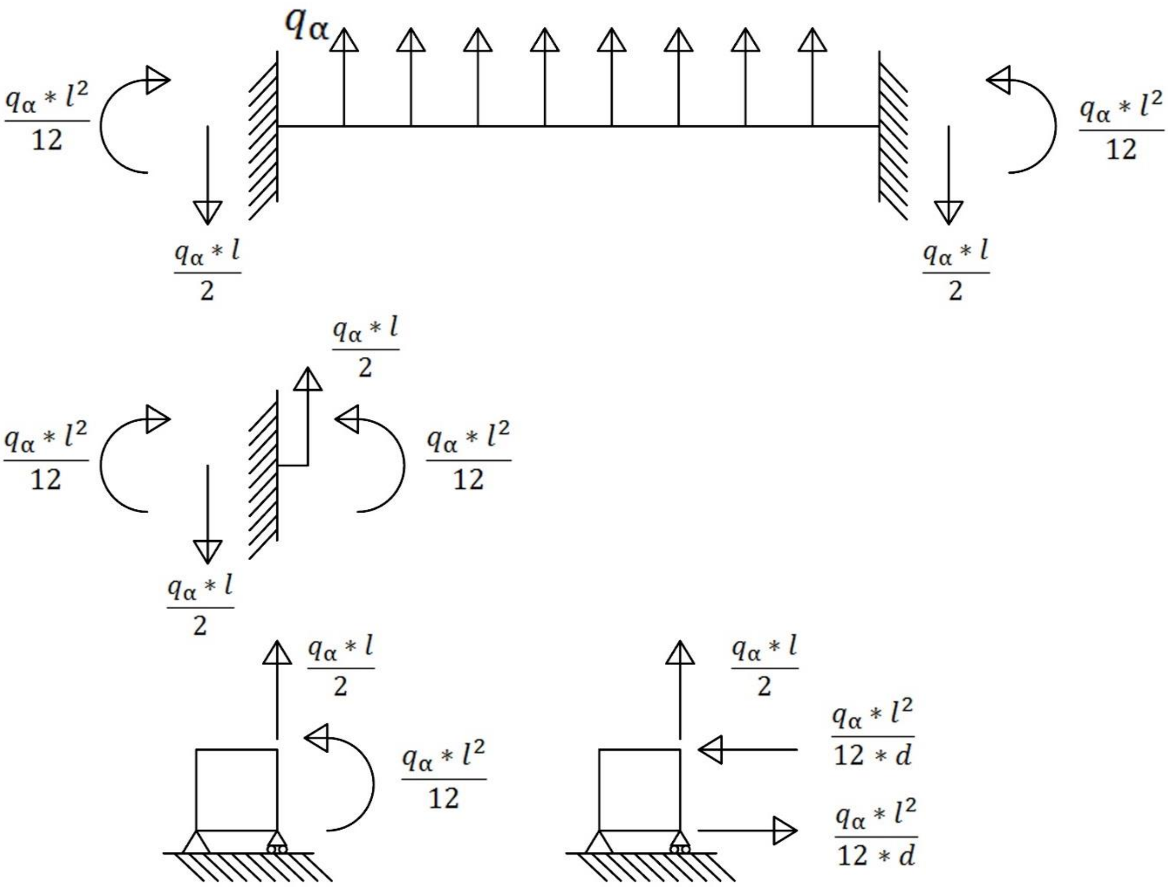

Figure 10-5 Hyperstatic scheme of the corner joint and actions from static scheme of the timber tie- beam

The new reaction in the scheme is the couple (from the bending moment Mchain) :

$$\text{Couple} = \frac{q_\alpha * l^2}{12 * d}$$

10.1.4 Hyperstatic rigid-jointed frame

In order to study the behavior of the corner joint composed by four crossed rafters it has been solved the following frame with the listed nomenclature of the forces.

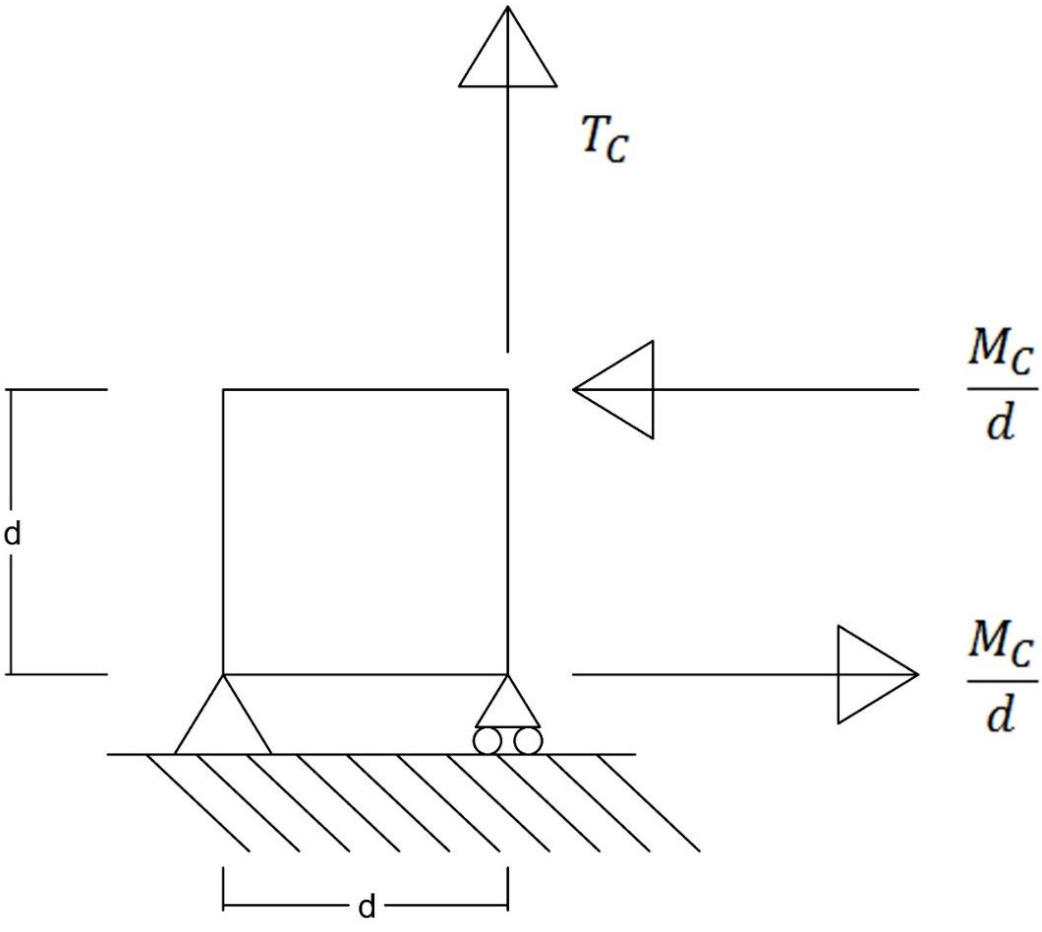

Figure 10-6 Hyperstatic rigid-jointed frame

Reactions used in the scheme :

- Seismic load :

$$q_\alpha = \frac{Mass_i * \alpha * g}{L}$$

- T chain, shear force :

$$T_c = \frac{q_\alpha * l}{2}$$

- M chain , bending moment :

$$M_c = \frac{q_\alpha * l^2}{12}$$

- Couple , bending moment

$$\frac{M_C}{d} = \frac{q_\alpha * l^2}{12 * d}$$

10.2 Force method with Müller-Breslau equations

The frame has been solved by the use of the force method using the Müller-Breslau equations. In the following sub-chapters they have been reported the steps for solving the structure and the solutions which have been fundamental for the flexible configuration analysis and the verifications of the timber elements.

10.2.1 Force method

Method Procedure :

1. Determine the degree of static indeterminacy.
   - Number of releases* equal to the degree of static indeterminacy are applied to the structure.
   - Released structure is referred to primary structure.
   - Primary structure must be chosen such that it is geometrically stable and statically determinate.
2. Calculate "errors" (displacements) at the primary structure redundants. These displacements are calculated using the method of virtual forces.
3. Determine displacements in the primary structure due to unit values of redundants (method of virtual forces). These displacements are required at the same location and in the same direction as the displacement errors determined in step 2.
4. Calculate redundant forces to eliminate displacement errors.
   - Use superposition equations (Müller-Breslau equations) in which the effects of the separate redundants are added to the displacements of the released structure.
   - Displacement superposition results in a set of n linear equations (n = number of releases) that express the fact that there is zero relative displacement at each release.
   - These compatibility equations guarantee a final displaced shape consistent with known support conditions, i.e., the structure fits together at the n releases with no relative displacements.
5. Hence, we find the forces on the original indeterminate structure. They are the sum of the correction forces (redundants) and forces on the released structure.

10.2.2 Degree of indeterminacy Rigid-Jointed Frame

Description of the Rigid-Jointed Frame

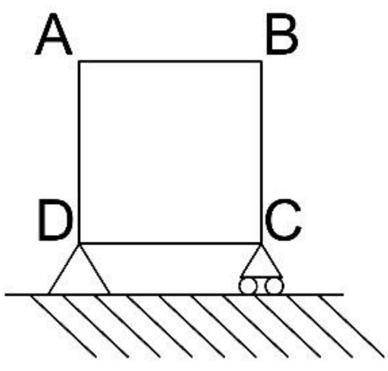

Figure 10-7 Rigid-Jointed Frame - names of the corners

The structure is externally statically determinate but internally statically indeterminate.

n : number of rigid joints n = 4

m : number members m = 4

r : support reactions r = 3

i : degree of indeterminacy i = ?

$$i = [(3 * m) + r] - 3 * n$$

$$i = [(3 * 4) + 3] - 3 * 4 = 3$$

The internal degree of indeterminacy is i = 3 .

10.2.2.1 Primary structure, from indeterminate system to a determinate one

Conversion of the indeterminate structure to a determinate one by removing 3 unknown forces and replacing them with (assumed) known / unit forces.

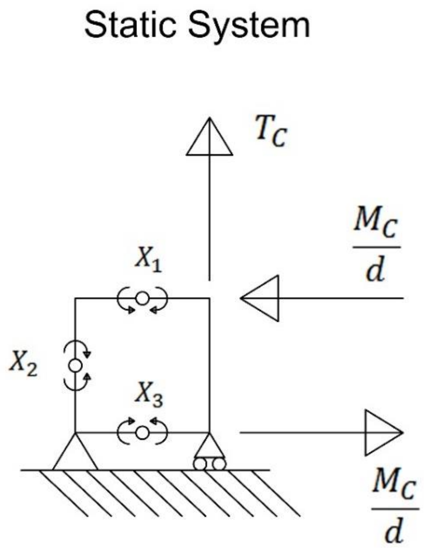

Figure 10-8 Primary structure - Static system

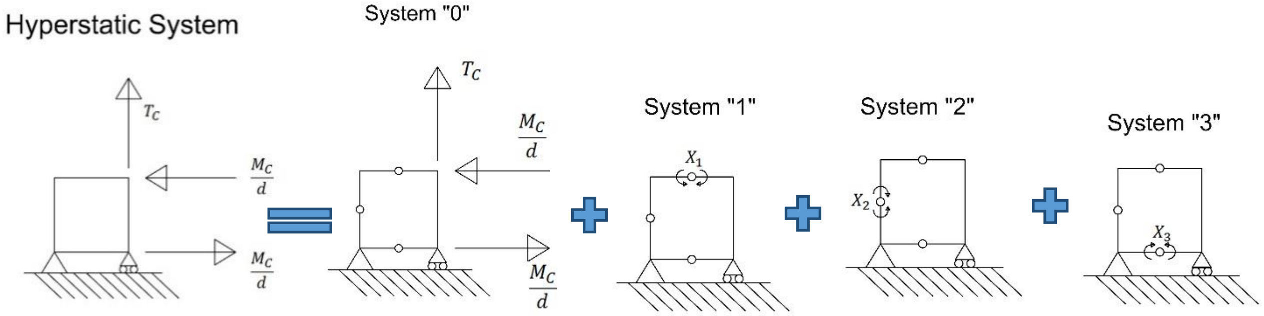

Figure 10-9 Decomposition of the redundant frame

10.2.3 Solved released systems

10.2.3.1 System 0

The primary structure is the released structure shown in the figure below and it is named System0.

They have been computed the reaction

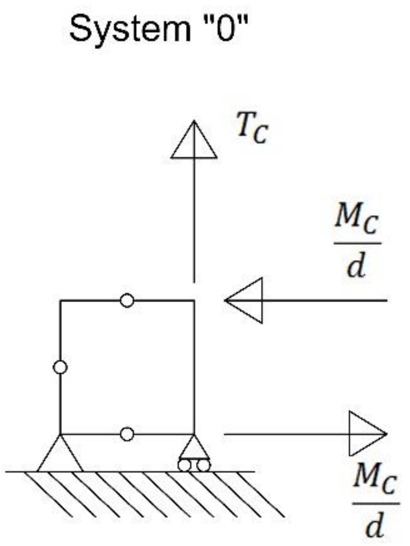

Figure 10-10 System

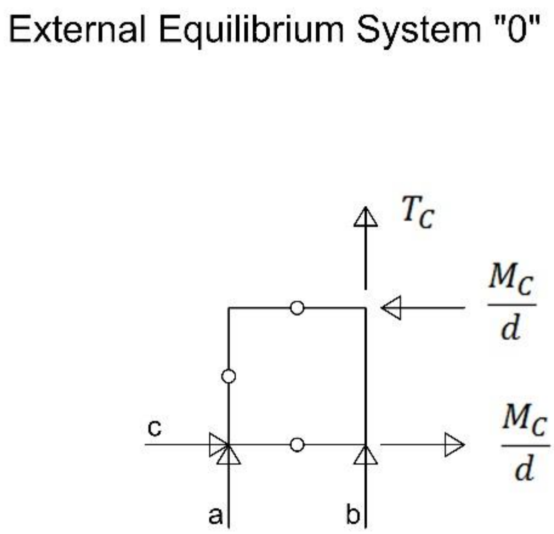

0 Figure 10-11 External Equilibrium System "0"

$$\begin{cases} a + b = -Tc \\ c = 0 \\ Tc * d + b * d + Mc = 0 \end{cases}$$

$$\begin{cases} a = \frac{Mc}{d} \\ c = 0 \\ b = -\frac{Mc}{d} - Tc \end{cases}$$

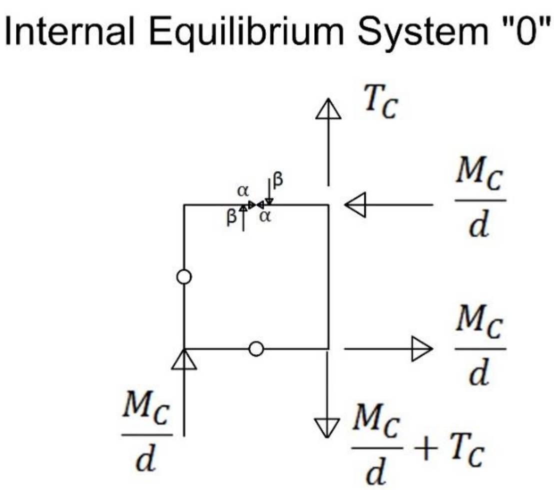

Figure 10-12 Internal Equilibrium System "0"

$$\begin{cases} -\alpha * \frac{d}{2} + \beta \frac{d}{2} = 0 \\ \alpha * d + Tc * \frac{d}{2} + Mc - \frac{Mc}{2} - Tc * \frac{d}{2} = 0 \end{cases}$$

$$\begin{cases} \alpha = -\frac{Mc}{2d} \\ \beta = -\frac{Mc}{2} \end{cases}$$

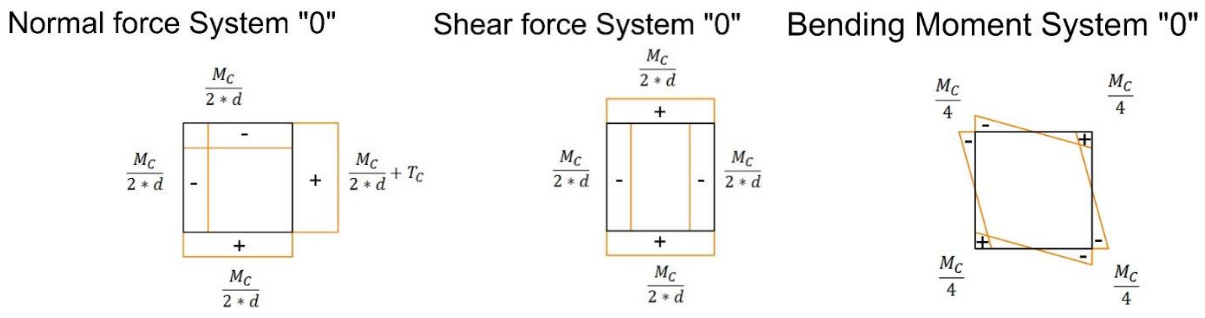

Figure 10-13 Internal reactions System "0"

10.2.3.2 System 1

The released structure with the addition of the the redoundant $X_1 = 1$ structure shown in the figure below and it is named System 1.

They have been computed the reaction

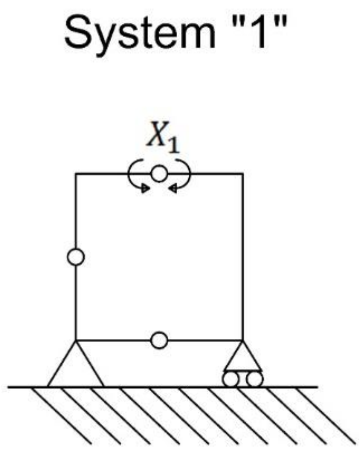

Figure 10-14 System 1

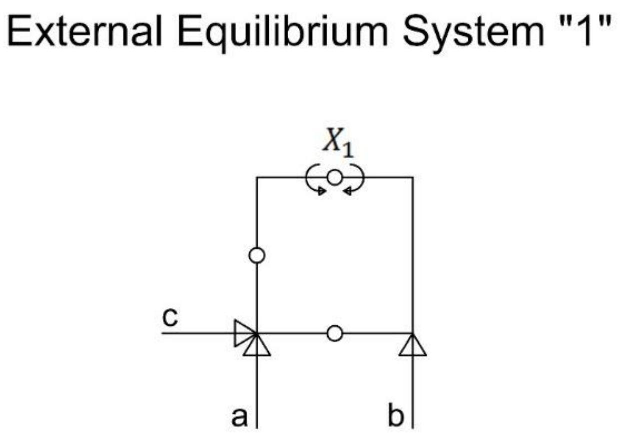

Figure 10-15 External Equilibrium System "1"

$$\begin{cases} a = 0 \\ b = 0 \\ c = 0 \end{cases}$$

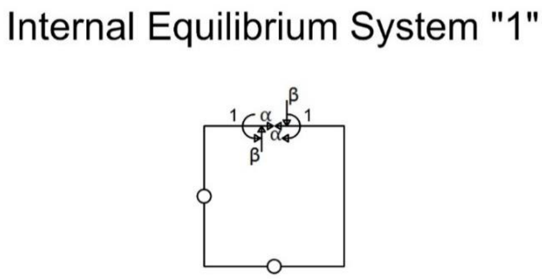

Figure 10-16 Internal Equilibrium System "1"

$$\begin{cases} \alpha * d - 1 = 0 \\ -\alpha * \dfrac{d}{2} + \beta * \dfrac{d}{2} = 0 \end{cases} \qquad \begin{cases} \alpha = \dfrac{1}{d} \\ \beta = -\dfrac{1}{d} \end{cases}$$

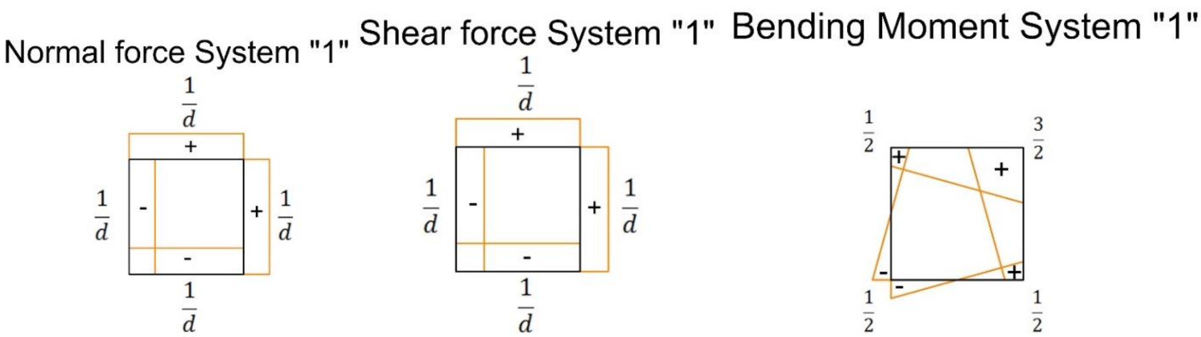

Figure 10-17 Internal Reactions System "1"

10.2.3.3 System 2

The released structure with the addition of the the redoundant $X_2 = 1$ structure shown in the figure below and it is named System 2.

They have been computed the reactions

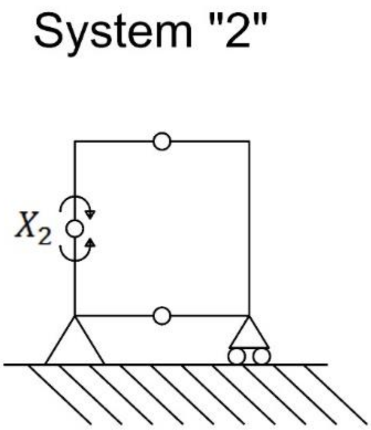

Figure 10-18 System 2

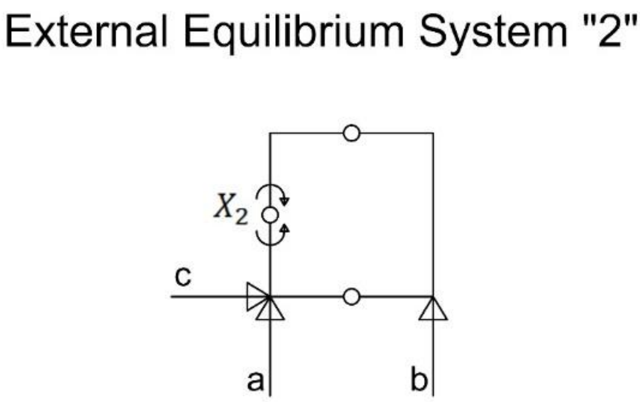

Figure 10-19 External Equilibrium System "2"

$$\begin{cases} a = 0 \\ b = 0 \\ c = 0 \end{cases}$$

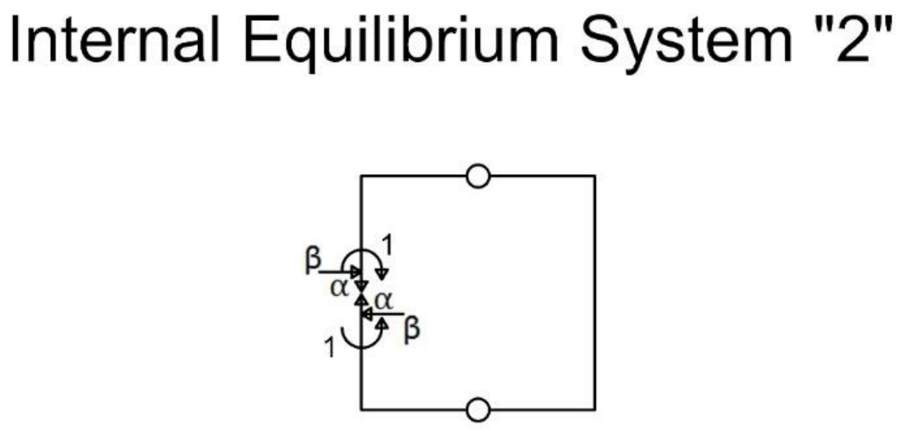

Figure 10-20 Internal Equilibrium System "2"

$$\begin{cases} \alpha * \dfrac{d}{2} - \beta * \dfrac{d}{2} - 1 = 0 \\ -\alpha * \dfrac{d}{2} - \beta * \dfrac{d}{2} + 1 = 0 \end{cases} \qquad \begin{cases} \alpha = \dfrac{2}{d} \\ \beta = 0 \end{cases}$$

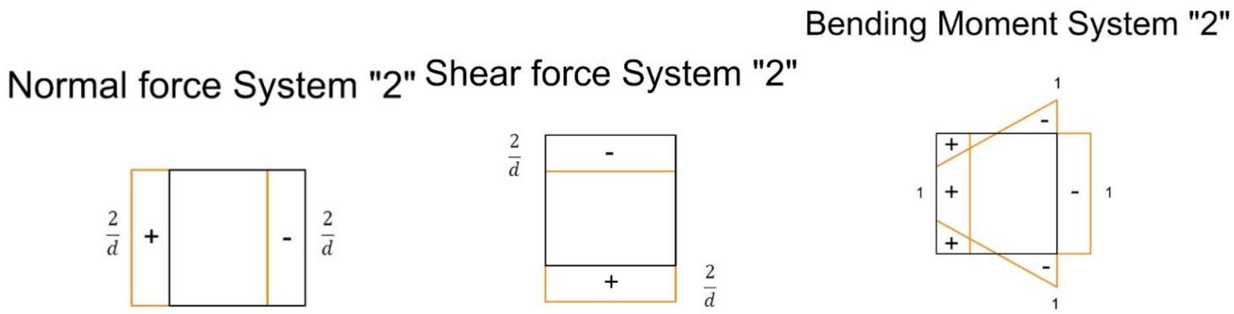

Figure 10-21 Internal Reactions System "2"

10.2.3.4 System 3

The released structure with the addition of the the redoundant $X_3 = 1$ structure shown in the figure below and it is named System 3.

They have been computed the reaction

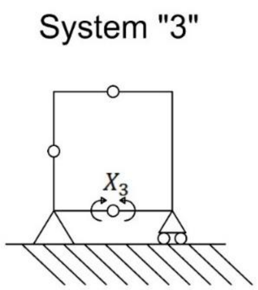

Figure 10-22 System "3"

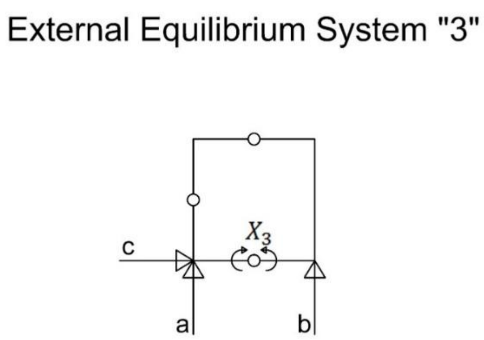

Figure 10-23 External Equilibrium System "3"

$$\begin{cases} a = 0 \\ b = 0 \\ c = 0 \end{cases}$$

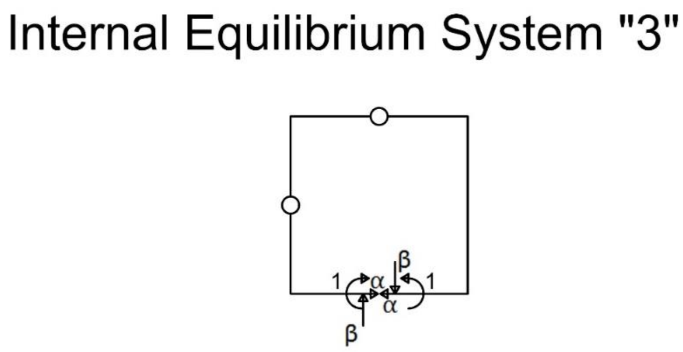

Figure 10-24 Internal Equilibrium System "3"

$$\begin{cases} \alpha * \dfrac{d}{2} - \beta * \dfrac{d}{2} - 1 = 0 \\ -\alpha * \dfrac{d}{2} - \beta * \dfrac{d}{2} + 1 = 0 \end{cases}$$

$$\begin{cases} \alpha = \dfrac{2}{d} \\ \beta = 0 \end{cases}$$

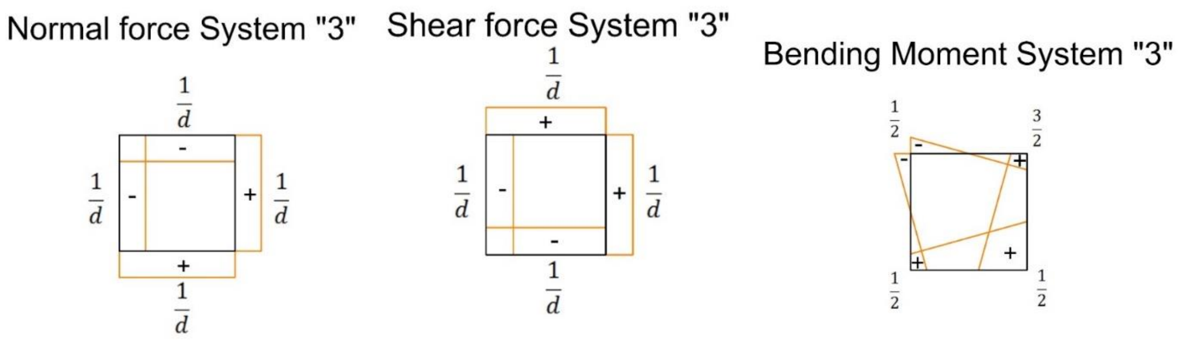

Figure 10-25 Internal reactions System "3"

10.2.4 Functions of the diagrams

For each system, they have been written the functions that describes the behavior of the forces, focus on each member.

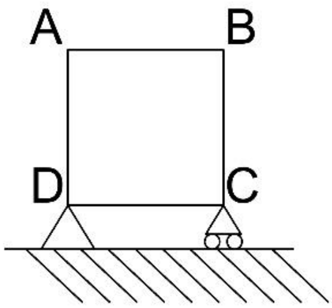

10.2.4.1 System 0

$N^0_{AB} = -\frac{Mc}{2d}$ $\quad N^0_{BC} = \frac{Mc}{2d} + Tc$ $\quad N^0_{CD} = \frac{Mc}{2d}$ $\quad N^0_{DA} = -\frac{Mc}{2d}$

$M^0_{AB} = \left(-\frac{1}{4} + \frac{s}{2d}\right) * Mc$ $\quad M^0_{BC} = \left(\frac{1}{4} - \frac{s}{2d}\right) * Mc$ $\quad M^0_{CD} = \left(-\frac{1}{4} + \frac{s}{2d}\right) * Mc$ $\quad M^0_{DA} = \left(\frac{1}{4} - \frac{s}{2d}\right) * Mc$

10.2.4.2 System 1

$N^1_{AB} = \frac{1}{d}$ $\quad N^1_{BC} = \frac{1}{d}$ $\quad N^1_{CD} = -\frac{1}{d}$ $\quad N^1_{DA} = -\frac{1}{d}$

$M^1_{AB} = \left(\frac{1}{2} + \frac{s}{d}\right)$ $\quad M^1_{BC} = \left(\frac{3}{2} - \frac{s}{d}\right)$ $\quad M^1_{CD} = \left(\frac{1}{2} - \frac{s}{d}\right)$ $\quad M^1_{DA} = \left(-\frac{1}{2} + \frac{s}{d}\right)$

10.2.4.3 System 2

$N^2_{AB} = 0$ $\quad N^2_{BC} = -\frac{2}{d}$ $\quad N^2_{CD} = 0$ $\quad N^2_{DA} = \frac{2}{d}$

$M^2_{AB} = \left(1 - \frac{2s}{d}\right)$ $\quad M^2_{BC} = -1$ $\quad M^2_{CD} = \left(-1 + \frac{2s}{d}\right)$ $\quad M^2_{DA} = 1$

10.2.4.4 System 3

$N^1_{AB} = -\frac{1}{d}$ $\quad N^1_{BC} = \frac{1}{d}$ $\quad N^1_{CD} = +\frac{1}{d}$ $\quad N^1_{DA} = -\frac{1}{d}$

$M^1_{AB} = \left(-\frac{1}{2} + \frac{s}{d}\right)$ $\quad M^1_{BC} = \left(\frac{1}{2} + \frac{s}{d}\right)$ $\quad M^1_{CD} = \left(\frac{3}{2} - \frac{s}{d}\right)$ $\quad M^1_{DA} = \left(\frac{1}{2} - \frac{s}{d}\right)$

10.2.5 Müller-Breslau equations

Base on the linearity of the problem they have been used the Müller-Breslau equations for the compatibility.

η_i : is the effective displacement in the effective structure

η_{i0} : is the displacement due to the primary system on the i released

X_i : is the unitary force in the position of the i released

η_{ik} : is the displacement of the point of application of the released X_i due to the redoundant $X_k = 1$

n : is the number of the released equal to the degree if indeterminacy i

$$\eta_i = \eta_{i0} + \sum_1^n \eta_{ik} * X_k$$

Thus, the 3 equation of Müller-Breslau that assures the compatibility are :

$$\begin{cases} \eta_1 = \eta_{10} + \eta_{11} * X_1 + \eta_{12} * X_2 + \eta_{13} * X_3 \\ \eta_2 = \eta_{20} + \eta_{21} * X_1 + \eta_{22} * X_2 + \eta_{23} * X_3 \\ \eta_3 = \eta_{30} + \eta_{31} * X_1 + \eta_{32} * X_2 + \eta_{33} * X_3 \end{cases}$$

Using the theorem of virtual work, it is possible to compute all the displacements as follows.

$$\eta_{i0} = \int \left(\frac{N_i * N_0}{EA} + \frac{T_i * T_0}{GK} + \frac{M_i * M_0}{EJ} \right) ds$$

$$\eta_{ik} = \int \left(\frac{N_i * N_k}{EA} + \frac{T_i * T_k}{GK} + \frac{M_i * M_k}{EJ} \right) ds$$

The contribution of the shear forces are negligible with the assumption that $GK = \infty$.

$$\eta_{i0} = \int \left(\frac{N_i * N_0}{EA} + \frac{M_i * M_0}{EJ} \right) ds$$

$$\eta_{ik} = \int \left(\frac{N_i * N_k}{EA} + \frac{M_i * M_k}{EJ} \right) ds$$

It is important to underline the following observations:

$$\eta_{ii} = \int \left(\frac{N_i * N_i}{EA} + \frac{M_i * M_i}{EJ} \right) ds = \int \left(\frac{{N_i}^2}{EA} + \frac{{M_i}^2}{EJ} \right) ds > 0$$

$\eta_{ik} = \eta_{ki}$ due to Maxwell Theorem

Then the coefficient matrix is symmetric and all the diagonal elements are positive.

10.2.5.1 Displacement coefficients

$$\eta_{10} = \int \left(\frac{N_1 * N_0}{EA} + \frac{M_1 * M_0}{EJ} \right) ds$$

$$= \int \left(\frac{N_{AB}^1 * N_{AB}^0 + N_{BC}^1 * N_{BC}^0 + N_{CD}^1 * N_{CD}^0 + N_{DA}^1 * N_{DA}^0}{EA} + \frac{M_{AB}^1 * M_{AB}^0 + M_{BC}^1 * M_{BC}^0 + M_{CD}^1 * M_{CD}^0 + M_{DA}^1 * M_{DA}^0}{EJ} \right) ds = \frac{Tc}{EA}$$

$$\eta_{20} = \int \left(\frac{N_2 * N_0}{EA} + \frac{M_2 * M_0}{EJ}\right) ds$$

$$= \int \left(\frac{N_{AB}^2 * N_{AB}^0 + N_{BC}^2 * N_{BC}^0 + N_{CD}^2 * N_{CD}^0 + N_{DA}^2 * N_{DA}^0}{EA} + \frac{M_{AB}^2 * M_{AB}^0 + M_{BC}^2 * M_{BC}^0 + M_{CD}^2 * M_{CD}^0 + M_{DA}^2 * M_{DA}^0}{EJ}\right) ds = -\frac{2}{EA} * \left(Tc + \frac{Mc}{d}\right)$$

$$\eta_{30} = \int \left(\frac{N_3 * N_0}{EA} + \frac{M_3 * M_0}{EJ}\right) ds$$

$$= \int \left(\frac{N_{AB}^3 * N_{AB}^0 + N_{BC}^3 * N_{BC}^0 + N_{CD}^3 * N_{CD}^0 + N_{DA}^3 * N_{DA}^0}{EA} + \frac{M_{AB}^3 * M_{AB}^0 + M_{BC}^3 * M_{BC}^0 + M_{CD}^3 * M_{CD}^0 + M_{DA}^3 * M_{DA}^0}{EJ}\right) ds = \frac{1}{EA} * \left(Tc + \frac{2Mc}{d}\right)$$

$$\eta_{11} = \int \left(\frac{{N_1}^2}{EA} + \frac{{M_1}^2}{EJ}\right) ds$$

$$= \int \left(\frac{{N_{AB}^1}^2 + {N_{BC}^1}^2 + {N_{CD}^1}^2 + {N_{DA}^1}^2}{EA} + \frac{{M_{AB}^1}^2 + {M_{BC}^1}^2 + {M_{CD}^1}^2 + {M_{DA}^1}^2}{EJ}\right) ds$$

$$= \frac{4}{d} * \frac{1}{EA} + \frac{7}{3} * \frac{d}{EJ}$$

$$\eta_{22} = \int \left(\frac{{N_2}^2}{EA} + \frac{{M_2}^2}{EJ}\right) ds$$

$$= \int \left(\frac{{N_{AB}^2}^2 + {N_{BC}^2}^2 + {N_{CD}^2}^2 + {N_{DA}^2}^2}{EA} + \frac{{M_{AB}^2}^2 + {M_{BC}^2}^2 + {M_{CD}^2}^2 + {M_{DA}^2}^2}{EJ}\right) ds$$

$$= \frac{8}{d} * \frac{1}{EA} + \frac{8}{3} * \frac{d}{EJ}$$

$$\eta_{33} = \int \left(\frac{{N_3}^2}{EA} + \frac{{M_3}^2}{EJ}\right) ds$$

$$= \int \left(\frac{{N_{AB}^3}^2 + {N_{BC}^3}^2 + {N_{CD}^3}^2 + {N_{DA}^3}^2}{EA} + \frac{{M_{AB}^3}^2 + {M_{BC}^3}^2 + {M_{CD}^3}^2 + {M_{DA}^3}^2}{EJ}\right) ds$$

$$= \frac{4}{d} * \frac{1}{EA} + \frac{7}{12} * \frac{d}{EJ}$$

$$\eta_{12} = \eta_{21} = \int \left(\frac{N_1 * N_2}{EA} + \frac{M_1 * M_2}{EJ} \right) ds$$

$$= \int \left(\frac{N_{AB}^1 * N_{AB}^2 + N_{BC}^1 * N_{BC}^2 + N_{CD}^1 * N_{CD}^2 + N_{DA}^1 * N_{DA}^2}{EA} + \frac{M_{AB}^1 * M_{AB}^2 + M_{BC}^1 * M_{BC}^2 + M_{CD}^1 * M_{CD}^2 + M_{DA}^1 * M_{DA}^2}{EJ} \right) ds = -\frac{4}{d} * \frac{1}{EA} - \frac{4}{3} * \frac{d}{EJ}$$

$$\eta_{13} = \eta_{31} = \int \left(\frac{N_1 * N_3}{EA} + \frac{M_1 * M_3}{EJ} \right) ds$$

$$= \int \left(\frac{N_{AB}^1 * N_{AB}^3 + N_{BC}^1 * N_{BC}^3 + N_{CD}^1 * N_{CD}^3 + N_{DA}^1 * N_{DA}^3}{EA} + \frac{M_{AB}^1 * M_{AB}^3 + M_{BC}^1 * M_{BC}^3 + M_{CD}^1 * M_{CD}^3 + M_{DA}^1 * M_{DA}^3}{EJ} \right) ds = \frac{1}{2} * \frac{d}{EJ}$$

$$\eta_{23} = \eta_{32} = \int \left(\frac{N_2 * N_3}{EA} + \frac{M_2 * M_3}{EJ} \right) ds$$

$$= \int \left(\frac{N_{AB}^2 * N_{AB}^3 + N_{BC}^2 * N_{BC}^3 + N_{CD}^2 * N_{CD}^3 + N_{DA}^2 * N_{DA}^3}{EA} + \frac{M_{AB}^2 * M_{AB}^3 + M_{BC}^2 * M_{BC}^3 + M_{CD}^2 * M_{CD}^3 + M_{DA}^2 * M_{DA}^3}{EJ} \right) ds = -\frac{4}{d} * \frac{1}{EA} - \frac{4}{3} * \frac{d}{EJ}$$

$$\begin{cases} \eta_1 = \frac{Tc}{EA} + \left(\frac{4}{d} * \frac{1}{EA} + \frac{7}{3} * \frac{d}{EJ}\right) * X_1 + \left(-\frac{4}{d} * \frac{1}{EA} - \frac{4}{3} * \frac{d}{EJ}\right) * X_2 + \left(\frac{1}{2} * \frac{d}{EJ}\right) * X_3 \\ \eta_2 = -\frac{2}{EA} * \left(Tc + \frac{Mc}{d}\right) + \left(-\frac{4}{d} * \frac{1}{EA} - \frac{4}{3} * \frac{d}{EJ}\right) * X_1 + \left(\frac{8}{d} * \frac{1}{EA} + \frac{8}{3} * \frac{d}{EJ}\right) * X_2 + \left(-\frac{4}{d} * \frac{1}{EA} - \frac{4}{3} * \frac{d}{EJ}\right) * X_3 \\ \eta_3 = \frac{1}{EA} * \left(Tc + \frac{2Mc}{d}\right) + \left(\frac{1}{2} * \frac{d}{EJ}\right) * X_1 + \left(-\frac{4}{d} * \frac{1}{EA} - \frac{4}{3} * \frac{d}{EJ}\right) * X_2 + \left(\frac{4}{d} * \frac{1}{EA} + \frac{7}{12} * \frac{d}{EJ}\right) * X_3 \end{cases}$$

They have been released internal actions this means the displacements are null because they are mutual.

$\eta_1 = 0$ $\eta_2 = 0$ $\eta_3 = 0$

$$\begin{cases} 0 = \frac{Tc}{EA} + \left(\frac{4}{d} * \frac{1}{EA} + \frac{7}{3} * \frac{d}{EJ}\right) * X_1 + \left(-\frac{4}{d} * \frac{1}{EA} - \frac{4}{3} * \frac{d}{EJ}\right) * X_2 + \left(\frac{1}{2} * \frac{d}{EJ}\right) * X_3 \\ 0 = -\frac{2}{EA} * \left(Tc + \frac{Mc}{d}\right) + \left(-\frac{4}{d} * \frac{1}{EA} - \frac{4}{3} * \frac{d}{EJ}\right) * X_1 + \left(\frac{8}{d} * \frac{1}{EA} + \frac{8}{3} * \frac{d}{EJ}\right) * X_2 + \left(-\frac{4}{d} * \frac{1}{EA} - \frac{4}{3} * \frac{d}{EJ}\right) * X_3 \\ 0 = \frac{1}{EA} * \left(Tc + \frac{2Mc}{d}\right) + \left(\frac{1}{2} * \frac{d}{EJ}\right) * X_1 + \left(-\frac{4}{d} * \frac{1}{EA} - \frac{4}{3} * \frac{d}{EJ}\right) * X_2 + \left(\frac{4}{d} * \frac{1}{EA} + \frac{7}{12} * \frac{d}{EJ}\right) * X_3 \end{cases}$$

10.2.5.2 Axial rigidity (EA) and flexural rigidity (EJ)

The Young modulus considered is the design Young modulus parallel to the fibers for the Shorea robusta timber.

$$E_{0,d} = 15.38 \left[\frac{kN}{mm^2}\right] = 15384615 \left[\frac{kN}{m^2}\right] = 15384615 * 10^3 \left[\frac{N}{m^2}\right]$$

It can be assumed that the rigid joint frames studied is composed by cross pieces. Following measures of the cross piece are in cm.

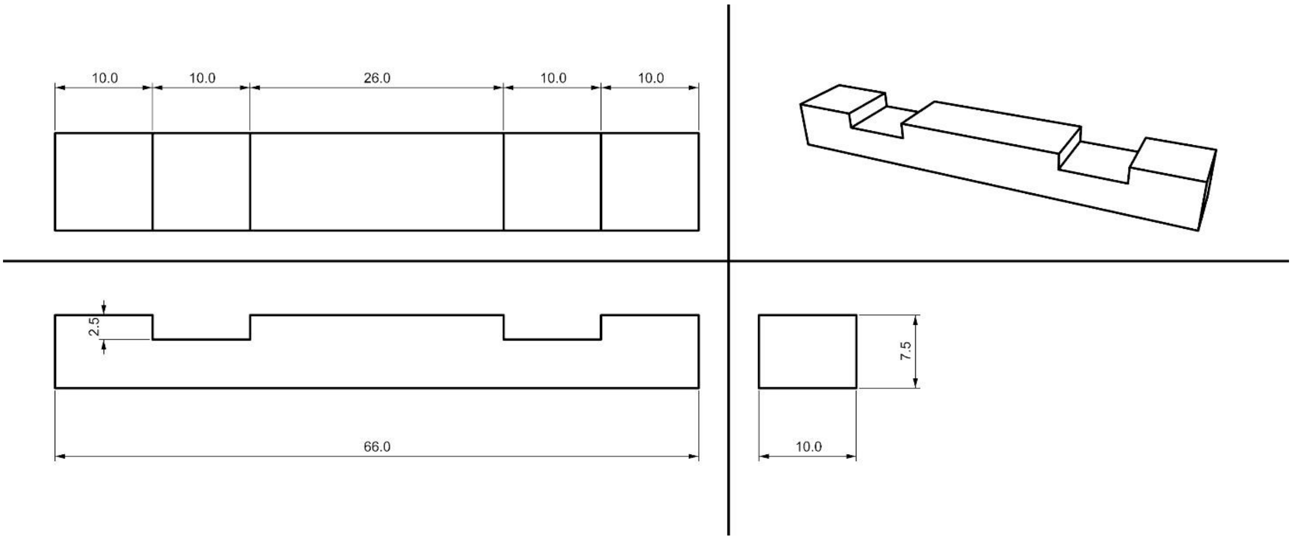

Data of the studied section:

$b = 0.075\ m$

$h = 0.1\ m$

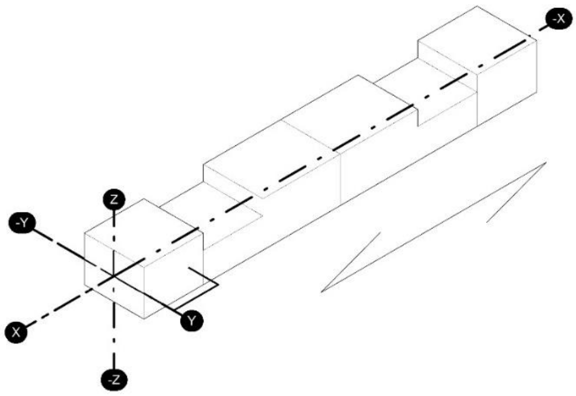

Moment of inertia around Z axis:

$$J_Z = \frac{b * h^3}{12} = \frac{0.075m * (0.1m)^3}{12} = 6.25 * 10^{-6} m^4$$

Area of the considered section A:

$$A = b * h = 0.075m * 0.1m = 7.5 * 10^{-3} m^2$$

10.2.5.3 Seismic distributed load q_α

The uniformly distributed load considered for the overturning with flexible body has been computed as following.

$$q_\alpha = \frac{Mass_i * g * \alpha}{L} \qquad \left[\frac{N}{m}\right]$$

Where

$Mass_i$: is the mass involved for the specific tie-timber beam

g: is the gravity accelleration

α : is the seismic load multiplier

L : is the length of the wall

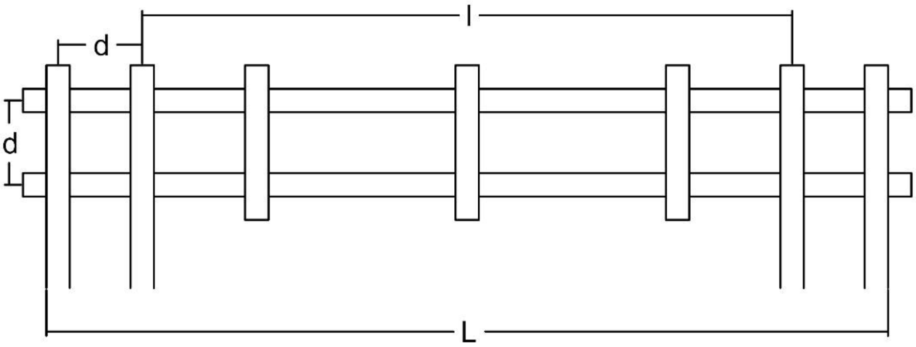

10.2.5.4 Seismic shear force (Tc) and Seismic bending moment (Mc)

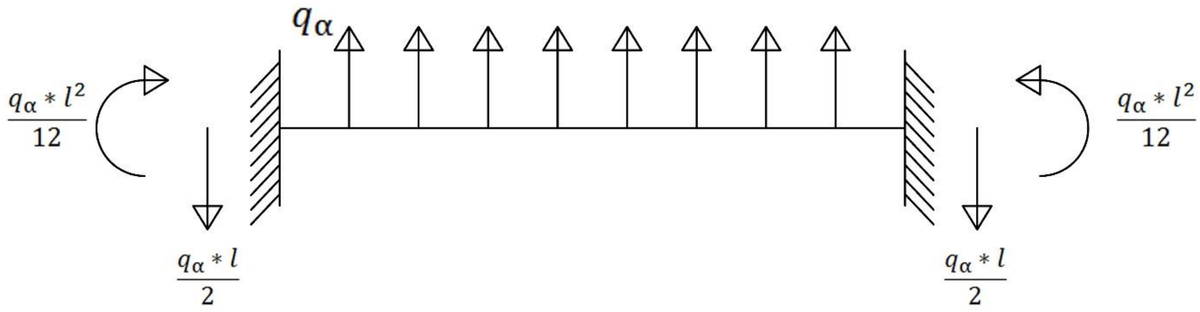

Seismic shear force is named Tc

$$T_C = \frac{q_\alpha * l}{2} \qquad [N]$$

Seismic bending moment is named Mc

$$M_C = \frac{q_\alpha * l^2}{12} \quad [Nm]$$

In order to have the homogenous coefficients depending on the seismic uniformly distributed load q_α , the actions have been written substituting the proper wall geometrical value.

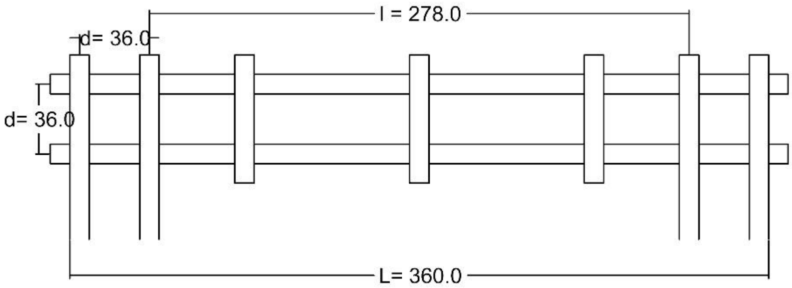

L : is the length of the wall equal to 3.6 m

l : is the length of the wall where the load is distributed, equal to 2.78 m

d : is the distances between all the timber elements, equal to 0.36 m

Thus

$$T_C = \frac{q_\alpha * l}{2} = q_\alpha \frac{2{,}78m}{2} = q_\alpha \frac{139}{100} \ [N]$$

$$M_C = \frac{q_\alpha * l^2}{12} = q_\alpha \frac{(2{,}78m)^2}{12} = q_\alpha \frac{19321}{30000} \ [Nm]$$

10.2.5.5 Solutions of Müller-Breslau equations

Substituting all the known values it has been obtained the following linear system in function of the seismic load.

$$\begin{cases} 0 = -185.33 * q_\alpha + (135881{,}48) * X_1 + (-78281{,}48) * X_2 + (28800{,}00) * X_3 \\ 0 = 847.73 * q_\alpha + (-78281{,}48) * X_1 + (156562{,}96) * X_2 + (-78281{,}48) * X_3 \\ 0 = -662.4 * q_\alpha + (28800{,}00) * X_1 + (-78281{,}48) * X_2 + (35081{,}48) * X_3 \end{cases}$$

The solutions of the system depends on the seismic load q_α.

$$\begin{cases} X_1 = 6.87 * 10^{-3} * q_\alpha \\ X_2 = 2.95 * 10^{-2} * q_\alpha \\ X_3 = 4.12 * 10^{-2} * q_\alpha \end{cases}$$

10.2.6 Solutions of the complete isostatic structure

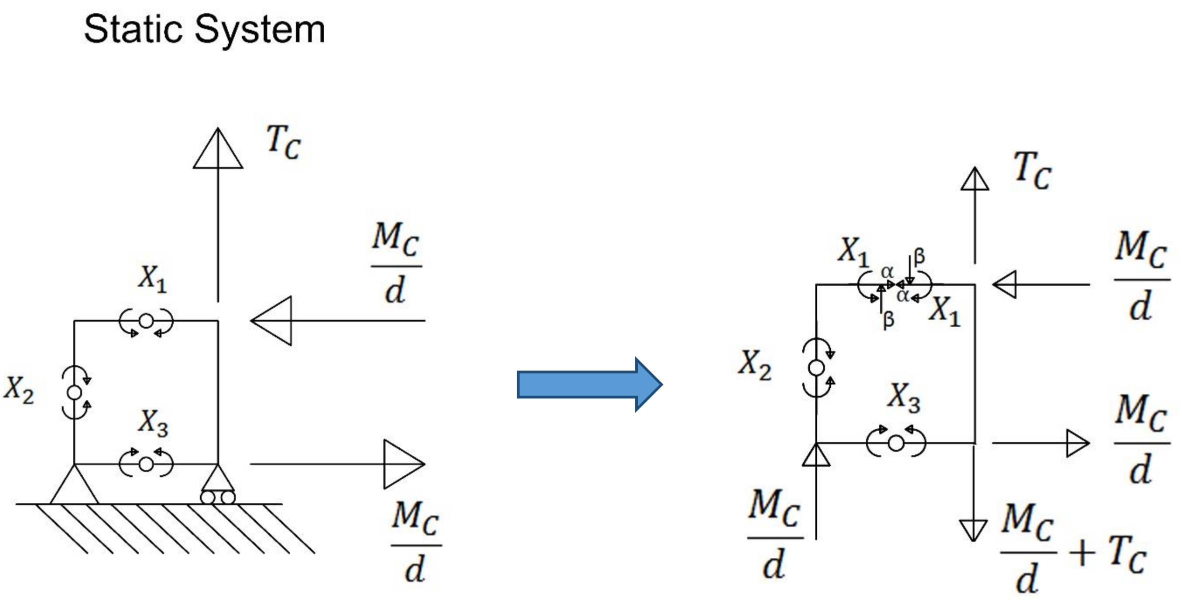

They have been obtained the internal forces by equilibrium.

$$\begin{cases} X_3 - \frac{Mc}{d} * \frac{d}{2} - Tc * \frac{d}{2} + Mc + Tc * \frac{d}{2} + \alpha * d \ - X_1 = 0 \\ -X_2 + X_1 - \alpha * \frac{d}{2} + \beta * \frac{d}{2} = 0 \end{cases}$$

$$\begin{cases} \alpha = \frac{X_1}{d} - \frac{X_3}{d} - \frac{Mc}{2d} \\ \beta = -\frac{X_1}{d} + 2 * \frac{X_2}{d} - \frac{X_3}{d} - \frac{Mc}{2d} \end{cases}$$

$$\begin{cases} \alpha = -0.99 * q_\alpha \\ \beta = -0.86 * q_\alpha \end{cases}$$

10.2.6.1 Normal, shear and bending moment diagrams in function of seismic load q_α

$T_C = \frac{139}{100} * q_\alpha \ [N]$

$M_C = \frac{19321}{30000} * q_\alpha \ [Nm]$

$X_1 = 6.87 * 10^{-3} * q_\alpha \ [Nm]$
$X_2 = 2.95 * 10^{-2} * q_\alpha \ [Nm]$
$X_3 = 4.12 * 10^{-2} * q_\alpha \ [Nm]$

$\alpha = -0.99 * q_\alpha \ [N]$
$\beta = -0.86 * q_\alpha \ [N]$

Normal forces

$N_{AB} = \alpha = -0.99 * q_\alpha \ [N]$

$$N_{BC} = Tc - \beta = \frac{139}{100} * q_\alpha + 0.86 * q_\alpha = 2.25 * q_\alpha [N]$$

$$N_{CD} = -\alpha = 0.99 * q_\alpha [N]$$

$$N_{DA} = \beta = -0.86 * q_\alpha [N]$$

Shear forces

$$T_{AB} = -\beta = 0.86 * q_\alpha [N]$$

$$T_{BC} = -\alpha - \frac{Mc}{d} = 0.99 * q_\alpha - \frac{19321}{30000} * \frac{100}{36} * q_\alpha = -0.8 * q_\alpha [N]$$

$$T_{CD} = \beta + \frac{Mc}{d} = -0.86 * q_\alpha + \frac{19321}{30000} * \frac{100}{36} * q_\alpha = 0.92 * q_\alpha [N]$$

$$T_{DA} = \alpha = -0.99 * q_\alpha [N]$$

Bending moments (in the corner rigid joints)

$$M_{inA} = X_1 + \beta * \frac{d}{2} = 6.87 * 10^{-3} * q_\alpha - 0.86 * \frac{36}{100} * \frac{1}{2} * q_\alpha = -0.15 * q_\alpha [Nm]$$

$$M_{inB} = X_1 - \beta * \frac{d}{2} = 6.87 * 10^{-3} * q_\alpha + 0.86 * \frac{36}{100} * \frac{1}{2} * q_\alpha = 0.16 * q_\alpha [Nm]$$

$$M_{inC} = X_1 - \beta * \frac{d}{2} - \alpha * d - Mc$$
$$= 6.87 * 10^{-3} * q_\alpha + 0.86 * \frac{36}{100} * \frac{1}{2} * q_\alpha + 0.99 * \frac{36}{100} * q_\alpha - \frac{19321}{30000} * q_\alpha$$
$$= -0.13 * q_\alpha [Nm]$$

$$M_{inD} = X_1 + \beta * \frac{d}{2} - \alpha * d = 6.87 * 10^{-3} * q_\alpha - 0.86 * \frac{36}{100} * \frac{1}{2} * q_\alpha + 0.99 * \frac{36}{100} * q_\alpha$$
$$= 0.21 * q_\alpha [Nm]$$

Normal force

$$N_{AB} = 0.99 * q_\alpha \ [N]$$

$$N_{DA} = 0.86 * q_\alpha [N]$$

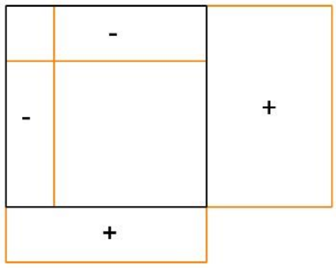

$$N_{BC} = 2.25 * q_\alpha [N]$$

$$N_{CD} = 0.99 * q_\alpha [N]$$

Shear force

$$T_{AB} = 0.86 * q_\alpha [N]$$

$$T_{DA} = 0.99 * q_\alpha [N]$$

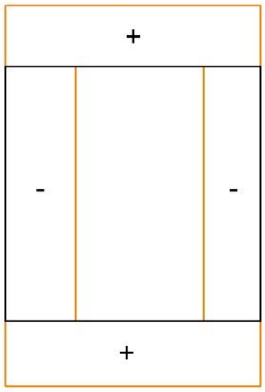

$$T_{BC} = 0.8 * q_\alpha [N]$$

$$T_{CD} = 0.92 * q_\alpha [N]$$

Bending Moment

$$M_{inA} = 0.15 * q_\alpha [Nm]$$

$$M_{inD} = 0.21 * q_\alpha [Nm]$$

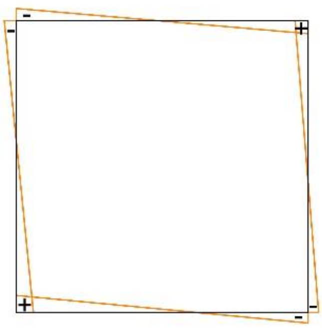

$$M_{inB} = 0.16 * q_\alpha [Nm]$$

$$M_{inC} = 0.13 * q_\alpha [Nm]$$

10.3 Triangular distribution of seismic load q_{α}

In the case of the bending behavior wall, the seismic forces has been set with the only triangular distribution over the height. This configuration is the only one possible for the hand calculation, other possible distribution would be possible with the modal analysis method but they would need a numerical approach.

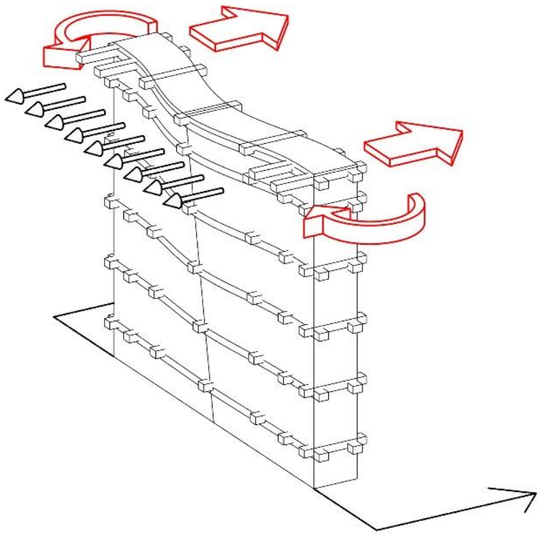

10.3.1 Scheme of wall Flexible response – Bendingbehavior~~flexible behavior~~

They have been named and numbered the analyzed beam in a similar way used for the rigid behavior.

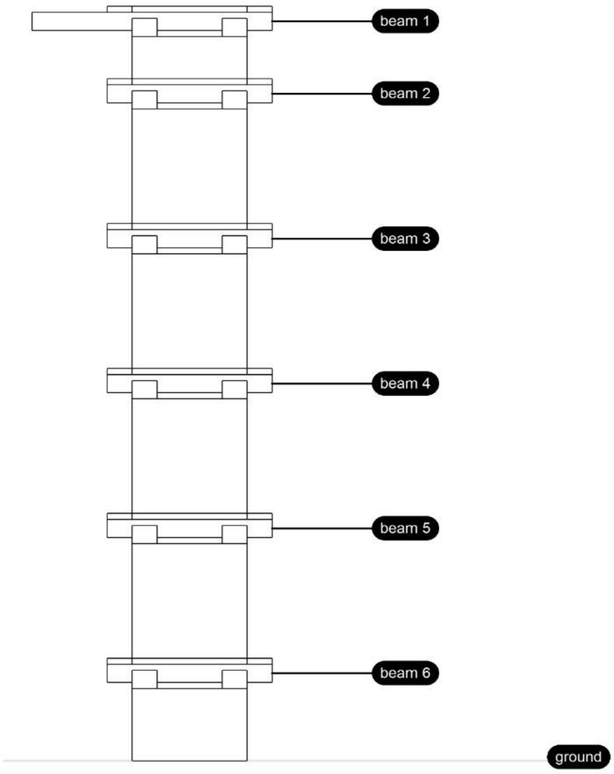

Figure 10-26 Flexible response – Bendingbehavior~~behavior~~ - Analyzed beams

10.3.2 Masses involved and heights of each timber beam

They have been assigned the pertinent masses at each timber band.

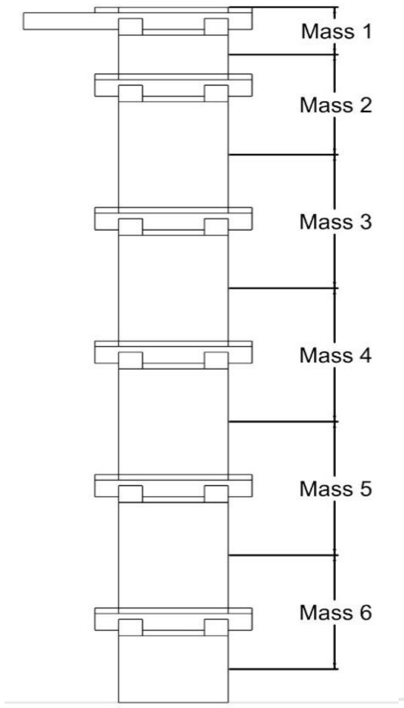

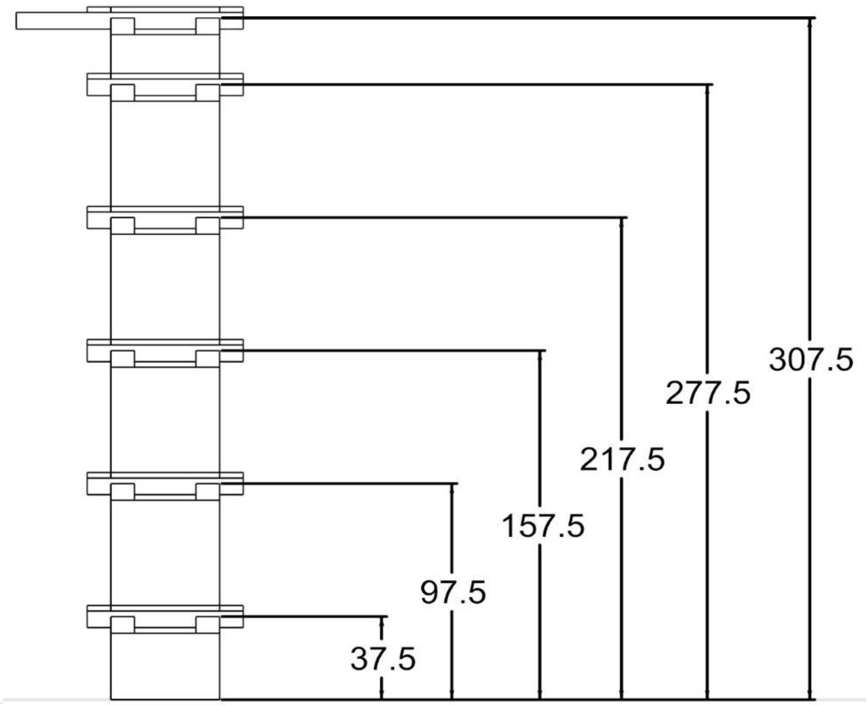

Figure 10-27 Bending behavior Pertinent masses for each timber band *Figure 10-28 Bending behavior Heights of each timber band*

Table 58 Pertinent masses foe each timber bands

	Mass for each Force 3 module		
		KN	Kg
Mass 1	Wroof module	51,23	5222,31
	W1	6,70	683,48
Mass 2	W2	14,52	1480,36
Mass 3	W3	19,05	1941,72
Mass 4	W4	19,05	1941,72
Mass 5	W5	19,05	1941,72
Mass 6	W6	16,17	1648,13
	W7	4,94	503,29

10.3.3 Seismic load q_α and Distribution factor β_j

The distribution factor for the triangular distribution has been obtained with the procedure descripted in the chapter 8.2.1.2 . Here are reported the main equations to compute the distribution factors and the corresponding seismic loads.

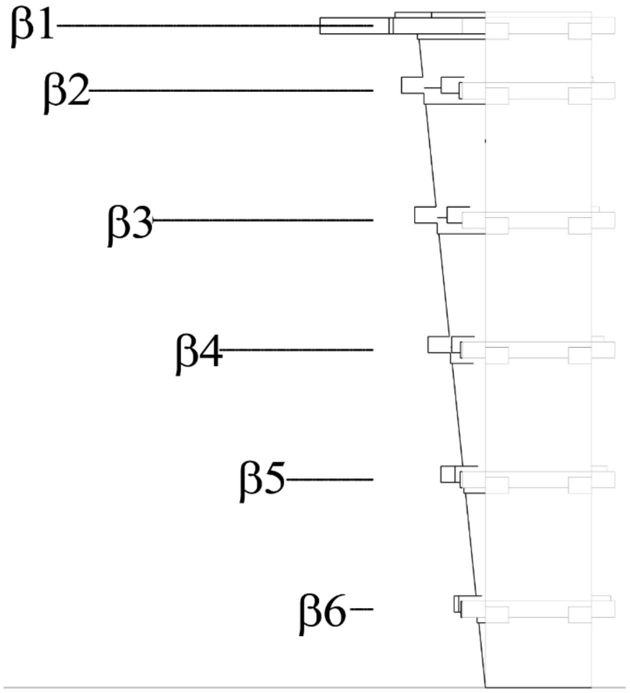

Figure 10-29 Bending behavior -Distribution factors

$$q = \frac{Mtot * g}{L} = \frac{Wtot}{L}$$

$$q_\alpha = q * \alpha = \frac{Mtot * g}{L} * \alpha = \frac{Wtot * g}{L} * \alpha$$

$$\beta_j = \frac{W_j * h_j}{\sum_{i=1}^{N} W_i * h_i + W_{roof} * H}$$

$$q_{\alpha j} = q_\alpha * \beta_j = q_\alpha * \frac{W_j * h_j}{\sum_{i=1}^{N} W_i * h_i + W_{roof} * H}$$

Table 59 Bending behavior - Distribution of the weight over the height

Distribution of the weight over the height			
	W	Height of Force : hi	Wi * hi
Wi	kN	m	kN*m
Wroof	51,23	3,075	157,53
W1	6,70	3,075	20,62
W2	14,52	2,775	40,30
W3	19,05	2,175	41,43
W4	19,05	1,575	30,00
W5	19,05	0,975	18,57
W6	16,17	0,375	6,06

Table 60 Bending behavior - Wall lenght

Wall length		
L	3,60	m

Table 61 Bending behavior - Distribution factors and seismic loads

Distribution factors and seismic loads		
qαj	βj	qαj=q*βj
qα1	0,57	23,71
qα2	0,13	5,36
qα3	0,13	5,51
qα4	0,10	3,99
qα5	0,06	2,47
qα6	0,02	0,81

10.4 Reactions for each beam

In this sub-chapter they have been recalled the results obtained by the force method and the seismic loads depending on the load multiplier in order to obtain the reactions on all the heads of the rafters which cross in the corner joint.

10.4.1 Rafter body reactions for each beam in the corner joint

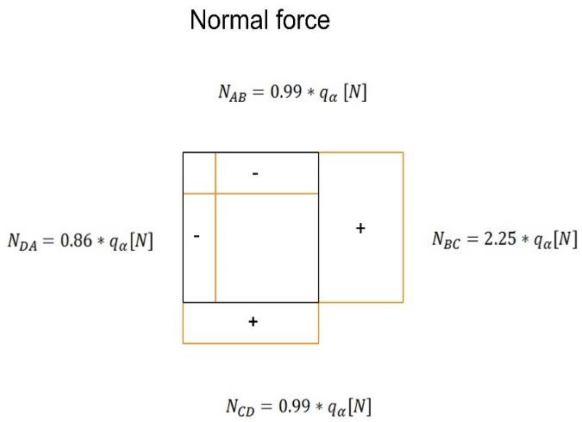

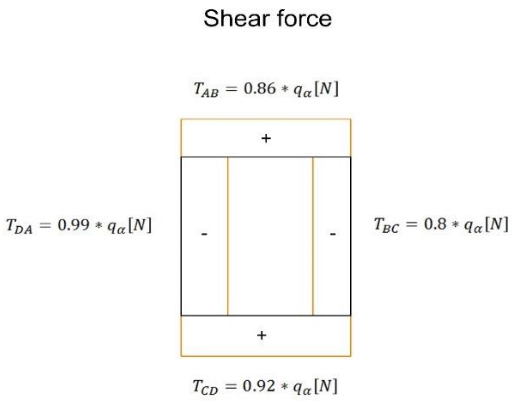

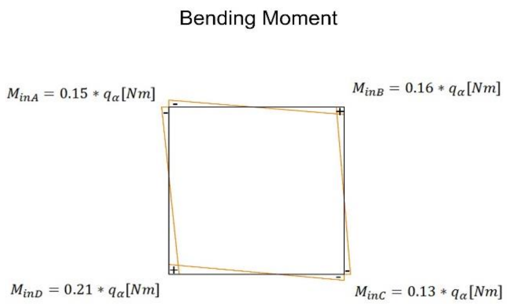

Table 62 Flexible behavior - Rafter body reactions for each beam

		Normal force				Shear force				Bending Moment			
Beam	q(α)j with α=1 [kN/m]	Nab [kN]	Nbc [kN]	Ncd [kN]	Nda [kN]	Tab [kN]	Tbc [kN]	Tcd [kN]	Tda [kN]	BM in A [kNm]	BM in B [kNm]	BM in C [kNm]	BM in D [kNm]
1	23,71	-23,47	53,46	23,47	-20,50	20,50	-18,95	21,92	-23,47	-3,53	3,85	-2,97	4,92
2	5,36	-5,31	12,09	5,31	-4,64	4,64	-4,29	4,96	-5,31	-0,80	0,87	-0,67	1,11
3	5,51	-5,46	12,43	5,46	-4,77	4,77	-4,41	5,10	-5,46	-0,82	0,90	-0,69	1,15
4	3,99	-3,95	9,00	3,95	-3,45	3,45	-3,19	3,69	-3,95	-0,59	0,65	-0,50	0,83
5	2,47	-2,45	5,57	2,45	-2,14	2,14	-1,98	2,29	-2,45	-0,37	0,40	-0,31	0,51
6	0,81	-0,80	1,82	0,80	-0,70	0,70	-0,64	0,75	-0,80	-0,12	0,13	-0,10	0,17

10.4.2 Rigid- jointed frame reactions for each beam

In this configuration, the computed values regard the whole longitudinal tie-timber beam composed by 2 rafters body. In order to have the values for 1 timber rafter body, 2 must divide the values in the following tables.

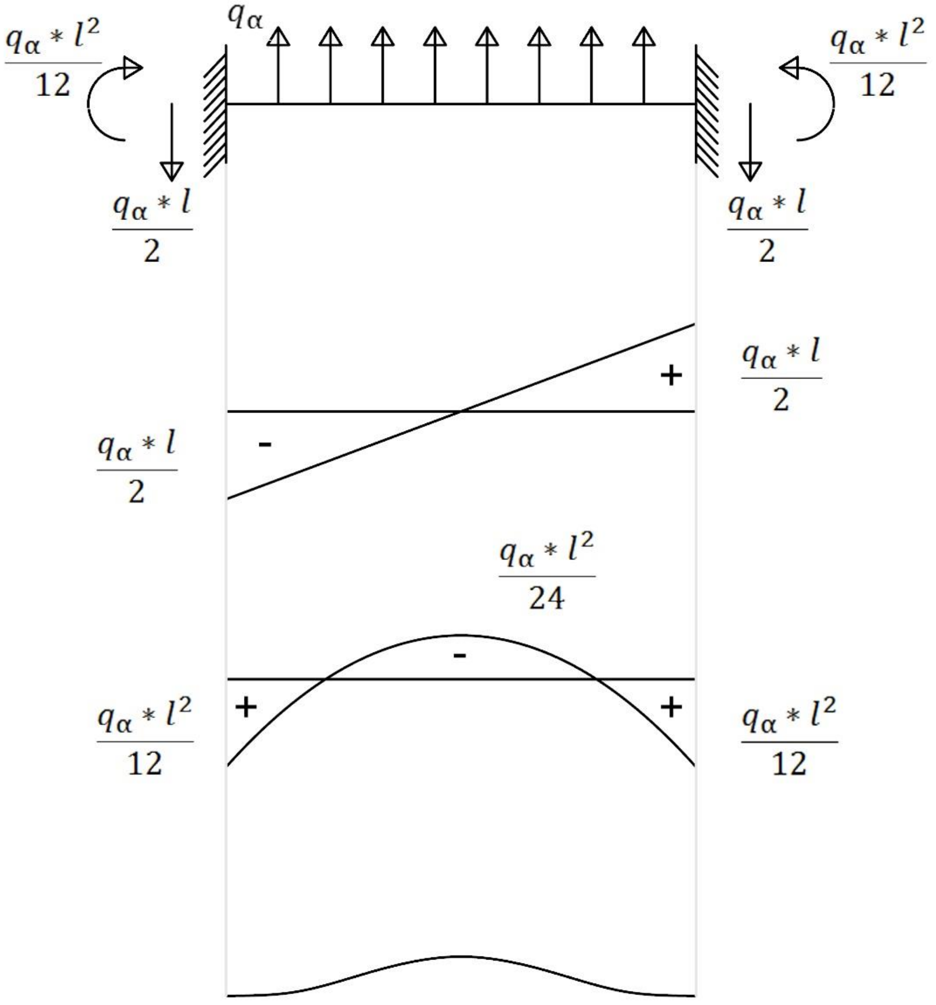

Figure 10-30 Bending behavior - Rigid- jointed frame reactions for each beam-

Table 63 Bending behavior - Rigid- jointed frame reactions for each beam

		Shear force [kN]		Bending Moment [kNm]		
		end left	end right	end left	midpoint	end right
Beam	q(α)j with α=1 [kN/m]	q(α)*(l)/2	q(α)*(l)/2	q(α)*(l^2)/12	q(α)*(l^2)/24=	q(α)*(l^2)/12
1	23,71	-32,96	32,96	15,27	-7,64	15,27
2	5,36	-7,46	7,46	3,45	-1,73	3,45
3	5,51	-7,67	7,67	3,55	-1,78	3,55
4	3,99	-5,55	5,55	2,57	-1,29	2,57
5	2,47	-3,44	3,44	1,59	-0,80	1,59
6	0,81	-1,12	1,12	0,52	-0,26	0,52

For the verifications of the rafters, belonging to the failing wall it has been used the following table

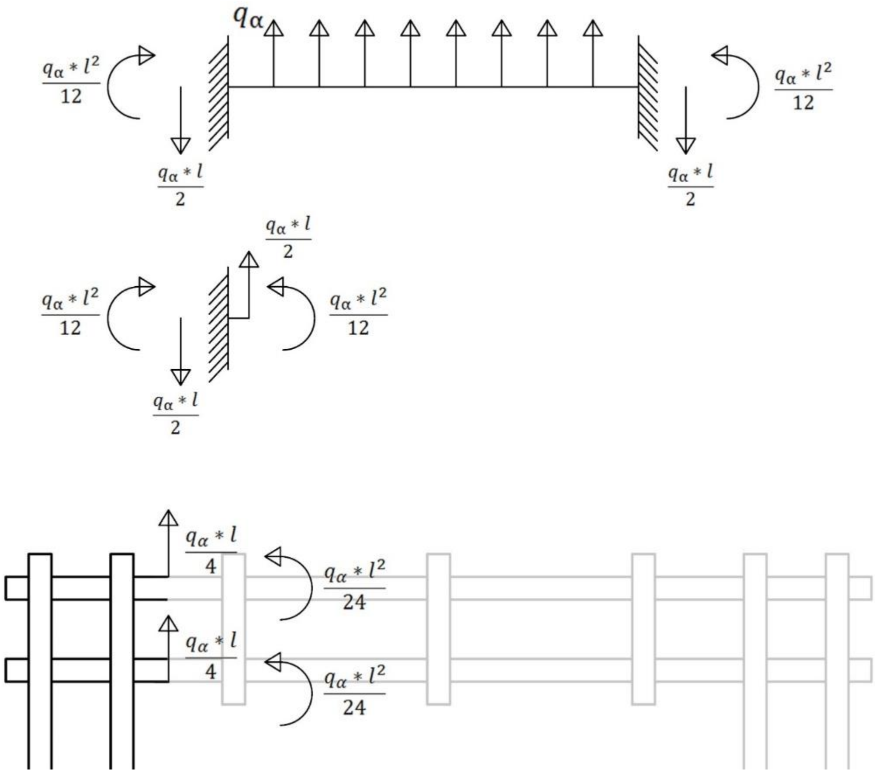

Figure 10-31 Bending behavior - Rigid- jointed frame reactions for each beam - Resisting rafters R

Table 64 Bending behavior - Rigid- jointed frame reactions for each beam - Resisting rafters R

		Shear force [kN]		Bending Moment [kNm]		
		end left	end right	end left	midpoint	end right
Beam	q(α)j with α=1 [kN/m]	q(α)*(l)/4	q(α)*(l)/4	q(α)*(l^2)/24	q(α)*(l^2)/48	q(α)*(l^2)/24
1	23,71	-16,48	16,48	7,64	-3,82	7,64
2	5,36	-3,73	3,73	1,73	-0,86	1,73
3	5,51	-3,83	3,83	1,78	-0,89	1,78
4	3,99	-2,78	2,78	1,29	-0,64	1,29
5	2,47	-1,72	1,72	0,80	-0,40	0,80
6	0,81	-0,56	0,56	0,26	-0,13	0,26

10.4.3 T1 in compression & T2 in tension

In the flexible configuration the external Rafter T1 is in compression, T1 = -(Mc/d) and T2 = Tc+Mc/d .

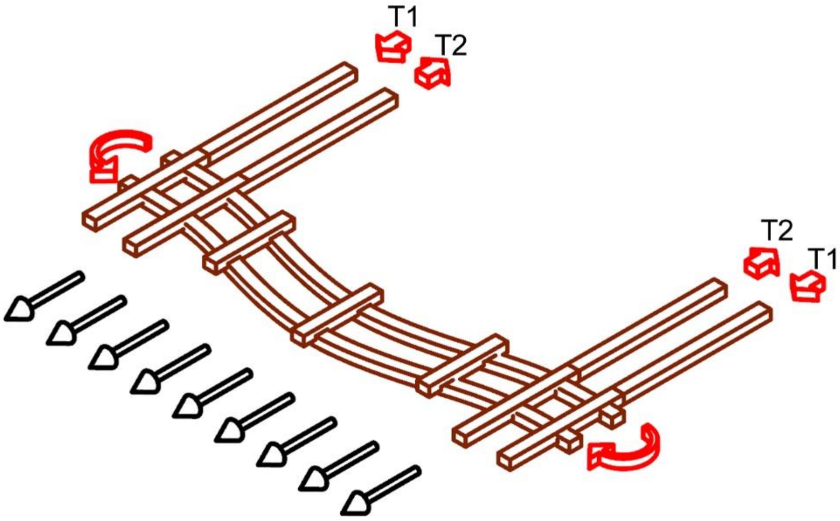

Figure 10-32 Bending behavior - Distribution of the forces on the rafters

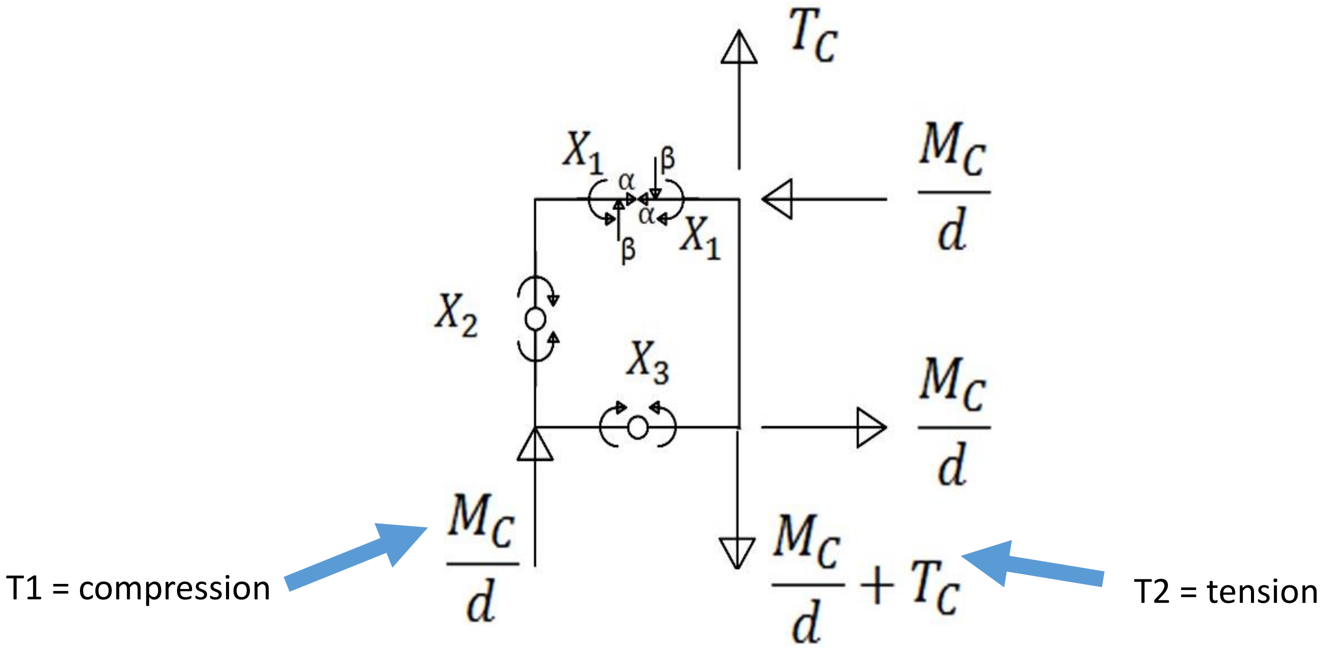

Figure 10-33 Bending behavior - Distribution of the forces on the rafters- corner joint

$$T_C = \frac{139}{100} * q_\alpha \ [N]$$

$$M_C = \frac{19321}{30000} * q_\alpha \ [Nm]$$

$$X_1 = 6.87 * 10^{-3} * q_\alpha \ [Nm]$$
$$X_2 = 2.95 * 10^{-2} * q_\alpha \ [Nm]$$
$$X_3 = 4.12 * 10^{-2} * q_\alpha \ [Nm]$$

In the flexible configuration the external Rafter T1 is in compression, T1 = -(Mc/d) and T2 = Tc+Mc/d .

Table 65 Bending behavior - External rafter T1 - compression

Rafter body T1		
Beam	q(α)j with α=1 [kN/m]	-Mc/d [kN/]
1	23,71	-42,42
2	5,36	-9,60
3	5,51	-9,87
4	3,99	-7,14
5	2,47	-4,42
6	0,81	-1,44

Table 66 Bending behavior - Internal rafter T2 - tension

Rafter body T2		
Beam	q(α)j with α=1 [kN/m]	Mc/d+Tc [kN]
1	23,71	75,38
2	5,36	17,05
3	5,51	17,53
4	3,99	12,69
5	2,47	7,86
6	0,81	2,57

10.5 Verifications for Flexible response – Bendingbehavior

10.5.1 Analyzing the worst case : Roof level with maximum Seismic load $q\alpha$ (α=1)

In the sub-chapter "10.3.3 Seismic load q_{α} and Distribution factor β_j" they have been computed the maximum distribution factor and seismic load which belong to the beam 1 , the one at the roof level.

All the beam bands are geometrically equal,thus the satisfied verifications on the most stressed beam ensure that the verification on the other beam bands subjected to smaller actions are satisfied as well.

The analysis have been made considering a seismic direction parallel to the roof rafter as well in the perpendicular direction in respect to the roof rafter.

10.5.2 Distribution of the reactions T1≠T2 and R1=R2

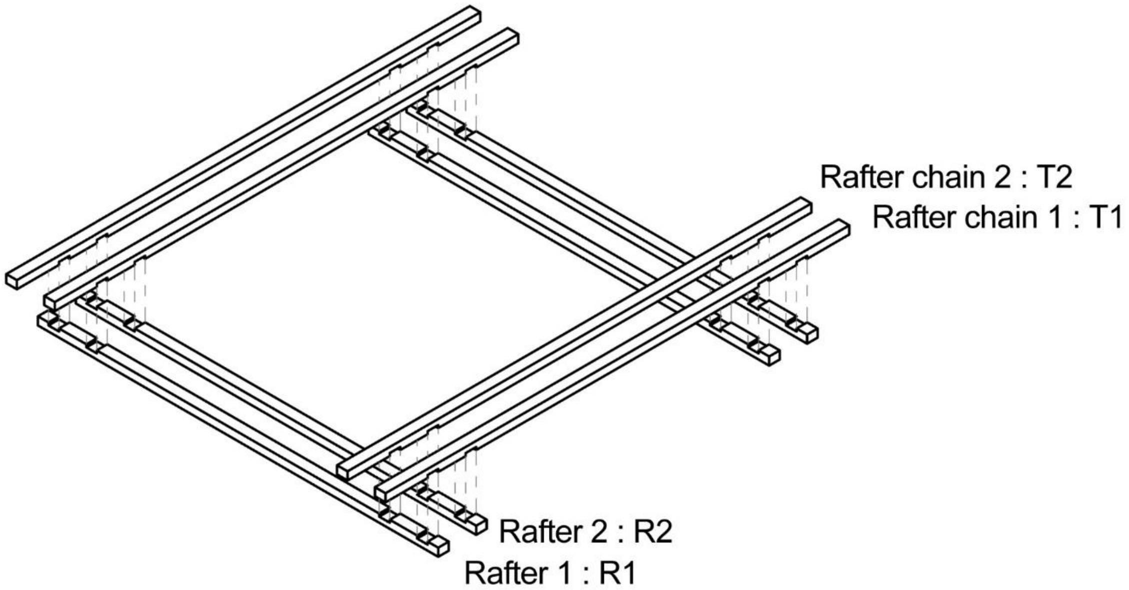

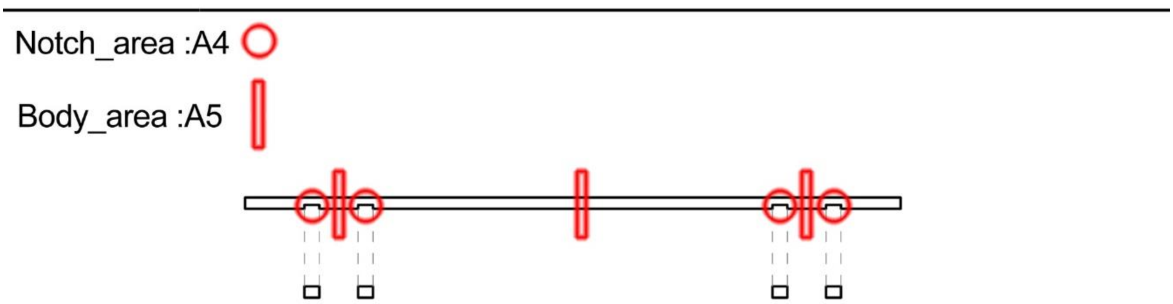

Thebehavior of the rafters chain 1 and 2 is different, thus the verifications on T1 and T2 have been performed separately. Thebehavior of rafters belonging to the bending wall is the same thus the verifications on R1 is equal to R2. The verifications have been performed on the biggest section of the rafters, the body, which refers to a section of area equal to A5. The same verifications have been performed considering the smallest section, the notch, of area equal to A4.

It has been reported the table Tab 51 Geometric dimensions for Notch and Body Areas:

	b	h	AREA net		
	mm	mm	mm^2	cm^2	m^2
A4	100	50	5000	50	0,005

	b	h	AREA net		
	mm	mm	mm^2	cm^2	m^2
A5	100	75	7500	75	0,0075

All the verifications have been done considering the highest load multiplier, thus α=1 .In the cases where the verification is not satisfied the load multiplier has been reduced until the verification was verified.

10.5.3 Verifications T1 - compression

10.5.3.1 Body

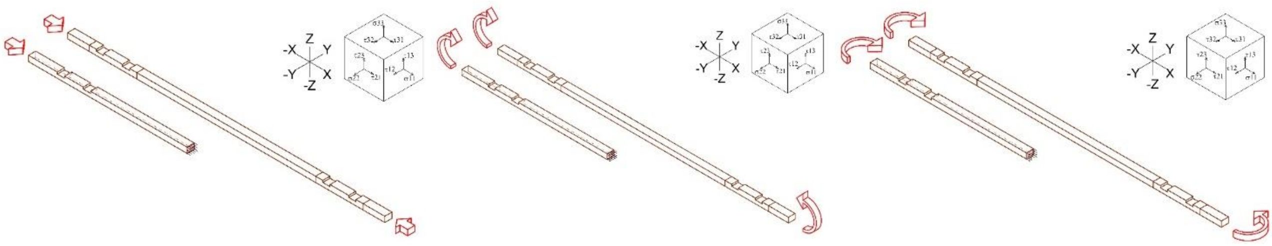

RB0comp		
N_0d	42421,64	N
b	100,00	mm
h	75,00	mm
A_(net)	7500,00	mm
σ_(c,0,d)	5,66	N/mm^2
f_(c,0,d)	24,93	N/mm^2
Verification	VERIFIED	
N_(0d)max	187,00	kN

RB0mY		
M_(y,d)	1612022,38	Nmm
K_m	0,70	
b	100,00	mm
h	75,00	mm
W_(y,d)	93750,00	mm^3
σ_(m,y,d)	17,19	N/mm^2
kh	1,15	
f_(m,d)	51,33	N/mm^2
f_(m,y,d)	58,97	N/mm^2
Verification	VERIFIED	
M_(y,d)max	5528110,83	Nmm
M_(y,d)max	5,53	kNm

RB0mZ		
M_(z,d)	0,00	Nmm
K_m	0,70	
b	100,00	mm
h	75,00	mm
W_(z,d)	125000,00	mm^3
σ_(m,z,d)	0,00	N/mm^2
kh	1,08	
f_(m,d)	51,33	N/mm^2
f_(m,z,d)	55,67	N/mm^2
Verification	VERIFIED	
M_(z,d)max	6958693,87	Nmm
M_(z,d)max	6,96	kNm

10.5.3.2 Body Combinations

Combined bending and axial compression

$$\left(\frac{\sigma_{c,0,d}}{f_{c,0,d}}\right)^2 + \frac{\sigma_{m,y,d}}{f_{m,y,d}} + k_m * \frac{\sigma_{m,z,d}}{f_{m,z,d}} \leq 1$$

$$\left(\frac{\sigma_{c,0,d}}{f_{c,0,d}}\right)^2 + k_m * \frac{\sigma_{m,y,d}}{f_{m,y,d}} + \frac{\sigma_{m,z,d}}{f_{m,z,d}} \leq 1$$

For solid timber, glued laminated timber and LVL:

- for rectangular sections: km = 0,7
- otherwise km = 1

Combination of RB0comp and RB0mY are satisfied for a load multiplier α = 1

Combination of RB0comp and RB0mZ are satisfied for a load multiplier α = 1

10.5.3.3 Notch

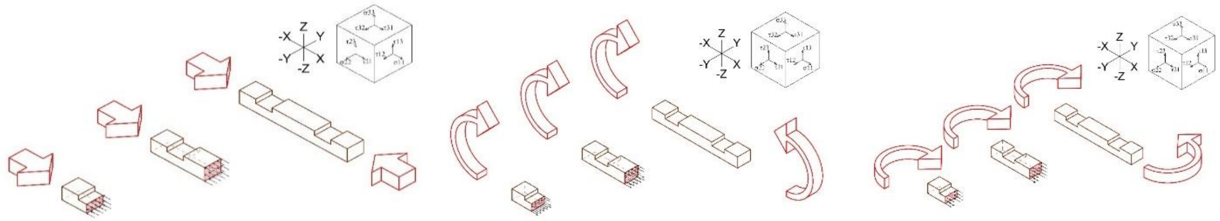

CPNotch0comp		
N_0d	42421,64	N
b	100,00	mm
h	50,00	mm
A_(net)	5000,00	mm^2
σ_(c,0,d)	8,48	N/mm^2
f_(c,0,d)	24,93	N/mm^2
Verification	VERIFIED	
N_(0d)max	124,67	kN

CPNotch0mY		
M_(y,d)	1612022,38	Nmm
K_m	0,70	
b	100,00	mm
h	50,00	mm
W_(y,d)	41666,67	mm^3
σ_(m,y,d)	38,69	N/mm^2
kh	1,25	
f_(m,d)	51,33	N/mm^2
f_(m,y,d)	63,95	N/mm^2
Verification	VERIFIED	
M_(y,d)max	2664480,07	Nmm
M_(y,d)max	2,66	kNm

CPNotch0mZ		
M_(z,d)	0,00	Nmm
K_m	0,70	
b	100,00	mm
h	50,00	mm
W_(z,d)	83333,33	mm^3
σ_(m,z,d)	0,00	N/mm^2
kh	1,08	
f_(m,d)	51,33	N/mm^2
f_(m,z,d)	55,67	N/mm^2
Verification	VERIFIED	
M_(z,d)max	4639129,24	Nmm
M_(z,d)max	4,64	kNm

10.5.3.4 Notch Combinations

Combined bending and axial compression

$$\left(\frac{\sigma_{c,0,d}}{f_{c,0,d}}\right)^2 + \frac{\sigma_{m,y,d}}{f_{m,y,d}} + k_m * \frac{\sigma_{m,z,d}}{f_{m,z,d}} \leq 1$$

$$\left(\frac{\sigma_{c,0,d}}{f_{c,0,d}}\right)^2 + k_m * \frac{\sigma_{m,y,d}}{f_{m,y,d}} + \frac{\sigma_{m,z,d}}{f_{m,z,d}} \leq 1$$

For solid timber, glued laminated timber and LVL:

- for rectangular sections: km = 0,7
- otherwise km = 1

Combination of CPNotch0comp and CPNotch0mY are satisfied for a load multiplier α = 1

Combination of CPNotch0comp and CPNotch0mZ are satisfied for a load multiplier α = 1

10.5.4 Verifications T2 - tension

10.5.4.1 Body

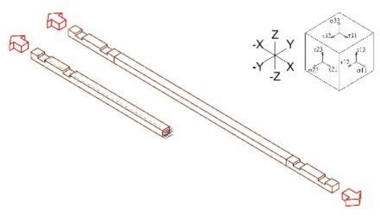
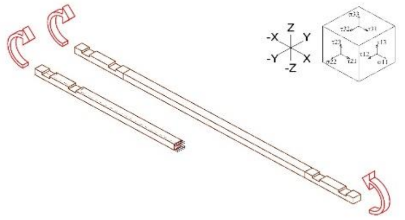
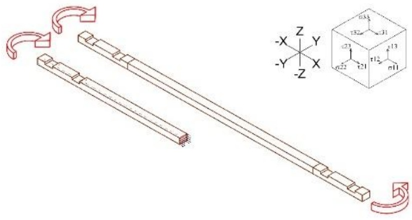

RB0tens		
N_0d	75382,34	N
b	100,00	mm
h	75,00	mm
A_(net)	7500,00	mm
σ_(t,0,d)	10,05	N/mm^2
kh	1,08	
f_(t,0,d)	30,80	N/mm^2
Verification	VERIFIED	
N_(0d)max	231,00	kN

Influence of keyed scarf joint		
Verification	NOT VERIFIED	
N_(0d)max	25,41	kN

RB0mY		
M_(y,d)	2864528,98	Nmm
K_m	0,70	
b	100,00	mm
h	75,00	mm
W_(y,d)	93750,00	mm^3
σ_(m,y,d)	30,55	N/mm^2
kh	1,15	
f_(m,d)	51,33	N/mm^2
f_(m,y,d)	58,97	N/mm^2
Verification	VERIFIED	
M_(y,d)max	5528110,83	Nmm
M_(y,d)max	5,53	kNm

RB0mZ		
M_(z,d)	0,00	Nmm
K_m	0,70	
b	100,00	mm
h	75,00	mm
W_(z,d)	125000,00	mm^3
σ_(m,z,d)	0,00	N/mm^2
kh	1,08	
f_(m,d)	51,33	N/mm^2
f_(m,z,d)	55,67	N/mm^2
Verification	VERIFIED	
M_(z,d)max	6958693,87	Nmm
M_(z,d)max	6,96	kNm

The verification about "Influence of keyed scarf joint" is satisfied for a load multiplier α = 0.3.

10.5.4.2 Body Combinations

Combined bending and axial tension

$$\frac{\sigma_{t,0,d}}{f_{t,0,d}} + \frac{\sigma_{m,y,d}}{f_{m,y,d}} + k_m * \frac{\sigma_{m,z,d}}{f_{m,z,d}} \leq 1$$

$$\frac{\sigma_{t,0,d}}{f_{t,0,d}} + k_m * \frac{\sigma_{m,y,d}}{f_{m,y,d}} + \frac{\sigma_{m,z,d}}{f_{m,z,d}} \leq 1$$

For solid timber, glued laminated timber and LVL:

- for rectangular sections: km = 0,7
- otherwise km = 1

Combination of RB0tens and RB0mY are satisfied for a load multiplier α = 1

Combination of RB0tens and RB0mZ are satisfied for a load multiplier α = 1

10.5.4.3 Notch

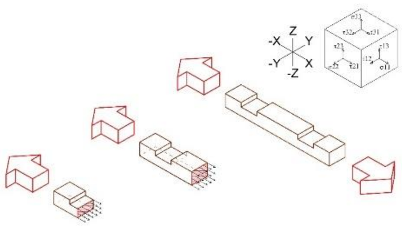
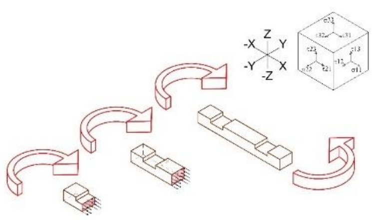
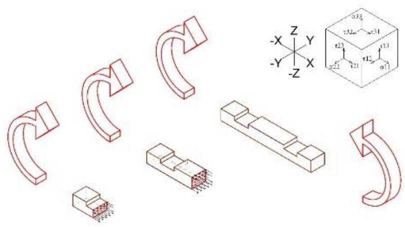

CPNotch0tens		
N_0d	75382,34	N
b	100,00	mm
h	50,00	mm
A_(net)	5000,00	mm^2
σ_(t,0,d)	15,08	N/mm^2
kh	1,08	
f_(t,0,d)	30,80	N/mm^2
Verification	VERIFIED	
N_(0d)max	154,00	kN

CPNotch0mY		
M_(y,d)	2864528,98	Nmm
K_m	0,70	
b	100,00	mm
h	50,00	mm
W_(y,d)	41666,67	mm^3
σ_(m,y,d)	68,75	N/mm^2
kh	1,25	
f_(m,d)	51,33	N/mm^2
f_(m,y,d)	63,95	N/mm^2
Verification	NOT VERIFIED	
M_(y,d)max	2664480,07	Nmm
M_(y,d)max	2,66	kNm

CPNotch0mZ		
M_(z,d)	0,00	Nmm
K_m	0,70	
b	100,00	mm
h	50,00	mm
W_(z,d)	83333,33	mm^3
σ_(m,z,d)	0,00	N/mm^2
kh	1,08	
f_(m,d)	51,33	N/mm^2
f_(m,z,d)	55,67	N/mm^2
Verification	VERIFIED	
M_(z,d)max	4639129,24	Nmm
M_(z,d)max	4,64	kNm

CPNotch0mY is satisfied for a load multiplier α = 0.9

10.5.4.4 Notch Combinations

Combined bending and axial tension

$$\frac{\sigma_{t,0,d}}{f_{t,0,d}} + \frac{\sigma_{m,y,d}}{f_{m,y,d}} + k_m * \frac{\sigma_{m,z,d}}{f_{m,z,d}} \leq 1$$

$$\frac{\sigma_{t,0,d}}{f_{t,0,d}} + k_m * \frac{\sigma_{m,y,d}}{f_{m,y,d}} + \frac{\sigma_{m,z,d}}{f_{m,z,d}} \leq 1$$

For solid timber, glued laminated timber and LVL:

- for rectangular sections: km = 0,7
- otherwise km = 1

Combination of CPNotch0tens and CPNotch0mY are satisfied for a load multiplier α = 0.9

Combination of CPNotch0tens and CPNotch0mZ are satisfied for a load multiplier α = 0.9

10.5.5 Verifications R1=R2

10.5.5.1 Body ends

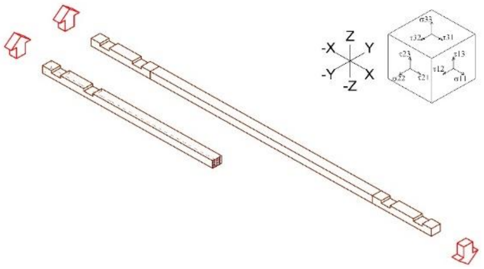

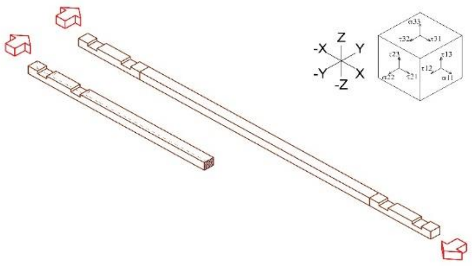

RB0shearZ with bending		
V_zd	0,00	N
K_cr	0,67	
A_(net)	5025,00	mm
τ_(d)	0,00	N/mm^2
f_(v,d)	3,67	N/mm^2
Verification	VERIFIED	
V_zd max	12,28	kN

RB0shearY with bending		
V_yd	16480,35	N
K_cr	0,67	
A_(net)	5025,00	mm
τ_(d)	4,92	N/mm^2
f_(v,d)	3,67	N/mm^2
Verification	NOT VERIFIED	
V_yd max	12,28	kN

RB0shearZ		
V_zd	0,00	N
A_(net)	7500,00	mm
τ_(d)	0,00	N/mm^2
f_(v,d)	3,67	N/mm^2
Verification	VERIFIED	
V_zd max	18,33	kN

RB0shearY		
V_yd	16480,35	N
A_(net)	7500,00	mm
τ_(d)	3,30	N/mm^2
f_(v,d)	3,67	N/mm^2
Verification	VERIFIED	
V_yd max	18,33	kN

RB0shearY with bending is satisfied for a load multiplier α = 0.7

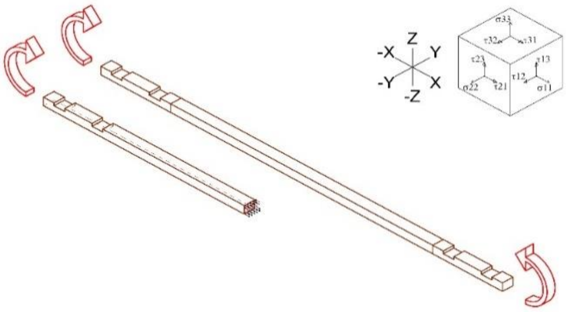

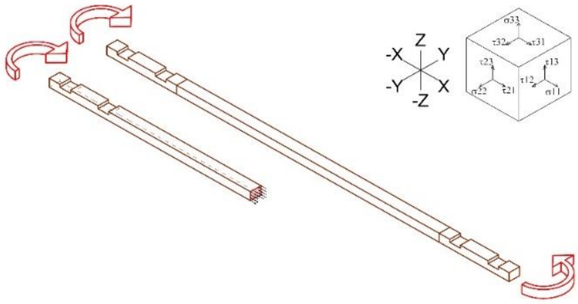

RB0mY		
M_(y,d)	7635895,48	Nmm
K_m	0,70	
b	100,00	mm
h	75,00	mm
W_(y,d)	93750,00	mm^3
σ_(m,y,d)	81,45	N/mm^2
kh	1,15	
f_(m,d)	51,33	N/mm^2
f_(m,y,d)	58,97	N/mm^2
Verification	NOT VERIFIED	
M_(y,d)max	5528110,83	Nmm
M_(y,d)max	5,53	kNm

RB0mZ		
M_(z,d)	0,00	Nmm
K_m	0,70	
b	100,00	mm
h	75,00	mm
W_(z,d)	125000,00	mm^3
σ_(m,z,d)	0,00	N/mm^2
kh	1,08	
f_(m,d)	51,33	N/mm^2
f_(m,z,d)	55,67	N/mm^2
Verification	VERIFIED	
M_(z,d)max	6958693,87	Nmm
M_(z,d)max	6,96	kNm

RB0mY with bending is satisfied for a load multiplier α = 0.7

10.5.5.2 Body midspan

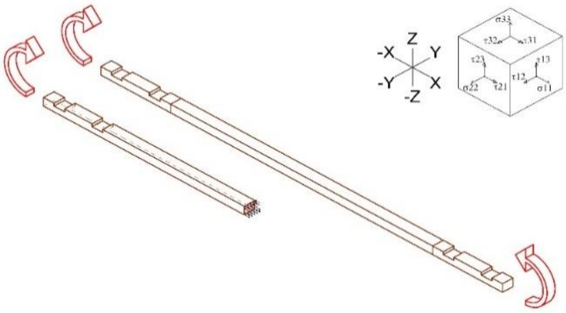

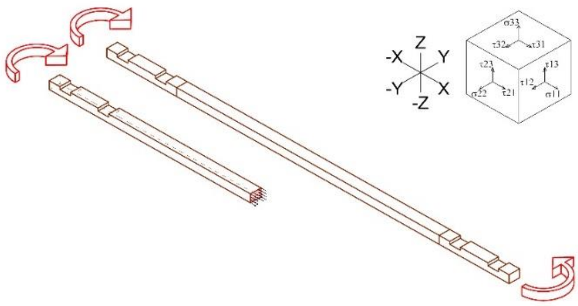

RB0mY		
M_(y,d)	3817947,74	Nmm
K_m	0,70	
b	100,00	mm
h	75,00	mm
W_(y,d)	93750,00	mm^3
σ_(m,y,d)	40,72	N/mm^2
kh	1,15	
f_(m,d)	51,33	N/mm^2
f_(m,y,d)	58,97	N/mm^2
Verification	VERIFIED	
M_(y,d)max	5528110,83	Nmm
M_(y,d)max	5,53	kNm

RB0mZ		
M_(z,d)	0,00	Nmm
K_m	0,70	
b	100,00	mm
h	75,00	mm
W_(z,d)	125000,00	mm^3
σ_(m,z,d)	0,00	N/mm^2
kh	1,08	
f_(m,d)	51,33	N/mm^2
f_(m,z,d)	55,67	N/mm^2
Verification	VERIFIED	
M_(z,d)max	6958693,87	Nmm
M_(z,d)max	6,96	kNm

10.5.5.3 Notch ends

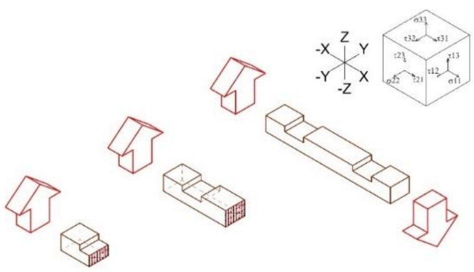

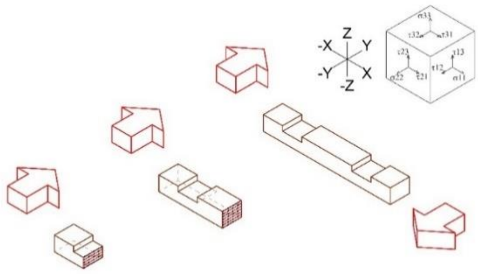

CPNotch0shearZ with bending		
V_zd	0,00	N
K_cr	0,67	
A_(net)	3350,00	mm^2
τ_(d)	0,00	N/mm^2
f_(v,d)	3,67	N/mm^2
Verification	VERIFIED	
V_zd max	8,19	kN

CPNotch0shearY with bending		
V_yd	16480,35	N
K_cr	0,67	
A_(net)	3350,00	mm^2
τ_(d)	7,38	N/mm^2
f_(v,d)	3,67	N/mm^2
Verification	NOT VERIFIED	
V_yd max	8,19	kN

CPNotch0shearZ		
V_zd	0,00	N
A_(net)	5000,00	mm
τ_(d)	0,00	N/mm^2
f_(v,d)	3,67	N/mm^2
Verification	VERIFIED	
V_zd max	12,22	kN

CPNotch0shearY		
V_yd	16480,35	N
A_(net)	5000,00	mm
τ_(d)	4,94	N/mm^2
f_(v,d)	3,67	N/mm^2
Verification	NOT VERIFIED	
V_yd max	12,22	kN

CPNotch0shearY with bending is satisfied for a load multiplier $\alpha = 0.4$

CPNotch0shearY is satisfied for a load multiplier $\alpha = 0.7$

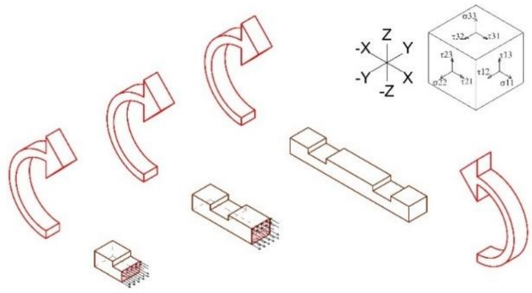

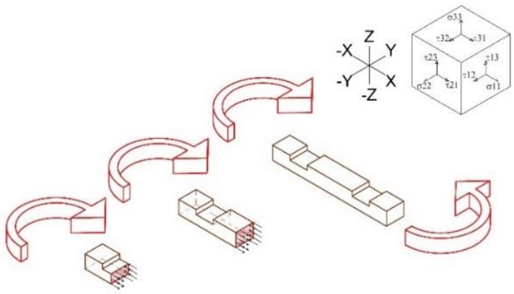

CPNotch0mY		
M_(y,d)	7635895,48	Nmm
K_m	0,70	
b	100,00	mm
h	50,00	mm
W_(y,d)	41666,67	mm^3
σ_(m,y,d)	183,26	N/mm^2
kh	1,25	
f_(m,d)	51,33	N/mm^2
f_(m,y,d)	63,95	N/mm^2
Verification	NOT VERIFIED	
M_(y,d)max	2664480,07	Nmm
M_(y,d)max	2,66	kNm

CPNotch0mZ		
M_(z,d)	0,00	Nmm
K_m	0,70	
b	100,00	mm
h	50,00	mm
W_(z,d)	83333,33	mm^3
σ_(m,z,d)	0,00	N/mm^2
kh	1,08	
f_(m,d)	51,33	N/mm^2
f_(m,z,d)	55,67	N/mm^2
Verification	VERIFIED	
M_(z,d)max	4639129,24	Nmm
M_(z,d)max	4,64	kNm

CPNotch0mY is satisfied for a load multiplier $\alpha = 0.3$

10.5.6 Verifications on corner joint, seismic event parallel to Roof Rafter

The verifications on the corner joint have been computed appling the actions resulted by the analysis of the scheme of the rigid frame solved in the sub-chapter 10.2.2.

All the verified sections have been defined in the previous chapters.

10.5.6.1 Scheme

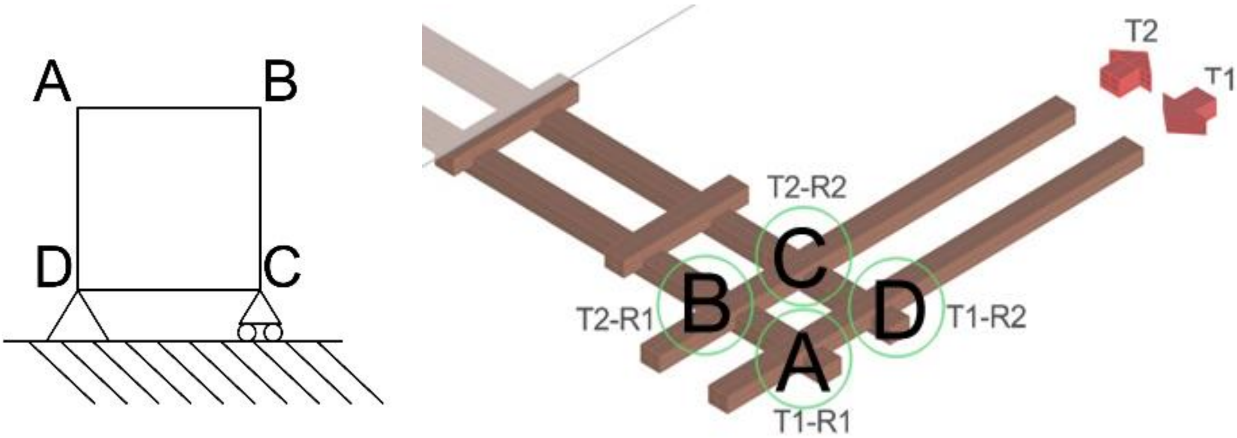

Figure 10-34 Rigid-Jointed Frame - names of the corners- scheme

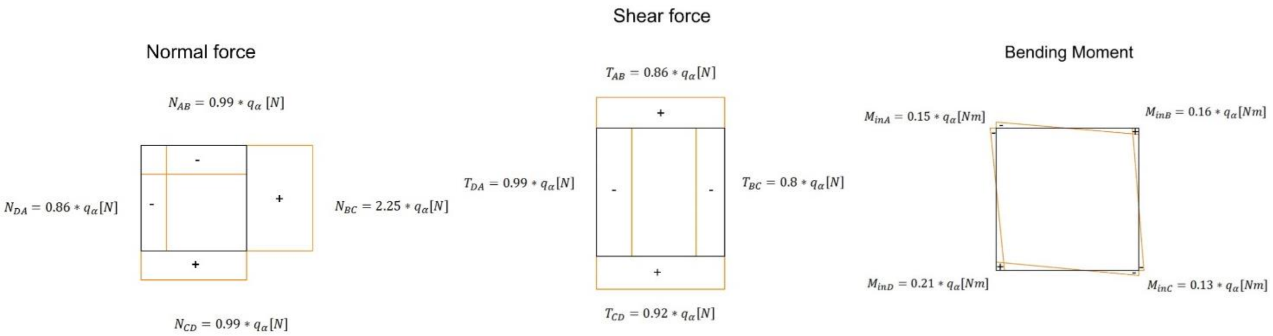

Table 67 Flexible behavior - Rafter body reactions for each beam - Verifications

		Nab/q(α)j	Nbc /q(α)j	Ncd /q(α)j	Nda /q(α)j	Tab /q(α)j	Tbc /q(α)j	Tcd /q(α)j	Tda /q(α)j	BM in A /q(α)j	BM in B /q(α)j	BM in C /q(α)j	BM in D /q(α)j
α	1,00	0,99	2,25	0,99	0,86	0,86	0,80	0,92	0,99	0,15	0,16	0,13	0,21
		Normal force				Shear force				Bending Moment			
Beam	q(α)j with α=1 [kN/m]	Nab [kN]	Nbc [kN]	Ncd [kN]	Nda [kN]	Tab [kN]	Tbc [kN]	Tcd [kN]	Tda [kN]	BM in A [kNm]	BM in B [kNm]	BM in C [kNm]	BM in D [kNm]
1	23,71	23,47	53,46	23,47	20,50	20,50	18,95	21,92	23,47	3,53	3,85	2,97	4,92
2	5,36	5,31	12,09	5,31	4,64	4,64	4,29	4,96	5,31	0,80	0,87	0,67	1,11
3	5,51	5,46	12,43	5,46	4,77	4,77	4,41	5,10	5,46	0,82	0,90	0,69	1,15
4	3,99	3,95	9,00	3,95	3,45	3,45	3,19	3,69	3,95	0,59	0,65	0,50	0,83
5	2,47	2,45	5,57	2,45	2,14	2,14	1,98	2,29	2,45	0,37	0,40	0,31	0,51
6	0,81	0,80	1,82	0,80	0,70	0,70	0,64	0,75	0,80	0,12	0,13	0,10	0,17

The table 56 and table 61 differ only for the sign, this because the verifications are specifically for cases of tension or compression.

10.5.6.2 Axial stresses : Compression and Tension

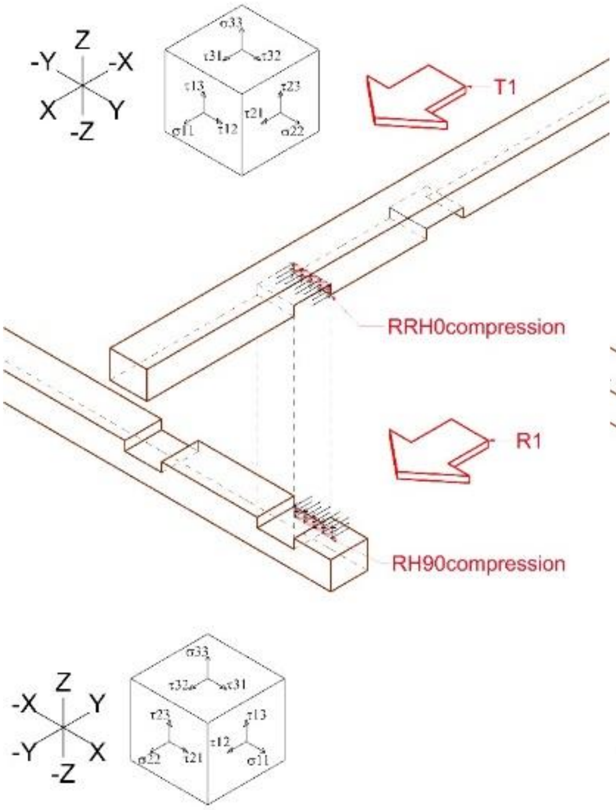

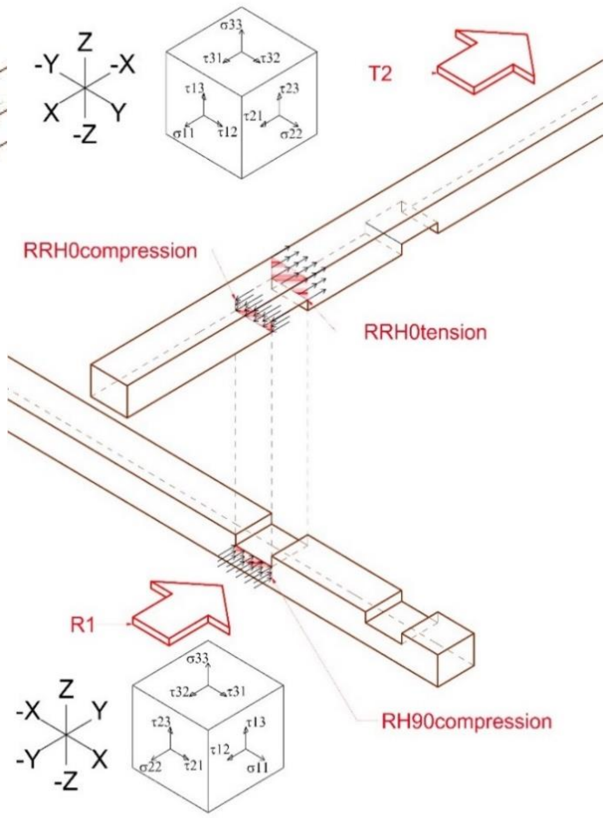

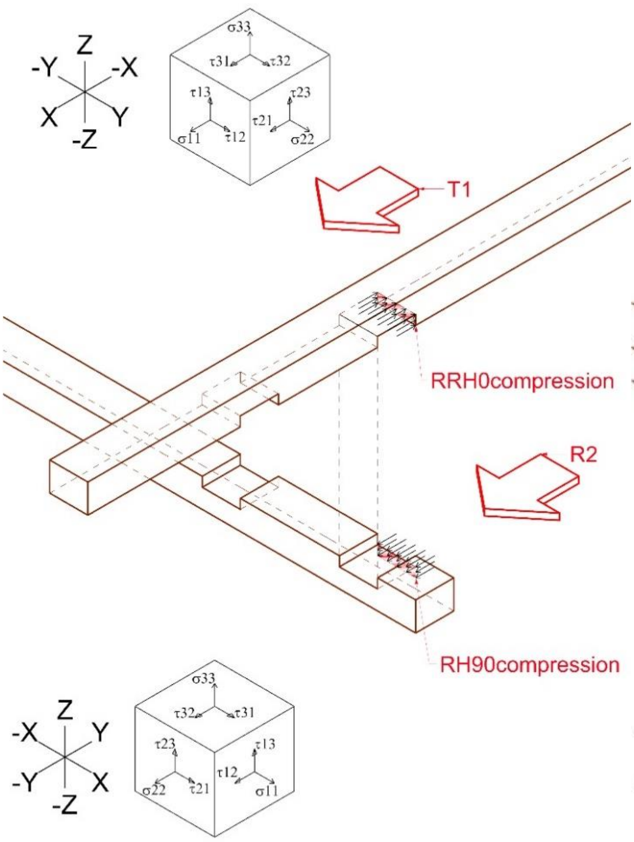

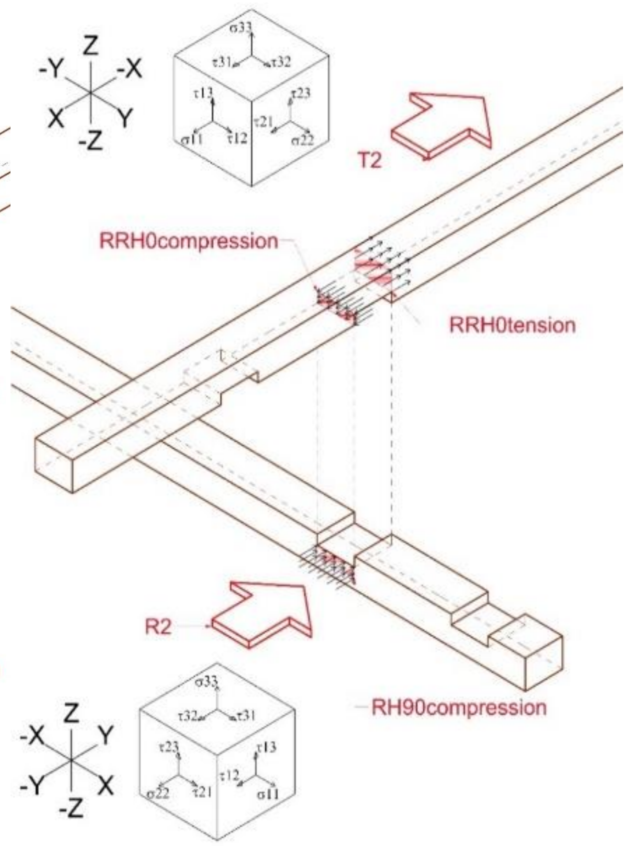

Nab [kN]
23,47

RRH0compression	A3	
N_0d	23475,00	N
b	100,00	mm
h	25,00	mm
A_(net)	2500,00	mm^2
σ_(c,0,d)	9,39	N/mm^2
f_(c,0,d)	24,93	N/mm^2
Verification	VERIFIED	
N_(od)max	62,33	kN

RRH0tension	A4	
N_0d	23475,00	N
b	100,00	mm
h	50,00	mm
A_(net)	5000,00	mm^2
σ_(t,0,d)	4,69	N/mm^2
kh	1,08	
f_(t,0,d)	30,80	N/mm^2
Verification	VERIFIED	
N_(od)max	154,00	kN

Nbc [kN]
53,46

RRH0compression	A3	
N_0d	53458,21	N
b	100,00	mm
h	25,00	mm
A_(net)	2500,00	mm^2
σ_(c,0,d)	21,38	N/mm^2
f_(c,0,d)	24,93	N/mm^2
Verification	VERIFIED	
N_(od)max	62,33	kN

RRH0tension	A4	
N_0d	53458,21	N
b	100,00	mm
h	50,00	mm
A_(net)	5000,00	mm^2
σ_(t,0,d)	10,69	N/mm^2
kh	1,08	
f_(t,0,d)	30,80	N/mm^2
Verification	VERIFIED	
N_(od)max	154,00	kN

Ncd [kN]
23,47

RRH0compression	A3	
N_0d	23475,00	N
b	100,00	mm
h	25,00	mm
A_(net)	2500,00	mm^2
σ_(c,0,d)	9,39	N/mm^2
f_(c,0,d)	24,93	N/mm^2
Verification	VERIFIED	
N_(od)max	62,33	kN

RRH0tension	A4	
N_0d	23475,00	N
b	100,00	mm
h	50,00	mm
A_(net)	5000,00	mm^2
σ_(t,0,d)	4,69	N/mm^2
kh	1,08	
f_(t,0,d)	30,80	N/mm^2
Verification	VERIFIED	
N_(od)max	154,00	kN

Nda [kN]
20,50

RRH0compression	A3	
N_0d	20497,51	N
b	100,00	mm
h	25,00	mm
A_(net)	2500,00	mm^2
σ_(c,0,d)	8,20	N/mm^2
f_(c,0,d)	24,93	N/mm^2
Verification	VERIFIED	
N_(od)max	62,33	kN

RRH0tension	A4	
N_0d	20497,51	N
b	100,00	mm
h	50,00	mm
A_(net)	5000,00	mm^2
σ_(t,0,d)	4,10	N/mm^2
kh	1,08	
f_(t,0,d)	30,80	N/mm^2
Verification	VERIFIED	
N_(od)max	154,00	kN

Tab [kN]
20,50

RH90compression	A3	
N_90d	20497,51	N
b	100,00	mm
h	25,00	mm
A_(net)	2500,00	mm^2
σ_(c,90,d)	8,20	N/mm^2
k_(c,90)	1,50	
f_(c,90,d)	9,90	N/mm^2
Verification	VERIFIED	
N_(90d)max	16,50	kN

Tbc [kN]
18,95

RH90compression	A3	
N_90d	18946,64	N
b	100,00	mm
h	25,00	mm
A_(net)	2500,00	mm^2
σ_(c,90,d)	7,58	N/mm^2
k_(c,90)	1,50	
f_(c,90,d)	9,90	N/mm^2
Verification	VERIFIED	
N_(90d)max	16,50	kN

Tcd [kN]
21,92

RH90compression	A3	
N_90d	21924,13	N
b	100,00	mm
h	25,00	mm
A_(net)	2500,00	mm^2
σ_(c,90,d)	8,77	N/mm^2
k_(c,90)	1,50	
f_(c,90,d)	9,90	N/mm^2
Verification	VERIFIED	
N_(90d)max	16,50	kN

Tda [kN]
23,47

RH90compression	A3	
N_90d	23475,00	N
b	100,00	mm
h	25,00	mm
A_(net)	2500,00	mm^2
σ_(c,90,d)	9,39	N/mm^2
k_(c,90)	1,50	
f_(c,90,d)	9,90	N/mm^2
Verification	VERIFIED	
N_(90d)max	16,50	kN

10.5.6.3 Tangential stresses : Shear

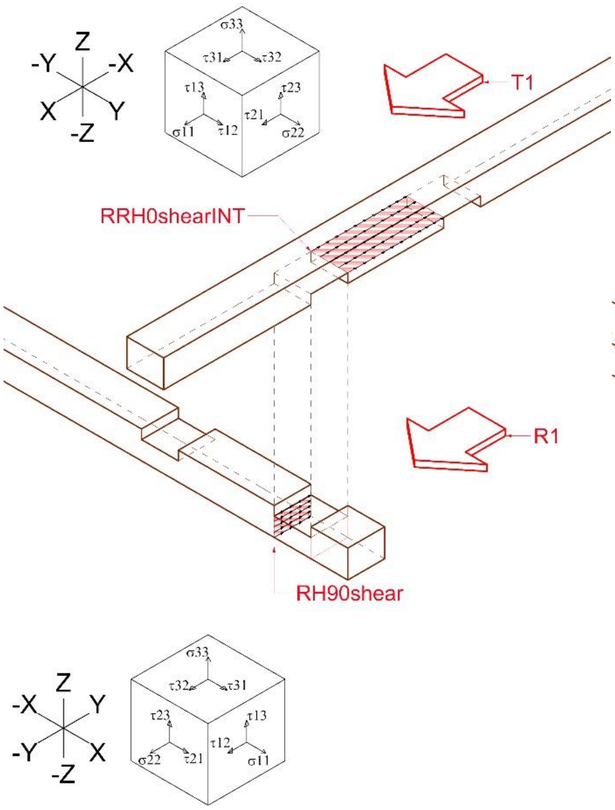

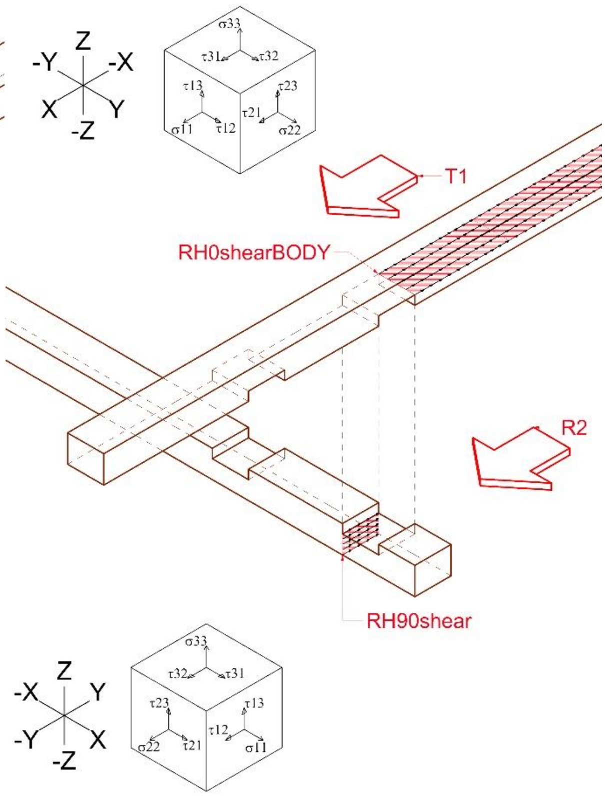

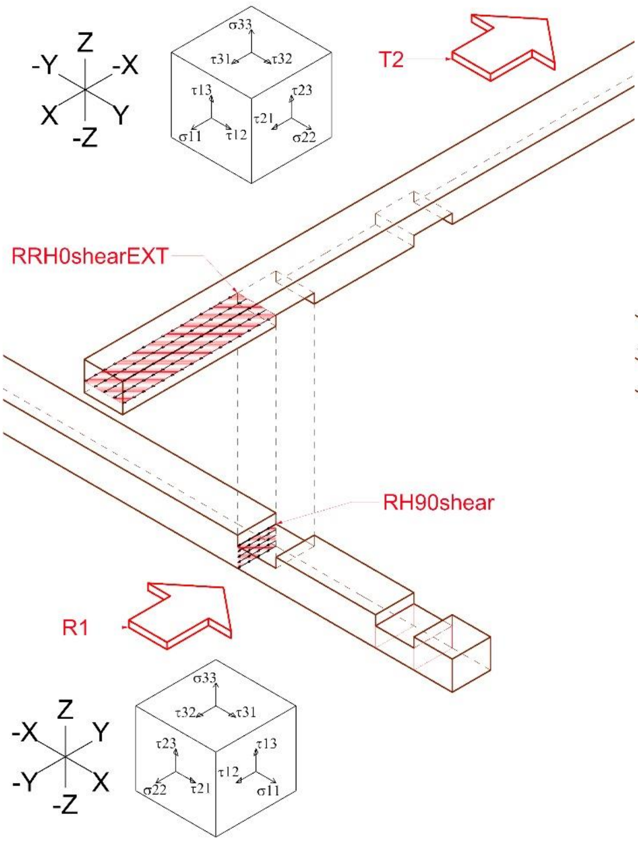

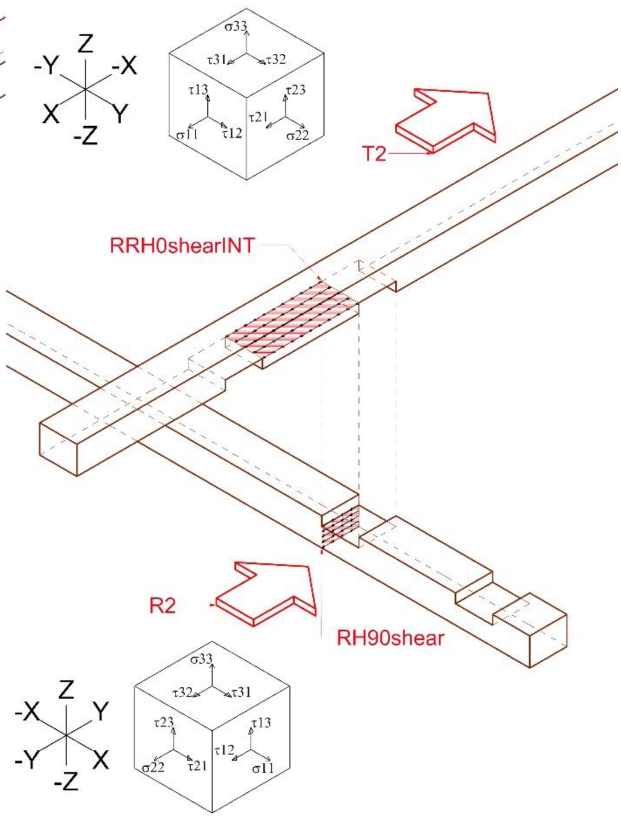

Nab [kN]	Nbc [kN]	Ncd [kN]	Nda [kN]
23,47	53,46	23,47	20,50

RRH0shearEXT	A7		RRH0shearEXT	A7		RRH0shearEXT	A7		RRH0shearEXT	A7	
with bending			with bending			with bending			with bending		
V_0d	23475,00	N	V_0d	53458,21	N	V_0d	23475,00	N	V_0d	20497,51	N
K_cr	0,67		K_cr	0,67		K_cr	0,67		K_cr	0,67	
A_(net)	26800,00	mm^2	A_(net)	26800,00	mm^2	A_(net)	26800,00	mm^2	A_(net)	26800,00	mm^2
τ_(d)	1,31	N/mm^2	τ_(d)	2,99	N/mm^2	τ_(d)	1,31	N/mm^2	τ_(d)	1,15	N/mm^2
f_(v,d)	3,67	N/mm^2	f_(v,d)	3,67	N/mm^2	f_(v,d)	3,67	N/mm^2	f_(v,d)	3,67	N/mm^2
Verification	VERIFIED		Verification	VERIFIED		Verification	VERIFIED		Verification	VERIFIED	
V_0d max	65,51	kN	V_0d max	65,51	kN	V_0d max	65,51	kN	V_0d max	65,51	kN

RRH0shearINT	A1		RRH0shearINT	A1		RRH0shearINT	A1		RRH0shearINT	A1	
with bending			with bending			with bending			with bending		
V_0d	23475,00	N	V_0d	53458,21	N	V_0d	23475,00	N	V_0d	20497,51	N
K_cr	0,67		K_cr	0,67		K_cr	0,67		K_cr	0,67	
A_(net)	17420,00	mm^2	A_(net)	17420,00	mm^2	A_(net)	17420,00	mm^2	A_(net)	17420,00	mm^2
τ_(d)	2,02	N/mm^2	τ_(d)	4,60	N/mm^2	τ_(d)	2,02	N/mm^2	τ_(d)	1,76	N/mm^2
f_(v,d)	3,67	N/mm^2	f_(v,d)	3,67	N/mm^2	f_(v,d)	3,67	N/mm^2	f_(v,d)	3,67	N/mm^2
Verification	VERIFIED		Verification	NOT VERIFIED		Verification	VERIFIED		Verification	VERIFIED	
V_0d max	42,58	kN	V_0d max	42,58	kN	V_0d max	42,58	kN	V_0d max	42,58	kN

RH0shearBODY	A6		RH0shearBODY	A6		RH0shearBODY	A6		RH0shearBODY	A6	
with bending			with bending			with bending			with bending		
V_0d	23475,00	N	V_0d	53458,21	N	V_0d	23475,00	N	V_0d	20497,51	N
K_cr	0,67		K_cr	0,67		K_cr	0,67		K_cr	0,67	
A_(net)	179560,00	mm^2	A_(net)	179560,00	mm^2	A_(net)	179560,00	mm^2	A_(net)	179560,00	mm^2
τ_(d)	0,20	N/mm^2	τ_(d)	0,45	N/mm^2	τ_(d)	0,20	N/mm^2	τ_(d)	0,17	N/mm^2
f_(v,d)	3,67	N/mm^2	f_(v,d)	3,67	N/mm^2	f_(v,d)	3,67	N/mm^2	f_(v,d)	3,67	N/mm^2
Verification	VERIFIED		Verification	VERIFIED		Verification	VERIFIED		Verification	VERIFIED	
V_0d max	438,92	kN	V_0d max	438,92	kN	V_0d max	438,92	kN	V_0d max	438,92	kN

RRH0shearINT	A1		RRH0shearINT	A1		RRH0shearINT	A1		RRH0shearINT	A1	
V_0d	23475,00	N	V_0d	53458,21	N	V_0d	23475,00	N	V_0d	20497,51	N
A_(net)	26000,00	mm^2	A_(net)	26000,00	mm^2	A_(net)	26000,00	mm^2	A_(net)	26000,00	mm^2
τ_(d)	1,35	N/mm^2	τ_(d)	3,08	N/mm^2	τ_(d)	1,35	N/mm^2	τ_(d)	1,18	N/mm^2
f_(v,d)	3,67	N/mm^2	f_(v,d)	3,67	N/mm^2	f_(v,d)	3,67	N/mm^2	f_(v,d)	3,67	N/mm^2
Verification	VERIFIED		Verification	VERIFIED		Verification	VERIFIED		Verification	VERIFIED	
V_0d max	63,56	kN	V_0d max	63,56	kN	V_0d max	63,56	kN	V_0d max	63,56	kN

RRH0shearINT with bending is satisfied for a load multiplier $\alpha = 0.8$

Tab [kN]
20,50

Tbc [kN]
18,95

Tcd [kN]
21,92

Tda [kN]
23,47

RH90shear	A5	
with bending		
V_90d	20497,51	N
K_cr	0,67	
A_(net)	5025,00	mm^2
τ_(d)	6,12	N/mm^2
ƒt,90,d	0,44	N/mm^2
f_(v,d)	0,88	N/mm^2
Verification	NOT VERIFIED	
V_90d max	2,95	kN

RH90shear	A5	
with bending		
V_90d	18946,64	N
K_cr	0,67	
A_(net)	5025,00	mm^2
τ_(d)	5,66	N/mm^2
ƒt,90,d	0,44	N/mm^2
f_(v,d)	0,88	N/mm^2
Verification	NOT VERIFIED	
V_90d max	2,95	kN

RH90shear	A5	
with bending		
V_90d	21924,13	N
K_cr	0,67	
A_(net)	5025,00	mm^2
τ_(d)	6,54	N/mm^2
ƒt,90,d	0,44	N/mm^2
f_(v,d)	0,88	N/mm^2
Verification	NOT VERIFIED	
V_90d max	2,95	kN

RH90shear	A5	
with bending		
V_90d	23475,00	N
K_cr	0,67	
A_(net)	5025,00	mm^2
τ_(d)	7,01	N/mm^2
ƒt,90,d	0,44	N/mm^2
f_(v,d)	0,88	N/mm^2
Verification	NOT VERIFIED	
V_90d max	2,95	kN

RH90shear	A5	
V_90d	20497,51	N
A_(net)	7500,00	mm^2
τ_(d)	4,10	N/mm^2
ƒt,90,d	0,44	N/mm^2
f_(v,d)	0,88	N/mm^2
Verification	NOT VERIFIED	
V_90d max	4,40	kN

RH90shear	A5	
V_90d	18946,64	N
A_(net)	7500,00	mm^2
τ_(d)	3,79	N/mm^2
ƒt,90,d	0,44	N/mm^2
f_(v,d)	0,88	N/mm^2
Verification	NOT VERIFIED	
V_90d max	4,40	kN

RH90shear	A5	
V_90d	21924,13	N
A_(net)	7500,00	mm^2
τ_(d)	4,38	N/mm^2
ƒt,90,d	0,44	N/mm^2
f_(v,d)	0,88	N/mm^2
Verification	NOT VERIFIED	
V_90d max	4,40	kN

RH90shear	A5	
V_90d	23475,00	N
A_(net)	7500,00	mm^2
τ_(d)	4,69	N/mm^2
ƒt,90,d	0,44	N/mm^2
f_(v,d)	0,88	N/mm^2
Verification	NOT VERIFIED	
V_90d max	4,40	kN

RH90shear for Tab, Tbc and Tcd are satisfied for a load multiplier $\alpha = 0.2$

RH90shear for Tda and RH90shear with bending for Tbc are satisfied for a load multiplier $\alpha = 0.15$

RH90shear with bending for Tab, Tcd and Tda are satisfied for a load multiplier $\alpha = 0.125$

10.5.6.4 Bending moments My and Mz

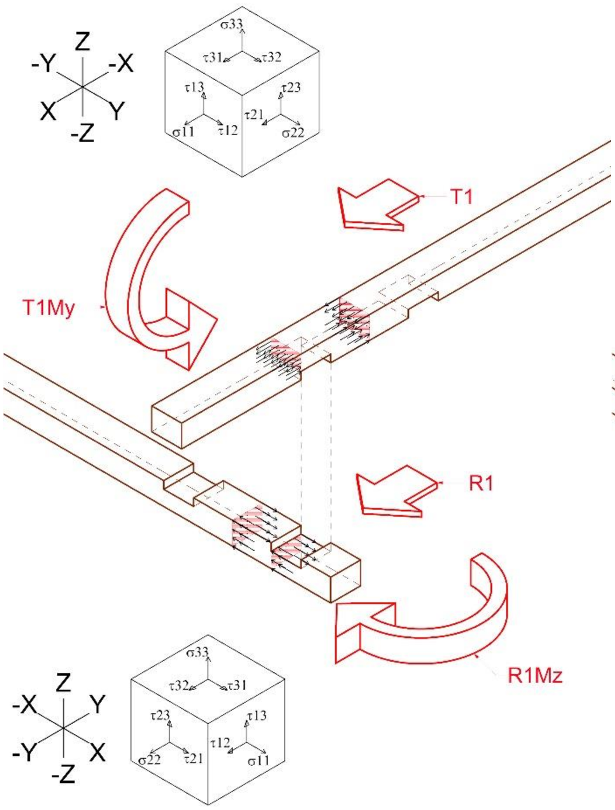

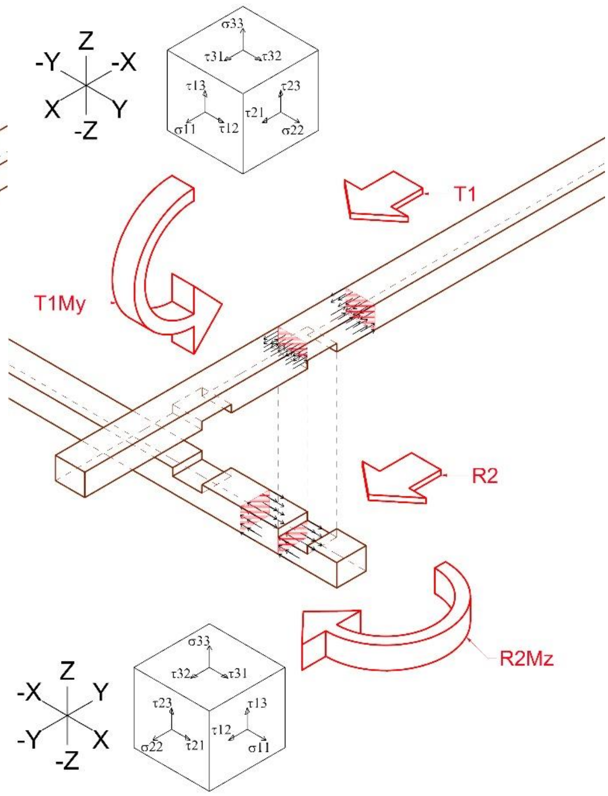

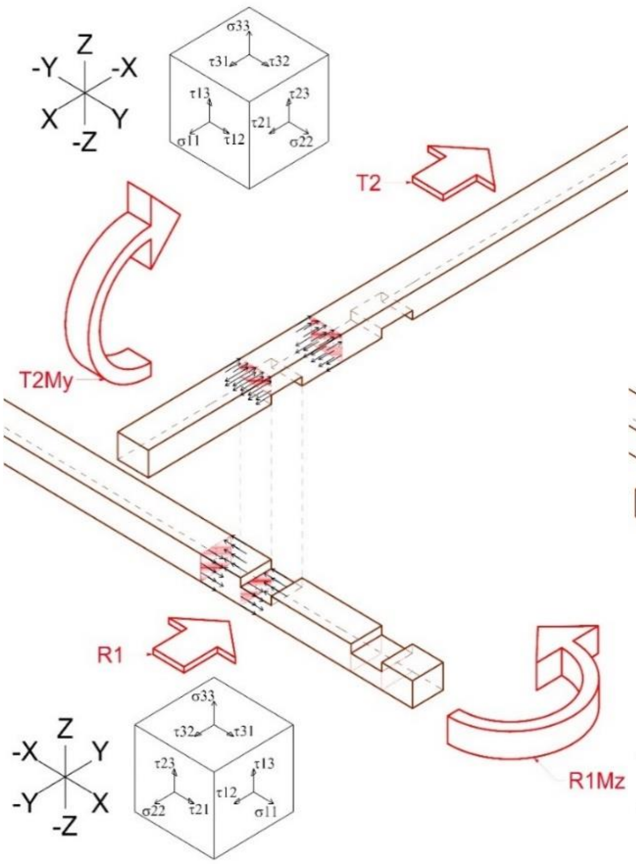

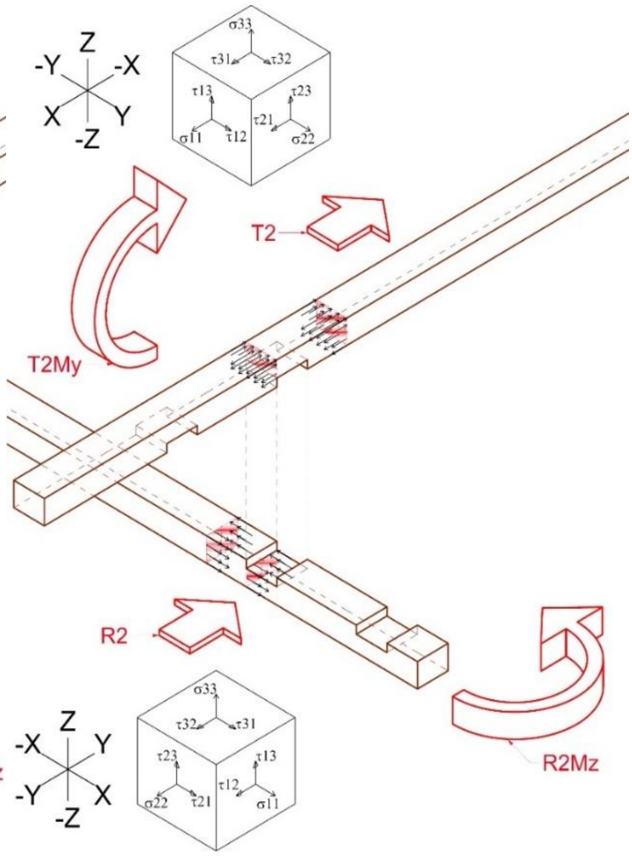

BM in A [kNm]
3,53

BM in B [kNm]
3,85

BM in C [kNm]
2,97

BM in D [kNm]
4,92

Body0mZ		
M_(z,d)	3526531,56	Nmm
K_m	0,70	
b	100,00	mm
h	75,00	mm
W_(z,d)	125000,00	mm^3
σ_(m,z,d)	28,21	N/mm^2
kh	1,08	
f_(m,d)	51,33	N/mm^2
f_(m,z,d)	55,67	N/mm^2
Verification	VERIFIED	
M_(z,d)max	6958693,87	Nmm
M_(z,d)max	6,96	kNm

Body0mZ		
M_(z,d)	3852573,21	Nmm
K_m	0,70	
b	100,00	mm
h	75,00	mm
W_(z,d)	125000,00	mm^3
σ_(m,z,d)	30,82	N/mm^2
kh	1,08	
f_(m,d)	51,33	N/mm^2
f_(m,z,d)	55,67	N/mm^2
Verification	VERIFIED	
M_(z,d)max	6958693,87	Nmm
M_(z,d)max	6,96	kNm

Body0mZ		
M_(z,d)	2968218,14	Nmm
K_m	0,70	
b	100,00	mm
h	75,00	mm
W_(z,d)	125000,00	mm^3
σ_(m,z,d)	23,75	N/mm^2
kh	1,08	
f_(m,d)	51,33	N/mm^2
f_(m,z,d)	55,67	N/mm^2
Verification	VERIFIED	
M_(z,d)max	6958693,87	Nmm
M_(z,d)max	6,96	kNm

Body0mZ		
M_(z,d)	4924468,05	Nmm
K_m	0,70	
b	100,00	mm
h	75,00	mm
W_(z,d)	125000,00	mm^3
σ_(m,z,d)	39,40	N/mm^2
kh	1,08	
f_(m,d)	51,33	N/mm^2
f_(m,z,d)	55,67	N/mm^2
Verification	VERIFIED	
M_(z,d)max	6958693,87	Nmm
M_(z,d)max	6,96	kNm

BM in A [kNm]
3,53

BM in B [kNm]
3,85

BM in C [kNm]
2,97

BM in D [kNm]
4,92

Notch0mZ		
M_(z,d)	3526531,56	Nmm
K_m	0,70	
b	100,00	mm
h	50,00	mm
W_(z,d)	83333,33	mm^3
σ_(m,z,d)	42,32	N/mm^2
kh	1,08	
f_(m,d)	51,33	N/mm^2
f_(m,z,d)	55,67	N/mm^2
Verification	VERIFIED	
M_(z,d)max	4639129,24	Nmm
M_(z,d)max	4,64	kNm

Notch0mZ		
M_(z,d)	3852573,21	Nmm
K_m	0,70	
b	100,00	mm
h	50,00	mm
W_(z,d)	83333,33	mm^3
σ_(m,z,d)	46,23	N/mm^2
kh	1,08	
f_(m,d)	51,33	N/mm^2
f_(m,z,d)	55,67	N/mm^2
Verification	VERIFIED	
M_(z,d)max	4639129,24	Nmm
M_(z,d)max	4,64	kNm

Notch0mZ		
M_(z,d)	2968218,14	Nmm
K_m	0,70	
b	100,00	mm
h	50,00	mm
W_(z,d)	83333,33	mm^3
σ_(m,z,d)	35,62	N/mm^2
kh	1,08	
f_(m,d)	51,33	N/mm^2
f_(m,z,d)	55,67	N/mm^2
Verification	VERIFIED	
M_(z,d)max	4639129,24	Nmm
M_(z,d)max	4,64	kNm

Notch0mZ		
M_(z,d)	4924468,05	Nmm
K_m	0,70	
b	100,00	mm
h	50,00	mm
W_(z,d)	83333,33	mm^3
σ_(m,z,d)	59,09	N/mm^2
kh	1,08	
f_(m,d)	51,33	N/mm^2
f_(m,z,d)	55,67	N/mm^2
Verification	NOT VERIFIED	
M_(z,d)max	4639129,24	Nmm
M_(z,d)max	4,64	kNm

Notch0mZ for BM in D satisfied for a load multiplier α = 0.9

They have been verified the "parasitic" bending moment as well.

Nab [kN]
23,47

Nbc [kN]
53,46

Ncd [kN]
23,47

Nda [kN]
20,50

Body0mY		
N_0d	23475,00	N
δ for My	38,00	mm
M_(y,d)	892049,96	Nmm
K_m	0,70	
b	100,00	mm
h	75,00	mm
W_(y,d)	93750,00	mm^3
σ_(m,y,d)	9,52	N/mm^2
kh	1,15	
f_(m,d)	51,33	N/mm^2
f_(m,y,d)	58,97	N/mm^2
Verification	VERIFIED	
M_(y,d)max	5528110,83	Nmm
M_(y,d)max	5,53	kNm

Body0mY		
N_0d	53458,21	N
δ for My	38,00	mm
M_(y,d)	2031412,10	Nmm
K_m	0,70	
b	100,00	mm
h	75,00	mm
W_(y,d)	93750,00	mm^3
σ_(m,y,d)	21,67	N/mm^2
kh	1,15	
f_(m,d)	51,33	N/mm^2
f_(m,y,d)	58,97	N/mm^2
Verification	VERIFIED	
M_(y,d)max	5528110,83	Nmm
M_(y,d)max	5,53	kNm

Body0mY		
N_0d	23475,00	N
δ for My	38,00	mm
M_(y,d)	892049,96	Nmm
K_m	0,70	
b	100,00	mm
h	75,00	mm
W_(y,d)	93750,00	mm^3
σ_(m,y,d)	9,52	N/mm^2
kh	1,15	
f_(m,d)	51,33	N/mm^2
f_(m,y,d)	58,97	N/mm^2
Verification	VERIFIED	
M_(y,d)max	5528110,83	Nmm
M_(y,d)max	5,53	kNm

Body0mY		
N_0d	20497,51	N
δ for My	38,00	mm
M_(y,d)	778905,50	Nmm
K_m	0,70	
b	100,00	mm
h	75,00	mm
W_(y,d)	93750,00	mm^3
σ_(m,y,d)	8,31	N/mm^2
kh	1,15	
f_(m,d)	51,33	N/mm^2
f_(m,y,d)	58,97	N/mm^2
Verification	VERIFIED	
M_(y,d)max	5528110,83	Nmm
M_(y,d)max	5,53	kNm

Notch0mY		
N_0d	23475,00	N
δ for My	38,00	mm
M_(y,d)	892049,96	Nmm
K_m	0,70	
b	100,00	mm
h	50,00	mm
W_(y,d)	41666,67	mm^3
σ_(m,y,d)	21,41	N/mm^2
kh	1,25	
f_(m,d)	51,33	N/mm^2
f_(m,y,d)	63,95	N/mm^2
Verification	VERIFIED	
M_(y,d)max	2664480,07	Nmm
M_(y,d)max	2,66	kNm

Notch0mY		
N_0d	53458,21	N
δ for My	38,00	mm
M_(y,d)	2031412,10	Nmm
K_m	0,70	
b	100,00	mm
h	50,00	mm
W_(y,d)	41666,67	mm^3
σ_(m,y,d)	48,75	N/mm^2
kh	1,25	
f_(m,d)	51,33	N/mm^2
f_(m,y,d)	63,95	N/mm^2
Verification	VERIFIED	
M_(y,d)max	2664480,07	Nmm
M_(y,d)max	2,66	kNm

Notch0mY		
N_0d	23475,00	N
δ for My	38,00	mm
M_(y,d)	892049,96	Nmm
K_m	0,70	
b	100,00	mm
h	50,00	mm
W_(y,d)	41666,67	mm^3
σ_(m,y,d)	21,41	N/mm^2
kh	1,25	
f_(m,d)	51,33	N/mm^2
f_(m,y,d)	63,95	N/mm^2
Verification	VERIFIED	
M_(y,d)max	2664480,07	Nmm
M_(y,d)max	2,66	kNm

Notch0mY		
N_0d	20497,51	N
δ for My	38,00	mm
M_(y,d)	778905,50	Nmm
K_m	0,70	
b	100,00	mm
h	50,00	mm
W_(y,d)	41666,67	mm^3
σ_(m,y,d)	18,69	N/mm^2
kh	1,25	
f_(m,d)	51,33	N/mm^2
f_(m,y,d)	63,95	N/mm^2
Verification	VERIFIED	
M_(y,d)max	2664480,07	Nmm
M_(y,d)max	2,66	kNm

10.5.6.5 Torsion

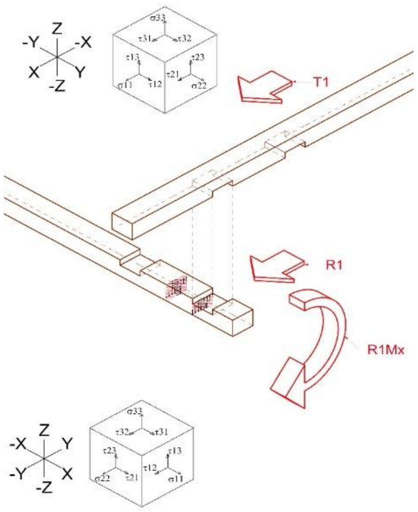

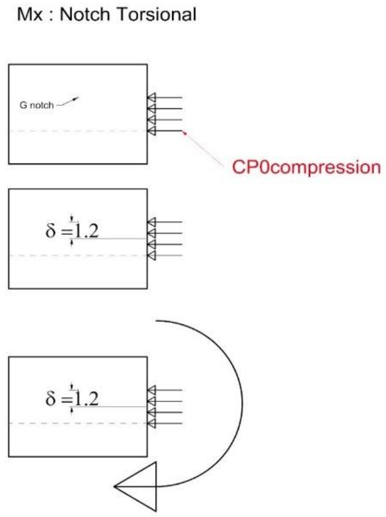

Tab [kN]
20,50

Tbc [kN]
18,95

Tcd [kN]
21,92

Tda [kN]
23,47

Body0mX		
V_90d	20497,51	N
δnotch for Mxnotch	12,00	mm
M_(x,d)	245970,16	Nmm
b	100,00	mm
h	75,00	mm
α	4,35	
τ_(tor,d)	1,90	N/mm^2
K_shape	1,02	
f_(v,d)	3,67	N/mm^2
k_shape*f_(v,d)	3,74	N/mm^2
Verification	VERIFIED	
M_(x,d) max	483620,69	Nmm
M_(x,d) max	0,48	kNm

Body0mX		
V_90d	18946,64	N
δnotch for Mxnotch	12,00	mm
M_(x,d)	227359,71	Nmm
b	100,00	mm
h	75,00	mm
α	4,35	
τ_(tor,d)	1,76	N/mm^2
K_shape	1,02	
f_(v,d)	3,67	N/mm^2
k_shape*f_(v,d)	3,74	N/mm^2
Verification	VERIFIED	
M_(x,d) max	483620,69	Nmm
M_(x,d) max	0,48	kNm

Body0mX		
V_90d	21924,13	N
δnotch for Mxnotch	12,00	mm
M_(x,d)	263089,54	Nmm
b	100,00	mm
h	75,00	mm
α	4,35	
τ_(tor,d)	2,03	N/mm^2
K_shape	1,02	
f_(v,d)	3,67	N/mm^2
k_shape*f_(v,d)	3,74	N/mm^2
Verification	VERIFIED	
M_(x,d) max	483620,69	Nmm
M_(x,d) max	0,48	kNm

Body0mX		
V_90d	23475,00	N
δnotch for Mxnotch	12,00	mm
M_(x,d)	281699,99	Nmm
b	100,00	mm
h	75,00	mm
α	4,35	
τ_(tor,d)	2,18	N/mm^2
K_shape	1,02	
f_(v,d)	3,67	N/mm^2
k_shape*f_(v,d)	3,74	N/mm^2
Verification	VERIFIED	
M_(x,d) max	483620,69	Nmm
M_(x,d) max	0,48	kNm

Notch0mX		
V_90d	20497,51	N
δnotch for Mxnotch	12,00	mm
M_(x,d)	245970,16	Nmm
b	100,00	mm
h	50,00	mm
α	3,90	
τ_(tor,d)	3,84	N/mm^2
K_shape	1,03	
f_(v,d)	3,67	N/mm^2
k_shape*f_(v,d)	3,78	N/mm^2
Verification	NOT VERIFIED	
M_(x,d) max	242094,02	Nmm
M_(x,d) max	0,24	kNm

Notch0mX		
V_90d	18946,64	N
δnotch for Mxnotch	12,00	mm
M_(x,d)	227359,71	Nmm
b	100,00	mm
h	50,00	mm
α	3,90	
τ_(tor,d)	3,55	N/mm^2
K_shape	1,03	
f_(v,d)	3,67	N/mm^2
k_shape*f_(v,d)	3,78	N/mm^2
Verification	VERIFIED	
M_(x,d) max	242094,02	Nmm
M_(x,d) max	0,24	kNm

Notch0mX		
V_90d	21924,13	N
δnotch for Mxnotch	12,00	mm
M_(x,d)	263089,54	Nmm
b	100,00	mm
h	50,00	mm
α	3,90	
τ_(tor,d)	4,10	N/mm^2
K_shape	1,03	
f_(v,d)	3,67	N/mm^2
k_shape*f_(v,d)	3,78	N/mm^2
Verification	NOT VERIFIED	
M_(x,d) max	242094,02	Nmm
M_(x,d) max	0,24	kNm

Notch0mX		
V_90d	23475,00	N
δnotch for Mxnotch	12,00	mm
M_(x,d)	281699,99	Nmm
b	100,00	mm
h	50,00	mm
α	3,90	
τ_(tor,d)	4,39	N/mm^2
K_shape	1,03	
f_(v,d)	3,67	N/mm^2
k_shape*f_(v,d)	3,78	N/mm^2
Verification	NOT VERIFIED	
M_(x,d) max	242094,02	Nmm
M_(x,d) max	0,24	kNm

Notch0mX for Tab, Tcd are satisfied for a load multiplier α = 0.9

Notch0mX for Tda is satisfied for a load multiplier α = 0.8

10.5.6.6 Combinations

The combinations for bending and tension have been computed for the weakest section, thus the notch.

Combined bending and axial tension

$$\frac{\sigma_{t,0,d}}{f_{t,0,d}} + \frac{\sigma_{m,y,d}}{f_{m,y,d}} + k_m * \frac{\sigma_{m,z,d}}{f_{m,z,d}} \leq 1$$

$$\frac{\sigma_{t,0,d}}{f_{t,0,d}} + k_m * \frac{\sigma_{m,y,d}}{f_{m,y,d}} + \frac{\sigma_{m,z,d}}{f_{m,z,d}} \leq 1$$

For solid timber, glued laminated timber and LVL:

- for rectangular sections: km = 0,7
- otherwise km = 1

Nbc [kN]	BM in B [kNm]
53,46	3,85

Verification	NOT VERIFIED
Verification	NOT VERIFIED

Notch0tens		
N_0d	53458,21	N
b	100,00	mm
h	50,00	mm
A_(net)	5000,00	mm^2
σ_(t,0,d)	10,69	N/mm^2
kh	1,08	
f_(t,0,d)	30,80	N/mm^2
Verification	VERIFIED	
N_(od)max	154,00	kN

Notch0mY		
N_0d	53458,21	N
δ for My	38,00	mm
M_(y,d)	2031412,10	Nmm
K_m	0,70	
b	100,00	mm
h	50,00	mm
W_(y,d)	41666,67	mm^3
σ_(m,y,d)	48,75	N/mm^2
kh	1,25	
f_(m,d)	51,33	N/mm^2
f_(m,y,d)	63,95	N/mm^2
Verification	VERIFIED	
M_(y,d)max	2664480,07	Nmm
M_(y,d)max	2,66	kNm

Notch0mZ2		
M_(z,d)	3852573,21	Nmm
K_m	0,70	
b	100,00	mm
h	50,00	mm
W_(z,d)	83333,33	mm^3
σ_(m,z,d)	46,23	N/mm^2
kh	1,08	
f_(m,d)	51,33	N/mm^2
f_(m,z,d)	55,67	N/mm^2
Verification	VERIFIED	
M_(z,d)max	4639129,24	Nmm
M_(z,d)max	4,64	kNm

Nbc [kN]	BM in C [kNm]
53,46	2,97

Verification	NOT VERIFIED
Verification	NOT VERIFIED

Notch0tens		
N_0d	53458,21	N
b	100,00	mm
h	50,00	mm
A_(net)	5000,00	mm^2
σ_(t,0,d)	10,69	N/mm^2
kh	1,08	
f_(t,0,d)	30,80	N/mm^2
Verification	VERIFIED	
N_(od)max	154,00	kN

Notch0mY		
N_0d	53458,21	N
δ for My	38,00	mm
M_(y,d)	2031412,10	Nmm
K_m	0,70	
b	100,00	mm
h	50,00	mm
W_(y,d)	41666,67	mm^3
σ_(m,y,d)	48,75	N/mm^2
kh	1,25	
f_(m,d)	51,33	N/mm^2
f_(m,y,d)	63,95	N/mm^2
Verification	VERIFIED	
M_(y,d)max	2664480,07	Nmm
M_(y,d)max	2,66	kNm

Notch0mZ2		
M_(z,d)	2968218,14	Nmm
K_m	0,70	
b	100,00	mm
h	50,00	mm
W_(z,d)	83333,33	mm^3
σ_(m,z,d)	35,62	N/mm^2
kh	1,08	
f_(m,d)	51,33	N/mm^2
f_(m,z,d)	55,67	N/mm^2
Verification	VERIFIED	
M_(z,d)max	4639129,24	Nmm
M_(z,d)max	4,64	kNm

Ncd [kN]	BM in C [kNm]
23,47	2,97

Verification	VERIFIED
Verification	NOT VERIFIED

Notch0tens		
N_0d	23475,00	N
b	100,00	mm
h	50,00	mm
A_(net)	5000,00	mm^2
σ_(t,0,d)	4,69	N/mm^2
kh	1,08	
f_(t,0,d)	30,80	N/mm^2
Verification	VERIFIED	
N_(od)max	154,00	kN

Notch0mY		
N_0d	23475,00	N
δ for My	38,00	mm
M_(y,d)	892049,96	Nmm
K_m	0,70	
b	100,00	mm
h	50,00	mm
W_(y,d)	41666,67	mm^3
σ_(m,y,d)	21,41	N/mm^2
kh	1,25	
f_(m,d)	51,33	N/mm^2
f_(m,y,d)	63,95	N/mm^2
Verification	VERIFIED	
M_(y,d)max	2664480,07	Nmm
M_(y,d)max	2,66	kNm

Notch0mZ2		
M_(z,d)	2968218,14	Nmm
K_m	0,70	
b	100,00	mm
h	50,00	mm
W_(z,d)	83333,33	mm^3
σ_(m,z,d)	35,62	N/mm^2
kh	1,08	
f_(m,d)	51,33	N/mm^2
f_(m,z,d)	55,67	N/mm^2
Verification	VERIFIED	
M_(z,d)max	4639129,24	Nmm
M_(z,d)max	4,64	kNm

Ncd [kN]	BM in D [kNm]
23,47	4,92

1,23

Verification	NOT VERIFIED
Verification	NOT VERIFIED

1,45

Notch0tens		
N_0d	23475,00	N
b	100,00	mm
h	50,00	mm
A_(net)	5000,00	mm^2
σ_(t,0,d)	4,69	N/mm^2
kh	1,08	
f_(t,0,d)	30,80	N/mm^2
Verification	VERIFIED	
N_(od)max	154,00	kN

Notch0mY		
N_0d	23475,00	N
δ for My	38,00	mm
M_(y,d)	892049,96	Nmm
K_m	0,70	
b	100,00	mm
h	50,00	mm
W_(y,d)	41666,67	mm^3
σ_(m,y,d)	21,41	N/mm^2
kh	1,25	
f_(m,d)	51,33	N/mm^2
f_(m,y,d)	63,95	N/mm^2
Verification	VERIFIED	
M_(y,d)max	2664480,07	Nmm
M_(y,d)max	2,66	kNm

Notch0mZ2		
M_(z,d)	4924468,05	Nmm
K_m	0,70	
b	100,00	mm
h	50,00	mm
W_(z,d)	83333,33	mm^3
σ_(m,z,d)	59,09	N/mm^2
kh	1,08	
f_(m,d)	51,33	N/mm^2
f_(m,z,d)	55,67	N/mm^2
Verification	NOT VERIFIED	
M_(z,d)max	4639129,24	Nmm
M_(z,d)max	4,64	kNm

Combination of Notch0tens, Notch0mY and Notch0mZ2 considering Nbc and BM in B are satisfied for a load multiplier α = 0.5

Combination of Notch0tens, Notch0mY and Notch0mZ2 considering Nbc and BM in C are satisfied for a load multiplier α = 0.6

Combination of Notch0tens, Notch0mY and Notch0mZ2 considering Ncd and BM in C are satisfied for a load multiplier α = 0.9

Combination of Notch0tens, Notch0mY and Notch0mZ2 considering Ncd and BM in D are satisfied for a load multiplier α = 0.6

The combinations for bending and compression have been computed for both sections, thus for the notch and the body section.

Combined bending and axial compression

$$\left(\frac{\sigma_{c,0,d}}{f_{c,0,d}}\right)^2 + \frac{\sigma_{m,y,d}}{f_{m,y,d}} + k_m * \frac{\sigma_{m,z,d}}{f_{m,z,d}} \leq 1$$

$$\left(\frac{\sigma_{c,0,d}}{f_{c,0,d}}\right)^2 + k_m * \frac{\sigma_{m,y,d}}{f_{m,y,d}} + \frac{\sigma_{m,z,d}}{f_{m,z,d}} \leq 1$$

For solid timber, glued laminated timber and LVL:

- for rectangular sections: km = 0,7
- otherwise km = 1

Nab [kN]	BM in A [kNm]
23,47	3,53

Verification	VERIFIED
Verification	NOT VERIFIED

Notch0comp		
N_0d	23475,00	N
b	100,00	mm
h	50,00	mm
A_(net)	5000,00	mm^2
σ_(c,0,d)	4,69	N/mm^2
f_(c,0,d)	24,93	N/mm^2
Verification	VERIFIED	
N_(od)max	124,67	kN

non esiste

Notch0mY		
N_0d	2,35E+04	N
δ for My	38,00	mm
M_(y,d)	892049,96	Nmm
K_m	0,70	
b	100,00	mm
h	50,00	mm
W_(y,d)	41666,67	mm^3
σ_(m,y,d)	21,41	N/mm^2
kh	1,25	
f_(m,d)	51,33	N/mm^2
f_(m,y,d)	63,95	N/mm^2
Verification	VERIFIED	
M_(y,d)max	2664480,07	Nmm
M_(y,d)max	2,66	kNm

Notch0mZ2		
M_(z,d)	3526531,56	Nmm
K_m	0,70	
b	100,00	mm
h	50,00	mm
W_(z,d)	83333,33	mm^3
σ_(m,z,d)	42,32	N/mm^2
kh	1,08	
f_(m,d)	51,33	N/mm^2
f_(m,z,d)	55,67	N/mm^2
Verification	VERIFIED	
M_(z,d)max	4639129,24	Nmm
M_(z,d)max	4,64	kNm

Nab [kN]	BM in B [kNm]
23,47	3,85

Verification	VERIFIED
Verification	VERIFIED

Body0comp		
N_0d	23475,00	N
b	100,00	mm
h	75,00	mm
A_(net)	5000,00	mm^2
σ_(c,0,d)	4,69	N/mm^2
f_(c,0,d)	24,93	N/mm^2
Verification	VERIFIED	
N_(od)max	124,67	kN

Body0mY		
N_0d	2,35E+04	N
δ for My	38,00	mm
M_(y,d)	892049,96	Nmm
K_m	0,70	
b	100,00	mm
h	75,00	mm
W_(y,d)	93750,00	mm^3
σ_(m,y,d)	9,52	N/mm^2
kh	1,15	
f_(m,d)	51,33	N/mm^2
f_(m,y,d)	58,97	N/mm^2
Verification	VERIFIED	
M_(y,d)max	5528110,83	Nmm
M_(y,d)max	5,53	kNm

Body0mZ2		
M_(z,d)	3852573,21	Nmm
K_m	0,70	
b	100,00	mm
h	75,00	mm
W_(z,d)	125000,00	mm^3
σ_(m,z,d)	30,82	N/mm^2
kh	1,08	
f_(m,d)	51,33	N/mm^2
f_(m,z,d)	55,67	N/mm^2
Verification	VERIFIED	
M_(z,d)max	6958693,87	Nmm
M_(z,d)max	6,96	kNm

Nda [kN]	BM in C [kNm]
20,50	2,97

Verification	VERIFIED
Verification	VERIFIED

Notch0comp		
N_0d	20497,51	N
b	100,00	mm
h	50,00	mm
A_(net)	5000,00	mm^2
σ_(c,0,d)	4,10	N/mm^2
f_(c,0,d)	24,93	N/mm^2
Verification	VERIFIED	
N_(od)max	124,67	kN

non esiste

Notch0mY		
N_0d	2,05E+04	N
δ for My	38,00	mm
M_(y,d)	778905,50	Nmm
K_m	0,70	
b	100,00	mm
h	50,00	mm
W_(y,d)	41666,67	mm^3
σ_(m,y,d)	18,69	N/mm^2
kh	1,25	
f_(m,d)	51,33	N/mm^2
f_(m,y,d)	63,95	N/mm^2
Verification	VERIFIED	
M_(y,d)max	2664480,07	Nmm
M_(y,d)max	2,66	kNm

Notch0mZ2		
M_(z,d)	2968218,14	Nmm
K_m	0,70	
b	100,00	mm
h	50,00	mm
W_(z,d)	83333,33	mm^3
σ_(m,z,d)	35,62	N/mm^2
kh	1,08	
f_(m,d)	51,33	N/mm^2
f_(m,z,d)	55,67	N/mm^2
Verification	VERIFIED	
M_(z,d)max	4639129,24	Nmm
M_(z,d)max	4,64	kNm

Nda [kN]	BM in D [kNm]
20,50	4,92

Verification	VERIFIED
Verification	VERIFIED

Body0comp		
N_0d	20497,51	N
b	100,00	mm
h	75,00	mm
A_(net)	5000,00	mm^2
σ_(c,0,d)	4,10	N/mm^2
f_(c,0,d)	24,93	N/mm^2
Verification	VERIFIED	
N_(od)max	124,67	kN

Body0mY		
N_0d	2,05E+04	N
δ for My	38,00	mm
M_(y,d)	778905,50	Nmm
K_m	0,70	
b	100,00	mm
h	75,00	mm
W_(y,d)	93750,00	mm^3
σ_(m,y,d)	8,31	N/mm^2
kh	1,15	
f_(m,d)	51,33	N/mm^2
f_(m,y,d)	58,97	N/mm^2
Verification	VERIFIED	
M_(y,d)max	5528110,83	Nmm
M_(y,d)max	5,53	kNm

Body0mZ2		
M_(z,d)	4924468,05	Nmm
K_m	0,70	
b	100,00	mm
h	75,00	mm
W_(z,d)	125000,00	mm^3
σ_(m,z,d)	39,40	N/mm^2
kh	1,08	
f_(m,d)	51,33	N/mm^2
f_(m,z,d)	55,67	N/mm^2
Verification	VERIFIED	
M_(z,d)max	6958693,87	Nmm
M_(z,d)max	6,96	kNm

Combination of Notch0tens, Notch0mY and Notch0mZ2 considering Nab and BM in A are satisfied for a load multiplier α = 0.9

The combinations for bending and compression have been computed for both sections, thus for the notch and the body section.

Combined Torsion and Shear - CNR-DT 206/2007

$$\frac{\tau_{tor,d}}{k_{shape} * f_{v,d}} + \left(\frac{\tau_d}{f_{v,d}}\right)^2 \leq 1$$

Tab [kN]	
20,50	
Verification	NOT VERIFIED

Notch90shearY		
V_90d	20497,51	N
A_(net)	5000,00	mm^2
τ_(d)	6,15	N/mm^2
ƒt,90,d	0,44	N/mm^2
f_(v,d)	0,88	N/mm^2
Verification	NOT VERIFIED	
V_90d max	2,93	kN

Notch0mX		
V_90d	2,05E+04	N
δnotch for Mxnotch	12,00	mm
M_(x,d)	245970,16	Nmm
b	100,00	mm
h	50,00	mm
α	3,90	
τ_(tor,d)	3,84	N/mm^2
K_shape	1,03	
f_(v,d)	3,67	N/mm^2
k_shape*f_(v,d)	3,78	N/mm^2
Verification	NOT VERIFIED	
M_(x,d) max	242094,02	Nmm
M_(x,d) max	0,24	kNm

Verification	VERIFIED

Body90shearY		
V_90d	20497,51	N
A_(net)	7500,00	mm^2
τ_(d)	4,10	N/mm^2
ƒt,90,d	0,44	N/mm^2
f_(v,d)	0,88	N/mm^2
Verification	NOT VERIFIED	
V_90d max	4,40	kN

Body0mX		
V_90d	2,05E+04	N
δnotch for Mxnotch	12,00	mm
M_(x,d)	245970,16	Nmm
b	100,00	mm
h	75,00	mm
α	4,35	
τ_(tor,d)	1,90	N/mm^2
K_shape	1,02	
f_(v,d)	3,67	N/mm^2
k_shape*f_(v,d)	3,74	N/mm^2
Verification	VERIFIED	
M_(x,d) max	483620,69	Nmm
M_(x,d) max	0,48	kNm

Tbc [kN]	
18,95	
Verification	NOT VERIFIED

Notch90shearY		
V_90d	18946,64	N
A_(net)	5000,00	mm^2
τ_(d)	5,68	N/mm^2
ƒt,90,d	0,44	N/mm^2
f_(v,d)	0,88	N/mm^2
Verification	NOT VERIFIED	
V_90d max	2,93	kN

Notch0mX		
V_90d	1,89E+04	N
δnotch for Mxnotch	12,00	mm
M_(x,d)	227359,71	Nmm
b	100,00	mm
h	50,00	mm
α	3,90	
τ_(tor,d)	3,55	N/mm^2
K_shape	1,03	
f_(v,d)	3,67	N/mm^2
k_shape*f_(v,d)	3,78	N/mm^2
Verification	VERIFIED	
M_(x,d) max	242094,02	Nmm
M_(x,d) max	0,24	kNm

Verification	VERIFIED

Body90shearY		
V_90d	18946,64	N
A_(net)	7500,00	mm^2
τ_(d)	3,79	N/mm^2
ƒt,90,d	0,44	N/mm^2
f_(v,d)	0,88	N/mm^2
Verification	NOT VERIFIED	
V_90d max	4,40	kN

Body0mX		
V_90d	1,89E+04	N
δnotch for Mxnotch	12,00	mm
M_(x,d)	227359,71	Nmm
b	100,00	mm
h	75,00	mm
α	4,35	
τ_(tor,d)	1,76	N/mm^2
K_shape	1,02	
f_(v,d)	3,67	N/mm^2
k_shape*f_(v,d)	3,74	N/mm^2
Verification	VERIFIED	
M_(x,d) max	483620,69	Nmm
M_(x,d) max	0,48	kNm

Tcd [kN]	
21,92	
Verification	NOT VERIFIED

Notch90shearY		
V_90d	21924,13	N
A_(net)	5000,00	mm^2
τ_(d)	6,58	N/mm^2
ƒt,90,d	0,44	N/mm^2
f_(v,d)	0,88	N/mm^2
Verification	NOT VERIFIED	
V_90d max	2,93	kN

Notch0mX		
V_90d	2,19E+04	N
δnotch for Mxnotch	12,00	mm
M_(x,d)	263089,54	Nmm
b	100,00	mm
h	50,00	mm
α	3,90	
τ_(tor,d)	4,10	N/mm^2
K_shape	1,03	
f_(v,d)	3,67	N/mm^2
k_shape*f_(v,d)	3,78	N/mm^2
Verification	NOT VERIFIED	
M_(x,d) max	242094,02	Nmm
M_(x,d) max	0,24	kNm

Verification	VERIFIED

Body90shearY		
V_90d	21924,13	N
A_(net)	7500,00	mm^2
τ_(d)	4,38	N/mm^2
ƒt,90,d	0,44	N/mm^2
f_(v,d)	0,88	N/mm^2
Verification	NOT VERIFIED	
V_90d max	4,40	kN

Body0mX		
V_90d	2,19E+04	N
δnotch for Mxnotch	12,00	mm
M_(x,d)	263089,54	Nmm
b	100,00	mm
h	75,00	mm
α	4,35	
τ_(tor,d)	2,03	N/mm^2
K_shape	1,02	
f_(v,d)	3,67	N/mm^2
k_shape*f_(v,d)	3,74	N/mm^2
Verification	VERIFIED	
M_(x,d) max	483620,69	Nmm
M_(x,d) max	0,48	kNm

Tda [kN]	
23,47	
Verification	NOT VERIFIED

Notch90shearY		
V_90d	23475,00	N
A_(net)	5000,00	mm^2
τ_(d)	7,04	N/mm^2
ƒt,90,d	0,44	N/mm^2
f_(v,d)	0,88	N/mm^2
Verification	NOT VERIFIED	
V_90d max	2,93	kN

Notch0mX		
V_90d	2,35E+04	N
δnotch for Mxnotch	12,00	mm
M_(x,d)	281699,99	Nmm
b	100,00	mm
h	50,00	mm
α	3,90	
τ_(tor,d)	4,39	N/mm^2
K_shape	1,03	
f_(v,d)	3,67	N/mm^2
k_shape*f_(v,d)	3,78	N/mm^2
Verification	NOT VERIFIED	
M_(x,d) max	242094,02	Nmm
M_(x,d) max	0,24	kNm

Verification	VERIFIED

Body90shearY		
V_90d	23475,00	N
A_(net)	7500,00	mm^2
τ_(d)	4,69	N/mm^2
ƒt,90,d	0,44	N/mm^2
f_(v,d)	0,88	N/mm^2
Verification	NOT VERIFIED	
V_90d max	4,40	kN

Body0mX		
V_90d	2,35E+04	N
δnotch for Mxnotch	12,00	mm
M_(x,d)	281699,99	Nmm
b	100,00	mm
h	75,00	mm
α	4,35	
τ_(tor,d)	2,18	N/mm^2
K_shape	1,02	
f_(v,d)	3,67	N/mm^2
k_shape*f_(v,d)	3,74	N/mm^2
Verification	VERIFIED	
M_(x,d) max	483620,69	Nmm
M_(x,d) max	0,48	kNm

The verifications about the combination of torsion and shear is strongly affected by the fragile behavior of the timber subjected to a shear force perpendicular to the fibers.

Combination of Notch90shearY and Notch0mX considering Tab and the pertinent torsional parasitic bending moment is satisfied for a load multiplier α = 0.7
Combination of Body90shearY and Body0mX considering Tab and the pertinent torsional parasitic bending moment is satisfied for a load multiplier α =1

Combination of Notch90shearY and Notch0mX considering Tbc and the pertinent torsional parasitic bending moment is satisfied for a load multiplier α = 0.7
Combination of Body90shearY and Body0mX considering Tbc and the pertinent torsional parasitic bending moment is satisfied for a load multiplier α = 1

Combination of Notch90shearY and Notch0mX considering Tcd and the pertinent torsional parasitic bending moment is satisfied for a load multiplier α = 0.6
Combination of Body90shearY and Body0mX considering Tcd and the pertinent torsional parasitic bending moment is satisfied for a load multiplier α = 1

Combination of Notch90shearY and Notch0mX considering Tda and the pertinent torsional parasitic bending moment is satisfied for a load multiplier α = 0.6
Combination of Body90shearY and Body0mX considering Tda and the pertinent torsional parasitic bending moment is satisfied for a load multiplier α = 1

It is important to underline that the verifications about the combination of torsion and shear result satisfied with the load multiplier shown above but the singular verifications about the shear is not verified. In order to obtaine the shear verification they are required the values of the load multipliers listed in the sub-chapter "10.5.6.3 Tangential stresses : Shear"

10.5.7 Verifications on corner joint, seismic event parallel to Rafter

It has been studied the case of a seismic event parallel to the normal rafter and perpendicular to the roof rafter in the tie-timber beam at the roof level. This has been done because the behavior is similar but normal rafter has few peculiar differences which made it weaker.

10.5.7.1 Scheme

The difference between the roof rafter and the rafter is the length of the head. The length of the normal rafter is shorter and the difference affects the longitudinal shear resistance of the element.

For all the other verifications nothing changes, that is why in the following, they are reported only the verifications about the shear resistance.

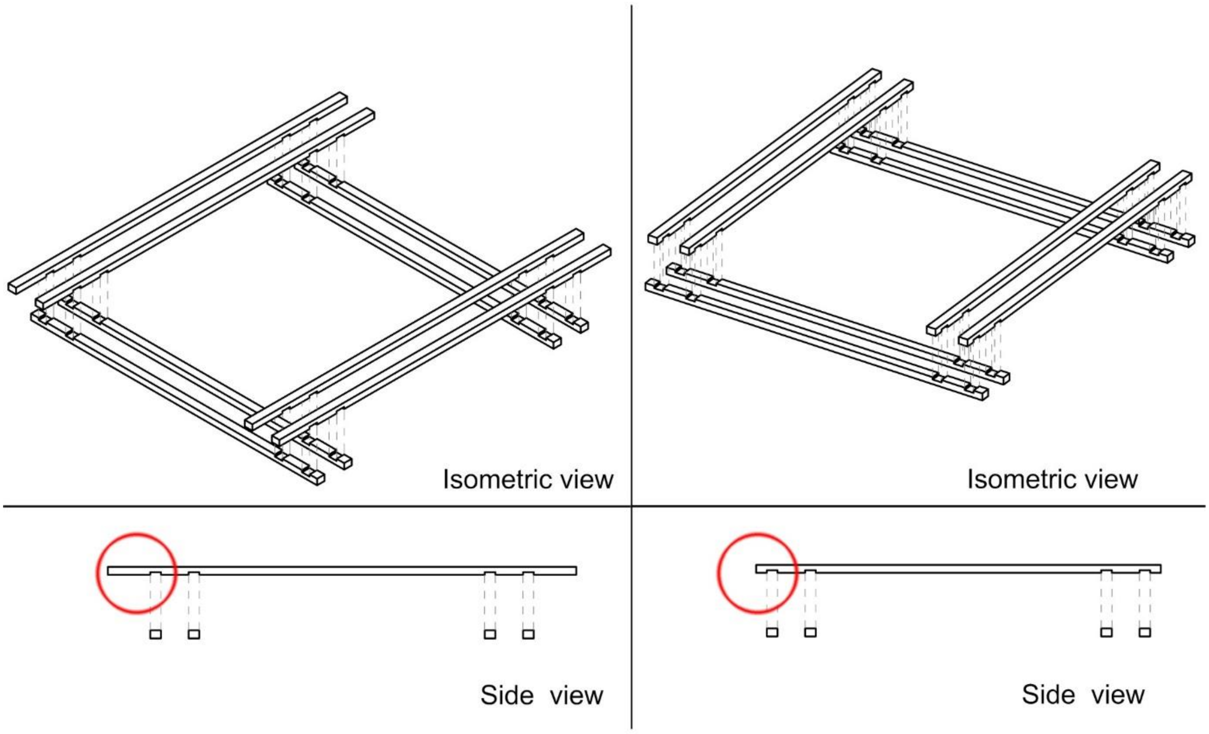

10.5.7.2 Tangential stresses : Shear

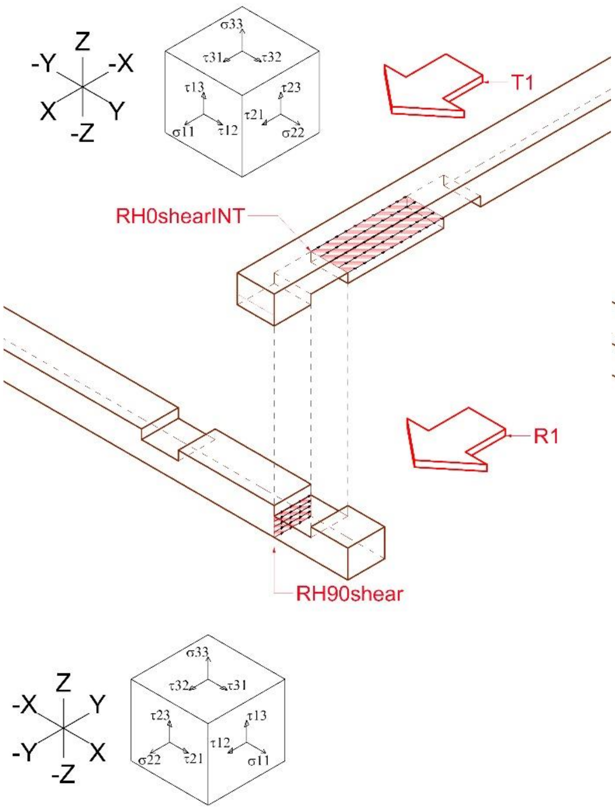

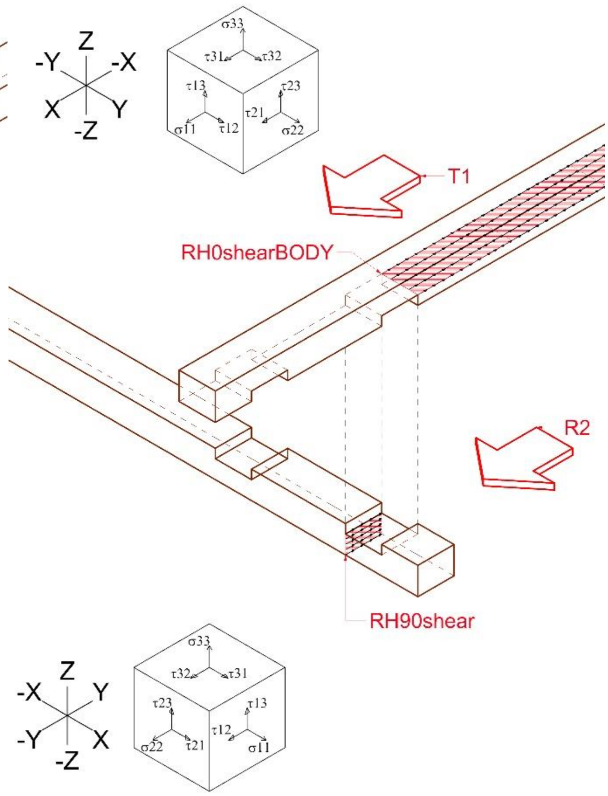

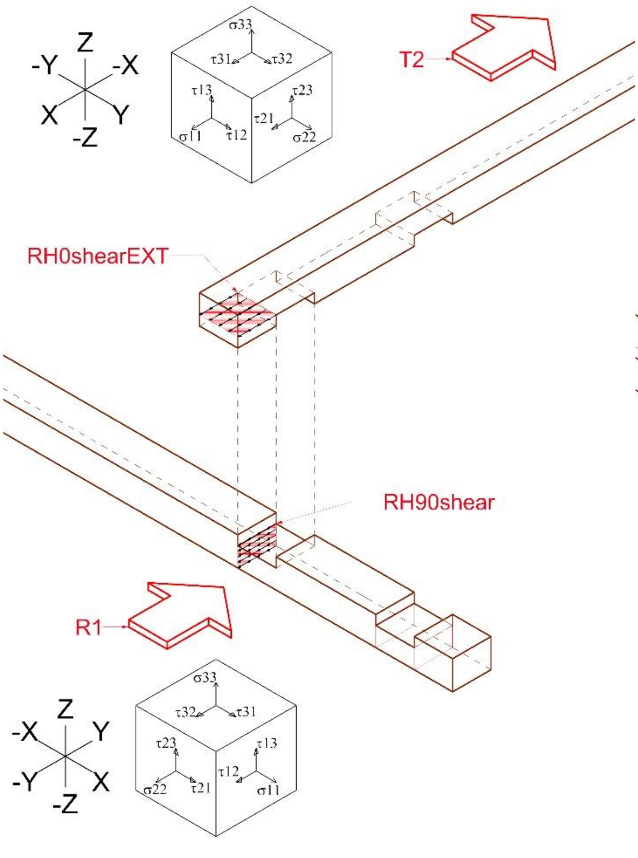

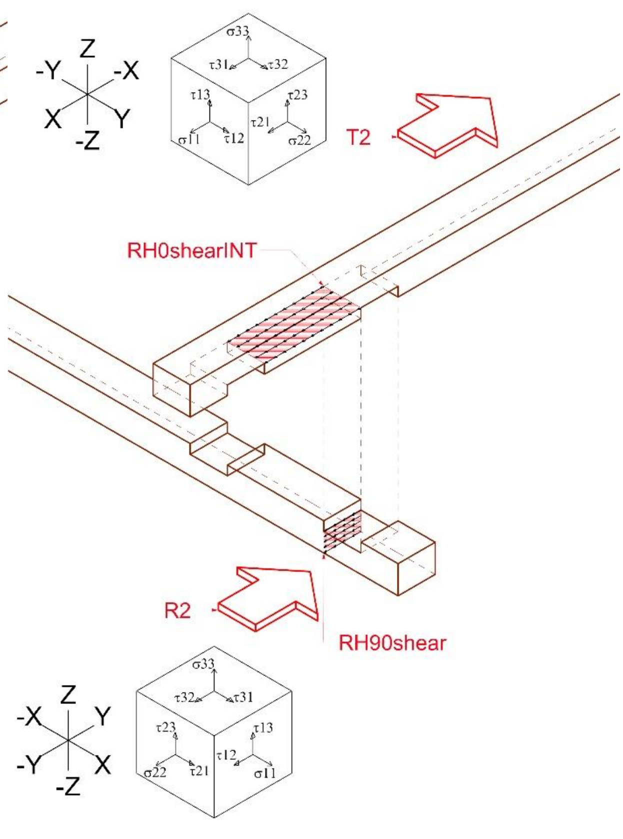

Nab [kN]	
23,47	

RH0shearEXT	A2	
with bending		
V_0d	23475	N
K_cr	0,67	
A_(net)	6700,0	mm^2
τ_(d)	5,26	N/mm^2
f_(v,d)	3,67	N/mm^2
Verification	NOT VERIFIED	
V_0d max	16,38	kN

Nbc [kN]	
53,46	

RH0shearEXT	A2	
with bending		
V_0d	53458,21	N
K_cr	0,67	
A_(net)	6700,00	mm^2
τ_(d)	11,97	N/mm^2
f_(v,d)	3,67	N/mm^2
Verification	NOT VERIFIED	
V_0d max	16,38	kN

Ncd [kN]	
23,47	

RH0shearEXT	A2	
with bending		
V_0d	23475,00	N
K_cr	0,67	
A_(net)	6700,00	mm^2
τ_(d)	5,26	N/mm^2
f_(v,d)	3,67	N/mm^2
Verification	NOT VERIFIED	
V_0d max	16,38	kN

Nda [kN]	
20,50	

RH0shearEXT	A2	
with bending		
V_0d	20497,51	N
K_cr	0,67	
A_(net)	6700,00	mm^2
τ_(d)	4,59	N/mm^2
f_(v,d)	3,67	N/mm^2
Verification	NOT VERIFIED	
V_0d max	16,38	kN

RH0shearBODY	A6	
with bending		
V_0d	23475	N
K_cr	0,67	
A_(net)	179560,00	mm^2
τ_(d)	0,20	N/mm^2
f_(v,d)	3,67	N/mm^2
Verification	VERIFIED	
V_0d max	438,92	kN

RH0shearBODY	A6	
with bending		
V_0d	53458,21	N
K_cr	0,67	
A_(net)	179560,00	mm^2
τ_(d)	0,45	N/mm^2
f_(v,d)	3,67	N/mm^2
Verification	VERIFIED	
V_0d max	438,92	kN

RH0shearBODY	A6	
with bending		
V_0d	23475,00	N
K_cr	0,67	
A_(net)	179560,00	mm^2
τ_(d)	0,20	N/mm^2
f_(v,d)	3,67	N/mm^2
Verification	VERIFIED	
V_0d max	438,92	kN

RH0shearBODY	A6	
with bending		
V_0d	20497,51	N
K_cr	0,67	
A_(net)	179560,00	mm^2
τ_(d)	0,17	N/mm^2
f_(v,d)	3,67	N/mm^2
Verification	VERIFIED	
V_0d max	438,92	kN

RH0shearINT	A1	
V_0d	23475	N
A_(net)	26000	mm^2
τ_(d)	1,35	N/mm^2
f_(v,d)	3,67	N/mm^2
Verification	VERIFIED	
V_0d max	63,56	kN

RH0shearINT	A1	
V_0d	53458,21	N
A_(net)	26000,00	mm^2
τ_(d)	3,08	N/mm^2
f_(v,d)	3,67	N/mm^2
Verification	VERIFIED	
V_0d max	63,56	kN

RRH0shearINT	A1	
V_0d	23475,00	N
A_(net)	26000,00	mm^2
τ_(d)	1,35	N/mm^2
f_(v,d)	3,67	N/mm^2
Verification	VERIFIED	
V_0d max	63,56	kN

RRH0shearINT	A1	
V_0d	20497,51	N
A_(net)	26000,00	mm^2
τ_(d)	1,18	N/mm^2
f_(v,d)	3,67	N/mm^2
Verification	VERIFIED	
V_0d max	63,56	kN

RRH0shearEXT with bending for Nab is satisfied for a load multiplier α = 0.6
RRH0shearEXT with bending for Nbc is satisfied for a load multiplier α = 0.3
RRH0shearEXT with bending for Ncd is satisfied for a load multiplier α = 0.6
RRH0shearEXT with bending for Nda is satisfied for a load multiplier α = 0.7

Tab [kN]	
20,50	

RH90shear	A5	
with bending		
V_90d	20497,51	N
K_cr	0,67	
A_(net)	5025,00	mm^2
τ_(d)	6,12	N/mm^2
ƒt,90,d	0,44	N/mm^2
f_(v,d)	0,88	N/mm^2
Verification	NOT VERIFIED	
V_90d max	2,95	kN
RH90shear	A5	
V_90d	20497,51	N
A_(net)	7500,00	mm^2
τ_(d)	4,10	N/mm^2
ƒt,90,d	0,44	N/mm^2
f_(v,d)	0,88	N/mm^2
Verification	NOT VERIFIED	
V_90d max	4,40	kN

Tbc [kN]	
18,95	

RH90shear	A5	
with bending		
V_90d	18946,64	N
K_cr	0,67	
A_(net)	5025,00	mm^2
τ_(d)	5,66	N/mm^2
ƒt,90,d	0,44	N/mm^2
f_(v,d)	0,88	N/mm^2
Verification	NOT VERIFIED	
V_90d max	2,95	kN
RH90shear	A5	
V_90d	18946,64	N
A_(net)	7500,00	mm^2
τ_(d)	3,79	N/mm^2
ƒt,90,d	0,44	N/mm^2
f_(v,d)	0,88	N/mm^2
Verification	NOT VERIFIED	
V_90d max	4,40	kN

Tcd [kN]	
21,92	

RH90shear	A5	
with bending		
V_90d	21924,13	N
K_cr	0,67	
A_(net)	5025,00	mm^2
τ_(d)	6,54	N/mm^2
ƒt,90,d	0,44	N/mm^2
f_(v,d)	0,88	N/mm^2
Verification	NOT VERIFIED	
V_90d max	2,95	kN
RH90shear	A5	
V_90d	21924,13	N
A_(net)	7500,00	mm^2
τ_(d)	4,38	N/mm^2
ƒt,90,d	0,44	N/mm^2
f_(v,d)	0,88	N/mm^2
Verification	NOT VERIFIED	
V_90d max	4,40	kN

Tda [kN]	
23,47	

RH90shear	A5	
with bending		
V_90d	23475,00	N
K_cr	0,67	
A_(net)	5025,00	mm^2
τ_(d)	7,01	N/mm^2
ƒt,90,d	0,44	N/mm^2
f_(v,d)	0,88	N/mm^2
Verification	NOT VERIFIED	
V_90d max	2,95	kN
RH90shear	A5	
V_90d	23475,00	N
A_(net)	7500,00	mm^2
τ_(d)	4,69	N/mm^2
ƒt,90,d	0,44	N/mm^2
f_(v,d)	0,88	N/mm^2
Verification	NOT VERIFIED	
V_90d max	4,40	kN

RH90shear for Tab, Tbc and Tcd are satisfied for a load multiplier α = 0.2
RH90shear for Tda and RH90shear with bending for Tbc are satisfied for a load multiplier α = 0.15
RH90shear with bending for Tab, Tcd and Tda are satisfied for a load multiplier α = 0.125.

10.6 Conclusions on seismic analysis out of plane – Flexible

10.6.1 Safetybehavior under seismic multiplier α=0,125

All the verifications have been computed in function of the seismic load multiplier α.

Summing up the results it can be noticed that in this configuration the timber elements with the function of chain is affected by the keyed scarf joint. This due to the fact that in the chain beam there is just un rafter under tension and the action is large compared to the overturning configuration.

The most critical section, again, is in the rafters of the timber beam belonging to failing wall.
This section has been named RH90shear but also RRH90shear.
The verification of this section is satisfied for a seismic load multiplier α = 0,125

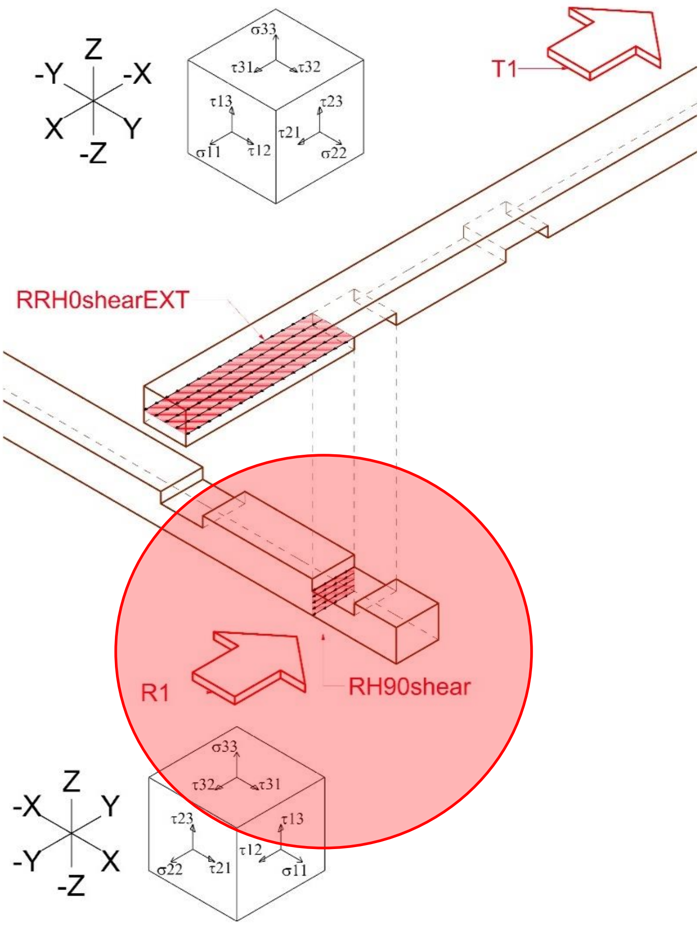

Figure 10-35 Flexible - RH90Shear most critical section

11 PRACTICAL RULES OF THUMB FOR CONSTRUCTION OF BHATAR SYSTEM

11.1 Arch Tom Schacher's rule of thumb an new specifications

The rules of thumb proposed by Arch Tom Schacher are valid but they do not ensure a perfectly earthquake proof behavior . From the results obtained in the analysis we can assert the structure may hold out against an earthquake with peack ground acceleration about 0.1 g.Some suggestions in reference to Tom shacher's rule of thumb are reported in the following.

11.1.1 Specifications on wall joints

With reference to the sub chapter "2.2.4 Wall – joints" it is specified that the keyed scarf joint (or Kashmir joint) must be placed in different position and not along a vertical line on the Z direction.

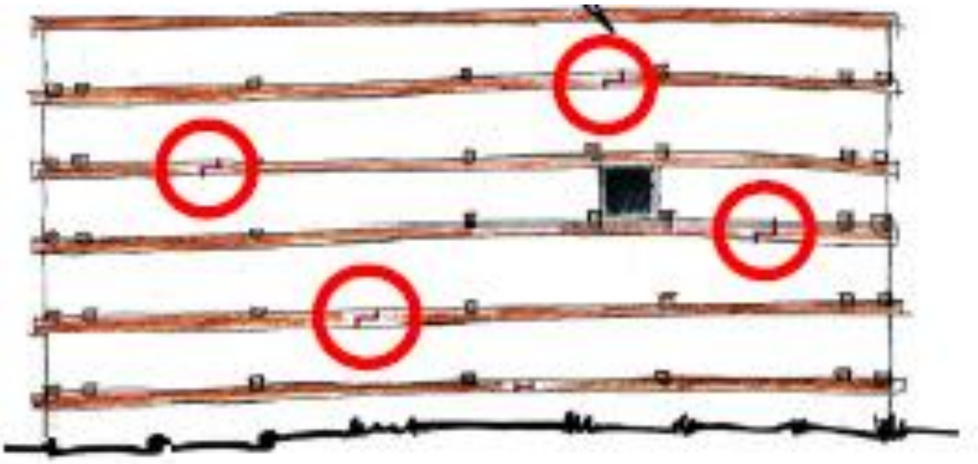

Figure 11-1 Spread the connection points.

The same specifications must be respected on the plane XY of the timber band, as shown in the topof figure 11-2. The joints have to be placed payng attention to do not have opening

A congruent pattern is shown in the figure 11-3, which shows the same wall , on the left the internal surface of the wall and on the right the external surface of the wall.

This kind of joint should be avoided on the rafters at the roof level, for a modul box of a 3.6m square plan If it is not possible it is necessary to respect the pattern described above.

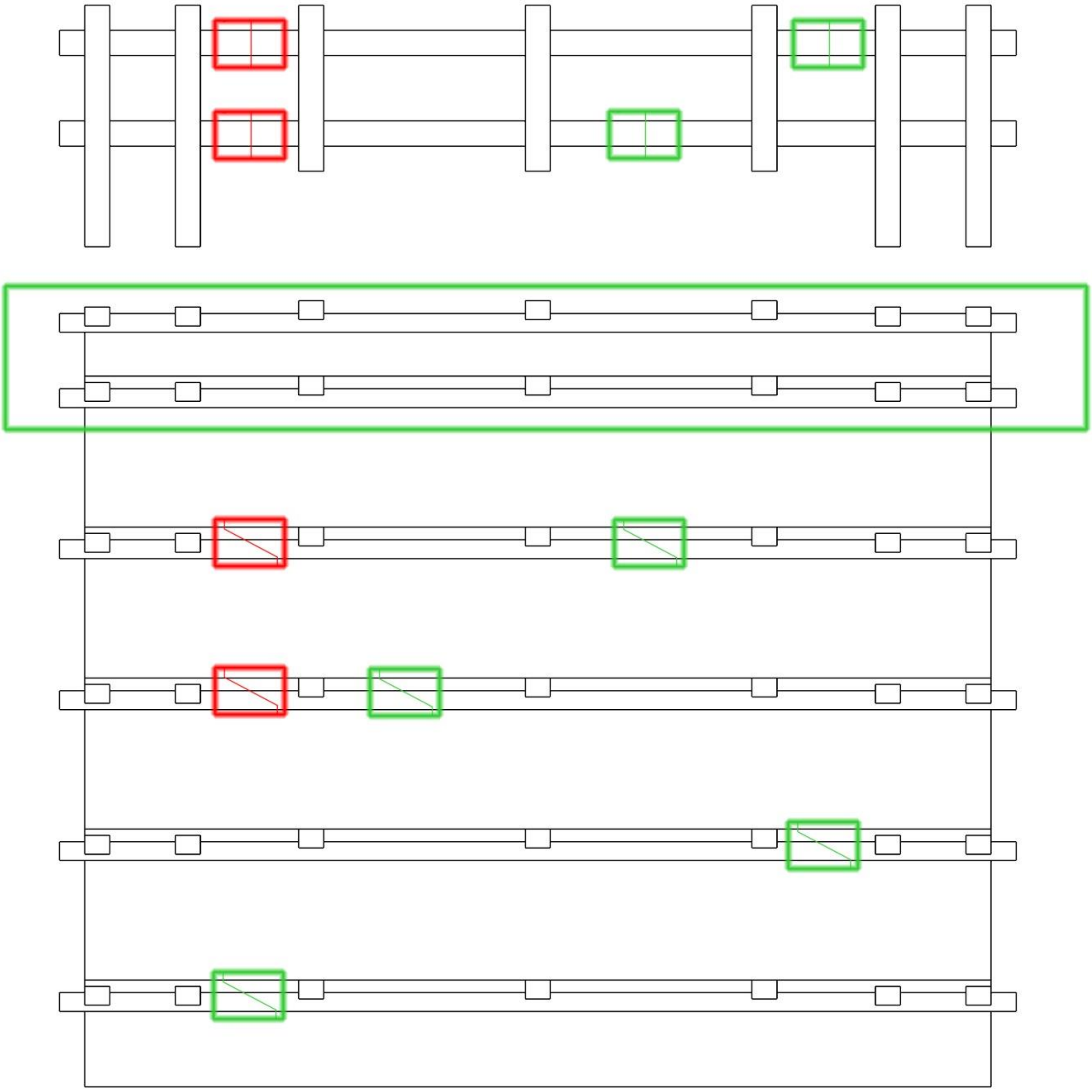

Figure 11-2 Pattern of Keyed scarf joint (or Kashmir joint)

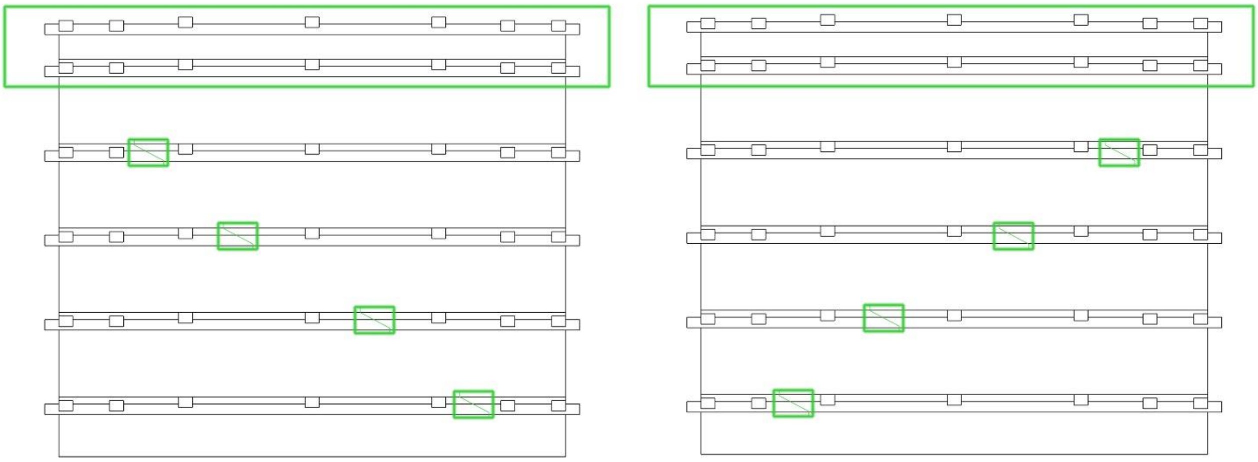

Figure 11-3Pattern for internal and external surface of the same wall

11.2 New Rules of thumb

11.2.1 Consideration about vertical component of the seismic event,

The analysis have been carried out considering the seismic actions applied on an horizontal plane parallel to the ground. Let us consider a spacial reference system with the Z axixs normal to the ground surface, the analysis were focused on the X and Y axis.The seismic action has a vertical component along the Z axis.

The vertical component of seismic action cannot be neglected. The in plane analysis is based on the Barton's model for rockfill which works properly if the surfaces of the rubble stones are in contact. The results of the in plane analysis are actually good even if any safety factors was applied neither to the actions or to the material. In order to ensure the behavior of bhatar analysed previously it is necessary to ensure that the stones composing the rockfill cannot be separated. The idea is to ensure a box behavior for each stone layers between the timber bands.

The connectors may be of different material like rope of vegetable fibersor cords, which are weaker but cheap, or rust preventer steel wire which is more expensive but stronger.

11.2.2 Steel wire connectors

In order to be able to sustain eventual vertical component of the seismic force, it is necessary to include some reinforcements where the tension stresses appear.
It can be notice from the picture that the wire is working in pure shear only at the bended part, elsewhere the wire is working in tension.

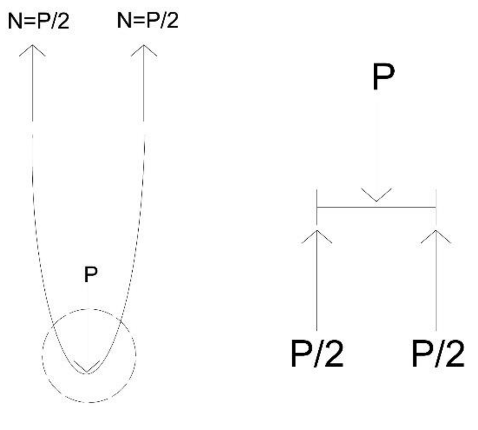

Figure 11-4 Forces acting on the steel wire connectors

"The magnitude of the shear yield stress in pure shear is (√3) times lower than the tensile yield stress in the case of simple tension" [4]. Thus, we have:

$$\tau \leq \frac{f_y}{\sqrt{3}}$$

The general shear stress for the forces acting on the wire is:

$$\tau \leq \frac{P}{2A}$$

Thus,

$$\frac{P}{2A} \leq \frac{f_y}{\sqrt{3}}$$

It has been assumed the yield stress of the steel as fy=3000kg/cm^2 and the diameter of the wire as Φ=3mm

11.2.2.1 *Vertical fasten connectors*

In order to constrict consecutive timber bands it is possible to take advantage of the cross pieces. The cross pieces stick out to the wall with a length about 10 cm. The cross piece end of the above timber band must be tied to end of the second below timber band, this must be done on the external surface of the wall and on the internal surface of the wall when it is possible.

The vertical connectors (purple line) are placed as shown in the figure below. Each connectors links just two cross pieces with the shown pattern.

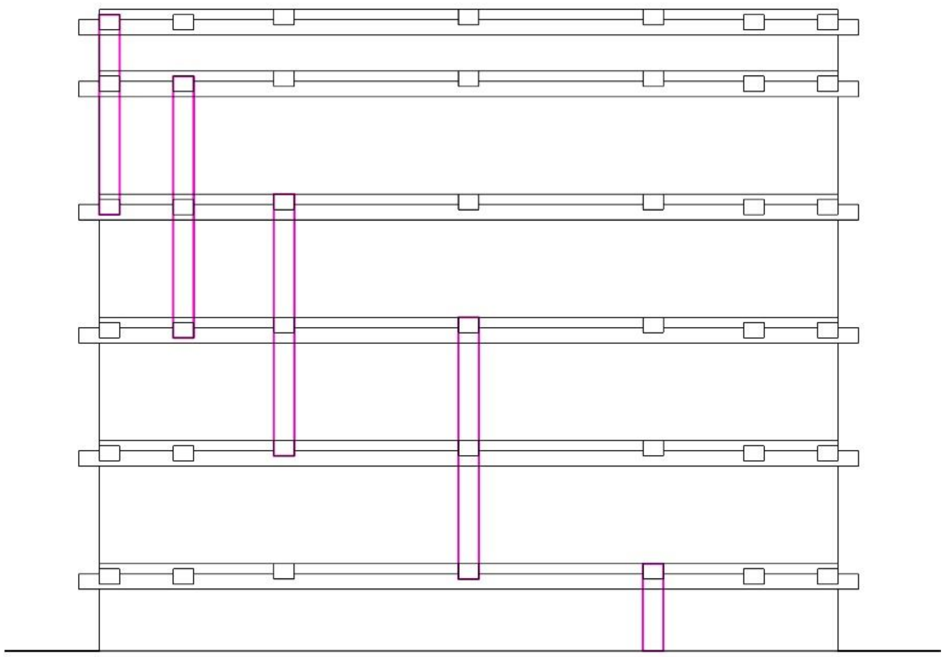

Figure 11-5 Pattern of vertical fasten connector

11.2.2.2 *Diagonal fasten connectors*

Similarly to the vertical fasten connectors it is usefull to install the diagonal fasten connectors.

The results in the conclusions of the seismic analysis in plane shows that the first four layers from the top may be subjected to sliding.The diagonal connectors guarantee a prevention against this event. The sliding may happen in the direction parallel to the wall and in two sense so the diagonal connectors must be installed with a right sense. In the following figures they are shown diagonal connectors with a positive rotation with respect to the vertical connectors (green line - figure 11-7) as well diagonal connectors with a negative rotation (red line - figure 11-8). Each connectors links just two cross pieces.

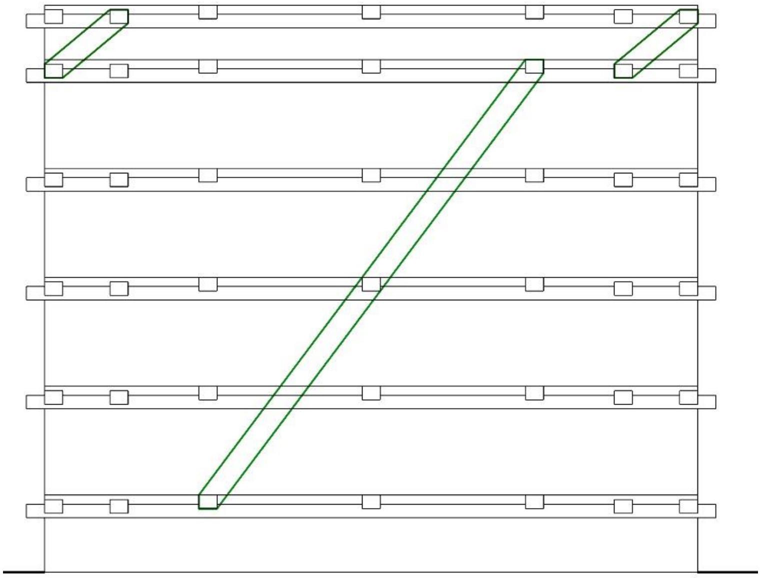

Figure 11-6 Example of single diagonal connector with positive orientation

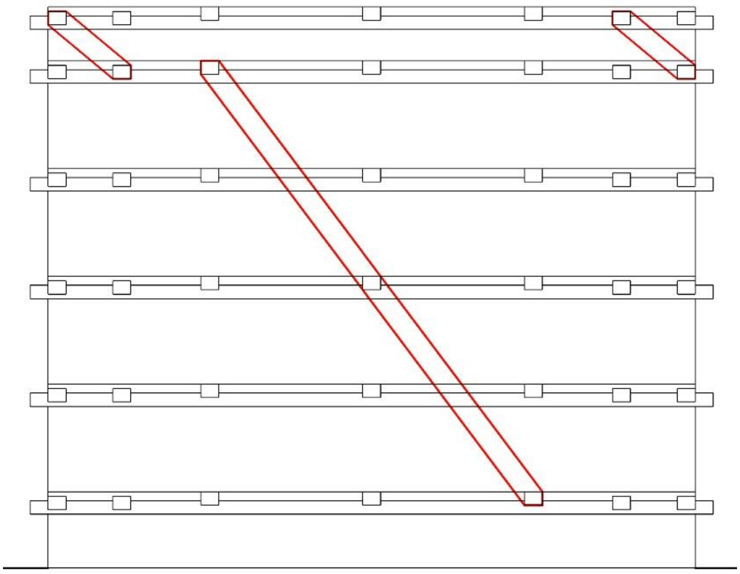

Figure 11-7 Example of single diagonal connector with negative orientation

11.2.2.3 Preliminary design of diagonal fasten connectors

The diagonal connectors at roof level have an inclination with respect to the horizontal of 40°, the main diagonal connectors in the central position The seismic force distribution have been recalled from the analysis below the timber bands.

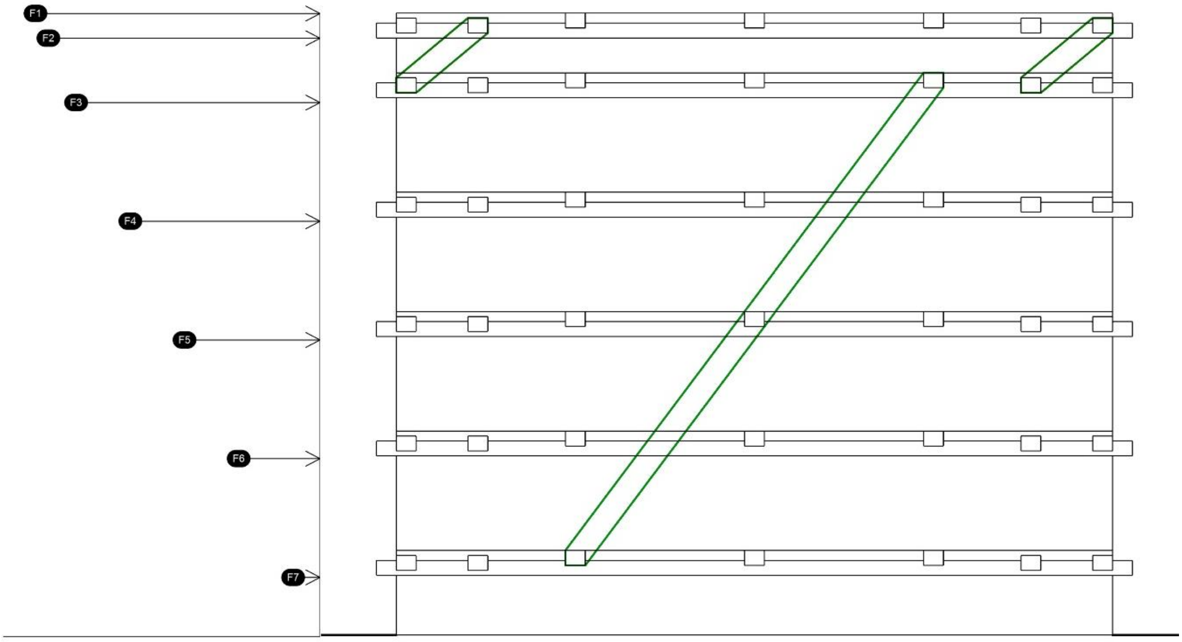

Figure 11-8 Preliminary design of diagonal connectors

The preliminary design of the diagonal connectors is pointed to obtain the numbers of connectors in each position.

The connectors at the roof level :are placed in the corners and they are subjected to a force called Froof. and have an inclination with respect to the horizontal of 40°.

$$F_{roof} = F_1 + F_2$$

$$\beta_{roof} = 40°$$

The connectors in the central position are subjected to a force called Fwall and have an inclination with respect to the horizontal of 53°.

$$F_{wall} = F_3 + F_4 + F_5 + F_6$$

$$\beta_{wall} = 53°$$

In order to know the number of connectors for each position it is required the verification of the shear stress τ acting on a single connector.The computation of the yeald shear stress has been shown in the sub-chapter “11.2.2 Steel wire connectors”.

The component of the seismic force vector acting on the connector at roof level is:

$$P = F_{roof} * \cos(\beta_{roof})$$

$$\tau = \frac{P}{2 * A} = \frac{F_{roof} * \cos(\beta_{roof})}{2 * A}$$

In order to know the numbers of connectors we can write:

$$\frac{\tau}{n} \leq \frac{f_y}{\sqrt{3}}$$

Where

n is the number of connectors.

In the case of the roof level it is necessary to consider that the connectors are at the both cornes, thus n must multiplied by 2

$$\frac{\tau}{2 * n} \leq \frac{f_y}{\sqrt{3}}$$

$$\frac{F_{roof} * \cos(\beta_{roof})}{n * 4 * A} \leq \frac{f_y}{\sqrt{3}}$$

Rearranging :

$$\frac{F_{roof} * \cos(\beta_{roof})}{n * 4 * A} \leq \frac{f_y}{\sqrt{3}}$$

$$n \geq \frac{F_{roof} * \cos(\beta_{roof}) * \sqrt{3}}{4 * A * f_y}$$

The component of the seismic force vector acting on the connector in the central position is:

$$P = F_{wall} * \cos(\beta_{wall})$$

$$\tau = \frac{P}{2 * A} = \frac{F_{wall} * \cos(\beta_{wall})}{2 * A}$$

In order to know the numbers of connectors we can write:

$$\frac{\tau}{n} \leq \frac{f_y}{\sqrt{3}}$$

Where

n is the number of connectors.

$$\frac{F_{roof} * \cos(\beta_{roof})}{n * 2 * A} \leq \frac{f_y}{\sqrt{3}}$$

It has been assumed the yield stress of the steel as fy=3000kg/cm^2 (0.294kN/mm^2) and the diameter of the wire as Φ=3mm

$$A_{\Phi 3} = \frac{\pi * (0.3)^2}{4} = 0.0707\ cm^2$$

Distribution factors and Forces		
Fj	βj	Fj=Fs*βj
	/	kN
F1	0,50	104,63
F2	0,09	18,38
F3	0,15	31,26
F4	0,12	24,32
F5	0,08	17,37
F6	0,05	10,42
F7	0,01	1,80

	P	β	P/2	P/2*cos(β)	P/(2A)*cos(β)	n
	kN	deg	kN	kN	kN/mm^2	
Froof=F1+F2=	123,02	40	61,50848	47,11822635	6,665865452	19,622089
Fwall=F3+F4+F5+F6=	83,37	53	41,68481	25,08654208	3,549019713	20,894265

The number of connectors at the roof corners must be at least 20, each corners.

The number of connectors in the center of the wall must be at least 21.

11.2.2.4 Foundation

The connectors which guarantee the fastening of the first line of the cross pieces to the ground must be installed in the initial step of the construction of the bhatar structure. The steel wire must be placed under the foundation paying attention to pass it under the first stone layer ,to b more clear the positions of the steel wire is shown in Figure11-5. The connectors on the corners of the box module plant cannot be placed at the foundation because of the impossibility of installing a straight steel wires without compenetrating the stones.

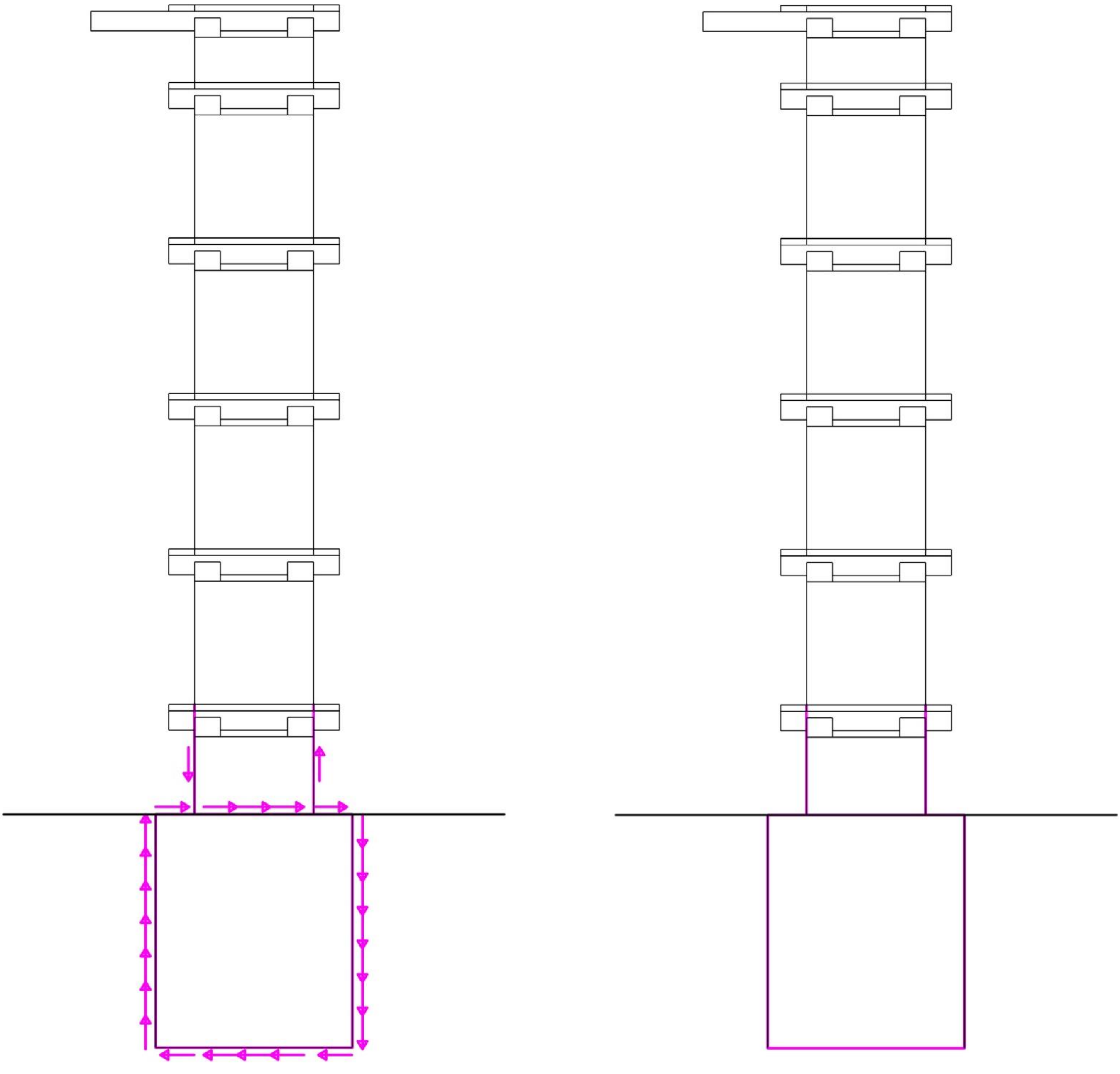

Figure 11-9 Connectors for foundation

11.2.2.5 Whole wall distribution of connectors

As written in the previuos sub-chapter the first four layers from the top are subjected to sliding so the priority is to install the vertical (Figure 11-6)and diagonal (Figure 11-8) connectors in order to avoid this event. In the vertical direction the connectors must be installed on all the wall height

The vertical connectors must be installed on the external surface of the wall and on the internal surface of the wall (Figure 11-7).

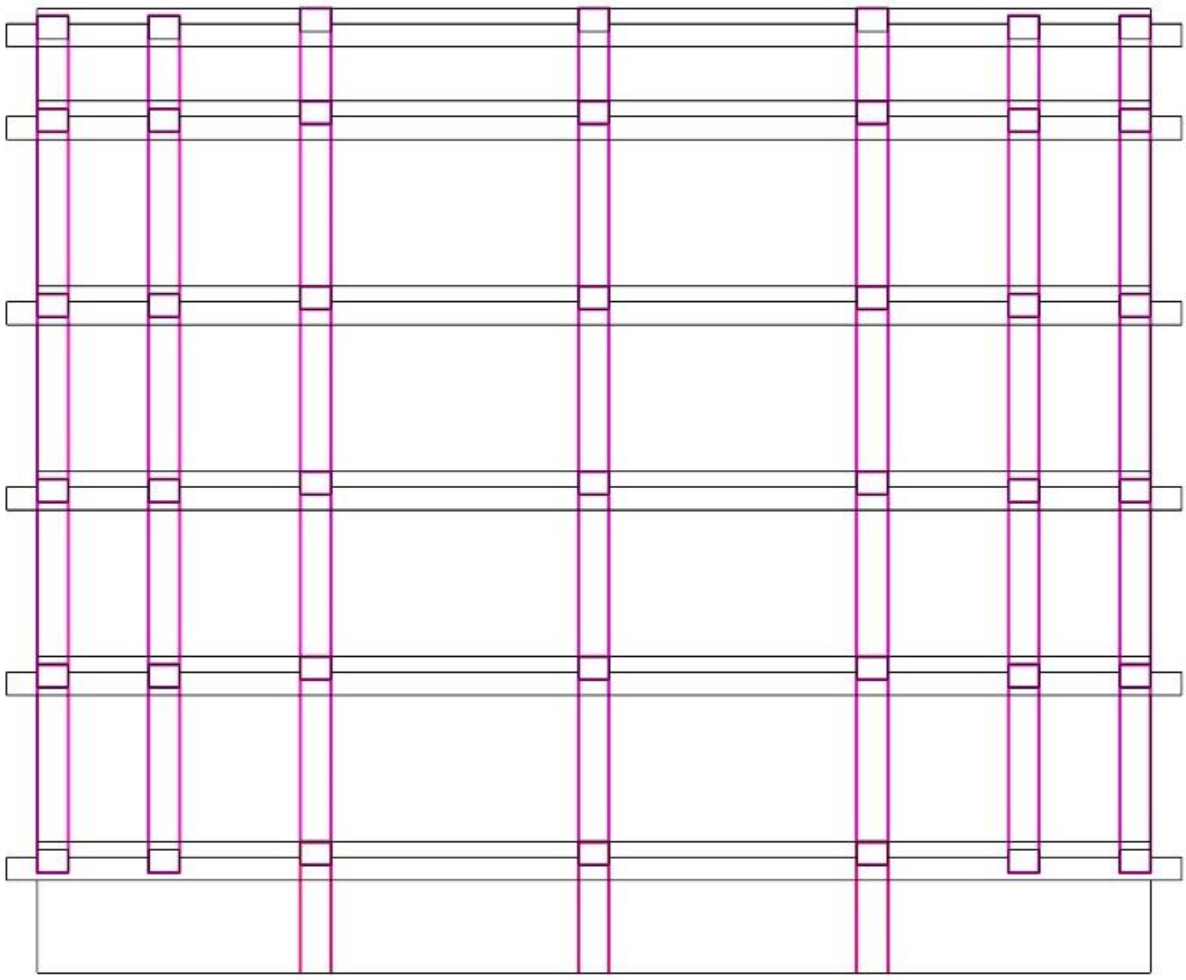

Figure 11-10 Vertical connectors total wall - external

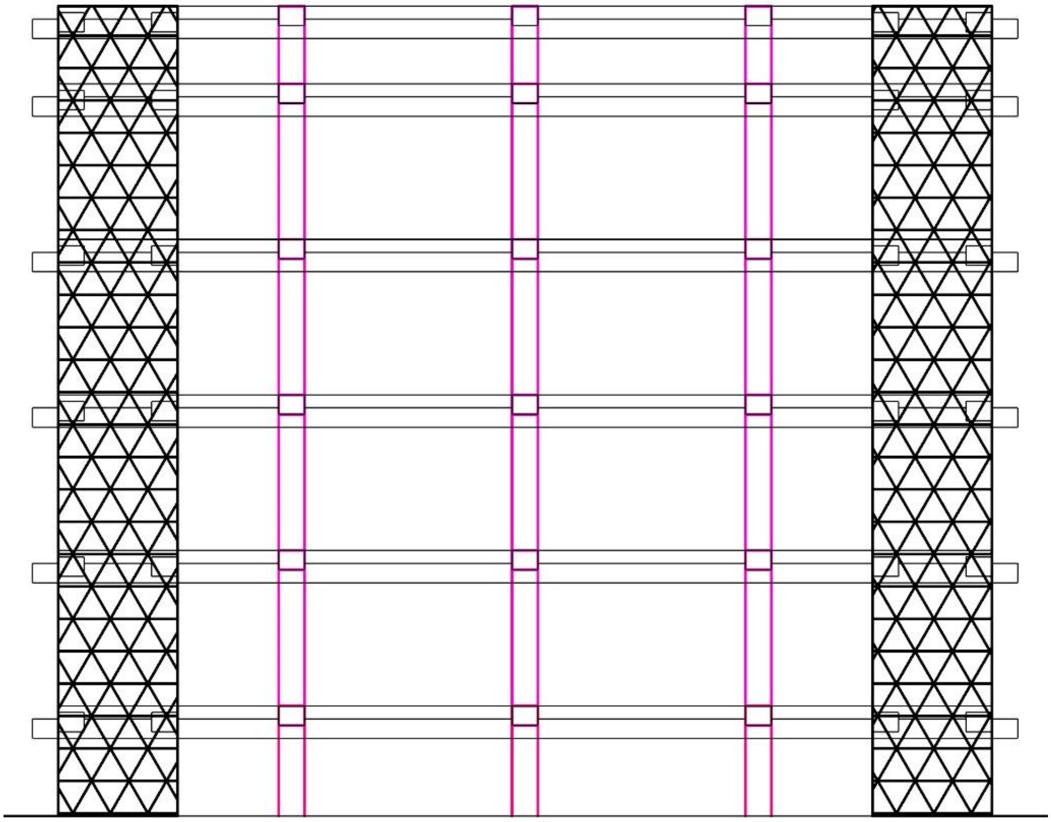

Figure 11-11 Vertical connectors total wall - internal

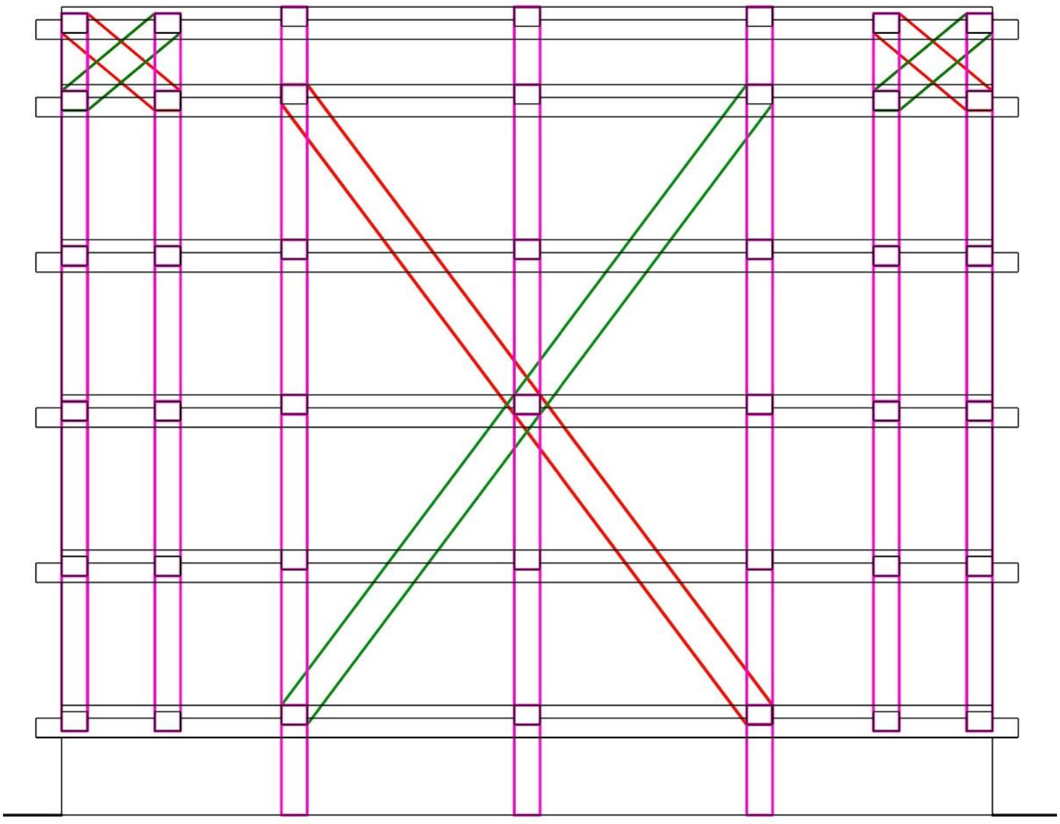

Figure 11-12 Connectors on total wall - external

11.2.1 Vertical rafters

The best solution from practical and economical point of view, is to install vertical timber rafters which are available and already known by the Bhatar users.

11.2.1.1 Single vertical rafter

The vertical rafters must be placed on the Bhatar structure as the last steps of the bulding process of the load-bearing elements , the walls. The dimension are approximatively

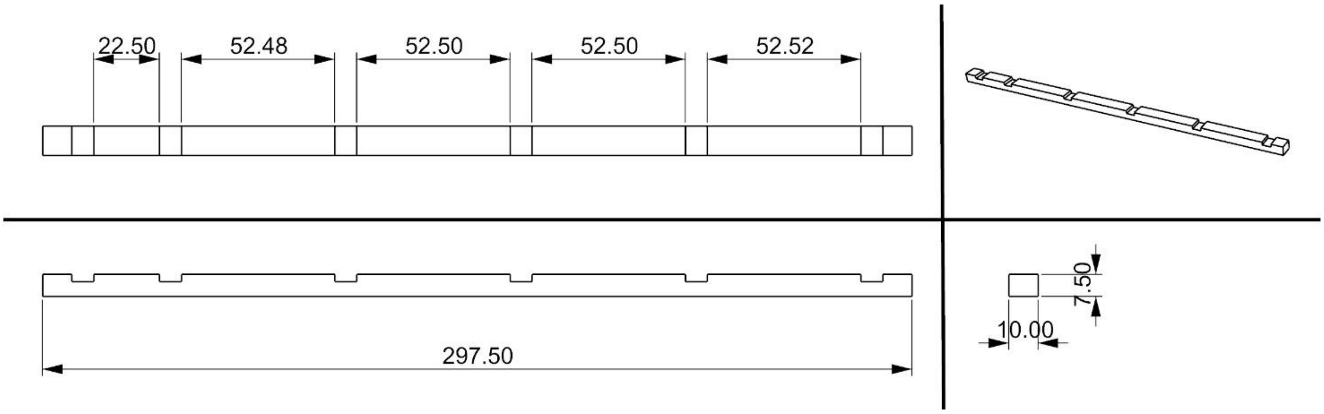

Figure 11-13 Vertical Rafters – gross measuraments in cm

The vertical rafters must be placed in order to embend all the cross pieces along a vertical line. For each line of cross piaces the vertical rafters must be placed at the right side and at the left side. It is also needed to set the vertical rafters externalside and internal side of the box walls. The vertical rafters must be embended to eachothers with connectors which may be of steel wire or rope.

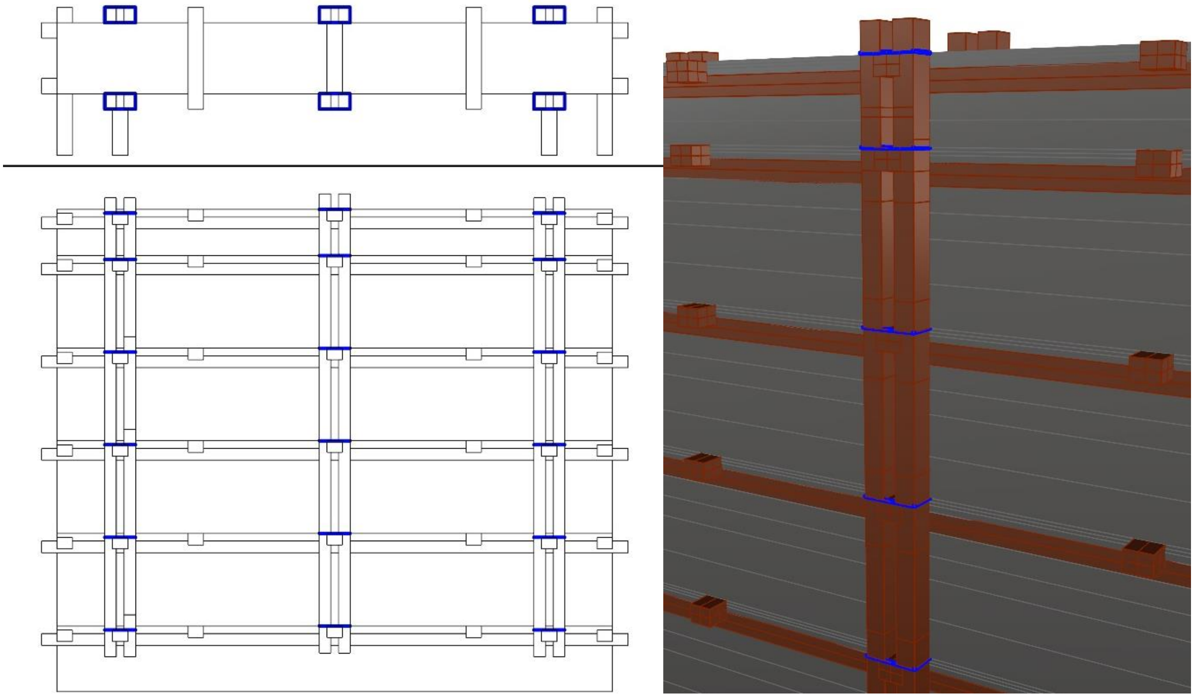

Figure 11-14 Connectors for vertical rafters.

In the next two pages are shown respectively one thrifty solution and one optimal solution for the placement of the vertical rafters.

11.2.1.2 Thrifty disposition of vertical rafters

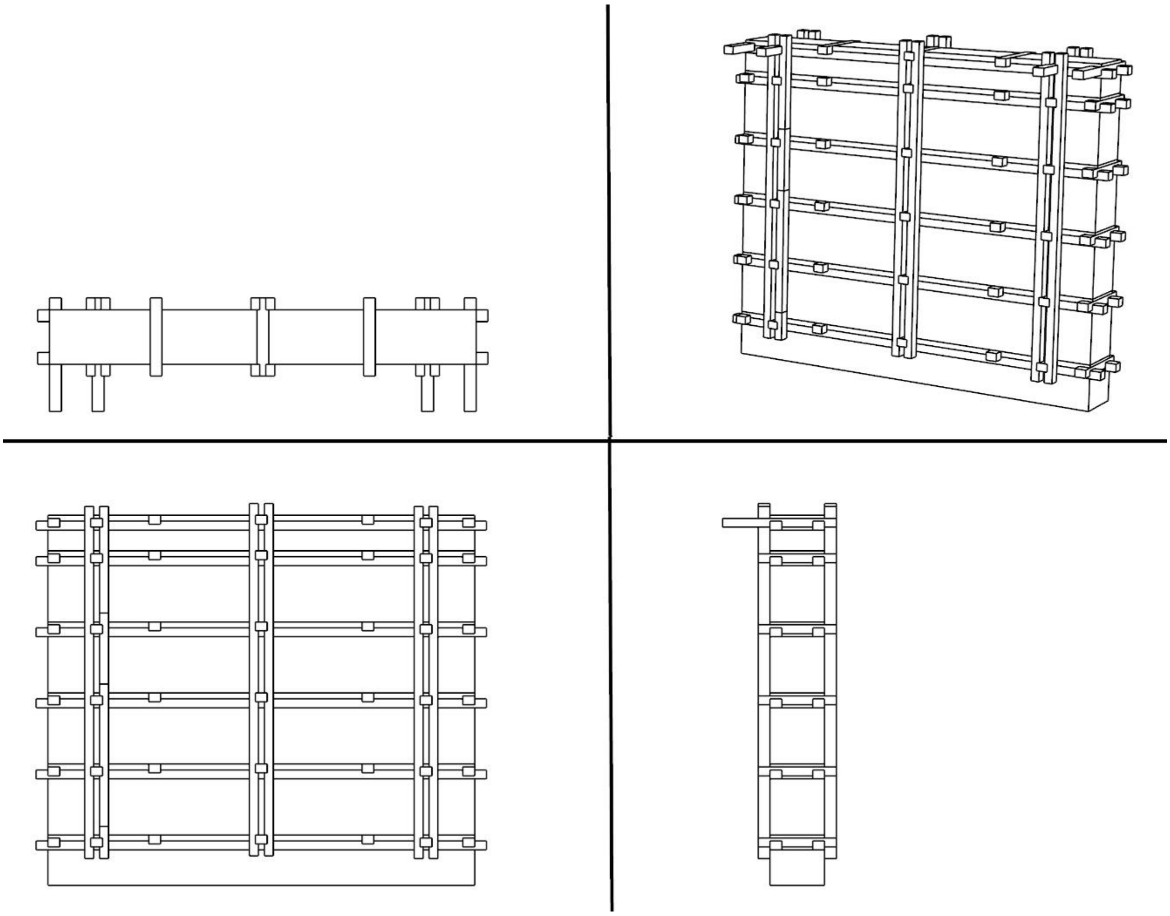

Figure 11-15 Thrifty Solution orthogonal projections

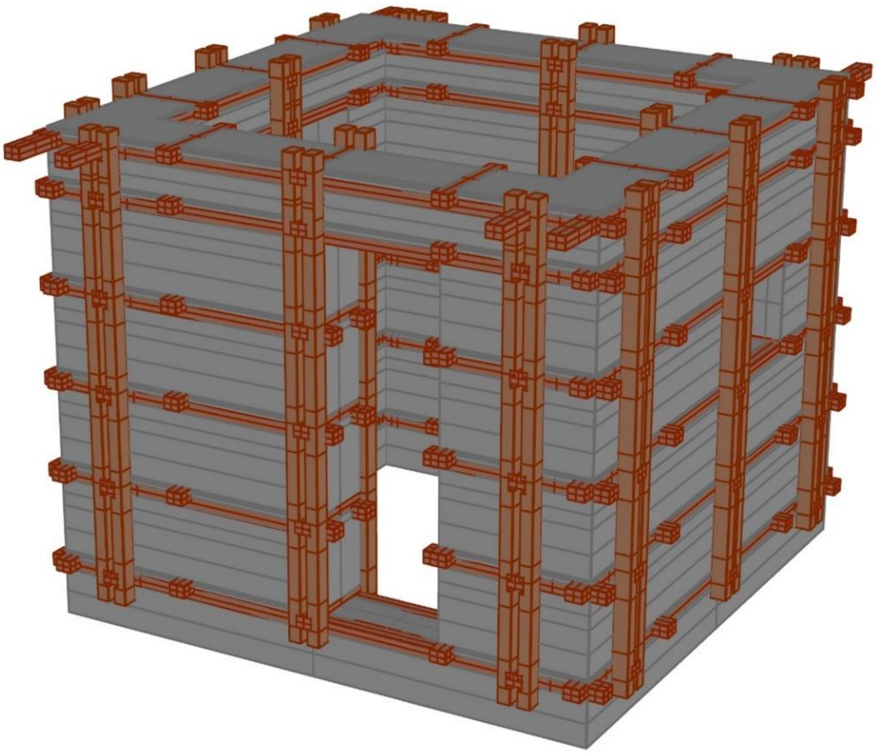

Figure 11-16 Thrifty solution

11.2.1.3 Optimal disposition for vertical rafters

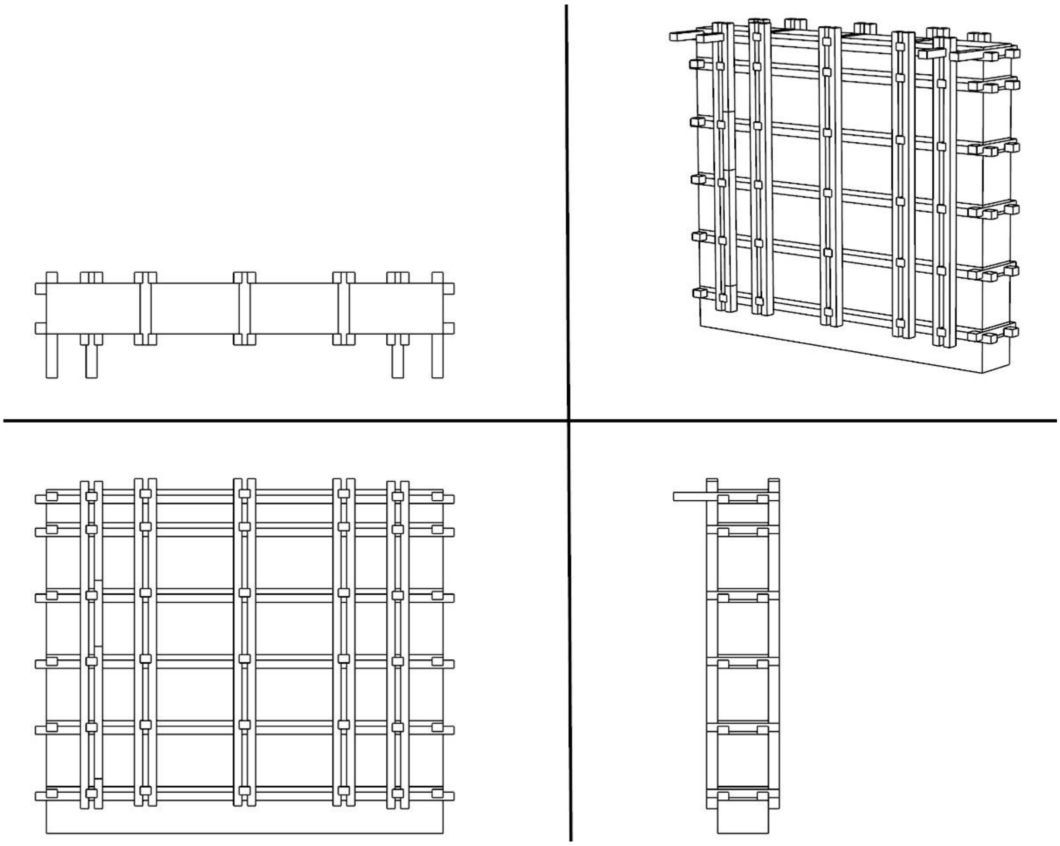

Figure 11-17 Optimal sSolution orthogonal projections

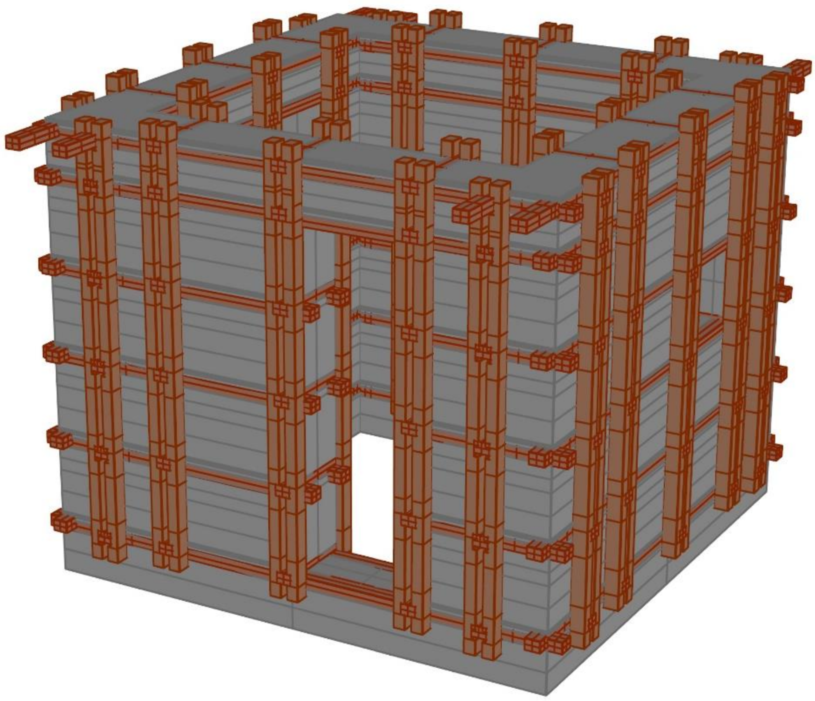

Figure 11-18 Optimal solution

11.2.2 Roof timber band

From the analysis it is clear that the most stressed timber band is the one where the heavy flat roof is placed. In order to renforce the last timber band on the top it is usefull to install two rafters instead of the two central cross pieces as shown in Figure 11-13.These new kind of rafters are generally equal to the rafter described in the previous chapter axept for the notch in the middle the length. The central joint is a half lap joint with depth of 5 cm as shown in Figure 11-14.

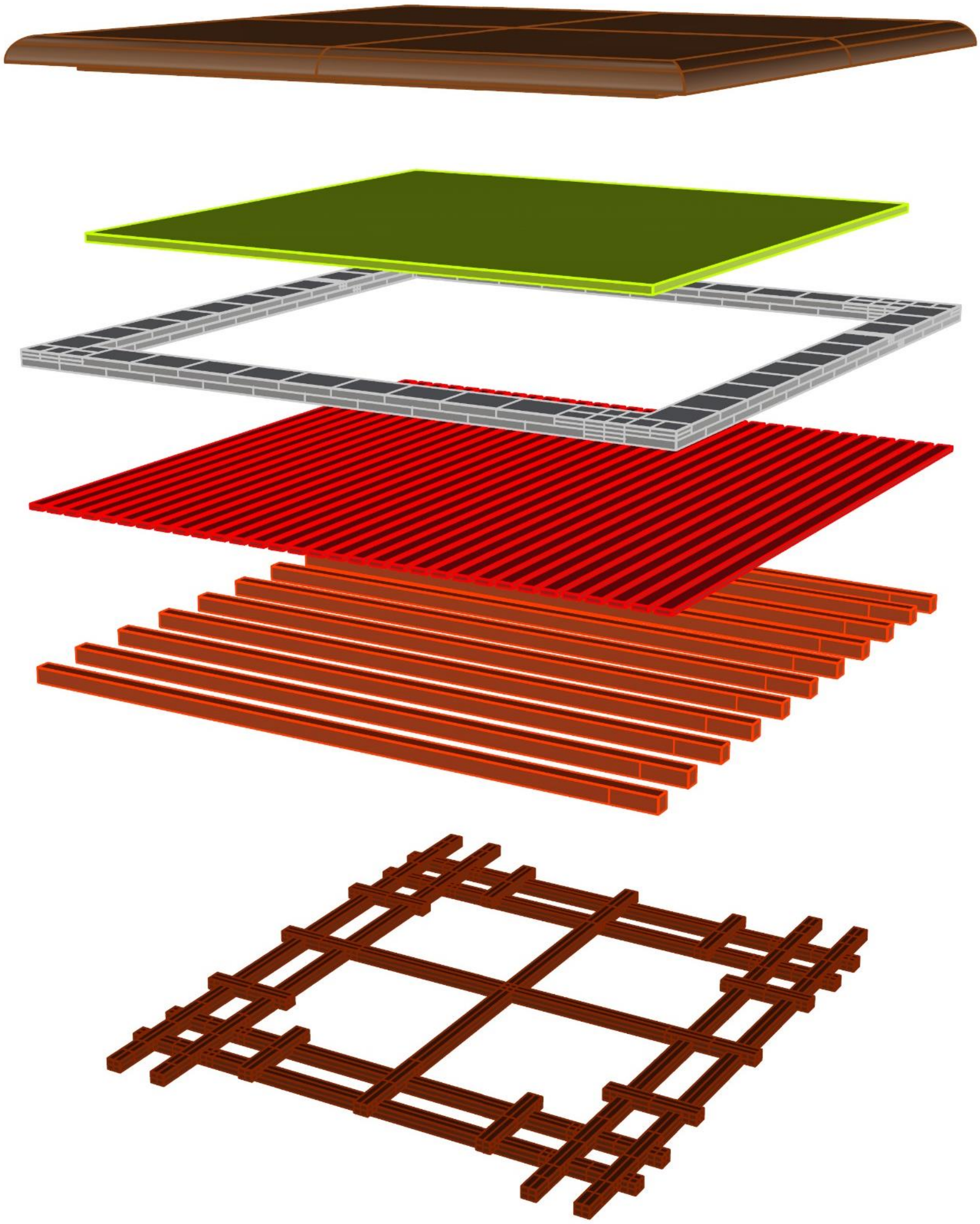

Figure 11-19 Rule of thumb for the roof

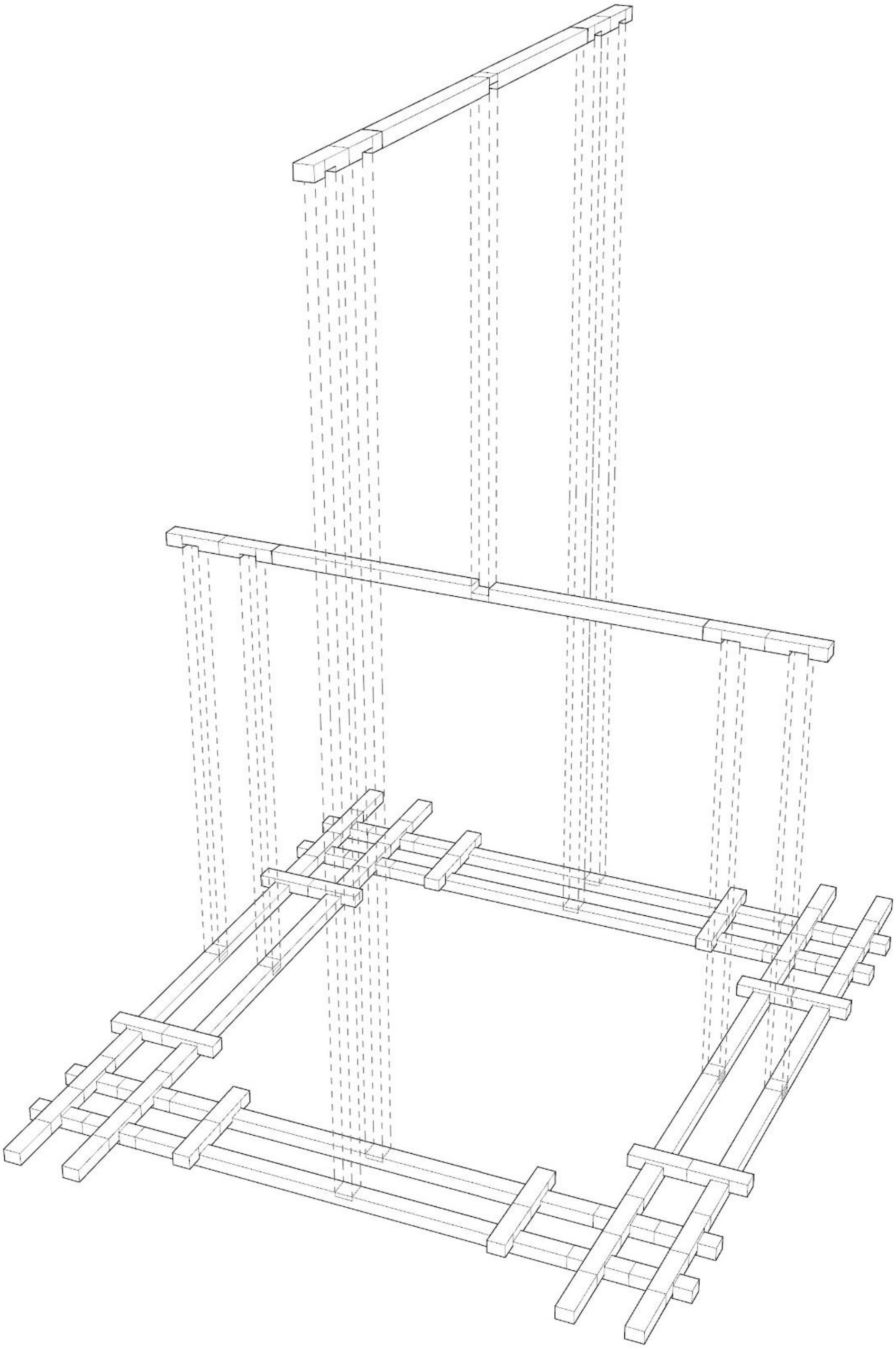

Figure 11-20 Rule of thumb for the roof - Timber band at roof level exploded

12 CONCLUSIONS

12.1 Analysis performed

After the initial observations on the bhatar box module they have been performed the main important seismic analysis used to describe the possible failure mechanisms on a dry-stacked masonry wall like the Bhatar: static, in-plane and out of plane analysis.

The analysis has been carried out starting from a research about materials properties commonly used in Nepal regions like shorea robusta wood and limestone rocks. The habitative unit has been decomposed in the elementar part. The basic geometric elements have been drawn with the Rhinoceros 3D computer graphics and computer-aided design (CAD) application software which allows to get information about volumes and other geometrical properties

The static analysis has been carried out studing the effect of the gravity acceleration on the mass of each layers. The effects of the vertical loads have been studied at different levels , e.g (i)in the middle of the stones layers and (ii)immediately below the timber bands

Generally the failure mechanism, in referenceto to the in plane resistance, mayhappen due to shear stresses.The shear stress may produce buckling , sliding or cracks. For the Bhatar system the only possible failure mechanism is the sliding between the stones. The buckling is a of secondary importance because the system is not compact enough, thus the failure happens before. The Bhatar system is characterized by the absence of mortar, the wall is composed by rubble stone masonry and timber beam which is naturally already cracked.

In order to study the sliding failure mechanism, the analysis have been conduct by the use of Barton model. The Barton model is a relationship between the normal stress and the shear stress developing in a gap filled with rocks. This method is used in the field of geotechnical engineering mostly in the studies of the stone dams.

The failure mechanism ,in reference to the out of plane resistance,may happen due to overturning with a rigid behavior or with a bending behavior.

The overturning with a rigid behavior has been studied considering the flat heavy earth roof as deformable slab and the absence of the bond-beam (or spreader-beam) at the roof level. The distribution of the reactions on the timber beam at the roof level has been studied as equal ditribuited on the timber rafters.

The timber elements embedded among them may be considered as bond beams, this is why the overturning with a bending behavior has been studied considering the flat heavy earth roof as deformable slab and the presence of the bond-beam (or spreader-beam) at the roof level.In this case,the distribution of the reactions on the timber beam at the roof level has been studied with a thoroughly analysis on the timber rafters connections in the corner joint.

12.2 Results

12.2.1 Results on seismic analysis in-plane

Recalling the results, they have been identified the critical layers for the in plane seismic analysis. The color red identified the critical load multiplier smaller than the Nepal peak ground acceleration, which is 0,5 g.

Table 68 Summary of results for the in-plane seismic analysis

	Critical Multiplier for inside stones layer case		Critical Multiplier below the timber band case	
Force applied at the top of the wall	**Layer**	**α <**	**Layer**	**α <**
	layer1	0,34	layer1	0,18
	layer2	0,41	layer2	0,21
	layer3	0,50	layer3	0,26
	layer4	0,58	layer4	0,31
	layer5	0,67	layer5	0,36
	layer6	0,74	layer6	0,40
	Layer_ground/Foundation	0,76	Layer_ground/Foundation	0,76
Triangular lateral distribution over the height of the wall	**Layer**	**α <**	**Layer**	**α <**
	Layer1	0,64	Layer1	0,37
	Layer2	0,63	Layer2	0,36
	Layer3	0,63	Layer3	0,35
	Layer4	0,65	Layer4	0,36
	Layer5	0,69	Layer5	0,38
	Layer6	0,74	Layer6	0,41
	Layer_ground/Foundation	0,76	Layer_ground/Foundation	0,76
Uniform lateral distribution over the height of the wall	**Layer**	**α <**	**Layer**	**α <**
	Layer1	0,89	Layer1	0,51
	Layer2	0,86	Layer2	0,49
	Layer3	0,82	Layer3	0,47
	Layer4	0,80	Layer4	0,46
	Layer5	0,78	Layer5	0,44
	Layer6	0,76	Layer6	0,43
	Layer_ground/Foundation	0,76	Layer_ground/Foundation	0,76

12.2.1.1 Critical Multiplier for inside stones layer case

Considering the Nepal peak ground acceleration given PGA = 0,5 g the seismic force results smaller than resisting shear force in both the sliding configurations.

The most critical one is the first configuration of «Force applied at the top of the wall» at the roof level, for layer 1 and layer 2 as shown in the following figure.

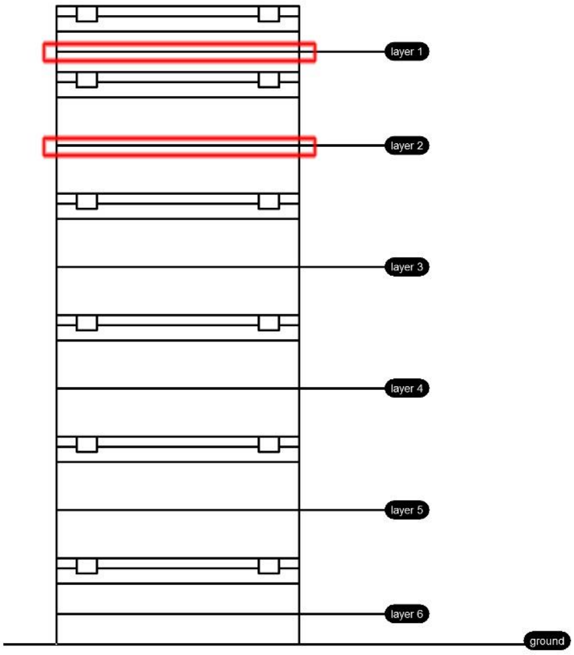

Figure 12-1 Critical layers for the in-plane seismic analysis. Sliding

12.2.1.2 Critical Multiplier below the timber band case

Considering the Nepal peak ground acceleration given PGA = 0,5 g the behavior shown is different in the sliding configurations examined considering an amplification of the action due by the safe factor γb = 1.5 . The most critical case is the first configuration of «Force applied at the top of the wall", which shows problems at all the layers. The sliding would occur starting from the roof level with a seismic load multiplier α =0.18 untill the layer ground/foundation with a seismic load multiplier α =0.43 The second critical case is the triangular lateral distribution over the height of the wall case, the sliding would occur for a seismic load multiplier α in a range between 0.37 : 0.43 .

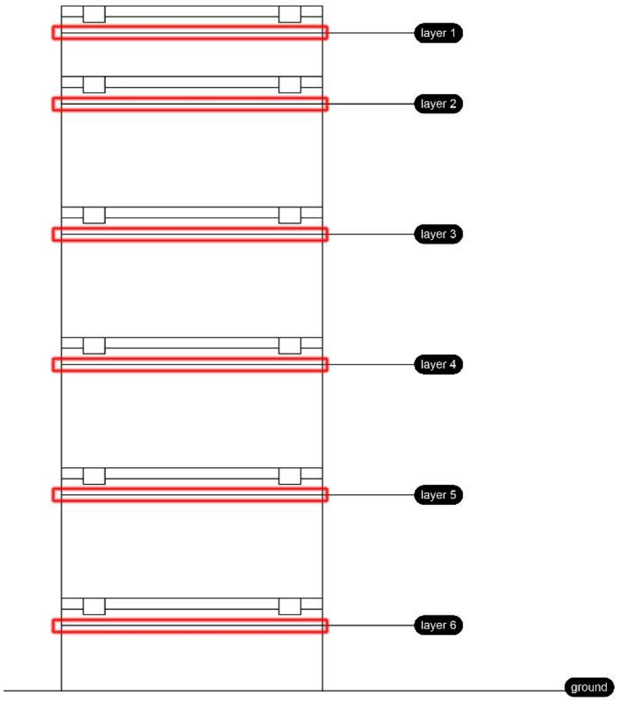

Figure 12-2 Critical layers for the in-plane seismic analysis. Sliding

12.2.2 Results on seismic analysis out of plane

12.2.2.1 Critical sections for a Nepal seismic event with a PGA=0.5g

The reference country of this thesis is Nepal, as it has been written the peak ground acceleration measured in the last decades in this country is around 0,5 g .

All the seismic load multipliers may be compared with the peak ground acceleration because they have been computed based on the unit measure of the gravity acceleration g. In this sub-chapter they are reported all the sections which do not satisfy the verification for a peak ground acceleration equal or larger to the seismic event expected in Nepal region. Thus, the critical sections are listed specifying the weakness form the most critical to the most safe. Indicators must be read with the following interpretation:

- Red : α < 0.5 g
- Yellow : α =0.5 g
- Green : α >0.5 g

RIGID	
α	
0,15	RH90shear with bending
0,15	RH90shear with bending
0,2	Combination of CPNotch0mX and CPNotch0shearY
0,2	CPNotch0shearY with bending and CPNotch0shearY
0,2	RH90shear
0,25	RH90shear
0,35	RB0shearY with bending and RB0shearY
0,5	Combination of CPNotch0mX and CPNotch0shearZ
0,5	CPNotch0mX
0,7	RB0tens
0,8	Combination of Notch0mX and Notch90shearY
0,8	Notch0mZ2
0,9	RH0shearEXT with bending

FLEXIBLE	
α	
0,125	RH90shear with bending for Tab, Tcd and Tda
0,125	RH90shear with bending for Tab, Tcd and Tda
0,15	RH90shear for Tda and RH90shear with bending for Tbc
0,15	RH90shear for Tda and RH90shear with bending for Tbc
0,2	RH90shear for Tab, Tbc and Tcd
0,2	RH90shear for Tab, Tbc and Tcd
0,3	CPNotch0mY
0,3	RRH0shearEXT with bending for Nbc
0,3	The verification about "Influence of keyed scarf joint" is satisfied for a load multiplier α = 0.3.
0,4	CPNotch0shearY with bending
0,5	Combination of Notch0tens, Notch0mY and Notch0mZ2 considering Nbc and BM in B
0,6	Combination of Notch0tens, Notch0mY and Notch0mZ2 considering Nbc and BM in C
0,6	Combination of Notch0tens, Notch0mY and Notch0mZ2 considering Ncd and BM in D
0,6	Combination of Notch90shearY and Notch0mX considering Tcd and the pertinent torsional parasitic bending moment
0,6	Combination of Notch90shearY and Notch0mX considering Tda and the pertinent torsional parasitic bending moment
0,6	RRH0shearEXT with bending for Nab
0,6	RRH0shearEXT with bending for Ncd
0,7	Combination of Notch90shearY and Notch0mX considering Tab and the pertinent torsional parasitic bending moment
0,7	Combination of Notch90shearY and Notch0mX considering Tbc and the pertinent torsional parasitic bending moment
0,7	CPNotch0shearY
0,7	RB0mY with bending
0,7	RB0shearY with bending
0,7	RRH0shearEXT with bending for Nda
0,8	Notch0mX for Tda
0,8	RRH0shearINT with bending
0,9	Combination of CPNotch0tens and CPNotch0mY
0,9	Combination of CPNotch0tens and CPNotch0mZ
0,9	Combination of Notch0tens, Notch0mY and Notch0mZ2 considering Nab and BM in A
0,9	Combination of Notch0tens, Notch0mY and Notch0mZ2 considering Ncd and BM in C
0,9	CPNotch0mY
0,9	Notch0mX for Tab, Tcd
0,9	Notch0mZ for BM in D

The critical sections verified for a load multiplier α < 0.5 are listed in the following figure:

RIGID	
α	
⊗ 0,15	RH90shear
⊗ 0,15	RH90shear
⊗ 0,2	Combination of CPNotch0mX and CPNotch0shearY
⊗ 0,2	CPNotch0shearY with bending and CPNotch0shearY
⊗ 0,2	RH90shear
⊗ 0,25	RH90shear
⊗ 0,35	RB0shearY with bending and RB0shearY

FLEXIBLE	
α	
⊗ 0,125	RH90shear with bending for Tab, Tcd and Tda
⊗ 0,125	RH90shear with bending for Tab, Tcd and Tda
⊗ 0,15	RH90shear for Tda and RH90shear with bending for Tbc
⊗ 0,15	RH90shear for Tda and RH90shear with bending for Tbc
⊗ 0,2	RH90shear for Tab, Tbc and Tcd
⊗ 0,2	RH90shear for Tab, Tbc and Tcd
⊗ 0,3	CPNotch0mY
⊗ 0,3	RRH0shearEXT with bending for Nbc
⊗ 0,3	The verification about "Influence of keyed scarf joint" is satisfied for a load multiplier α = 0.3.
⊗ 0,4	CPNotch0shearY with bending

Figure 12-3 Critical sections on the bhatar construction

Basically all the criticalities refer to the notch section of the timber elements with the exeption for the keyed scarf joint.

12.2.2.2 Analysis out of plane – Overturning rigidbehavior

The most critical section is in the rafters of the timber beam belonging to overturning wall.
This section has been named RH90shear and it is shown in the figure below.
The verification of this section is satisfied for a seismic load multiplier α = 0,15

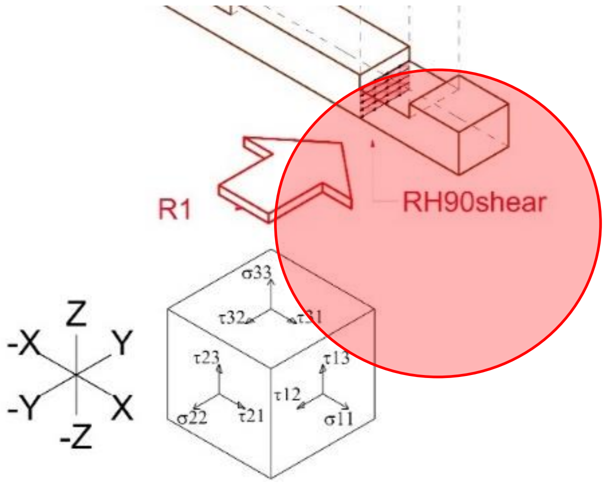

Figure 12-4 RH90Shear most ctitical section

12.2.2.3 Analysis out of plane – Flexible response – Bendingbehavior

The most critical section, again, is in the rafters of the timber beam belonging to failing wall.
The verification of this section is satisfied for a seismic load multiplier α = 0,125

12.3Possible research developemnts

This work reports a full analytical study on the static and seismic behavior, anyhow many subject about this topic need to be examined. In the list below are reported the main important subjects suggested to be thorough :

- Experimental tests on different kind of stones in order to define the specific parameter for the Bartom model for each different kind of stones
- Lab tests on a scale model in order to verify the reliability of the Barton Model for this kind of structure (IN PLANE LAB TESTS)
- Lab tests on Shorea robusta timber, mechanical properties.
- Lab tests on a scale model in order to verify the resistance of the timber elements and the carpentry connections.
- Lab tests on a box module in scale to verify the whole structure behavior.
- Definition of parameters of Barton model for rockfill in order to study the bhatar with a numerical approach.
- Definition of a DEM program in order to verified the hand calculation analysis done.
- Deep study on the horizontal timber bands working as a grounp and the influence on the fragile behavior of the timber.

Thumb rules:

- Definition of the dimensioning for design of the vertical and diagonal connectors . This means the diameter of the steel wire and the number of connectors for each cross piece couple. This is because it is needed to ensure a good strength for vertical component of the seismic event and also in order to avoid the sliding of the 4 top timber bands.
- Definition of the dimensioning for design vertical elements at the foundation level for the steel wire or rope case and for vertical rafter case in order to ensure a global scatolar behavior.

BIBLIOGRAPHY

[1] DON’T TEAR IT DOWN - PRESERVING THE EARTHQUAKE RESISTANT - Text and Photographs by Randolph Langenbach - First published in India by: Vernacular Architecture of Kashmir - United Nations Educational, Scientific and Cultural Organization (UNESCO)

[2] MECHANICAL PROPERTIES AND DURABILITY OF SOME SELECTED TIMBER SPECIES - M. Bellal Hossain1 and A.S.M. Abdul Awal2

[3] STUDIES ON TENSILE STRENGTH PROPERTY OF COMMERCIAL TIMBER SPECIES OF SOLAN DISTRICT - Himachal Pradesh SEEMA BHATT, BUPENDER DUTT, RAJESH KUMAR MEENA and TASRUF AHMAD*

[4] COMPARISON OF TEST RESULTS OF VARIOUS AVAILABLE NEPALESE TIMBERS FOR SMALL WIND TURBINE APPLICATIONS - R. Sharma1 1 1 , R. Sinha , P. Acharya , L. Mishnaevsky Jr. 2, P. Freere3

[5] TECNOLOGIA DEL LEGNO - G. Giordano, UTET, Torino 1988.

[6] NBC 203 Guidelines for Earthquake Resistant Building Construction: Low Strength Masonry UNDP/UNCHS (Habitat) Sub-project Nep 88/054/21.03, His Majesty's Government of Nepal, Ministry of House and Physical Planning 1994

[7] Appendix-A: Prototype Building inventory; the Development of Alternative Building Materials and Technologies for Nepal UNDP/UNCHS (Habitat) Sub-project Nep 88/054/21.03, His Majesty's Government of Nepal, Ministry of House and Physical Planning 1994

SITOGRAPHY

[1] BHATAR , ARCH. TOM SCHACHER : http://www.archidev.org/IMG/pdf/Battar-handout_English-07-06-04.pdf

[2]BHATAR , ARCH. TOM SCHACHER : http://www.traditional-is-modern.net/LIBRARY/SCHACHER-lessons/07(12)SCHACHER-Bhatar%20handout.pdf

[3]TIMBER, SHOREA ROBUSTA : http://civil.utm.my/mjce/files/2013/10/Mechanical-Properties-And-Durability-Of-Some-Selected-Timber-Species.pdf

[4] TIMBER, SHOREA ROBUSTA : http://www.inflibnet.ac.in/ojs/index.php/IJFS/article/download/3432/2703

[5] TIMBER, SHOREA ROBUSTA : http://solar.org.au/papers/08papers/241.pdf

[6] THE WORLD HOUSING ENCYCLOPEDIA (WHE) - http://db.world-housing.net/building/74/

[7] MINERAL RESOURCES OF NEPAL AND THEIR PRESENT STATUS - Krishna P. Kaphle, Former Superintending Geologist, Department of Mines and Geology, Kathmandu, Nepal Former President, Nepal Geological Society : http://ngs.org.np/geodetail/4

[8] Shear Strength of Rockfill, Interfaces and Rock Joints, and their Points of Contact in Rock Dump Design :https://www.researchgate.net/publication/242456636

[9] Shear strength criteria for rock, rock joints, rockfill and rock masses: Problems and some solutions:

- Journal of Rock Mechanics and Geotechnical Engineering : http://www.sciencedirect.com/science/article/pii/S1674775513000449
- Researchgate : https://www.researchgate.net/publication/278703795_Shear_Strength_Criteria_for_Rock_Rock_Joints_Rockfill_Interfaces_and_Rock_Masses
- Nick Barton and associate : http://www.nickbarton.com/downloads_03.asp